GEOLOGICAL SURVEY OF CANADA

OPEN FILE 2169

This document was produced
by scanning the original publication.

Ce document a été produit par
numérisation de la publication originale.

Mineral deposits of the northern Canadian Cordillera, Yukon - northeastern British Columbia (Field Trip 14)

edited by
J.G. Abbott
R.J.W. Turner

1991

Energy, Mines and Resources Canada
Énergie, Mines et Ressources Canada

Canada

GEOLOGICAL SURVEY OF CANADA

OPEN FILE 2169

Mineral deposits of the northern Canadian Cordillera, Yukon - northeastern British Columbia (Field Trip 14)

edited by
J.G. Abbott
R.J.W. Turner

1991

Energy, Mines and Resources Canada
Énergie, Mines et Ressources Canada

Canada

GEOLOGICAL SURVEY OF CANADA

OPEN FILE 2169

MINERAL DEPOSITS OF THE NORTHERN CANADIAN CORDILLERA, YUKON - NORTHEASTERN BRITISH COLUMBIA

[FIELD TRIP 14]

EDITED BY

J.G. ABBOTT and R.J.W. TURNER

With Contributions from:

J.G. Abbott, S.M. Abercrombie, D. Atkinson, D.J. Baker, R.J. Beckett, M.S. Cathro, K.M. Dawson, B.W. Downing, J.L. Duke, W.D. Goodfellow, S.P. Gordey, J.D. Hughes, D.G.F. Long, J.M. Peter, L.C. Pigage, D. Rhodes, S.S. Scott, D.J. Tempelman-Kluit, R.J.W. Turner and M.P. Webster

8TH IAGOD SYMPOSIUM

FIELD TRIP GUIDEBOOK

8th IAGOD SYMPOSIUM

FIELD TRIPS COMMITTEE

Chairman and Guidebook Technical Editor:	**W.D. GOODFELLOW**
Guidebook Reviewer:	**W.D. SINCLAIR**
Field Trip Committee Members:	**B.I. CAMERON** **A. DOUMA** **C.W. JEFFERSON** **A.R. MILLER** **N. PRASAD** **D.G. RICHARDSON** **A.L. SANGSTER** **J.M. SHAW**
Word Processing:	**P. BROWN** **B. GIESE**

TABLE OF CONTENTS

REGIONAL GEOLOGICAL SETTING OF SELECTED MINERAL DEPOSITS OF THE NORTHERN CORDILLERA

Kenneth M. Dawson
Geological Survey of Canada
Mineral Resources Division
100 West Pender Street
Vancouver, B.C. CANADA
V6B 1R8

INTRODUCTION

This paper attempts to provide an overview of the geological context for some of the mineral deposits in the northern Canadian Cordillera. The mineral deposits emphasized are those visited by the I.A.G.O.D. field trip #14 "Mineral deposits of the northern Canadian Cordillera" and discussed by various papers in this field guide.

From east to west the northern Canadian Cordillera is composed of:

(1) autochthonous miogeoclinal strata of Middle Proterozoic to Late Paleozoic age;

(2) displaced continental margin; and
(3) accreted collage of allochthonous terranes of the central and western Cordillera.

This paper emphasizes the miogeocline as it is host to most of the deposits visited (i.e. Anvil district, Jason, Tom, Mactung). Discussion of displaced continental margin terranes and allochthonous terranes is limited to those that host mineral deposits visited on this trip. The structure of the paper is as follows:

AUTOCHTHONOUS NORTH AMERICAN MIOGEOCLINE

A. Middle Proterozoic passive margin - Wernecke Supergroup; Mackenzie Mountains Assemblage

B. Late Proterozoic Rifted Margin - Windermere Supergroup

C. Cambrian to Middle Devonian passive margin - Late Precambrian to Middle Devonian platform-basin assemblage - Sedimentary-exhalative Zn-Pb deposits - Anvil District (Stop #6); Howards Pass district - Skarn and replacement deposits - Mactung W skarn deposit (Stop #4)

D. Middle Devonian to Mississippian clastic wedge - Earn Group - Tom and Jason sedimentary exhalative Zn,Pb,Ag barite deposits (Stops #2,3)

DISPLACED CONTINENTAL MARGIN

Cassiar Terrane - Ketza River Au manto deposit (Stop #5)

ACCRETED TERRANES

Alexander Terrane - Windy Craggy volcanogenic massive sulphide deposit (Stop #1)

OVERLAP ASSEMBLAGES

Grew Creek epithermal Au,Ag deposit (Stop #7)

AUTOCHTHONOUS NORTH AMERICAN MIOGEOCLINE

A. Middle Proterozoic passive margin

Middle Proterozoic clastic and carbonate sequences are included in at least two assemblages more than 10 km thick, of miogeoclinal character and passive marginal setting. The older sequence comprises the Purcell (Belt) Supergroup in the southern Cordillera, the Wernecke Supergroup in the Wernecke and Ogilvie mountains, possibly the Muskwa Ranges succession in the northern Rocky Mountains, and represent an interval between 1.7 and 1.2 Ga.

The younger assemblage, the Mackenzie Mountains Supergroup, occurs only north of latitude 60° and may include the Pinguicula Group

in the Wernecke and Ogilvie mountains. It is younger than 1.2 Ga and older than 770 Ma, the age of diabase dykes which intrude the sequence in the Mackenzie Mountains. In the southern part of the Cordilleran orogen and perhaps in the northern Rocky Mountains, the older sequence of Middle Proterozoic rocks may have been deposited in one of several southwestward opening aulacogenes indenting a northwest-trending rifted continental margin (Gabrielse and Yorath, 1989).

Wernecke Supergroup

The Middle Proterozoic Wernecke Supergroup of the Wernecke and Ogilvie mountains of northern Yukon Territory is at least 14 km thick and consists dominantly of fine-grained terrigenous clastics which grade upwards to carbonate strata (Delaney, 1978, 1981). It has been broadly correlated with the Purcell Supergroup (Young et al., 1979) and is considered older than 1.2 Ga on the basis of crosscutting breccia pipes, isotopically dated by Archer and Schmidt (1978) and Archer et al. (1986). Bell's (1982) proposal that the Wernecke Supergroup may be a displaced terrane incorporating continental margin sediments dextrally displaced in Late Proterozoic (Windermere) time is further expanded by Aitken and McMechan (in press) as the distal part of the Hornby Bay-Dismal Lakes miogeoclinal wedge. The aulacogen depositional environment proposed for the Hornby basin (Kerans et al., 1981; Dewey and Burke, 1973), in which an elongate rift opens westward to the continental margin, is similar to the setting of a structurally- controlled Purcell embayment in the continental margin supported by Aitken and McMechan (in press).

The most significant mineral deposits hosted by rocks of the Wernecke Supergroup (Figure 1) are the more than forty U occurrences, mainly brannerite, $(U,Ca,Fe)_3Ti_5O_{16}$, accompanied by several assemblages of Cu, Fe, U, Ba, Co, and Au minerals. They occur in narrow discontinuous vein-zones peripheral to metre- to kilometre-scale monolithic and heterolithic breccia bodies that commonly cut the lower parts of the sedimentary sequence (Archer and Schmidt, 1978; Bell, 1978, 1982). A pre-displacement age of U mineralization is proposed, related to a synsedimentary rifting event which occurred at about 1.2 Ga, prior to dextral displacement of the Wernecke Supergroup in Windermere time. Local remobilization of uranium within the occurrences took place during later deformation.

Also located near the top of the Wernecke Supergroup but possibly unrelated to breccias, is the Hart River massive sulphide deposit hosted by black argillite 50 m below pillow basalt flows (Abbott, 1987). Both Hart River (1.24-1.28 Ga; Morin, 1978) and Sullivan (1.43 Ga; LeCouteur, 1979) are Middle Proterozoic products of exhalative activity within distal sedimentary facies possibly related to faulting (Aitken and McMechan, in press; Hoy, 1982).

Mackenzie Mountains Assemblage

An extensive pericratonic platformal succession composed of at least 4000 m of predominantly shallow water quartzite, shale, and partly stromatolitic carbonates (Aitken et al., 1978a; Gabrielse et al., 1973) was deposited in the Mackenzie Mountains region between about 1.2 and 0.8 Ga. The upper sequence of Middle Proterozoic rocks, the Mackenzie Mountains Supergroup, appears to have accumulated upon a deeply subsiding epicratonic platform. Assuming that the Muskwa Ranges succession belongs to the older Purcell (Belt) Assemblage, much of the Cordillera throughout British Columbia and the United States contains no record of the interval between 1.2 and 0.8 Ga, the age of the basal part of the overlying Windermere Supergroup. Fragmentary evidence for deformation, metamorphism and granitic intrusion in the Purcell rocks suggests one or two episodes of tectonism prior to Windermere deposition. The lack of an associated clastic wedge renders an unknown significance to these events (Gabrielse and Yorath, 1989).

Proterozoic rocks of this age are not known in the central and southern Canadian Cordillera, but correlation of the lower formations of the Mackenzie Mountains Supergroup with the Rae Group of the Coppermine Homocline, Northwest Territories, has been established by Young (1977) and Aitken et al. (1978b).

The most significant mineral deposits known in the Mackenzie Mountains Supergroup are the carbonate-hosted (Mississippi Valley-type) Zn,Pb deposits of the Gayna River region hosted by dolostones of the Little Dal Group (Figure 1). The district, comprising some 18 deposits and

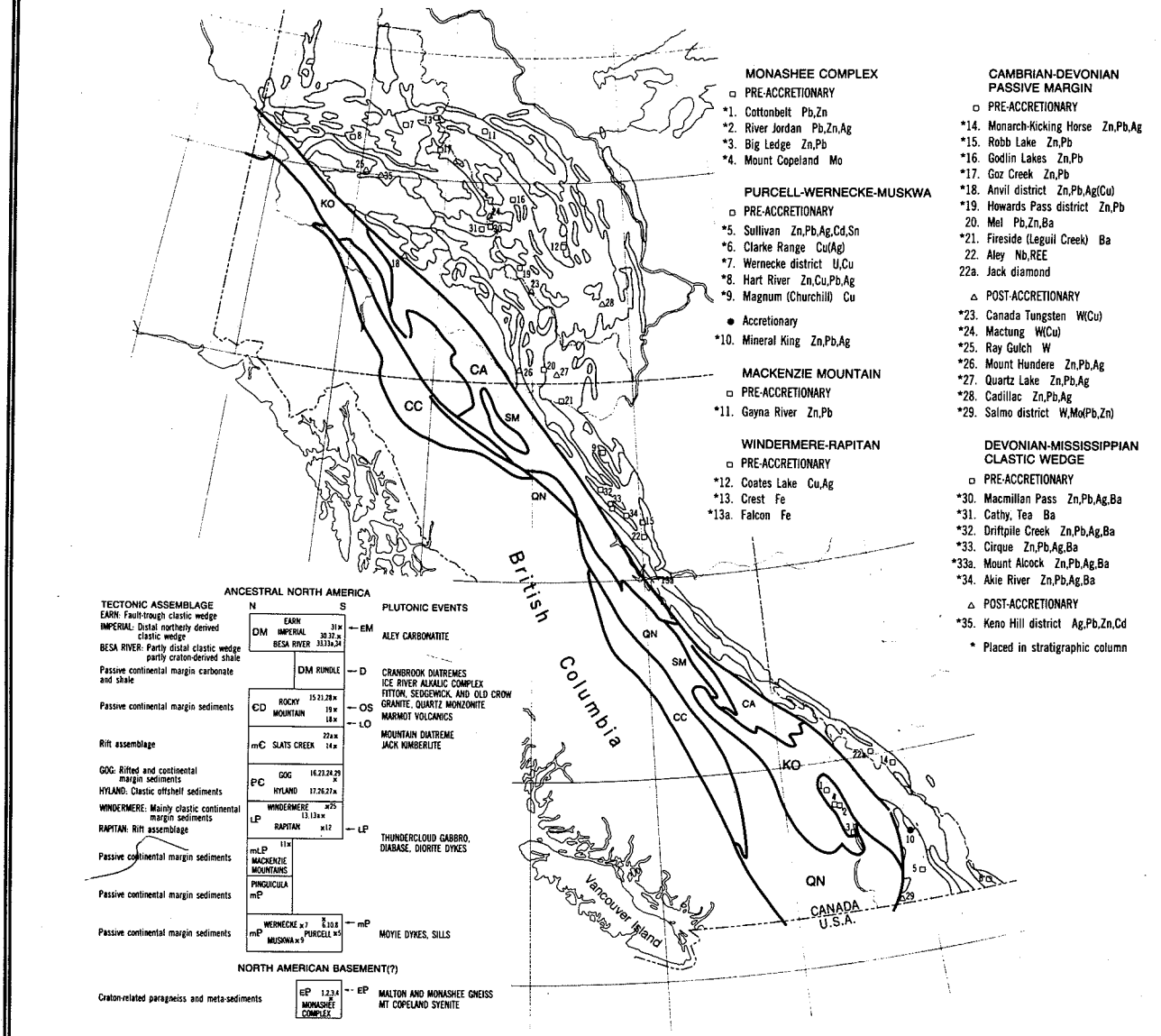

Figure 1 Ancestral North America and (?) Basement (from Dawson et al., in press.)

more than 100 occurrences, has estimated potential resources of more than 50 million tonnes of greater than 5% combined Zn + Pb (Hewton, 1982).

B. Late Proterozoic Rifted Margin

In contrast to the areally restricted Middle

Proterozoic assemblages, thick, dominantly clastic strata of the Upper Proterozoic Windermere Supergroup occur throughout the full length of the Cordillera and bear close spatial relationships with lower Paleozoic miogeoclinal rocks.

Windermere Supergroup

The dominantly clastic rocks of the Upper Proterozoic Windermere Supergroup, in contrast to the areally restricted Middle Proterozoic assemblages, are exposed almost continuously from Alaska, through Yukon Territory and British Columbia southward into California (Figure 1) and contain the depositional record of a major rifting event along the western continental margin of North America (Stewart, 1972; Eisbacher, 1981; Young, 1982; Gabrielse and Campbell, in press). Lowest and easternmost units, i.e. the Rapitan Assemblage, best reflect a rift environment with rapid facies and thickness changes, a suite of rift-related igneous intrusions and extrusions whose isotopic ages centre on 770 Ma, and the local presence of evaporites. Throughout the eastern Cordillera the Windermere Supergroup is unconformably overlain by Lower Cambrian sandstone, indicating a minimum age of about 570 Ma. Diamictite, in part glaciogenic, occurs at several localities and stratigraphic levels, notable at two well defined horizons in eastern Mackenzie Mountains, one of which also contains jaspilite-hematite iron formation of probable volcanic exhalative origin. One of the largest hematite-jaspilite iron deposits in North America, the Crest iron deposit at Snake River (Figure 1), in its richest central part, contains 5.6 billion tonnes of iron formation averaging 47.2% Fe (Stuart, 1963), whereas the regional resource is estimated to exceed 18.6 billion tonnes (Yeo, 1986).

Significant stratabound copper deposits are hosted by rocks of the Coates Lake Group, an unconformity-bounded rift assemblage which occurs mainly in six synsedimentary fault-controlled depositional embayments over a 300 km long arcuate belt marking the eastern limit of Upper Proterozoic strata in the Mackenzie Mountains (Jefferson and Ruelle, 1986). An interval of evaporitic mudstones and algal laminites, transitional from underlying redbeds to basinal turbiditic limestone sequences of the Coppercap Formation (Gabrielse et al., 1973), includes up to eight repetitive sabkha sequences at Coates Lake (Figure 1) containing Cu, Fe, and less abundant Pb and Zn sulphides disseminated in algal limestone beds (Jefferson and Ruelle, 1986). The lowest copper-bearing bed in this transition zone, the only one that approaches economic proportions, averages 1 m thick and contains 37 million tonnes of 3.92% Cu and 11.3 g/t Ag within an area of about 12 km^2 (Ruelle, 1982).

C. Cambrian to Middle Devonian passive margin

Late Precambrian to Middle Devonian platform-basin assemblage

From the late Precambrian to Middle Devonian the Foreland Belt of the eastern Cordillera was segmented into two contrasting facies belts. On the northeast were deposited shallow water sandstone, dolostone, and limestone that define the Mackenzie Platform. To the southwest, time-equivalent rocks comprise turbiditic sandstone, deep water limestone, shale, and chert of the Selwyn Basin. Within the Selwyn Basin, euxinic black shale of Early Silurian age is host to important stratiform lead-zinc deposits. The platform-basin boundary shifted with time so that a transitional region exists where formations of basin and platform affinity are interstratified. Numerous fossil collections, particularly conodonts, allow accurate correlation between platform and basin facies. Important unconformities occur beneath the Upper Cambrian, middle Lower Devonian, and lowermost Middle Devonian. The aggregate thickness of Lower Cambrian to Middle Devonian platform and thick basinal near-platform strata is about 4200 m, while that of equivalent outer basin strata is about 1600 m (Gordey, in press-a).

The oldest exposed strata within Selwyn Basin consist of latest(?) Precambrian turbiditic quartz sandstone at least 3000 m thick. They are younger than the Windermere Supergroup of Mackenzie Mountains with which they have previously been correlated. They may represent a younger Eocambrian rift event, as has been interpreted for similar strata in the southern Cordillera.

Sedimentary lithofacies exerted a primary control upon the localization of sediment-hosted mineral deposits. Carbonate-hosted Mississippi Valley-type (MV) Zn,Pb deposits, e.g. Goz Ck., Gagna R., Godlin Lks., occur commonly at the tectonically unstable western margin of lower

Paleozoic platformal carbonate successions. Younger skarn and replacement deposits, e.g. Mactung, Ketza River, (Figure 1) are located in essentially the same setting, where relatively thick and pure limestone beds were intruded by late Mesozoic to early Cenozoic felsic granitoid rocks. Sedimentary exhalative (sedex) Zn,Pb deposits, e.g. Howards Pass, Anvil district, are hosted commonly by fine cherty, calcareous and/or carbonaceous clastic successions within linear sub-basins whose development was controlled by synsedimentary extensional block faulting near the shelf-slope transition.

Sedimentary-exhalative Zn-Pb deposits

The most significant stratiform shale-hosted sedimentary-exhalative Zn,Pb deposits of the Cambrian to Middle Devonian passive margin, termed "sedex" by Carne and Cathro (1982), are contained within the Anvil and Howards Pass districts, which occupy linear belts on opposite sides of Selwyn Basin in the northern Cordillera (Abbott et al., this volume). Selwyn Basin was established as a major negative tectonic element by latest Proterozoic time, flanked to the north and east by the Ogilvie and Redstone arches, and on the southeast by MacDonald Platform (Gabrielse, 1967). The western part of the basin was overridden by allochthonous upper Paleozoic and Mesozoic rocks (Tempelman-Kluit, 1979) and truncated by the Tintina Fault. Accordingly, age and stratigraphic correlation of the metamorphosed pelitic rocks hosting the Anvil district deposits, which lie directly east of allochthonous units and Tintina Fault, are not known with certainty. The tectonic setting, stratigraphy, and regional correlation of Cambrian to Silurian assemblages of Selwyn Basin are described by Fritz et al. (in press) and Abbott et al. (1986).

Stop 6 Anvil District

The first major sedimentary exhalative event is represented by the sedex deposits of the Anvil district (Pigage, this volume). They occur in a 150 m succession that is located at the transition between the informally named Mount Mye formation and conformably overlying Vangorda formation which comprise at least 3 km of non-calcareous and calcareous phyllites. The five sub-units of the Vangorda formation are correlated lithologically by Jennings and Jilson (1986) with Lower Cambrian limestone conglomerate and pelite mapped in eastern Selwyn Basin (Gordey, in press-a) and with the Cambro-Ordovician Rabbitkettle Formation in the same general area (Gabrielse et al., 1973). A 1 km-thick metabasaltic sequence, the informally named Menzies Creek formation (Jennings and Jilson, 1986), is interleaved with the upper shaly part of the Vangorda formation which contains Early Ordovician to Early Silurian graptolites (Gordey, 1983; Tempelman-Kluit, 1972), indicating a correlation with the Road River Group of Selwyn Basin.

Mineralization in the Anvil District was pre-accretionary with respect to the Mesozoic attachment of the allochthonous Slide Mountain and Kootenay terranes immediately to the southwest. Primary and deformational textures support a synsedimentary, pre-metamorphic age of mineralization.

Five stratiform pyritic Zn,Pb,Ag(Au,Cu,Ba) deposits and two stratiform pyritic Cu,Zn occurrences which extend over a strike length of 45 km constitute an aggregate pre-mining reserve of 120 million tonnes of 5.6% Zn, 3.7% Pb, and 45-50 g/t Ag (Jennings and Jilson, 1986). Faro, the largest deposit, is the only one mined prior to 1990, when Vangorda is slated for production.

The seven deposits are hosted by a distinctive graphitic phyllite unit which serves as a district-wide metallotect. Coincidence of marked southwestward thickening in graphitic phyllite with a linear array of centres of alkaline basaltic volcanism indicates that rift-related synsedimentary faults may have served as conduits for sedimentary exhalative fluids, however demonstrable feeder zones have not been observed. The accumulation of stratiform sulphide deposits in lower Paleozoic basinal facies of the outer Cordilleran miogeocline and spatially associated basaltic volcanism apparently are related to episodic Middle Cambrian to Early Ordovician extension and synsedimentary block faulting. Elongate tectonic sub-basins were postulated to have confined exhalative metalliferous brines in a reducing environment where base metal sulphides were precipitated (Jennings and Jilson, 1986).

Howards Pass district

A second major sedimentary exhalative

event was localized in eastern Selwyn Basin at Howards Pass where large stratiform bodies of Zn,Pb,Fe sulphides were deposited in Lower Silurian (Norford and Orchard, 1983) carbonaceous and limy mudstone and chert. Deep basinal clastic sedimentation adjacent to the Mackenzie carbonate platform was contemporaneous with two Early Paleozoic extensional episodes: the opening of Misty Creek Embayment in Early to Middle Cambrian time and the opening of Meilleur River Embayment in Early to Middle Ordovician time (Fritz et al., in press). Alkalic basaltic volcanism was widespread during the latter episode, notably in the Menzies Creek and upper Rabbitkettle formations.

Laminated sulphidic sediments of the XY, Anniv, and OP deposits of the Howards Pass district, which extend discontinuously southeastward for over 20 km, were localized within elongate sub-basinal depressions at the base of the slope 10-20 km southwest of the carbonate platform margin (Morganti, 1979, 1981). The XY mineralized zone, a lens up to 50 m thick decreasing gradually in thickness over its 3-4 km length, is composed of fine-grained, well bedded sphalerite, galena, and pyrite, with traces of chalcopyrite, molybdenite, and other sulphides thinly interlaminated with carbonaceous and limy mudstone and chert (Morganti, 1979). The XY and Anniv deposits combined contain indicated reserves of 113 million tonnes of 5% Zn and 2% Pb, plus a further 363 million tonnes of inferred reserves at a similar grade (Placer Development Ltd. Annual Report, June, 1982).

The Howards Pass deposits were formed from Pb- and Zn-rich fluids which discharged episodically into a stable, starved marine basin during a period of restricted seawater circulation and resultant sulphidic, anoxic bottom waters. The anoxic conditions corresponded to an episode of rifting, volcanism, basinal subsidence, local marine transgression, and related hydrothermal activity (Goodfellow and Jonasson, 1986).

2. Skarn and replacement deposits

Skarn and replacement deposits in the northern Canadian Cordillera are abundant, diverse, and economically significant (Figure 2). Skarn deposits of the miogeocline are localized commonly where mid-Cretaceous, generally S-type granitoid plutons of the Selwyn, Cassiar and Tombstone suites (Woodsworth et al., in press) discordantly intrude the lowest and(or) thickest limestone beds of an upper Proterozoic to lower Paleozoic shelf carbonate-pelite sequence. The broad thermal aureole at the contact between a Cretaceous quartz monzonite stock and a Lower Cambrian limestone is a typical setting.

Northern Cordilleran W,Cu(Zn,Mo) skarns are typically stratabound bodies adjacent to unaltered coarse-grained porphyritic quartz monzonite or granodiorite plutons. Relatively deep-seated passive plutonic emplacement is evidenced by wide hornfelsed aureoles, the presence of migmatite and pegmatite, the chemically reduced states of the mineral assemblages (e.g. graphite, pyrite and high Fe^2/Fe^3 ratios) and the absence of brecciation, breccia pipes, intense stockwork fracturing and(or) dyke swarms. Prograde almandine garnet-hedenbergitic pyroxene-scheelite skarn has overprinted contact calc-silicate hornfels. Subsequent cooling and influx of meteoric water has caused hydrous retrograde alteration of the skarn to an assemblage of amphibole-biotite-chlorite with redistribution of scheelite, including both depletion and upgrading, and deposition of sulphides (Dawson, in Eckstrand, 1984, p. 55).

In the Early Cretaceous, northeast-southwest compression of competent carbonate strata of Mackenzie Platform formed large open folds typical of the Mackenzie Fold Belt, whereas the largely incompetent Selwyn Basin strata formed smaller open to tight folds with pervasive axial-planar slaty cleavage (Selwyn Fold Belt) (Gordey, in press-b). Folded strata are intruded and hornfelsed by granite and granodiorite intrusions of the mid-Cretaceous Selwyn Plutonic Suite (Figure 3). Two major pluton types are distinguished by the presence or absence of hornblende. Tungsten skarns are associated with some of the latter in association with biotite and muscovite plus garnet, andalusite and tourmaline in tungsten-rich marginal phases and satellitic intrusions. Isotopic ages (mineral K-Ar and whole rock-mineral Rb-Sr isochrons) for the suite range from 88-114 Ma, with average ages for Mactung and Cantung plutons centred at 89 and 94 Ma, respectively (Anderson, 1983).

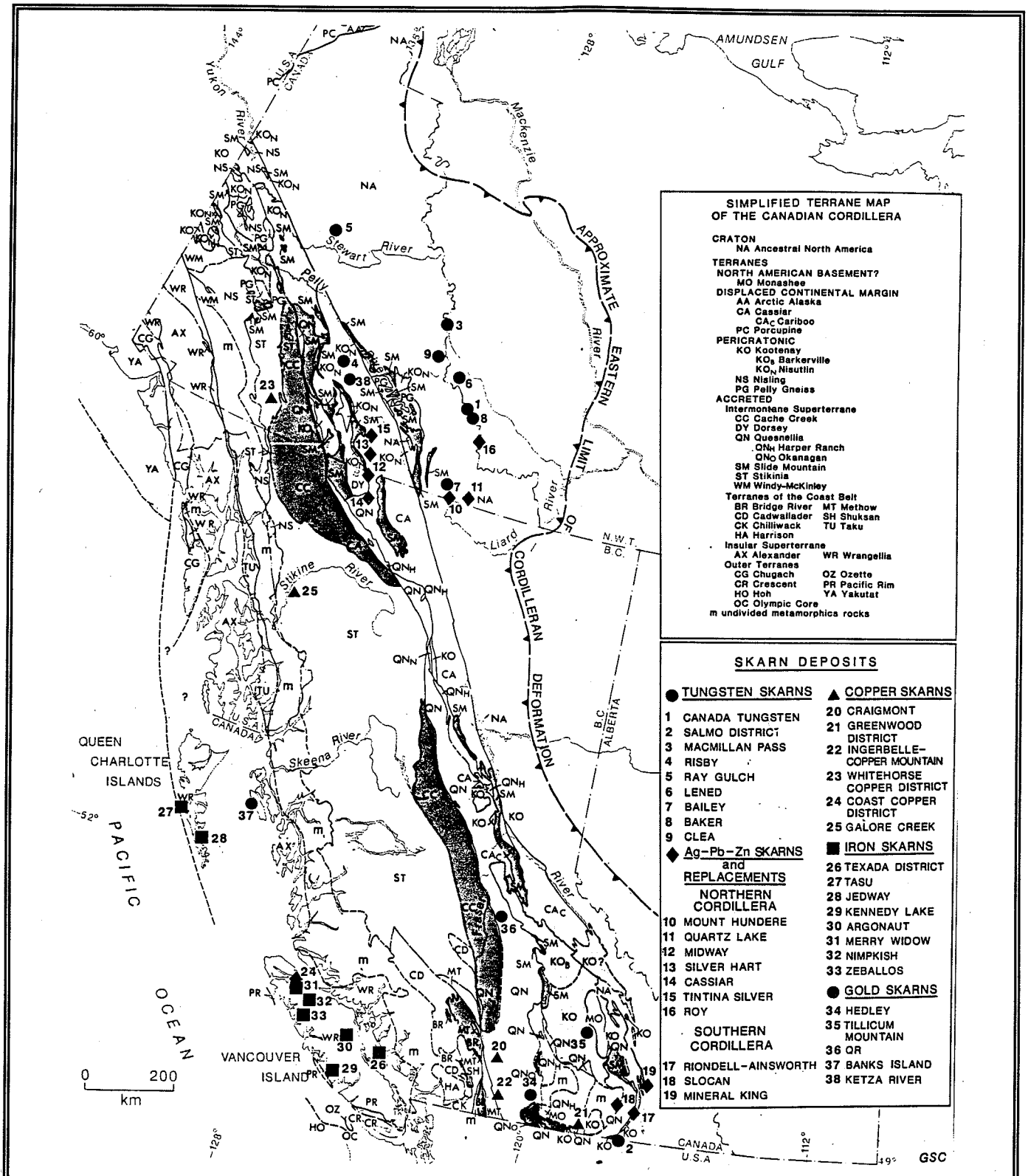

Figure 2 Skarn deposits of the Canadian Cordillera (from Dawson et al., in press).

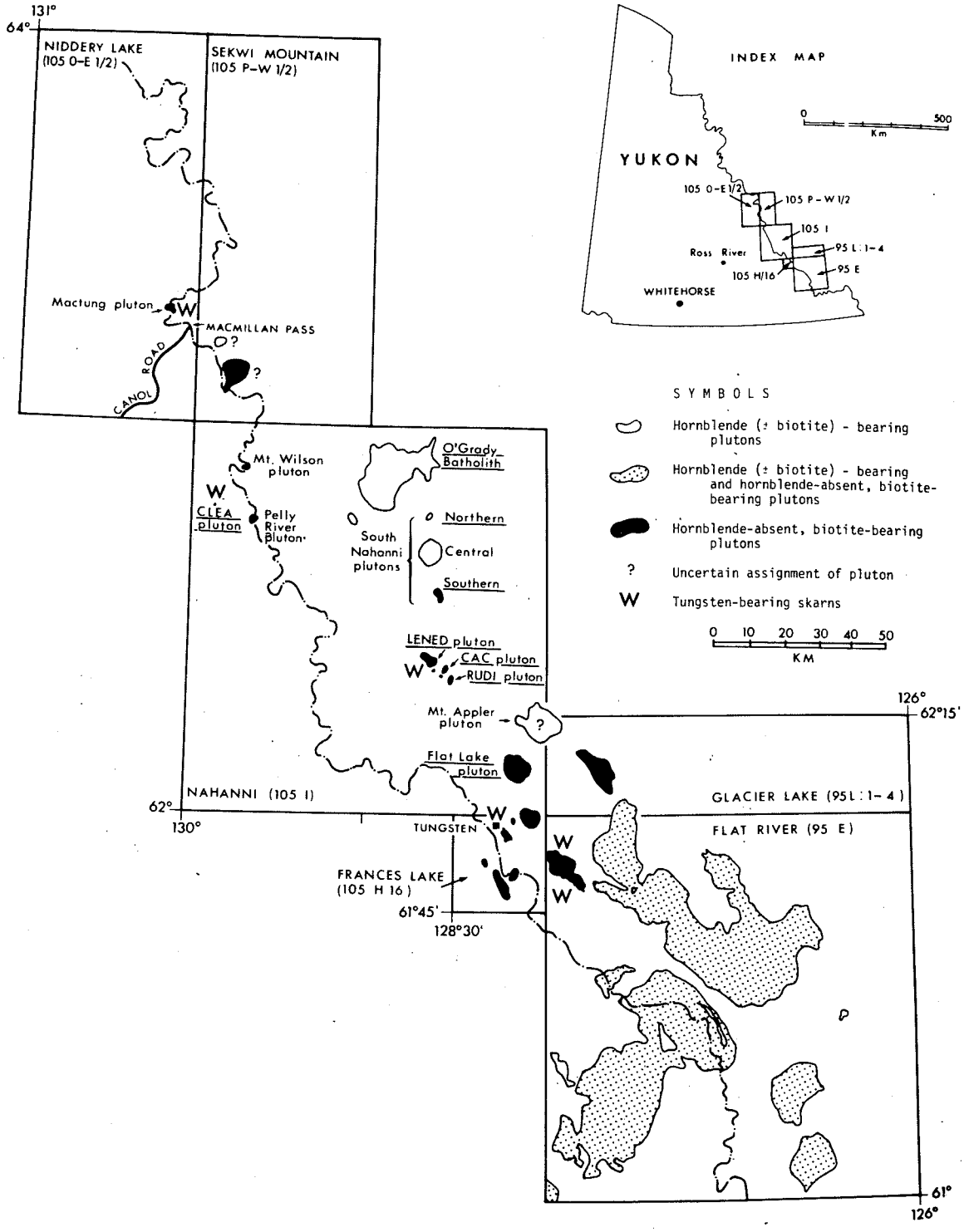

Figure 3 Southeastern Selwyn Plutonic Suite (from Anderson, 1983).

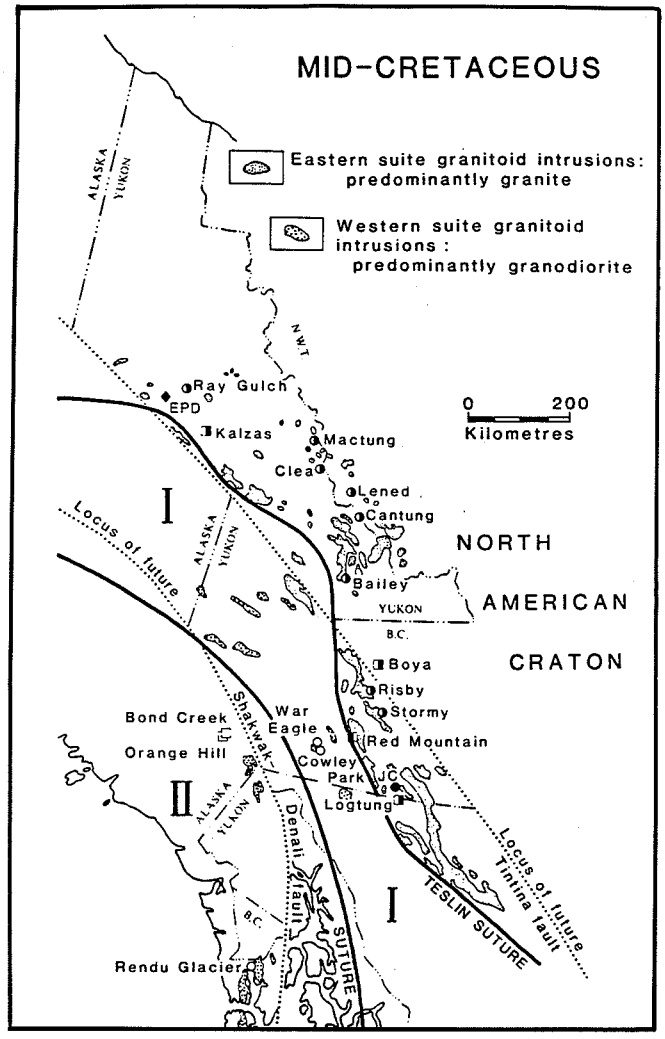

Figure 4 Distribution of mid-Cretaceous granitoid intrusions and associated deposits in the northern Cordillera (from Sinclair, 1986).

Stop 4 Mactung W skarn deposit

A belt of W,Cu(Zn,Mo) skarns centred on the Selwyn Plutonic Suite that follows an arcuate trend of similar, generally small, mid-Cretaceous granitoid plutons from southeastern Yukon Territory and southwestern District of Mackenzie, Northwest Territories, northwestward to the Dublin Gulch district (Figure 4) (Sinclair, 1986) contains one of the world's largest reserves and resources of skarn tungsten, mainly in the Canada Tungsten mine at Tungsten, Northwest Territories, and in the Mactung deposit at Macmillan Pass, Yukon Territory, 175 km northwest of Tungsten. The large, high-grade E-zone orebody at Canada Tungsten (Mathieson and Clark, 1984) contains geological (i.e. total of proven, probable, and possible) reserves of 7 million tonnes of 1.5% WO_3 and 0.2% Cu (Canada Tungsten Mining Corp. Ltd., pers. comm., 1986). Scheelite orebodies are hosted by basinal facies of two outer-shelf limestone members of the Lower Cambrian Sekwi Formation (Fritz, in press; Blusson, 1968) which form an overturned anticline whose lower limb is truncated by a quartz monzonite pluton spatially related to skarn ore.

Similar shelf rocks describe an arcuate belt that flanks Selwyn Basin on the east and northeast and hosts the world-class Mactung deposit at Macmillan Pass (Figure 1). Geological reserves of the developed prospect are 32 million tonnes of 0.92% WO_3 (Atkinson and Baker, 1986, this volume). Two scheelite- chalcopyrite ore zones have replaced limestone breccia and interbedded limestone-pelite in a gently dipping, locally folded Cambro-Ordovician outer shelf sequence which is both flanked on the north and inferred to be underlain by mid-Cretaceous granitoid stocks. Quartz vein densities, skarn and ore mineral zonation and location of pegmatite and aplite dykes are cited by Atkinson and Baker (1986, this volume), in support of a source of hydrothermal fluids at depth to the south of the orebody. Other potentially economic tungsten skarn deposits in this belt include, from southeast to northwest: Bailey, Baker, Lened, Clea, and Ray Gulch, whose reserves range between 1 and 5 million tonnes and grades between about 0.7 and 1.5% WO_3 (Dawson and Dick, 1978; Godwin et al., 1980; Glover and Burson, 1986; Figure 4).

In addition to tungsten skarns, base-metal and gold skarn and replacement deposits are the other skarn subtypes of economic significance in autochthonous and displaced (i.e. Cassiar Terrane) parts of the North American miogeocline. Numerous subeconomic Zn,Pb,Ag(Cu,W) skarns are adjacent to the Mount Billings Batholith in southeastern Yukon Territory and the Coal River stock in southwestern Northwest Territories in a tectonic setting essentially identical to that of the nearby, in part overlapping, belt of tungsten skarns described previously (Dawson and Dick, 1978). Zn,Pb skarns in some cases developed along lithologic and structural pathways more distant from an intrusion than W,Cu skarns. Some pass

distally into replacement manto and chimney deposits that are significantly higher in Ag content and total ore tonnage than the skarn (Dawson, 1987). Sphalerite and the prograde skarn minerals hedenbergite and andradite are Fe-rich, whereas the retrograde skarn minerals epidote, actinolite, and chlorite are Mn-rich.

Two relatively large and potentially economic Zn,Pb,Ag replacement deposits are located in southeastern Yukon Territory at Mount Hundere and Quartz Lake, whereas the main belt of such deposits, which includes Midway, Silver Hart, Tintina Silver and distal Ag,Pb-rich parts of the Ketza River Au district, lies 100 km westward within the Cassiar Terrane (Figure 2). Both Mount Hundere and Quartz Lake stratabound Zn,Pb,Ag deposits replace carbonate members of a folded upper Proterozoic to Cambrian clastic-carbonate shelf sequence (Gabrielse, 1966; Gabrielse and Blusson, 1969; Vaillancourt, 1982a,b). The deposits exhibit marked stratigraphic and structural control of mineralization (Hamilton et al., 1982; Morin, 1981; Abbott, 1981). Both deposits are relatively distant from granitoid plutons but are closely associated with faults interpreted to have served as conduits to underlying plutons (Dawson and Dick, 1978; Hamilton et al., 1982; Morin, 1981).

D. Middle Devonian to Mississippian clastic wedge

Earn Group

Devono-Mississippian tectonism in the miogeocline involved local uplift and granitic intrusion in northern Yukon, volcanism in central Yukon and south-central British Columbia, and a dramatic change in sedimentation patterns throughout the northern Cordillera as shelf carbonate-clastic platforms were drowned and starved of clastic sediments before being inundated by fine- to coarse-grained, mainly turbiditic chert-rich clastics derived from the west and north (Gordey, in press-b). The abrupt change from passive-margin to variably coarsening-upward clastic sedimentation represented by the Earn Group has been attributed to local block uplift as a consequence of regional extension or strike-slip faulting (Gordey, in press-b); ensialic arc magmatism, uplift and foreland clastic wedge deposition (Gabrielse et al., 1982); rifting, Mississippian volcanism, and graben sedimentation (Tempelman-Kluit, 1979); syndepositional extensional and (or) wrench faulting (Abbott, 1986a); and Paleozoic sinistral transcurrent faulting along the cratonal margin (Eisbacher, 1983).

Stop 2 and 3 Tom and Jason sedimentary exhalative Zn,Pb,Ag, barite deposits

Stratiform barite-rich deposits hosted by cratonal Devono-Mississippian clastic strata form part of the world's largest barite metallogenic province, which follows the eastern Cordilleran miogeocline from the Arctic to Mexico (Dawson, 1983).

In the Macmillan Pass area, Yukon Territory, sedex barite occurrences (e.g. Cathy, Pete) and Zn,Pb,Ag,Ba deposits (e.g. Tom, Jason) occupy three or more stratigraphic levels, ranging from Middle to Late Devonian age, in the lower Earn Group and one Early Mississippian level (e.g. Tea) in the upper Earn Group. The lower Upper Devonian (Frasnian) barite interval is a metallotect of regional extent that corresponds to the principal stratiform Zn,Pb,Ag,Ba horizon at Macmillan Pass (Dawson and Orchard, 1982). Most sedex deposits are spatially related to syndepositional faults which bound a westerly trending pull-apart basin (Abbott and Turner, this volume), filled successively with dark siliceous shale and chert, turbiditic siltstone, shale, sandstone, and chert conglomerate, and silver-blue-weathering siliceous shale of the lower Earn Group (Abbott, 1986a).

Pyritic siliceous argillite of the uppermost (Frasnian) unit hosts the Tom West and Jason Zn,Pb,Ag,Ba deposits (Dawson and Orchard, 1982). The two structurally- separated zones of the deformed Tom deposit, with an aggregate geological reserve of 15.7 million tonnes of 7.0% Zn, 4.6% Pb, and 49.1 g/t Ag, originally constituted one stratigraphically continuous body (McClay and Bidwell, 1986). The distribution of principal ore facies at Tom, including Cu,Ag-rich footwall stockwork overlain by Pb,Zn-rich massive sulphide facies grading upward and laterally to Zn,Fe-rich laminated sulphide facies, and distally to Ba-rich ore represents primary zonal deposition from hydrothermal brines exhaled into an anoxic sub-basin (McClay and Bidwell, 1986; Carne, 1979; Large, 1983).

Near the southern limit of the deposit a vent complex with scarp talus breccias and thinned pre-ore rock units indicate that localization of vents and abrupt termination of stratiform mineralization were controlled by syn-sedimentary faulting.

Zonation of ore lenses about the vent is due, in part, to subsequent replacement and infilling of hydrothermal sediments by vent fluids (Goodfellow and Lydon, 1990; Goodfellow and Rhodes, this volume).

The Jason Pb,Zn,Ag,Ba deposits, 5 km southwest of Tom, possess similar ore facies and are associated with extensive sedimentary breccias, slump and debris flows (Turner et al., 1989; Turner, this volume). Three ore zones contain an aggregate geological reserve of 14.1 million tonnes grading 7.09% Pb, 6.57% Zn, and 79.9 g/t Ag (Bailes et al., 1986). The Jason South/Main stratiform deposit occurs in a faulted, southwest-plunging syncline. Laminated ore is replaced adjacent to a syndepositional normal fault by massive, vein and breccia ore rich in ferroan carbonate that represents the upflow of late-stage hydrothermal fluid (Turner et al., 1990; Turner, this volume).

DISPLACED CONTINENTAL MARGIN

Cassiar Terrane

Cassiar Terrane, together with Cariboo Subterrane, extends along the western margin of the North American miogeocline from the Cariboo district of east-central British Columbia 1350 km northwestward to central Yukon Territory (Figure 5; Dawson et al., in press). It comprises an Upper Proterozoic to Upper Triassic miogeoclinal succession of sedimentary strata similar to platformal- and shelf-facies rocks farther east. Cassiar Terrane was displaced as a coherent block from its original position by 500-1000 km of dextral displacement along the Tintina and Northern Rocky Mountain Trench fault systems in Late Mesozoic to Early Tertiary time (Gabrielse et al., in press).

Most skarn and replacement deposits in Cassiar Terrane are associated with a suite of small felsic stocks and dykes of mid-Cretaceous to Eocene age. Both intrusion and related replacement mineralization were controlled by discordant north, northwest, and east-west faults in a transtensional environment ascribed to late movement on the Tintina, Kechika, and Cassiar faults (Abbott, 1983; Gabrielse, 1985). Significant similarities between these replacement deposits and the manto and chimney deposits of northeastern Mexico, in addition to morphology and mineralogy, include cratonal basement, post-orogenic F-rich granitoids and extensional setting (Dawson, 1987).

Stop 5 Ketza River Au manto deposit

A belt of economically significant replacement deposits hosted by lower Paleozoic carbonate/clastic successions of Cassiar Terrane includes the Ketza River Au mine (Abercrombie, this volume; Cathro, this volume), and the Tintina Silver, Midway and Silver Hart developed Ag,Pb,Zn prospects. At Ketza River, reserves of proven plus possible oxide ore are 230,406 tonnes of 13.91 g/t Au (Canamax Annual Report, 1988).

The Ketza River district is underlain by Late Proterozoic to Triassic miogeoclinal clastic, volcanic and carbonate rocks deformed during the accretion of the Intermontane Superterrane in the early Mesozoic (Tempelman-Kluit, 1979). The structural framework is dominated by a few large thrust faults and the Ketza-Seagull Arch. Normal faults containing veins postdate some thrust faults, and may be related to buried intrusions (Abbott, 1986b). Hornfelsed lower Cambrian host pelites yield a K-Ar whole rock age of 101 ± 4 Ma, similar to the mid-Cretaceous ages of the northern lobe of the adjacent Nisutlin Batholith and White Creek stock (Dawson, unpub. data, 1986). Mineralization, however, may be younger and possibly related to Eocene minor intrusions, as in the Tintina Silver and YP deposits. Metals are zoned about the centre of the Ketza Uplift from: quartz-arsenopyrite-gold veins; to auriferous pyrrhotite-arsenopyrite mantos and veins; to barren pyrrhotite-siderite mantos and veins; all hosted by Upper Proterozoic and Lower Cambrian strata; and finally to galena-siderite veins and replacements of mainly Upper Cambrian and younger strata on the perimeter (Cathro, 1988).

ACCRETED TERRANES

Alexander Terrane

Clastic, volcanic and carbonate rocks of Alexander Terrane, ranging in age from Middle Devonian to Late Triassic, accumulated in island arc and ultimately, rift environments (Figure 6). A Permo-Triassic unconformity common to all terranes of island-arc affinity, separates upper Paleozoic from Upper Triassic rocks. Middle Pennsylvanian plutons intrude basement rocks of both Alexander Terrane and Wrangellia, indicating amalgamation of the two terranes in the Late Paleozoic (Gardner et al., 1988) prior to their accretion to the previously accreted Intermontane

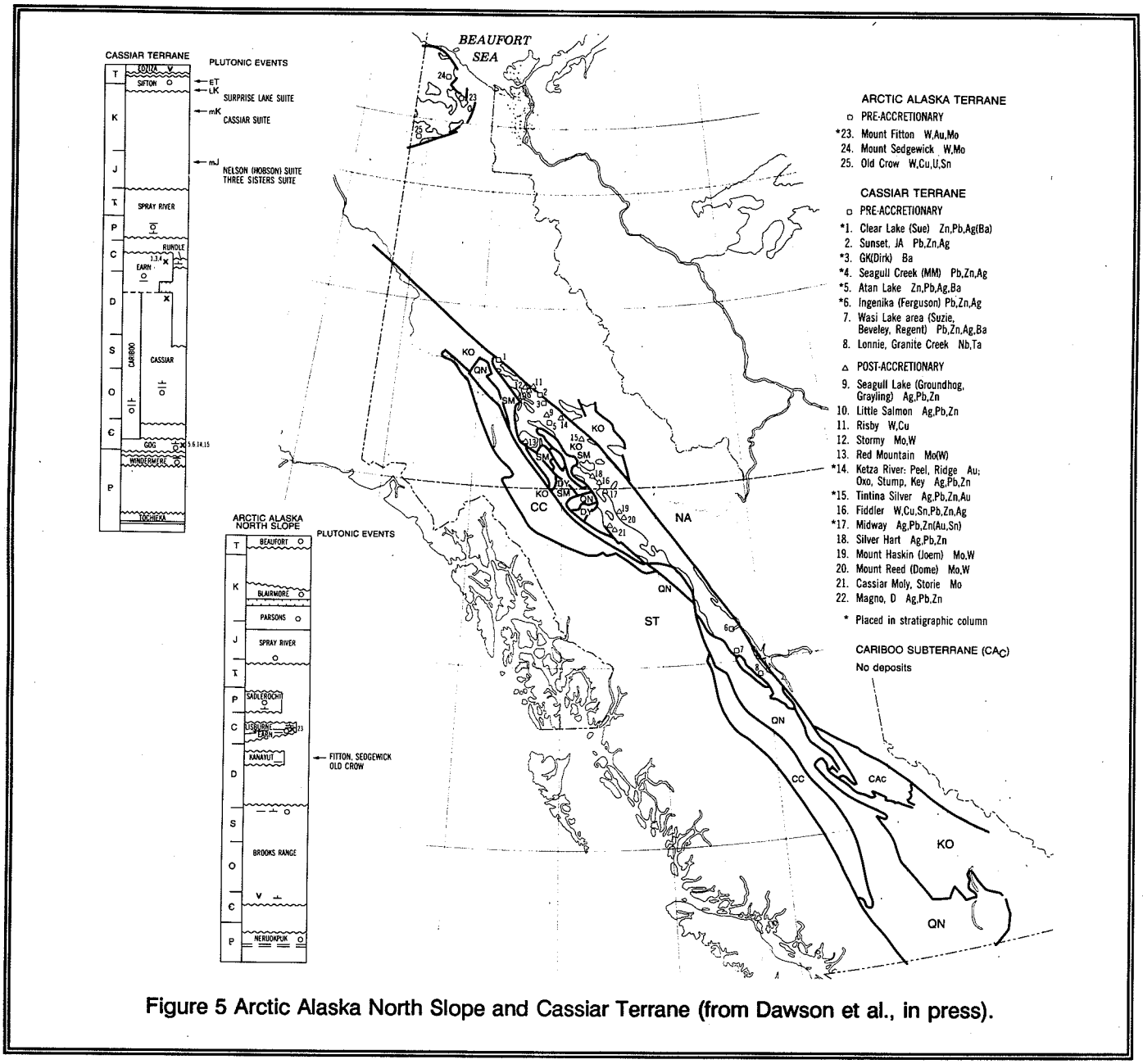

Figure 5 Arctic Alaska North Slope and Cassiar Terrane (from Dawson et al., in press).

Superterrane by mid-Cretaceous time.

Stop 1 Windy Craggy volcanogenic massive sulphide deposit

Upper Triassic rocks in Alexander Terrane are best documented in the Tatshenshini River area near the developed Windy Craggy Cu,Co(Au,Ag,Zn) volcanogenic massive sulphide prospect. A basal limestone and turbiditic siltstone unit of unknown age and thickness is in fault contact with deformed Middle Devonian carbonates. It is overlain by and partly interfingered with a 1000 m thick lower division of tholeiitic, massive amygdaloidal to pillowed basalt flows, diorite sills, minor chert, and argillite ('Lower Tats Volcanics' and 'Argillite' Figures 7,8,9). A middle division, 2000 m thick, which hosts the Windy Craggy orebody in its lower

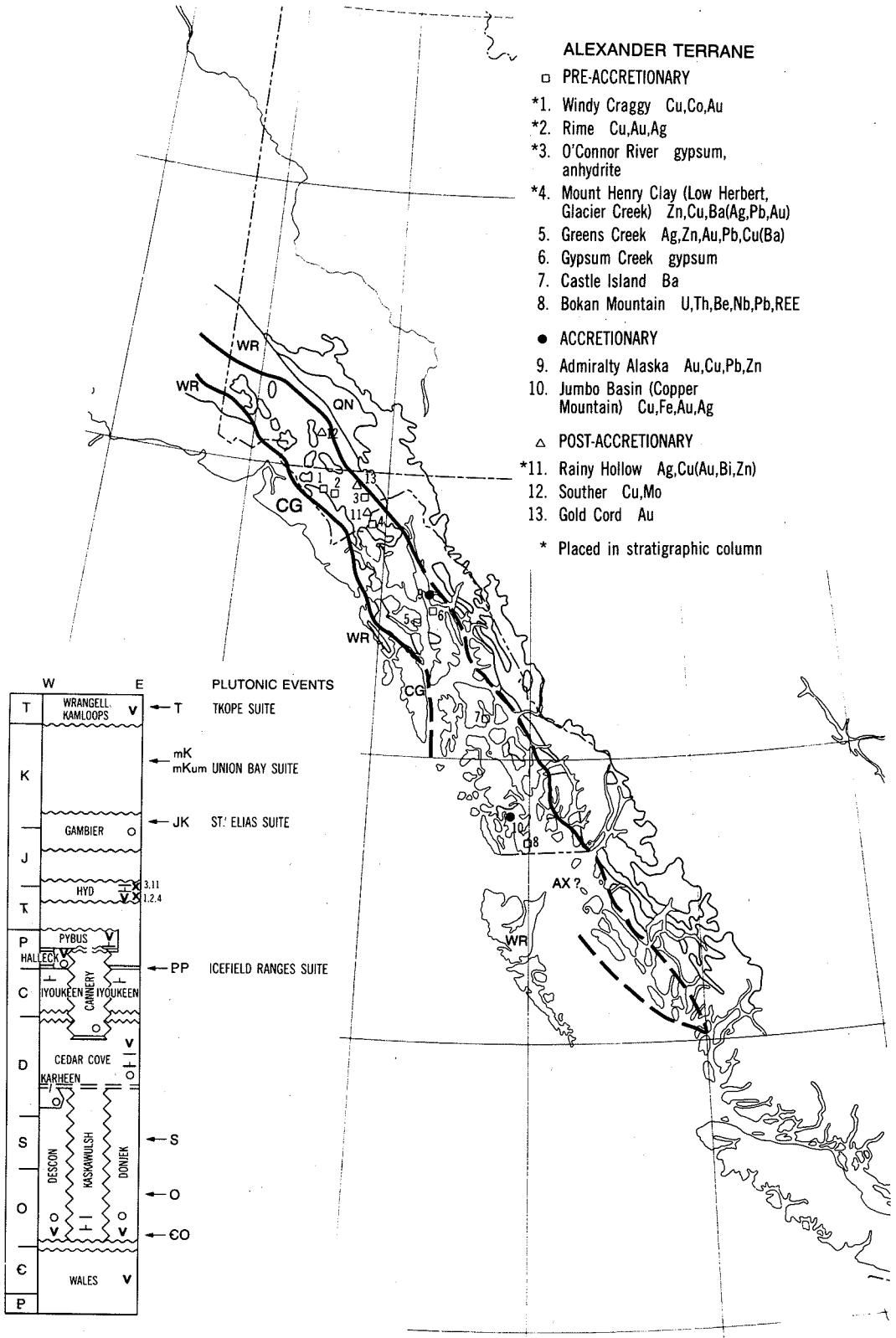

Figure 6 Accreted volcanic-sedimentary terrane of Insular Superterrane: Alexander (from Dawson et al., in press).

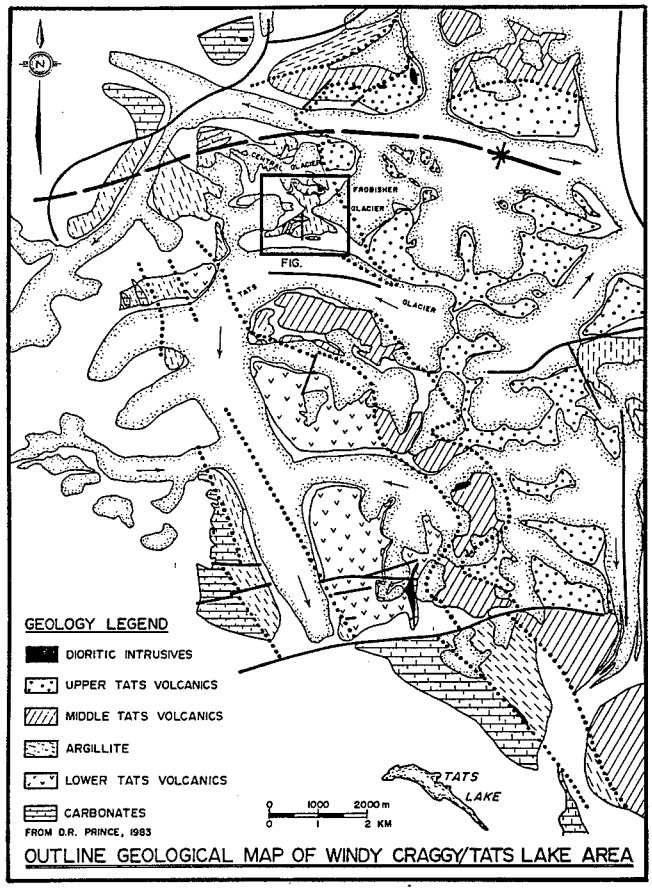

Figure 7 Distribution of main rock units in the vicinity of Windy Craggy (from Gammon and Chandler, 1986).

part, includes limy argillite, chert, calc-alkaline dioritic sills and dykes, mafic to intermediate, massive amygdaloidal to pillowed flows, tuff, agglomerate, and limestone ('Middle Tats Volcanics'). Conodonts from the middle division, including orebody host rocks, have determined its age to be Early Norian or mid-Late Triassic (M.J. Orchard, pers. comm., 1983). An upper volcanic division ('Upper Tats Volcanics') consists of at least 1500 m of calc-alkaline pillow basalts of Early to Middle Norian age (Gammon and Chandler, 1986; MacIntyre, 1984) (Figure 8).

The large cupriferous pyrite deposit, which contains proven and probable reserves of 114 million tonnes of 1.9% Cu, 0.08% Co, and 0.20 g/t Au and 3.7 g/t Ag, (Downing et al., this volume) shows some similarities to Cyprus-type deposits, yet the dominantly alkaline to subalkaline compositions of the host volcanics (MacIntyre, 1986) and the abundant cratonally-derived clastic sediments are more characteristic of Besshi-type mineralization (Fox, 1984). Pb isotopes from Windy Craggy sphalerites plot within the field of the Besshi-type ores of the Sambagawa belt, Japan (Sato and Sasaki, 1976, 1980; Dawson, unpub. data, 1986). The tectonic setting of the Upper Triassic rocks in the Tatshenshini River area, as deduced from adjacent miogeoclinal sediments, the progression from tholeiitic to calc-alkaline volcanism, turbiditic clastics, and Besshi-type mineralization, is interpreted to have been one of epicontinental rifting subsequent to amalgamation with Wrangellia in Carboniferous(?) time, and prior to collision between the Insular Superterrane and North America in Cretaceous time.

The Windy Craggy orebody is composed of two or more sulphide bodies that have been folded, faulted and, in part, sheared (Downing et al., this volume; Peter and Scott, this volume).

OVERLAP ASSEMBLAGES

Stop 7 Grew Creek epithermal Au,Ag deposit

A bimodal suite of rhyolite intrusions and flows and olivine basalt flows, tuff and tuff breccia occurs along and immediately north of Tintina Fault from near Faro to Tuchitua in east-central Yukon (Jackson et al., 1986; Figure 10). They have been dated as mid-Eocene by K-Ar on basalt and by pollen spores in volcaniclastic rocks Duke and Godwin (1986). Similar Eocene K-Ar dates were obtained from different volcanic units along Tintina Fault by Jackson et al. (1986).

Similar bimodal suites of calc-alkaline to transitional tholeiitic volcanics are commonly ascribed to crustal extension and normal faulting (Ewart, 1979). Volcanics presumably were deposited within transtensional grabens formed by transcurrent slip along Tintina Fault (Hughes and Long, this volume). The volcanic rocks constitute an overlap assemblage to lower Paleozoic phyllite, argillite and chert of Cassiar Terrane southwest of Tintina Fault and upper Paleozoic metabasalt and marble of the allochthonous Slide Mountain and Kootenay terranes northeast of Danger Creek fault (Duke, this volume). Upper Tertiary block faulting

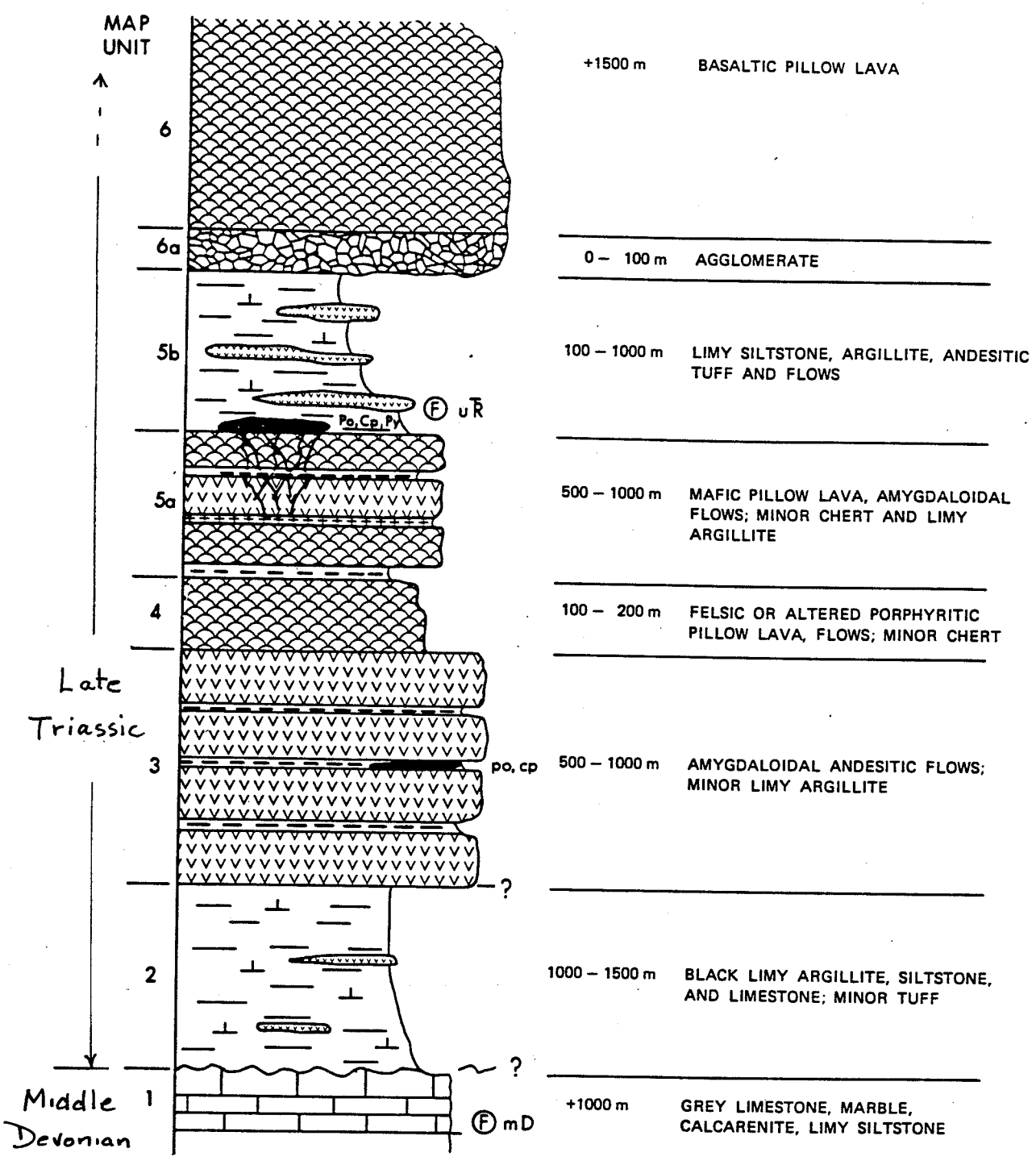

Figure 8 Preliminary stratigraphic column for the Alsek-Tatshenshini map area (from MacIntyre, 1984).

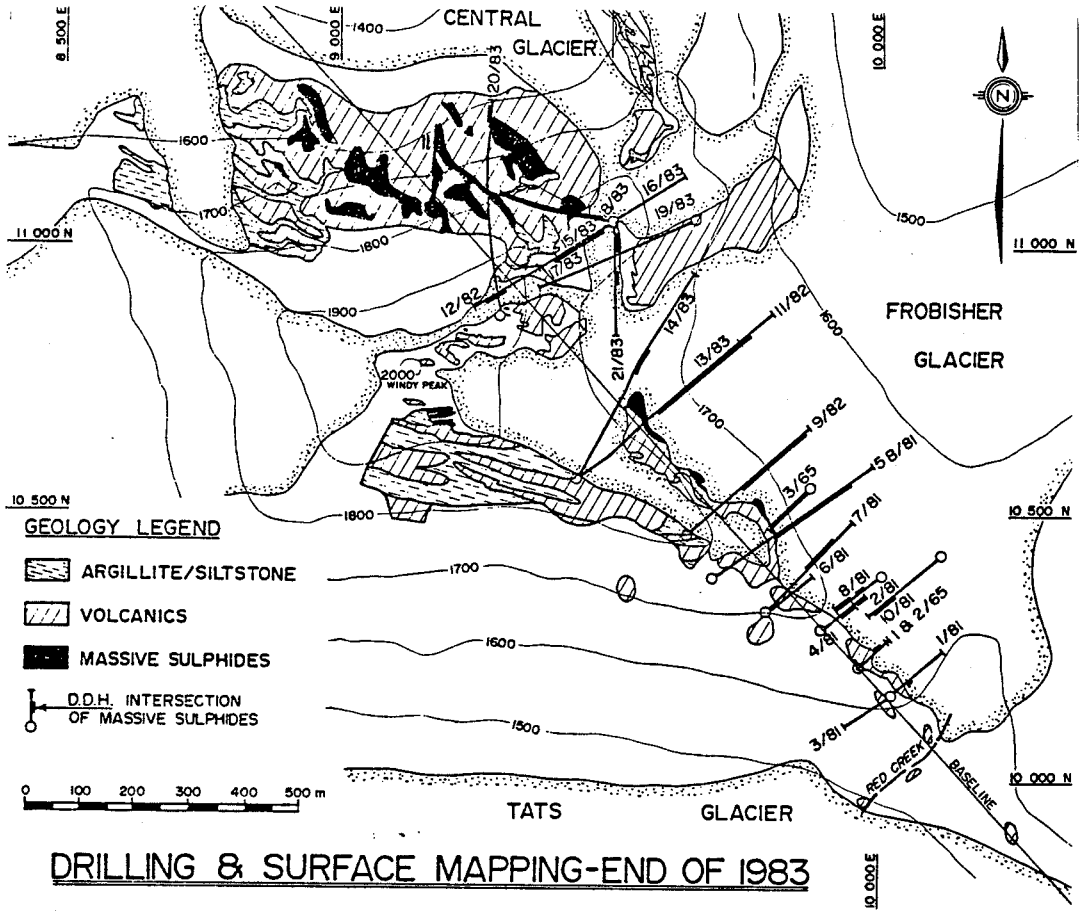

Figure 9 Outcrop geology and geology projected to surface from 1965-1983 drill holes (from Gammon and Chandler, 1986).

preserved the Eocene host rocks between these major tectonic elements (Duke, this volume).

The deposit is a stockwork, within a host of rhyolitic tuff, of chalcedonic quartz with fine-grained electrum in a gangue of clay, calcite and adularia.

Reserves prior to 1989 drilling were estimated to be 773,000 tonnes of 8.3 g/t Au and 31.3 g/t Ag (Duke, this volume). The deposit, the first reported gold occurrence in Tertiary volcanics in the Tintina Trench, indicates that rocks of similar types, age and setting have potential for gold mineralization.

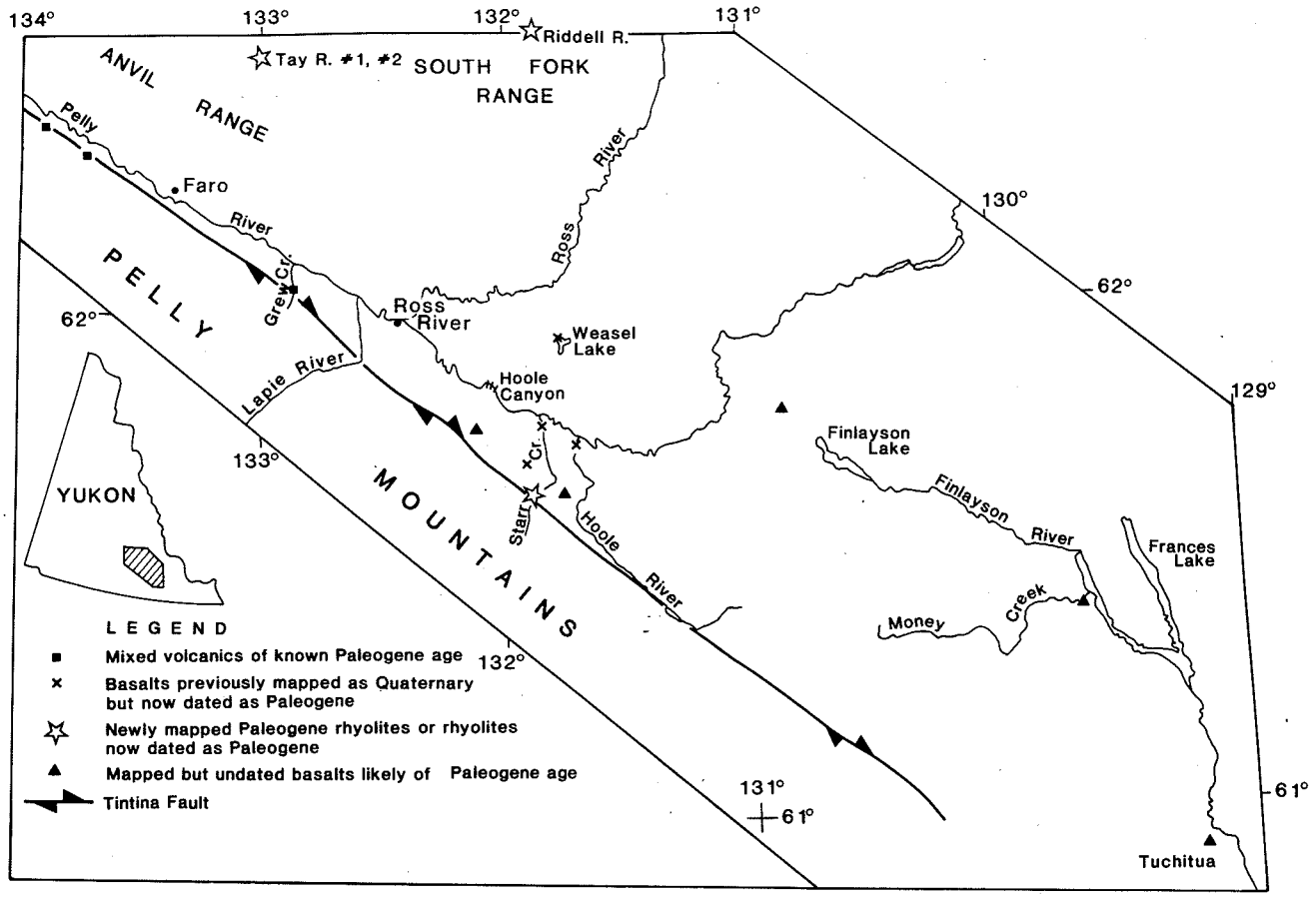

Figure 10 Occurences of Paleogene volcanics in the upper Pelly and Liard (Frances Lake basin) river basins (from jackson et al., 1986).

REFERENCES

Abbott, J.G. 1981: A new geological map of Mt. Hundere and the area north; in Yukon Geology and Exploration 1979-80, Indian and Northern Affairs Canada, p. 45-50.

Abbott, J.G. 1983: Geology, Macmillan Fold Belt, 105O/SW and parts of 105P/SW; Indian and Northern Affairs Canada, Open File 1983.

Abbott, J.G. 1986a: Devonian extension and wrench tectonics near Macmillan Pass, Yukon Territory, Canada; in The Genesis of Stratiform Hosted Lead and Zinc Deposits, R.J.W. Turner and M.T. Einaudi (ed.), Conference Proceedings, Stanford University Press, p. 85-89.

Abbott, J.G. 1986b: Epigenetic mineral deposits of the Ketza-Seagull district, Yukon; in Yukon Geology, v. 1, J.A. Morin and D.S. Emond (ed.), Exploration and Geological Services Division, Yukon, Indian and Northern Affairs Canada, p. 56-66.

Abbott, J.G. 1987: Field Activities, 1986; in 1986 Yukon Mining and Exploration Overview, Mineral Resources Directorate, Northern Affairs Program, Yukon Department of Indian Affairs and Northern Development, p. 32-33.

Abbott, J.G. and Turner, R.J.W.(this volume): Character and paleotectonic setting of Devonian stratiform sediment-hosted Zn-Pb-barite deposits, Macmillan Fold Belt, Yukon.

Abbott, J.G., Gordey, S.P., and Tempelman-Kluit, D.J.1986: Setting of stratiform sediment-hosted lead-zinc deposits in Yukon and northeastern British Columbia; in Mineral Deposits of Northern Cordillera, J.A. Morin (ed.), Canadian Institute of Mining and Metallurgy, Special Volume 37, p. 1-18.(this volume): Setting of stratiform, sediment-hosted lead-zinc deposits in Yukon and northeastern British Columbia.

Abercrombie, S.M.(this volume): Geology of the Ketza River gold mine.

Aitken, J.D. and McMechan, M.E.(in press): Middle Proterozoic assemblages of the Canadian Cordillera; in Geology of the Cordilleran Orogen in Canada; DNAG Volume G2, H. Gabrielse and C.J. Yorath (ed.), Chapter 5.

Aitken, J.D., Long, D.G.F., and Semikhatov, M.A.1978a: Progress in Helikian stratigraphy, Mackenzie Mountains; in Current Research, Part A, Geological Survey of Canada, Paper 78-1A, p. 481-484.

Aitken, J.D. 1978b: Correlation of Helikian strata, Mackenzie Mountains-Brock Inlier-Victoria Island; in Current Research, Part A, Geological Survey of Canada, Paper 78-1A, p. 485-486.

Anderson, R.G.1983: Selwyn plutonic suite and its relationship to tungsten skarn mineralization, southeastern Yukon and District of Mackenzie; in Current Research, Part B, Geological Survey of Canada, Paper 83-1B, p. 151-163.

Archer, A.R. and Schmidt, U.1978: Mineralized breccias of Early Proterozoic age, Bonnet Plume River district, Yukon Territory; Canadian Institute of Mining and Metallurgy, Bulletin, v. 71, no. 796, p. 53-58.

Archer, A., Bell, R.T., and Thorpe, R.I. 1986: Age relationships from U-Th-Pb isotope studies of uranium mineralization in Wernecke breccias, Yukon Territory; in Current Research, Part A, Geological Survey of Canada, Paper 86-1A, p. 385-391.

Atkinson, D. and Baker, D.J. 1986: Recent developments in the geologic understanding of Mactung; in Mineral Deposits of Northern Cordillera, J.A. Morin (ed.), Canadian Institute of Mining and Metallurgy, Special Volume 37, p. 234-244.

Atkinson, D. and Baker, D.J. (this volume): Geology of the Mactung tungsten skarn.

Bailes, R.J., Smee, B.W., Blackadar, D.W., and Gardner, W.D.1986: Geology of the Jason lead-zinc-silver deposits, Macmillan Pass, eastern Yukon; in Mineral Deposits of Northern Cordillera, J.A. Morin (ed.), Canadian Institute of Mining and Metallurgy, Special Volume 37, p. 87-99.

Bell, R.T. 1978: Breccias and uranium mineralization in the Wernecke Mountains, Yukon Territory - a progress report; in Current Research, Part A, Geological Survey of Canada, Paper 78-1A, p. 317-322.

Bell, R.T. 1982: Comments on the geology and uraniferous mineral occurrences of the Wernecke Mountains, Yukon and District of Mackenzie; in Current Research, Part B, Geological Survey of Canada, Paper 82-1B, p. 279-284.

Blusson, S.L. 1968: Geology and tungsten deposits near the headwaters of Flat River, Yukon Territory and southwestern District of Mackenzie; Geological Survey of Canada, Paper 67-22, 77 p.

Carne, R.C. 1979: Upper Devonian stratiform barite-lead-zinc-silver mineralization at Tom claims, Macmillan Pass, Yukon Territory; M.Sc. thesis, University of British Columbia, Vancouver, 149 p.

Carne, R.C. and Cathro, R.J. 1982: Sedimentary exhalative (sedex) zinc-lead-silver deposits, northern Canadian Cordillera; Canadian Institute of Mining and Metallurgy, Bulletin, v. 75, no. 840, p. 66-78.

Cathro, M.S. 1988: Gold and silver, lead deposits of the Ketza River district, Yukon preliminary results of fieldwork; in Yukon Geology, v. 2, G. Abbott (ed.), Exploration and Geological Services Division, Yukon, Indian and Northern Affairs Canada, p. 8-26.

Cathro, M.S. (this volume): Gold and silver, lead deposits of the Ketza River district, Yukon: preliminary results of field work.

Dawson, K.M. 1983: A review of barite in the northern Canadian Cordillera; Canadian Institute of Mining and Metallurgy Symposium, Mineral Deposits of Northern Cordillera, Whitehorse, Program and Abstracts, p. 18.

Dawson, K.M. 1987: Silver-rich base metal skarn and replacement deposits of the northern Canadian Cordillera and Mexico; Northwest Mining Association 93rd Annual Convention, Spokane, Washington, Program and Abstracts, p. 28.

Dawson, K.M. and Dick, L.A. 1978: Regional metallogeny in the northern Cordillera: tungsten and base metal-bearing skarns in southeastern Yukon and southwestern Mackenzie; in Current Research, Part A, Geological Survey of Canada, Paper 78-1A, p. 289-292.

Dawson, K.M. and Orchard, M.J. 1982: Regional metallogeny of northern Cordillera: biostratigraphy, correlation and metallogenic significance of bedded barite occurrences in eastern Yukon and western District of Mackenzie; in Current Research, Part C, Geological Survey of Canada, Paper 82-1C, p. 31-38.

Dawson, K.M., Panteleyev, A., Sutherland Brown, A., and Woodsworth, G.J. (in press): Regional metallogeny; in Geology of the Cordilleran Orogen in Canada; DNAG Volume G-2, H. Gabrielse and C.J. Yorath (ed.), Chapter 19.

Delaney, G.D. 1978: A progress report on stratigraphic investigations of the lowermost succession of Proterozoic rocks, northern Wernecke Mountains, Yukon Territory; Department of Indian and Northern Affairs, Open File EGS 1978-10.

Delaney, G.D. 1981: The mid-Proterozoic Wernecke Supergroup, Wernecke Mountains, Yukon Territory; in Proterozoic Basins of Canada, F.H.A. Campbell (ed.), Geological Survey of Canada, Paper 81-10, p. 1-23.

Dewey, J.F. and Burke, K. 1973: Plume generated triple junctions; Eos (Transactions, American Geophysical Union), v. 54, p. 239.

Downing, B.W., Webster, M.P., and Beckett, R.J. (this volume): The Windy Craggy massive sulphide deposit.

Duke, J.L. (this volume): The Grew Creek gold-silver deposit in south-central Yukon Territory.

Duke, J.L. and Godwin, C.I. 1986: Geology and alteration of the Grew Creek epithermal gold-silver prospect, south-central Yukon; in Yukon Geology, v. 1, J.A. Morin and D.S. Emond (ed.), Exploration and Geological Services Division, Yukon, Indian and Northern Affairs Canada, p. 72-82.

Eckstrand, O.R. (ed.) 1984: Canadian mineral deposit types: a geological synopsis; Geological Survey of Canada, Economic Geology Report 36, 86 p.

Eisbacher, G.H. 1981: Sedimentary tectonics and glacial record in the Windermere Supergroup, Mackenzie Mountains, northwestern Canada; Geological Survey of Canada, Paper 80-27, 40 p.

Eisbacher, G.H. 1983: Devonian-Mississippian sinistral transcurrent faulting along the cratonic margin of western North America: A hypothesis; Geology, v. 11, p. 7-10.

Ewart, A. 1979: A review of mineralogy and chemistry of Tertiary-Recent dacitic, latitic, rhyolitic and related salic volcanic rocks; in Trondhjemites, Dacites and Related Rocks, F. Barker (ed.), Developments in Petrology, Chapter 2, p. 13-121.

Fox, J.S. 1984: Besshi-type volcanogenic sulphide deposits - a review; Canadian Institute of Mining and Metallurgy, Bulletin, v. 77, no. 864, p. 57-68.

Fritz, W.H., Cecile, M.P., Norford, B.S., Morrow, D., and Geldsetzer, H. (in press): Cambrian to Middle Devonian Assemblages of the Canadian Cordillera; in Geology of the Cordilleran Orogen in Canada; DNAG Volume G-2, H. Gabrielse, and C.J. Yorath (ed.), Chapter 7.

Gabrielse, H. 1966: Watson Lake map-area, Yukon Territory; Geological Survey of Canada, Map 19-1966.

Gabrielse, H. 1967: Tectonic evolution of the northern Canadian Cordillera; Canadian Journal of Earth Sciences, v. 4, p. 271-298.

Gabrielse, H. 1985: Major dextral transcurrent displacements along the Northern Rocky Mountain Trench and related lineaments in north-central British Columbia; Geological Society of America Bulletin, v. 96, p. 1-14.

Gabrielse, H. and Campbell, R.B. (in press): Upper Proterozoic assemblages of the Canadian cordillera; in Geology of the Cordilleran Orogen in Canada; DNAG Volume G-2, H. Gabrielse and C.J. Yorath (ed.), Chapter 6.

Gabrielse, H. and Blusson, S.L. 1969: Geology of Coal River map-area, Yukon Territory and District of Mackenzie (95D); Geological Survey of Canada, Paper 68-38, 22 p.

Gabrielse, H. and Yorath, C.J. 1989: DNAG #4: The Cordilleran orogen in Canada; Geoscience Canada, v. 16, no. 2, p. 67-83.

Gabrielse, H., Blusson, S.L., and Roddick, J.A. 1973: Geology of Flat River, Glacier Lake and Wrigley Lake map-areas, District of Mackenzie and Yukon Territory; Geological Survey of Canada, Memoir 366, Part 1, 153 p., Part 2, 268 p.

Gabrielse, H., Loveridge, W.D., Sullivan, R.W., and Stevens, R.D.1982: U-Pb measurements of zircon indicate middle Paleozoic plutonism in the Omineca Crystalline Belt, north-central British Columbia; in Current Research, Part C, Geological Survey of Canada, Paper 82-1C, p. 139-146.

Gabrielse, H., Monger, J.W.H., and Wheeler, J.O. (in press): Tectonic framework of the Canadian Cordillera; in Geology of the Cordilleran Orogen in Canada; DNAG Volume G-2, H. Gabrielse and C.J. Yorath (ed.), Chapter 2.

Gammon, J.B. and Chandler, T.E. 1986: Exploration of the Windy Craggy massive sulphide deposit, British Columbia, Canada; in Geology in the Real World - The Kingsley Dunham Volume, E.W. Nesbitt and I. Nichol (ed.), Institute of Mining and Metallurgy, p. 131-141.

Gardner, M.C., Bergman, S.C., Cushing, G.W., MacKevett, E.M., Jr., Plafker, G., Campbell, R.B., Dodds, C.J., McLelland, W.C., and Mueller, P.A. 1988: Pennsylvanian pluton stitching of Wrangellia and the Alexander Terrane, Wrangell Mountains, Alaska; Geology, v. 16, p. 967-971.

Glover, J.K. and Burson, M.J. 1986: Geology of the Lened tungsten skarn deposit, Logan Mountains, Northwest Territories; in Mineral Deposits of Northern Cordillera, J.A. Morin (ed.), Canadian Institute of Mining and Metallurgy, Special Volume 37, p. 255-265.

Godwin, C.I., Armstrong, R.L., and Tompson, K.M. 1980: K-Ar and Rb-Sr dating and the genesis of tungsten at the Clea tungsten skarn property, Selwyn Mountains, Yukon Territory; Canadian Institute of Mining and Metallurgy, Bulletin, v. 73, no. 821, p. 90-93.

Goodfellow, W.D. and Jonasson, I.R. 1986: Environment of formation of the Howards Pass (XY) Zn-Pb deposit, Selwyn Basin, Yukon; in Mineral Deposits of Northern Cordillera, J.A. Morin (ed.), Canadian Institute of Mining and Metallurgy, Special Volume 37, p. 19-50.

Goodfellow, W.D. and Lydon, J. 1990: Geology geochemistry and origin of the Tom Zn-Pb-Ag-barite deposit, Selwyn Basin, Yukon; Minerals Colloquium, Ottawa, 17-18 January, 1990, Geological Survey of Canada, Program with Abstracts, p. 21.

Goodfellow, W.G. and Rhodes, D. (this volume): Geology and geochemistry of the Tom stratiform lead-zinc deposit.

Gordey, S.P. 1983: Thrust faults in the Anvil Range and a new look at the Anvil Range Group, south-central Yukon Territory; in Current Research, Part A, Geological Survey of Canada, Paper 83-1A, p. 225-227.

Gordey, S.P. (in press-a): Evolution of the northern Cordilleran miogeocline, Nahanni map-area (105I), Yukon Territory and District of Mackenzie; Geological Survey of Canada, Memoir.

Gordey, S.P. (in press-b): In Upper Devonian to Middle Jurassic assemblages: Part a - Ancestral North America; in Geology of the Cordilleran Orogen in Canada; DNAG Volume G-2, H. Gabrielse, and C.J. Yorath (ed.), Chapter 8.

Hamilton, J.M., Bishop, D.T., Morris, H.C., and Owens, O.E. 1982: Geology of Sullivan orebody, Kimberley, B.C. Canada; in Precambrian Sulphide Deposits, The H.S. Robinson Memorial Volume, R.W. Hutchinson, C.D. Spence and J.M. Franklin (ed.), Geological Association of Canada, Special Paper 25, p. 597-665.

Hewton, R.S. 1982: Gayna River: a Proterozoic Mississippi Valley-type zinc-lead deposit; in Precambrian Sulphide Deposits, H.S. Robinson Memorial Volume, R.W. Hutchinson, C.D. Spence and J.M. Franklin (ed.), Geological Association of Canada, Special Paper 25, p. 667-700.

Hoy, T. 1982: The Purcell Supergroup in southeastern British Columbia: sedimentation, tectonics and stratiform lead-zinc deposits; in Precambrian Sulphide Deposits, The H.S. Robinson Memorial Volume, R.W. Hutchinson, C.D. Spence and J.M. Franklin (ed.), Geological Association of Canada, Special Paper 25, p. 127-147.

Hughes, J.D. and Long, D.G.F. (this volume): Geology of the Ross River coal deposits.

Jackson, L.E., Gordey, S.P., Armstrong, R.L., and Harakal, J.E. 1986: Bimodal Paleogene volcanics near Tintina Fault, east-central Yukon and their possible relationship to placer gold; in Yukon Geology, v. 1, J.A. Morin and D.S. Emond (ed.), Exploration and Geological Services Division, Yukon, Indian and Northern Affairs Canada, p. 139-147.

Jefferson, C.W. and Ruelle, J.C.L. 1986: The Late Proterozoic Redstone Copper Belt, Mackenzie Mountains, Northwest Territories; in Mineral Deposits of Northern Cordillera, J.A. Morin (ed.), Canadian Institute of Mining and Metallurgy, Special Volume 37, p. 154-168.

Jennings, D.S. and Jilson, G.A. 1986: Geology and sulphide deposits of Anvil Range, Yukon; in Mineral Deposits of Northern Cordillera, J.A. Morin (ed.), Canadian Institute of Mining and Metallurgy, Special Volume 37, p. 319-361.

Kerans, C., Ross, G.M., Donaldson, J.A., and Geldsetzer, H.J. 1981: Tectonism and depositional history of the Helikian Hornby Bay and Dismal Lakes Groups, District of Mackenzie; in Proterozoic Basins of Canada, F.H.A. Campbell (ed.), Geological Survey of Canada, Paper 81-10, p. 157-182.

Large, D.E. 1983: Sediment-hosted massive sulphide lead-zinc deposits: an empirical model; in Short Course in Sediment-Hosted Stratiform Lead-Zinc Deposits, D.F. Sangster (ed.), Mineralogical Association of Canada Handbook, v. 8 (sic v.9), p. 1-29.

LeCouteur, P.C. 1979: Age of the Sullivan lead-zinc deposit; in Evolution of the Cratonic Margin and Related Mineral Deposits, Geological Association of Canada, Cordilleran Section Symposium, Program and Abstracts, p. 19.

McClay, K.R. and Bidwell, G.E. 1986: Geology of the Tom deposit, Macmillan Pass, Yukon; in Mineral Deposits of Northern Cordillera, J.A. Morin (ed.), Canadian Institute of Mining and Metallurgy, Special Volume 37; p. 100-114.

MacIntyre, D.G. 1984: Geology of the Alsek-Tatshenshini Rivers area (114P); in Geological Fieldwork 1983, British Columbia Ministry of Energy, Mines and Petroleum Resources, Paper 1984-1, p.173-184.

MacIntyre, D.G. 1986: The geochemistry of basalts hosting massive sulphide deposits, Alexander Terrane, northwest British Columbia (114P); in Geological Fieldwork 1985, British Columbia Ministry of Energy, Mines and Petroleum Resources, Paper 1986-1, p. 197-210.

Mathieson, G.A. and Clark, A.H. 1984: The Cantung E Zone scheelite skarn orebody, Tungsten, Northwest Territories: a revised genetic model; Economic Geology, v. 79, p. 883-901.

Morganti, J.M. 1979: The geology and ore deposits of the Howards Pass area, Yukon and Northwest Territories: the origin of basinal sedimentary stratiform sulphide deposits; Ph.D. thesis, University of British Columbia, Vancouver, 317 p.

Morganti, J.M. 1981: Ore deposit models - 4. Sedimentary-type stratiform ore deposits: some models and a new classification; Geoscience Canada, v. 8, p. 65-75.

Morin, J.A. 1978: A preliminary report on Hart River (116A/10) - a Proterozoic massive sulphide deposit; in Mineral Industry Report 1977, Yukon Territory, EGS 1978-9, Indian and Northern Affairs Canada, p. 22-25.

Morin, J.A. 1981: The McMillan deposit - a stratabound lead-zinc-silver deposit in sedimentary rocks of Upper Proterozoic age; in Yukon Geology and Exploration 1979-80, Department of Indian and Northern Affairs, p. 105-109.

Norford, B.S. and Orchard, M.J. 1983: Early Silurian age of rocks hosting lead-zinc mineralization at Howards Pass, Yukon Territory and District of Mackenzie: local biostratigraphy of Road River Formation and Earn Group; Geological Survey of Canada, Paper 83-18, 35 p.

Peter, J.M. and Scott, S.D. (this volume): The Windy Craggy massive sulphide deposit.

Pigage, L.C. (this volume): Field Guide, Anvil Pb-Zn-Ag district, Yukon Territory, Canada.

Ruelle, J.C.L. 1982: Depositional environments and genesis of stratiform copper deposits of the Redstone Copper Belt, Mackenzie Mountains, N.W.T.; in Precambrian Sulphide Deposits, H.S. Robinson Memorial Volume, R.W. Hutchinson, C.D. Spence and J.M. Franklin (ed.), Geological Association of Canada, Special Paper 25, p. 701-737.

Sato, K. and Sasaki, A. 1976: Lead isotopic evidence on the genesis of pre-Cenozoic stratiform sulphide deposits in Japan; Geochemical Journal, v. 10, p. 197-203.

Sato, K. and Sasaki, A. 1980: Lead isotope features of the Besshi-type deposits and its bearing on the ore lead evolution; Geochemical Journal, v. 14, p. 303-315.

Sinclair, W.D. 1986: Molybdenum, tungsten and tin deposits and associated granitoid intrusions in the northern Canadian Cordillera and adjacent parts of Alaska; in Mineral Deposits of the Northern Cordillera, J.A. Morin (ed.), Canadian Institute of Mining and Metallurgy, Special Volume 37, p. 216-233.

Stewart, J.H. 1972: Initial deposits in the Cordilleran geosyncline: evidence of a Late Precambrian (<850 m.y.) continental separation; Geological Society of America, Bulletin, v. 83, p. 1345-1360.

Stuart, R.A. 1963: Geology of the Snake River iron deposit; Department of Indian Affairs and Northern Development Assessment Files, Yellowknife, N.W.T., 18 p.

Tempelman-Kluit, D.J. 1972: Geology and origin of the Faro, Vangorda and Swim concordant zinc-lead deposits, central Yukon Territory; Geological Survey of Canada, Bulletin 208, 73 p.

Tempelman-Kluit, D.J. 1979: Transported cataclasite, ophiolite and granodiorite in Yukon: evidence of arc-continent collision; Geological Survey of Canada, Paper 79-14, 27 p.

Turner, R.J.W. (this volume): Jason stratiform Zn-Pb-barite deposit, Selwyn Basin, Canada (NTS 105-O-1): Geological setting, hydrothermal facies, and genesis.

Turner, R.J.W., Goodfellow, W.D., and Taylor, B.E. 1989: Isotopic geochemistry of the Jason stratiform sediment-hosted zinc-lead deposit, Macmillan Pass, Yukon; in Current Research, Part E, Geological Survey of Canada, Paper 89-1E, p. 21-30.

Turner, R.J.W., Taylor, B.E., and Goodfellow, W.D. 1990: The Jason stratiform Zn-Pb-Ag-barite deposit: exhalative and replacement processes along a Devonian syndepositional fault; Forum 1990, Ottawa, January 15-17, 1990, Geological Survey of Canada, Program with Abstracts, p. 22.

Vaillancourt, P. de G. 1982a: Geology of pyrite-sphalerite-galena concentrations in Proterozoic quartzite at Quartz Lake, southeastern Yukon; in Yukon Exploration and Geology 1982, Indian and Northern Affairs Canada, Exploration and Geological Services, Whitehorse, Yukon, p. 73-77.

Vaillancourt, P. de G. 1982b: Geology and genesis of pyrite-sphalerite-galena concentrations in Proterozoic quartzite at Quartz Lake, Yukon Territory; M.Sc. thesis, University of Western Ontario, London, 177 p.

Woodsworth, G.J., Anderson, R.G., Armstrong, R.L., and Struik, L.C. (in press): Plutonic regimes; in Geology of the Cordilleran Orogen in Canada; DNAG Volume G-2, H. Gabrielse and C.J. Yorath (ed.), Chapter 15.

Yeo, G.M. 1986: Iron-formation in the late Proterozoic Rapitan Group, Yukon and Northwest Territories; in Mineral Deposits of Northern Cordillera, J.A. Morin (ed.), Canadian Institute of Mining and Metallurgy, Special Volume 37, p. 142-153.

Young, G.M. 1977: Stratigraphic correlation of upper Proterozoic rocks of northwestern Canada; Canadian Journal of Earth Sciences, v. 14, p. 1771-1787.

Young, G.M. 1982: The late Proterozoic Tindir Group, east-central Alaska; evolution of a continental margin; Geological Society of America, Bulletin, v. 93, p. 759-783.

Young, G.M., Jefferson, C.W., Delaney, G.D., and Yeo, G.M. 1979: Middle and late Proterozoic evolution of the northern Canadian Cordillera and Shield; Geology, v. 7, p. 125-128.

THE WINDY CRAGGY MASSIVE-SULPHIDE DEPOSIT NORTHWESTERN BRITISH COLUMBIA, CANADA

B.W. Downing and M.P. Webster, R.J. Beckett
Geddes Resources Ltd.
Suite 1080, 1055 West Hastings St.,
Vancouver, B.C., Canada V6E 2E9

R.J. Beckett
Beckett Geological Services
Suite 208, 744 West Hastings St.
Vancouver B.C., Canada V6C 1A5

Introduction

The Windy Craggy Cu-Co-Au-Ag-Zn massive sulphide deposit is located within the St. Elias Mountains of northwestern British Columbia at 59° 44' N and 137° 44' W, approximately 200 kilometres southwest of Whitehorse, Yukon (Fig 1).

Property History

1957 - prospecting discovery (J.J. McDougall), Frobisher Ltd.

1958 to 1980 - surface drilling, Falconbridge Nickel Mines Ltd.

1981 to 1986 - surface drilling, mapping, airborne geophysical survey, airstrip construction

1981 - joint venture between Falconbridge Ltd. and Geddes Resources Limited. 1983 - Geddes Resources Limited acquires 100% interest subject to Falconbridge net profits interest.

1987 to 1990 - underground development: drifting, drilling, bulk sampling; surface drilling; metallurgical, engineering, and environmental studies.

Exploration to December 1989 includes 4139 metres (13,580 feet) of underground development on the 1400-metre level; 50,362 metres (165,230 feet) of drilling in 34 surface and 121 underground drill holes; and bulk sampling. Preliminary results indicate high copper recoveries with conventional crushing, grinding, and flotation methods. Continuous massive-sulphide mineralization extends a minimum strike length of 1.6 kilometres, at least 600 vertical metres, and greater than 200 metres in width. The deposit remains open at depth and along strike (Fig. 2.).

Table 1: Estimated Geological reserves at the 1.0% copper cut-off (March 1990)

	Tonnes	Cu%	Co%	g/t Au	g/t Ag
Proven	32,904,000	2.12	0.083	0.16	3.30
Probable	81,424,000	1.84	0.082	0.22	3.84
Total	114,328,000	1.92	0.082	0.20	3.69
Possible	51,903,000	1.82	0.082	0.21	4.28

Regional Geology

The Windy Craggy deposit is within the fault-bounded Alexander Terrane of the

Figure 1 Location map of Windy Craggy deposits.

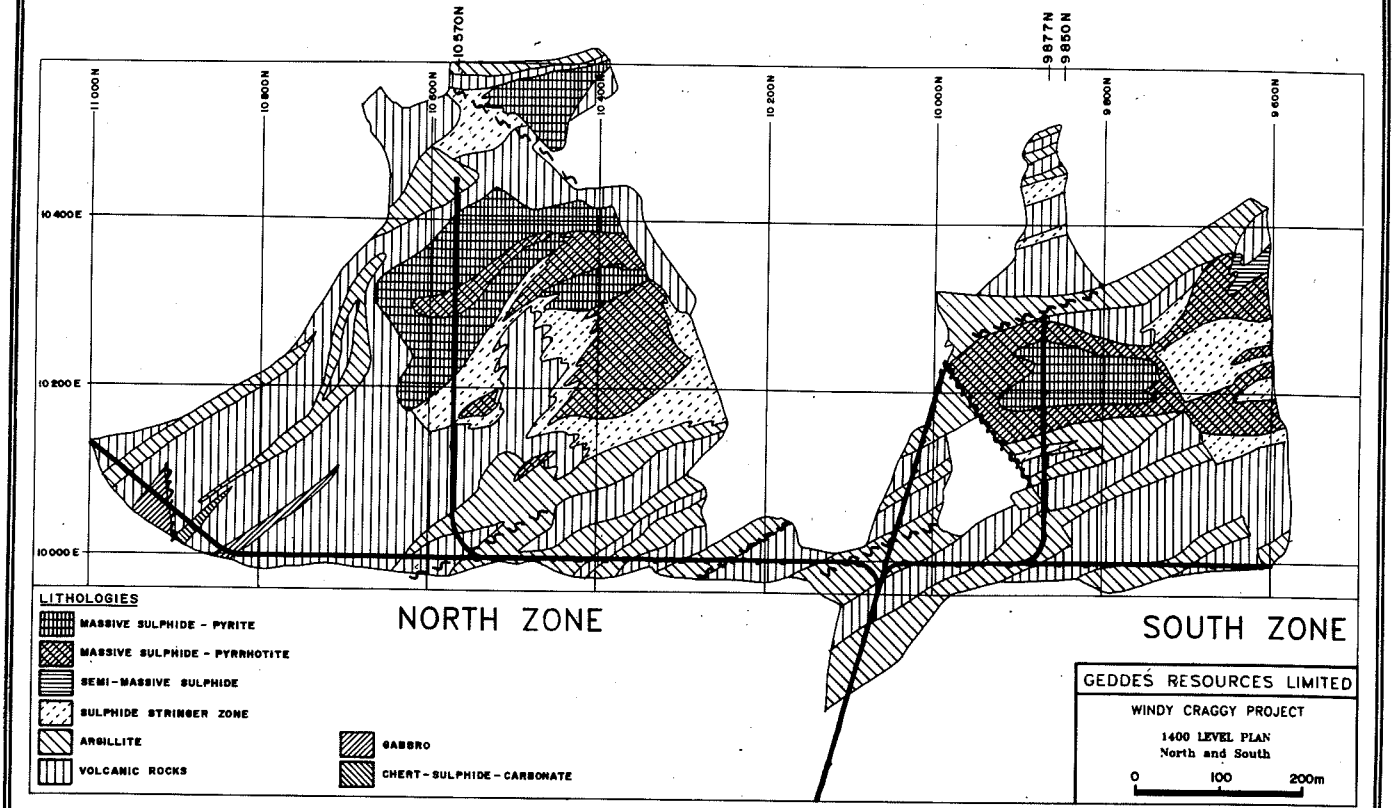

Figure 2 Geology of 1400 level, Windy Craggy deposit

Cordilleran Insular Belt. Lithologies include: Paleozoic carbonates to calcareous clastics and Triassic marine clastics and volcanics. All these lithologies are intruded by Jurassic-Cretaceous granitoid stocks and batholiths.

Deposit Geology

Overview

The Windy Craggy deposit is hosted by Triassic (Norian) clastic sediments and mafic flows and sills. Massive sulphide mineralization occurs near the transition from predominantly clastic units to overlying volcanic assemblages. Clastic sediments include calcareous, carbonaceous, and sulphidic units. Intermediate to mafic volcanic units are carbonate- and chlorite-altered. Metamorphic rank is greenschist. The deposit has similarities with both Besshi-type and Cyprus-type massive-sulphide deposits.

Structure

Major faults dip steeply, strike northwesterly, and trend subparallel to contacts between enclosing lithologies. Two phases of folding, isoclinal and open, occur in both massive sulphides and host rocks. Tectonic foliation, minor folding, boudinage and microstructural evidence for ductile and brittle deformation indicate that the massive sulphides accommodated significant strain.

Massive Sulphide Mineralization

Massive sulphide mineralization occurs as two discrete (northern and southern bodies) but possibly contiguous zones of massive, fine-grained

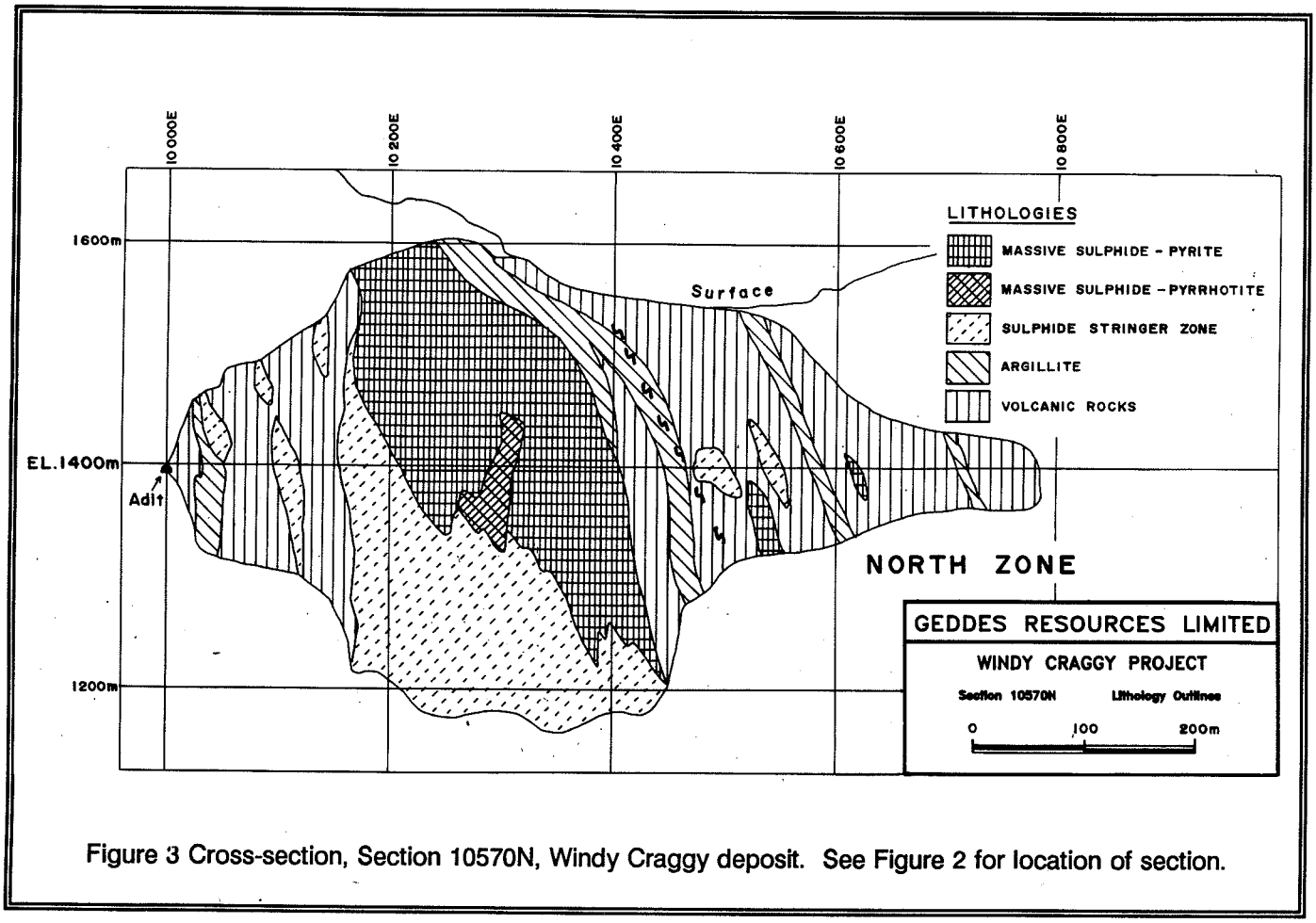

Figure 3 Cross-section, Section 10570N, Windy Craggy deposit. See Figure 2 for location of section.

pyrite, pyrrhotite, and chalcopyrite (Fig. 3 and 4). Gold, partly as native gold occurs within both massive sulphide bodies and averages 0.22 grammes per tonne. Cobalt content of the massive sulphides averages about 0.09 per cent. Gangue components include quartz, iron carbonates, chlorite, and calcite.

The tabular to lenticular, stratiform, northern body trends WNW and dips moderately steeply to the NNE (Fig. 3). The tabular to lensoid southern body plunges steeply to the southeast, and extends southeastwards as a series of 15-metre to 60-metre wide massive sulphide bodies (Fig. 4). Stockwork mineralization is associated with both bodies. The strike of the main part of the southern body is discordant in a gross sense with host rock stratigraphy.

Zoning

Stratigraphic sulphide zoning, recognized in both northern and southern bodies, passes upwards from footwall stringer mineralization to massive pyrrhotite, to massive pyrrhotite-pyrite, to massive pyrite, to massive pyrite-calcite-sphalerite, and ends in discontinuous chert-carbonate-sulphides (Fig. 5). Zoning has been modified by subsequent mineralization and structural deformation.

Stringer Zone

A significant sulphide-stringer stockwork is developed around the northern body and intermittently around the southern body. The stockwork is comprised of irregular sulphide veins within pervasively chlorite- and silica-altered wallrock. The stockwork mineralization grades northeast into massive sulphides, supporting

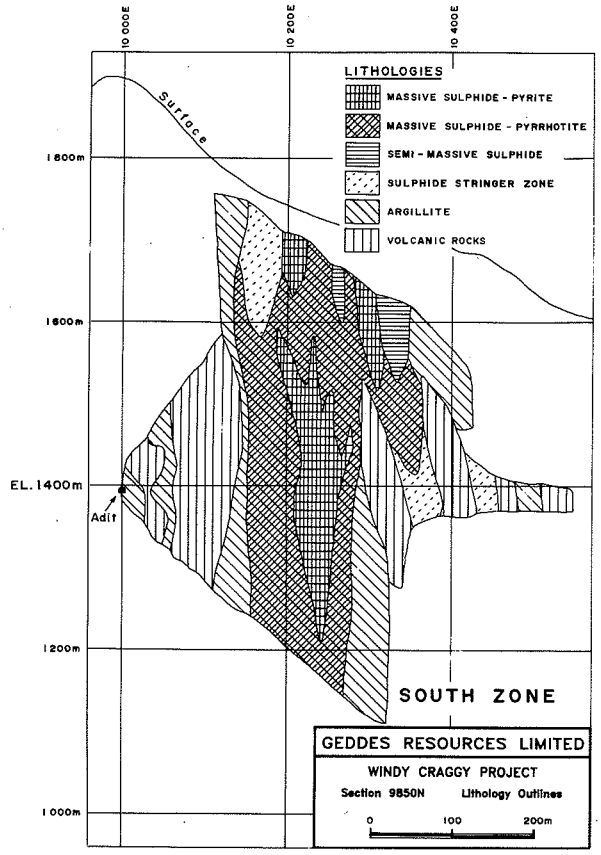

Figure 4 Cross-section, Section 9850N, Windy Craggy deposits. See Figure 2 for location of section.

stratigraphic facing directions.

Chert-Carbonate-Sulphide Zone

Significant gold is associated with the chert-carbonate-sulphide unit (drill hole 83-14, 29.7 metres of 14.72 grams gold/tonne). The chert-carbonate-sulphide unit often shows a laminated fabric and comprises fine- to medium-grained ankerite and siderite, white and black calcite, red hematitic to grey silica, and banded to disseminated sulphides. Within the sulphides pyrite is dominant over pyrrhotite. The chalcopyrite occurs as fracture fillings, fine-grained disseminations, and banded grain aggregates. Copper values consistently average just under two per cent. Spatially related, anomalous trace elements include bismuth, molybdenum, arsenic, nickel, and zinc. Visible gold grains up to 0.5 millimetres in diameter have been observed in core from drill holes 83-14 and 88-50. Microscopic gold and electrum, generally occur as free grains in the range of seven to eight microns in diameter.

Supergene Zone

A supergene zone has been identified up to 90-metres thick, where intersected. This zone comprises pyritic mud, chalcocite, cuprite, native copper, hematite, and sphalerite. Assays up to 12 percent copper over two metres occur. Approximately two million tonnes of supergene-zone reserves have been delineated.

Outlook

Reserve delineation, environmental studies, metallurgical testing, mine, and infrastructure design are continuing with a view toward development of the Windy Craggy Project after completion of a full feasibility study in 1990.

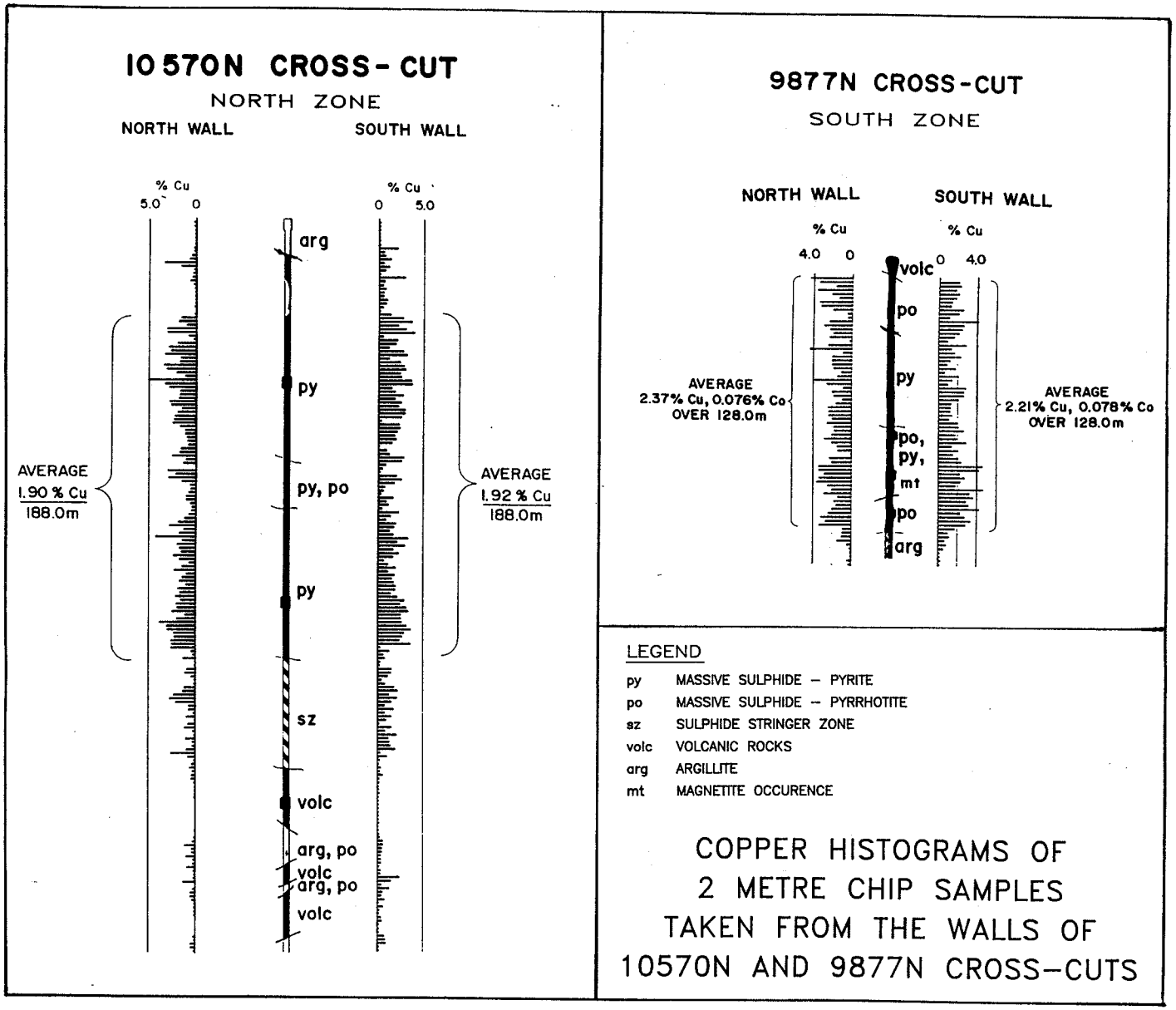

Figure 5 Copper histograms of 2 metre chip samples taken from the walls of 10570 and 9877N cross-cuts, Windy Craggy deposit.

MINERALOGY AND GEOCHEMISTRY OF THE WINDY CRAGGY COPPER-COBALT-GOLD MASSIVE SULPHIDE DEPOSIT, NORTHWESTERN BRITISH COLUMBI CANADA

Jan M. Peter and Steven D. Scott
Department of Geology, Earth Sciences Centre,
University of Toronto, 22 Russell St.,
Toronto, Ontario, Canada, M5S 3B1

Introduction:

The Windy Craggy copper-cobalt-gold massive sulphide deposit is located at 59°44' north latitude and 137°44' west longitude in the Alsek-Tatshenshini River area of the St. Elias Mountains in extreme northwestern British Columbia (see Fig. 1 of Downing et al., this volume). Proven, probable, and possible reserves currently (March 1990) are 165,400,00 metric tonnes at 1.89% Cu, 0.08% Co, 0.2 g/t Au, and 3.9 g/t Ag, with further reserves presently being delineated. This paper is complementary to Downing et al.(1990, this volume) which describes the exploration history and provides a geological overview of this very large Besshi-type deposit. We describe the mineralogy and geochemistry of the mineralization and volcanic host rocks to the deposit. Our continuing research includes stable isotope geochemistry of sulphides and gangue minerals, fluid inclusion microthermometry, lead isotope geochemistry of mineralization and igneous and sedimentary host rocks, and geochemistry of sedimentary host rocks.

Regional Geological Setting:

The Windy Craggy area is within the allochthonous Alexander terrane of the Insular tectonic belt in the extreme northwest part of British Columbia (Fig. 1). This terrane includes a thick succession of complexly deformed Precambrian to Permian basinal and platformal carbonate and clastic rocks with a subordinate volcanic component. These rocks are of relatively low metamorphic grade and are unconformably overlain by Late Triassic calcareous turbidites and a bimodal volcanic suite (Berg, 1979; Campbell and Dodds, 1979, 1983; MacIntyre, 1983, 1984; Prince, 1983). Paleomagnetic data indicate that this terrane has migrated northward from low paleolatitudes (Hillhouse, 1980).

Geological Setting of the Deposit:

The Late Triassic section in the Windy Craggy area is comprised of mafic submarine volcanics with variable amounts of interbedded calcareous argillaceous sedimentary rocks. MacIntyre (1984) has presented a stratigraphic section for the informally-named "Tats Volcanic Complex" in the Windy Craggy area (see Fig. __ of Dawson, 1990). MacIntyre (1983, 1984, 1986) and Prince (1983) have defined five major subdivisions of the Tats Complex:

1) Upper Tats-mainly pillow basalt of Upper Triassic age (at least 1500 m thick);

2) Middle Tats-interbedded graphitic and calcareous argillites, pillowed and massive mafic amygdaloidal to pillowed flows, tuff, agglomerate, and limestone of Upper Triassic age, based on conodont faunal assemblages (Orchard, 1986)(≈2000 m thick);

3) Lower Tats-mafic flows and sills of Upper Triassic age (≈1000 m thick);

4) Graphitic Shale Unit-calcareous and graphitic shale, argillite, and limestone of unknown age;

5) Limestone Unit-grey limestone of (?) Siluro-Devonian age in fault contact.

The lower part of the Middle Tats Group hosts the Windy Craggy deposit. At present, the deposit is thought to consist of two discrete sulphide bodies, but on-going exploration and drilling may lead to a refinement of this conclusion. Recent drilling has indicated the possible presence of a third sulphide body.

Host Rocks:

A description of the host rocks, taken mainly from Peter (1989) is given below:

Volcanic Rocks:

Volcanic flows are fine grained and range in

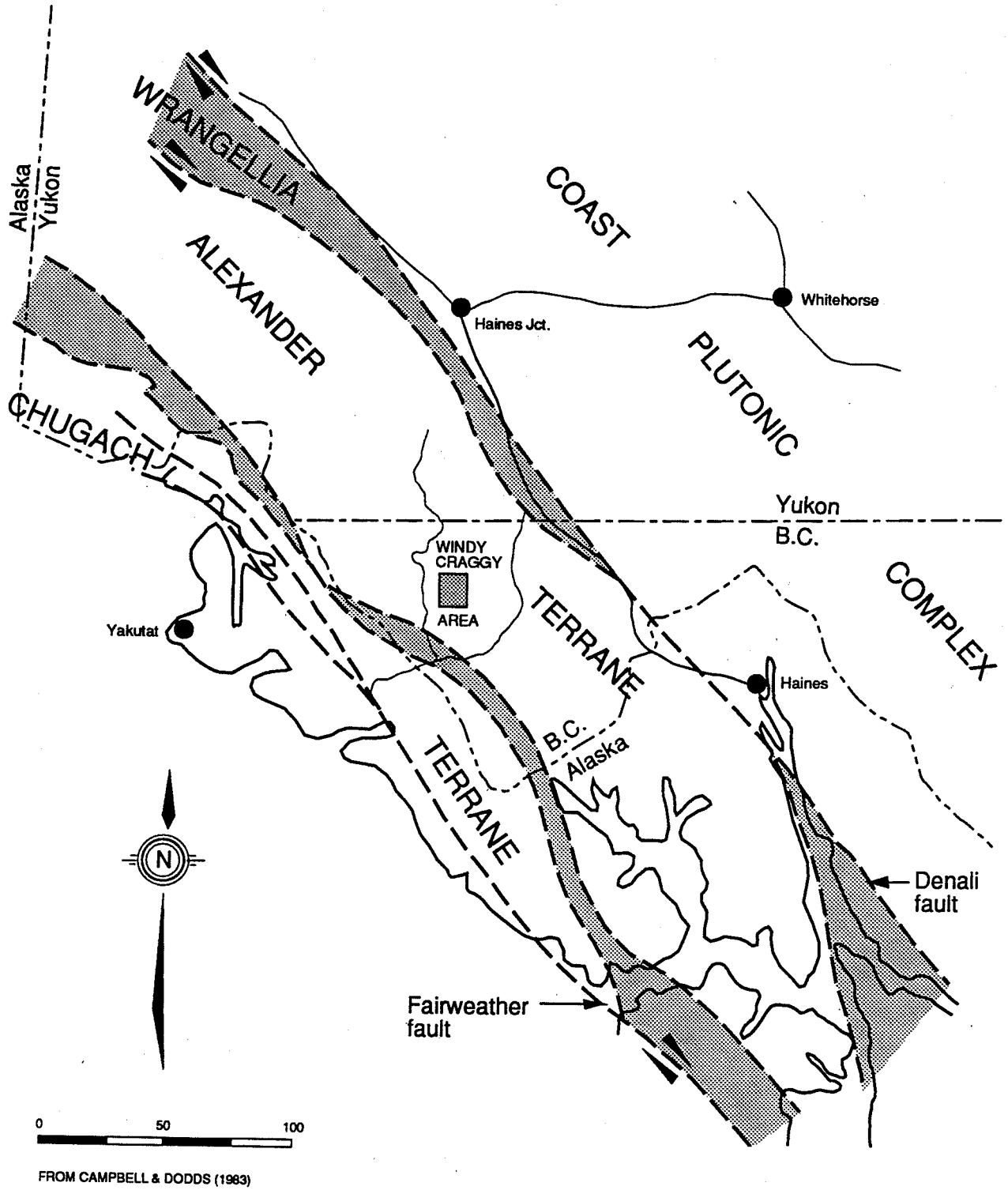

Figure 1 Tectonic setting of the Windy Craggy area (after Campbell and Dodds, 1983, and modified from Gammon and Chandler, 1986).

colour from medium grey to dark green. They are commonly amygdaloidal with spherical to amoeboid amygdules 1 to 5 millimetres in diameter composed of white, fine-grained calcite and, rarely, fine-grained pyrrhotite. In places amygdules comprise up to 4 volume per cent of the rock. Less commonly, the flows are porphyritic, with euhedral phenocrysts of plagioclase 3 to 8 millimetres in diameter and/or hornblende 0.5 to 3.0 millimetres in diameter. The hornblende phenocrysts are variably pseudomorphed by chlorite. Flows are pervasively chloritized and carbonatized. Much of this alteration is related to a regional greenschist facies metamorphic event. Flows are generally only slightly foliated. Where they are present, pillows vary from 10 to 70 centimetres in diameter and generally have finer grained chloritized rims. Drill core examination indicates individual flows are up to 100 metres thick and average 10 to 15 metres in thickness. In the North Cross-cut, a flow immediately overlies graphitic argillite which caps the North Sulphide Body; this flow has an unusual scalloped lower contact with the argillite which indicates that it was deposited on unconsolidated, wet sediments.

Sills are distinguished from dikes on the basis of field relationships and geochemistry (discussed below). Sills are conformable with bedding, medium-grained, medium to dark green in colour and have a diabasic texture. Dikes cross-cut all lithologies, including massive mineralization. However, dikes that cross-cut mineralization are geochemically distinct from those which cross-cut all other lithologies (see below). Dikes are generally lighter coloured (light grey-green) and finer grained than sills, and they range from less than 10 cm to several metres wide. They generally possess a 1 to 20 cm wide chloritic chilled margin, and may contain biotite pseudomorphs after hornblende phenocrysts. All dikes are variably foliated and, therefore, were emplaced prior to folding and tectonism.

In a few drill hole intersections, diabase bodies of limited extent occur spatially and stratigraphically beneath massive mineralization. Intersection widths vary from 1 to 40 metres. The diabases are green-black in colour, medium to coarse-grained, and have homogeneous meshwork textures of intergrown plagioclase, amphibole and pyroxene and, in part, display an ophitic texture (Harris, 1988). They are moderately to extremely altered and contain calcite, chlorite, and epidote. In places, diabase is host to stockwork or stringer mineralization and predates mineralization. These diabase bodies are geochemically similar to overlying footwall and hanging wall flows (see below) and likely the feeder conduits for these overlying units.

Sedimentary Rocks:

Argillites are dark grey-black to light grey-buff in colour and range from non-calcareous to calcareous. They are indistinctly to well laminated (less than 1 millimetre to 20 centimetres) and are dominantly fine- to very fine-grained. Thin, sandy lenses or beds containing lighter grey calcareous grains are an extremely minor component. In places the argillites contain a tuffaceous component consisting of chlorite-rich beds and laminae. Individual argillite units vary in thickness from less than a metre to 40 metres, and on average are 10 to 15 metres thick. Sedimentary structures including normal graded bedding and lamination, soft-sediment deformation and slump structures, scours, pebble dents and concretions and boudins occur within argillite.

"Nodular argillite" is a field term used to describe a locally common variant consisting of augen-shaped boudins of lighter grey calcareous siltstone, 5 millimetres to 3 centimetres in diameter in a darker, finer-grained matrix. Concretions are also rarely present within argillite; they are round to ovoid, concentrically zoned, and comprise about 10 to 30 per cent of the rock. Concretions are 3 to 15 centimetres in diameter, with 3 to 10 millimetre thick monomineralic layers of pyrrhotite, light grey calcite and rare blebs of chalcopyrite.

Mineralization within the argillites consists predominantly of minor, very fine- to coarse-grained (up to 8 millimetres in diameter), disseminated euhedral cubes of pyrite and/or fine-grained pyrrhotite. These sulphides appear to be secondary, and probably formed during diagenesis. Sulphide-rich beds and laminae occur in a few places, and textural evidence indicates that these are primary. In some places, epigenetic sulphides occur as discrete layers that have selectively replaced certain beds. Some argillites display a well-developed foliation which is defined by pyrrhotite plates that are aligned in an axial planar orientation. A slatey cleavage is variably developed within graphitic argillite.

Mineralization:

To date, drilling and underground development has identified two main sulphide masses, the North and South Sulphide Bodies, each with a variably developed stockwork/stringer zone (see Fig. 2 of Downing et al., this volume). One or more smaller massive sulphide lenses are also present. The current interpretation is that these are distinct from the main massive bodies,

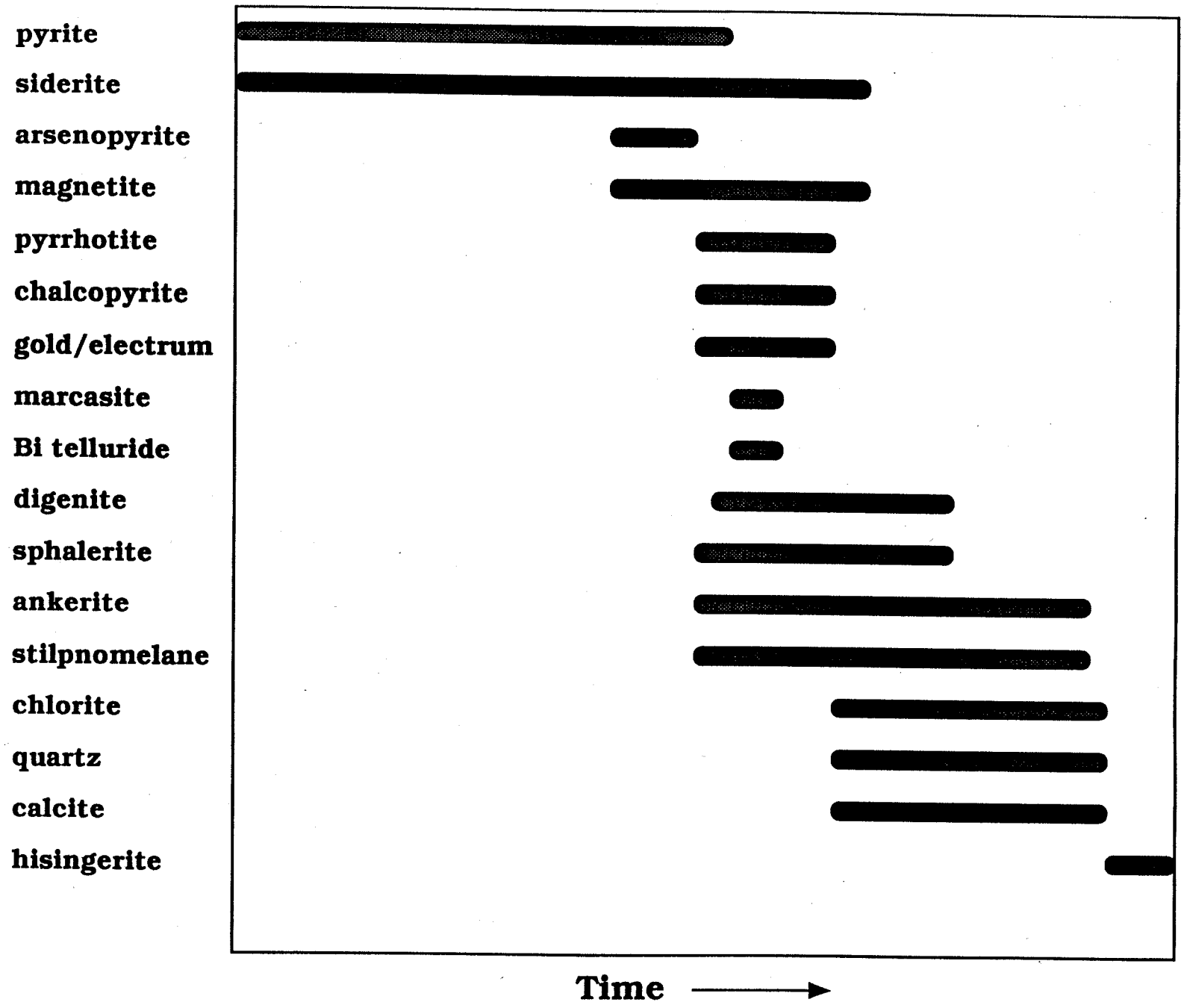

Figure 2 Generalized paragenetic sequence for massive sulphide mineralization in the Windy Craggy deposit.

however, it is possible that these are faulted and displaced portions of the two main bodies. The North Sulphide Body is about 120-150 metres thick by 500 metres in diameter (true dimensions)(see Fig. 3. of Downing et al., this volume), and has a well-developed stockwork/alteration zone within both volcanic and sedimentary rocks. The South Sulphide Body (see Fig. 4 of Downing et al., this volume) is relatively more deformed, and deformation/translation has altered the primary morphology of this lens.

Three principal types of massive sulphide mineralization exist:

1) massive pyrrhotite with lesser chalcopyrite;

2) massive pyrite with lesser chalcopyrite;

3) massive pyrrhotite and pyrite with lesser chalcopyrite and magnetite.

The North Sulphide Body is mineralogically zoned from a pyrrhotite-rich core to a pyrite-rich outer/upper portion (see Fig. 3. of Downing et al., this volume). Magnetite occurs at the transition zone from pyrrhotite to pyrite, as fine-grained wisps, blebs, and patches. This zonation appears to be a primary feature.

Massive sulphide displaying breccia textures is common in the North Sulphide Body. Clasts typically comprise a few to tens of per cent of the total volume of mineralization and are matrix supported. Clasts are commonly pyritic and the matrix is predominantly pyrrhotite. Clasts range in size from 1 to 30 centimetres in diameter. In some places, the clasts are slightly to intensely deformed (stretched). In places, particularly in the North Cross-cut (shown on Fig. 2 of Downing et al., this volume), relatively undeformed, angular breccia sulphides can be traced into extremely deformed/foliated sulphides displaying fine layering, with the layers representing extremely deformed sulphide clasts. Thus, within the massive sulphide body, there are domains of intense structural deformation juxtaposed with areas that are relatively undeformed. Generally, foliated sulphide textures are much more prevalent in the South Sulphide Body.

A stockwork/feeder zone is present beneath both sulphide bodies, although it is better developed and/or less deformed in the North Sulphide Body. These stockwork zones have been translated (tectonically rotated) to varying degrees. However, in the North Sulphide Body, the cross-cutting nature of the stockwork zone to the volcanic stratigraphy is evident (see Fig. 3 of Downing et al., this volume). Stockwork and stringer mineralization occur within all footwall host lithologies and consist of veinlets of sulphides less than 1 millimetre to about 50 centimetres wide within brecciated host rock. Stockwork mineralization extends at least 200 metres stratigraphically beneath massive mineralization in the North Sulphide Body. Sulphides within the stockwork zone consist predominantly of pyrrhotite with lesser chalcopyrite and, in places, pyrite. In general, the percentage of sulphides, and number and density of sulphide veins increases upward from the bottom or "root" to the top of the stockwork zone. Gangue minerals include quartz, carbonate, chlorite, and albite.

The stockwork/stringer zone displays distinct mineralogical zonation. The most intensely altered zones are characterized by moderate to extreme bleaching and silicification of host rocks. Accompanying this silicification is slight to intense brecciation of the host rocks and veining by sulphides (pyrite, pyrrhotite, chalcopyrite and in places minor quartz and/or sphalerite). Host rock breccia fragments have been slightly to intensely chloritized and/or bleached and silicified. Fragments are angular, 1 to 10 centimetres in diameter, translucent, and milky white in colour. Intensely altered rocks resemble cryptocrystalline chert. In places, sulphides have infilled pillow interstices and radial shrinkage or cooling cracks within pillows. The narrowest and most closely spaced veinlets of sulphides are associated with the most intense silicification, giving the appearance of a "crackle breccia". These strongly silicified areas presumably represent the most intensive fossil hydrothermal fluid upflow zones.

This silicification grades into a zone of intense chloritization. The most intense chloritization typically occurs adjacent to the zone of silicification and is characteristically a distinct, bright, apple-green colour. This variety of chlorite grades laterally away from the stockwork zone to a darker olive-green coloured chlorite. There may be a concomitant variation in chlorite composition, although this has not yet been investigated.

Stockwork mineralization in argillite consists of light to dark grey fragments in a fine-grained sulphide matrix whereas similar mineralization in tuff generally contains dark grey-green fragments. Tuff fragments commonly contain more chlorite and reflect their original mineralogy and composition. Intensely altered argillite and tuff fragments appear to be cryptocrystalline and milky white in colour. Pyrrhotite and chalcopyrite occur along selected laminae and beds within individual fragments and as a breccia matrix between clasts.

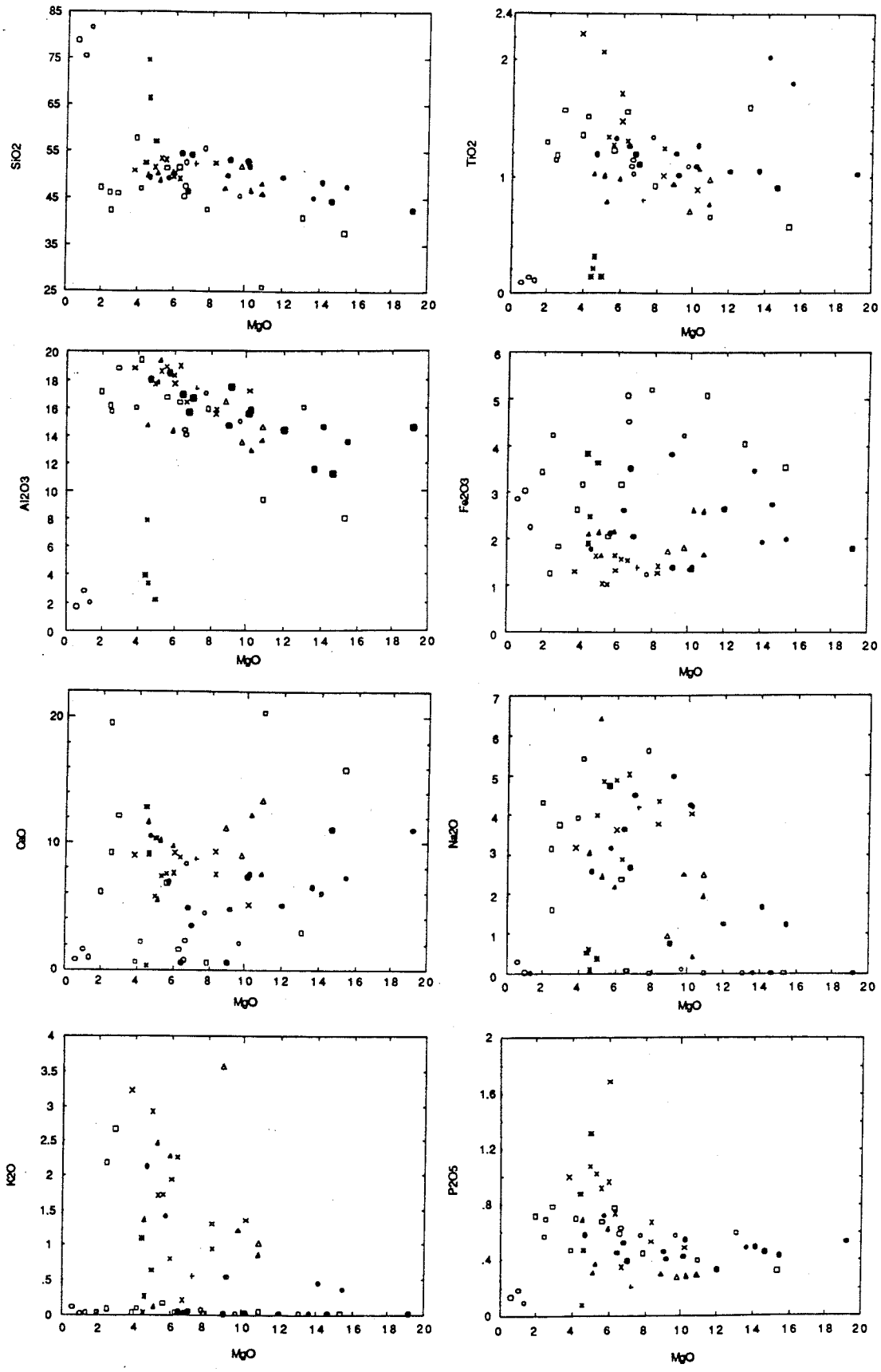

Figure 3 MgO versus major and minor element plots for Windy Craggy igneous rocks.

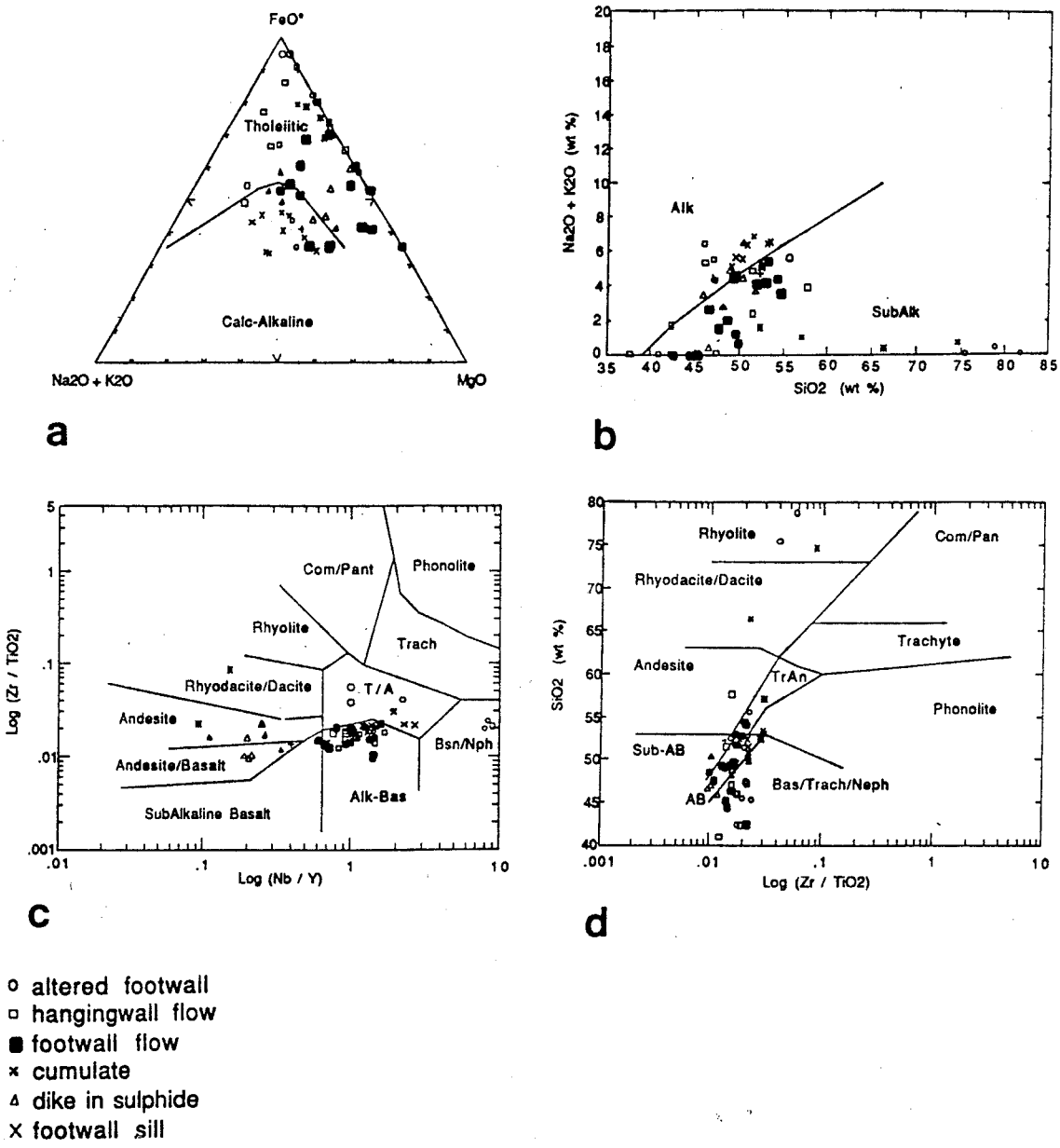

Figure 4. a) AFM plot showing calc-alkaline and tholeiitic fields. Note Fe enrichment; b) Plot of SiO_2 versus Na_2O+K_2O for igneous rocks showing alkaline and subalkaline fields of Irvine and Baragar (1971); c) Log (Nb/Y) versus Log (Zr/TiO_2) plot of (Winchester and Floyd, 1977) showing alkaline nature of Windy Craggy basalts; d) SiO_2 versus Zr/TiO_2 plot showing classification of (Floyd and Winchester, 1977).

Relict lamination and bedding can be seen in both argillite and tuff. Sulphide laminae and beds are interconnected by sulphide veinlets. Sulphides have preferentially replaced coarser-grained laminae and beds.

Chert-Carbonate-Sulphide Exhalite:

A chert-carbonate-sulphide exhalite consisting of finely interlaminated to interbedded (less than 1 millimetre to 5 centimetres) calcite, siderite, ankerite, chert, chlorite, sericite, hematite, magnetite, pyrrhotite, pyrite, chalcopyrite, and, rarely, sphalerite is present in several places within the deposit. This unit is thought to be present both at the base of the South Sulphide Body as well as immediately overlying the North Sulphide Body, where several thin beds are intercalated with hanging wall volcanic flows. Individual units are generally narrow (0.1 to about 3 metres). The chlorite and sericite probably reflect a tuffaceous/sedimentary component. In places, the chert-carbonate-sulphide unit is brecciated and contains angular clasts of fine-grained, hematitic quartz in a hematitic quartz ± sulphide matrix. This brecciation may have occurred relatively recently after deposition of this unit. The chert-carbonate-sulphide unit at Windy Craggy is not typically auriferous, although in several places it contains anomalous values between 1 and 10 grams per tonne Au.

Exhalite of similar appearance to the laminated chert-carbonate-sulphide unit at Windy Craggy commonly overlies massive mineralization in a number of sulphide deposits (e.g., "Tetsusekiei" or ferruginous chert of the Japanese Kuroko deposits: Kalogeropoulos and Scott, 1983; the Main Contact and "C" tuff of the Noranda area: Kalogeropoulos and Scott, 1986; Gibson et al., 1983; and the Key tuffite of Mattagami: Roberts, 1975). At the Okuki mine in western Shikoku, Japan, a typical Besshi-type deposit, the massive sulphide horizon is overlain by a thin "red chert" composed of alternating hematite and aluminosilicate minerals (Watanabe, 1970).

Mineralogy:

In the North Sulphide Body, where deformation is not as intense as in the South Sulphide Body, two generations of pyrite are recognized:

1) early, colloform to framboidal spheres and colloform layers;

2) later, recrystallized(?) euhedral, equant cubes and pyritohedrons intergrown in a boxwork fashion.

These crystals may be incipiently fractured and veined by chalcopyrite and pyrrhotite. In places, the latter variety of pyrite is seen to overgrow the colloform variety with little or no replacement. In the South Sulphide Body, pyrite is present as the latter variety and commonly occurs as trails of cataclased grains.

Pyrrhotite is coeval with chalcopyrite and is predominantly later than pyrite. It commonly occurs interstitially to pyrite and as fracture fillings (with chalcopyrite) within pyrite. Minor pyrrhotite occurs as small inclusions within pyrite. In the South Sulphide Body, pyrrhotite grains have been elongated and may display deformation twin lamellae. In certain places in both the North and South Sulphide Bodies, pyrrhotite is completely recrystallized and displays a crystalloblastic texture with 120° grain boundaries. Marcasite is prevalent only within the South Sulphide Body. It occurs as minute, rounded blebs in pyrrhotite.

Chalcopyrite displays mutual boundaries with coeval pyrrhotite and is predominantly later than pyrite. It usually occurs interstitially to pyrite and as fracture fillings together with pyrrhotite in pyrite. A small amount of chalcopyrite occurs as small inclusions within pyrite. In places, early pyrite spheres are partly pseudomorphed by chalcopyrite.

Sphalerite is rarely present in the South Sulphide Body; where, it occurs as small, isolated, anhedral grains within carbonate and as narrow veinlets cross-cutting other sulphides. In transmitted light it is translucent and deep orange-brown in colour due to the presence of appreciable iron. In the North Sulphide Body, sphalerite is much more common, occurring as anhedral crystals that are interstitial to euhedral pyrite. Here, it displays mutual boundaries with pyrrhotite.

Digenite has only been observed in the North Sulphide Body. It occurs as irregular, anhedral blebs with chalcopyrite and sphalerite, with which it displays mutual boundaries interstitial to, and as overgrowths on pyrite. It is also found as inclusions within chalcopyrite.

Arsenopyrite is exceedingly rare, and has only been identified in the North Sulphide Body. It occurs as euhedral rhombohedral or lozenge-shaped crystals that have chalcopyrite and pyrrhotite overgrowths.

Graphite is present as very fine foliae and disseminations deflected around sulphides, quartz, and plagioclase grains within semi-massive to massive sulphide, particularly in stockwork mineralization developed in argillite.

Native gold and electrum occur not only in the gold-enriched zone, but are also present in the North and South Sulphide Bodies. These minerals are difficult to distinguish optically; gold is distinguished from electrum here by its darker yellow colour. Gold and electrum occur as:

1) blebs associated with chalcopyrite and pyrrhotite fracture fillings in pyrite within massive sulphides;

2) anhedral inclusions within recrystallized, euhedral pyrite in massive sulphides;

3) as inclusions within, and intergrowths with, calcite in the gold-enriched portions of the chert-carbonate-sulphide exhalite unit.

Bismuth telluride occurs as very small rounded blebs included in pyrrhotite. Its presence was identified by scanning electron microscopy, and optical properties suggest one of the following minerals: wehrlite (BiTe), hedleyite ($Bi_{14}Te_6$), or tellurobismuthinite (Bi_2Te_3).

Several types and generations of carbonate are present:

1) early, "dirty", inclusion-bearing, brownish coloured, anhedral crystals and patches of siderite which occur as colloform to botryoidal overgrowths on sulphides;

2) euhedral brownish siderite rhombs that commonly display growth zoning;

3) optically clear, white, interstitial (late) anhedral calcite;

4) dark grey to black, interstitial, anhedral calcite which occurs as discrete patches or is intergrown with white calcite.

In the South Sulphide Body, carbonates typically display deformed cleavages and may be somewhat elongated or cataclased.

In the North Sulphide Body, magnetite occurs as euhedral dodecahedrons and octahedrons included within pyrite, pyrrhotite, chalcopyrite, carbonate, and rarely, sphalerite. In the South Sulphide Body, bifurcating veinlets of magnetite cross-cut massive pyrrhotite+pyrite+chalcopyrite. These are particularly well exposed in the South Cross-cut.

Quartz occurs as discrete grains interstitial to sulphides and commonly intergrown with carbonate. In the South Sulphide Body, quartz occurs in discrete trains or patches, with some grains displaying pressure shadows.

Hisingerite ($Fe_2Si_2O_5(OH)_4.2H_2O$) is an amber to dark brown coloured, conchoidally fracturing mineral present in anastomosing or horsetail veins and veinlets cross-cutting massive sulphides in the South Sulphide Body; good exposures of this mineral are in the South Cross-cut. When sampled, the mineral crumbles due to desiccation. The mineral does not give a good x-ray diffraction pattern, and positive identification was made with an electron microprobe.

Hisingerite has been noted in several other sulphide deposits (including the Wilcox Mine, Parry Sound, Ontario and Montauban Mines, Quebec) where the mineral is closely related to sulphide ore deposition (Osborne and Archambault, 1950; Schwartz, 1924; Whelan and Goldich, 1961). In these deposits it is thought to represent late-stage hydrothermal activity, whereas at Windy Craggy, hisingerite probably formed during deformation or metamorphism of the massive sulphides.

Stilpnomelane, a brittle mica, occurs as fibres intergrown with pyrrhotite, chalcopyrite, chlorite, and quartz and is also interstitial to sulphides within mineralization. It varies in colour from brownish green to orange-brown. The mineral may have been formed from precursor Fe- and Al-oxyhydroxides.

Chlorite is present within massive sulphide as later overgrowths on sulphides.

Cordierite is present as large, well-developed porphyroblasts within mafic tuff beds. This mineral formed during hydrothermal alteration and sulphide deposition. The magnesium was probably derived from chlorite in the mafic tuff, and the argillaceous sedimentary component supplied the necessary alumina and silica. From experimental and theoretical studies, the stability of cordierite requires temperatures in excess of 350°C, irrespective of pressure (Schreyer et al., 1964; Schreyer and Yoder, 1964).

Mineral Paragenesis:

A generalized paragenetic sequence for massive mineralization is shown in Figure 2. In the North Sulphide Body, primary textures are better preserved and are better suited to paragenetic studies than mineralization in the South Sulphide Body. Pyrite is generally the first sulphide to have been deposited and, in places, good evidence of primary textures such as framboids and colloform bands are preserved. Pyrite is generally accompanied by early siderite. Pyrrhotite, chalcopyrite, gold and electrum, marcasite, sphalerite, digenite, and ankerite are deposited later and were generally precipitated as epitaxial growths on pyrite, although they can occur as rarer inclusions within pyrite.

Stilpnomelane, chlorite, quartz and calcite

generally occur as overgrowths on these minerals, and rarely as intergrowths with sulphides. Some of these inter- and overgrowths may be related to deformation and recrystallization of the sulphide mass. Hisingerite most likely formed late syn- to post-deformation and metamorphism. Within the stockwork zone, quartz was precipitated in zones of intense silicification where the mineral pseudomorphs primary igneous minerals. Discrete quartz-sulphide veins are rare, but can be seen underground (e.g., in the North Cross-cut). Within relatively undeformed stockwork mineralization, chalcopyrite occurs as fracture fillings in pyrite, and this texture is thought to be primary. Cordierite "porphyroblasts" occur within stockwork developed in argillite.

In the South Sulphide Body, most of the mineral textures are the result of deformation. Secondary metamorphic and deformational textures include quartz fibres developed on recrystallized pyrite cubes; such textures are reminiscent of those formed by crack-seal deformation (Ramsay, 1980). Other deformation textures include:

1) recrystallized pyrite cubes;

2) deformation/twin lamellae in pyrrhotite;

3) elongation of pyrrhotite crystals;

4) chalcopyrite ± pyrrhotite filling fractures in pyrite;

5) cataclased and comminuted pyrite grains;

6) 120° grain boundaries in pyrrhotite.

Some of the recrystallization of pyrite within massive mineralization may have taken place during the late stages of sulphide deposition as hydrothermal fluids circulated through porous, pre-existing sulphide mass.

Sulphide Geochemistry:

Within the North Sulphide Body, several 70-75 m portions of the North Cross-cut contain zinc values up to 5 weight percent and concomitant anomalous gold concentrations up to about 2 g/t. Zinc correlates positively with cadmium, arsenic, antimony, lead, gold, and silver. High values of the above elements are not correlatable with copper, cobalt, or iron contents. Furthermore, high cobalt values do not necessarily correlate with high copper concentrations.

The average cobalt grade of proven and probable reserves at Windy Craggy is 0.082 wt%. However, no discrete, primary cobalt-bearing phase has been identified. Muir (1980) reported a pyrrhotite analysis of 0.29 wt% Co and two analyses of pyrite containing 0.32 wt% Co. Mainwaring (1983) analyzed pyrrhotite and pyrite from six samples and found that pyrite contains from <0.03 to 3.2 wt% Co (mean=1 wt%), and coexisting pyrrhotite contains from <0.03 to 0.2 wt% Co (mean=0.1 wt%). Cobalt enrichment is also observed in pyrite from Japanese Besshi-type deposits (Kase and Yamamoto, 1988), and Co-rich pentlandite, Co-bearing mackinawite, and cobaltite have been noted at the Shimokawa deposit (Bamba and Motoyoshi, 1985).

The average gold content of massive sulphide is 0.22 grams per tonne; the chert-carbonate-sulphide unit for the most part is not gold-bearing; however, certain intersections contain elevated gold (1 to 10 grams per tonne). A zone of significant gold enrichment has been intersected at the margin of the South Sulphide Body in several drill holes. The drill hole which first intersected this zone assayed 4.46 grams gold and 3.43 grams silver per tonne and 0.62 per cent copper over 61.3 metres. Within this section, 5.5 metres assayed 11.66 grams gold and 3.09 grams silver per tone and 0.98 per cent copper. However, this is probably not a true width.

This gold-bearing zone contains fragments and bands or beds of milky white, very fine-grained rock with the appearance of chert. Less commonly, clasts of fine-grained mafic volcanic rock and rare laminated to banded argillite fragments are also present. Volcanic clasts commonly display a thin rim of darker green chlorite indicative of hydrothermal alteration. Clasts comprise about 40 per cent of the rock and are supported by a fine-grained, mottled sulphide and carbonate matrix consisting of intergrown pyrite, pyrrhotite, chalcopyrite, magnetite, brown-grey siderite and milky white calcite. Sulphides are present as fine-grained disseminations intergrown with carbonate. Rare visible gold is associated with sulphides and carbonates and occurs as discrete grains 30 to 80μ in diameter. Electrum and native silver have also been identified (Buchan, 1984; Gasparrini, 1983).

Within this zone are clasts and fragments of volcanics and argillite that are rimmed by chlorite. In some places, pyrrhotite and minor chalcopyrite bands occur in dark grey, fine-grained quartzose argillite. These bands are interconnected by narrow sulphide veinlets which crosscut the argillite. This texture suggests that sulphides have selectively replaced beds and laminae.

Little is known of the distribution of precious metals in Besshi-type deposits. Maeda et al.(1981) reported on the occurrence of electrum in the Shimokawa mine, Hokkaido, Japan. The deposit has many similarities with Windy Craggy and is situated at the boundary between diabase and phyllite of the Mesozoic Hidaka Supergroup. Here, electrum occurs as irregular grains less than 30 μ diameter. The mineral is intimately associated with sphalerite and pyrrhotite and contains between 13 and 56 weight per cent Ag.

Petrography:

All samples were examined in thin section, and table 1 gives their capsule description and mineralogy. Although host rocks have been metamorphosed to greenschist facies, primary textures and structures are typically well preserved. Greenschist facies alteration minerals include chlorite, albite, epidote, actinolite, sphene, and leucoxene. Epidote, chlorite, and calcite have replaced feldspar, and chlorite, epidote and calcite have replaced mafic minerals. Amygdules are filled with chlorite, epidote, calcite and albite. Rocks have also been hydrothermally altered to varying degrees. Plagioclase laths have been typically altered to albite and the mafic phases to a pale or darker green chlorite and fine-grained sphene. All of the samples are fine- to medium-grained and exhibit predominantly pilotaxitic and intersertal textures. Most samples are massive or, less commonly, vesicular to amygdaloidal.

Geochemistry of Igneous Rocks:

Fifty-eight samples of volcanic flows, sills and dikes were collected from drill core, surface, and underground workings in the immediate area of the deposit from both the hanging wall and footwall of the deposit (Table 1). Samples were pulverized in an alumina mill/shatterbox at the University of Toronto and analyzed for major elements, H_2O+, H_2O-, CO_2, and S on fused glass discs by X-Ray Assay Laboratories Ltd. of Don Mills, Ontario. Trace element analyses (Zr, Y, Rb, Sr, Cr, and Ni) were performed at the University of Toronto on pressed powder pellets.

The precision was estimated, from repeated analyses and from counting statistics, to be better than 5% for Zr, La, Ce, Sm, Yb, Y, Sc, and Co; better than 10% for Hf, Eu, Cr, Ni, and Rb; and better than 20% for Th, Nd, Tb, Ta, and Ba. Rare earth element (REE), Ta, Th, Hf, Sc, and Co analyses were performed at the University of Toronto. Samples were irradiated at the University's Slowpoke reactor and counted in the Department of Geology using the method of Barnes and Gorton (1984). CIPW norms were calculated according to the method of Kelsey (1965) by the computer program NEWPET (Clarke 1989). Iron oxides were recalculated to $Fe^{3+}/(Fe^{3+} + Fe^{2+})=0.15$, and the analyses were subsequently recalculated to 100% on an H_2O and CO_2-free basis.

Major, trace and rare earth element compositions of selected samples are given in Table 2, along with the calculated Mg number and selected element ratios. To ameliorate problems of identifying primary compositions, alteration effects associated with regional metamorphism were lessened by recalculating all analyses on a CO_2 and H_2O-free basis. Mg-numbers vary from ≈69 to ≈6 (Table 2) and indicate that most samples have undergone fractionation involving a decrease in Mg number since their separation from source materials in the mantle. However, the Mg number for some samples has been modified by hydrothermal alteration and metamorphism.

CIPW norm compositions for each sample are shown in Table 3. Norm calculations were performed on the CO_2 and H_2O-free analyses. Additionally, these analyses were recalculated on a pyrite-free basis by attributing all sulfur and the requisite Fe to pyrite. Figure 3 displays some of the salient geochemical aspects of these samples. Plots of MgO show clearer trends than Mg number because of the iron enrichment associated with mineralization. Plots of MgO versus CaO, K_2O, and Na_2O show scatter due to depletions or enrichments unrelated to primary trends, and these are discussed later. The plot of MgO versus TiO_2 shows that the flows are low in titanium and that there is an antipathetic variation, consistent with crystal fractionation (Walker et al., 1979). The footwall sills are generally higher in titanium. The plot of MgO versus Al_2O_3 is consistent with fractionation of olivine and plagioclase at low pressures.

Figure 4a is a Na_2O+K_2O vs. FeO* vs MgO (AFM) diagram of Irvine and Baragar (1971). Samples of sills within footwall argillites plot distinctly within the calc-alkaline field. Footwall and hanging wall flows plot predominantly in the tholeiitic field and display varying degrees of iron enrichment, although a few samples lie within the calc-alkaline field. On the SiO_2 vs. Na_2O+K_2O plot (Fig. 4b) of Irvine and Baragar (1971), the sills plot predominantly within the alkalic field, with some samples plotting on the dividing line. Most of the flow samples plot within the subalkalic field, although some of the hanging wall samples are within the alkalic field. A number of the samples, particularly those that have been hydrothermally altered, display a severe depletion

Table 1. Description and mineralogy of Windy Craggy igneous rock samples.

Sample No.	Description	Mineralogy
footwall flows and intrusives		
88-32;001.5 (*)	green-grey, massive, stratigraphically beneath stockwork zone.	plagioclase, chlorite, calcite, sericite, opaques.
88-33;066.4	green-grey, massive, ≈60 m wide intersection, stratigraphically well beneath stockwork zone.	clinopyroxene, chlorite, calcite, sphene, biotite.
88-36;066.3	medium grey-green, fine grained, chloritized, massive; ≈55 m wide intersection.	plagioclase, chlorite, calcite, biotite, sericite, albite, sphene, opaques.
88-42;191.6	dark green, medium to coarse grained diabasic texture.	plagioclase, chlorite, calcite, sphene.
88-44;241.6	medium green, amygdaloidal, within stockwork zone.	chlorite, calcite, quartz, epidote, biotite, opaques.
altered footwall flows		
WCU89-42	bright green, from chloritized stockwork zone, underground, 152 m from entrance of North Cross-cut, south wall.	chlorite, epidote, carbonate, albite, quartz, pyrite, chalcopyrite.
WCU89-43	bright green, from chloritized stockwork zone, underground, 140 m from entrance of North Cross-cut, north wall.	chlorite, carbonate, epidote, albite, quartz.
WCU89-44	bright green, from chloritized stockwork zone, underground, 132 m from entrance of North Cross-cut, north wall.	chlorite, albite, epidote, quartz, carbonate, pyrite, chalcopyrite.
88-42;265.8	milky green to white, brecciated, chalcopyrite and pyrrhotite veined, from silicified stockwork zone.	quartz, carbonate, chlorite, pyyrrhotite, chalcopyrite.

(Table 1 Continued)

88-46;106.9	milky green to white, brecciated, with pyrrhotite and chalcopyrite veinlets, from silicified stockwork zone.	quartz, carbonate, chlorite, pyrrhotite, chalcopyrite.
88-77;270.6	milky green, crackle brecciated, with pyrrhotite and chlorite veinlets, from silicified stockwork zone.	quartz, chlorite, carbonate, pyrrhotite.
hangingwall flows		
88-40;436.5	medium green, fine grained, massive to amygdaloidal, minor disseminated sulfides.	plagioclase, chlorite, calcite, sericite, sphene, opaques.
88-44;339.6	dark green, fine grained, stratigraphically immediately overlying massive sulphides.	chlorite, calcite, quartz.
88-46;336.8	medium green-grey, fine grained, amygdaloidal, stratigraphically immediately overlying massive sulfides.	plagioclase, chlorite, quartz, calcite, opaques.
footwall sills		
X-14	surface, southwest ridge, Windy Peak.	plagioclase, chlorite, sericite, clinopyroxene, amphibole, biotite, epidote, sphene, apatite.
X-51	coarse grained, hornblende-phyric, surface, northwest ridge, Windy Peak at 1630m elevation.	plagioclase, apatite, chlorite, hornblende, sericite, opaques, titanomagnetite.
WCU88-20	underground, main adit at 581m.	plagioclase, calcite, chlorite, opaques, sphene, epidote, actinolite.

(Table 1 Continued)

dikes cross-cutting massive sulphides		
88-30;381.0	green-grey, near hangingwall.	calcite, chlorite, actinolite, quartz, apatite?, opaques.
88-37;243.0	medium green, ≈1 m wide.	hornblende, chlorite, epidote, calcite, clinopyroxene, albite, sphene, opaques.
88-44;291.3	massive to porphyritic, with 10 cm wide chloritized margins.	calcite, chlorite, quartz, sericite, apatite.
88-46;261.2	medium green-grey, fine grained, biotite pseudomorphs after clinopyroxene phenocrysts, chloritized margins.	biotite, chlorite, calcite, opaques, sericite, quartz.
cumlates		
88-29;207.0	dark green-black, hydrothermally altered.	orthoamphibole-tremolite, chlorite, quartz?, pyrrhotite, chalcopyrite.

* denotes year, drill hole number, and down-hole meterage.

of Na and K, and this is discussed later.

On the log (Zr/TiO_2) vs. log (Nb/Y) (Fig. 4c) and SiO_2 vs. log (Zr/TiO_2) diagrams (Fig. 4d) of Winchester and Floyd (1977), all unaltered flows and most of the sill samples plot within the alkaline basalt field. A few of the sill samples fall within the trachyandesite field; several extremely altered samples also fall within these fields, however, these show evidence of extreme mobility of these elements as well as the rare earth elements (REE); this is also discussed further below. The diagram clearly distinguishes the dikes which cross-cut massive sulphide from the flows and sills, with the former plotting in the andesite and andesite/basalt fields.

Major element abundances, which discriminate magma types in recent volcanic rocks, are susceptible to modification during low-grade metamorphism. These are, therefore, of limited value for determining magmatic affinities. Certain trace elements (Ti, Cr, Ni, Zr, Y, Nb, Co, Sc, U, Th, Ta, Hf, and the rare earth elements (REE) are believed to be immobile in water-rock interactions including those involved in ore genesis (Campbell et al., 1984; Costa et al., 1983; Finlow-Bates and Stumpfl, 1981; Floyd and Winchester, 1978; Garcia, 1978; Gibson, et al. 1983; Hall, 1982; MacGeehan and MacLean, 1980a,b; MacLean and Kranidiotis, 1987;

Table 2 Major, trace, and rare earth element content of selected igneous host rocks to the Windy Craggy deposit. All analyses have been recalculated to 100% H_2O- and CO_2-free

Sample No.	88-32; 1.5	88-33; 66.4	88-36; 66.3	88-42; 191.6	88-44; 241.6	X-14	X-51
Description	footwall flow	footwall flow	footwall flow	footwall flow	footwall flow	footwall sill	footwall sill
(wt. %)							
SiO2	49.40	42.80	44.00	47.00	44.00	51.40	49.20
TiO2	0.94	1.62	1.84	1.15	1.06	1.23	2.16
Al2O3	16.30	12.20	13.30	14.40	16.10	18.30	18.20
Fe2O3*	8.54	11.90	11.70	8.31	10.50	6.49	8.25
MnO	0.10	0.20	0.18	0.18	0.16	0.13	0.14
MgO	8.52	13.90	12.80	9.29	4.16	5.38	3.68
CaO	4.45	6.56	5.51	6.83	9.42	7.33	8.73
Na2O	4.62	1.10	1.51	3.82	2.30	4.60	3.08
K2O	0.51	0.33	0.41	0.03	1.90	1.67	3.13
P2O5	0.38	0.39	0.45	0.50	0.52	0.89	0.97
H2O+	4.50	6.30	6.30	4.90	3.90	2.20	2.00
H2O-	0.10	0.20	0.10	0.10	0.10	0.10	<0.1
CO2	1.76	2.94	2.64	4.17	6.63	0.04	0.08
S	0.02	0.00	0.00	0.00	0.03	0.00	0.00
Total	100.14	100.44	100.75	100.68	100.78	99.77	99.63
Mg Number	66.40	69.82	68.42	68.89	43.97	62.15	46.90
(ppm)							
Ba	357	111	94	86	390	535	888
Rb	17.0	27.0	15.0	18.0	39.0	16.0	60.0
Sr	334	179	182	493	290	1260	1640
Zn	60	107	0	87	115	72	84
Sc	37.0	23.0	24.7	27.5	35.3	22.7	22.4
Cr	365	610	476	393	38	72	0
Co	35	64	63	38	32	23	23
Ni	106	320	260	202	19	66	20
V	239	211	226	217	278	151	213
La	24	24	28	33	23	74	84
Ce	48	59	68	72	52	141	178
Nd	16	25	30	26	22	49	65
Sm	3.53	5.13	5.73	5.12	4.80	8.01	11.14
Eu	1.0	1.6	1.7	1.7	1.1	2.3	3.2
Tb	0.6	0.5	0.5	0.7	0.6	0.9	1.0
Yb	1.7	1.3	1.3	2.0	1.6	2.4	2.7
Lu	0.29	0.23	0.24	0.34	0.31	0.37	0.38
Y	19	16	17	22	18	23	27
Zr	95	103	107	118	80	224	278
Nb	19.9	21.7	23.1	23.0	12.4	43.6	71.9
Hf	2.0	2.5	2.5	2.9	1.9	4.4	6.3
Ta	1.1	1.3	1.5	1.3	0.6	2.7	4.1
Th	2.6	1.4	1.5	2.6	1.0	7.1	5.8
U	0.6	0.2	0.2	0.6	0.2	1.7	1.2
Ti/Zr	99.10	157.04	171.34	97.32	133.03	54.84	77.60
Zr/Y	4.9	6.6	6.4	5.4	4.6	9.9	10.3
Zr/Hf	47.4	41.3	43.3	40.9	42.4	50.5	44.1
Nb/Ta	18.1	16.5	15.9	18.0	20.4	16.4	17.5
La/Th	9.1	17.3	18.3	12.8	23.1	10.5	14.5
La/Ta	21.5	18.3	18.9	25.9	37.9	28.0	20.4
La/Nb	1.2	1.1	1.2	1.4	1.9	1.7	1.2
La/Yb	13.7	18.9	21.6	16.9	14.4	31.5	31.4
La/Sm	6.7	4.7	4.8	6.5	4.8	9.3	7.5

Analyses are not recalculated.
Mg number [molar 100 MgO/(MgO+FeO)] is calculated from total Fe contents assuming Fe2O3/FeO=0.15.

(Table 2 Continued)

Sample No.	WCU88-20	88-40; 436.5	88-44; 339.6	88-46; 336.8	WCU89-42	WCU89-43	WCU89-44
Description	footwall sill	hangingwall flow	hangingwall flow	hangingwall flow	altered footwall flow	altered footwall flow	altered footwall flow
(wt. %)							
SiO2	45.10	40.80	29.00	47.00	43.20	41.30	41.50
TiO2	1.20	1.39	0.44	1.12	1.04	0.99	0.99
Al2O3	17.40	16.70	6.16	15.30	12.80	13.10	13.70
Fe2O3*	9.51	10.80	18.20	12.40	27.50	30.90	25.80
MnO	0.16	0.24	0.37	0.24	0.11	0.18	0.10
MgO	5.82	2.56	11.80	5.11	6.05	5.98	8.83
CaO	8.14	10.80	12.20	6.23	2.10	0.71	1.93
Na2O	2.65	3.34	0.00	4.33	0.07	0.07	0.09
K2O	2.08	2.37	0.02	0.15	0.02	0.02	0.02
P2O5	0.68	0.70	0.25	0.62	0.58	0.54	0.53
H2O+	3.60	3.10	3.80	4.20	6.50	7.00	7.30
H2O-	<0.1	<0.1	0.10	0.10	0.10	0.10	0.10
CO2	3.54	7.84	18.60	4.11	1.83	0.79	1.99
S	0.08	0.00	0.04	0.02	0.40	0.11	0.00
Total	99.96	100.65	100.98	100.93	102.30	101.79	102.88
Mg Number	54.79	31.95	56.22	44.94	30.35	27.71	40.40
(ppm)							
Ba	456	372	49	114	72	109	61
Pb	36.0	28.0	23.0	15.0	36.0	17.0	11.0
Sr	669	258	353	189	51	20	58
Zn	98	64	80	111	0	0	0
Sc	36.5	33.8	15.6	30.8	27.6	25.9	26.4
Cr	28	166	33	186	321	113	118
Co	38	14	70	22	0	0	0
Ni	15	41	841	66	0	0	0
V	296	252	99	258	0	0	0
La	30	37	14	36	34	31	23
Ce	65	87	31	78	0	0	0
Nd	31	32	10	30	22	22	16
Sm	6.57	6.06	2.21	5.34	3.96	3.88	3.76
Eu	2.1	1.3	0.9	1.6	0.0	0.0	0.0
Tb	0.7	0.6	0.3	0.6	0.5	0.5	0.5
Yb	2.0	1.8	0.9	1.8	1.7	1.6	1.7
Lu	0.36	0.36	0.13	0.34	0.28	0.27	0.35
Y	22	20	10	20	5	5	5
Zr	101	149	50	137	130	141	117
Nb	15.0	34.4	9.3	28.3	45.0	42.0	40.0
Hf	2.3	3.4	1.2	2.8	-	-	-
Ta	0.7	1.9	0.6	1.6	-	-	-
Th	1.7	2.7	1.1	3.5	3.1	2.8	2.5
U	0.5	0.5	0.3	0.9	0.0	0.3	0.3
Ti/Zr	118.27	93.01	88.84	81.50	80.00	70.21	84.62
Zr/Y	4.7	7.3	4.9	6.7	26.0	28.2	23.4
Zr/Hf	44.2	44.0	40.6	49.1			
Nb/Ta	21.8	18.2	14.7	17.1			
La/Th	17.3	13.8	12.6	10.4	10.8	11.3	9.2
La/Ta	43.1	19.7	22.1	22.1			
La/Nb	2.0	1.1	1.5	1.3	0.7	0.7	0.6
La/Yb	14.6	20.6	15.3	19.8	19.6	19.2	13.5
La/Sm	4.5	6.1	6.3	6.8	8.5	8.1	6.1

(Table 2 Continued)

Sample No.	88-42;	88-46;	88-77;	88-29;	88-30;	88-46;	88-37;
Description	265.8 altered footwall flow	106.9 altered footwall flow	270.6 altered footwall flow	207 cumulate	381 dike in sulphide	261.2 dike in sulphide	243 dikes in sulphide
(wt. %)							
SiO2	71.00	77.80	69.60	45.30	43.10	43.90	50.10
TiO2	0.08	0.10	0.12	0.12	0.69	0.85	0.68
Al2O3	1.52	1.92	2.61	3.41	17.10	12.50	13.10
Fe2O3*	17.10	14.20	18.60	22.10	9.59	12.50	11.70
MnO	0.07	0.07	0.20	0.26	0.29	0.29	0.14
MgO	0.53	1.25	0.93	3.83	4.62	5.15	9.45
CaO	0.76	0.91	1.51	11.10	9.02	8.51	8.74
Na2O	0.26	0.00	0.02	0.45	2.17	1.91	2.42
K2O	0.10	0.03	0.02	0.95	2.18	1.99	1.18
P2O5	0.12	0.09	0.17	0.76	0.33	0.55	0.27
H2O+	0.40	1.00	1.40	4.80	4.00	3.20	2.50
H2O-	0.10	<0.1	<0.1	1.20	0.10	0.10	0.10
CO2	1.15	0.00	2.97	8.29	6.96	9.23	0.25
S	5.88	2.72	2.64	0.22	0.00	0.00	0.04
Total	99.07	100.09	100.79	102.79	100.15	100.69	100.67
Mg Number	5.78	14.85	9.01	25.55	48.82	44.93	61.53
(ppm)							
Ba	390	32	5	408	1070	1010	922
Rb	248.0	359.0	252.0	30.0	48.0	66.0	23.0
Sr	34	28	14	154	342	524	674
Zn	0	0	0	54	89	203	109
Sc	1.5	2.3	2.8	5.0	24.5	44.4	38.0
Cr	280	117	108	57	24	238	509
Co	0	0	0	54	32	34	39
Ni	0	0	0	14	10	68	171
V	0	0	0	154	284	320	236
La	2	0	1	5	11	25	14
Ce	0	0	0	6	26	60	31
Nd	1	0	1	5	12	30	12
Sm	0.50	0.24	0.55	1.65	3.82	7.89	3.70
Eu	0.0	0.0	0.0	0.3	1.1	2.2	1.3
Tb	0.1	0.0	0.1	0.3	0.5	0.8	0.5
Yb	0.3	0.2	0.4	2.0	1.6	1.6	1.6
Lu	0.08	0.06	0.10	0.37	0.29	0.34	0.28
Y	5	5	5	16	18	23	17
Zr	27	23	29	20	66	113	69
Nb	5.0	5.0	11.0	0.0	1.9	5.9	4.5
Hf	-	-	-	0.5	1.8	3.1	1.8
Ta	-	-	-	0.1	0.2	0.4	0.4
Th	0.2	0.3	0.4	0.4	1.2	3.3	2.6
U	1.0	0.8	0.9	0.7	0.4	1.5	1.0
Ti/Zr	29.63	43.48	41.38	58.59	104.31	75.04	98.12
Zr/Y	5.4	4.6	5.8	1.3	3.8	4.9	4.0
Zr/Hf				40.2	37.4	36.1	38.5
Nb/Ta				0.0	8.4	16.0	12.6
La/Th	9.8	1.2	2.6	12.7	9.0	7.5	5.4
La/Ta				56.7	47.0	66.8	39.2
La/Nb	0.4	0.1	0.1		5.6	4.2	3.1
La/Yb	6.0	1.9	2.4	2.6	6.7	15.6	8.9
La/Sm	3.8	1.7	1.8	3.1	2.8	3.1	3.8

Table 3 CIPW norms for selected Windy Craggy igneous rock samples.

Sample No.	88-46; 337	WCU89-42	WCU89-43	WCU89-44	88-42; 266	88-37; 243
Quartz	0.00	16.89	15.53	11.44	67.02	0.00
Corundum	0.00	10.93	13.83	12.07	0.00	0.00
Zircon	0.03	0.03	0.03	0.03	0.01	0.01
Orthoclase	0.95	0.13	0.13	0.12	0.75	7.16
Albite	39.60	0.59	0.59	0.85	2.37	20.90
Anorthite	23.67	7.15	0.01	6.53	2.93	21.95
Nepheline	0.00	0.00	0.00	0.00	0.00	0.00
Diopside	4.57	0.00	0.00	0.00	0.41	17.16
Hypersthene	12.61	51.46	56.48	57.29	14.87	20.15
Olivine	10.69	0.00	0.00	0.00	0.00	7.21
Wollastonite	0.00	0.00	0.00	0.00	0.00	0.00
Magnetite	2.91	6.28	7.13	6.00	2.32	2.59
Calcite	0.04	0.07	0.03	0.03	0.07	0.11
Ilmenite	2.30	2.11	2.01	2.01	0.17	1.33
Rutile	0.00	0.00	0.00	0.00	0.00	0.00
Apatite	1.59	1.47	1.38	1.35	0.31	0.67

Sample No.	88-46; 107	88-77; 271	88-29; 207	88-30; 381	88-46; 261
Quartz	70.31	59.95	9.79	0.00	0.00
Corundum	0.44	0.21	0.00	0.00	0.00
Zircon	0.00	0.01	0.00	0.01	0.03
Orthoclase	0.32	0.22	6.40	14.50	13.39
Albite	0.00	0.17	4.32	17.69	18.36
Anorthite	4.09	6.82	5.05	34.24	22.32
Nepheline	0.00	0.00	0.00	1.60	0.00
Diopside	0.00	0.00	44.46	11.61	18.34
Hypersthene	17.55	23.54	20.00	0.00	13.44
Olivine	0.00	0.00	0.00	14.97	6.77
Wollastonite	0.00	0.00	0.00	0.00	0.00
Magnetite	2.44	3.55	5.38	2.34	3.08
Calcite	0.03	0.02	0.01	0.01	0.06
Ilmenite	0.19	0.25	0.27	1.46	1.82
Rutile	0.00	0.00	0.00	0.00	0.00
Apatite	0.21	0.43	2.04	0.88	1.48

Sample No.	88-32; 2	88-33; 66	88-36; 66	88-42; 192	88-44; 242
Quartz	0.00	0.00	0.00	0.00	0.00
Corundum	0.96	0.00	1.51	0.00	0.00
Zircon	0.02	0.02	0.02	0.03	0.02
Orthoclase	3.20	2.14	2.67	0.18	12.49
Albite	41.71	10.24	13.96	35.28	21.58
Anorthite	21.12	30.11	26.72	24.17	31.11
Nepheline	0.00	0.00	0.00	0.00	0.00
Diopside	0.00	2.38	0.00	7.62	14.29
Hypersthene	13.51	35.84	41.75	13.12	1.71
Olivine	13.95	0.11	4.62	13.27	11.79
Wollastonite	0.00	0.00	0.00	0.00	0.00
Magnetite	1.97	2.84	2.77	1.97	2.52
Calcite	0.08	0.14	0.11	0.09	0.01
Ilmenite	1.90	3.38	3.82	2.39	2.24
Rutile	0.00	0.00	0.00	0.00	0.00
Apatite	0.98	1.02	1.16	1.31	1.38

(Table 3 Continued)

Sample No.	X-14	X-51	WCU88-20	88-40; 437	88-44; 340
Quartz	0.00	0.00	0.00	0.00	0.00
Corundum	0.00	0.00	0.00	0.00	0.00
Zircon	0.05	0.06	0.02	0.03	0.01
Orthoclase	10.11	19.00	13.25	15.62	0.00
Albite	39.94	26.24	24.20	5.20	0.00
Anorthite	25.08	27.34	31.79	26.33	21.34
Nepheline	0.00	0.27	0.00	14.23	0.00
Diopside	5.58	9.41	6.06	24.11	14.64
Hypersthene	0.26	0.00	0.28	0.00	0.00
Olivine	12.67	8.95	17.24	6.16	44.02
Wollastonite	0.00	0.00	0.00	0.00	0.00
Magnetite	1.45	1.84	2.21	2.62	5.03
Calcite	0.02	0.00	0.01	0.04	0.01
Ilmenite	2.39	4.20	2.45	2.94	1.06
Rutile	0.00	0.00	0.00	0.00	0.00
Apatite	2.17	2.37	1.74	1.85	0.76

CIPW norms (calculated on a water, carbon dioxide, and pyrite free basis. (Fe2O3/FeO=0.15)

Pearce and Cann, 1973; Pearce et al., 1975; Riverin and Hodgson, 1980; Roberts and Reardon, 1978; Robinson, 1984; Winchester and Floyd, 1976).

These elements show distinctive trends that, in most cases where contamination is not severe, allow ocean-floor basalts to be discriminated from most volcanic arc basalts. The general tectonic environments that can be delineated by their geochemical features are: 1) divergent plate margins (ocean-ridge basalt), 2) convergent plate margins (island-arc series), and 3) intraplate settings (ocean-island and continental-rift basalts).

On the Zr-Ti/100-Y*3 diagram (Fig 5a) of Pearce and Cann (1973), most samples fall within the calc-alkaline basalt (CAB) and within-plate basalt (WPB) fields; however, the diagram is not particularly useful in discrimination of the Windy Craggy basalts. On the Zr vs. Ti diagram (Fig. 5b) of Pearce and Cann (1973), samples plot in the calc-alkaline basalt (CAB), ocean floor basalt (OFB), and low K tholeiite (LKT) fields. The data points define a broad linear array that projects toward the origin. Such a trend also occurs on other incompatible element plots (e.g., Zr versus Nb; not shown). These are primary fractionation trends with superposed concentration or dilution of these immobile elements by subtraction or addition of other components. Thus, the ratios between immobile elements have been preserved, but the concentrations of these components have been altered by secondary processes. The implications of this are discussed more fully later. Some scatter in the data could reflect analytical uncertainties and minor elemental mobility.

The Hf-Th-Ta ternary plot of Wood (1980) (Fig. 5c) is extremely useful in discriminating the Windy Craggy basalts because Th is stable up to at least greenschist facies metamorphism, and Th and Ta behave coherently in non subduction-related oceanic basalts and are only decoupled in the subduction environment (Wood, 1980). All of the flow and sill samples plot in the alkaline within-plate basalt (WPB) field, with the exception of a few which plot in the enriched-type mid ocean ridge basalt (E-MORB) field. Dikes that cross-cut mineralization plot in the volcanic-arc basalt (VAB) field. This distinction of dikes from flows and sills is very pronounced on the Ti/100 versus V diagram of Shervais (1982) (Figure 5d), on which flows and sills plot as non-arc derived and are separated from the dikes which plot in the arc field.

This distinction is again expressed on the Zr/4 versus Nb*2 versus Y ternary plot (Figure 5e) of Meschede (1986), in which flows and sills plot in the within-plate alkaline basalt (WPA) fields whereas the dikes fall in the volcanic-arc basalt (VAB) fields. Frey et al. (1978) drew attention to the strong correlation

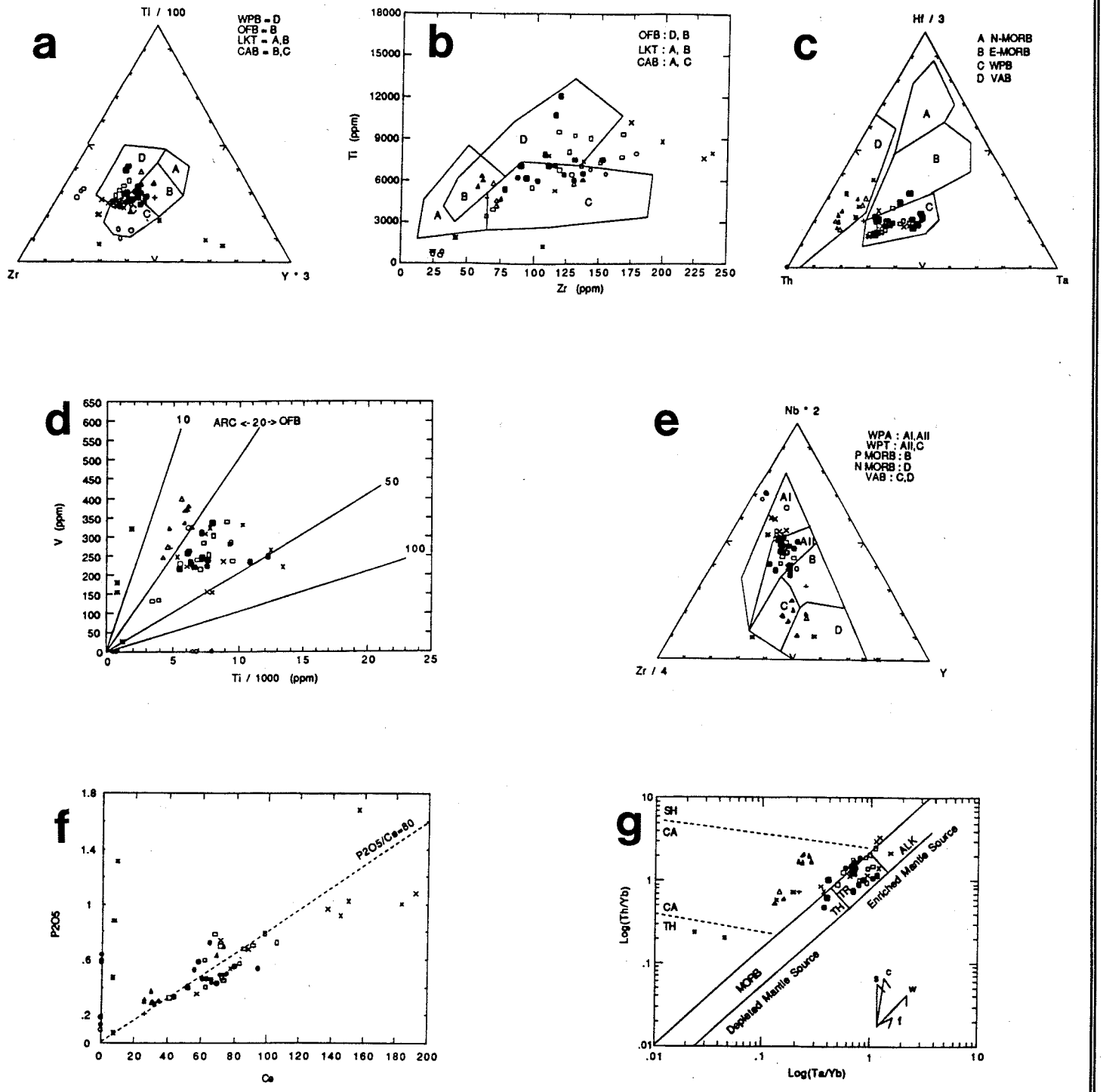

Figure 5. a) Zr versus Ti/100 versus Y*3 diagram of Pearce and Cann (1973); b) Ti/1000 versus Zr plot of Pearce and Cann, (1973) showing ocean floor basalt (OFB), low-K tholeiite (LKT), and calc-alkaline basalt (CAB; c) Hf/3-Th-Ta ternary plot of (Wood, 1980) showing N-MORB (A), E-MORB (B), alkaline, within-plate basalts (C), and destructive plate margin basalts (D) fields; d) Plot of Ti/1000 versus V of (Shervais, 1982) showing arc and ocean floor basalt fields; e) Nb*2-Zr/4-Y ternary plot of (Meschede, 1986) showing within-plate alkaline basalt (WPA), within-plate tholeiite (WPT), plume-type mid-ocean ridge basalt (P-MORB), normal mid-ocean ridge basalt (N-MORB), and volcanic arc basalt (VAB) fields; f) P_2O_5 versus Ce plot; g) Log (Ta/Yb) versus Log (Th/Yb) plot of Pearce (1983) showing distinction between flows and sills and dikes which cross-cut sulphide mineralization. Vectors shown indicate the influence of different components and processes. The former group are derived from enriched mantle sources, whereas the latter show a subduction or crustal contamination influence from a less enriched mantle source. Fields are as follows: TH=tholeiitic, TR=transitional, ALK=alkaline, SHO=shoshonitic, and CA=calc-alkaline. See Figure 4 for explanation of symbols

between P_2O_5 and the light rare earth elements (LREE), as well as the incompatible behavior of P_2O_5 during partial melting, and used P_2O_5 as an index of degree of partial melting. These authors considered a P_2O_5/Ce value of 75 to be typical of primary alkali basalts. On Figure 5f, Windy Craggy flows plot along an estimate line with P_2O_5/Ce ≈80, very close to such a value. The sills have lower P_2O_5/Ce values and may have originated from a different magma.

Figure 5g, a plot of Ta/Yb versus Th/Yb again illustrates the transitional nature of the flows and sills and distinguishes these from the dikes which cross-cut mineralization. The vectors on the diagram illustrate the relative effects of certain processes on the primary geochemical signature.

Figures 6a-g are MORB-normalized geochemical patterns for a selected range of elements. The shape of patterns on such "Pearce" diagrams or "spidergrams" is little affected by differences in partial melting and fractional crystallization histories (Pearce, 1983); therefore, the variations between the patterns are best explained in terms of heterogeneities in the mantle source. The main incompatible element-depleted reservoir of convecting upper mantle is thus thought to yield flat patterns of N-type MORB, whereas the humped patterns are thought to be derived from the incompatible element-enriched portions of this reservoir such as those associated with "mantle plumes" (e.g., Schilling, 1973; Tarney et al., 1980).

It has been argued that such large ion lithophile element (LILE) enrichment can be due to secondary alteration (e.g., Hart et al., 1974; Mitchell and Aumento, 1977). However, Th is one of the few LILE which is relatively immobile during alteration of basalt, and it can be determined with high precision by neutron activation analysis. The good linear correlation passing through the origin on a plot of Zr versus Th (not shown), illustrates the immobility of Th in this study and demonstrates that the Th (and other LILE) enrichments are due to primary magmatic processes.

Figure 6g is in contrast with Figures 6a-f. All figures show the selective enrichment in certain elements (Sr, K, Rb, Ba, Th, Ce, and Sm); however, the figure 6g also shows a relative depletion of Ta, and Nb. This feature has been attributed to the modification of the mantle source region for island-arc basalts by a "subduction component", i.e., by aqueous and siliceous fluids derived from an underlying subduction zone e.g. (Pearce, 1983; Saunders and Tarney, 1979). Thus, the shape of the patterns in Figures 6a-g can be explained in terms of the two components in the mantle source: a "mantle component" which represents the composition of the mantle prior to subduction and the subduction component which causes an additional selective enrichment in elements that are in high concentration in the fluids derived from the subduction zone.

Figure 7 shows chondrite normalized rare earth element (REE) abundance patterns. The samples have moderate to steep REE patterns with significant variation in the extent of light rare earth element (LREE) enrichment ((La/Yb)n = 7.1 to 25.4). Most of the REE patterns are characteristically parallel between La and Sm, but the slopes vary slightly between the different groups. This is illustrated by the average (La/Sm)n ratios and their standard deviations (hanging wall flows: 5.71±3.67; n=12, footwall flows: 3.87±0.87; n=15, footwall sills: 4.59±0.85; n=11, dikes in sulphide: 1.99±0.31; n=9, cumulates: 2.34±1.22; n=4). The ratio for dikes which cross-cut sulphide mineralization is significantly lower than all other groups. Many of the samples show a slightly positive or negative Eu anomaly, but the magnitude of this anomaly is within the analytical error for Eu (±10%) and does not necessarily indicate plagioclase accumulation or removal, respectively.

The cause of LILE and LREE enrichment may be an enriched (i.e., undepleted) mantle source (for example, oceanic island basalt; Morris and Hart, 1983), variation in degree of partial melting, fluids derived from the subducted slab, sediments from the subducted slab incorporated into the source, and crustal assimilation.

The variation in heavy rare earth element (HREE) abundances is relatively small. Average chondrite-normalized values for Yb are: hanging wall flows: 6.9±1.6; n=12, footwall flows: 6.8±0.9; n=15, footwall sills: 10.0±1.9; n=11, dikes in sulphide: 5.9±1.2; n=9, cumulates: 6.6±1.3; n=4. The small variations in HREE and low Yb values suggest that the effect of crystal fractionation on the REE abundances of the samples is small. For some samples, there is also a tendency for the HREE portion of the pattern, from Tb to Yb, to cross over. These characteristics of the HREE pattern suggest that garnet was residual in the mantle source during initial generation of the basalt melts.

Implications for Tectonic Setting of the Windy Craggy deposit:

Transitional to alkaline volcanics from the submerged parts of ocean basins have been described by several investigators (e.g., Aumento, 1968; Bonatti et al., 1971; Melson et al., 1967; Frey, 1970; Batiza, 1977; Stebbins and Thompson, 1978). De Long (1975) noted that sodic alkaline lavas occur at specific sites in arc

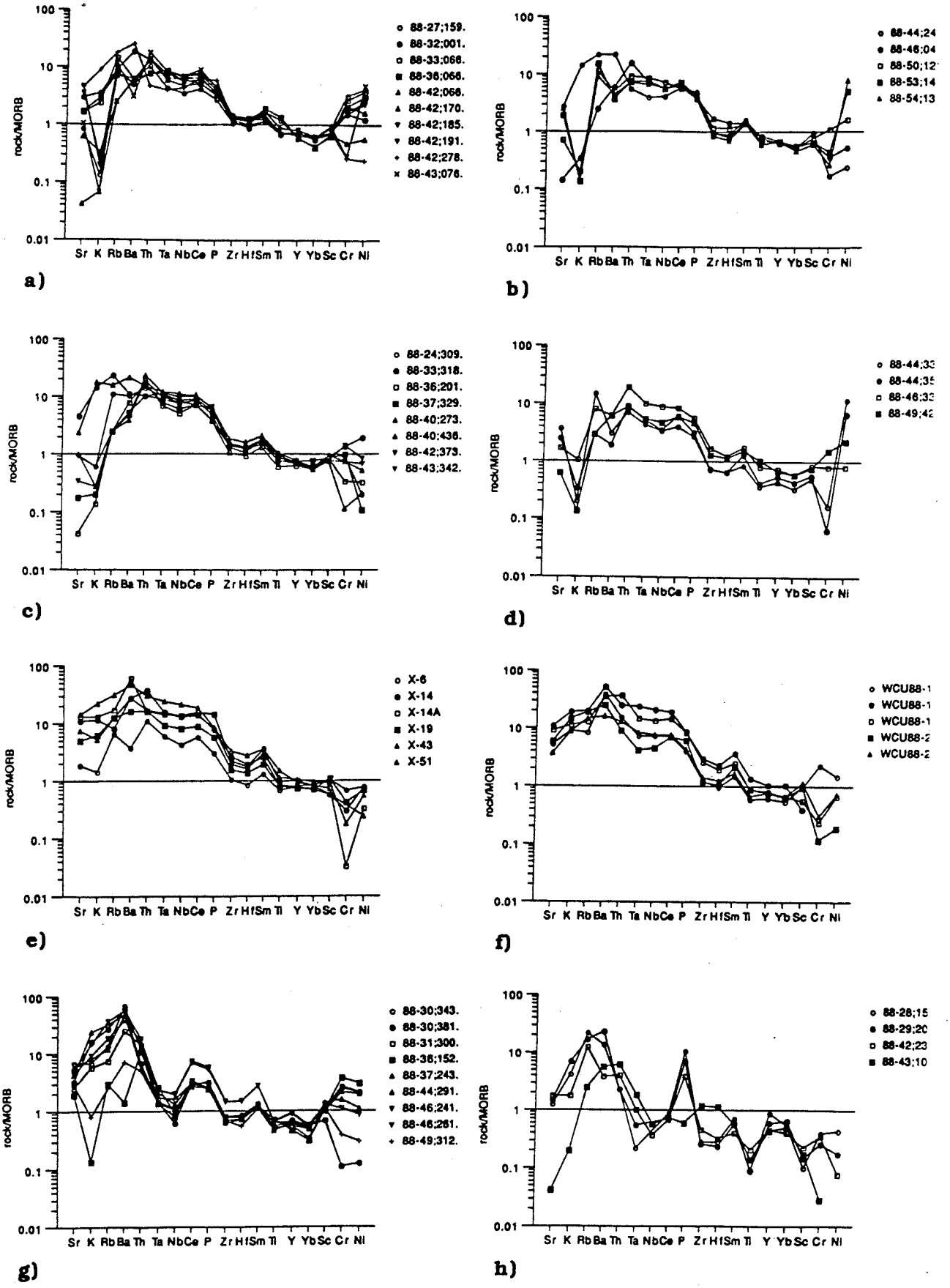

Figure 6. Spidergram of igneous host rocks normalized to MORB (Pearce, 1983). a) and b) footwall flows; c) and d) hanging wall flows; e) and f) footwall sills; g) dikes cross-cutting mineralization; h) cumulates. Note theTa and Nb troughs in patterns for dikes (g) within sulphide mineralization; these are characteristic of arc-related (subduction zone) magmas. Other basalts do not show this feature.

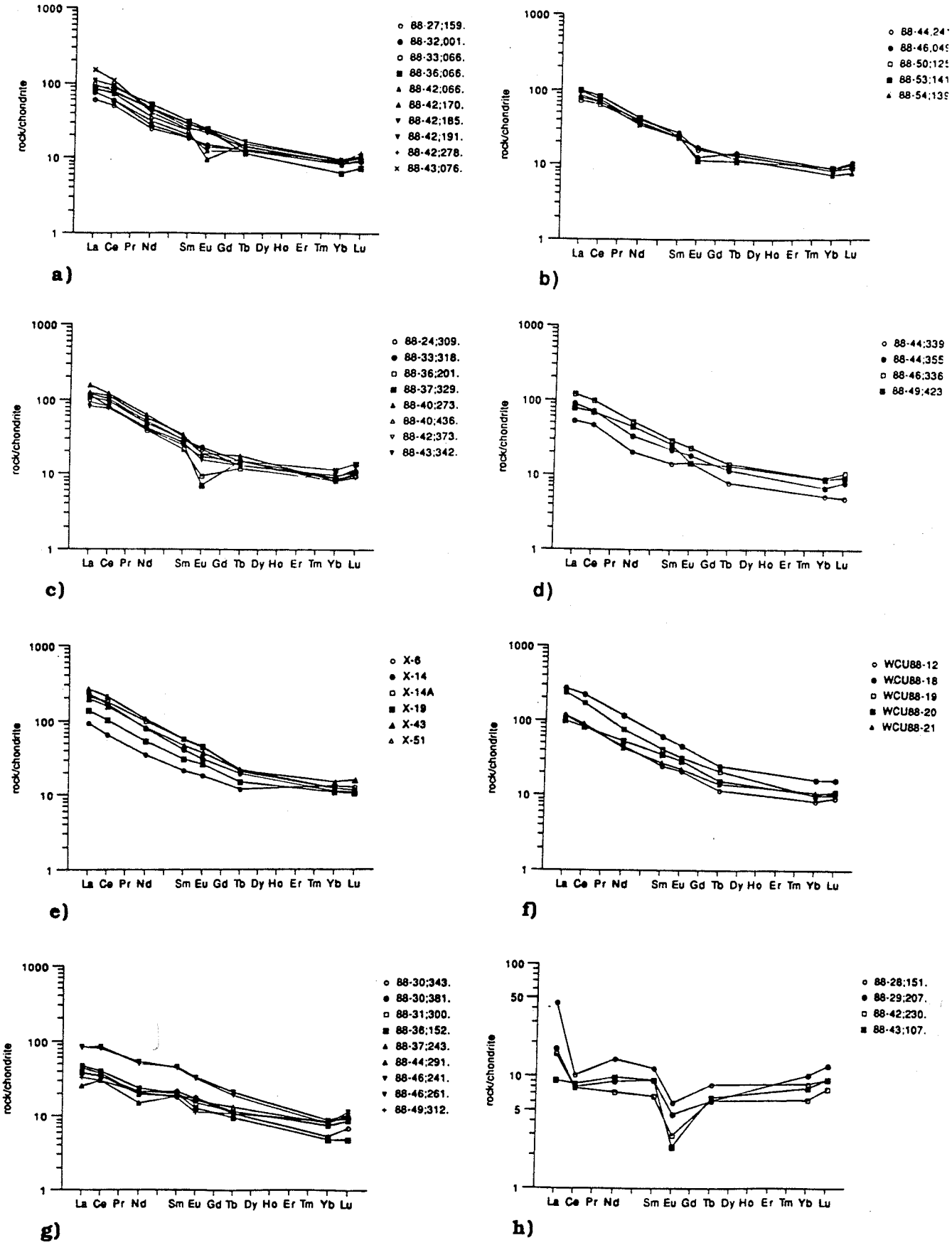

Figure 7. Chondrite normalized rare earth element plot for igneous host rocks of the Windy Craggy deposit. Normalizing values are from Nakamura (1974). a) and b) footwall flows; c) and d) hanging wall flows; e) and f) footwall sills; g) dikes cross-cutting mineralization; h) cummulates. Note the Ta and Nb troughs in patterns for dikes (g) within sulphide mineralization

systems, e.g., along lateral edges of subduction zones, or where a fracture zone perpendicular to the trench is being subducted. Similar anomalous magmas have been found close to continents during the initial stages of back arc spreading or back arc rifting, e.g., Penguin Island (Weaver et al., 1979) and in southern Chile (Saunders et al., 1979). The Pearce spidergrams (Fig. 6) show that the footwall and hanging wall flows and the footwall sills are somewhat similar to back-arc basalts. However, the Windy Craggy rocks, with their higher Ta and Nb contents, show a closer affinity with intraplate basalts.

Most igneous rocks recovered from the floors of back-arc basins are basaltic in composition, usually olivine- (more rarely nepheline- or quartz-normative) tholeiites, and are virtually indistinguishable from ocean ridge tholeiites on the basis of their mineralogy and major element geochemistry (e.g., Hart et al., 1972; Hawkins, 1976, 1977; Saunders and Tarney, 1979; Wood et al., 1981; Mattey et al., 1980; Marsh et al., 1980).

Relative enrichments in K, Rb, Sr, Ba, LREE, CO_2, and Cl have been documented in some back arc basin basalts (Hart et al., 1972; Gill, 1976; Saunders and Tarney, 1979; Tarney et al., 1977; Garcia et al., 1979; Muenow et al., 1980; Fryer, 1981; Wood et al., 1981). Fryer (1981) suggested that such volatile and other incompatible element-enriched lavas represent a distinct magma type characteristic of back arc basins and referred to this type as back arc basin basalt (BABB). More recently, Hawkins and Melchior (1985), Sinton et al. (1986), and Sinton and Fryer (1987) documented a spectrum of compositions from N-MORB to variably enriched BABB and other lava types in the Lau, North Fiji, and Manus back arc basins.

Several authors have pointed out the variable chemistry of back-arc basin basalt (BABB), and have proposed that variability is due to different degrees of partial melting, heterogeneity of the mantle source, and high-level crystal fractionation in addition to a variable influence of fluids derived from the subducting plate. It has been suggested that the influence of subduction zone fluids should be greatest during the early stages of basin opening, and that this influence lessens as the basin widens (Tarney et al., 1977).

The variation in chemistry of basalts in back-arc marginal basins or spreading centres is so great (e.g., Saunders and Tarney, 1984; Tarney and Windley, 1981) that it is hazardous to designate them as marginal basin or back-arc rocks on their chemistry alone. Moores (1982) has suggested that the type of sedimentary sequences overlying submarine volcanic rocks may allow back-arc spreading volcanic rocks to be distinguished from those generated at mid-ocean ridges. He suggested that in a back-arc basin setting volcanics might typically be overlain by volcaniclastic sequences, whereas mid-ocean ridge volcanics would typically be overlain by deep-sea pelagic sediments which would tend to indicate an open ocean environment. Additionally, the abundance of sediments is more likely to occur during the initial stages of back-arc rifting when the juvenile basin will be subjected to sediment influx from the immediately adjacent arc or continental margin.

MacIntyre (1986) favoured a back-arc basin formed in continental crust as the tectonic setting for the host rocks and mineralization in the Windy Craggy area. Dawson (1990), this volume) suggests that the Upper Triassic Windy Craggy host rocks formed as a result of epicontinental rifting subsequent to amalgamation with Wrangellia in Carboniferous time, and prior to collision between the Insular Superterrane and North America in Cretaceous time. He based this conclusion, in part, on the presence of adjacent miogeoclinal sediments, the progression from tholeiitic to calc-alkaline volcanics, and the presence of turbiditic clastics. The geochemical data presented herein cannot, alone, unequivocally distinguish between these possibilities, and both are considered tenable

The dikes which cross-cut mineralization are not volumetrically important within the immediate deposit area, although they may be important within rocks that are stratigraphically above the Windy Craggy deposit. These dikes relate to subduction processes that post-date the formation of the footwall and hanging wall basalts and the deposit itself.

Geochemistry of Hydrothermal Alteration Associated with Mineralization:

Within the recognizable stockwork/feeder zone, plagioclase has been partly to completely replaced by quartz and/or sulphides. Chemical alteration has been moderately intense, as evidenced by water content, which ranges from 1.9 to 8.6% and the highly variable CO_2 contents of some samples which range from 0 to 21.6%. However, some of this may be due to regional metamorphism. Therefore, in order to evaluate the relative gains and losses of elements due to the effects of hydrothermal alteration associated with mineralization, analyses of samples from the chloritic and silicified parts of the feeder/stockwork zone have been normalized to basalt that is distant from the stockwork zone. The results of this normalizing procedure for selected elements is shown in Fig. 8. The normalizing composition was obtained by using mean element

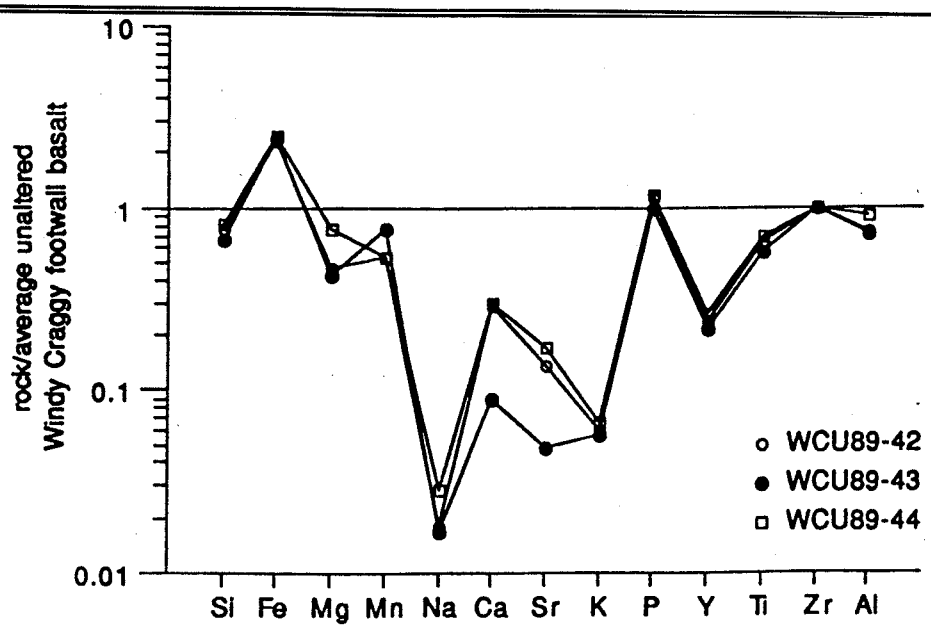

a)

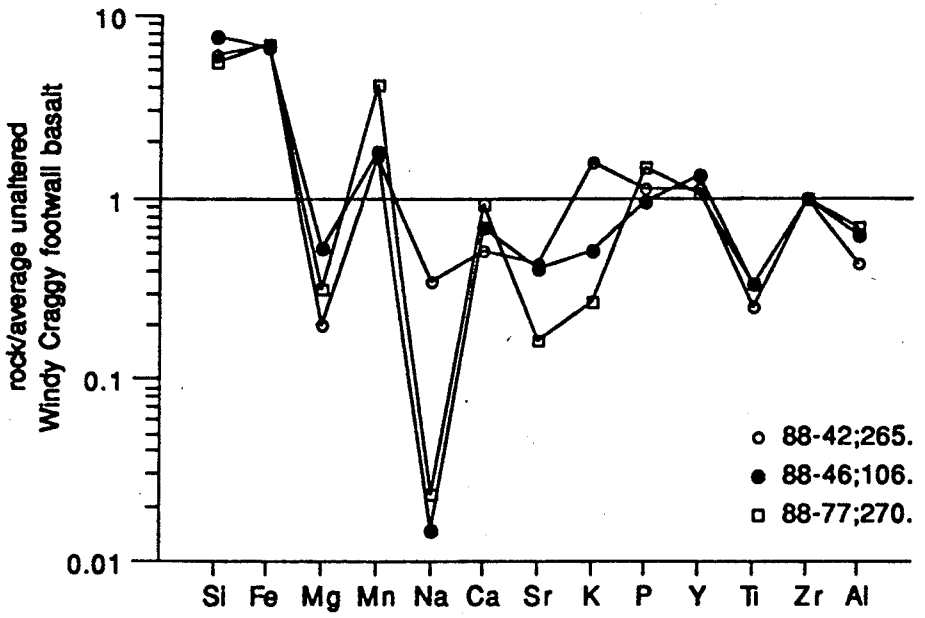

b)

Figure 8 Spidergrams showing gains and losses of altered basalts from the chloritic (a) and silicified (b) portions of the stockwork/feeder zone. Samples have been normalized to average unaltered footwall basalt (n=5; 88-32;001.5, 88-33;066.4, 88-36;066.3, 88-42;185.9, and 88-42;191.6) and doubly normalized to the Zr content of this unaltered footwall basalt

values for 5 samples of footwall basalt. In these figures, samples have been doubly normalized to a common Zr content, based on the assumption that this element was not mobilized. This double normalization is an attempt to correct for apparent enrichments or depletions that are caused by volume or density changes and dilution effects attendant with alteration.

Within the chloritic part of the stockwork zone there is a moderate degree of Fe enrichment and a slight Mg depletion. Strong depletions of Na, Ca, Sr, and K are also noted. Slight depletions in Si, Mn, Y, and Ti are evident, but these may be the result of different degrees of fractionation between the normalizing standard and the samples; any calculation for which it is necessary to designate a parent-daughter relationship between samples is fraught with problems, and thus the observed mobility of these latter elements could simply result from an inappropriate choice of a parental composition (e.g., Roberts and Reardon, 1978).

Within the silicified portion of the stockwork zone there is a strong enrichment in Si, Fe, and Mn. This is due to the introduction of fine-grained quartz , iron chlorite, and iron sulphides. The Mn enrichment is likely due to its presence in the chlorite. A strong depletion of Na and moderate variable depletions of Ca, Sr, K, Ti, and Al are also noted. Previous studies have also documented the mobility of Al_2O_3 during alteration associated with volcanogenic mineralization (e.g., Larson, 1984; Wynne and Strong, 1984). P is not appreciably mobilized in either the chloritic or silicified rocks.

Figure 9a is a rare earth element plot of chloritized rocks from the stockwork zone normalized to the REE values for average Windy Craggy footwall basalt discussed above. This figure shows that within the chloritized rocks, the REE have not been mobilized to any degree and display primary magmatic abundances. However, a similar plot for the silicified stockwork zone rocks (Fig. 9b) reveals that all REE (including the HREE) have been mobilized, with the LREE displaying greater mobility than the HREE.

This observation is in keeping with the data of Michard et al. (1983), who analyzed hydrothermal vent fluids from the 13°N, East Pacific Rise sulphide deposit and noted that these solutions were very enriched in LREE. Based on their analyses of fluid and basalt from this site, Michard et al. (1983) suggested that in order for significant amounts of REE to be driven off from the basalt during hydrothermal alteration, extremely large water/rock ratios (W/R) are required. Furthermore, variations in hydrothermal fluid (modified seawater)/rock ratios are known to influence greatly the alteration assemblages during high temperature interaction between seawater and basalt (Mottl, 1983). Low (W/R) results in chlorite and albite dominated rocks and high W/R produces chlorite-quartz assemblages. Therefore, the abundance of quartz in the silicified rocks is also suggestive of high W/R.

End member (i.e., no entrained ambient seawater is mixed with the fluid) hydrothermal vent fluids associated with modern sea floor sulphide deposits are characterized by a conspicuous absence of Mg (Edmond et al., 1979; Von Damm et al., 1985). The depletion of Mg in the Windy Craggy stockwork zone indicates that this upflow zone may have formed from Mg-poor fluids similar in composition to those sampled at modern sea floor sulphide deposits, and that Mg was deposited elsewhere in the hydrothermal system (i.e., in the recharge zone).

Lead Isotope Geochemistry of Sulphides:

Lead isotope ratios of sulphide minerals can aid in identifying the source of Pb and associated metals in ore deposits and may be a useful criterion for comparison of modern and ancient analogues. Lead was extracted from the sulphides by leaching 20 to 30 mg. of hand-picked, crushed sulphide with a mixture of concentrated HCl and HNO_3. Lead isotope analyses were performed on a conventional 90°, 30 cm radius mass spectrometer in the Department of Physics at the University of Toronto. Lead ions were produced using the standard Re filament, silica gel-phosphoric acid technique of Cameron et al.(1969). The data, shown in Table 4, represent averages of 20-30 scans of the lead mass spectrum, corrected for mass fractionation of 0.145% per mass unit based on replicate analyses of lead standard SRM-981.

Figure 10 is a $^{207}Pb/^{204}Pb$ vs. $^{206}Pb/^{204}Pb$ diagram for Windy Craggy bulk sulphides. For comparison, the lead isotopic composition of modern basalt (Church and Tatsumoto, 1975; Brevart et al., 1981; Vidal and Clauer, 1981) and pelagic sediment (Reynolds and Sinclair, 1971; Church, 1976; Meijer, 1976; Sun, 1980; Vidal and Clauer, 1981) as well as sulphides from Besshi-type deposits of Japan (Sato and Sasaki, 1980) are also shown. Volcanogenic massive sulphides typically have $^{238}U/^{204}Pb$ ratios less than 0.1 (e.g., Roddick, 1984), and a simple calculation indicates that changes in the isotopic ratios $^{207}Pb/^{204}Pb$ and $^{206}Pb/^{204}Pb$ over a period of approximately 220 Ma. are much less than the analytical uncertainties in our data.

The data in Figure 10 define a linear trend extending from the field for MORB to that for pelagic

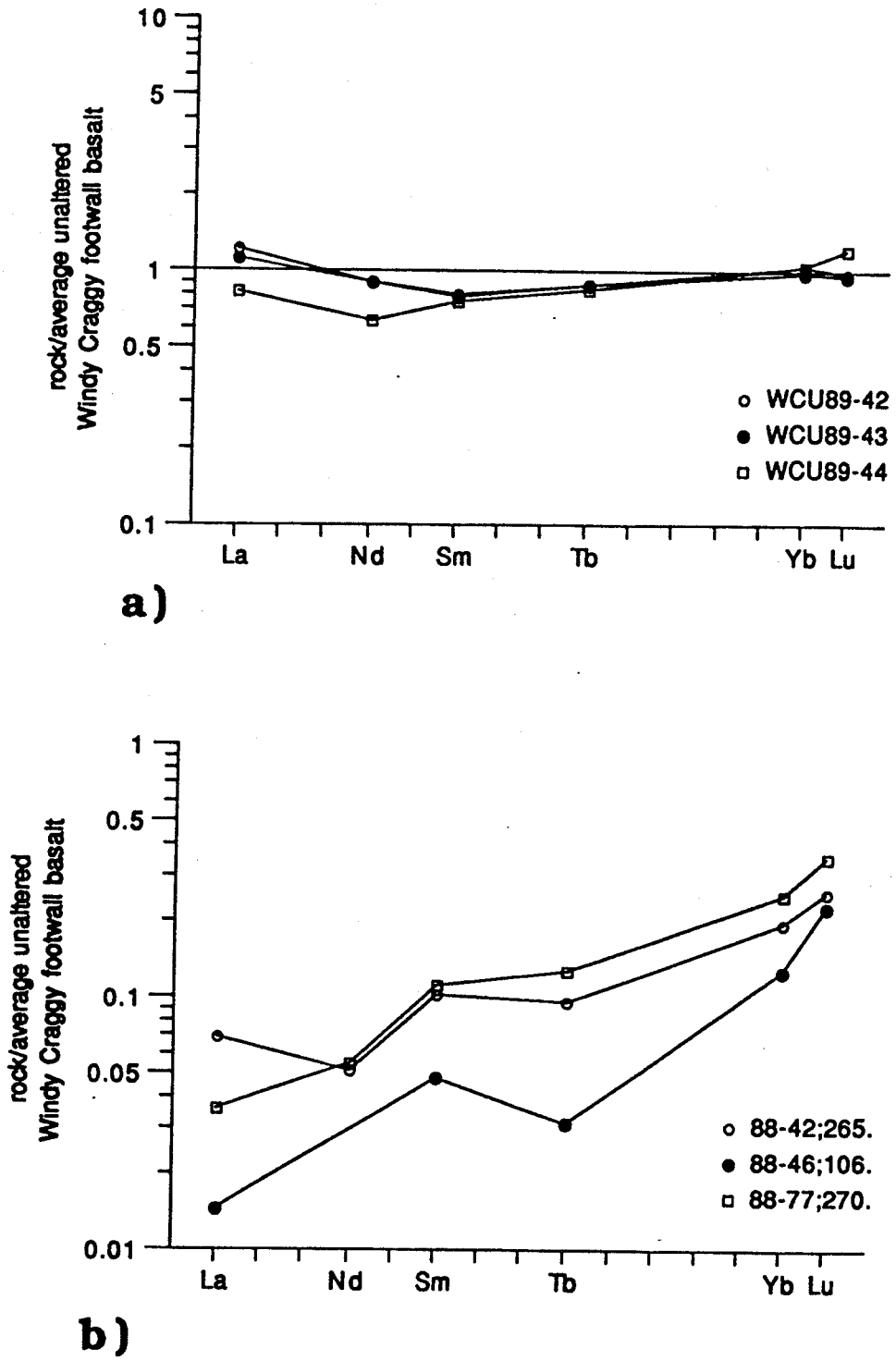

Figure 9. Rare earth element plot of rocks from a) the chloritic part of the stockwork zone and b) the silicified part of the stockwork zone. Normalizing values are average unaltered Windy Craggy footwall basalt - see caption for Figure 8

Table 4. Lead isotopic composition of Windy Craggy sulphides.

Sample No.	$^{206}Pb/^{204}Pb$	$^{207}Pb/204Pb$	$^{208}Pb/^{204}Pb$
88-36;370.8M[a]	18.705	15.599	38.263
88-46;103.4M[b]	18.600	15.504	37.891
88-75;317.3M[c]	18.762	15.628	38.344
DDH11;1669FT[d]*	18.703	15.573	38.285
DDH11;1691FT[e]*	18.703	15.579	38.306

[a]finely laminated chert-sulphide (pyrrhotite, pyrite, and chalcopyrite)-carbonate ("exhalite").

[b]pyrrhotite-chalcopyrite-quartz veinlet in bleached and silicified mafic volcanic ("silicified stockwork zone").

[c]fine grained pyrrhotite and pyrite with blebs of dark, iron-rich sphalerite (massive sulphide zone).

[d]rounded clasts of chalcopyrite and pyrite in matrix of pyrrhotite, sphalerite, and iron carbonate.

[e]large angular clasts of pyrite with interstitial and vein chalcopyrite in sphalerite-iron carbonate-pyrrhotite matrix.

*analyzed by Geospec Consultants.

marine sediments. This trend is interpreted as resulting from the mixing of lead from a mantle source (the footwall basalts) with that of an upper crustal end member (the terrigenous sediments intercalated with the footwall basalts). It is interesting to note that the least radiogenic analysis (sample 88-46;103.4) is from sulphides within silicified stockwork in mafic volcanics. However, we stress that these are only preliminary results, and further work is in progress.

Thus, a significant fraction of the Pb in the Windy Craggy sulphides was derived from a sedimentary source. This is consistent with observations that significant proportions of stockwork mineralization and alteration are developed within bedded argillite in the North Sulphide Body. Therefore, the hydrothermal fluids from which the sulphides were precipitated have interacted with sediments prior to discharge onto the paleo-ocean floor.

Conclusions:

The Windy Craggy deposit is an unusually large (world class) deposit formed within both volcanic and sedimentary host rocks. The deposit consists of two or more massive sulphide lenses, each with a stockwork/feeder zone which cross-cuts both the

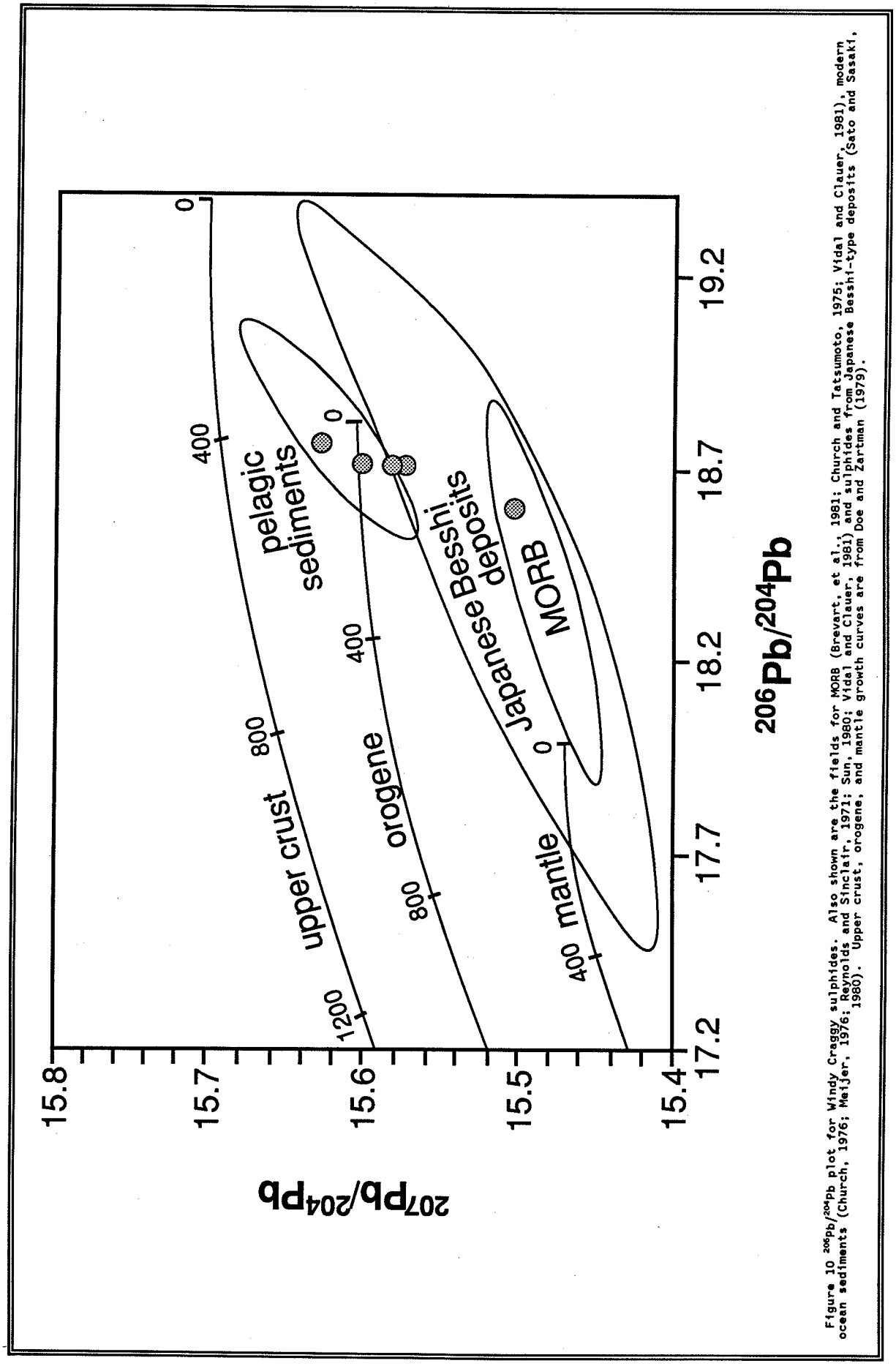

Figure 10 $^{206}Pb/^{204}Pb$ plot for Windy Craggy sulphides. Also shown are the fields for MORB (Brevart, et al., 1981; Church and Tatsumoto, 1975; Vidal and Clauer, 1981), modern ocean sediments (Church, 1976; Maijer, 1976; Reynolds and Sinclair, 1971; Sun, 1980; Vidal and Clauer, 1981) and sulphides from Japanese Besshi-type deposits (Sato and Sasaki, 1980). Upper crust, orogene, and mantle growth curves are from Doe and Zartman (1979).

volcanic and sedimentary rocks. Principal "ore" minerals include pyrrhotite, pyrite, chalcopyrite, and magnetite, with lesser digenite, sphalerite, and rare gold, electrum, marcasite, and arsenopyrite.

Although the host rocks have been altered to greenschist facies, their incompatible element and REE chemistry allows their primary affinity to be determined. Footwall and hanging wall volcanic flows are geochemically related to footwall sills. Dikes which cross-cut mineralization are geochemically distinct from these units and are, therefore, not cogenetic. The geochemical characteristics and geological relationships suggest that the Windy Craggy host basalts formed in a rift setting from an undepleted mantle source. The footwall and hanging wall flows and sills do not show any typical subduction zone geochemical signature, whereas the later dikes which cross-cut mineralization do show such an "arc" signature. Possible tectonic settings include either a back-arc basin or rifted continental margin/shelf setting. Within the recognizable stockwork alteration zone, volcanic rocks have been intensely chloritized and silicified. During silicification of these volcanic rocks, rare earth elements have been completely mobilized (leached). However, such REE mobility has occurred to only a limited extent within the chloritized parts of the stockwork zone. Lead isotope geochemistry of the sulphides indicates that a variable but significant portion of the lead (and presumably other metals) was derived from the footwall sedimentary rocks in addition to lead derived from volcanic rocks.

Acknowledgements:

We thank Geddes Resources Ltd. for generously providing free access to the deposit and for providing logistical support. In particular, we thank N.J. Callan, B. Downing, G. Harper, J.D. Little, G. Webster, M.P. Webster of Geddes Resources Ltd. and R.J. Beckett of Beckett Geological Services for discussion and ideas. However, we remain responsible for all interpretations and conclusions presented. We thank M.P. Gorton for assistance with neutron activation analysis and trace element geochemistry. The assistance of P.E. Smith and R. Farquhar with lead isotope analyses is greatly appreciated. Kenneth Dawson of the Geological Survey of Canada, Vancouver kindly provided two unpublished lead isotope analyses. The British Columbia Ministry of Energy, Mines and Petroleum Resources are thanked for generously providing a contract supporting initial research at Windy Craggy. Continuing research is supported by the Natural Sciences and Engineering Research Council of Canada.

References

Aumento, F., 1968, The Mid-Atlantic ridge near 45N. II. Basalts from the area of Confederation Peak: Can. Jour. Earth Sci., v. 5, p. 1-21.

Bamba, T. and Motoyoshi, Y., 1985, Study on massive sulfide ores from the Shimokawa mine, Hokkaido, Japan: Min. Geol., v. 35, p. 211-225.

Barnes, S. J. and Gorton, M. P., 1984, Trace element analysis by neutron activation with a low flux reactor (Slowpoke-II): results for international reference rocks: Geostandard Newsletter, v. 8, p. 17-23.

Batiza, R. 1977, Age, volume, compositional and spatial relations of small isolated oceanic central volcanoes: Mar. Geol., v. 24, p. 169-183.

Berg, H. C., 1979, Significance of Geotectonics in the Metallogenesis and Resource Appraisal of Southeastern Alaska: A Progress Report, The United States Geological Survey in Alaska: Accomplishments During 1978, Circular 804-B, U.S.G.S., pp. B116-B118.

Bonatti, E., Honnorez, J. and Ferrara, G., 1971, Peridotite-gabbro-basalt complex from the equatorial Mid-Atlantic Ridge: Phil. Trans. R. Soc. Lond., v. A268, p. 385-402.

Brevart, O., Dupre, B. and Allegre, C. J., 1981, Metallogenesis at spreading centers: lead isotope systematics for sulfides, manganese-rich crusts, basalts, and sediments from the CYAMEX and ALVIN areas: Econ. Geol., p. 1205-1210.

Buchan, R. 1984, Reconnaissance Petrographic Examination and Photomicrography of 18 samples from Windy Craggy, B.C. Falconbridge Metallurgical Laboratories unpublished report.

Cameron, A. E., Smith, D. E. and Walker, R. L., 1969, Mass spectrometry of nanogram size samples of lead: Anal. Chem., v. 41, p. 525-526.

Campbell, I. H., Lesher, C. M., Coad, P., Franklin, J. M., Gorton, M. P. and Thurston, P. C., 1984, Rare-earth element mobility in alteration pipes below massive Cu-Zn sulfide deposits: Chem. Geol., v. 45, p. 181-202.

Campbell, R. B., and Dodds, C. J., 1979, Operation Saint Elias, British Columbia: Geological Survey of Canada, Current Research, p. 17-20.

Campbell, R. B. and Dodds, C. J. 1983, Geology of Tatshenshini River Map Area (114P), British Columbia. Geological Survey of Canada.

Church, S. E. 1976, The Cascade Mountains revisited: a re-evaluation in light of new lead isotope data: Earth Planet. Sci. Lett., v. 29, p. 175-188.

Church, S. E. and Tatsumoto, M., 1975, Lead isotope relations in oceanic ridge basalts from the Juan de Fuca-Gorda Ridge area, N.E. Pacific Ocean: Contrib. Mineral. Petrol., v. 53, p. 253-279.

Clarke, D., 1989, NEWPET computer program. Memorial University of Newfoundland.

Costa, U. R., Barnett, R. L. and Kerrich, R., 1983, The Mattagami Lake Mine Archean Zn-Cu sulfide deposit, Quebec: hydrothermal coprecipitation of talc and sulfides in a sea-floor brine pool-evidence from geochemistry, $^{18}O/^{16}O$, and mineral chemistry: Econ. Geol., v. 78, p. 1144-1203.

Dawson, K., 1990, Regional Geological Setting of Selected Mineral Deposits of the Nortthern Cordillera. IAGOD Ottawa Guidebook #14, p. 1-24.

DeLong, S.E., Hodges, F.N. and Arculus, R.J., 1975, Ultramafic and mafic inclusions, Kanaga Island, Alaska, and the occurrence of alkaline rocks in island arcs: Jour. Geol., v. 83, p. 721-736.

Doe, B. R., and Zartman, R. E., 1979, Plumbotectonics I, the Phanerozoic, in Barnes, H. L., Geochemistry of Hydrothermal Ore Deposits: New York, John Wiley and Sons Publ., p. 22-69.

Downing, B. W., Webster, M. P. and Beckett, R. J., 1990, The Windy Craggy massive-sulphide deposit, northwestern British Columbia, Canada, IAGOD, Ottawa, Guidebook #14 p. 25-30.

Edmond, J. M., Measures, C., McDuff, R. E., Chan, L. H., Collier, R. and Grant, B., 1979, Ridge crest hydrothermal activity and the balances of the major and minor elements in the ocean: the Galapagos data: Earth Planet. Sci. Lett., v. 46, p. 1-19.

Finlow-Bates, T., and Stumpfl, E. F., 1981, The behavior of so-called immobile elements in hydrothermally altered rocks associated with volcanogenic submarin-exhalative ore deposits: Mineral. Dep., v. 16, p. 319-328.

Floyd, B. A., and Winchester, J. A., 1978, Identification and discrimination of altered and metamorphosed volcanic rocks using immobile elements: Chem. Geol., v. 21, p. 291-306.

Frey, F.A., 1970, Rare earth and potassium abundances in St. Paul's rocks: Earth Planet. Sci. Lett., v.7 p.351-360.

Frey, F.A., Green, D.H. and Roy, S.D., 1978, Integrated models of basalt petrogenesis: a study of quartz tholeiites and olivine melilites from south eastern Australia utilizing geochemical and experimental petrological data, Jour. Petrol., v. 19, p. 463-513.

Fryer, P. 1981 Petrogensis of basaltic rocks from the Mariana Trough, PhD. Thesis, University of Hawaii, Honolulu, 157 p.

Gammon, J. B. and Chandler, T. E., 1986, Exploration of the Windy Craggy Massive Sulphide Deposit, British Columbia, Geology in the Real World - The Kingsley Dunham Volume: IMM, p. 131-141.

Garcia, M. O., 1978, Criteria for the identification of ancient volcanic arcs: Earth Sci. Rev., v. 14, p. 147-165.

Garcia, M. O., Liu, N. K. W. and Muenow, D. W., 1979, Volatiles in submarine volcanic rocks from the Mariana island arc and trough: Geochim. Cosmochim. Acta, v. 43, p. 305-312.

Gasparrini, C., 1983, Study of the Gold, Silver, and Cobalt Distribution in Two Samples of Core from the Windy Craggy Deposit. unpublished report, Geddes Resources Ltd.

Gibson, H. L., Watkinson, D. H. and Comba, C. D. A., 1983, Silicification: Hydrothermal Alteration in an Archean Geothermal System within the Amulet Rhyolite Formation, Noranda, Quebec: v. 78, p. 954-971.

Gill, J. B., 1976, Composition and age of Lau Basin and Ridge volcanic rocks: implications for evolution of an interarc basin and remnant arc: Geol. Soc. Amer. Bull., v. 87, p. 1384-1395.

Hall, B. V., 1982, Geochemistry of the alteration pipe at the Amulet Upper A deposit, Noranda, Quebec: Can. Jour. Earth Sci., v. 19, p. 2060-2084.

Harris, J. F. 1988, Petrographic Study of Rocks from the Windy Craggy Area, Atlin Mining District, B.C., unpublished report, Geddes Resources Ltd.

Hart, S. R., Glassley, W. E. and Karig, D. E., 1972, Basalts and sea floor spreading behind the Mariana Island arc: Earth Planet. Sci. Lett., v. 15, p. 12-18.

Hart, S. R., Erlank, A. J. and Kable, E. J. D., 1974, Sea floor basalt alteration: some chemical and Sr isotopic effects: Contrib. Mineral. Petrol., v. 44, p. 219-230.

Hawkins, J. W., Jr., 1976, Petrology and geochemistry of basaltic rocks of the Lau Basin: Earth Planet. Sci. Lett., v. 28, p. 283-297.

Hawkins, J. W., Jr., 1977, Petrologic and geochemical characteristics of marginal basin basalts, in Talwani, M., and Pittman, W. C., Island arcs, deep sea trenches and back-arc basins: American Geophysical Union, p. 355-365.

Hawkins, J. W., and Melchior, J., 1985, Petrology of Mariana Trough and Lau Basin basalts: Jour. Geophys. Res., v. 90, p. 11431-11468.

Hillhouse, J. W. and Gromme, C. S., 1980, Paleomagnetism of the Triassic Hound Island volcanics, Alexander Terrane, southeastern Alaska; Jour. Geophys. Res., v. 85, p. 2594-2602.

Irvine, T. N. and Baragar, W. R. A., 1971, a guide to the chemical classification of the common volcanic rocks: Can. Jour. Earth Sci., v. 8, p. 523-548.

Kalogeropoulos, S. I. and Scott, S. D., 1983, Mineralogy and Geochemistry of Tuffaceous Exhalites (Tetsusekiei) of the Fukazawa Mine, Hokuroku District, Japan: Econ. Geol. Mon. 5, p. 412-432.

Kalogeropoulos, S. I., and Scott, S. D., 1986, Mineralogy and geochemistry of an Archean tuffaceous exhalite: the Main Contact Tuff, Millenbach mine area, Noranda, Quebec: Can. Jour. Earth Sci., v. 26, p. 88-105.

Kase, K. and Yamamoto, M., 1988, Minerals and geochemical characteristics of ores from the Besshi-type deposits in the Sanbagawa belt, Japan: Min. Geol., v. 38, p. 203-214.

Kelsey, C. H., 1965, Calculation of the C.I.P.W. norm: Min. Mag., v. 34, p. 276-282.

Larson, P. B., 1984, Geochemistry of the alteration pipe at the Bruce Cu-Zn volcanogenic massive sulfide deposit, Arizona.: Econ. Geol., v. 79, p. 1880-1896.

MacGeehan, P. J. and MacLean, W. H., 1980a, Tholeiitic basalt-rhyolite magmatism and massive sulfide deposits at Matagami, Quebec: Nature, v. 283, p. 153-157.

MacGeehan, P. J. and MacLean, W. H., 1980b, An Archean sub-seafloor geothermal system, "calc-alkali" trends, and massive sulfide genesis: Nature, v. 286, p. 767-771.

MacIntyre, D. G., 1983, A comparison of stratiform massive sulphide deposits of the Gataga District with the Midway and Windy Craggy Deposits, Northern British Columbia: B.C. Ministry of Energy, Mines and Petroleum Resources, Paper 1983-1, p. 149-170.

MacIntyre, D. G., 1984, Geology of the Alsek-Tatshenshini Rivers Area (114P): B.C. Ministry of Energy, Mines and Petroleum Resources, Paper 1984-1, p. 173-184.

MacIntyre, D. G., 1986, The geochemistry of basalts hosting massive sulphide deposits, Alexander Terrane, Northwest British Columbia: B.C. Ministry of Energy, Mines and Petroleum Resources, Paper 1987-1, p. 197-210.

MacLean, W. H. and Kranidiotis, P., 1987, Immobile elements as monitors of mass transfer in hydrothermal alteration: Phelps Dodge massive sulfide deposits, Matagami, Quebec: Econ. Geol., v. 82, p. 951-962.

Maeda, H., Ito, Y., Aragane, T. and Sato, J., 1981, Modes of occurrence and properties of electrum from the Shimokawa cupriferous iron sulphide deposits-in comparison with those from the Kuroko deposits: Min. Geol., v. 10, p. 193-202.

Mainwaring, P. R., 1983, Initial mineralogical characterization of the Windy Craggy Cu-Co deposit, British Columbia. unpublished report, CANMET, Ottawa.

Marsh, N. G., Saunders, A. D., Tarney, J. and Dick, H. J. B., 1980, Geochemistry of basalts from the Shikoku and Daito Basins, Deep Sea Drilling Project Leg 58, in DeVries Klein, G., Kobayashi, K., et al., Initial Reports of the Deep Sea Drilling Project Leg 58: Washington, D.C., U.S. Government Printing Office, p. 805-842.

Mattey, D. P., Marsh, N. G. and Tarney, J., 1980, The geochemistry, mineralogy and petrology of basalts from the West Philippine and Parece Vela Basins and from the Palau-Kyushu and West Mariana Ridges, Deep Sea Drilling Project Leg 58, in Kroenke, L., and Scott, R., Initial Reports of the Deep Sea Drilling Project Leg 59: Washington, D.C., U.S. Government Printing Office, p. 805-842.

Meijer, A., 1976, Pb and Sr isotopic data bearing on the origin of volcanic rocks from the Mariana island-arc system: Geol. Soc. Amer. Bull., v. 87, p. 1358-1369.

Melson, W. G., Jarosewich, E., Cifelli, R. and Thompson, G., 1967, Alkali olivine basalt dredged near St. Paul's Rocks, Mid-Atlantic Ridge: Nature, v. 215, p. 381-382.

Meschede, M., 1986, A method of discriminating between different types of mid-ocean ridge basalts and continental tholeiites with the Nb-Zr-Y diagram: Chem. Geol., v. 56, p. 207-218.

Michard, A., Albarede, F., Michard, G., Minster, J. F. and Charlou, J. L., 1983, Rare-earth elements and uranium in high-temperature solutions from East Pacific Rise hydrothermal vent field (13°N): Nature, v. 303, p. 795-797.

Mitchell, W. S. and Aumento, F., 1977, Uranium in oceanic rocks: Deep Sea Drilling Project Leg 37: Can. Jour. Earth Sci., v. 14, p. 794-808.

Moores, E. M., 1982, Origin and emplacement of ophiolites: Rev. Geophys. Space Phys., v. 20, p. 735-760.

Morris, J. D. and Hart, S. R., 1983, Isotopic and incompatible element constraints on the genesis of island arc volcanics from Cold Bay and Amak Island, Aleutians, and implications for mantle structure: Geochim. Cosmochim. Acta., v. 47, p. 2015-2030.

Mottl, M.J., 1983, Metabasalts, axial hot springs, and the structure of hydrothermal systems at mid-ocean ridges, Geol. Soc. Amer. Bull., v. 94, p. 161-180.

Muenow, D. W., Liu, N. W. K., Garcia, M. O. and Saunders, A. D., 1980, Volatiles in submarine volcanic rocks from the spreading axis of the East Scotia Sea back-arc basin: Earth Planet. Sci. Lett., v. 47, p. 272-278.

Muir, J. E., 1980, Mineralogical examination of a suite of mineralized samples from the area of the Alsek (Windy Craggy) copper deposit, Northwestern B.C., Unpublished report, Falconbridge Metallurgical Laboratories.

Nakamura, N., 1974, Determination of REE, Ba, Fe, Mg, Na, and K in carbonaceous and ordinary chondrites, Geochim. Cosmochim. Acta, v. 38, p. 757-773.

Orchard, M. J., 1986, Conodonts from Western Canadian Chert: Their Nature, Distribution and Stratigraphic Application, Conodonts: Investigative Techniques and Applications: Chichester, Ellis Horwood Ltd., p. 94-119.

Osborne, F. F. and Archambault, 1950, Hisingerite from Montauban-les-mines: Le Naturaliste Canadien, v. 77, p. 283-290.

Pearce, J. A., 1983, The role of sub-continental lithosphere in magma genesis at destructive plate margins, in Hawkesworth, C. J., and Norry, M. J., Continental Basalts and Mantle Xenoliths: Nantwich, Shiva, p. 230-249.

Pearce, J. A. and Cann, J. R., 1973, Tectonic setting of basic volcanic rocks determined using trace element analysis: Earth Planet. Sci. Lett., v. 19, p. 290-300.

Pearce, T. H., Gorman, B. E., and Birkett, T.C., 1975, The TiO_2-K_2O-P_2O_5 diagram: a method of discriminating between oceanic and non-oceanic basalts: Earth Planet. Sci. Lett., v. 24, p. 419-426.

Peter, J. M., 1989, The Windy Craggy copper-cobalt-gold massive sulphide deposit, northwestern British Columbia; British Columbia Ministry of Energy, Mines and Petroleum Resources, Geological Fieldwork, 1988, Paper 1989-1, p. 455-466.

Prince, D. R., 1983, Report on reconnaissance geological mapping of the Windy Craggy Area, B.C., NTS 114P. Falconbridge Ltd.

Ramsay, J. G., 1980, The crack-seal mechanism of rock deformation: Nature, v. 284, p. 135-139.

Reynolds, P. H. and Sinclair, A. J., 1971, Rock and ore-lead isotopes from the Nelson Batholith and the Kootenay Arc, British Columbia, Canada: Econ. Geol., v. 66, p. 259-266.

Riverin, G. and Hodgson, C. J., 1980, Wall-rock alteration at the Millenbach Cu-Zn mine, Noranda, Quebec: Econ. Geol., v. 75, p. 424-444.

Roberts, R. G., 1975, The geological setting of the Mattagami Lake mine, Quebec: a volcanogenic massive sulphide deposit: Econ. Geol., v. 70, p. 115-129.

Roberts, R. G. and Reardon, E. J., 1978, Alteration and ore-forming processes at Matagami Lake, Quebec: Can. Jour. Earth Sci., v. 15, p. 1-21.

Robinson, D. J., 1984, Silicate facies iron-formation and stratabound alteration: tuffaceous exhalites derived by mixing-evidence from Mn garnet-stilpnomelane rocks at Redstone, Timmins: Econ. Geol., v. 79, p. 1796-1817.

Roddick, J., 1984, Emplacement and metamorphism of Archean mafic volcanics at Kambalda, Western Australia-geochemical and isotopic constraints: Geochim. Cosmochim. Acta, v. 48, p. 1305-1318.

Sato, K. and Sasaki, A., 1980, Lead isotopic features of the Besshi-type deposits and their bearing on the ore lead evolution: Geochem. Jour., v. 14, p. 303-315.

Saunders, A. D. and Tarney, J., 1979, The geochemistry of basalts from a back-arc spreading centre in the East Scotia Sea: Geochim. Cosmochim. Acta, v. 43, p. 555-572.

Saunders, A. D. and Tarney, J., 1984, Geochemical characteristics of basaltic volcanism within back-arc basins, in Kokelaar, B. P., and Howells, M. F., Marginal Basin Geology: London, Geological Society, p. 59-76.

Saunders, A. D. Tarney, J., Stern, C. R., and Dalziel, I. W. D., 1979, Geochemistry of Mesozoic marginal basin floor igneous rocks from southern Chile: Geol. Soc. Amer. Bull., v. 90, p. 237-258.

Schilling, J.-G., 1973, Iceland mantle plume: geochemical evidence along the Reykjanes Ridge, Nature, v. 242, p. 565-571.

Schreyer, W. and Yoder, H. S., Jr., 1964, The system Mg-cordierite-H_2O and related rocks: Neues Jahrb. Mineral., v. 101, p. 271-342.

Schreyer, W., Kullerud, G. and Ramdohr, P., 1964, Metamorphic conditions of ore and country rock of the Bodenmais, Bavaria, sulfide deposit: Neues Jahrb. Mineral., v. 101, p. 1-26.

Schwartz, G. M., 1924, On the nature and origin of hisingerite from Parry Sound, Ontario: Amer. Mineral., v. 9, p. 141-144.

Shervais, J. W., 1982, Ti-V plots and the petrogenesis of modern and ophiolitic lavas: Earth Planet. Sci. Lett., v. 57, p. 101-118.

Sinton, J. M. and Fryer, P., 1987, Mariana Trough lavas from 18°N: implications for the origin of back arc basin basalts: Jour. Geophys. Res., v. 92, p. 12782-12802.

Sinton, J. M., Liu, L., B., T. and Chappell, B., 1986, Petrology, magmatic budget and tectonic setting of Manus back-arc basin lavas: Eos, Trans. Amer. Geophys. Union, v. 67, p. 377-378.

Stebbins, J. and Thompson, G., 1978, The nature and petrogenesis of intra-ocean plate alkaline eruptive and plutonic rocks: King's Trough, north-east Atlantic: Jour. Volc. Geotherm. Res., v. 4, p. 333-361.

Sun, S.-S., 1980, Lead isotope study of young volcanic rocks from mid-ocean ridges, ocean islands and island arcs: Phil. Trans. R. Soc. Lond., v. A297, p. 409-445.

Tarney, J. and Windley, B., 1981, Marginal basins through geologic time: Phil. Trans. R. Soc. Lond., v. A301, p. 217-232.

Tarney, J., Saunders, A. D. and Weaver, S. D., 1977, Geochemistry of volcanic rocks from the island arcs and marginal basins of the Scotia Arc region, in Talwani, M., and Pitman, W. C., III, Island Arcs, Deep Sea Trenches and Back Arc Basins: Washington, D.C., American Geophysical Union, p. 367-377.

Vidal, P. H. and Clauer, N., 1981, Pb and Sr isotopic systematics of some basalts and sulphides from the East Pacific Rise at 21°N (project RITA): Earth Planet. Sci. Lett., v. 55, p. 237-246.

Von Damm, K. L., Edmond, J. M., Measures, C. I. and Grant, B., 1985, Chemistry of submarine hydrothermal solutions at Guaymas Basin, Gulf of California: Geochim. Cosmochim. Acta, v. 49, p. 2221-2237.

Walker, D., Shibita, T. and DeLong, S. E., 1979, Abyssal tholeiites from the Oceanographer fracture zone: Contrib. Mineral. Petrol., v. 70, p. 111-125.

Watanabe, T., 1970, Volcanism and ore genesis, in Tatsumi, T., Volcanism and Ore Genesis: Tokyo, University of Tokyo Press, p. 423-432.

Weaver, S. D., Saunders, A. D., Pankhurst, R. J. and Tarney, J., 1979, A geochemical study of magmatism associated with the initial stages of back-arc spreading: Contrib. Mineral. Petrol., v. 68, p. 151-169.

Whelan, J. A. and Goldich, S. S., 1961, New data for hisingerite and neotocite: Amer. Mineral., v. 46, p. 1412-1423.

Winchester, J. A. and Floyd, P. A., 1976, Geochemical magma type discrimination: application to altered and metamorphosed basic igneous rocks: Earth Planet. Sci. Lett., v. 28, p. 459-469.

Winchester, J. A. and Floyd, P. A., 1977, Geochemical discrimination of different magma series and their differentiation products using immobile elements: Chem. Geol., v. 20, p. 325-343.

Wood, D. A., 1980, The application of a Th-Hf-Ta diagram to problems of tectonomagmatic classification and to establishing the nature of crustal contamination of basaltic lavas of the british tertiary volcanic province: Earth Planet. Sci. Lett., v. 50, p. 11-30.

Wood, D. A., Marsh, N. G., Tarney, J., Joron, J.-L., Fryer, P. and Treuil, M., 1981, Geochemistry of igneous rocks recovered from a transect across the Mariana Trough, Arc, Fore-arc, and Trench, Sites 453 through 461, Deep Sea Drilling Project Leg 60, Init. Rep. Deep Sea Drill. Proj. 60, Washington, D.C., U.S. Government Printing Office, pp. 611-645.

Wynne, P. J. and Strong, D. F., 1984, The Strickland prospect of southwestern Newfoundland: a lithogeochemical study of metamorphosed and deformed volcanogenic massive sulfides.: Econ. Geol., v. 79, p. 1620-1642.

SETTING OF STRATIFORM, SEDIMENT-HOSTED LEAD-ZINC DEPOSITS IN YUKON AND NORTHEASTERN BRITISH COLUMBIA[1]

J.G. ABBOTT
Exploration and Geological Services Division
Indian and Northern Affairs Canada
Whitehorse, Yukon

S.P. GORDEY and D.J. TEMPELMAN-KLUIT
Geological Survey of Canada
Vancouver, British Columbia

ABSTRACT

In Yukon and northeastern British Columbia, sediment-hosted, stratiform, zinc, lead (silver), (barite) deposits of Cambrian to Mississippian age occur in two of four dominantly clastic assemblages that make up the outer part of the Upper Proterozoic rifting and deposition of the Windermere Supergroup along the North American continental margin. In the inner miogeocline, basal glaciomarine siliciclastic rocks, diamictite and overlying cyclic shale and carbonate rocks prograded westward from a hinge line defined by Ogilvie and Mackenzie Arches. In the outer miogeocline, possible equivalents of these rocks are largely hidden in the subsurface.

Early Cambrian to Devonian 'passive' margin sedimentation began with subsidence, following the end of prolonged Windermere rifting or separate earliest Cambrian rifting. In the inner miogeocline, quartzose sandstone unconformably overlies Windermere strata and forms the base of a westward thickening prism of Cambrian to Middle Devonian shelf carbonates. In the outer miogeocline, thick sequences of gritty quartzose clastics, and maroon and green to dark weathering shale and minor sandstone, are probably equivalent to basal Cambrian sandstone of the inner miogeocline. A relatively thin basinal assemblage of the outer miogeocline is transitional to shelf carbonates of the inner miogeocline. Lower and Middle Cambrian shale, siltstone, and minor limestone, are locally identified. Cambro-Ordovician argillaceous limestone in the southeast correlates with calcareous and non-calcareous phyllite and basalt farther west. A succeeding Lower Ordovician to Middle Devonian assemblage is dominated by chert, black graptolitic siliceous shale and local, mafic volcanics of the Road River 'Group.' Siluro-Devonian shallow-water, shelf carbonate and clastic rocks form an elongate belt along the present western margin of the miogeocline. Periodic crustal extension and tectonic instability is indicated by scattered mafic alkalic volcanic rocks, aberrant Middle Cambrian and Middle Ordovician changes in position of the carbonate-shale transition, Late Cambrian, Middle Ordovician, Early Silurian, and sub-Devonian unconformities, and deposition of Siluro-Devonian shelf carbonate rocks along the western margin of the outer miogeocline.

Middle Devonian to Mississippian deposition of thick westerly derived coarse clastic turbidites of the Earn Group also includes black, graphitic shale and chert, and in the Pelly Mountains, Mississippian alkalic volcanic and sub-volcanic rocks. Platformal carbonate deposition ceased in the Middle Devonian and shale extends far to the east across the inner miogeocline. Uplift and erosion leading to the large influx of clastic rocks has been variously attributed to rifting, large-scale strike-slip faulting and collisional orogeny.

Mississippian to Triassic shale, sandstone, chert and lesser limestone mark a return to normal, clastic, marine, shelf sedimentation in both the inner and outer miogeocline. A few barren barite deposits are near the base, but are notably absent from the rest of the assemblage.

---

[1](Reprinted from Abbott et al., 1986)

The sediment-hosted zinc, lead deposits vary greatly in age, distribution, composition and host rock but all are in the Cambrian to Mississippian clastic strata of the outer miogeocline. In contrast, sediment-hosted copper deposits are in rift strata at the base of the Windermere Supergroup of the inner miogeocline, iron formation is in glaciogenic sediments of the Windermere Supergroup, and carbonate-hosted zinc-lead deposits are in Lower Cambrian to Middle Devonian strata of the inner miogeocline. Widespread, periodic crustal extension and tectonic instability are broadly related to the clastic-hosted zinc-lead deposits, but local stratigraphic and structural controls on their formation are poorly understood. Abrupt changes in stratigraphy near some Devonian deposits indicate syndepositional faulting, but generally, differences between strata near deposits and elsewhere are not obvious.

Introduction

One of the world's largest concentrations of sediment-hosted, stratiform zinc, lead deposits is in the northern Canadian Cordillera. The deposits considered here are Cambrian to Mississippian in age [the Helikian Hart River deposit (Morin, 1979) is older]. Like other deposits of their type (Large, 1981, 1983), they occur in thick sequences of clastic rocks overlying continental crust. Most are thought to have been precipitated from brines exhaled on to the sea floor near faults active during mineralization, and at least some are related to specific regional tectonic events with associated local high heat flow, such as rifting or wrench faulting. In the northern Canadian Cordillera, relationships between the regional tectonic framework and deposits can be broadly defined, but specific ties remain obscure.

Most writers (Blusson, 1976; Carne, 1979; Carne and Cathro, 1982; Dawson, 1977; Large, 1981, 1983; Lydon et al., 1979; McIntyre, 1983; Morganti, 1981; and Tempelman-Kluit, 1981) have described the deposits in terms of Selwyn Basin and its bounding tectonic elements, Cassiar, Mackenzie, and MacDonald Platforms (Fig. 1). Implied, is the concept that Selwyn Basin is a fault-bounded intracratonic basin with a different Paleozoic tectonic history than other parts of the Cordillera. This unique history has been regarded as the controlling factor in deposit formation.

This outline considers Selwyn Basin, and Cassiar, Mackenzie and MacDonald Platforms to be integral parts of the cordilleran miogeocline. It briefly describes the stratigraphic and structural framework of the miogeocline in the northern Cordillera, and attempts to relate the sediment-hosted deposits to its evolution. All of the large stratabound, sediment-hosted zinc, lead deposits in the northern Canadian Cordillera are concentrated in the Anvil, MacMillan Pass, Howard's Pass, and Gataga districts. Most are described in this volume; those that are not are briefly characterized here, where the regional setting is the focus.

The Cordilleran Miogeocline: Summary of Evolution

The Cordilleran miogeocline is a prism of sedimentary rocks of Precambrian to Middle Jurassic age deposited along the relatively stable continental margin of western North America. The latest phase of miogeoclinal sedimentation began no later than 730 Ma ago with rifting reflected in dyke intrusion, synsedimentary faulting, and the progradation of a thick wedge of clastic rocks (Windermere Supergroup) (Stewart, 1972; Eisbacher, 1981; Evenchick and Gabrielse, 1984; Thompson and Eisbacher, 1984). At this time, the Cordilleran basin first shows clearly west-deepening polarity. In Yukon, rifting was preceded by at least two periods of epicratonic sedimentation of about 400 Ma each [Wernecke Assemblage (12+ km); Pinguicula Group/Mackenzie Mountains Supergroup (5-7+ km) (Eisbacher, 1981; Young et al., 1979)], separated by regional deformation (Eisbacher, 1981). Deposition during these periods may have occurred in an intracratonic basin or may have been miogeoclinal. The extent of these old epicratonic strata beneath much of the younger miogeocline is unknown, but appears to be widespread in northern Rocky and Mackenzie Mountains.

'Passive' margin sedimentation was interrupted during the late Devonian and ended by collision of a Mesozoic island-arc with the outer miogeocline in the Middle Jurassic (Tempelman-Kluit, 1979). The outer miogeocline was overthrust by mylonite, ophiolite, and granitic rocks and was itself imbricated and folded during decollement-style deformation. Jura-Cretaceous molasse that spread ahead of the eastward-growing mountain belt was itself progressively deformed, elevated, and eroded. Widespread mid-Cretaceous granite, possibly formed by crustal thickening and heating as a result of continental underplating intruded the deformed strata of the outer miogeocline. Deformation of the inner miogeocline in eastern and northern Mackenzie Mountains occurred later and involved Paleocene coarse clastic strata (Aitken et al., 1982). Transcurrent movement along Tintina Fault,

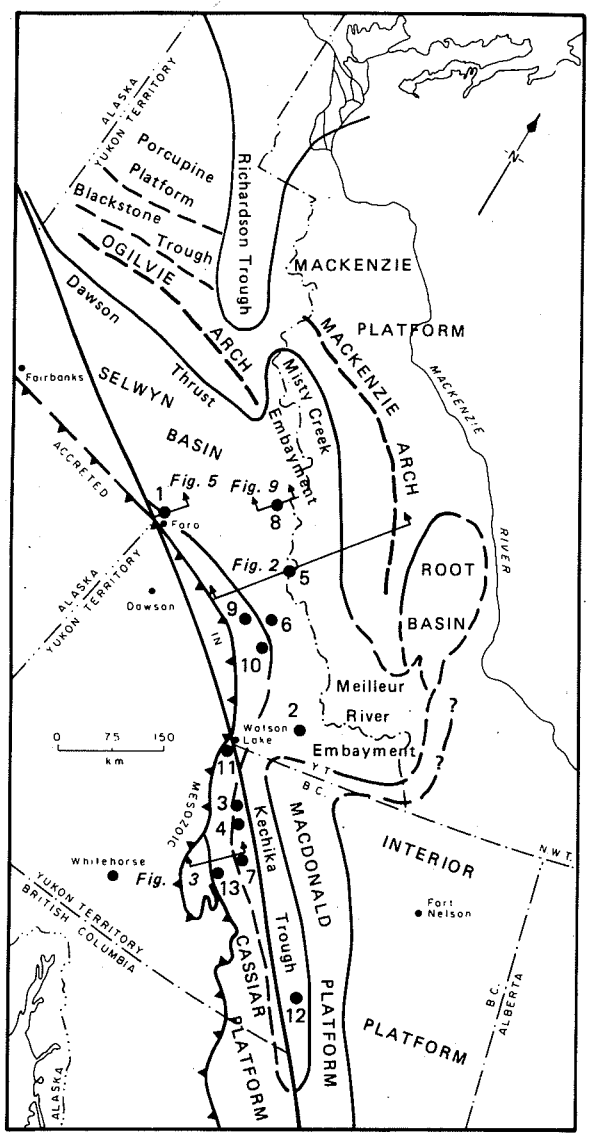

1	Anvil district	8	MacMillan Pass district
2	Mel deposit	9	Fin occurrence
3	JA occurrence	10	Matt Berry occurrence
4	Sunset occurrence	11	Clear lake deposit
5	Howards Pass district	12	Gataga district
6	Maxi occurrence	13	MM deposit, Bnob, Chzerpnough occurrence
7	Angie occurrence		

FIGURE 1. Tectonic elements of the northern Canadian Cordillera and location of sediment-hosted, stratabound deposits. Modified from Cecile, 1982. A total of 450 km of right-lateral strike-slip is restored on Tintina Fault.

northern Rocky Mountain Trench Fault and related structures, in latest Cretaceous or early Tertiary time was at least 450 km judging from offset of Mesozoic structural elements (Tempelman-Kluit, 1979), and as much as 750 km as indicated by possible offset facies of Lower Paleozoic rocks (Gabrielse, 1984).

For most of its length, the Cordilleran miogeocline is bounded east of a hinge, by relatively thin platformal sequences of the Interior Platform (Fig. 1). In the northern Cordillera, however, the late Proterozoic and lower Cambrian hinge was farther west, and is represented by Ogilvie and Mackenzie Arches in Yukon and Northwest Territories, and is unnamed in northern British Columbia (Fig. 1). The three segments are disrupted by the latest Early Cambrian to Early Silurian Misty Creek Embayment, and Ordovician to Middle Devonian Meilleur River Embayment (Bassett and Stout, 1967; Morrow, 1984).

In northern British Columbia, east of the hinge, thin Silurian and Devonian shelf carbonate rocks of MacDonald Platform (Gabrielse, 1967, pers. comm., 1985) unconformably overlie Helikian strata. Southeast of Mackenzie Arch, Ordovician to Middle Devonian platform and shelf carbonates of Mackenzie Platform (Lenz, 1972), partially enclose Root Basin, an inner shelf embayment of relatively thick sequences of carbonate rocks of the same age. Ogilvie Arch is bounded to the north by relatively deep water Cambrian to Devonian clastic and carbonate rocks in Richardson Trough and by similar Middle Ordovician to Middle Devonian strata in Blackstone Trough.

Accreted assemblages bound the miogeocline in the west.

What is Selwyn Basin?

This review is about that part of the miogeocline southwest of Ogilvie and Mackenzie Arches, and is based on figure 2, a version of Gordey's (1981b, 1982) structure and stratigraphic sections across the south-central Mackenzie and Selwyn Mountains, and figure 3, Tempelman-Kluit's (1977a) schematic stratigraphic section across the Pelly Mountains south of Tintina Fault. A number of terms have been used to describe parts of the miogeocline included in these sections and this terminology is currently in a state of flux.

Selwyn Basin was first defined by Gabrielse (1967), who considered it to be a basin in the tectonic sense; a negative element defined by unusually thick

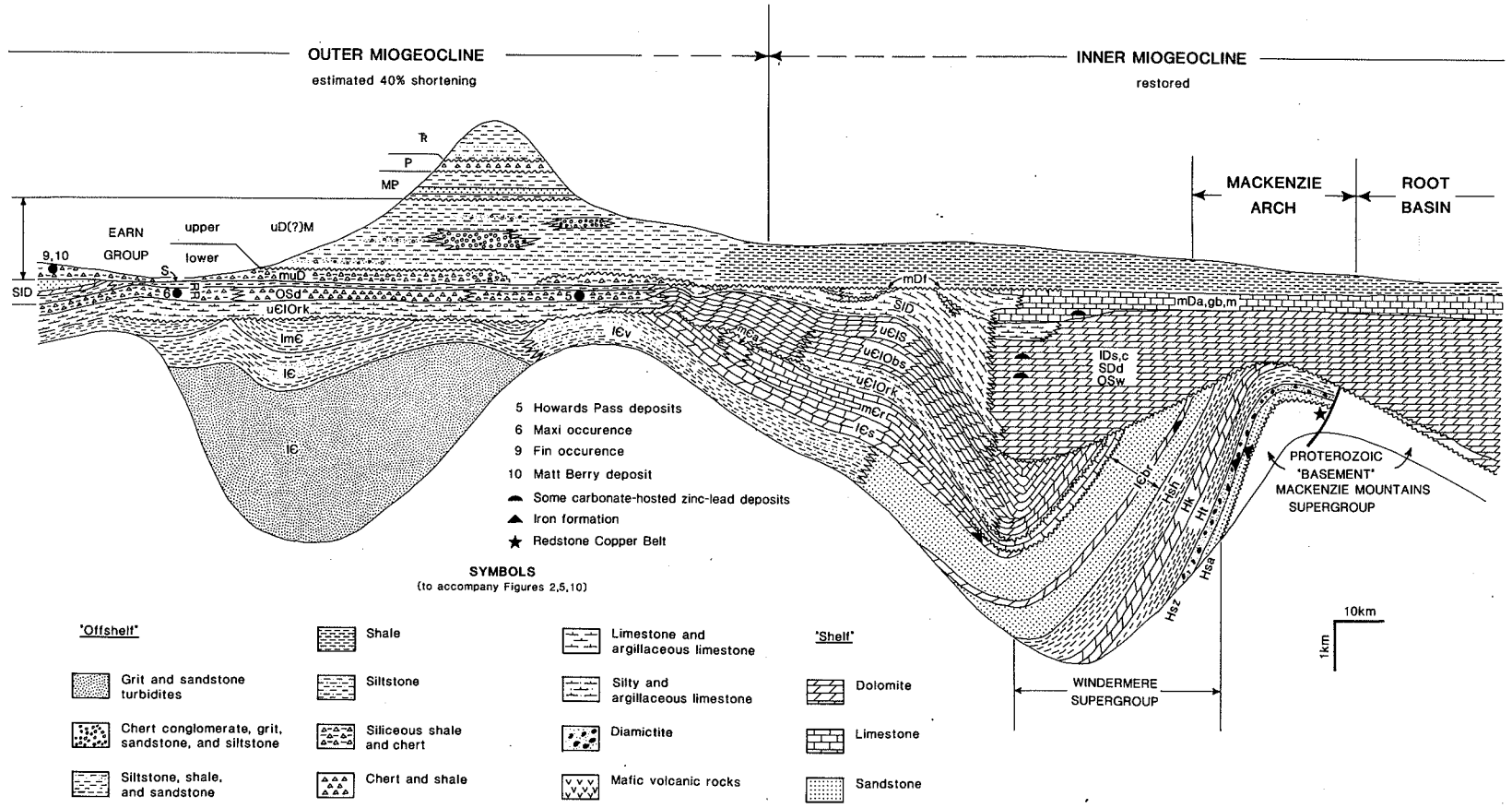

FIGURE 2. Restored stratigraphic section across the Cordilleran miogeocline in Yukon and Northwest Territories, modified from Gordey (1981b, 1982). Location shown in Figure 1. Hsa - Sayunei Fm, Hsz - Shezal Fm., Ht - Twitya Fm, Hk - Keele Fm, Hsh - Sheepbed Fm, lCbr - Backbone Ranges Fm, lCs - Sekwi Fm, lCv - Vampire Fm, mCr - Rockslide Fm, lCObs - Broken Skull Fm, uCOrk - Rabbitkettle Fm, OSd - Duo Lakes Fm, OSw - Whittaker Fm, SDd - Delorme Fm, - lDs - Sombre Fm, lDc - Camsell Fm, mDa - Arnica Fm, mDgb - Grizzlie Bear Fm, mDm - Manetoe Fm, mDln - Nahanni Fm, nDh - Headless Fm, mDl - Landry Fm, mDf - Funeral Fm, mDna - Natla Fm.

successions of carbonate and clastic strata of late Precambrian through Middle Devonian age, bounded to the east and north by Redstone Arch (part of Mackenzie Arch) and Ogilvie Arch (Fig. 4). Silurian and Devonian shallow-water carbonate and clastic rocks as well as strata as old as late Precambrian (some of deep water affinity), along the western margin of Selwyn Basin and west of Tintina and Rocky Mountain Trenches were called Cassiar Platform. Upper Devonian and younger strata were unnamed.

West of MacDonald Platform, thick Cambrian to Middle Devonian carbonate and clastic rocks and their offshelf, shaley equivalents were named Kechika Trough (Douglas et al., 1972) and are equivalent to those Gabrielse included in Selwyn Basin farther north. All shelf carbonates in the area have been included in MacDonald Platform and only the offshelf facies has in turn, been included in Selwyn Basin (i.e.

Tempelman-Kluit, 1977a,b).

Tempelman-Kluit (1982) used Selwyn Basin and Cassiar Platform in a depositional rather than a tectonic sense. Only Upper Cambrian to Devonian relatively deep water clastic rocks of the outer miogeocline were included in Selwyn Basin because only strata of this age are thought to have been bounded on the west by relatively shallow water strata, which he considered to be Cassiar Platform (Fig. 3 and 4). Basin in this sense refers to a marine arm where sediments were deposited, rather than a thick succession of sediments which may or may not have been deposited in deep water surrounded by relatively shallow water or land. He also used the term Mackenzie Platform, to encompass those shallow water carbonate rocks of late Precambrian to Middle Devonian age north and east of the carbonate-shale boundary.

Gordey (in prep.) prefers to include all late Precambrian through Middle Devonian relatively deep water clastic and carbonate rocks of offshelf or deeper water facies in Selwyn Basin (Fig. 4).

Aside from these different perceptions of Selwyn Basin, the term has also been used informally to refer to the geographical area roughly delineated by the Paleozoic carbonate-shale boundary and Tintina Fault. In this use, all rocks of any age, including Cretaceous granitic rocks, have and could be included in Selwyn Basin.

Disagreement about Selwyn Basin is clearly semantic and not rooted in any basic disagreement about the rocks.

Sedimentary Sequences of the Miogeocline

Sedimentary facies in the miogeocline can be conveniently grouped into four assemblages of different ages and these groups can, in turn, be divided into inner and outer parts.

1. The late Proterozoic Windermere Supergroup comprises a westward thickening, clastic-dominated sequence of which the lower part, at least, is thought to reflect initial rifting.

2. Early Cambrian to Middle Devonian westward thickening shallow water clastic and shelf carbonate rocks in the inner miogeocline and thinner, deeper water clastic-dominated strata in the outer miogeocline were deposited in a 'passive' environment which underwent intermittent extension.

3. Middle Devonian and Mississippian transgressive, northerly and westerly derived shale and siltstone in the inner miogeocline and a complex assemblage of chert, shale and locally derived coarse clastic turbidites (Earn Group) within the outer miogeocline reflect a tectonic event of uncertain origin.

4. Mississippian to Triassic strata, preserved locally, are mainly fine-grained clastic rocks and chert that indicate stable marine shelf sedimentation.

Late Proterozoic (Windermere Supergroup)

The Windermere Supergroup is preserved west of Mackenzie Arch, and was either removed by early Proterozoic erosion or never deposited farther to the east. In the inner miogeocline (Fig. 2), Eisbacher (1981) has shown that a phase of syn-depositional regional faulting began with the onset of deposition of the lower Windermere Supergroup. Basaltic volcanic rocks in dolostone of the uppermost part of the Little Dal Group, abrupt thickness and facies changes in redbeds, evaporites, and carbonates of the overlying Redstone River and Coppercap Formations, and in siliciclastic laminates of the Sayunei Formation, indicate rifting at this time. Contemporaneous normal faults with as much as 800 m displacement form a northerly-trending fan across the area of Mackenzie Platform. Diabase dykes in or parallel to the faults may be feeders to the basalt

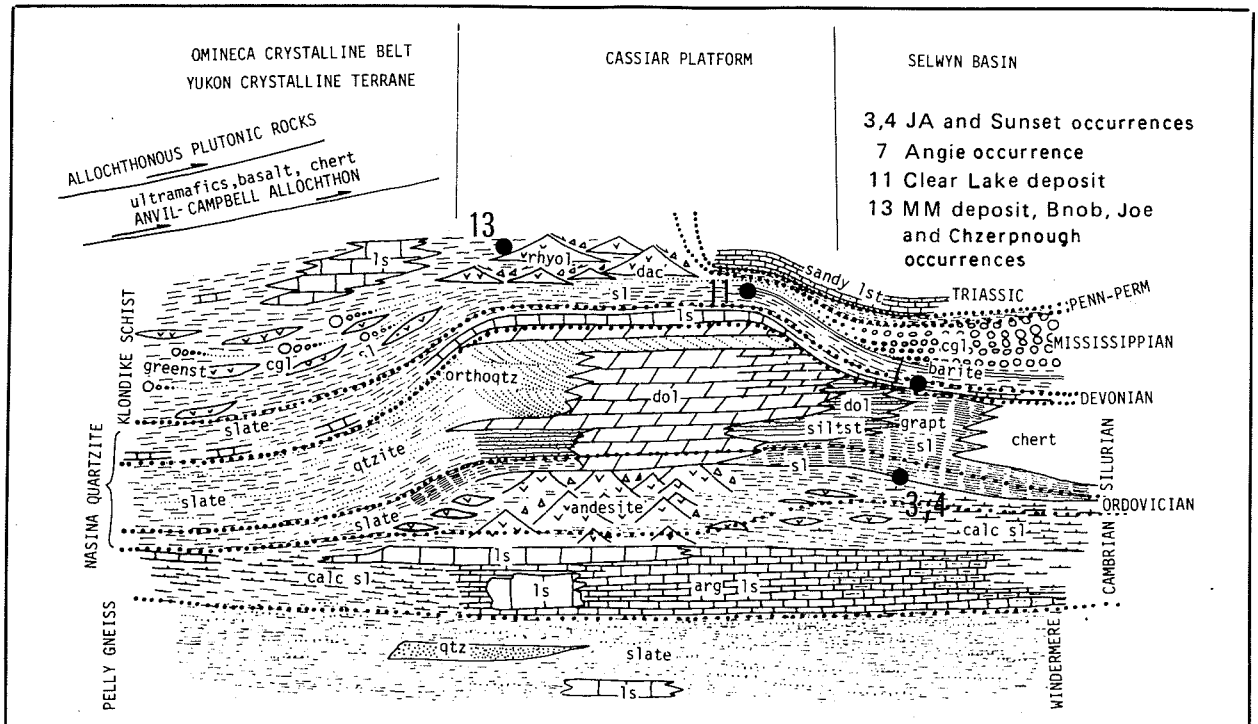

FIGURE 3. Schematic stratigraphic section across Cassiar Platform south of Tintina Fault, modified from Tempelman-Kluit, 1977. Cassiar Platform as defined by Tempelman-Kluit is shaded. Location shown in Figure 1. Shale-hosted zinc-lead deposits are both above Cassiar Platform and along its northern margin.

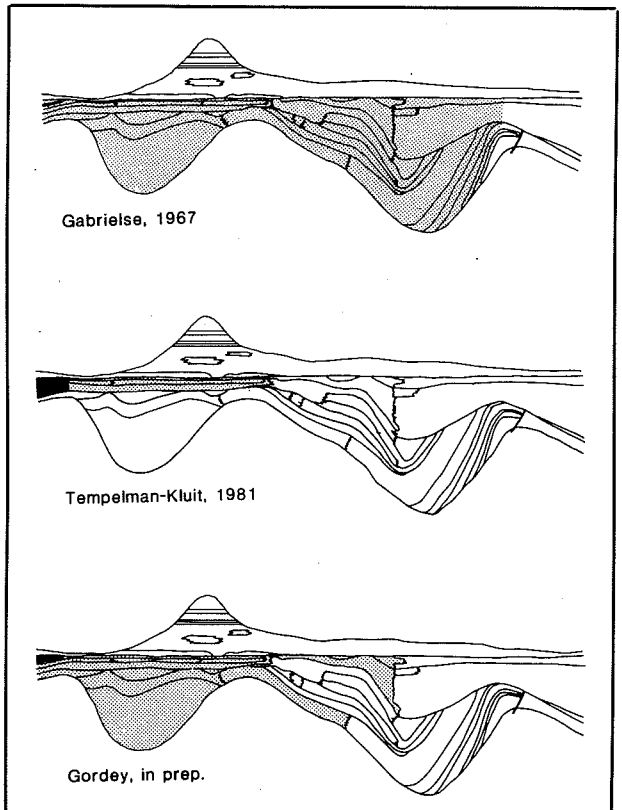

FIGURE 4. The different definitions of Selwyn Basin (grey) and Cassiar Platform (black).

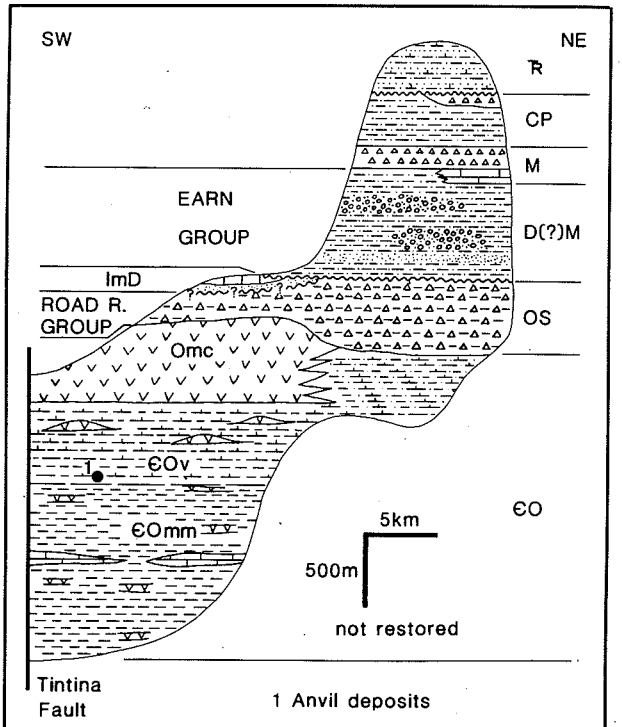

FIGURE 5. Schematic stratigraphic section across the Anvil Range (not restored). Location shown in Figure 1. COmc - Menzie Creek Fm, COv - Vangorda Fm, COmm - Mount Mye Fm. The Anvil deposits are at the transition between the Mt. Mye and Vangorda Formations. These units broadly resemble strata seen elsewhere in the outer miogeocline.

flows in the Little Dal Group. Radiometric ages of 766 and 769 Ma (Armstrong et al., 1982) from the dykes suggest a maximum age for onset of Windermere sedimentation. However, Eisbacher (1981) suggested that the dykes might also be related to widespread iron formation higher within the upper Windermere Supergroup.

At least 3000 m of younger strata thin eastward by thinning of units, and by eastward bevelling of Paleozoic unconformities (Eisbacher, 1981). Siliciclastic laminates, argillite, and hematite-jaspillite of the Sayunei Formation, and overlying tillite and diamictite of the Shezal Formation are in part glaciogenic. Above the Shezal Formation, shale, siltstone, and sandstone of the Twitya Formation grade upward to shallow-water carbonate and quartzite of the Keele Formation. Shale of the Sheepbed Formation comprises the uppermost member of the Windermere Supergroup. Current indicators and facies changes indicate that sediments were deposited centripetally into a westward deepening basin from the east and north (Eisbacher, 1981).

In northern British Columbia, only remnants of basal(?) diamictite are preserved beneath unconformably Lower Cambrian strata (Taylor et al., 1979; Eisbacher, 1981).

South of Ogilvie Arch, latest(?) Proterozoic basalt and proximal carbonate conglomerate, fill half-grabens in pre-Windermere carbonates and are unconformably overlain by lower Cambrian carbonate (Roots, 1982; Thompson and Roots, 1982; Thompson and Eisbacher, 1984).

At the western end of Ogilvie Arch, in eastern Alaska, Payne and Allison (1981), Young (1982) and others have correlated mafic volcanics, maroon rythmite, diamictite, iron formation, shale, and carbonate of the Upper Tindir Group with the Windermere Supergroup of the Mackenzie Mountains. However, a Lower Cambrian age for part of the Upper Tindir Group is indicated from microfossil evidence (Payne and Allison, 1982).

In the outer miogeocline of northern British Columbia, east of Northern Rocky Mountain Trench, Evenchick et al. (1984) have shown that siliciclastic grit, associated diamictic and volcanic rocks were deposited on granite that gave a radiometric age of 728 Ma. West of the trench, similar strata, but with not diamictite, unconformably overlie crystalline basement giving a radiometric age of 1.85 Ga (Evenchick et al., 1984).I n central Yukon, the oldest exposed rocks are coarse, quartzofeldspathic turbidites, and shale at least 3000 m thick. The grits have traditionally been assigned to the lower 'grit unit' of the Windermere Supergroup (Eisbacher, 1981). Recent work in the northern Mackenzie Mountains and near Howard's Pass by Fritz et al. (1983), has shown that the upper part is Lower Cambrian, and the lower parts could also be of post-Windermere age.

Tectonic Interpretation

Eisbacher (1981) has correlated the Windermere assemblage of the northern Cordillera to similar assemblages that can be traced the length of the North American Cordillera. Evidence cited by Stewart (1972, 1976), Eisbacher (1981), Evenchick and Gabrielse (1984), Thompson and Eisbacher (1984), and Young et al. (1979) indicates that deposition occurred along a newly rifted margin of western North America. Continental crust was thinned during rifting , but development of true oceanic crust at this time has not been demonstrated (Eisbacher, 1981, p. 36).

Mineral Deposits

No sediment-hosted stratabound lead zinc deposits are known in the Windermere Supergroup of the northern Cordillera, but other types of stratabound metal deposits are known and include the Redstone copper belt (Ruelle, 1982; Jefferson and Ruelle, 1986), and the Snake River iron formation (Yeo, 1981, 1986).

In this Redstone copper belt, stratiform zones, less than a metre thick, of disseminated bornite, chalcopyrite, and chalcocite are confined to beds of cryptalgal carbonate in the rift assemblage that marks the onset of Windermere sedimentation (Fig. 2). The deposits are in the transition zone between underlying non-marine fanglomerates, redbeds, and evaporites of the Redstone River Formation, and overlying transgressive, shallow marine dolomite, limestone and shale of the Coppercap Formation. Syn-depositional northeast-trending normal fault, superimposed on a northwest-trending shoreline produced complex, abrupt facies and thickness changes in both the Redstone River and Coppercap Formations. The faults show no direct relationship to the deposits, but controlled the complex facies relationships which resulted in mineralization. Ruelle (1982) postulated that the copper came from

basalt in the Little Dal Formation, beneath the Redstone River Formation, was dissolved in saline, oxidized groundwater in the redbeds and evaporites of the Redstone River Formation, and was precipitated in overlying reduced algal dolomites during compaction and dewatering.

Iron formation is part of the Shezal, and to a lesser extent, the Sayunei Formations, near the base of the Windermere Supergroup (Fig. 2). The Crest deposit, near the Snake River at the north end of Mackenzie Arch, is the largest with a minimum size of 20 billion tonnes, of which 5.44 billion tonnes grading 47.2% iron is amenable to open-pit mining (Yeo, 1981, 1986). The deposit is about 150 m above the base of the Shezal Formation, and includes more than 10 zones up to 24 m thick, in an interval of about 150 m (Yeo, 1981). The deposit is mainly laminated jasper and hematite. Jasper also forms nodules and irregularly shaped lenticles in laminated to massive hematite. Yeo (1981) considered the hematite and jasper to be chemical precipitates derived from the fumarolic waters, and proposed that the deposits are related to faults and possibly volcanism that were part of the rifting and continental separation that accompanied the onset of Windermere sedimentation.

Latest Proterozoic to Middle Devonian

The latest Proterozoic to Middle Devonian inner miogeocline is typically a westward thickening prism of basal shallow-water clastic rocks and overlying shelf carbonates like that shown in figure 2. The outer miogeocline includes generally thinner transitional (slope) and fine clastic (basinal) facies, and along its western margin, relatively shallow-water Silurian and Devonian carbonates. The depositional environment was essentially passive, but periodic extension and tectonic instability are indicated by several internal unconformities, scattered volcanic rocks in the outer miogeocline, and widespread migration of the hinge and carbonate-shale transition with time. Figures 5 to 8 summarize the resultant complex paleogeography. Some of the more important aspects of the paleogeography are described here.

Inner Miogeocline. From Mackenzie Arch southward into British Columbia (Fig. 5), easterly derived, transgressive latest Proterozoic and Lower Cambrian non-marine to shallow-water
marine quartz arenite, feldspathic sandstone, and dolostone (Backbone Ranges Formation in Fig. 2), overlie the Windermere Supergroup (Fig. 5). Mafic volcanics occur in clastics and carbonates north of the British Columbia border in Coal and Flat River map area. An angular unconformity separates the sandstones from older strata in most places, but conformable relations are seen in parts of the northern Mackenzie Mountains.

Over most of Ogilvie Arch, Lower Cambrian clastic rocks are absent and Lower Cambrian carbonate rocks unconformably overlie a faulted substrate of older carbonate strata of uncertain age and correlation (Norris, 1982; Thompson and Roots, 1982; Thompson and Eisbacher, 1984).

Lower Cambrian to Devonian shelf dolomite and limestone comprise numerous formations in the inner miogeocline. Some from the west side of Mackenzie Arch are shown in figure 2, where the thickest part of the prism attains 6.5 km thickness. In most places, Upper Cambrian (Fig. 5), sub-Upper Ordovician (Fig. 6), and late Silurian-Lower Devonian unconformities remove strata and commonly bevel the section eastward. In Kechicka Trough, a sub-late Early Silurian unconformity locally removes strata (M. Cecile, pers. comm., 1985).

Northward from the section in figure 2, the prism thins as it bends around Mackenzie Arch to join Ogilvie Arch. There, Early Ordovician to Late Silurian limestone and dolomite rest unconformably upon strata as old as pre-Windermere. Thicknesses reach 1.5 km (Green, 1972). Late Silurian to Middle Devonian dolomite is preserved locally.

The south end of Mackenzie Arch is terminated by the thick Upper Cambrian to Middle Devonian carbonates, which merge with equivalent strata of Root Basin (Gabrielse, 1967). In northern British Columbia, the carbonate prism on MacDonald Platform resembles the one on Mackenzie Arch. Farther west, the rocks thicken and change facies into Kechicka Trough (Gabrielse, 1967).

Outer Miogeocline. Near the thickest part of the wedge, most formations undergo a transition to thinner, deeper water, fine-grained clastic facies of the outer miogeocline. The Cambrian and Lower Ordovician transition is broad and others are fairly sharp. South of Ogilvie Arch, shelf and basin facies of most ages are in abrupt contact across the 'Dawson Thrust' (Fig. 1) (Tempelman-Kluit, 1981), a fault zone mapped by Green (1972) as Mesozoic. Tempelman-Kluit (1981) and Thompson (pers. comm., 1984) interpreted it as a late

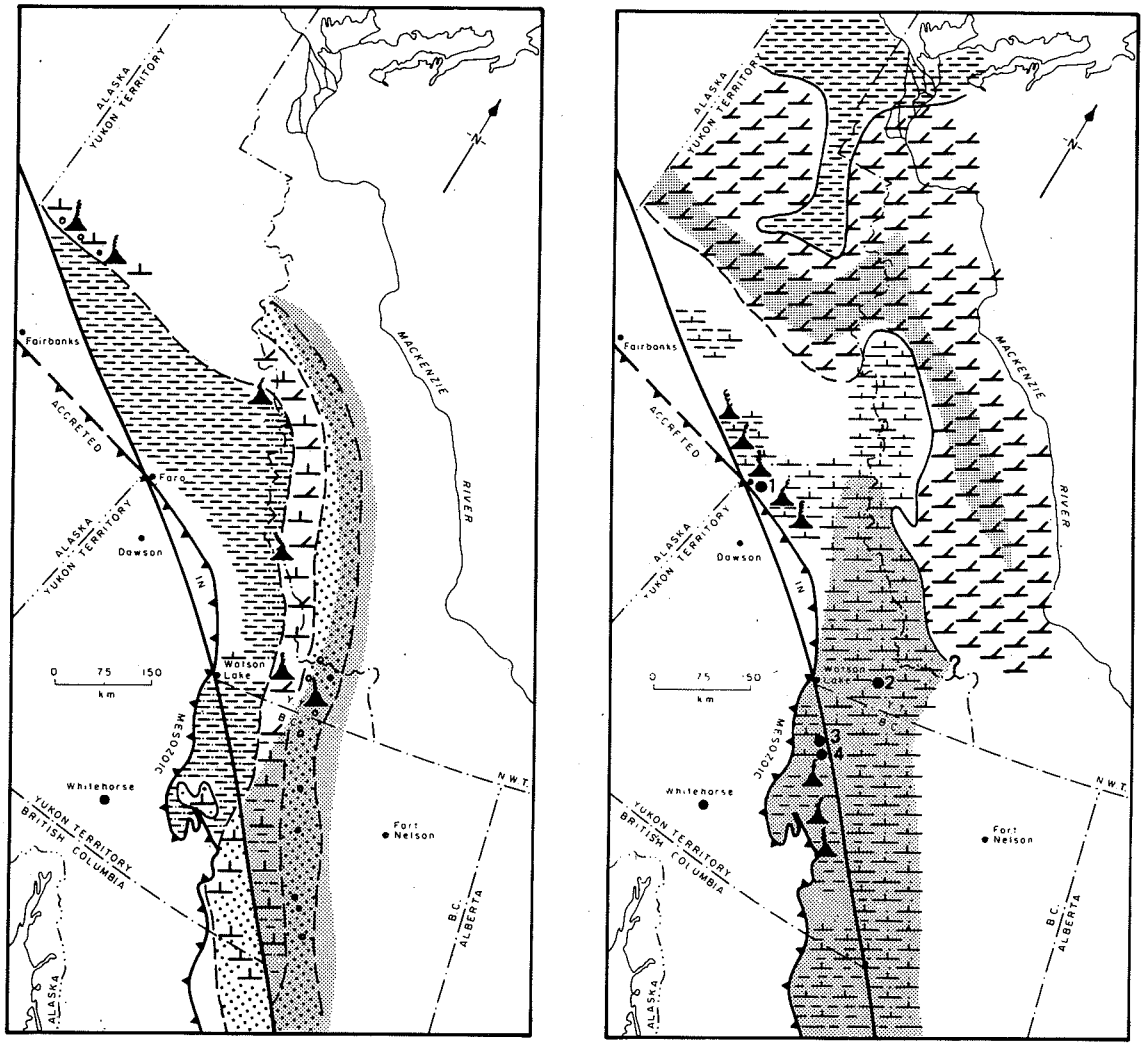

FIGURE 6. Early Cambrian and Late Cambrian to Early Ordovician paleogeography. Based on reconstructions by Gabrielse (1973) and Cecile (1982), unpublished reconstructions by Cecile and Norford, and Geological Survey of Canada reports and maps.

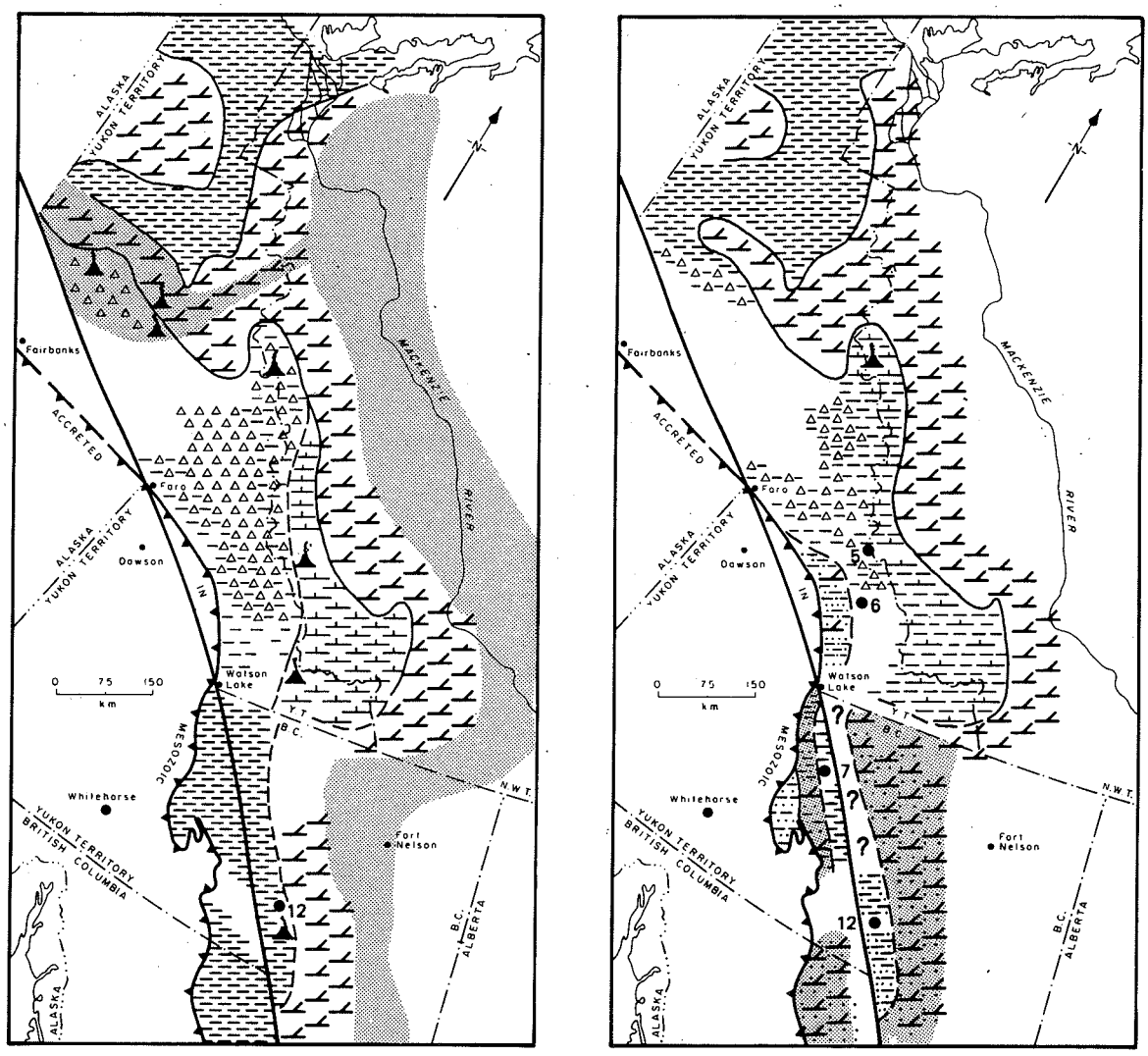

MIDDLE ORDOVICIAN

EARLY SILURIAN

Shelf dolomite. eS in B.C. includes quartz arenite

Offshelf limestone, argillaceous limestone

Platy dolomitic siltstone and quartz arenite, with dolomite buildups in Cassiar Platform

Black siliceous shale, locally with chert

Shale and chert

Mainly chert with shale interbeds

Mafic volcanic rocks

Strata of designated age unconformably overlie older strata

Strata of designated age removed beneath unconformities or were never deposited

5 Howards Pass district
6 Maxi occurrence
7 Angie occurrence (early Devonian)
12 Reb, Aikie-Sika occurrences (middle (?) Ordovician)
12 Ern, Ct occurrences (early Silurian)

FIGURE 7. Middle Ordovician and Early Silurian paleogeography. Based on reconstructions by Cecile (1982), unpublished reconstructions by Cecile and Norford, and Geological Survey of Canada reports and maps.

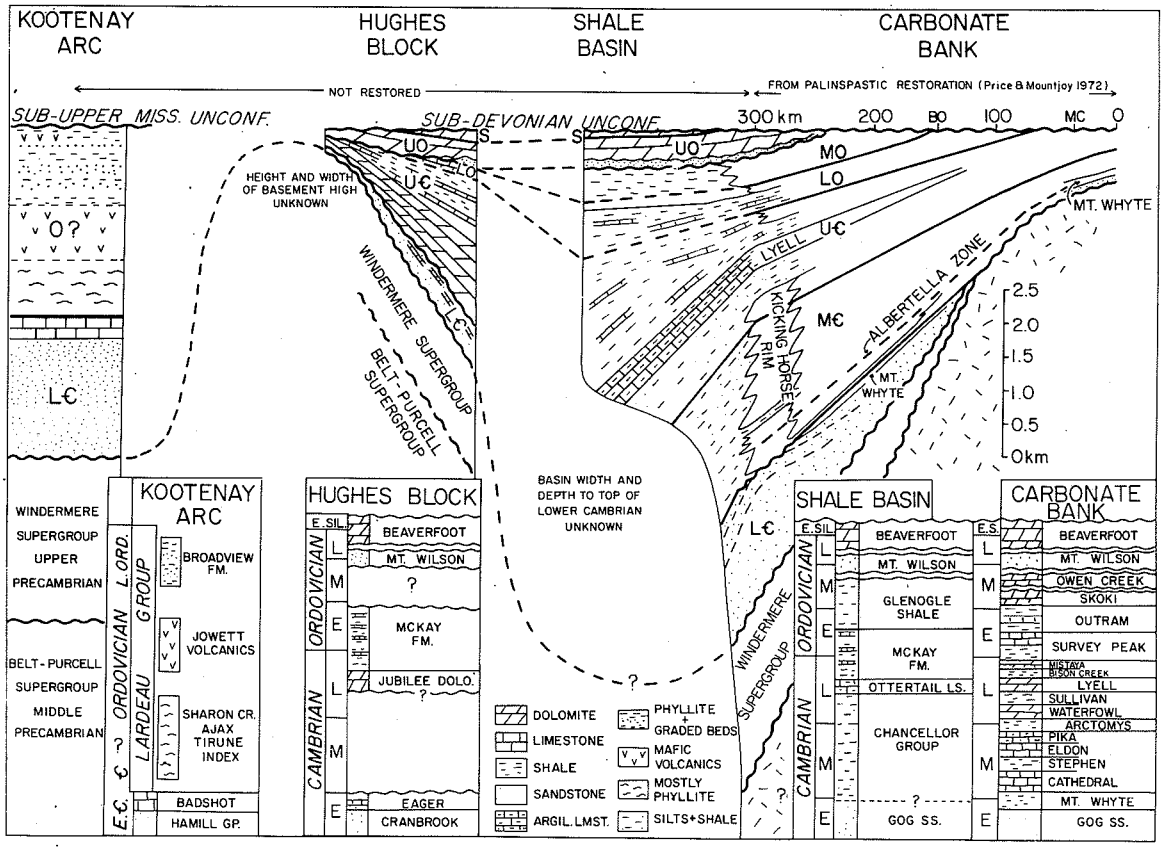

FIGURE 8, Diagrammatic cross section of the southern Cordilleran miogeocline west of Calgary, by Bond and Komintz (1984). The late Proterozoic to Devonian miogeocline in the southern Canadian Cordillera broadly resembles that in the north (Fig. 2). The southern miogeocline has a relatively narrow, poorly preserved outer part (shale basin). The Hughes Block may correspond to Cassiar Platform in the north.

Proterozoic or Earliest Cambrian rift which controlled Paleozoic facies changes and the style of Mesozoic deformation. Aberrant changes in position of the facies boundary resulted in the development of Misty Creek Embayment, Richardson and Blackstone Troughs (Cecile, 1982), and Meilleur River Embayment (Morrow, 1984) during the late Early Cambrian to Middle(?) Ordovician. All but the Misty Creek Embayment persisted as negative elements until the Middle Devonian.

The predominantly clastic basinal assemblage is 2 km to 3 km thick, and characteristically thinner than equivalent carbonates of the inner miogeocline. Older units tend to be thicker than younger units. Upper Cambrian, Middle Ordovician, and Middle Devonian unconformities are widespread. The relatively shallow-water Silurian to Middle Devonian Cassiar Platform bounds the western margin of the outer miogeocline.

Lowest Cambrian strata in the outer miogeocline belong to the 'grit unit'. Fritz et al. (1983), tentatively correlated discontinuous limestone near the top of the coarse clastic lower 'grit unit' to the middle dolomite member of the Backbone Ranges Formation. Near Howard's Pass, the upper 'grit unit' comprises distinctive maroon and green shale with less brown shale and sandstone which grades to brown shale and sandstone of the transitional Vampire Formation which in turn grades eastward to the upper member of the Backbone Ranges Formation. Equivalents to the Lower Cambrian Sekwi Formation include about 1 km of brown weathering shale and siltstone near Howard's Pass (Gordey, in press), and thick shale and alkalic mafic volcanic rocks north of MacMillan Pass, in northwest Niddery map area (M. Cecile, 1984b; pers. comm.,

1984). In most areas, Lower and Middle Cambrian strata younger than the 'grit unit' have not been recognized, or are no longer preserved.

Middle Cambrian strata in northern British Columbia define sharp northerly-trending facies belts indicative of bloc faulting and rifting(?) (Taylor et al., 1979; Fritz, 1979b; Gabrielse, 1981). Conglomerate, which characterizes one belt, can be related to faults with vertical displacements above 500 m (Taylor et al., 1979, p. 230). The conglomerate belt is bounded on the east by siltstone, sandstone, and shale and to the west by mixed fine-grained clastics and limestone. West of the mixed facies lies a reef or intrabasinal (?) platform (Gabrielse, 1981, p. 205). In most of northern British Columbia and southeast Yukon, Middle and locally, Lower Cambrian strata have been removed by Late Cambrian erosion (Fig. 5). Cecile (1982), showed that the Late Cambrian unconformity is absent in Misty Creek Embayment, where Lower Cambrian Sekwi shelf carbonate is overlain by dark shale and siliciclastic flysch (Middle Cambrian Hess River Formation), which grades to Upper Cambrian and Lower Ordovician Rabbitkettle silty limestone. Unlike most basinal facies, Cecile's units are thicker than their platformal counterparts; they are at least 2500 m and 950 m thick, respectively. Cecile (1982) proposed that Misty Creek Embayment reflects rifting and extension that began in the late Early Cambrian. The subsidence that formed Misty Creek Embayment, and the coeval uplift and erosion seen in northern British Columbia and southeastern Yukon may be related.

Upper Cambrian and Lower Ordovician strata are generally distinctive, homogeneous silty limestone of the Rabbitkettle Formation in the Mackenzie Mountains and calcareous shale and silty limestone of the Kechika Group in northern British Columbia and central Yukon (Fig. 5). Mafic volcanic rocks are locally intercalated near Howard's Pass. The most southwestern exposures of the Kechika Group, on both sides of Tintina Fault, include a second facies of basalt and tuff interbedded with non-calcareous shale, siltstone, and locally sandstone (Tempelman-Kluit, 1970, 1977a,b; Gordey, 1981a, 1983). This assemblage, which Tempelman-Kluit included in Cassiar Platform, grades laterally to typical calcareous strata of the Kechika Group and to younger black graptolitic shales of the Road River Group.

From Faro southeastward, the outer miogeocline is apparently bounded by a narrow belt of Ordovician and early Silurian black shale, chert, and grey phyllite of the Road River Group, and overlying Silurian to Middle Devonian dolomitic siltstone, quartz arenite, dolomite of Cassiar Platform. The shelf carbonates thicken southeastward from about 50 m near Faro, to 400 m in northeast Finlayson Lake map area (Fig. 3), to more than 1400 m southwest of Tintina Fault (Gordey, 1981). Tempelman-Kluit (1977a,b), on evidence seen southwest of Tintina Fault in Quiet Lake and Finlayson Lake map areas, considered the carbonates to form a narrow belt grading southwest and northeast to time-equivalent shale. Also southwest of Tintina Fault, in British Columbia, Gabrielse (1984), on the basis of facies and current indicators, correlates the Siluro-Devonian carbonate rocks with those of MacDonald Platform. The carbonate rocks apparently form a peninsula (Fig. 6), although Gabrielse (1984), on the basis of offset of the Lower Cambrian shale-quartzite boundary and Devonian fossil zones, has suggested the possibility that all of the Siluro-Devonian carbonate rocks southwest of Tintina Fault are displaced from MacDonald Platform. If so, displacement on Tintina Fault totalled more than 750 km, and additional movement took place on a splay located southwest of the main fault, between the carbonates and intervening shales.

Mafic volcanic flows, volcaniclastic breccias, and tuffs are volumetrically small, but widespread members of the Road River Group and its transitional facies. The Middle Ordovician Marmot Formation, in central Misty Creek Embayment (Cecile, 1982), at 500 m, is by far the thickest and most extensive accumulation. Middle Ordovician volcanics in the Sunblood limestone in Glacier Lake and Coal river map areas, southeastern Yukon (Gabrielse and Blusson, 1969; Gabrielse, et al., 1973), and in black shales in northeastern British Columbia are near the carbonate-shale transition. South of the Dawson "thrust", widespread mafic volcanic and ultramafic rocks of probable Ordovician age may be related to that feature (Tempelman-Kluit, 1970, 1981; Green, 1972; Roots, 1982; Roots and Moore, 1983). Near MacMillan Pass, Silurian (?) and Middle Devonian volcanics are confined to a narrow Middle and Late Devonian rift (Abbott, 1982). Southwest of Tintina Fault (Tempelman-Kluit, 1977b), Silurian tuff and volcanic breccia are intercalated with a platformal dolomite, and Devonian flows and breccias are in calcareous shale along the northeast margin of Cassiar Platform.

The Road River Group conformably overlies older strata in most places, but south of the "Dawson thrust", black shale and mafic volcanic rocks rest

unconformably on the 'grit unit' (Tempelman-Kluit, 1970, R. Thompson, pers. comm., 1984). Gordey has observed similar relationships northeast of the Anvil Range. The black shale and chert in these areas are not dated, but the absence of the Rabbitkettle Formation, and similarity of the black shale and chert to the basal Road River Group elsewhere suggests a Lower or Middle Ordovician unconformity between Road River and older strata. Early and Middle (?) Ordovician uplift and erosion in western Yukon, contrasts with subsidence, transgressive onlap of the basinal facies, and foundering of part of platform and shelf to form Root Basin and Meilleur River Embayment in southeastern Yukon.

At the northwest end of Cassiar Platform, near Faro, the Anvil deposits (Jennings and Jilson, 1986), (Fig. 5), are in a thick succession of Cambrian and Early Ordovician phyllites and volcanic rocks (Tempelman-Kluit, 1972). Early Ordovician graptolites were collected by Gordey (1983) from shale in the upper volcanics, and at least the upper part of the assemblage correlates with the Kechika Group, but the age of strata which host the Anvil deposits, other than Cambrian, is unknown and the subject of speculation. Tempelman-Kluit (1972), correlated the host rocks with the Kechika Group. Jennings and Jilson (1986) divided the assemblage into a lower non-calcareous phyllite with lenses of limestone and tuff (Mount Mye Formation), a middle thinly laminated calcareous phyllite interbedded with volcanic flows (Vangorda Formation), and an upper thick basalt (Menzie Creek Formation). The Anvil deposits occur in black phyllite between the Mount Mye and Vangorda Formations. Southeast of Faro, near Watson Lake, archaeocyathid-bearing Lower Cambrian limestone lenses, interbedded with non-calcareous shale and tuff resemble the Mount Mye Formation, and overlying silty limestone correlated with the Kechika Group resembles the Vangorda Formation (Abbott, 1981).

Ordovician to Middle Devonian basinal facies are characterized by black graptolitic shale and chert of the Road River Group. In Meilleur River Embayment, the Road River Group comprises undifferentiated, late Ordovician to Middle Devonian argillaceous limestone and variably calcareous shale (Gabrielse et al., 1973; Morrow, 1984). In Misty Creek Embayment, Cecile (1982) included Early to Late Ordovician black shale and chert in Duo Lakes Formations; Late Ordovician to Early Silurian silty limestone and shale in the Cloudy Formation, and Early Devonian silty limestone in the Natla(?) Formation. He suggested that all of these formations be included in the Road River Group. Near MacMillan Pass and Howard's Pass, three subdivisions are Early Ordovician to Early Silurian black, graptolitic, siliceous shale and chert (Duo Lakes Formation equivalent), Silurian orange weathering, pyritic, dolomitic mudstone, and Early Devonian silty limestone (Natla Formation equivalent), (Gordey, 1981b; Abbott, 1983b). The Devonian limestone is a transitional facies that thins westward to shale, and is not included in the Road River Group by Bordey (in prep.). In northern British Columbia, the Road River 'Formation' includes transitional facies with a large proportion of transported clastic carbonate and sandstone derived from MacDonald Platform (Cecile and Norford, 1979; Gabrielse, 1981; MacIntyre, 1983). Three divisions, broadly similar to those near Howards Pass and MacMillan Pass, are late Early to Upper Ordovician black shale with lesser limestone, dolomite, and quartzite, Early Silurian limestone, and Middle Silurian to Early Devonian orange weathering, argillaceous dolomite, shale, and siltstone.

Tectonic Interpretation

Tectonic subsidence curves constructed for the of pre-Devonian miogeocline in the southern Canadian Cordillera (Bond and Kominz, 1984), (Fig. 8), show that transgression and unconformable deposition of Lower Cambrian quartz arenite on the Windermere Supergroup reflect initial cooling and subsidence of a newly rifted continental margin. Whether rifting associated with initial deposition of the Windermere Supergroup is a separate, older event, or part of one process that ended in Lower Cambrian time is unresolved. Bond and Kominz (1984, p. 168) favour the second alternative. Thompson and Eisbacher (1984) postulated a similar origin for the Windermere Supergroup in the northern Cordillera.

The Late Proterozoic to Devonian miogeocline of figure 2 resembles the section (Fig. 8) by Bond and Komintz (1984) from the southern Cordillera. Both can be divided into inner and outer parts. The inner miogeocline, in both, comprises a westward thickening prism of clastic and carbonate rocks which reaches a minimum thickness of 9 km outboard of coincident hinges. Clastic sequences of the Windermere Supergroup mark onset of sedimentation, and are overlain by transgressive Lower Cambrian clastic rocks. Cambrian to Devonian shelf carbonates of the inner miogeocline change to deeper-water carbonate and shale of the outer miogeocline. The outer miogeocline,

north and south, is bounded on the west margin by shallow-water facies. Unconformities bevel progressively younger strata toward the hinge within the inner miogeocline and are also seen within the outer miogeocline. Unconformities in the outer miogeocline in the south are Late Cambrian, Middle Ordovician, and sub-Devonian as in the north. In the south, little of the outer miogeocline is preserved, but descriptions of Middle Cambrian through Middle Ordovician strata generally resemble those in the north (Aitken, 1966). Extensive chert is absent, but much of the outer miogeocline is not preserved, and such a facies may have existed. Late Ordovician and Silurian strata are relatively shallow-water carbonate unlike shale to the north. Lower Devonian strata, are no longer preserved. Discontinuity of the hingeline, aberrant migration of the shelf-basin transition with time, and variations of thickness of the inner miogeocline are more pronounced in the north, suggesting more tectonic instability. Despite these differences, the sedimentation pattern within the miogeocline is similar.

Tempelman-Kluit (1981) interpreted Selwyn Basin and Cassiar Platform to reflect rifting, crustal extension, and subsidence that began with Cambro-Ordovician mafic volcanism, and continued with intermittent volcanism through Silurian and Devonian time. In this interpretation, the volcanics formed an edifice upon which the platformal carbonate rocks were deposited. Selwyn Basin, in this version, is an 'aulacogen' that opened to the west and died in northern British Columbia where Siluro-Devonian carbonates of Cassiar Platform join MacDonald Platform. This interpretation implies that Selwyn Basin represents a unique tectonic element in the Cordilleran miogeocline. However, the similarity of this 'Selwyn Basin' to the outer miogeocline in the southern Cordillera suggests that the extensional processes to which it may be related probably affected other parts of the miogeocline and analogs may have formed elsewhere and are not recognized or are no longer preserved.

Continued, intermittent crustal extension in the northern Cordillera is indicated by late Early Cambrian development of Misty Creek Embayment, Middle(?) Ordovician development of Meilleur River Embayment and Root Basin, volcanism and possibly, by Late Cambrian, Middle or Late Ordovician, Early Silurian, and sub-Devonian unconformities. Although these unconformities may relate to eustatic sea level changes, they do indicate relatively high areas, and changes in their location are possible indicators of tectonism, particularly in the outer miogeocline, where sedimentation was in relatively deep water. Like the Lower Cambrian unconformity, these might reflect uplift caused by crustal thinning and resulting high heat flow.

Mineral Deposits

As mentioned above, the age of the Anvil massive sulphide deposits (Fig. 5 and 6), other than Cambrian, is not known and their relationship to regional events uncertain. Two possibilities are likely. Middle Cambrian block faulting, uplift, and extension preceded deposition of the Kechicka Group elsewhere in the miogeocline. Although the deposits have been included in the Upper Cambrian and Lower Ordovician Kechicka Group, strata below the deposits are lithologically similar to Lower Cambrian strata seen elsewhere and the deposits could be related to the Middle Cambrian event. If not, they are most likely younger and related to continued intermittent rifting that likely accompanied deposition of the volcanic-rich parts of the Kechika Group.

The XY, Anniv, and OP deposits near Howard's Pass (Morganti, 1981), (Fig. 3 and 7) are Early Silurian, and hosted by graphitic shale and chert of the Road River Group. The Road River near the deposits and elsewhere is broadly similar. No nearby regional tectonic event of that age is known, but in northern British Columbia. Early Silurian strata generally overlie older strata unconformably.

The Maxi deposits (Fig. 3 and 7) is in Ordovician or Silurian siliceous, graphitic phyllite of the Road River Group (Blusson, 1978). Intensely transposed laminations and a few bands of coarse-grained sphalerite, less galena, and quartz form discontinuous zones up to several metres wide. A few zones assayed about 3% combined lead and zinc across 1 m to 2 m and one zone assayed about 28% combined lead and zinc across 0.75 m (Brock et al., 1977).

Several small, low-grade occurrences are in shaley off-shelf facies along the northern margin of Cassiar Platform, southwest of Tintina Fault. The JA and Sunset (Fig. 2 and 6) are the most significant of several skarn-related and stratiform occurrences and are found over a strike length of 11 km in Cambro-Ordovician argillaceous limestone, calcareous siltstone, and quartz sandstone of the Kechika Group, and Ordovician-Silurian black calcareous phyllite of the Road River Group

(D.I.A.N.D., 1980, p. 41; Scott, 1978). The showings are in the metamorphic aureole of a Cretaceous stock. Five occurrences are in argillaceous limestone, about 250 m below the top of the Kechika Group, and two less significant occurrences are in black phyllite about 120 m above the Kechika Group. Stratiform galena- and sphalerite-bearing, garnet, siderite, magnetite, and pyrrhotite skarn up to 30 m thick forms two zones in the Kechika Group, the upper Sunset and the lower Piglet. The skarns are lead-rich and return erratic assays ranging from 1% to 21% combined Pb-Zn and 15 - 100 g/t Ag across widths of less than 2 m. About 15 m stratigraphically below the skarn, are stratiform galena- and sphalerite-bearing zones of the lower Sunset occurrence, and along strike at the same stratigraphic position, the main JA and Wayne occurrences. These are well defined, laterally persistent laminations and bands of coarse-grained sphalerite, quartz, minor galena and carbonate in hornfelsed calcareous siltstone. Zones as wide as 5 m assay up to 2% Pb-Zn and no silver. Black shale of the Road River Group hosts two other small occurrences, the upper JA and the main Piglet. These are thin bands of sphalerite, quartz, and siderite up to 10 cm wide. The largest can be traced for about 60 m. High-grade specimens typically assay several per cent Zn and no silver.

The Angie occurrence (Fig. 2 and 7) (D.I.A.N.D., 1980, p. 39; Foster and Holland, 1979), in the same belt as the JA and Sunset, is the largest of several in Early or Middle Devonian sooty limestone and calcareous shale over a strike length of 5 km. Sphalerite, smithsonite, and native silver form pelletoidal disseminations concentrated in bands parallel to bedding and as secondary replacement and vein fillings. The largest zone is 280 m long, lenticular, and erratic. High-grade portions assayed 5.8% Zn and 122.5 g/t Ag across 3.2 m.

In the Gataga district (Fig. 7), MacIntyre (1983) reported two deposits in Middle to Late Ordovician black shale and two in dolomite of Early Silurian age. The Reb occurrence is a 20 m interval of massive, coarse-grained and finely laminated pyrite in probable Middle to Late Ordovician black shale, chert, and siltstone. The Aikie-Sika occurrence is a 0.5 to 1 m thick bed of white crystalline barite that overlies quartz wacke turbidites and is overlain by late Middle to Late Ordovician black shale. On the same property, are several Early Silurian to Middle Devonian bedded and nodular barite horizons. The Early Silurian(?) Ern Prospect is a 10 m to 12 m thick zone of interbedded pyritic quartzite and dolostone, granular pyrite and minor sphalerite mixed with fine-grained silica and barite, baritic- and sphalerite-bearing black cherty mudstone, and breccia comprised of dolomite and quartzite clasts in a pyrite, dolostone, quartz matrix. The zone overlies graptolitic black shale and is overlain by Silurian dolomitic siltstone. The CT prospect is 3 m thick, with massive pyrite and sphalerite at the base, dolostone, pyrite, and sphalerite breccia in the centre, and massive barite and sphalerite at the top. Dolostone in the footwall correlates with that on the Ern prospect and overlying mudstone and siltstone is Early Silurian.

Carbonate-hosted zinc-lead deposits of the inner miogeocline contrast with the sediment-hosted deposits of the outer miogeocline. Deposits at Robb Lake in northern British Columbia and at Goz Creek in the northern Mackenzie Mountains are the largest, with 6 100 000 tonnes grading 7.3% combined Zn-Pb and 1 360 000 tonnes grading 10% combined Zn-Pb respectively (Northcote et al., 1983, p. 201; Sangster and Lancaster, 1976). Numerous occurrences and a few other small deposits (Dawson, 1975) are scattered in Lower Cambrian to Middle Devonian shelf dolomite and less commonly, limestone, mainly near the carbonate-shale transition (MacQueen and Thompson, 1978; McLaren and Godwin, 1979) (Fig. 2). Sphalerite and small amounts of galena are the main sulphides, and white dolomite and some quartz, the gangue. Associated minerals include pyrite, marcasite, calcite, barite, and pyrobitumen (Dawson, 1975; MacQueen and Thompson, 1978). Morphologies of deposits include erratic replacements of host dolomite disseminations and pore fillings in host dolomite, vein fillings of fractures and faults, and stratiform and cross-cutting breccias that resemble those of Mississippi Valley deposits. Dawson (1975) and Sangster and Lancaster (1976) proposed that the breccias are related to solution collapse and karst development, and that the deposits are primarily Mississippi-Valley type, but are remobilized along younger faults in many places. Godwin et al. (1982) concluded from lead isotope data that deposits in Lower Cambrian strata are of that age, whereas those in younger rocks are Devonian. MacQueen and Thompson (1978) proposed that breccias and veins in the Robb Lake deposits are related to Early Mesozoic(?) hydrofracturing and high pore pressures that accompanied dewatering of adjacent shale of the Besa River Formation under deep subsurface conditions.

Middle Devonian to Mississippian

Middle Devonian sedimentation changed dramatically as transgressive shale and chert replaced shelf carbonates of the inner miogeocline, Cassiar Platform and the Interior Platform, and as thick chert conglomerate and related clastic sediments of the Earn Group accumulated in fault-controlled troughs on the outer miogeocline (Fig. 9). On the inner miogeocline and platforms, late Middle and Upper Devonian dark siliceous shale [Hare Indian, Canol formation and other members of the Horn river Group in northern Yukon and District of Mackenzie (Pugh, 1983)], sandstone, siltstone, and silty shale (Imperial Formation in northern and northeastern Yukon), and siliceous siltstone and shale (Besa River Formation in southeastern Yukon and northern British Columbia) reflect this change. The Imperial Formation, unlike the fine-grained formations, is a flysch sequence that was transported southerly and southeasterly form orogenic highlands in northern Yukon and Alaska.

In the outer miogeocline, the latest Early Devonian to Mississippian Earn Group (Gordey et al., 1982) is characterized by a complex internal stratigraphy with internal unconformities and extreme changes in lithology, weathering colour, thickness and facies. Near Howards Pass (Gordey 1981b), upper and lower divisions of shale, chert, quartz sandstone, grit and chert pebble conglomerate locally exceed a combined thickness of 1500 m. The Lower Earn Group spans most of the Devonian and is distinguished regionally by its gun-blue weathering siliceous shale and chert. The Upper Earn Group is Fammenian to Early(?) Mississippian and is mainly brown weathering and less siliceous (Gordey et al., 1982). In the Gataga District, informally named formations comprise Middle and Upper Devonian blue weathering shale, sandstone, and chert conglomerate of the Warneford Formation. In other areas, the two subdivisions of the Earn Group are absent or unrecognized, but the characteristic rocks and complex internal stratigraphy are generally the same. Late Devonian and Early Mississippian alkalic volcanic rocks and related intrusions interfinger with black shale in the Pelly Mountains, south of Tintina Fault (Tempelman-Kluit, 1977a,b; Gordey, 1981a; Mortensen, 1982).

Regional depositional patterns in the Earn Group are poorly understood (Fig. 9). Coarse clastic rocks are concentrated around the margins of the outer miogeocline, and in places lap onto shelf carbonates of the inner miogeocline and Cassiar Platform. Turbidites were deposited as submarine fans(?) in sequences of

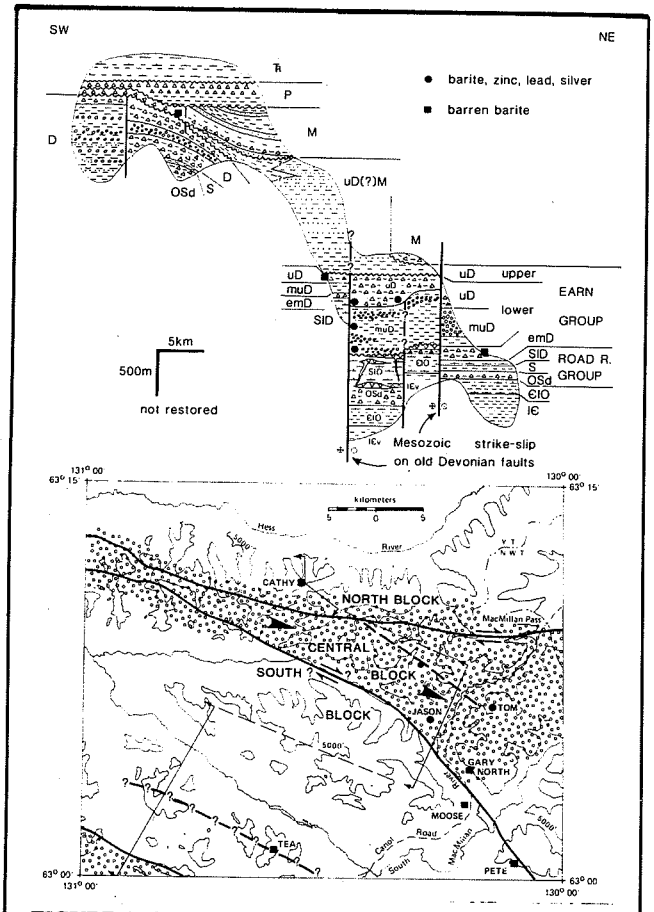

FIGURE 9. Stratigraphic section across the MacMillan Fold Belt (not restored). Location shown in Figure 1. lCv - Vampire FM, ClO - Sekwi, Hess River and Rabbitkettle Fms, OSd - Duo Lakes Fm. Abrupt lateral changes in the stratigraphy reflect syndepositional extensional and/or wrench faults. Mesozoic strike-slip of relatively small, but unknown magnitude along some faults complicates paleogeographic interpretations. Arrows show generalized paleoflow of Devonian turbidites. Barite-zinc-lead deposits are spatially related to the faults.

black shale and chert. A few measured paleocurrent indicators near MacMillan Pass (Bailes et al., 1986), near Howard's Pass (Gordey, 1979) and in northern British Columbia (Gabrielse et al., 1977) suggest westerly sources. Clast composition suggests derivation from the 'grit unit', the Road River Group and other units of outer miogeocline. Subaerial erosion at source is indicated by an abundance of rounded chert clasts. No source areas have been identified, but central regions in the outer miogeocline where Devonian and younger strata are absent are candidates. Near Misty Creek Embayment and MacMillan Pass, westerly derived members of the Earn Group are overlapped by northerly

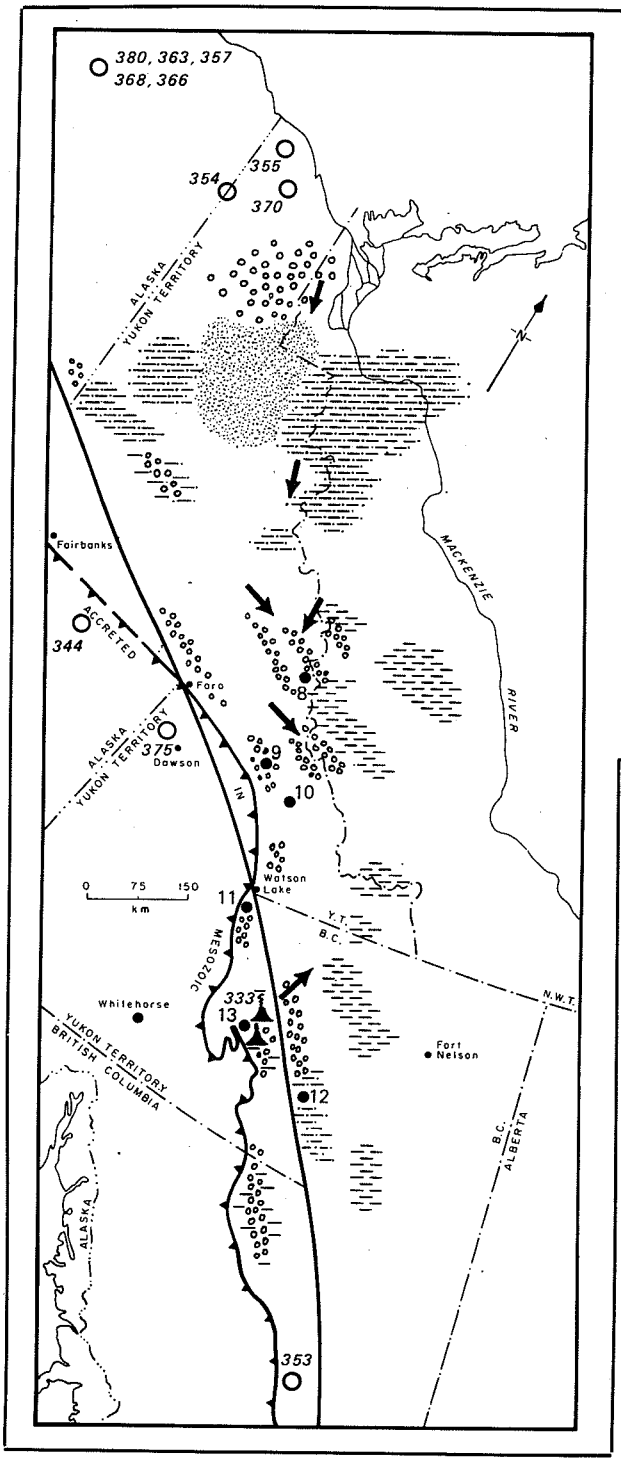

LATE DEVONIAN

- Mainly chert conglomerate with sandstone, siltstone and shale. In northern Yukon, nonmarine in part.
- Mainly sandstone, siltstone and shale of the Imperial Formation
- Siltstone and shale
- Mainly shale, lesser siltstone, and minor sandstone
- Felsic volcanic rocks
- 333 Radiometric ages of intrusions and volcanic rocks

8	MacMillan Pass district
9	Fin occurrence
10	Matt Berry occurrence
11	Clear Lake deposit
12	Gataga district
13	MM deposit, Bnob, Chzer pnough, Joe occurrence

FIGURE 10. Late Devonian paleogeography and location of radiometric ages from middle Paleozoic intrusions and volcanic rocks. Based on Gordey's (1981) reconstruction, Geological Survey of Canada maps and reports, and age determinations summarized by Gabrielse, 1983 and Mortenson, 1982. Arrows show generalized paleoflow.

derived sandstones of the Imperial Formation.

There is little direct evidence for the faulting, uplift and subsidence which must have accompanied erosion and subsequent deposition of the coarse clastics. The MacMillan Pass area is one of the few where the Earn Group has been studied in detail (Abbott, 1982, 1983a, b; Carne, 1979; McClay, 1983; Turner, 1983). There, a complex and prolonged history of Devonian and Mississippian(?) extensional and/or wrench faulting is indicated by variations in thickness, internal stratigraphy, and external stratigraphic relations of the Earn Group (Fig. 10). Faulting occurred mainly in a west-trending Devonian rift, more than 50 km long, whose Mesozoic tectonic expression is the MacMillan Fold Belt (Abbott, 1982, 1983). To the southwest, other faults have been interpreted near the Mississippian Tea barite deposit.

The Lower Earn Group includes five members that are either blue-weathering and siliceous, or brown weathering and clastic-dominated (Fig. 10). Three members in the MacMillan Fold Belt are late Lower to Middle Devonian, dark blue weathering siliceous shale and chert (emDpt of Abbott, 1983b), Middle(?) and Upper Devonian, westerly derived turbidites comprised of brown weathering shale, siltstone, sandstone and chert conglomerate (muDps, muDcg of Abbott 1983b; units 1, 2, 3a of Carne, 1979) and Upper Devonian, silver blue weathering siliceous shale (uDpt of Abbott 1983b, unit 3a of Carne 1979). Near the Tea barite deposit

(Fig. 10), blue weathering siliceous shale and chert conglomerate (units emDps, emDcg of Abbott, 1983b), is abruptly juxtaposed against a brown weathering, coarse clastic sequence (units muDps, muDcg of Abbott, 1983b). Both are included in the Lower Earn Group, but are poorly dated, and cannot be correlated confidently with similar strata in the MacMillan Fold Belt.

In the MacMillan Fold Belt, the Devonian fault zone or Central Block, is bounded by the North and South Blocks (Abbott, 1982). In the North Block, more than 200 m of late Early to Middle Devonian siliceous shale of the lower member conformably overlies the Road River Group. Above the siliceous shale, a well defined, westerly derived, turbidite fan of the middle member is confined to the southern margin of the block. In the Central Block, siliceous shale of the lower member is locally preserved beneath an unconformity above which isolated patches of mafic volcaniclastic rocks as young as Middle Devonian (Givetian) unconformably overlie strata as old as Ordovician. A discontinuity in level of erosion beneath the unconformity which trends northwest from the Tom deposit (Fig. 10) is thought to be a fault related to early uplift and erosion. The middle turbidite member includes brown weathering shale, siltstone, sandstone, and chert conglomerate 50 m to 500 m thick. Local changes in thickness and facies indicate the probability of syn-depositional faults inside the Central Block (Abbott, 1982; K. McClay, pers. comm., 1984). Blue weathering siliceous shale (up to 500 m thick of the upper member) sharply overlies the coarse clastic rocks. In the South Block, the entire Lower Earn Group is less than 300 m thick, and the middle member) contains almost no coarse clastic rocks. Only in the Central Block does the Lower Earn Group record a history of uplift and erosion, mafic volcanism, subsidence, and deposition of relatively thick sequences of coarse clastic rocks.

The Upper Earn Group in the MacMillan Fold Belt (Msp of Abbott, 1983a,b; Unit 4 of Carne, 1979), unconformably overlies the Lower Earn Group, and includes up to 1200 m of northerly derived sandstone, siltstone and shale. Southeastward from MacMillan Pass, the sandstone appears to change facies to shale that is more typical of the Earn Group, and near Tea Deposit, is missing beneath Mississippian quartz arenite, shale and chert. Gordey et al. (1982) considered the unit to be Early Mississippian, but a more recent conodont collection by Abbott indicates that the unit is late Devonian (Fammenian) and time equivalent to the Imperial Formation.

In the MacMillan Fold Belt, Devonian structures affect Mesozoic deformation so that the structural style of each block differs, and the over-all westerly trend is anomalous with the regional northwesterly structural grain. Southerly directed thrusts in the North Block contrast with complex northerly directed folds and high-angle reverse faults, and overprinted north to northwest-trending folds and faults in the Central Block, and relatively simple west-trending folds in the South Block. Right lateral strike-slip along reactivated Devonian faults (Fig. 9) is indicated by truncated Mesozoic folds along the southern margin of the Central Block (K. McClay, pers. comm.), and by juxtaposition of dissimilar Early Paleozoic strata along the northern margin of the Central Block. The amount of displacement is likely to be less than a few kilometres. There is no evidence that contrasts in Devonian stratigraphy across the faults result only from Mesozoic offset.

Interpretation of Devonian paleogeography and style of tectonism is hindered by the late strike-slip movement. In the Central Block, in addition to uplift, erosion, volcanism and subsidence, weak Devonian compression is indicated near the Tom deposit and rarely north-trending folds and axial plane cleavage found only in the Lower Earn Group and older strata (K. McClay, 1983, pers. comm., 1984). this complex tectonic history is perhaps best explained by rifting and wrench faulting. Wrench or strike-slip movement could also account for the absence of an apparent local source area for the tremendous volume of coarse clastic rocks. However, no Devonian strike-slip movement is yet documented. Continued faulting may be indicated by the abrupt changes of thickness and facies(?) in the Upper Earn Group.

Tectonic Interpretation

The dramatic change to coarse clastic sedimentation represented by the Earn Group has been attributed to rifting (Tempelman-Kluit, 1979), strike-slip faulting (Eisbacher, 1983) and collisional orogeny (Gabrielse et al., 1982). Mortensen (1982), in support of Tempelman-Kluit, considers the trace element signature of felsic metavolcanic rocks in the Pelly Mountains to most closely resemble peralkaline volcanics found in other extensional environments.

Eisbacher (1982) speculated that apparent offset and lithologic differences in middle and upper Proterozoic sequences across the north-trending Richardson Fault Array, within and parallel to Richardson

Trough, result from Devonian sinistral strike-slip. However, Cecile (1984a), has traced Lower and Middle Paleozoic strata across the fault zone and discounts Paleozoic displacement. The possibility of northwest-trending strike-slip or wrench faults, confined to the outer miogeocline cannot be discounted, although none of that age are known.

Granitic intrusions from widespread parts of the Cordillera, and the Brooks Range in northern Alaska have yielded mid-Paleozoic U-Pb zircon ages and K/Ar ages (Gabrielse et al., 1982; Mortensen, 1982). Some invade assemblages accreted to North America, but those in the Brooks Range and northern British Columbia intrude North American strata. In the Brooks Range, mainly Middle and Late Devonian ages have been obtained from large stocks and plutons of intermediate composition which form an east-trending belt 300 km long (Dillon et al., 1980). South of the intrusions are a belt of felsic metavolcanic rocks which also give Devonian ages. Dillon et al. concluded that the intrusions and volcanic rocks indicate a mid-Paleozoic magmatic arc. The relationship between the Brooks Range and the Cordilleran orogen is unclear and these intrusions may not relate to the Earn Group. In northern British Columbia, Silurian (429 Ma) and Early Mississippian (353 Ma) zircon ages from a quartz monzonite sill and dyke intruded in late Proterozoic metasediments led Gabrielse (1967) to suggest that the Earn Group represents a westerly derived clastic wedge eroded from an uplifted, ensialic magmatic arc.

Whatever its origin, the Earn Group does not represent an event confined to Selwyn Basin. In central and southern British Columbia, Devonian and Mississippian strata are generally absent in the outer miogeocline, but Struik (1981) correlated locally preserved chert conglomerate, greywacke, sandstone and black shale of the Upper Devonian Guyet Formation with the Earn Group.

Although carbonate deposition continued in the inner miogeocline, the Earn Group may have been more widespread than its present distribution. Widespread Devonian magmatism, in the Brooks Range and northern Yukon, and subsequent deposition of thick westerly and northerly derived flysch suggest a far-ranging and significant tectonic event.

Mineral Deposits

Late Devonian deposits of the Gataga District (Fig. 9) include more than eleven deposits in a linear, northwest-trending belt 180 km long (MacIntyre, 1983). Deposits are at or near the top of the Middle(?) and Upper Devonian Gunsteel 'formation', a unit of blue weathering black chert, and siliceous shale which unconformably overlies the Road River Group. Grey to brown weathering shale and siltstone of the Akie 'formation' are laterally equivalent to and overlie the Gunsteel strata. Westerly derived, grey to brown weathering chert conglomerate, shale, siltstone and sandstone of the Warneford 'formation' are laterally equivalent to and overlie the Akie shales (Jefferson et al.,1983).

The deposits comprise a continuum of mineral facies that include: barren barite; laminated barite, pyrite, sphalerite, and galena; massive pyrite with sphalerite and some galena; and laminated, shaley pyrite with sparse sphalerite and galena (MacIntyre, 1983). These facies are also seen in individual deposits and are well documented in the Cirque deposit (Pigage, 1986). No feeder or stockwork facies or alteration haloes have been recognized, although all deposits are presumed to have been accompanied by a vent (Jefferson et al., 1983).

MacIntyre (1983) and Gabrielse (1981) present evidence that Lower and Middle Devonian carbonate rocks on both sides of the southeast portion of the district may have formed high-standing northwest-trending belts, separated from each other and the main carbonate shelf to the east by shale. Apparently, faults controlled Middle Devonian facies, and later deposition of Upper Devonian sulphide deposits. More local controls of sulphide deposition, although presumed to be fault-controlled sub-basins, have not yet been clearly defined (Jefferson et al., 1983).

In the MacMillan Fold Belt (Fig. 9 and 10), barren and metalliferous barite deposits are at three or more stratigraphic levels in the Lower Earn Group. The deposits show a spatial relationship to the Devonian faults described earlier. In the North Block, barren barite deposits such as the Cathy Deposit are Middle Devonian (Givetian) and occur as lenses as thick as 30 m in siliceous shale of unit emDpt (Abbott, 1981c). In the Central Block, the Tom East and West zones and Jason Main zone are at the top of the coarse clastic turbidite sequence (unit muDps). The Jason South and End zones maybe at the same stratigraphic level or could be slightly older and in the coarse clastics (Turner, 1983; Bailes et al., 1986). The Jason deposits

are apparently localized along the south boundary of the South Block. The Tom deposit is in South Block and may be related to the possible pre-Earn Group fault shown in figure 10. Barren barite deposits such as the Gary North, Moose, and Pete form lenses in siliceous shale of unit uDpt along the southern margin of the Central Block.

In Central Yukon, southwest of Tintina Fault, the Clear Lake massive sulphide deposit (Fig. 2 and 9) is in graphitic, siliceous-shale, chert, sandstone, siltstone and minor chert conglomerate of the Earn Group (Morin, 1981, pp. 85-87). There are no exposures near the deposit and its precise age and stratigraphic position within the Earn Group are unknown. The deposit consists primarily of massive pyrite with variable amounts of sphalerite and galena. A few meters stratigraphically below the deposit are several metres of baritic, tuffaceous phyllite and lapilli tuff. A unit of laminar barite, tuffaceous chert, and chert is spatially associated with the deposit, but the exact relationship to the sulphides is unclear (K. Grapes, pers. comm.). Host rocks and sulphides closely resemble the Driftpile deposit in the Gataga district (R. Carne, pers. comm., 1984).

The Fin occurrence in central Yukon (Fig. 3 and 9), is in an assemblage of chert conglomerate, siltstone, sandstone, black shale, and varicoloured chert of the Earn Group (D.I.A.N.D., 1982, p. 144; Hodgson, 1981). Sphalerite and galena laminae form several zones up to 0.5 m thick in black mudstone. Assays are erratic. One 0.5 m intersection returned grades of 2.90% Pb, 11.40% Zn and 57.1 g/t Ag which are typical for this occurrence (Lane, 1980).

The Matt Berry deposit (Fig. 3 and 9) is in the metamorphic aureole of a Cretaceous batholith and hosted by dark grey to black phyllite and tuffaceous quartz-sericite schist (Ikona, 1977), tentatively assigned to the Devono-Mississippian Earn Group (Blusson, 1966). The schist is about 150 m thick and enclosed by phyllite. A 10 m interval near the upper phyllite-schist contact includes three bands of massive sulphides comprised of galena, sphalerite, pyrite, and minor chalcopyrite in a quartz-siderite gangue (Findlay, 1969, p. 48). The largest band is 1 m to 2 m thick and contains inferred reserves of 533 316 tonnes grading, 6.1% Pb, 4.6% Zn, and 102.63 g/t Ag (Ikona, 1977).

Mississippian alkalic volcanic rocks, in the Pelly Mountains southwest of Tintina Fault (Fig. 2 and 9), host four small massive sulphide deposits and a number of more distal, barren barite deposits. The deposits are in a thrust panel comprised of about 600 m of submarine volcaniclastic rocks and trachytic lava flows which are intercalated with black shale and intruded by coeval hypabyssal syenite plugs (Morin, 1977). The deposits are volcanogenic and resemble Kuroko deposits (Mortensen and Godwin, 1982). The MM, which is the largest and only one studied in detail consists of several narrow lenses up to 2 m thick in volcaniclastic rocks near the flanks of a trachyte plug (Morin, 1977; Mortensen and Godwin, 1982). Sulphides are mainly pyrite and pyrrhotite with varying amounts of galena, sphalerite, chalcopyrite stringers. Other small sulphide lenses occur throughout 75 m of strata above the main lens and persist laterally for over 3 km. Barite and pyrite content increases away from the plug. The similar Bnob, Chzerpnough, and Joe occurrences are nearby.

Mississippian to Triassic

Locally preserved, fine-grained clastics and chert of relatively shallow water, stable marine origin define three regionally distinct Carboniferous, Permian, and Triassic units separated by unconformities. There is no sharp distinction between inner and outer miogeocline.

In northern British Columbia and southeast Yukon, Mississippian formations, reach a maximum thickness of about 600 m and include limestone, calcareous shale, and sandstone of the Early Mississippian Flett Formation in the north, time-equivalent limestone, dolomite, and chert of the Prophet Formation in the south, and overlying easterly derived terrigenous and shallowmarine clastic and carbonate rocks of the Upper Mississippian Stoddart Group (Bamber et al., 1968; Bamber and Mamet, 1978). All grade westward to shales of the Besa River Formation along a north-trending facies boundary which migrates upward stratigraphically to the west.

Unconformably above the Mississippian strata are thin calcareous and siliceous shale, siltstone, and sandstone of the Permian Kindle Formation, and overlying chert, the Permian Fantasque Formations reach maximum thicknesses of about 200 m and 40 m, respectively (Bamber et al., 1968; Bamber and Mamet, 1978).

Disconformably(?) above the condensed Permian are thick Triassic calcareous sandstone,

siltstone, shale and limestone of the Toad, Grayling, Liard, and other formations. The Triassic assemblage thickens to a minimum 1500 m and fines westward (Pelletier, 1964).

Near MacMillan and Howard's Pass, the succession includes three formations (Gordey, in prep., Abbott, in prep.). Unconformably above the Earn Group, Mississippian dark siliceous shale and siltstone up to 500 m thick have discontinuous marine quartz sandstone members up to 30 m thick. Late Mississippian, bioclastic limestone is locally preserved near the top. Southwest of MacMillan Pass near the Tea barite deposit, a few conodont collections indicate that the quartzite unit changes abruptly westward to thin chert. Unconformably above the Mississippian rocks are about 250 m of dark weathering quartz siltstone and pale green weathering shale overlain by orange weathering green chert and shale. Lower Permian conodonts were found in the chert and the units may correlate with the Kindle and Fantasque Formations. More than 750 m of Triassic calcareous sandstone, siltstone, shale, and silty limestone unconformably(?) overlies the Permian chert. In the Anvil Range, broadly similar strata include Lower Mississippian limestone and orange weathering chert, an overlying sequence of dark shale, siltstone, and minor chert (containing Permian conodonts), and well bedded Triassic silty limestone and calcareous shale. In the Pelly Mountains, southwest of Tintina Fault are about 100 m of Mississippian orange weathering chert and shale, 30 m of Permian shale and sandstone, and 500 m of Upper Triassic silty limestone and shale (Tempelman-Kluit, 1977a,b; Gordey, 1981a). Northeast of Dawson, near the Alaska border, Permian limestone of the Takhandit Formation, about 30 m thick, unconformably overlie Earn Group and Road River strata. It is overlain by about 70 m of Triassic siltstone and limestone. Upper Jurassic shale and siltstone more than 500 m thick disconformably overlie the Triassic limestone (Tempelman-Kluit, 1970).

Tectonic Interpretation

The Mississippian to Triassic marine strata indicate relative tectonic stability in comparison to the volcanic-bearing Cambro-Devonian assemblage of the outer miogeocline and the complex, coarse clastic Devono-Mississippian Earn Group.

Mineral Deposits

The Tea barite deposit (Fig. 10) and several nearby barite occurrences are apparently Early Mississippian (Dawson and Orchard, 1982) and of the same age as the lowest part of the Mississippian quartzite unit. Relations between the deposit and that formation are not yet clear because fossil control is poor, but the barite seems to occur where the unit changes abruptly westward from quartz arenite and siliceous shale to chert. Host rocks are blue-weathering siliceous shale and chert that are indistinguishable from those of the Earn Group.

Elsewhere, no sediment-hosted deposits are known from the Mississippian to Triassic assemblage.

Discussion and Summary

Links between sediment-hosted stratiform zinc, lead deposits in the northern Canadian Cordillera and their regional setting are tenuous. Deposits are known to occur within Cambrian to Mississippian strata of the outer Cordilleran miogeocline but not in older strata of the Late Proterozoic Windermere Supergroup, or in most late Paleozoic or Early Mesozoic strata. Prerequisites for deposit formation include the thick sequences of Late Proterozoic and Lower Cambrian clastic rocks, which may have been the source of metals (Lydon, 1983), and the underlying, thin, tectonically unstable continental crust.

Periodic Cambrian to Middle Devonian tectonic instability, crustal extension, and local high heat flow in the outer part of the miogeocline is indicated by: late-Cambrian, middle(?) Ordovician, early Silurian and sub-Devonian(?) unconformities, scattered volcanism, aberrant middle Cambrian and middle(?) Ordovician migration of the shelf-basin transition, development of Cassiar Platform, and linear reefoidal limestone deposits of Middle Cambrian and Middle Devonian age. These features can be related broadly to the deposits, but specific ties are lacking.

In contrast, deposits in the Earn Group appear related to an important, more specific event marked by local uplift and subsidence, extension and, possibly, local compression, which resulted in Middle(?) and Late Devonian to Mississippian sedimentation characterized by westerly derived coarse clastic turbidites, and destruction of older sedimentation patterns. Some deposits in the Earn Group are clearly related to syndepositional faults. The Earn Group has been variously attributed to rifting, collisional orogeny, and strike-slip faulting.

Comparison of partially restored cross sections through the northern and southern Cordilleran miogeocline suggest that Cambrian to Middle Devonian deposits occur in a tectonic setting that may have extended the length of the western continental margin of North America. Strata equivalent to the Earn Group was deposited locally at least in the south, but is no longer preserved in most places.

Acknowledgments

We are grateful to H. Gabrielse, M. Cecile, and R. Carne for critical reviews that improved the manuscript. Discussions with many people, too numerous to mention, added to our knowledge of the Cordilleran miogeocline and its mineral deposits. In particular, we thank Bob Thompson.

REFERENCES

Abbott, J.G., 1971, Structure and stratigraphy of the Mount Hundere area, southeastern Yukon; unpublished M.A.Sc. thesis, Queen's University, Kingston, Ontario, 111 p.

Abbott, J.G., 1981a, A new geological map of Mount Hundere and the area north; in Yukon Geology and Exploration 1979-80; Department of Indian Affairs and Northern Development Canada, Northern Affairs Program, Exploration and Geological Services Division, Whitehorse, Yukon, p. 45-50.

Abbott, J.G., 1981b, Walt property description; in Yukon Geology and Exploration 1979-80; Department of Indian Affairs and Northern Development Canada, Northern Affairs Program, Exploration and Geological Services Division, Whitehorse, Yukon, p. 216-217.

Abbott, J.G., 1982, Structure and stratigraphy of the MacMillan Fold Belt: evidence for Devonian faulting; in Yukon Geology and Exploration 1981; Department of Indian Affairs and Norther Development Canada, Norther Affairs Program, Exploration and Geological Services Division, Whitehorse, Yukon, p. 22-23.

Abbott, J.G., 1983a, Possible mid-Paleozoic faults near barite and metalliferous barite deposits, Macmillan Pass, Yukon; in Geological Association of Canada and Mineral Association of Canada (program with abstracts); Vol. 8.

Abbott, J.G., 1983b, Geology, MacMillan Fold Belt; Department of Indian Affairs and Northern Development Canada, Northern Affairs Program, Exploration and Geological Services Division, Whitehorse, Yukon, Open File Maps.

Armstrong, R.L., Eisbacher, G.H., and Evans, P.D., 1982, Age and stratigraphic-tectonic significance of Proterozoic diabase sheets, Mackenzie Mountains, northwestern Canada; Canadian Journal of Earth Sciences, Vol. 19, p. 316-323.

Bailes, R.J., Smee, B.W., Blackadar, D.W., Gardner, H.D., 1986, Geology of the Jason lead-zinc-silver deposits, Macmillan Pass, Yukon Territory, *in* Morin, J.A., ed., Mineral deposits of the Northern Cordillera: Canadian Institute of Mining and Metallurgy. Special Volume 37, p. 87-99

Bamber, E.W., Taylor, G.C., and Proctor, R.M., 1968, carboniferous and Permian stratigraphyof northeastern British Columbia; Geological Survey of Canada, Paper 68-15, 25 p.

Bamber, E.W. and Mamet, B.L., 1978, Carboniferous biostratigraphy and correlation, northeastern British Columbia and southwestern district of Mackenzie; Geological Survey of Canada, Bull. 266, 65 p.

Basset, H.G., and Stout, J.G., 1967, Devonian of Western Canada; in International Symposium on the Devonian System, Calgary, 1967; Alberta Soc. of Petr. Geol., Vol. 1. p. 717-752.

Blusson, S.L., 1966, Frances Lake, Yukon Territory and District of Mackenzie; Geological Survey of Canada, Map 6-1966.

Blusson, S.L., 1976, Selwyn Basin, Yukon and District of Mackenzie, in Report of Activities; Geological Survey of Canada, Paper 76-1A, p. 131-132.

Blusson, S.L., 1978, Regional geologic setting of lead-zinc deposits in Selwyn Basin, Yukon; in Current Research, Part A; Geological Survey of Canada, Paper 78-1A p. 77-80.

Bond, G.C., and Kominz, M.A., 1984, Construction of tectonic subsidence curves for the early Paleozoic miogeocline, southern Canadian Rocky Mountains: Implications for subsidence mechanisms, age of breakup, and crustal thinning; Geol. Soc. Amer. Bull. Vol. 95, No. 2, p. 155-173.

Brock, J.S., Guild, J.D., McArthur, G.F., and McArthur, M.L., 1977, Preliminary investigation of the Maxi zinc-lead occurences and surrounding region; Department of Indian and Northern Affairs Canada, Northern Affairs Program, Exploration and Geological Services Division, Whitehorse, Yukon, Assessment Rpt. 061654, 25 p.

Campbell, R.B., 1967, Reconnaissance geology of Glenlyon map area, Yukon Territory; Geological Survey of Canada, Mem. 352.

Campbell, R.B., Mountjoy, E.W., and Struik, L.C., 1982, Structural cross section through south-central Rocky and Cariboo mountains to the Coast Range; Geological Survey of Canada, Open File 844.

Carne, R.C., 1976, Stratabound barite and lead-zinc-barite deposits in eastern Selwyn Basin; Department of Indian and Northern Affairs Canada, Northern Affairs Program, Exploration and Geological Services Division, Whitehorse, Yukon, Open File Rpt. EGS 1976-16, p. 1-41.

Carne, R.C., 1979, Geological setting and stratiform mineralization, Tom claims, Yukon Territory; Department of Indian Affairs and Northern Development Canada, Northern Affairs Program, Exploration and Geological Services Division, Whitehorse, Yukon, Rpt. EGS 1979-4, 30 p.

Carne, R.C. and Cathro, R.J., 1982, Sedimentary exhalative (sedex) zinc-lead-silver deposits, northern Canadian Cordillera; CIM Bulletin, Vol. 75, No. 840, p. 66-78.

Cecile, M.P., 1981 Geology of northeast Niddery Lake map area, NTS 105 0 9, 10, 15, 16; Geological Survey of Canada, Open File 765.

Cecile, M.P., 1982, the Lower Paleozoic Misty Creek Embayment, Selwyn Basin, Yukon and Northwest Territories; Geological Survey of Canada, Bull. 335, 78 p.

Cecile, M.P., 1984a, Evidence against large-scale strike-slip separation of Paleozoic strata along the Richardson-Hess fault system, northern Canadian Cordillera; Geology, Vol. 12, No. 7, p. 385-448.

Cecile, M.P., 1984b, Geology of Northeast Niddery map area; Geological Survey of Canada, Open File 1006.

Cecile, M.P., and Norford, B.S., 1979, Basin to platform transition, lower Paleozoic strata of Ware and Trutch map area, northeastern British Columbia, in Current Research, Part A; Geological Survey of Canada, Paper 79-1A, p. 219-226.

Dawson, K.M., 1975, Carbonate-hosted zinc-lead deposits of the northern Canadian Cordillera; in Report of Activities; Geological Survey of Canada, Paper 75-1A, p. 239-242.

Dawson, K.M., 1977, Regional metallogeny of the northern Cordillera; in Report of Activities, Part A; Geological Survey of Canada, Paper 77-1A, p. 1-4.

Dawson, K.M. and Orchard, M.J., 1982, Regional metallogeny of the northern Cordillera: biostratigraphy, correlation and metallogenic significance of bedded barite occurrences in eastern Yukon and western District of Mackenzie; in Current Research, Part C; Geological Survey of Canada, Paper 82-1C, p. 31-38.

Department of Indian Affairs and Northern Development, 1980, Mineral Industry Report 1978; Department of Indian Affairs and Northern Development Canada, Northern Affairs Program. Exploration and Geological Services Division, Whitehorse, Yukon, p.

Department of Indian Affairs and Northern Development, 1981, Yukon Exploration and Geology 1979-80; Department of Indian Affairs and Northern Development Canada, Northern Affairs Program, Exploration and Geological Services Division, Whitehorse, Yuko, 364 p.

Department of Indian Affairs and Northern Development, 1982, Yukon Exploration and Geology 1981; Department of Indian Affairs and Northern Development Canada, Northern Affairs Program, Exploration and Geological Services Division, Whitehorse, Yukon, 281 p.

Dillon, J.T., Pessel, G.H., Chen, J.H., and Veach, N.C., 1980, Middle Paleozoic magmatism and orogenesis in the Brooks Range, Alaska; Geology, Vol. 8, No. 7, p. 338-343.

Eisbacher, G.H., 1981, Sedimentary tectonics and glacial record in the Windermere Supergroup, Mackenzie Mountains, northerwestern Canada; Geological Survey of Canada, Paper 80-27.

Eisbacher, G.H., 1983, Devonian-Mississippian sinistral transcurrent faulting along the cratonic margin of western North America: A hypothesis; Geology, Vol. 11, No. 1. p. 7-10.

Evenchick, C.A., and Gabrielse, H., 1984, Basement gneisses and late Proterozoic paleogeography in the northern Canadian Cordillera; Geological Society of America (program with abstracts), Vol. 16, No. 5, p. 282.

Evenchick, C.A., Parrish, R.R., and Gabrielse, H., 1984, Precambrian gneiss and late Proterozoic sedimentation in northcentral British Columbia; Geology, Vol. 12, No. 4, p. 233-237.

Findlay, D.C., 1969, The mineral industry of Yukon and southwest District of Mackenzie, 1968; Geological Survey of Canada, Paper 69-55, 71 p.

Foster, H.F. and Holland, R.T., 1979, Woodside project, chapter 2; Department of Indian Affairs and Northern Development Canada, Northern Affairs Program, Exploration and Geological Services Division, Whitehorse, Yukon Assessment Rpt. 090463.

Fritz, W.H., 1979b, Cambrian Stratigraphy in the northern rocky Mountains, British Columbia; in Current Research, Part B; Geological Survey of Canada, Paper 79-1B, p. 99-109.

Fritz, W.H., Narbonne, G.M., and Gordey, S.P., 1983, Strata and trace fossils near the Precambrian-Cambrian boundary, Mackenzie, Selwyn, and Wernecke Mountains, Yukon and Northwest Territories; in Current Research, Part B; Geological Survey of Canada, Paper 83-1B p. 365-375.

Gabrielse, H., 1967, Tectonic evolution of the northern Canadian Cordillera, Canadian Journal of Earth Sciences, Vol. 4, p. 271-298.

Gabrielse, H., 1975, Geology of Fort Grahame E 1/2 map are, British Columbia; Geological Survey of Canada, Paper 75-33.

Gabrielse, H., 1981, Stratigraphy and structure of Road River and associated strata in Ware (west half) map area, northern Rocky Mountains, British Columbia; Geological Survey of Canada, Paper 81-1A, p. 201-207.

Gabrielse, H., 1984, Major dextral transcurrent displacements along the northern Rocky Mountain trench and related lineaments in north central British Columbia; Geological Society of America Bulletin, Vol. 96, p. 1-24.

Gabrielse, H., and Blusson, S.L., 1969, Geology of Coal River map area, Yukon Territory and District of Mackenzie (95 D); Geological Survey of Canada, Paper 68-38, 22 p.

Gabrielse, H., Blusson, S.L., and Roddick, J.A., 1973, Geology of Flat River, Glacier Lake, and Wrigley Lake map areas, District of Mackenzie and Yukon Territory; Geological Survey of Canada, Mem. 366.

Gabrielse, H., Loveridge, W.D., Sullivan, R.W., and Stevens, R.D., 1982, U-Pb measurements on zircon indicate middle Paleozoic plutonism in the Omineca Crystalline Belt, north-central British Columbia; in Current Research, Part C; Geol. Surv. Can., Paper 82-1C, pp. 139-146.

Godwin, C.I., Sinclair, A.J., and Ryan, B.J., 1982, Lead isotope models for the genesis of carbonate-hosted Zn-Pb, shale-hosted Ba-Zn-Pb, and silver-rich deposits in the northern Canadian Cordillera; Econ. Geol., Vol. 77, p. 82-94.

Gordey, S.P., 1979, Stratigraphy of southeastern Selwyn Basin in the Summit Lake area, Yukon and Northwest Territories, in Current Research, Part A; Geol. Surv. Can., Paper 78-1A, pp. 43-48.

Gordey, S.P., 1981a, Stratigraphy, structure and tectonic evolution of southern Pelly Mountains in the Indigo Lake area, Yukon Territory; Geol. Surv. Can., Bull. 318, p.

Gordey, S.P., 1981b, Geology of Nahanni Map Area, Yukon Territory and southern District of Mackenzie; Geol. Surv. Can., Open File 780.

Gordey, S.P., 1982, Structure section, south central Mackenzie Mountains, N.W.T.; Geol. Surv. Can., Open File 809.

Gordey, S.P., 1983, Thrust faults in the Anvil Range and a new look at the Anvil Range Group, south-central Yukon Territory; in Current Research, Part A; Geol. Surv. Can., Paper 83-1A, pp. 225-227.

Gordey, S.P., in prep., Geology of Nahanni map-area; Geol. Surv. Can.

Gordey, S,P., Abbott, J.G., and Orchard, M.J., 1982, Devono-Mississippian (Earn Group) and younger strata in east-central Yukon; in Current Research, Part B; Geol. Surv. Can., Paper 82-1B, pp. 93-100.

Green, L.H., 1972, Geology of Nash Creek, Larsen Creek and Dawson map-areas, Yukon; Geol. Surv. Can., Mem. 364, p.

Hodgson, T.W., 1981, Geology, geochemistry, Fin property; Dept. of Indian Affairs and Northern Development (Canada), Northern Affairs Program, Expl. and Geol. Serv. Div., Whitehorse, Yukon, Assessment Rept. 909877, 6 p.

Ikona, C.K., 1977, Report on Barb 1 to 15 mineral claims; Dept. of Indian Affairs and Northern Development (Canada), Northern Affairs Program, Expl. and Geol. Serv. Div., Whitehorse, Yukon, Assessment Rept. 061798, 14 p.

Jefferson, C.W., and Ruelle, J.C.L., 1986, the Late Proterozoic Redstone Copper Belt, Mackenzie Mountains, Northwest Territories, *in* Morin, J.A., ed., Mineral deposits of the northern Cordillera: Canadian institute of Mining and Metallurgy, Special Volume 37, p. 154-168.

Jefferson, C.W., Kilby, D.B., Pigage, L.C., and Roberts, W.J., 1983, The Cirque barite-lead-zinc deposits, northeast British Columbia, in Short Course in Sediment-hosted Stratiform Lead-zinc Deposits, D.F. Sangster, ed.; Min. Assoc, Can. Short Course Handbook, Vol. 8, pp. 121-140.

Jennings, D.S. and Jilson, G.A., Geology and sulphide deposits of Anvil Range, Yukon, *in* Morin, J.A., ed., Mineral deposits of the northern Cordillera: Canadian Institute of Mining and Metallurgy, Special Volume 37, p. 319-361.

Lane, R.W., 1980, Diamond drilling, Fin property; Dept. of Indian Affairs and Northern Development (Canada), Northern Affairs Program, Expl. and Geol. Serv. Div., Whitehorse, Yukon, Assessment Rept. 090658.

Large, D.E., 1981, Sediment-hosted submarine exhalative lead-zinc deposits - a review of their geological characteristics and genesis; in Handbook of Stratabound and Stratiform Ore Deposits, Vol. 9, K.H. Wolf, ed.; pp. 459-507.

Large, D.E., 1983, Sediment-hosted massive sulphide lead-zinc deposits: an empirical model, in Short Course in Sediment-hosted Stratiform Lead-zinc Deposits, D.F. Sangster, ed.; Min. Assoc. Can. Short Course Handbook Vol. 8, pp. 1-29.

Lenz, A.C., 1972, Ordovician to Devonian history of northern Yukon and adjacent District of Mackenzie; Can. Petr. Geol. Bull., Vol. 20, No. 2, pp. 321-336.

Lydon J.W., 1983, Chemical parameters controlling the origin and deposition of sediment-hosted, stratiform lead-zinc deposits; in Short Course in Sediment-hosted Stratiform Lead-zinc Deposits (D.F. Sangster ed.); Min. Assoc. Can. Short Course Handbook, pp. 175-250.

Lydon, J.W., Lancaster, R.D., and Karkkainen, P., 1979, Genetic controls of Selwyn Basin stratiform barite/sphalerite/galena deposits: an investigation of the dominant barium mineralogy of the Tea Deposit, Yukon; in Current Research, Part B; Geol. Surv. Can., Paper 79-1B, pp. 223-229

MacIntyre, D.G., 1983, Geology and stratiform barite-sulphide deposits of the Gataga District, northeastern British Columbia; in Short Course in Sediment-hosted Stratiform Lead-zinc Deposits, D.F. Sangster, ed.; Min. Assoc. Can., Short Course Handbook, pp. 85-120.

MacQueen, R.W. and Thompson, R.I., 1978, Carbonate-hosted lead-zinc occurrences in northeastern British Columbia with emphasis on the Robb Lake deposit; Can. Jour. Earth Sci., Vol. 15, pp. 1737-1762.

McClay, K.R., 1983, Structure of the Tom Deposit, Yukon Territory; Geol. assoc. of Can. (program with abstract), Vol. 8, p. A45.

McLaren, G.P. and Godwin, C.I., 1979, Stratigraphic framework of lead-zinc deposits in the northern Cordillera northeast of the Tintina Trench; Can. Jour. Earth Sci., Vol. 16, No. 2, pp. 380-386.

Morganti, J.M., 1981, Sedimentary-type stratiform ore deposits; Some models and a new classification; Geoscience Canada, Vol. 8, No. 2, pp. 65-75.

Morin, J.A., 1977, Ag-Pb-Zn mineralization in the MM deposit and associated Mississippian felsic volcanic rocks in the St. Cyr Range, Pelly Mountains; in Mineral Industry Report 1976; Dept. of Indian Affairs and Northern Development (Canada), Northern Affairs Program, Expl. and Geol. Serv. Div. Whitehorse, Yukon, Rpt. EGS 1977-1, pp. 83-97.

Morin, J.A., 1979, A preliminary report on Hart River (116 A 10) -- A Proterozoic massive sulphide deposit; in Mineral Industry Report 1977, Yukon Territory, Dept. of Indian Affairs and Northern Development (Canada), Northern Affairs Program, Expl. and Geol. Serv. Div. Whitehorse, Yukon, E.G.S. 1978-9, pp. 22-24.

Morin, J.A., 1981, A note on rock geochemistry of the Clear Lake Massive Sulphide; in Yukon Geology and Exploration, 1979-80, Dept. of Indian Affairs and Northern Development (Canada), Northern Affairs Program, Expl. and Geol. Serv. Div., Whitehorse, Yukon, 364 p.

Morrow, D.W., 1984, Sedimentation in Root Basin and Prairie Creek Embayment-Siluro-Devonian, Northwest Territories, Can. Petr. Geol. Bull. Vol. 32, No. 2, pp. 162-189.

Mortensen, J.K., 1982, Geological setting and tectonic significance of Mississippian felsic metavolcanic rocks in the Pelly Mountains, southeastern Yukon Territory; Can. Jour. Earth Sci., Vol. 19, pp. 8-22.

Mortensen, J.K. and Godwin, C.I., 1982, Volcanogenic massive sulfide deposits associated with highly alkaline rift volcanics in the southeastern Yukon Territory; Econ. Geol., Vol. 77, pp. 1225-1230.

Norris, D.K., 1982, Geology, Wind, River, Yukon Territory, Geol. Surv. Can. Map 1528A.

Payne, M.W. and Allison, C.W., 1981, Paleozoic continental-margin sedimentation in east-central Alaska; Geology, Vol. 9, pp. 274-279.

Pelletier, B.R., 1964, Triassic stratigraphy of the Rocky Mountain Foothills between Peace and Muskwa Rivers, northeastern British Columbia; Geol. Surv. Can., Paper 63-33, 89 p.

Pugh, D.C., 1983, Pre-Mesozoic geology in the subsurface of Peel River map area, Yukon Territory and District of Mackenzie; Geol. Surv. Can., Mem. 401, 61 p.

Roots, C.F., 1982, Ogilvie Mountains Project: Part B. Volcanic rocks in north-central Dawson map area; in Current Research, Part A; Geol. Surv. Can., Paper 82-1A, pp. 411-414.

Roots, C.F. and Moore, J.M., 1983, Proterozoic and early Paleozoic volcanism in the Ogilvie Mountains: an example from Mount Harper, west-central Yukon; in Yukon Exploration and Geology 1982; Dept. of Indian Affairs and Northern Development (Canada), Northern Affairs Program, Expl. and Geol. Serv. Div., Whitehorse, Yukon.

Ruelle, J.C.L., 1982, Depositional environments and genesis of stratiform copper deposits of the Redstone Copper Belt, Mackenzie Mountains, N.W.T.; in Precambrian Sulphide Deposits (R.W. Hutchinson, C.D. Spence and J.M. Franklin, eds.); Geol. Assoc. Can., Special Paper 25, pp. 701-738.

Sangster, D.F. and Lancaster, R.D., 1976, Geology of Canadian lead and zinc deposits; in Report of Activities, Part A, Geol. Surv. Can., Paper 76-1A, pp. 301-310.

Scott, G.H., 1977, Report on the geological, geochemical and geophysical surveys and diamond drilling and trenching on the MONI, PMJ, JANE, TELE, KIRK, AL RIM, EEL, and ANGIE mineral claims; Dept. of Indian Affairs and Northern Development (Canada), Northern Affairs Program, Expl. and Geol. Serv. Div., Whitehorse, Yukon, Assessment Rpt. 090351.

Stewart, J.H., 1972, Initial deposits in the Cordilleran geosyncline: evidence of a late Precambrian (<850 m.y.) continental separation; Geol. Soc. Amer. Bull., Vol. 83, pp. 1345-1360.

Stewart, J.H., 1976, Late Precambrian evolution of North America: plate tectonic implications; Geology, Vol. 4, pp. 11-15.

Struik, L.C., 1981, A re-examination of the type area of the Devono-Mississippian Cariboo Orogeny, central British Columbia; Can. Jour. Earth Sci., Vol. 18, pp. 1767-1775.

Taylor, G.C., 1979, Trutch and Ware east half map-areas; Geol. Surv. Can., Open File Rpt. 606.

Taylor, G.C. and Stott, D.F., 1973, Tuchodi Lakes map-area, British Columbia; Geol. Surv. Can., Mem. 373.

Taylor, G.C., Cecile, M.P., Jefferson, C.W., and Norford, B.S., 1979, Stratigraphy of Ware (east half) map area, northeastern British Columbia; in Current Research, Part A; Geol. Surv. Can., Paper 79-1A, pp. 227-231.

Tempelman-Kluit, D.J., 1970, Stratigraphy and structure of the "Keno Hill Quartzite" in Tombstone River-Upper Klondike River map-areas, Yukon Territory (116B/7, B/8); Geol. Surv. Can., Bull. 180, 102 p.

Tempelman-Kluit, D.J., 1972, Geology and origin of the Faro, Vangorda, and Swim concordant zinc-lead deposits, central Yukon Territory, Geol. Surv. Can., Bull. 208.

Tempelman-Kluit, D.J., 1977a, Stratigraphy and structural relations between the Selwyn Basin, Pelly Cassiar Platform, and Yukon Crystalline Terrane in the Pelly Mountains, Yukon; in Report of Activities, Part A; Geol. Surv. Can., Paper 76-1A, pp. 223-227.

Tempelman-Kluit, D.J., 1977b, Geology of Quiet Lake and Finlayson Lake map areas, Yukon Territory (105 F and G); Geol. Surv. Can., Open File 486.

Tempelman-Kluit, D.J., 1979, Transported ophiolite, cataclasite, and granodiorite in Yukon: evidence of arc-continent collision; Geol. Surv. Can., Paper 79-14, 27 p.

Tempelman-Kluit, D.J., 1981, Craig Property description: in Yukon Geology and Exploration 1979-80; Dept. of Indian Affairs and Northern Development (Canada), Northern Affairs Program, Expl. and Geol. Serv. Div., Whitehorse, Yukon, pp. 225-230.

Tempelman-Kluit, D.J., Gordey, S.P., and Read, B.C., 1976, Stratigraphy and structural studies in the Pelly Mountains, Yukon Territory; in Current Research, Part A, Geol. Surv. Can., Paper 76-1A, pp. 97-106.

Tempelman-Kluit, D.J. and Wanless, R.K., 1980, Zircon ages for the Pelly gneiss and Klotassin granodiorite in western Yukon; Can. Jour. Earth Sci., Vol. 17, No. 3, pp. 297-306.

Thompson, R.I. and Eisbacher, G.H., 1984, Late Proterozoic rift assemblages, northern Canadian Cordillera; Geol. Soc. of Amer., (program with abstracts), Vol. 16, No. 5, p. 336.

Thompson, R.I. and Roots, C.F., 1982, Ogilvie Mountains Project, Yukon; Part A: A new regional mapping program; in Current Research, Part A; Geol. Surv. Can., Paper 82-1A, pp. 403-411.

Turner, R., 1983, Geology of the South Zone deposits, Jason Property, MacMillan Pass area, Yukon; in Yukon Exploration and Geology 1983; Dept. of Indian Affairs and Northern Development (Canada), Northern Affairs Program, Expl. and Geol. Serv. Div., Whitehorse, Yukon, pp. 105-114.

Walker, S.E., 1982, A petrographic study of volcanic rocks of MacMillan Pass Area, Yukon; unpubl. M.Sc. thesis, Queen's University, Kingston, Ont.

Wheeler, J.O., Aitken, J.D., Berry, M.J., Gabrielse, H., Hutchinson, W.W., Jacoby, W.A., Monger, J.W.H., Niblett, E.R., Norris, D.K., Price, R.A., and Stacey, R.A., 1972, The Cordilleran structural province; in Variations in Tectonic Styles in Canada, R.A. Price and R.J.W. Douglas, eds.; Geol. Assoc. Can., Special Paper No. 11, pp. 1-82.

Yeo, G.E., 1981, The late Proterozoic Rapitan glaciation in the northern Cordillera; in Proterozoic Basin of Canada, F.H.A. Campbell, ed.; Geol. Surv. Can., Paper 81-10, pp. 25-46.

Yeo, G.M. 1986, Iron-Formation in the Late proterozoic Rapitan Group, Yukon and Northwest Territories *in* Morin, J.A., ed., Mineral deposits of the northern Cordillera: Canadian Institute of Mining and Metallurgy, Special Volume 37, p. 142-153.

Young, G.M., 1982, The late Proterozoic Tindir Group, east-central Alaska: evolution of a continental margin; Geol. Soc. Amer. Bull., Vol. 93, pp. 759-783.

Young, G.M., Jefferson, C.W., Delaney, G.D., and Yeo, G.M., 1979, Middle and Late Proterozoic evolution of the northern Canadian Cordillera and Shield; Geology, Vol. 7, pp. 125-128.

CHARACTER AND PALEOTECTONIC SETTING OF DEVONIAN STRATIFORM SEDIMENT-HOSTED ZN, PB, BA DEPOSITS, MACMILLAN FOLD BELT, YUKON

J.G. Abbott
Exploration and Geological Services Division
Indian and Northern Affairs, Canada
200 Range Road, Whitehorse, Yukon
Y1A 3V1

R.J. Turner
Geological Survey of Canada
100 West Pender Street
Vancouver, British Columbia
V6B 1R8

INTRODUCTION

Near Macmillan Pass in east-central Yukon (Fig. 1), carbonaceous and siliciclastic marine strata of the Devono-Mississippian Earn Group contain the TOM, JASON, and BOUNDARY CREEK zinc lead prospects, and more than 15 stratiform barite deposits. The Earn Group is widespread in central Yukon and northern British Columbia and probably represents an episode of rifting and/or wrench faulting of the outer continental margin of western North America (Gordey et al., 1982; Gordey et al., in press). This summary focusses on the stratigraphic and structural setting of stratiform sediment-hosted zinc, lead, barite deposits in the Macmillan Pass district, and is based primarily on regional mapping by Abbott(1983) and detailed studies near selected mineral deposits by Turner (Turner, 1986; Turner and Rhodes, 1990; Turner and Goodfellow, 1990). Other studies in the area include those by Bailes et al, 1986; Carne, 1979; Goodfellow and Rhodes, this volume; McClay, 1983; McClay and Bidwell, 1986; Turner, 1985; Turner et al, 1989; and Winn and Bailes, 1987.

At Macmillan Pass, Devonian strata are well exposed, metamorphic grade is low, and Devonian age base metal and barite deposits are numerous and diverse. As a result, the stratigraphy of the Earn Group and related Devonian tectonism and metallogeny are more clearly displayed and better documented there than anywhere else in the northern Canadian Cordillera.

Anomalous, intense Mesozoic deformation both provides evidence for, and inhibits precise definition of Devonian tectonism. The Macmillan Fold Belt(MFB) (Abbott, 1982), is more than 125 km long and dominates the local stratigraphic and structural framework. It trends conspicuously west across the northwest-trending regional grain (Fig. 1), roughly coincides with facies changes in the Earn Group, and is thought to reflect a deep-seated Devonian fault zone (Abbott, 1982). Near Macmillan Pass, contrasts in Paleozoic stratigraphy and style of Mesozoic structures divide the Macmillan Fold Belt into the North, Central and South Blocks (Abbott, 1982; Fig. 2, this paper). The Central Block is bounded by the Macmillan and Hess fault zones. Most Lower and Middle Paleozoic strata differ sharply across the Macmillan fault zone and to a lesser degree, Middle Paleozoic strata differ across the Hess Fault. Most of these differences, and associated changes in structural style, are attributed to Mesozoic right lateral strike-slip of about 30 km along the Macmillan fault zone, and possibly up to 25 km along the Hess fault zone.

Variations in thickness, internal stratigraphy, and external stratigraphic relations in the Earn Group record a complex history of repeated uplift and subsidence that indirectly suggest Devonian extension, rifting and wrench faulting along an ancestral Central Block that roughly coincides with the Mesozoic Central Block defined above (Figure 4). The Hess fault zone in particular dissects the ancestral Central Block so that parts of it are now in the Mesozoic South Block. The terms North, Central, and South Blocks here refer to Mesozoic features unless otherwise indicated.

Devonian features that have been identified are

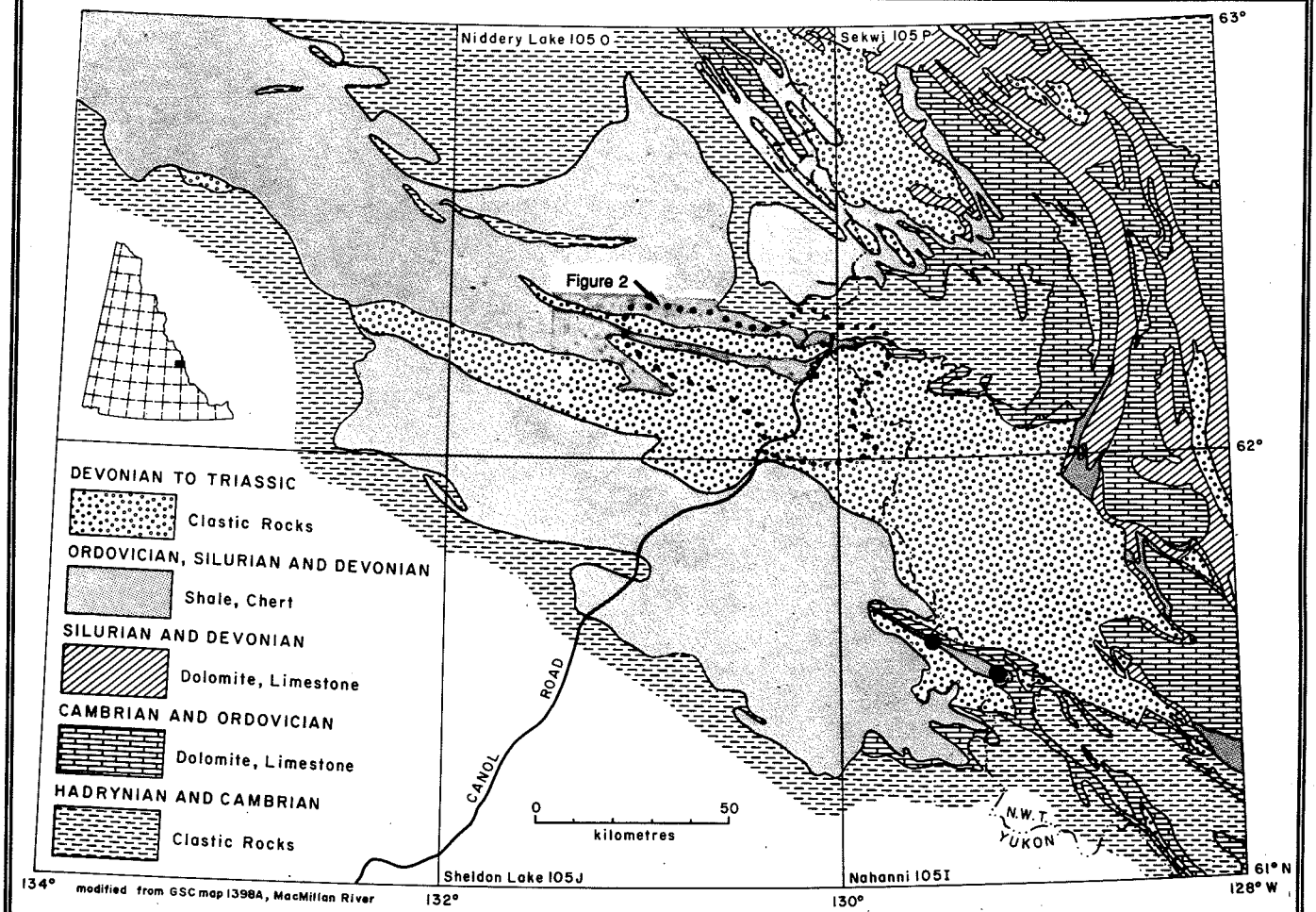

Figure 1 Location and regional geological setting of the Macmillan Pass District and the Macmillan Fold Belt.

shown in figure 4. The ancestral Central Block is not yet completely defined, but is thought to represent a Devonian rift zone or pull-apart basin which localized coarse clastic turbidites derived from a separate(?) subaerial source that lay to the west of the Macmillan Pass District. Local features confined to the ancestral block include Devonian volcanic rocks, base metal deposits, sedimentary breccias, and syndepositional faults. The syndepositional faults clearly controlled deposition of the volcanic rocks, diamictites, and the Boundary Creek, Tom, and Jason Pb, Zn deposits.

STRATIGRAPHY OF THE EARN GROUP

Figure 5 outlines the internal and external stratigraphic relations, and current terminology of the Earn Group near Macmillan Pass. The Earn Group ranges in age from late Early to latest Devonian. It both conformably overlies silty limestone in the Road River Group that is as young as late Early Devonian, and also unconformably overlies strata as old as Ordovician. Overlying Early Mississippian shale and quartzite of the Tsichu formation (Gordey, in press), marks a return to normal offshelf marine sedimentation. Total thickness of the Earn Group varies greatly, but exceeds 2 km in places. Paleontological control in the Earn Group, based largely on conodont microfossil collections, is summarized in Figure 5.

Strata that Gordey et al. (1982) included in the Earn Group have been divided in several different ways (Fig. 5), and this terminology is still in a state of flux.

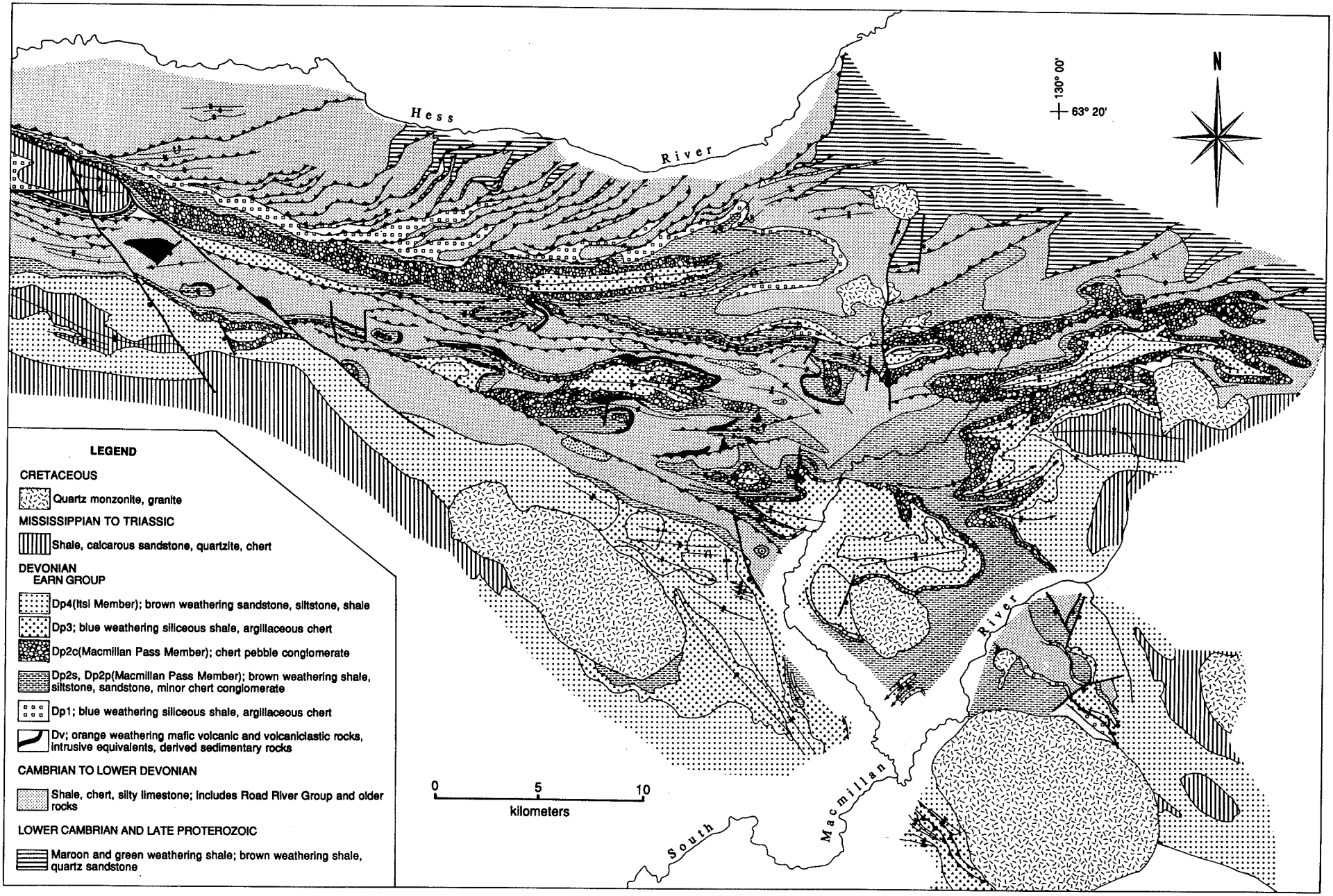

Figure 2 Geological map of the Macmillan Fold Belt.

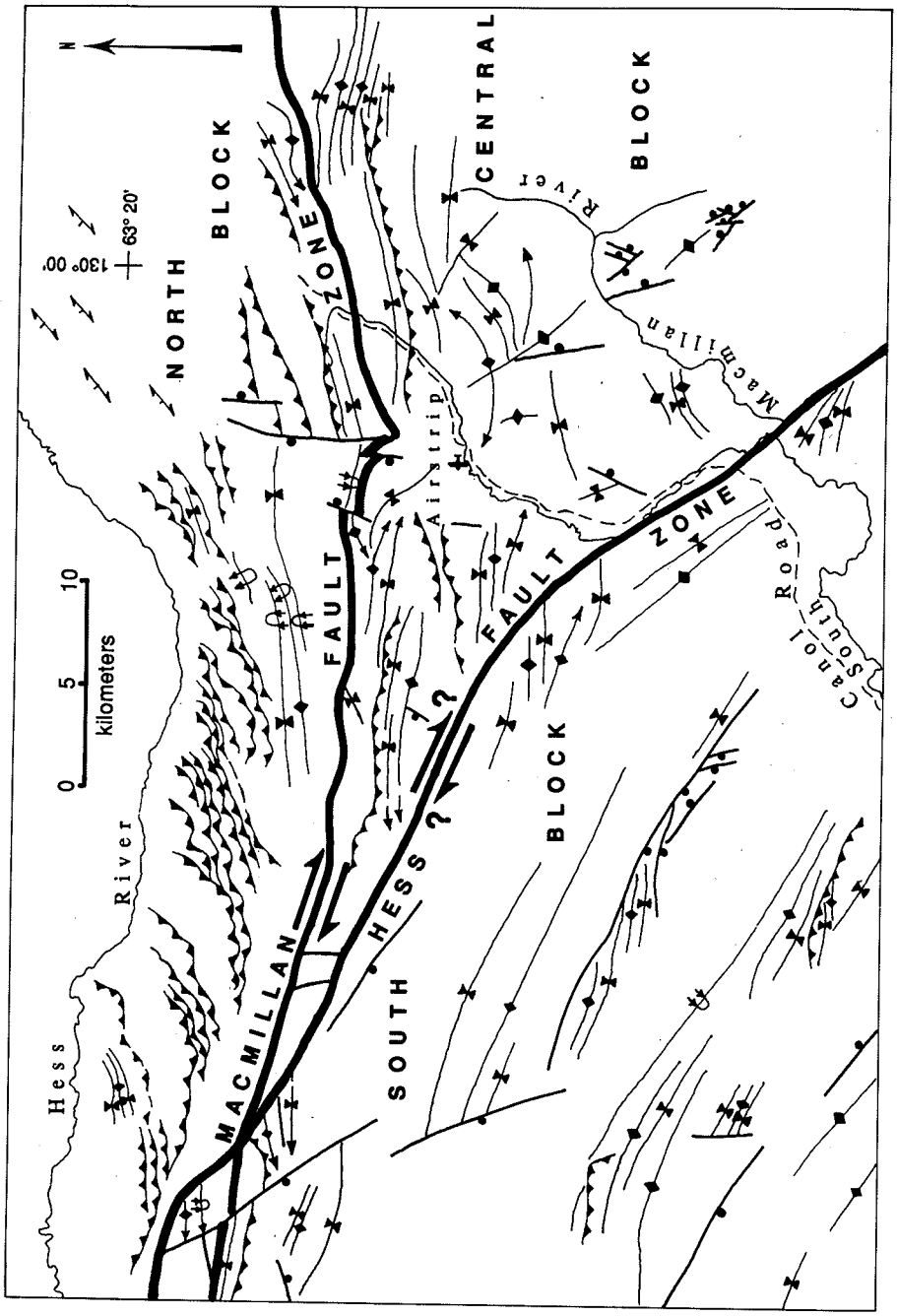

Figure 3 Main tectonic elements and Mesozoic structures in the Macmillan Fold Belt. (NB) North Block, (CB) Central Block, (SB) South Block, (MFZ) Macmillan fault zone, (HFZ) Hess fault zone.

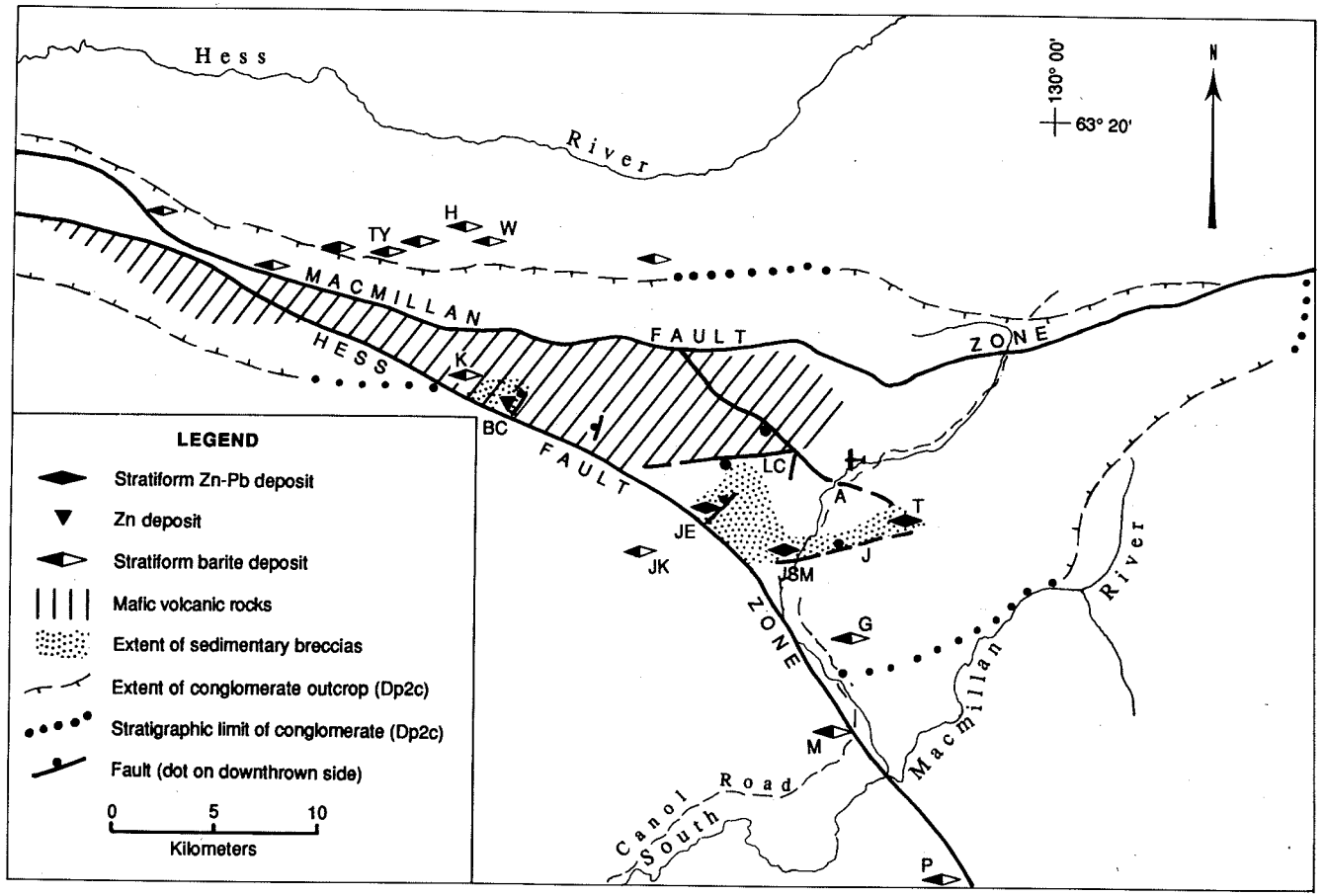

Figure 4 Distribution of Devonian age features in the Macmillan Fold Belt such as coarse clastic rocks in the Macmillan Pass member, syndepositional faults, sedimentary breccias, volcanic rocks, base metal deposits, and stratiform barite deposits. The extent of ferroan carbonate alteration within sedimentary strata of the Earn Group and Road River Group is approximately coextensive with the distribution of sedimentary breccias. Zinc-lead prospects noted on the map are Boundary Creek (BC), Jason End zone (JE), Jason South/Main (JSM), and Tom (T). Barite prospects noted on the map are Tyrala (TY), Hess (H), Walt (W), K (Kobuk), JK (JK), Gary (G), Moose (M), and Pete (P). Synsedimentary faults noted on the map are Airstrip (A), Lower Conglomerate (LC), Jason (J), Jason End Zone (JE), Boundary Creek (BC).

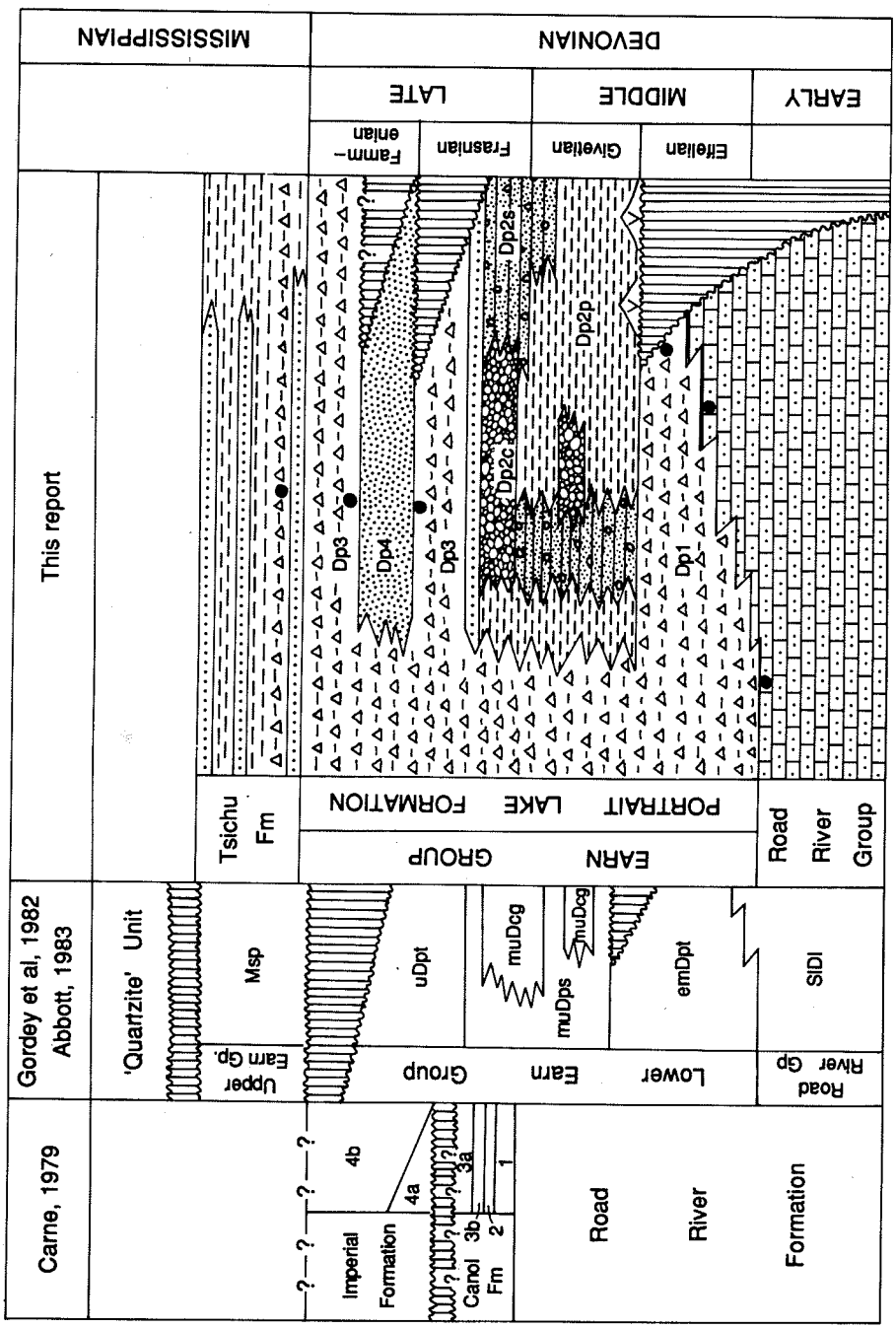

Figure 5 Terminology and stratigraphic relations of the Earn Group near Macmillan Pass. Dots indicate fossil control, primarily by conodont microfossils.

Here, the Earn Group is divided into Devonian volcanics, and the Portrait Lake Formation. The Portrait Lake Formation near Macmillan Pass includes the Macmillan Pass and Itsi Members and three other informal units. The term Portrait Lake Formation has been formally introduced by Gordey (in press) and the terms Macmillan Pass Member, Itsi Member and other units of the Portrait Lake Formation by Abbott (in prep).

Strata included in the Portrait Lake Formation have been informally correlated with the Canol Formation by Blusson (1978) and Carne (1979) , divided into units 1, 2, 3a and 3b by Carne (1979), and into units emDpt, muDps, muDcg, and uDpt by Abbott (1983). Strata included in the Itsi Member were informally correlated by Blusson (1978) and Carne (1979) with the Imperial Formation, mapped as units 4a and 4b by Carne (1979), as unit Msp by Abbott(1983), and included in the upper Earn Group by Gordey et al. (1982).

Portrait Lake Formation

The Portrait Lake Formation near Macmillan Pass comprises blue weathering siliceous shale and argillaceous chert (units Dp1 and Dp3), a brown-weathering, westerly derived shale, conglomerate, and sandstone turbidite assemblage named the Macmillan Pass Member(Dp2), and brown-weathering, northerly derived, resistant, quartz sandstone, siltstone, and shale named the Itsi Member (Dp4). South of Macmillan Pass, in western Nahanni map area, blue weathering siliceous shale with a minor coarse clastic component characterizes the Portrait Lake Formation (Gordey, in press). The Macmillan Pass and Itsi Members are confined to the Macmillan Fold Belt.

Unit Dp1

The lower part of the Earn Group (unit Dp1) comprises uniform, dark blue-weathering, thin-bedded siliceous, carbonaceous shale and argillaceous chert up to 200 meters thick. Stratigraphic relations vary across the map area (Figure 6). North of the Macmillan Fault Zone(North Block), the unit overlies the Road River Group with apparent conformity. A diachronous relationship is suggested by scant fossil evidence and thinning of the unit from west to east, and with corresponding thickening of underlying Siluro-Devonian limestone. Near the Macmillan Fault Zone, the siliceous shale is sharply overlain by brown-weathering shale of the Macmillan Pass Member. This contact could be conformable or unconformable. In most of the Central

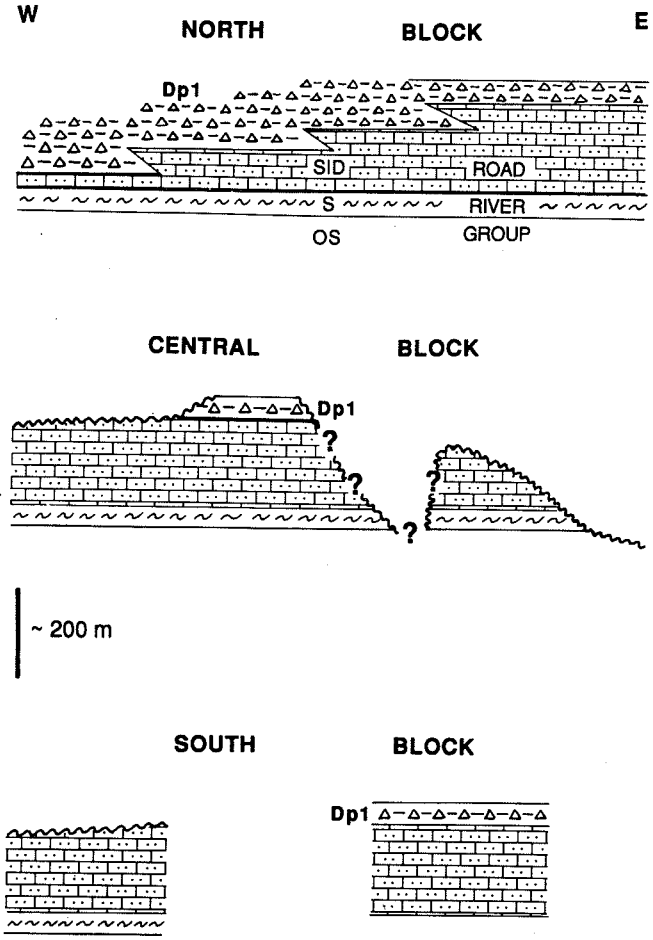

Figure 6 Stratigraphic relations of unit Dp1 near Macmillan Pass. Variations in thickness of unit Dp1 between the North and Central Blocks probably reflect juxtaposition by Mesozoic right lateral strike-slip. Variations in level of erosion of unit Dp1 beneath the unconformity reflects Devonian differential uplift and faulting prior to subsidence and deposition of coarse clastic turbidites of the Macmillan Pass member.

Block, the unit is missing or less than 10 meters thick beneath an unconformity at the base of the Macmillan Pass Member. At the eastern end of the map area, and possibly north of the Tom deposit, the unconformity cuts down to Ordovician strata. In the South Block, the unit is about 50 m thick near the Jason Deposits and is missing farther west, possibly beneath the same unconformity.

Macmillan Pass Member (Unit Dp2)

The Macmillan Pass Member is confined to the Macmillan Fold Belt (Fig. 7), and lies primarily in the Central Block, but extends across the Macmillan Fault Zone into the North Block, across the Hess Fault into the South Block, and out of the map area to the west and east. The thickness of the Macmillan Pass member exceeds 500 meters in most of the North Block and the eastern portion of the Central Block, but is about 100-200 meters both in the Central Block west of the Macmillan airstrip (Fig. 3 and 4), and throughout the South Block.

Shale, siltstone, chert pebble conglomerate and lesser amounts of sandstone and grit comprise the Macmillan Pass Member. The coarse clastic detritus consists of variable proportions of quartz and chert. Conglomerate clasts include mainly pebbles and some cobbles of angular to subrounded, light to dark grey chert, lesser amounts of green and white chert, black argillaceous chert, and minor quartz sand, chert sand, quartz sandstone and shale. Authigenic pyrite is a common accessory. Fragments of black chert resemble unit Dp1 and others resemble Ordovician chert located west of the district in the Road River Group. The quartz sand, and sandstone and shale clasts resemble other nearby lower Paleozoic units.

The Macmillan Pass Member includes three main lithologic divisions with complex lateral and vertical stratigraphic relationships: well-bedded shale and silty shale with minor sandstone and conglomerate (Dp2p), well-bedded shale, sandstone, and conglomerate (Dp2s), and massive conglomerate with minor sandstone grit and shale (Dp2c). Shale of unit Dp2p characteristically displays pinstripes defined by thin silty laminae spaced a few centimeters apart. Sandstone and siltstone, are locally important. Unit Dp2s is characterized by well-defined bedding and dominace of sandstone. Grain size increased with bed thickness. Most conglomerate beds are 30 cm to 2 meters thick, and sandstone beds are 10 to 50 centimeters thick. Thinning and fining upward cycles on the order of ? m thich have been noted in some sequences of interbedded conglomerate, sandstone and siltstone (Turner, this volume). Tool marks, grooves and flute casts occur in well-bedded sandstone and shale, but are not common. Most conglomerate clasts are pebble-sized or smaller, and are commonly supported in a sandy or muddy matrix. Massive conglomerate (Dp2c) up to 400 meters thick is composed of clast supported grains with quartz cement and appears to be structureless. However, black lichen characterizes its weathered surfaces and therefore, subtle internal structure is hard to recognize.

Locally derived slump breccias or diamictites are associated with the Boundary Creek, Jason(South, Main, End), and Tom deposits. These heterolithic breccias contain mudstone and siltstone, chert pebbles, and minor fragments of sandstone and chert pebble conglomerate. The matrix of the breccias is a variable mixture of mud, silt, and sand.

The internal stratigraphy of the Macmillan Pass Member is complex, but many sections are composed of: (1) a lower thick interval of pinstriped shale and silty shale with variable, but small amounts of sandstone, grit and conglomerate (Dp2p), (2) a middle interval of sharply defined massive conglomerate (Dp2c), and (3) an upper few meters of thin-bedded sandstone and siltstone (Fig. 5 and 8). These are units 1, 2 and 3a of Carne (1979). Alternatively, the lower shale interval grades stratigraphically upward into sandstone and siltstone of unit Dp2s, which is sharply overlain by conglomerate. Unit Dp2s also undergoes abrupt lateral transitions to both shale (Dp2p) and conglomerate (Dp2c) in the upper part of the sequence. Only north of the Jason Deposits was unit Dp2s seen to comprise most of the assemblage below the upper conglomerate (Turner, this volume).

Conglomerate (Dp2C) appears to form a laterally continuous horizon near the top of the Macmillan Pass Member over much of the Macmillan Fold Belt (Fig. 7 and 8). Only north of the Jason deposits and east of the Tom deposit were two massive conglomerate horizons seen in one section. The two occurences of a lower conglomerate lie on an east-west trend and could be part of a single channel deposit.

Thicknesses and stratigraphic details of the Macmillan Pass Member are different in each of the North, Central and South Blocks (Figure 8). In the western part of the North Block, about 100 meters of shale, overlain by up to 400 meters conglomerate form a narrow belt along the north side of the Macmillan Fault Zone. Going east, the lower shale unit thickens to more than 500 meters, and the conglomerate changes to well-bedded sandstone, grit, conglomerate, and shale (Dp2s). Both the conglomerate and coarse clastic rocks appear to change to shale going north. These rocks represent an eastward fining fan complex along the

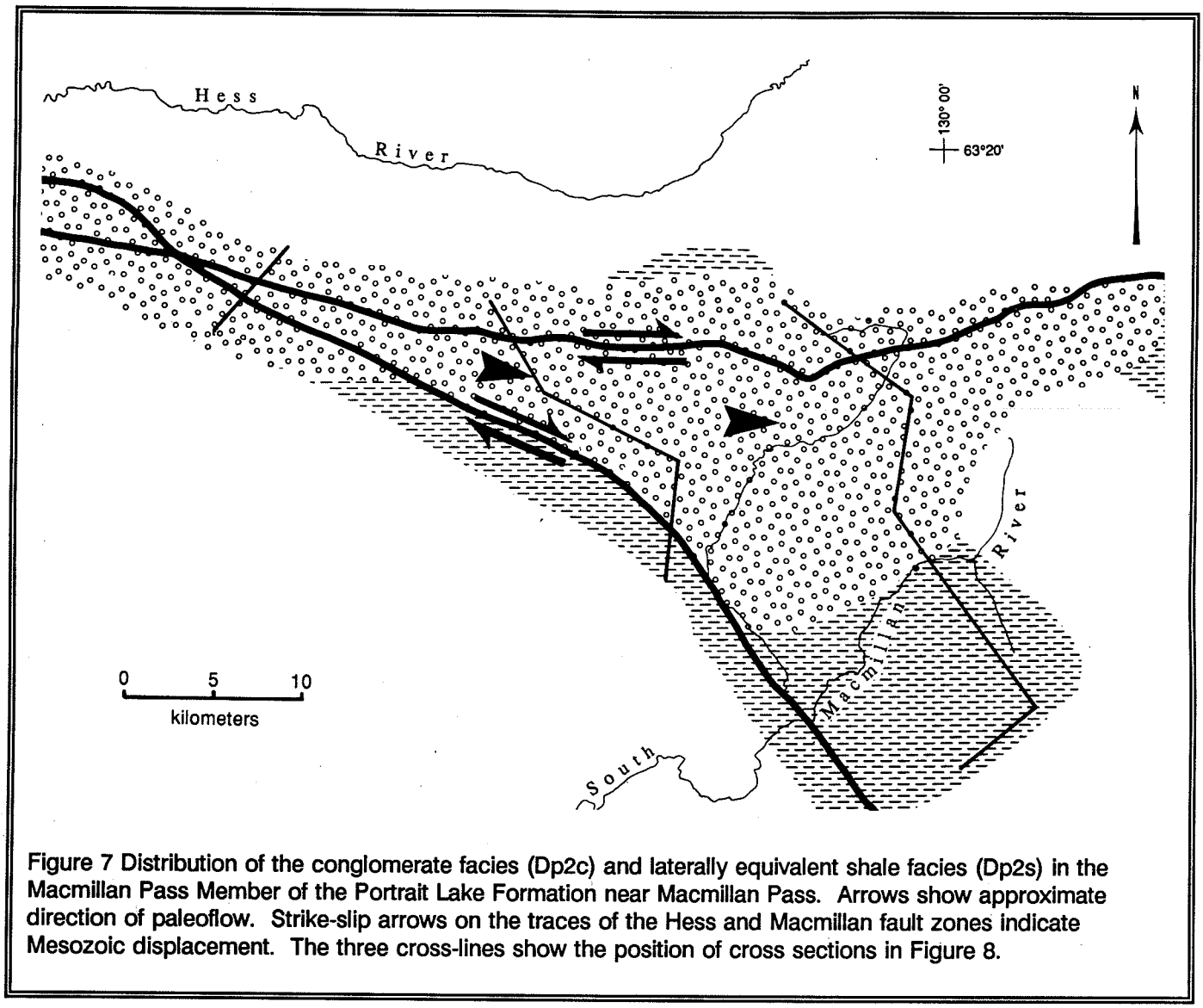

Figure 7 Distribution of the conglomerate facies (Dp2c) and laterally equivalent shale facies (Dp2s) in the Macmillan Pass Member of the Portrait Lake Formation near Macmillan Pass. Arrows show approximate direction of paleoflow. Strike-slip arrows on the traces of the Hess and Macmillan fault zones indicate Mesozoic displacement. The three cross-lines show the position of cross sections in Figure 8.

northern depositional boundary of the turbidite system.

In the Central Block, facies relationships are more complex than in the North Block. At the west end, shale and conglomerate with a combined thickness of less than 100 meters are juxtaposed against the similar, but much thicker strata on the north side of the Macmillan Fault Zone. At the eastern end of the Central Block, the shale thins and about 200 meters of conglomerate comprises all or most of the Macmillan Pass Member. The easternmost exposures of the conglomerate are more sand rich and are interbedded with sandstone. Near the central part of the Central Block, the combined thickness of shale and conglomerate reaches several hundred meters, and well-bedded sandstone, shale and conglomerate of unit Dp2s underlies a small area about 6 kilometers to the west and east of the Macmillan airstrip. Conglomerate near the base of the unit in this area is thick enough to map separately. Unit Dp2s in part of this area is bounded on the north by a steep east-trending fault which juxtaposes it against shale in the same stratigraphic position (Lower conglomerate syndepositional fault, Figure 4). The fault is probably a reactivated Devonian structure which controlled deposition of the coarse clastic rocks. South of the Tom

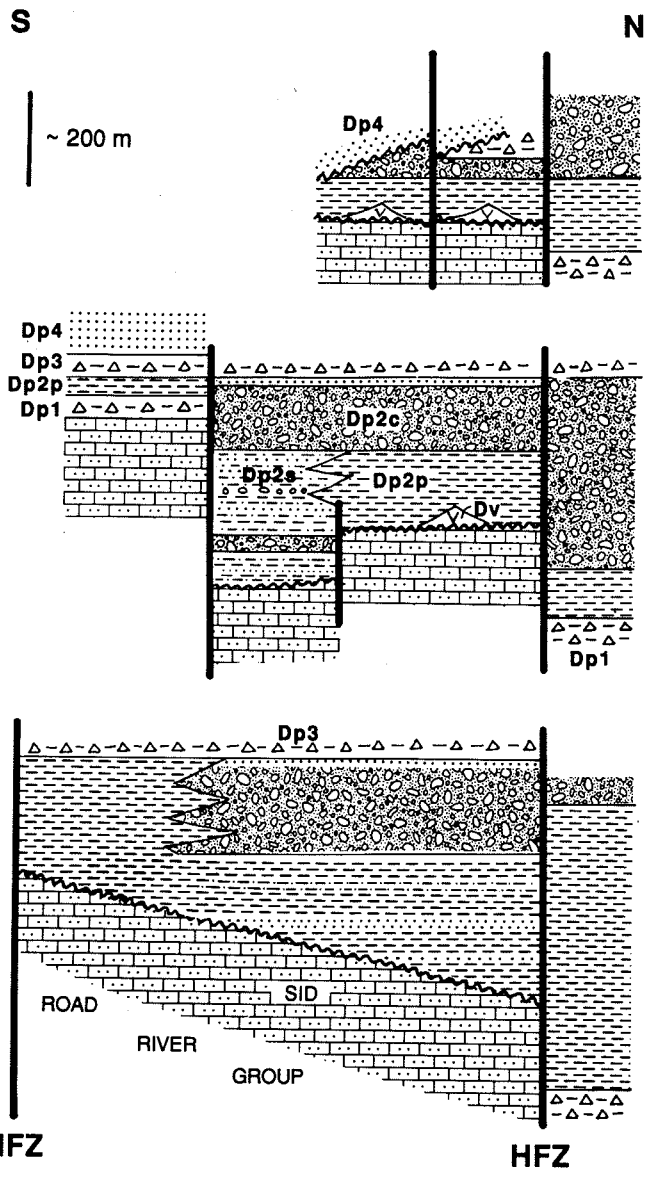

Figure 8 Restored, schematic cross-sections throughout the Macmillan Pass Member. Location of sections shown on Figure 7. MFZ-Macmillan fault zone; HFZ-Hess fault zone. Contrasts in internal and external stratigraphic relations of the Macmillan Pass member across the Hess and Macmillan fault zones in part reflect juxtaposition by Mesozoic strike-slip and in part reflect differential Devonian movement.

deposit, the chert conglomerate thins and eventually pinches out, whereas shale, siltstone, and sandstone of unit Dp2p thicken and comprise the entire Macmillan Pass Member.

In the South Block, at the west end, the Macmillan Pass Member consists of shale overlain by conglomerate. Erosional remnants of conglomerate are preserved as lenses beneath the unconformably overlying Itsi Member(Figure 8), and the preserved sequence is less than 100 meters thick. Near the Jason deposits, shale and minor sandstone about 100 meters thick comprise the entire Macmillan Pass Member.

Paleogeography

The present distribution of the Macmillan Pass Member is probably little changed from the Devonian. Cecile (1984) traced the Macmillan Pass Member for about 10 kilometers west of the map area (Figure 2). Farther west, strata are poorly exposed, but appear to be mainly blue weathering shale. To the southwest, south, and east beyond the area shown in Figure 2, limited exposures suggest that the coarse clastic rocks change to blue weathering siliceous shale. Neither the Macmillan Pass Member, nor its equivalents, are preserved along the northern margin of the Macmillan Fold Belt, but the coincidence of the coarse clastic rocks with the structurally anomalous Macmillan Fold Belt, and the northward change from conglomerate into shale in one preserved locality suggest that the Macmillan Pass member was never deposited north of the Macmillan Fold Belt.

Most of the Macmillan Pass Member appears to have been derived from the west, although current indicators are rare. Winn et al. (1981), Bailes et al. (1986) and Turner (1985) reported that current indicators in sandstone north of the Jason deposits indicated sediment transport from the northwest to the southeast. Abbott (unpublished data) measured a few toolmarks of similar orientation in the same area, as well as two flute casts north of the Macmillan Fault Zone that suggested southwesterly derivation (northeast paleoflow). Carne (1979), reported that current indicators in turbidites of unit 2 (Dp2c) near the Tom deposit indicated sediment transport from the west or northwest to the east to south east. The nearest possible source for the chert from the Road River Group which makes up most of the clastic component of the Macmillan Pass Member is about 20 kilometers west of the map area, near Niddery Lake (Cecile, 1984).

The Macmillan Pass Member does not fit the standard model for turbidite deposition, in which a fan of sediments was built out from the mouth of a single

feeder channel. The three part stratigraphy of the Macmillan Pass Member suggests a telescoped prograde and retrograde cycle in which advance and retreat of depositional environments took place rapidly. Channelized deposition of conglomerate and sandstone is suggested by the massive nature of the former and the fining upward/thinning upward cycles of the latter. The lower conglomerate lens located north of the Jason deposits is composed of thinning and fining upward sequences suggesting channel deposition. Shale rich rocks are laterally equivalent to the channel. Conglomerate forms a sheetlike deposit near the top of the member that is at least 50 km long and 15 km wide. Along its northern, southern (near the Jason Deposits) and eastern margin, the conglomerate changes laterally to bedded sand-rich strata.

Pinstriped shale, sand laminated argillite and banded siltstone suggest outer fan or basin plane deposition. The absence of recognized coarsening upward sequences in sand-rich strata which might indicate mid-fan deposition, suggests the transition from channel deposits to "outer fan" took place over a short distance and likely reflects the bimodal (gravel, silt) sediment of the Devonian distributary system.

The lack of similarity of the Macmillan Pass member to classic fan models may result from some combination of the following possibilities. (1)Mesozoic strike-slip on the Macmillan and Hess Faults and possibly other structures has destroyed the original distribution of facies in the Macmillan Pass Member. (2)The elongate configuration of the Macmillan Pass Member as it is now distributed, and its apparent relationship to anomalous Mesozoic structures suggests that deposition occurred in a fault-controlled trough in which typical fans could not develop. (3)Sandstone is generally the main component of turbidite fans, and definitions of the fan model depend on its presence (Walker, 1984). The Macmillan Pass Member is shale- and conglomerate-rich and sand-poor. The bimodal distribution probably reflects the shale- and chert-rich nature of the source terrane. Though Portrait Lake strata east or southeast of the map area are little studied, a few reconnaissance traverses by Abbott in this area indicated that the Macmillan Pass Member is mainly shale. (4) The upper conglomerate may represent a series of coalescing lenses derived from many point sources or a moving point source that originated from a fault scarp located somewhere to the west of the Central Block. The Hess Fault, at least in the map area (Fig. 2) is not a candidate, as Devonian silty limestone underlies the Earn Group for the exposed length of the fault, whereas in the source terrane, Ordovician chert and older clastic rocks must have been subaerially exposed and eroded.

Unit Dp3

Silver to blue-black-weathering platey, graphitic, siliceous mudstone, siliceous shale, and local chert of Unit Dp3 (Fig. 5) sharply overlies the Macmillan Pass Member, and encloses the Itsi Member. Slump breccias and diamictite interbedded with mudstone and siltstone occur in the basal part of Dp3 near all known base metal deposits(Jason South, Main, End; Tom; Boundary Creek). These deposits are interpreted to have formed along syndepositional faults with active resedimentation from the submarine fault scarp (Bailes et al., 1986; Turner, 1986, this volume) The unit resembles Unit Dp1, but is less siliceous and more silvery-weathering. Bailes et al. (1986) and Turner (1985) described debris flows intercalated with the lower parts of the member near the Jason Deposits, but none have been seen elsewhere.

The siliceous shale is at least several hundred meters thick west of the Tom Deposit, and abruptly thins to about 100 meters one kilometer east of the Tom Deposit. This thickness change may be depositional. In the South Block, the shale is about 100 meters thick near the Jason Deposits and thins westward. At the west end of the Macmillan Fold Belt, unit Dp3 appears to be cut out beneath an unconformity at the base of the Itsi Member (Fig. 8). Variations in thickness elsewhere could be either depositional or reflect erosion beneath this unconformity.

Blue weathering shale about 80m thick above the Itsi Member and below quartzite of the Tsichu formation in the Central Block (Fig. 5) is also correlated with unit Dp3. In the North Block, a sample from a thin limestone bed an unknown distance from the top of the unit yielded middle Fammenian conodonts. This age is younger than early Fammenian conodonts collected from blue shale which overlies the Itsi Member in the South Block. The Itsi Member is absent in the North Block, and Unit Dp3 in that area may be either a stratigraphically continuous unit that is, in part, time equivalent to the Itsi Member, or less probably, two units separated by an unconformity which has removed the Itsi Member.

Itsi Member (Unit Dp4)

The Itsi Member is early to middle Fammenian

in age and consists of distinctive, northerly-derived, resistant, brown-weathering, quartz sandstone, siltstone, and shale. It unconformably overlies units Dp2 and Dp3, is overlain by, and probably laterally equivalent to blue weathering shale of unit Dp3.

The Itsi Member is characterized by siltstone and fine grained sandstone that tends to form thick to very thick, resistant intervals separated by thin beds of silty shale. The sandstone intervals comprise alternating plane parallel laminated sandstone and ripple cross-laminated sandstone of variable thickness. Plane parallel laminations are more abundant than cross-laminations. Cross-laminations consistently indicate a southerly to south south-westerly directed current direction. Without detailed study, the sedimentary structures could be interpreted to indicate either deposition by turbidity currents or by normal bottom currents.

The Itsi Member appears to form a lobe or prism confined to the Central and South Blocks (Fig. 10 and 11) and derived from the north. Thicknesses vary dramatically from 175 meters near Macmillan Pass to more than 1300 meters south of the Jason deposits. Farther to the south and southwest the sandstone appears to change to shale and siltsone. Still farther, beyond the area shown in Figure 2, the member is absent.

In the North Block, siliceous shale mapped as unit Dp3 overlies chert conglomerate of the Macmillan Pass member, but contains middle Fammenian conodonts that are younger than other conodonts collected from similar blue-black shale that overlies the Itsi Member. The discordance can be explained by dextral strike-slip offset on the Macmillan Fault Zone. Fifty kilometers to the northeast of Macmillan Pass, in Sekwi map area, sandstone of unit 26b (Blusson, 1971) resembles the Itsi Member, and may be it's offset equivalent. In this interpretation, Unit 26b is laterally equivalent to black shale of Unit Dp3 in the North Block. Alternatively, the Itsi Member in the North Block was removed beneath an unconformity that is hidden in the blue shales of member Dp3.

Devonian volcanics and related intrusions (Dv)

Orange-weathering hyaloclastic breccias, volcaniclastic sandstone, a few volcanic flows, and related sills and dikes are confined to the Central Block west and north of the Macmillan airstrip. The volcanic and volcaniclastic rocks form thin, intermittent lenses 1 to 70 meters thick that occupy more than one stratigraphic position near the base of the Earn Group. In most places the volcanics are at the basal contact of the Earn Group and sharply overlie Siluro-Devonian silty limestone, but they also appear to be intercalated with the uppermost part of the silty limestone, and are also intercalated with or overlie a few meters of blue weathering shale of unit Dp1. Five kilometers northwest of the Macmillan airstrip, the volcanics appear to unconformably overlie Ordovician black shale and chert. This unconformity may account for the absence of unit Dp1 from much of the Central Block. Brown-weathering clastic rocks of member Dp2 of the Portrait Lake Formation generally sharply overlie the volcanic rocks, but in drill core from the Boundary Creek deposit, the volcanic rocks are clearly intercalated with chert conglomerate and diamictite in the Macmillan Pass member. One collection of conodonts from a limestone lens in the volcanics in sharp contact with underlying Siluro-Devonian limestone and overlying brown shale of the Macmillan Pass member are of middle Eifelian to early Givetian (Middle Devonian) age, younger than the age of the base of unit Dp1, thereby indicating deposition during or immediately following deposition of unit Dp1.

Hyaloclastic breccias, the dominant rock type, contain uniform, angular, dark green, locally vesicular, volcanic clasts, and a few shale clasts, 1 or 2 centimeters across, in an orange weathering ferroan carbonate-rich matrix. On weathered surfaces, fragments stand out to produce a distinctive nubbly texture. Orange weathering, well-bedded calcareous volcaniclastic sandstone and siltstone, and/or tuff are locally intercalated with the breccias. Near the west end of the Central Block, massive, resistant, dark green vesicular flows reach 70 meters in thickness, but elsewhere, are either absent or a small part of the unit. Several dark weathering, massive greenstone sills up to 2 kilometers long and 20 meters thick appear to be intrusive equivalents to the volcanic rocks.

STRUCTURAL GEOLOGY

The Macmillan Fold Belt is a structural anomaly in the Mackenzie and Selwyn Fold Belts (Fig. 1). It trends west-northwest across the northwest-trending regional grain, and can be traced for 120 kilometers.

The style of deformation varies greatly between the North, Central and South Blocks (Fig. 3). The North Block is characterized by southeasterly directed

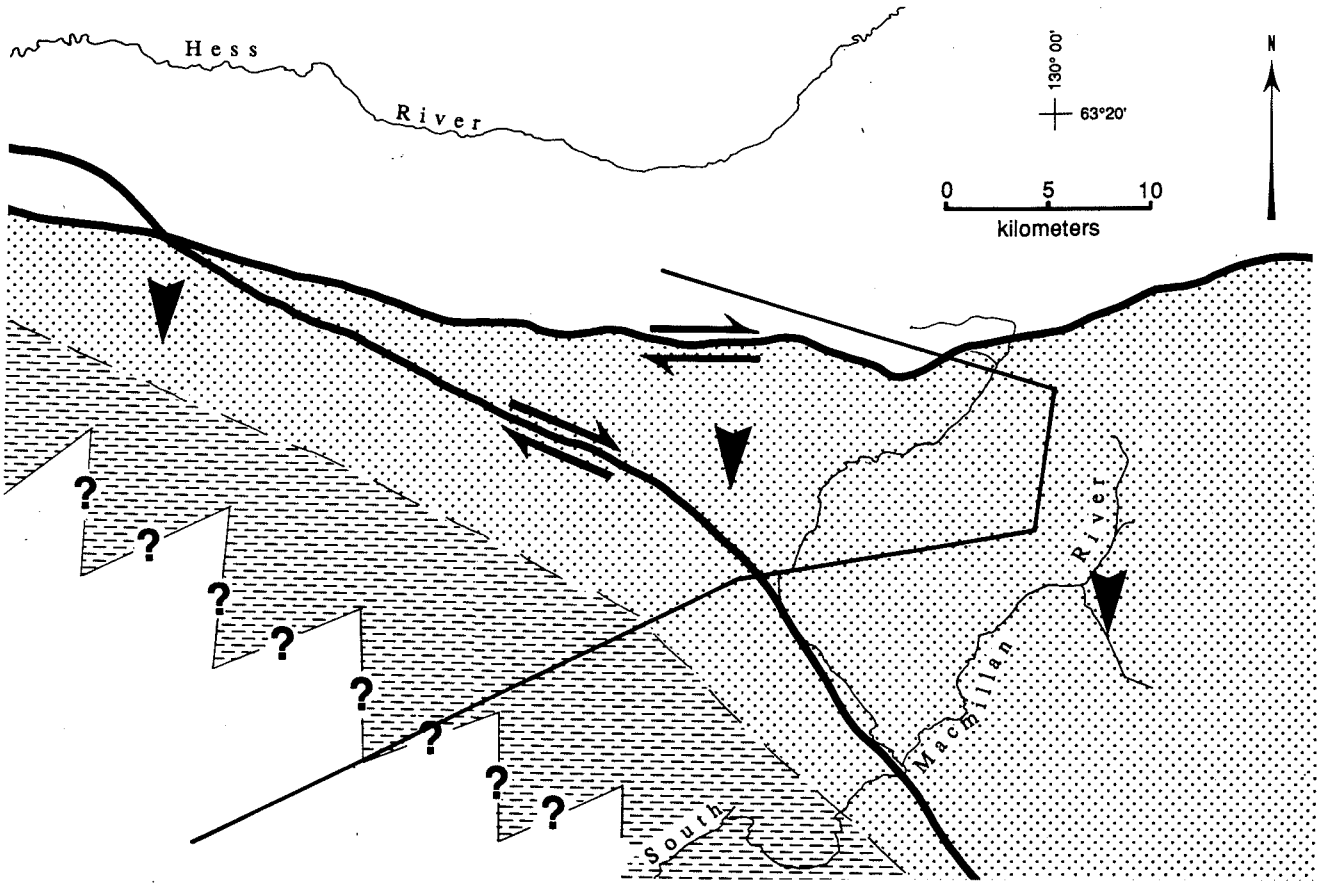

Figure 9 Distribution of the Itsi Member of the Portrait Lake Formation near Macmillan Pass. The absence of the Itsi Member in the North Block is attributed to Mesozoic right-lateral offset of about 30 km on the Macmillan fault zone. The absence of the member in the southwest part of the area and to the southeast beyond the map area suggest that late Devonian subsidence in parts of the ancestral Central and South Blocks controlled deposition of the Itsi member. Arrows show generalized paleoflow. Cross-line shows location of Figure 10.

imbricate thrust faults; the Central Block, by complex structures that include at least three phases of folds and faults; and the South Block, by two phases of relatively simple northwesterly and north trending folds.

The Hess and Macmillan Fault Zones, which bound the Central Block, are thought to broadly reflect primary Devonian structures which controlled the style of Mesozoic deformation, the development of the Macmillan Fold Belt and the complex structures in it. The complex structures in the Central Block are thought to reflect interference with Devonian structures.

North Block

In the North Block, moderately to steeply dipping, southerly to southeasterly directed imbricate thrust faults form a broad arc along the south side of the Hess River. Bedding generally dips northwest, intersects thrusts at low angles, and is cut by a poorly developed, steep dipping cleavage. The angle between thrusts and bedding seems to increase steadily upsection, with no

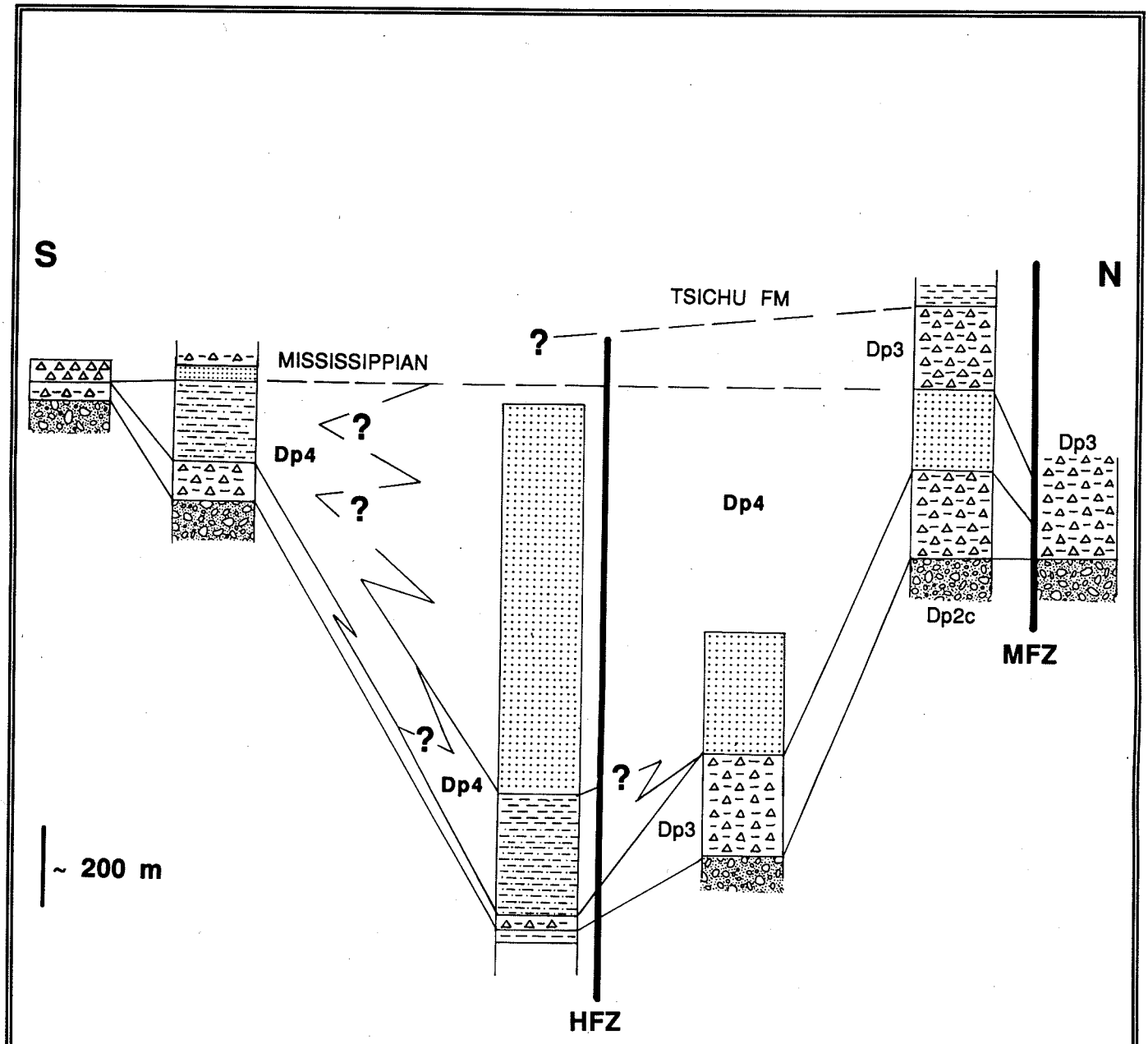

Figure 10 Restored schematic cross-section through the Itsi Member. Location of sections shown on Figure 9. The dramatic southward thickening of the Itsi member may reflect late Devonian subsidence in parts of the ancestral Central and south Blocks. MFZ-Macmillan fault zone; HFZ-Hess fault zone.

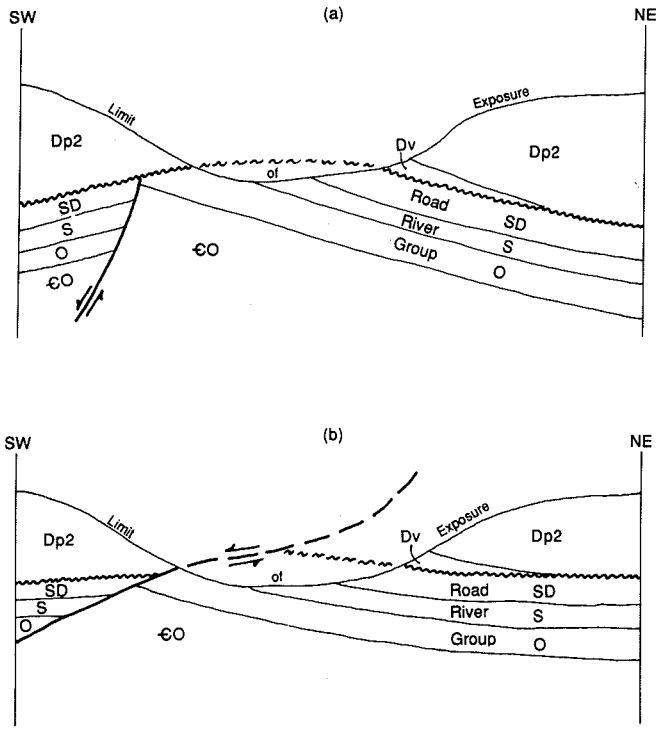

Figure 11 Two possible interpretations of the Airstrip syndepositional fault. (a) A hidden, southwest-side-down, steeply dipping normal fault coincident with uplift and erosion and volcanism at the base of the Macmillan pass Member. (b) A southwest-side-down low angle normal fault coincident with formation of the sulphide deposition at the top of the Macmillan Pass Member.

abrupt changes. Folds are known only at the extreme ends of the imbricate zone. The faults place rocks as old as earliest Cambrian on rocks as young as Middle Devonian, with a maximum stratigraphic omission of about one kilometer. West of Mactung, the amount of stratigraphic throw, and therefore displacement, decreases to the west along each fault. The faults also tend to coalesce to the west, and ultimately steepen and die in the cores of tight anticlines beneath or against the rib of chert conglomerate in the Portrait Lake Formation (Unit Dp2c), along the southern boundary of the North Block. The thrusts do not intersect the Macmillan Fault. Immediately west of Mactung, the thrust belt curves northeastward away from the Macmillan Fault Zone and is bounded to the southeast by southeasterly overturned folds in thick shale of the Portrait Lake Formation.

Structure cross-sections suggest that the thrusts coalesce at depth and root in a single detachment somewhere near the top of the lowermost Cambrian strata. Minimum shortening must be about 10 kilometers within the map area.

The thrust belt is part of a larger zone of intense shortening and imbrication that Cecile (1981; 1983; 1984) has traced across central Niddery map area in thin Lower and Middle Paleozoic sedimentary units of Selwyn Basin. This 'duplex' generally trends northwest, parallel to typical, northeasterly-directed regional structures of the Mackenzie Fold Belt, but bends in a broad arc to the southwest to join the thrust belt in the North Block of the Macmillan Fold Belt, where it terminates along the Macmillan Fault Zone.

Central Block

In the Central Block, three phases of superposed structures are recognized. West-trending, upright, tight folds and parallel, high angle reverse faults of the second phase dominate. McClay (1983, 1985), from detailed studies near the Tom deposit, has shown that an early, weakly developed north trending cleavage axial planar to the south plunging Tom anticline (Goodfellow and Rhodes, this volume) is deformed by the west trending folds and cleavage. These structures are, in turn, deformed by a third set of small scale, north trending folds and cleavage that have little effect on map patterns. A broad zone of large, southeast and beyond the map area. These folds are also younger than the west trending second phase structures, but their relationship to the north trending third phase is not known.

The early north-trending structures seen in the Tom anticline are not in the Itsi Member or younger strata, and McClay (1983) surmised that they are Devonian. None were recognized elsewhere by the writer, and they have only been seen locally in the Central Block by McClay (pers. com., 1984). The age and significance of the early north trending cleavage and related folds are still uncertain.

South Block

Much of the South Block is deformed by a single, relatively simple northwest-to west-trending folds and axial plane cleavage. Folds verge to the northeast, and are locally overturned in that direction. A second

phase of more northerly trending folds occurs near the northeast margin along the Canol Road. Northwest to north-northwest trending normal(?) faults cut folds and probably have displacements as large as several hundred meters.

Macmillan and Hess Fault Zones

The Macmillan and Hess fault zones each consist of one to three parallel, steeply south and southeast dipping faults, spaced up to 2 km apart. Stratigraphic and structural evidence suggests Mesozoic right lateral strike-slip displacement on the Macmillan, and possibly the Hess fault zones.

Macmillan Fault Zone

Across the Macmillan fault, north-trending facies boundaries in Lower and Middle Paleozoic strata are offset, suggesting about 30 km of right lateral movement. Stratigraphic evidence for Mesozoic, rather than older offset is based on the absence of the Late Devonian Itsi Member in the North Block and the marked difference between Carboniferous strata across the west end of the Macmillan fault (not described in this report).

Structural evidence for Mesozoic strike-slip on the Macmillan fault zone consists primarily of the southwest-trending thrust faults in the North Block, which make an angle of about 45° with the Macmillan fault zone (Fig. 3), in contrast to the dominant west-trending folds and high angle reverse faults in the Central Block. Some west-trending folds in the Central Block are truncated against the Macmillan fault. The apparent sense of displacement on the Macmillan fault is reverse, but the amount of throw varies significantly from place to place, thereby suggesting strike-slip movement.

Hess Fault Zone

The Hess fault zone could be either a series of branching reverse faults or have as much as 25 km of right-lateral displacement on it. Much of the Hess fault zone follows valley floors and is covered, but the general sense of apparent movement seems to be reverse. However, west-trending folds on both sides of the fault, north and south of the Jason deposits are truncated, and significant differences in the amount of apparent throw from place to place suggest strike slip.

Only the Macmillan Pass member displays significant differences in facies and thicknesses of units along strike and across the Hess fault zone that may indicate strike-slip offset. These differences(figures 4,8) divide the fault zone into three segments. Southeast of the Jason deposits, a thick shale sequence overlain by chert pebble conglomerate, on the northeast side, is juxtaposed against thinner shale on the southwest side. West of the Boundary Creek deposit, on both sides of the fault zone, about 100 m of shale is overlain by conglomerate. Devonian volcanic rocks include flows on the south side and are hyaloclastic breccias and reworked sandstones on the north side. Between the Jason and Boundary Creek deposits, thickness and facies differ significantly across the fault. On the north side, up to several hundred meters of shale, sandstone, and chert conglomerate are interbedded with significant quantities of anomalous diamictites interpreted to be locally derived slump material. The Boundary Creek and Jason deposits, and large areas of cogenetic ferroan carbonate alteration are also near the fault zone. Volcanic rocks and volcanic clasts occur thoughout the Macmillan Pass Member only in the Boundary Creek deposit. On the southwest side of the Hess fault zone, the Macmillan Pass Member is about 100 m of unaltered shale, with no chert conglomerate, diamictites, or volcanic rocks.

If about 25 km of right- lateral offset along the Hess fault zone is restored, the discordance in the Macmillan Pass member is largely removed. In the Central Block, the southern pinchout of chert pebble conglomerate which intersects the Hess Fault south of the Tom deposit, would match a similar pinchout in the South Block, which intersects the Hess fault south of the Boundary Creek deposit (Fig. 4). The South Block would be a possible source for the diamictites and volcanic debris in the Central Block, between the Jason and Boundary Creek deposits. Unlike strata now south of the Boundary Creek-Jason segment, in the postulated source west of the Boundary Creek deposit; volcanic flows up to 70 meters thick are at the base of the Macmillan Pass member, the Macmillan Pass member contains significant chert conglomerate, and the unconformity at the base of the Itsi member removes strata as old as the Macmillan Pass member, thereby suggesting that erosion may have coincided with deposition of diamictites in unit Dp3 along the north side of the fault. Facies and thicknesses of strata along otherparts of the Hess fault zone are compatible with this reconstruction.

SYNDEPOSITIONAL FAULTS IN THE CENTRAL BLOCK

Macmillan Fault

The nature of Devonian movement on the Macmillan fault cannot be accurately determined. Mesozoic right lateral strike-slip of 30 km must first be restored. However, 30 km west of the map area (Fig. 2), stratigraphy south of the fault is not well enough understood to compare accurately with that in the map area north of the fault, and 30 km east of the map area, only Lower Cambran and older strata are preserved on the northern side of the fault. Middle Devonian movement on the Macmillan fault is indirectly indicated by the contrast between conformable(?) deposition of the Macmillan Pass Member on unit Dp1 in the North Block; and uplift and erosion of unit Dp1 and older strata, prior to subsidence, extensive volcanism, and unconformable deposition of the Macmillan Pass Member in the Central Block. Movement may have included both normal and small amounts of right-lateral strike-slip offset.

Hess Fault

The Hess fault zone cuts across the east-west trending southern margin of coarse clastic rocks in the Macmillan Pass member (fig. 4) and parts, but not all of the fault zone may represent reactivated Devonian structures. Their interpretation depends upon the interpretation of Mesozoic movement on the Hess fault zone.

If no Mesozoic strike-slip occured on the Hess fault zone, the middle segment of the fault between the Boundary Creek and Jason deposits must have exerted a strong control on the southern margin of deposition of coarse clastic rocks in the Macmillan Pass Member. However, west of the Boundary Creek Deposit, the Hess fault zone juxtaposes similar sequences of clastic rocks and shows no evidence of Devonian movement, and the southern boundary of the coarse clastic rocks trends west, away from the Hess fault zone. Similarly, southeast of the Jason Deposits, the southern boundary of coarse clastic rocks trends east away from the Hess Fault zone. In this case, perhaps the Hess fault zone is primarily a Mesozoic feature that coincides with a more easterly-trending Devonian fault zone between the Jason and Boundary Creek deposits.

With 25 km of restored Mesozoic displacement, the Macmillan Pass Member would display little contrast in thickness or facies across the eastern and western segments of the Hess fault zone, and therefore little evidence for Devonian movement. Along the middle segment, between the Jason and Boundary Creek deposits, the contrast in facies would be less abrupt, but the linear array of sulphide deposits, diamictites, alteration, and volcanic rocks in the Macmillan Pass member still suggests proximity to a Devonian fault. Such a fault would be inside the restored "Central Block" as defined by the limit of coarse clastic rocks in the Macmillan Pass member. Movement would be normal with the northeast side down.

Airstrip syndepositional fault

An enigmatic feature that trends northwest from the Tom deposit to the Macmillan fault represents the most significant Devonian structure recognized so far in the Central Block (Fig. 4). Described under stratigraphy as a possible unconformity, it is a narrow northwest-trending belt along which Devonian volcanic rocks and the Macmillan Pass Member appear to unconformably overlie Ordovician strata. In contrast, the same strata on either side appear to unconformably overlie either unit Dp1 or Siluro-Devonian limestone. Such an abrupt contrast in the level of erosion suggests the presence of a Devonian normal fault. No such fault is exposed and if it does exit, much be buried beneath the southwestern boundary of the zone (Fig. 11). Alternatively, the contact itself is a southwesterly-dipping low angle normal fault. In this case movement would not coincide with volcanism at the base of the Macmillan Pass Member as in the first case, but would be younger, postdate deposition of the Macmillan Pass member, and possibly correspond with formation of the Tom deposit and thickening of carbonaceous shale of unit Dp3 across the Tom anticline. The axis of the Tom anticline, the unusual and complex structure which contains the Tom deposit, is aligned with this feature. The Tom anticline, in this interpretation, would represent Mesozoic reactivation of the Devonian extensional fault.

Lower conglomerate syndepositional fault

Another clearly defined Devonian fault is a steep, south-dipping east trending fault located north of the Jason deposits (Fig. 4) which juxtaposes well bedded sandstone, siltsone and conglomerate of Unit Dp2s on the south side against shale of unit Dp2s on the north side. The basal contact with underlying Siluro-Devonian limestone is exposed on both sides and the two different facies are clearly in the same stratigraphic position. The sense of Mesozoic movement is reverse with the north side down. The Devonian sense of movement was probably normal with south side down.

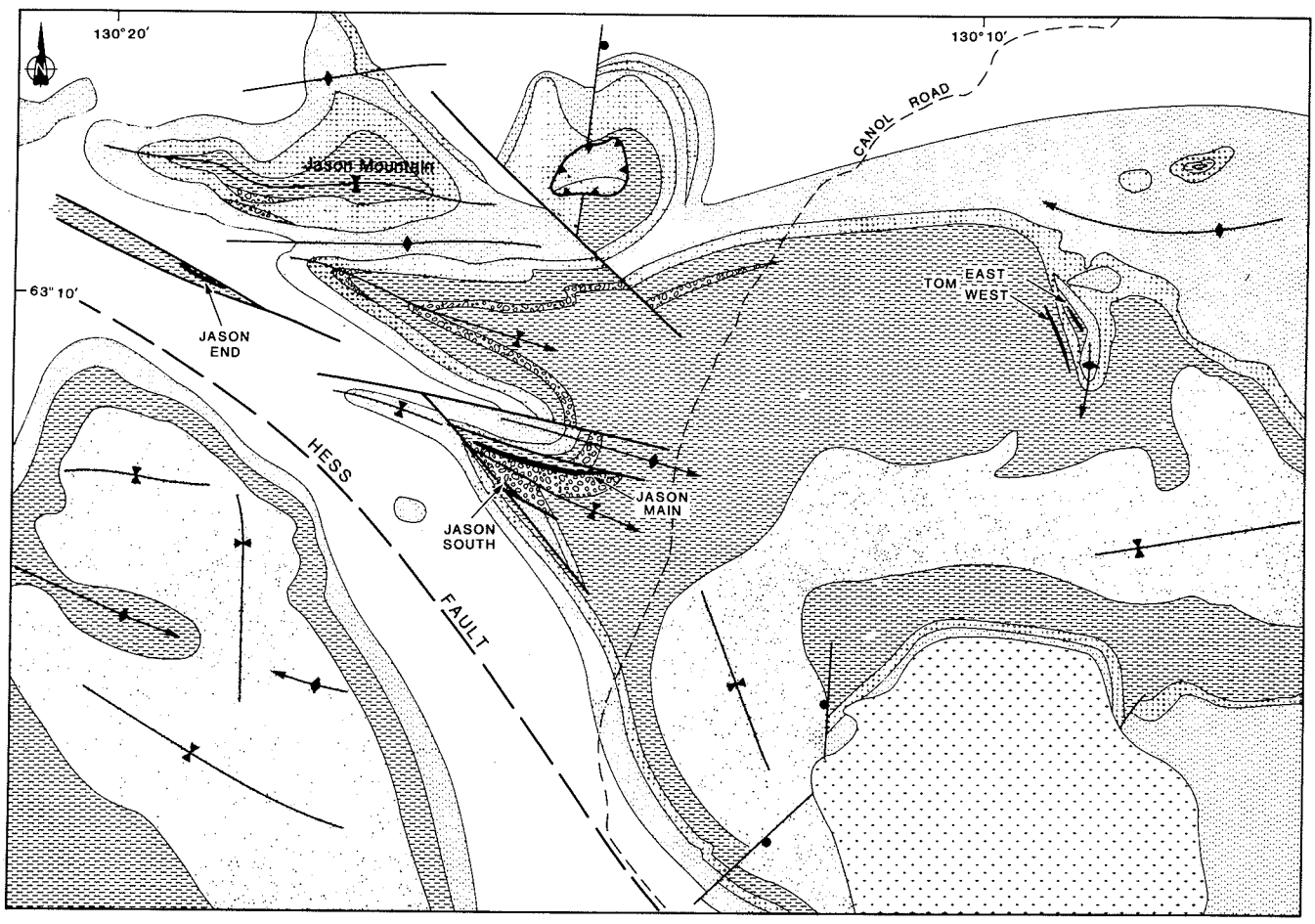

Figure 12 Bedrock geological map of the Tom and Jason deposit area (modified after Abbott, 1983; McClay and Bidwell, 1986).

Jason syndepositional fault

Setting

The Jason stratiform Zn-Pb-Ba deposit is located along the southern margin of the Central Block near the Hess fault (Figure 4). Portrait Lake strata are exposed in a series of upright tight west-trending, shallowly east-plunging folds north of the Hess fault on the Jason property (Figure 12). The Jason deposit occurs in the Jason syncline, southernmost of these folds (Turner, this volume). The Jason syncline is a

faulted, south-east plunging syncline; stratiform sulphide-barite occurs on both the south (South zone) and north (Main zone) limbs (Fig. 13). Within the syncline, Dp2 conglomerate, sandstone and siltstone are overlain by a sequence at least 270 m thick of interbedded matrix-rich heterolithic diamictites, sedimentary breccias, and conglomerate interbedded with siltstone and siliceous shale. Two stacked stratiform sulphide-barite lenses terminate up-dip against the steeply-dipping Jason fault on the south side of the syncline. Stratiform sulphide-barite is interbedded with the basal part of the diamictite-rich sequence as well as the uppermost siltstone of unit Dp2.

The Jason fault is a steeply-dipping, northwest-trending structure that juxtaposes older Road River strata to the south against Dp2, diamictite-rich strata, and stratiform sulphide-barite strata to the north. A younger subparallel reverse fault has offset all but a sliver of strata on the south side of the Jason fault (Fig. 13).

Diamictite-rich strata

Diamictites include a diverse suite of coarse-grained, poorly-sorted fragmental rocks composed of subangular to subrounded clasts of siltstone, mudstone, sandstone and chert conglomerate, and chert pebbles, in a poorly-sorted carbonaceous mud-rich matrix (Winn et al., 1981; Bailes et al., 1986; Turner, this volume). Diamictites include intraclast-rich breccias, pebbly mudstones, muddy conglomerates, and sandy mudstones. Many siltstone and mudstone clasts are 10 to 30 cm in diameter, some exceed a meter. These diverse clasts of the diamictite lithofacies have all been derived from underlying Dp2.

Interbedded diamictite, conglomerate and sandstone beds form discrete stratigraphic units referred to as "diamictite units". Isopach thicknesses of three diamictite units within the Jason syncline over an area 1200 m by 1200 m indicate deposition as northwest-trending lobes normal to the trend of the Jason fault (Turner, this volume). Individual lobes exceed 800 m in length, vary from 200 to 600 m in width and thicken to as much as 90 m where they terminate against the Jason fault. Diamictite lobes are wedge-shaped in longitudinal profile. With increasing distance from the Jason fault, diamictite beds thin and the average clast size decreases. Conglomerate, intraclast-rich conglomerate and sandstone occur together as lenticular, channel-like bodies parallel to the axis of the distal portions of diamictite lobes.

These patterns, and the textural and compositional character of the Jason fault (see below) suggest that the source of the diamictite lobes was across the Jason fault to the south or the submarine scarp of the Jason fault itself.

Syndepositional fault

The Jason fault does not crop out on surface but has been intersected in 13 drill holes over a strike length of 450 m and a dip extent of 400m (Turner, this volume). Stratigraphic throw amounts to about six hundred meters. Younger faults in the Jason area are composed of graphitic or muddy gouge that lack significant base metal content; however the Jason fault zone is indurated and composed of altered mudclasts and siderite vein fragments in an altered and sulphide-bearing matrix. Clasts are characterized by rounded to subrounded fragments of coarse-grained siderite, shale or siltstone cut by siderite veinlets or breccia. The matrix is massive fine-grained clay, quartz, muscovite and siderite with minor disseminated pyrite, sphalerite, galena, chalcopyrite and pyrrhotite.

The structure and composition of the Jason fault changes with depth (Turner, this volume). In the deepest portions, the fault zone is narrow, sharply defined, and associated with altered and sulphide-rich wall rocks. At shallower stratigraphic levels, the Jason fault is a broad, more diffuse zone of faults, pervasive ductile shear, spaced small-offset faults and veinlets that cut bedding at high angle. Here, the fault zone is clay-rich and only weakly altered; some siderite-pyrite veins in the hanging wall cut strata at high angle and show normal offset while others are folded, suggesting veining of unlithified sediment and then folding during compaction of the sediment.

Pre-Mesozoic orientation of Jason fault, and relationship to the Tom stratiform deposit

If the Jason syncline is unfolded about its gently east-plunging axis, the restored Jason fault trends east-northeast and dips about 40 degrees northwest (Turner, this volume). This restored orientation trends toward the present location of the Tom stratiform sulphide-barite deposit. The Tom deposit, like the Jason deposit, is adjacent to a west-side-down normal syndepositional fault (see Goodfellow and Rhodes, this volume) suggesting that both the Tom and Jason

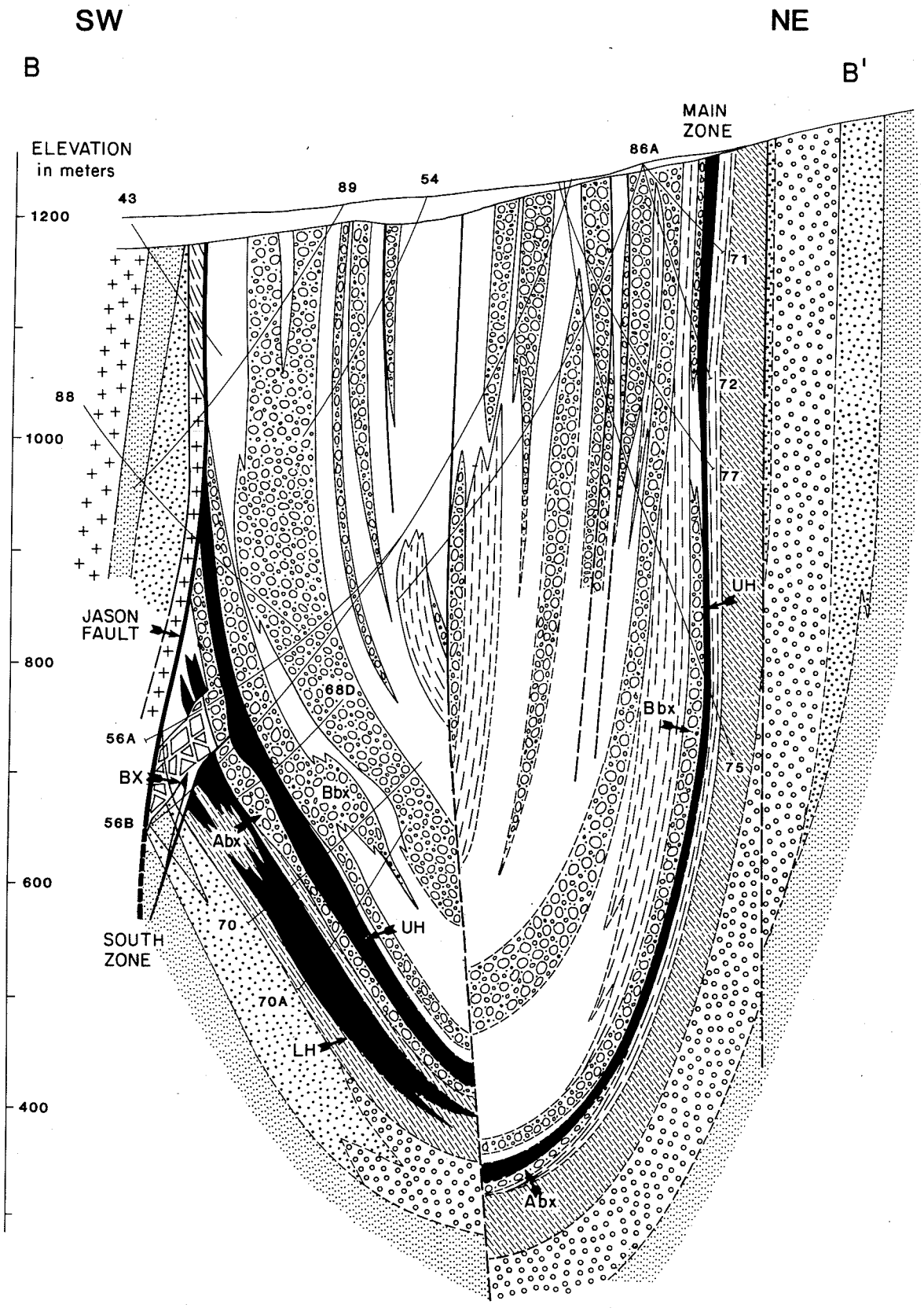

Figure 13 Geological cross-section looking west across the South and main zones. Several features are indicated: upper lens (UH), lower lens (LH), and individual diamicitite units (Abx, Bbx) (Turner, 1986).

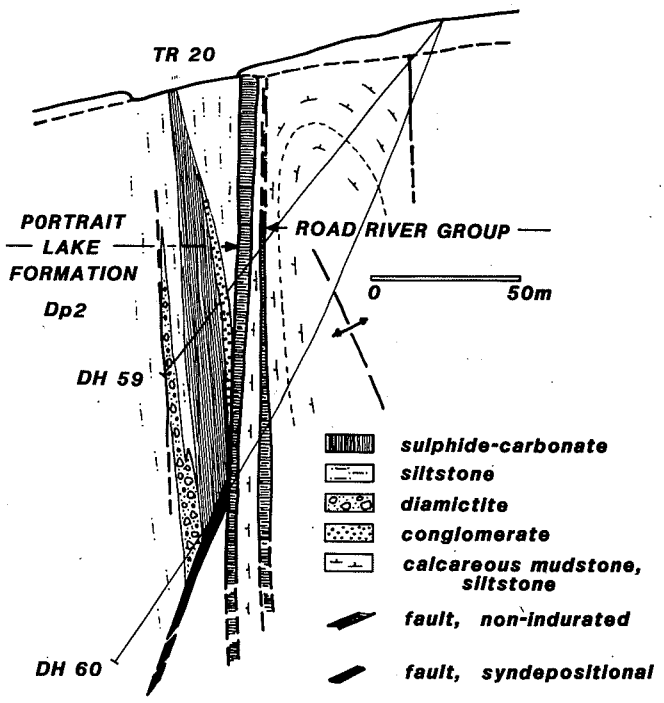

Figure 14 Geological cross-section of the Jason End zone deposit.

deposit formed adjacent to the same ENE-trending syndepositional fault.

Jason End zone syndepositional fault

Setting

The Jason End zone stratiform Pb, Zn deposit occurs within a fault-bound block (i.e. "End zone block") of Dp2 siltstone, sandstone and conglomerate of the Portrait Lake Formation, 5 km NW of the Jason South/Main deposit (Fig. 12). Knowledge of the stratigraphic setting of the End zone is complicated by this faulting.

Syndepositional fault

The steeply-dipping End zone sulphide deposit occurs along the northern margin of the fault-bound block of Portrait Lake Formation (Fig. 14). The sulphide body is separated from the fault by 2 m of conglomerate or interbedded siltstone and sandstone, and is successively overlain stratigraphically by a locally developed diamictite up to 5m thick, and ripple cross-laminated sand-banded siltstone at least 50 m thick. The End zone terminates down-dip, in DH 60, against a 1m wide, indurated, siderite fragmental zone interpreted to be a syndepositional fault. This structure is interpreted to dip south more shallowly than the sulphide body, and it is likely offset updip by the younger NW-trending fault. This zone is interpreted to be a syndepositional fault based on textural and compositional similarity to the Jason fault and thinning of diamictite away from the zone. The dominance of massive and vein-rich ferroan carbonate and lead-rich Pb, Zn, Fe facies indicate that the End zone represents a vent complex sulphide body, formed above a hydrothermal upflow zone (see Turner, this volume). Like the Jason South/Main sulphide body relative to the Jason fault, Pb/Pb+Zn ratios within the End zone sulphide body increase toward the proposed syndepositional fault.

Road River Group calcareous mudstone and sandstone turbidite (Fig. 12) immediately to the north are highly altered. Alteration includes intense silicification, replacement of calcareous strata by siderite bands, pods and disseminated euhedra ("buckshot" siderite), veins of siderite, ankerite, pyrite and minor pyrrhotite, sphalerite and galena, and brecciated silicified mudstone with siderite matrix. This alteration is thought to be related to the upflow of hydrothermal fluids on and near the End zone syndepositional fault.

Trend of the End zone fault; stratigraphic level of the Jason End zone deposit

Diamictite-rich units occur to the west, northeast and east of the End zone. Three hundred meters west of the End zone, a 100 m thick sequence of sandstone, diamictite and conglomerate overlies the Road River Group. One kilometer northeast of the End zone, a 50 m thick unit of diamictite is exposed at the base of the Dp2c conglomerate unit. The conglomerate is overlain successively by a thin siltstone unit and at least 10 m of diamictite. About 1 km east of the End zone on a south-trending ridge ("Crystal Ridge"), siltstone-clast-rich conglomerate, muddy conglomerate and diamictite with an aggregate thickness of at least 50 m occur at the base and top of the conglomerate unit. These diamictite-rich conglomeratic units are interpreted to interfinger with the regional Dp2c conglomerate. The End zone deposit overlies conglomerate, near or slightly below the stratigraphic level of the Jason South/Main deposit, and is interpreted to have formed just following conglomerate deposition. The east to northeast elongate distribution of diamictite-rich strata suggests the End

zone structure also trended east to northeast.

Boundary Creek syndepositional fault

The Boundary Creek prospect is located 15 kilometers northwest of the Jason South/Main deposit (Fig. 4) below a drift-covered valley bottom. Portrait Lake strata occur within a tight west-trending syncline cut by steep west-trending faults (Fig. 15) 1 km north of the Hess fault zone.

Anomalous diamictite-rich strata

In the immediate area of the Boundary Creek prospect, Portrait Lake Formation is composed of (1) a thick sequence over 400 m thick of conglomerate interbedded with muddy conglomerate, volcanic diamictite, volcanic tuffs, siltstone and mudstone overlain by (2) carbonaceous mudstone (Fig. 16) (Turner and Rhodes, 1990). The lower coarse clastic package is correlated with Dp2 and the overlying carbonaceous siliceous mudstone with Dp3. These anomalous diamictite-rich lower strata extend 1.5 km along strike (east-west) and about 2 km in a NE direction (3 km when Mesozoic shortening due to folding is removed). To the west and east, Portrait Lake strata lack diamictite and volcanic rock. Alteration and mineralization is limited to the anomalous diamictite-rich strata (see "Boundary Creek zinc prospect" below).

Units of muddy conglomerate, chert pebble diamictite and mudstone diamictite up to 30 m thick suggest local resedimentation of chert pebble gravels and interbedded muds. Volcanic diamictite with ferroan carbonate-altered volcanic clasts up to boulder size mixed with chert pebbles and mudstone fragments indicate resedimentation of volcanic rocks and sediments. The association of resedimented materials, volcanic rocks, and alteration and mineralization suggests proximity to a syndepositional fault that localized hydrothermal and volcanic activity.

Syndepositional fault

A steeply north-dipping zone of cataclastite, vein and breccia juxtaposes diamictite-rich Portrait Lake strata against older Road River Group in one hole at the Boundary Creek prospect (Turner and Rhodes, 1990) (Fig. 16). This nine meter interval is composed of two cataclastic zones that bracket and are overlain by highly altered rock with banded carbonate-sulphide veins up to 50 cm thick. The contact between the lower cataclastic zone and the Road River Group is a gouge zone indicating later fault reactivation, likely during Mesozoic deformation. The cataclastic zones consist of a foliated matrix of fine-grained quartz, clay, and ferroan carbonate with rounded to angular fragments of ankerite veins, fine-grained siderite and siliceous mudstone. Veins associated with the fault zone are rich in chalcopyrite and galena relative to the zinc-rich nature of the rest of the Boundary Creek deposit. Volcanic rocks adjacent to the fault zone are altered to an anomalous assemblage of black chlorite, ferroan carbonate and quartz found only in the fault zone.

Structural elevation on the Boundary Creek fault is reflected in the map pattern by a northward bulge of the upper contact with the Road River Group (Fig. 15). Reactivation of this fault may account for some of this offset.

The abundance of resedimented and locally derived coarse clastic rocks in the Portrait Lake Formation suggests fault movement during the Middle to Late Devonian. The northeasterly distribution of diamictite, alteration, and sulphides in the Boundary Creek area indicates a northeasterly trend of the Boundary Creek syndepositional fault.

STRATIFORM ZN-PB DEPOSITS

Jason South/Main stratiform deposit

The Jason South/Main stratiform Pb-Zn-sulphide-barite deposit (63°10' N; 130°15' W) is strongly zoned from a ferroan carbonate vent complex adjacent to the Jason syndepositional fault outwards to a laminated body of barite, chert, sphalerite, galena and pyrite (see Turner, this volume for expanded discussion). The Jason Main zone was discovered in 1975 by drilling a geochemical anomaly on a drift covered knoll 100 m above the valley. The South zone was discovered in 1978 drill testing a geochemical anomaly 400 m to the south. The property was optioned by Abermin Corporation (then Pan Ocean Oil Ltd., and later Aberford Resources Ltd.) in 1979. Approximately 30,000 m of surface diamond drilling from 1975 to 1982 has defined total geological reserves in the South, Main and End zones of 14.1 million tonnes grading 7.09% lead, 6.57% zinc and 79.9 g/tonne silver using a cut-off grade

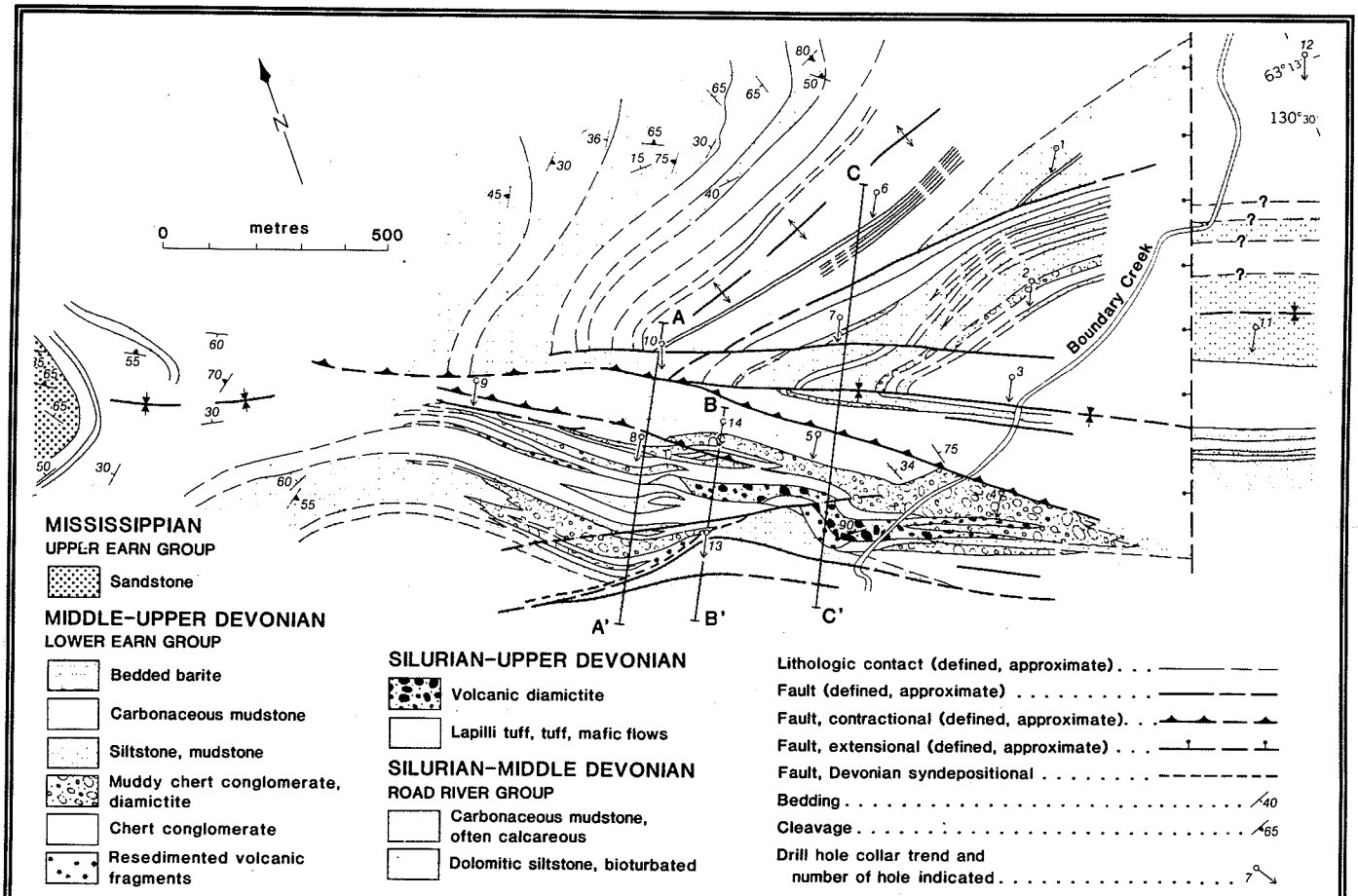

Figure 15 Generalized geologic map of the Boundary Creek area (Turner and Rhodes, 1990). Location of cross section (Figure 16) is indicated.

of 8% zinc plus lead (Bailes et al., 1986).

The Jason South/Main zone deposit is composed of two stacked lenses of sulphide-barite-ferroan carbonate. The upper lens extends from the Jason fault on the south limb to the north limb. The lower lens occurs only on the south limb. A breccia pipe merges with the Jason fault at depth, cuts the lower lens, and extends to the base of the upper lens. The lower lens is interbedded with siltstone, the upper lense with diamictite and carbonaceous mudstone.

Hydrothermal facies

Two distinct ore types occur within the Jason deposit: (1) veined and massive iron carbonate-sulphide adjacent to the Jason fault interpreted to be a vent complex and (2) widespread laminated barite, sulphide, and chert interpreted to be sedimentary exhalative in orgin. The barite-sulphide facies comprises most of the Jason deposit and is composed of millimeter-scale laminae of barite, chert, sphalerite or galena. Finely laminated pyrite and sphalerite interbedded with carbonacous chert form the distal fringe. Near the Jason fault, laminae of the barite-sulphide facies are interbedded with massive beds of sphalerite+galena, or galena+pyrite. Locally, sulphide strata show erosional scour and resedimentation.

Next to the Jason fault, vent complex ferroan carbonate rocks comprise much of the upper and lower horizons. In the upper lens, massive, mottled and veined ankerite contains a complex assemblage of galena, pyrite, pyrrhotite, quartz and minor fragments of silicified

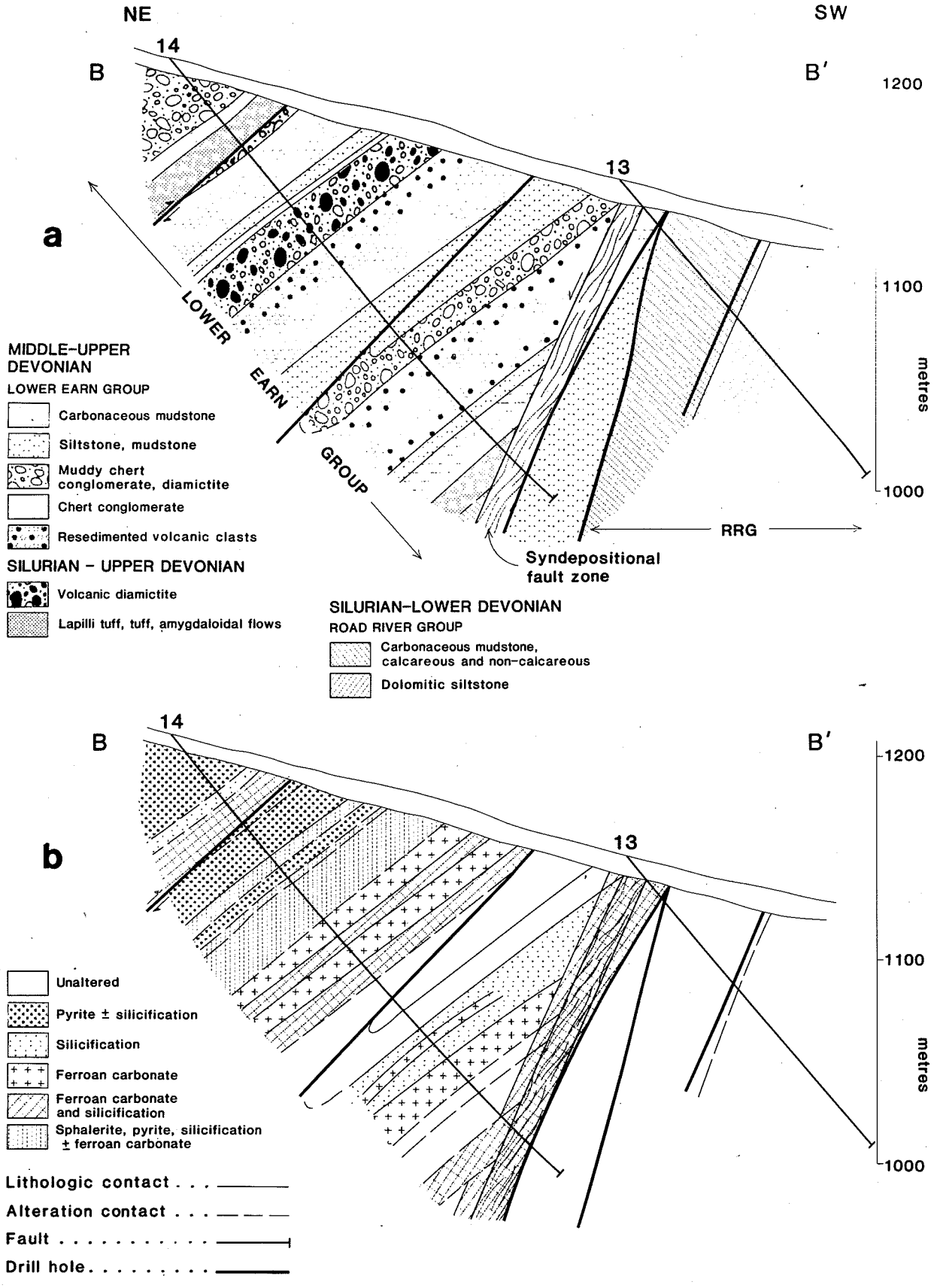

Figure 16 North-south structural cross-section through Boundary Creek deposit illustrating distribution of (a) lithologies and (b) alteration/mineralization types (Turner and Rhodes, 1990).

siltstone. The average mean homogenization temperature for fluid inclusions within ankerite, siderite and quartz is 250° C; salinity is interpreted to have been about 9 equivalent wt% NaCl (Gardner and Hutcheon, 1985). On the fringe of the vent complex, laminated barite-sulphide is silicified and replaced by banded and massive ankerite. The breccia pipe underlies this ferroan carbonate facies in the upper lens and is composed of angular fragments of silicified siltstone in a variable matrix of siderite, ankerite, muscovite, pyrrhotite, quartz, galena, and pyrite.

Based on stable and strontium isotopic data, the fluid that formed the Jason South/Main deposit was a radiogenic, highly evolved basinal or metamorphic fluid derived from continental strata; sulphide and sulphate sulphur was largely derived from ambient reduced seawater (Turner, this volume). Carbon in carbonates may reflect a mantle source or a mixture of organic and carbonate carbon from underlying strata (Turner, this volume).

Jason End zone stratiform deposit

The Jason End zone, 5 km northwest of the Jason South/Main zone, was discovered in 1980 by trenching a coincident soil geochemistry-gravity anomaly. The End zone deposit is a steeply dipping body that has been traced for 150 m on surface by trenching, and has been drilled by 4 drill holes to a maximum depth of 150 m (Bailes et al., 1986). The End zone is a small tonnage, high Pb+Zn grade deposit (very high Pb/Pb+ Zn ratio) that lacks associated bedded barite.

Setting

The End zone deposit occurs on the north margin of a fault-bound block of Portrait Lake Formation. The stratigraphy exposed in the fault block is (1) lowermost chert pebble conglomerate (>2m thick) or siltstone (>15m thick) with a faulted base; (2) End zone; (3) diamictite up to 5m thick; (4) siltstone, mudstone at least 50 m thick.

Mineral facies

Immediately adjacent to the End zone syndepositional fault, the End zone is composed of mottled siderite-pyrite-galena overlain by banded galena-pyrite (DH 60). Further from the fault (DH 59), the deposit is composed of (1) a basal breccia bed of banded chert-sphalerite fragments in a chert-pyrite matrix; (2) overlying mottled siderite-galena-pyrite with quartz pods and cut by veinlets of pyrrhotite, pyrite, sphalerite and galena (very similar to vent complex ferroan carbonate facies of the Jason South/Main deposit); and (3) an upper breccia bed of chert, pyrite, sphalerite and galena. The basal and upper breccia beds are interpreted to be resedimented sediments based on delicate interdigitating outlines of some chert-sulphide clasts that suggest soft-sediment deformation. Furthest from the syndepositional fault and exposed in surface trenches is high-grade massive to banded galena, sphalerite and pyrite.

Mineral chemistry

No fluid inclusion data exist for the Jason End zone. Limited sulphur isotope analyses exist from irregular veinlets of pyrite, pyrrhotite, sphalerite and galena (Gardner and Hutcheon, 1985). These $\delta^{34}S$ sulphide values are: sphalerite (20.0, 22.5), galena (17.7, 20.2), and pyrite (20.0). The calculated fractionation temperature for sphalerite-galena pairs are 315° C and 318° C +/- 25° C (Gardner and Hutcheon, 1985). Microprobe analyses of these sphalerite grains indicate an average composition of 13.3 wt% FeS (3 samples; Gardner and Hutcheon, 1985).

Tom stratiform deposit

The Tom stratiform Pb-Zn sulphide-barite deposit, like the Jason South/Main deposit, is strongly zoned from a ferroan carbonate vent complex adjacent to a syndepositional fault outwards to a laminated body of barite, chert, sphalerite, galena and pyrite. The laminated portion of the deposit composes the bulk of the deposit. The Tom stratiform zinc-lead-barite deposit is underlain by diamictite and resedimented conglomerate derived from Devonian sediments exposed on a syndepositional fault scarp. Geological reserves for the Tom deposit are 15.7 m tonnes averaging 7% Zn, 4.6% Pb and 49.1 g/tonne Ag (McClay and Bidwell, 1986). See Goodfellow and Rhodes, (this volume) for expanded discussion.

BOUNDARY CREEK (NIDD): A DEVONIAN EPIGENETIC ZINC DEPOSIT

The Boundary Creek deposit on the Nidd property occurs 15km northwest of the Jason deposit (Fig. 4). The Nidd property was staked in 1976 by Cominco Ltd., and between 1982 and 1989 fourteen

holes totalling 4665 m were drilled at the Boundary Creek prospect.

The Boundary Creek zinc deposit is defined by the extent of ferroan carbonate, pyrite, minor sphalerite and trace galena that occur within conglomerate, muddy conglomerate, diamictite and volcanic rocks adjacent to the Late Devonian syndepositional fault (Turner and Rhodes, 1990). This large tonnage, very low grade zinc deposit very likely represents an epigenetic variant of sedimentary exhalative deposits that formed synchronously with the nearby stratiform Zn-Pb-barite deposits. Mineralization coincided with latest activity of a small basaltic volcanic center at Boundary Creek.

Alteration and mineralization

Altered, sulphide-rich rock occurs within the anomalous Dp2 unit and underlying Road River Group calcareous mudstone over a stratigraphic thickness of 400 m and along a northeast trend of at least 1500 m. East and west of the Boundary Creek area, Portrait Lake strata lack diamictites and volcanics, multiple conglomerate horizons, and alteration or sulphide content (Fig. 15). Altered and mineralized rocks are variably silicified and contain ferroan carbonate, clay, pyrite, sphalerite, and minor galena, chalcopyrite and sericite. These minerals occur as interstitial cements within conglomerates, as replacement bodies, or as vein filling.

The Boundary Creek deposit is both texturally and compositionally zoned with increasing stratigraphic depth (Fig. 16). Hydrothermal minerals occur as cement within conglomerate and as replacement of diamictite at shallower stratigraphic levels, as veins and replacement of all rock types at greater depths, and as large banded sphalerite-carbonate veins and carbonate breccias locally along the syndepositional fault. The widest and most abundant veins are associated with the syndepositional fault. This vertical zonation suggests formation in a hydrothermal upflow zone along the syndepositional fault. Pyrite is the dominant sulphide in the shallowest part of the deposit, while sphalerite occurs with quartz as a cement in conglomerates, as replacement of volcanic rocks, or in veins interbanded with ferroan carbonate at intermediate and deeper levels. Galena is only significant in the deeper portions of the deposit, and chalcopyrite is limited to the syndepositional fault. Silicification is common throughout the intermediate and deep portion of the deposit. Ferroan carbonate occurs as cement, "buckshsot siderite", fine-grained bands, and veins in the intermediate and deep portion of the deposit.

Syndepositional fault zone

The syndepositional fault zone consists of multiple cataclastic zones within a 10 m wide zone of veined and altered rock (Fig. 16). The cataclastic zones have a matrix of fine-grained quartz, ferroan carbonate, and sulphides with angular to rounded fragments of fine-grained ferroan carbonate, ankerite veins, and siliceous mudstone. Sugary sphalerite veins; breccia veins of ankerite, chalcopyrite and pyrite; and veins of banded sugary sphalerite and pink, buff and reddish ferroan carbonate up to 50 cm thick cut the cataclastic zones and intervening silicified rock. Veins characteristically lack alteration selvages.

Origin of the Boundary Creek deposit

The presence within the Portrait Lake at Boundary Creek of (1) abundant resedimented sedimentary and volcanic material locally derived from uplifted Portrait Lake sediments, (2) a fault zone associated with major base metal veins representing a hydrothermal fluid upflow zone, (3) structural elevation of the Road River Group along this fault, and (4) the presence of volcanic tuffs rare elsewhere in the Lower Earn Group collectively argue for the existence of a submarine syndepositional fault that was the locus of basaltic eruptions and a conduit for hydrothermal fluids during Late Devonian time.

Possible interpretations of the formation of the Boundary Creek deposit include (1) exhalative sulphide deposition coincident with deposition of Dp2, (2) sulphide deposition at a shallow depth below the seabottom during the Late Devonian, or (3) post Late Devonian (e.g Cretaceous, Tertiary) epigenetic origin. The abundance of hydrothermal minerals as replacements and veins indicates a post-sedimentary formation. In addition, an exhalative model would predict the occurrence of laminated base metal sulphides within fine-grained mudrock interbeds within Dp2; such laminated suphides are absent. A shallow sub-seafloor diagenetic epithermal origin is consistent with the strong vertical textural and mineralogical zonation within the deposit, and evidence for strong permeability control during mineralization. Pyrite laminae in basal Dp3 mudstones may be syngenetic in origin and reflect venting of the hydrothermal fluids on the seafloor. If so, hydrothermal activity at Boundary Creek was

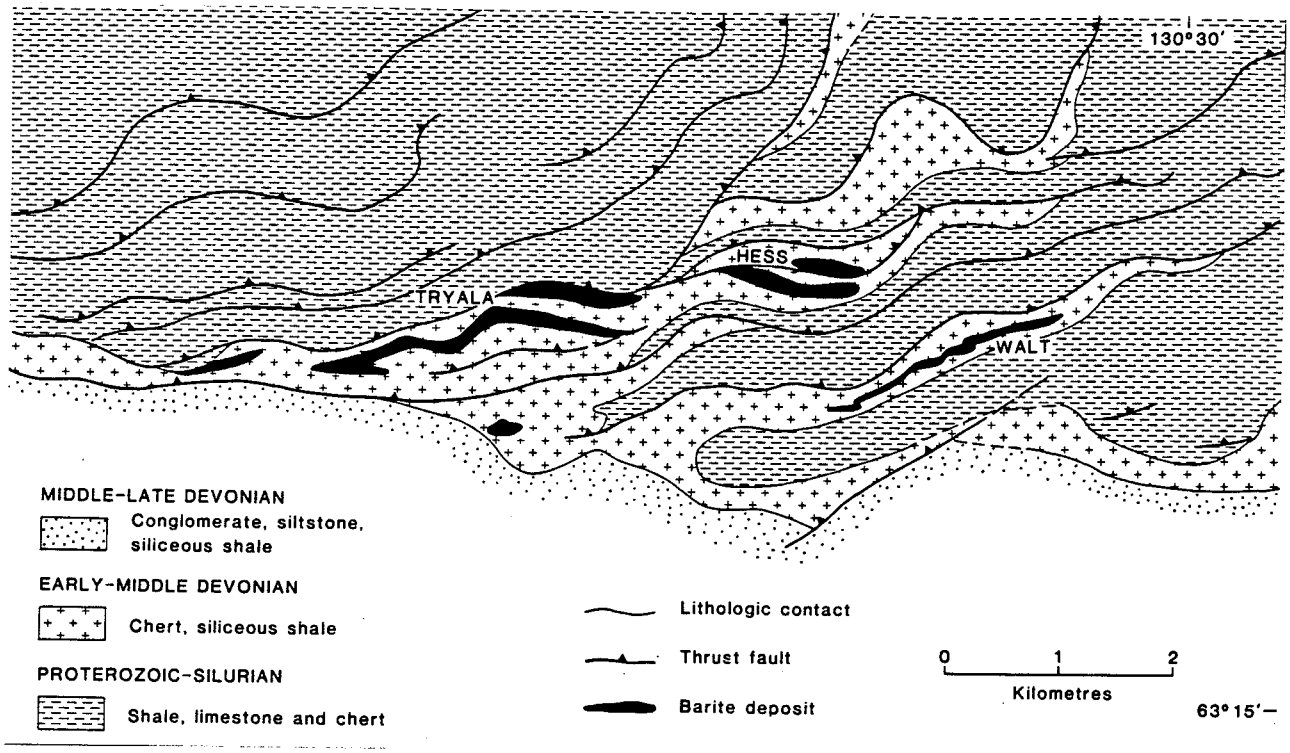

Figure 17 Geological map of a southern portion of the North Block showing distribution of stratiform barite deposits (modified after Abbott, 1983).

approximately coeval with formation of the nearby stratiform deposits.

Comparison to stratiform ZnPb deposits

Widespread silicification, abundant ferroan carbonate and minor sericite, and the presence of pyrite, sphalerite and galena at Boundary Creek as well as the Jason and Tom deposits suggests formation from similar hydrothermal fluids. Boundary Creek, however, has a much higher ratio of sphalerite to galena, and lacks pyrrhotite and pyrobitumen. The mineralized system at Boundary Creek may contain a similar tonnage of Zn but subordinate Pb when compared to the exhalative Tom and Jason deposits. Metal precipitated below rather than at the seafloor, probably due to rapid cooling related to either subseafloor boiling or mixing with seawater in permeable gravels.

STRATIFORM BARITE DEPOSITS

Thirteen stratiform barite deposits of Middle to Late Devonian age occur within the MacMillan Fold Belt (Fig. 4). In the South and Central Blocks, stratiform barite deposits typically occur in siliceous shale of unit Dp3, and in the North Block and northernmost western Central Block, in siliceous shale and chert of unit Dp1.

In the North Block, eight barite deposits occur in four separate thrust panels over a strike length of 13 km (Fig. 17). Whether or not these barite deposits were part of a single barite body prior to faulting is unclear.

Walt stratiform barite deposit

The Walt deposit (63°17'N, 130°33'W) crops out along the crest of an alpine ridge at about 1700 m elevation about 25 km northwest of the Jason South/Main deposit. In 1980, Baroid of Canada Ltd drilled 10 holes (899m) that outlined a zone up to 30 m thick and 150 m long containing 450,000 tonnes of

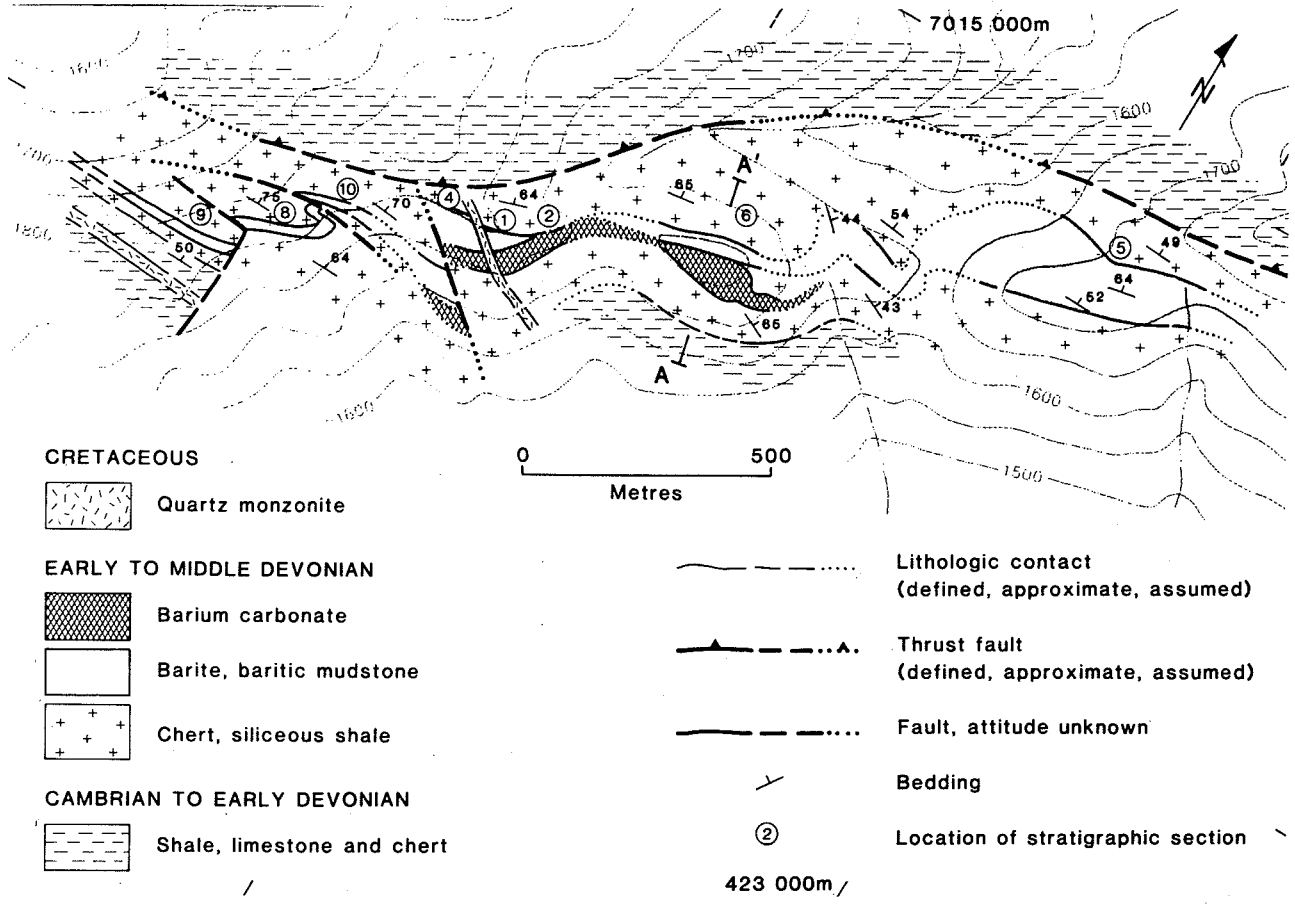

Figure 18 Geological map of the Walt property (from turner and Goodfellow, 1990).

baritic rock with a specific gravity above 4.25 (Abbott, 1981).

Structure and stratigraphy

The Walt barite deposit occurs on the eastern side and at the lowest structural level of the trend of barite deposits in the North Block (Fig. 17). This barite-carbonate body occurs at the top of a northwest-dipping thrust panel of Cambrian to Devonian strata, in black chert and siliceous shale of unit Dp1, near the thrust fault contact with structurally overlying Cambro-Ordovician strata (Abbott, 1983). The deposit includes concordant, cliff-forming carbonate bodies up to 60 m thick and continuous over at least 2 km, that are flanked and overlain by more recessive bedded barite (Fig. 18 and 19). The deposit forms an east northeast-trending ridge, the north slope of which is a dip-slope of barite beds. Carbonate in the barite body yielded conodonts of Eifelian to Givetian age (Middle Devonian) (Dawson and Orchard, 1982). XRD analyses of samples from the Walt property (Dawson and Orchard, 1982) identified barytocalcite, witherite, calcite, and gypsum.

Barite strata

Barite strata is more extensive than barium carbonate strata in the Walt deposit (Turner and Goodfellow, 1990). Sequences of finely-laminated dark grey barite up to 25 m thick are composed of dark grey

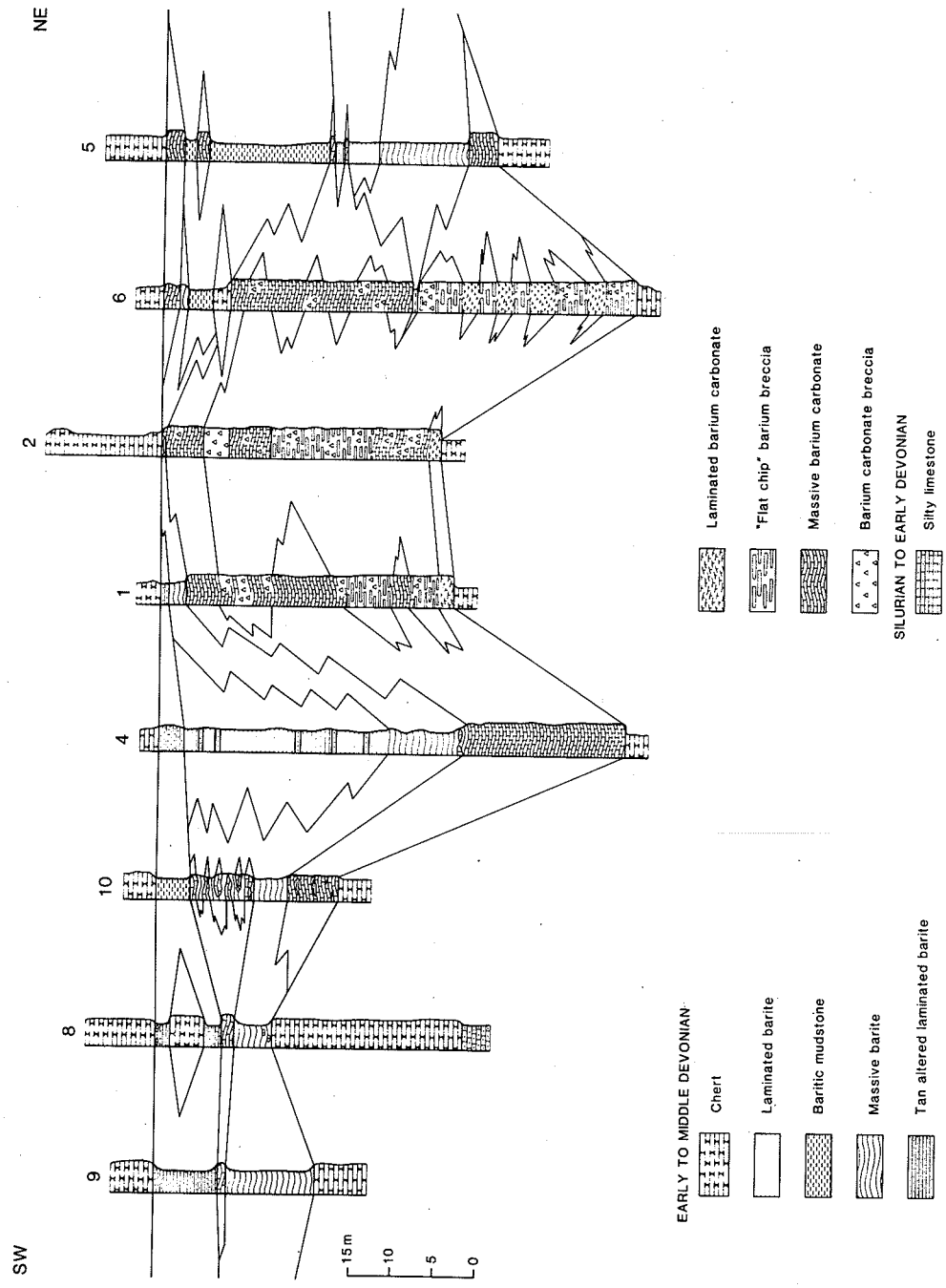

Stratigraphic fence diagram of the Walt deposit (from Turner and Goodfellow, 1990). Location of stratigraphic sections indicated on Figure 19.

organic-rich barite laminae 0.5 to 2 mm thick interbedded with minor black chert laminae (Fig. 19). Baritic mudstone and argillaceous barite, mixtures of barite, detrital quartz and clay, occur near the top of the barite horizon. At the nearby Hess property (Fig. 17), cross-laminated baritic sandstone beds up to 1 cm thick are interbedded with baritic mudstone suggesting resedimentation of baritic sediment.

Massive to faintly-banded, pale grey to black, sucrosic barite forms units up to 10 m thick. Massive barite is the common form of barite at the contact between barite and barium carbonate strata (Fig. 19).

Barium carbonate strata

Barium carbonate strata form cliff-forming bodies over a strike length of 800 m. Massive fine- to medium-grained barium carbonate forms units up to 20 m thick and is most abundant at the upper and lateral margins of the barium carbonate body, in a transitional position between carbonate breccias and barite (Turner and Goodfellow, 1990) (Fig. 19). Irregular discordant, locally concordant breccias up to 3 m thick occur in the core of the cliff- forming barium carbonate body. Clasts are angular to subrounded, sub-equant in shape, and typically 2-3 cm in diameter .

The contact between massive barium carbonate and barite facies is interdigitating and complex. Within this transition zone, massive barite is interbanded with bands and pods of carbonate. Locally, banded barium carbonate rock is transitional to laminated barite and laminae are noted to pass though a discordant reaction front. These textures suggest replacement of massive barite by massive barium carbonate (Turner and Goodfellow, 1990).

Origin of the Walt deposit

The stratiform nature of the barite strata suggests a sedimentary origin for the barite (Fig. 20). Interbedded carbonaceous chert and siliceous shale indicates hemipelagic and pelagic deposition within a basin starved of clastic input. The organic-rich nature of chert and barite, and the absence of bioturbation indicate sedimentation below a reduced watermass. Evidence suggests that barium carbonate strata formed by the replacement of a part of the sedimentary barite strata (Turner and Goodfellow, 1990) (Fig. 20). This replacement of barite by barium carbonate is interpreted to be related to vent processes coincident with deposition of the barite as there is no evidence for the association of carbonate replacement with younger faults or intrusives. This carbonate metasomatism is similar to ferroan carbonate replacement of bedded barite-sulphide at the Jason and Tom deposits (Turner, this volume; Goodfellow and Rhodes, this volume). Brecciation may have resulted from CO_2 effervescence in the hydrothermal fluids, hydraulic fracturing during hydrothermal fluid discharge, or tectonic movement on a syndepositional fault. A syndepositional fault is presumed to have been the focus of hydrothermal discharge; however no sedimentary breccias or other evidence for such a fault have been recognized and presumably it was small.

Hess stratiform barite deposit

The Hess barite-carbonate deposit lies a kilometer northwest of the Walt barite deposit in higher thrust panels but hosted in the same Dp1 chert (Fig. 4). The deposit has been repeated by a south-directed thrust. In the lower panel, it is very well exposed for a kilometer along a west-trending spur. Much of the body is stratabound massive to brecciated carbonate that is overlain and laterally equivalent to massive and laminated dark grey barite. The contact between carbonate and barite is interdigitating and shows replacement textures of carbonate after barite. The Hess deposit closely resembles the Walt deposit and the two are may be structural repetitions of one body.

Kobuk stratiform barite deposit

The Kobuk barite deposit (63°13'N, 130°34'W) occurs on the ridge immediately west of the Boundary Creek deposit (Fig. 4). Buff weathering, light grey bedded barite up to 75 m thick with a minimum strike length of 0.5 km occurs with carbonaceous shale of Dp3 (Fig. 15) near the contact with overlying Itsi Member. Bedded pyrite occurs in the barite (Morin et al., 1978; pg.9).

Moose stratiform barite deposit

The Moose stratiform barite deposit crops out on a south-trending ridge on the west side of the MacMillan River valley 10 km south southeast of the Jason South/Main deposit (Fig. 4). The deposit varies in thickness from 2 to 50 m , is at least 400 m long, and is deformed into a tight, north-trending anticline. The anticline is overturned to the east and both limbs dip to the southwest. The west limb appears offset and

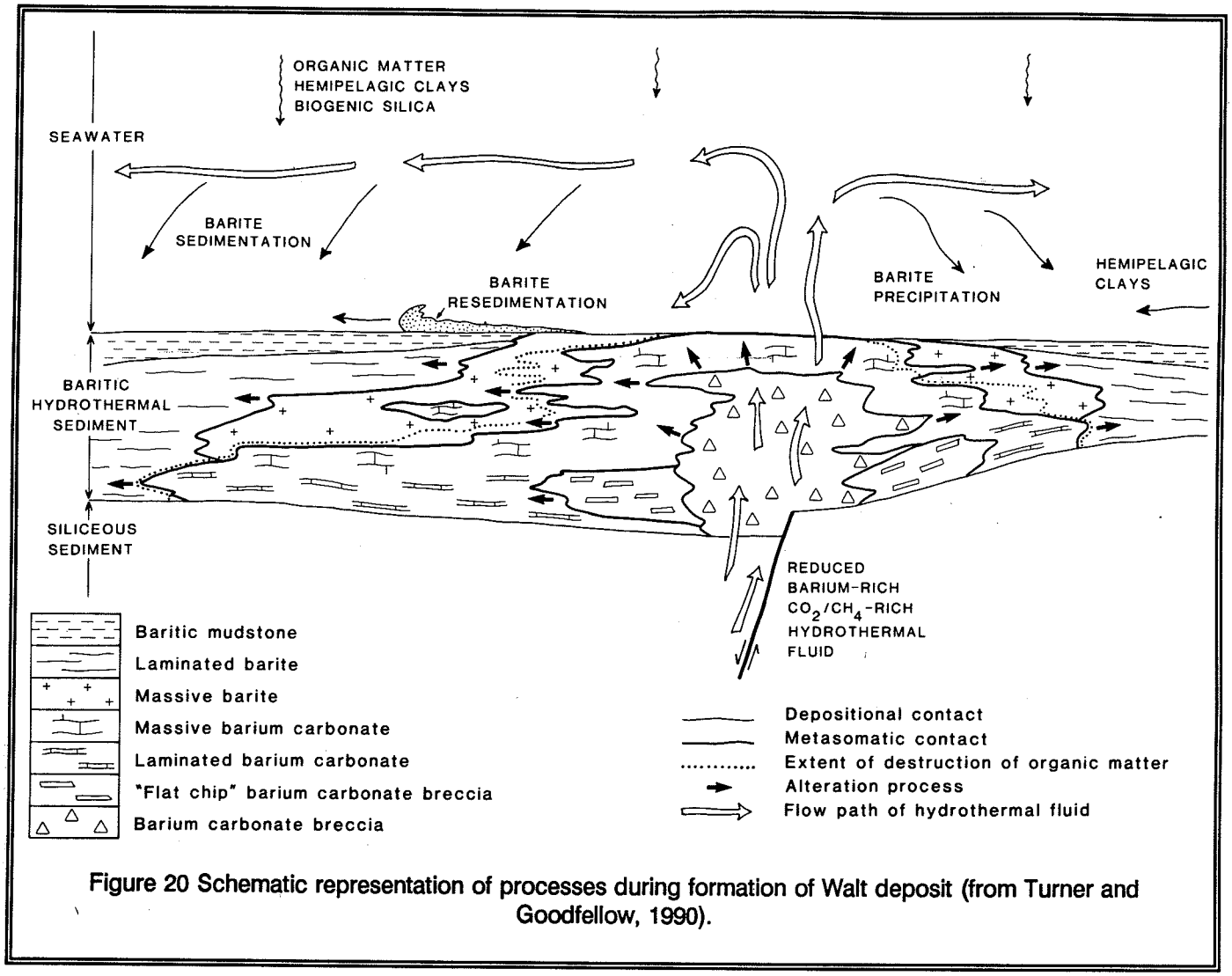

Figure 20 Schematic representation of processes during formation of Walt deposit (from Turner and Goodfellow, 1990).

elevated by a west-side-up reverse fault trending parallel to the fold axial plane. The deposit occurs within carbonaceous mudstones of Dp3, but is underlain and overlain by more chert-rich rocks. The lower cherty unit is a 5 to 15 m thick black siliceous shale and chert sequence that contains nodular barite and minor disseminated pyrite within 2 m of the overlying bedded barite. White laminated barite with some iron oxide stainning is interbedded with black siliceous shale up to a meter thick form a stratiform barite lens that thickens from 2 to 50 m towards the southwest along a strike length of 250 m. The barite is overlain by grey pyritic siliceous shale and chert interlaminated with minor barite laminae that decrease in abundance up section. This upper cherty unit appears to thicken to the northwest coincident with thinning of the barite body.

North Gary stratiform barite deposit

The North Gary stratiform barite deposit (63°02'N; 130°11'W) crops out on the steep mountain slope on the east side of the MacMillan River valley southeast of the Jason South/Main deposit. Statiform and nodular barite occur over a strike length of 3 km within Dp3 carbonaceous argillites just below the contact with the overlying Itsi Formation. The southern end of the deposit is within a kilometer of a granitic stock and unit Dp3 is hornfelsed to andalusite (chiastolite)-bearing

argillites.

The stratigraphy exposed on the mountain slope on the east side of the MacMillan River valley from oldest to youngest is: (1) greater than 100 m of siliceous laminated to thinly-bedded siltstone and argillites (Dp2p); (2) 30 to 60 m of diamictite containing chert and siltstone fragments in a mud-rich matrix, and interbedded with bedded sandstone; (3) black carbonaceous massive argillite about 70m thick; (4) several meters of black argillaceous chert with nodules and laminae of barite, and disseminated pyrite; (5) laminated white barite, celsian, and/or carbonate interbedded with black argillaceous chert; (6) black argillaceous chert up to 15 m thick with minor laminae of barite and disseminated pyrite; (7) carbonaceous argillite about 70m thick; and (8) sandstone and argillite of the Itsi Member. Within the chert unit overlying the barite body and near the uppermost laminae of barite in chert (about 10 to 25 m above the barite body) is a thin bed (10 to 50 cm) of coarsely crystalline grey limestone similar to that noted at the Pete and JK barite deposits. The limestone yielded middle Frasnian conodonts similar to those from the limestone immediately below the Pete deposit (Dawson and Orchard, 1982).

The stratiform barite deposit is up to 50 m thick near the southern limit of exposure where strata are deformed into an open northwest-plunging syncline cut by northeast-trending faults. Strata of the north limb are truncated by granite, strata on the southwest limb form a dip slope. Laminated barium carbonate occurs in outcrop at the base of slope to the southwest. To the northwest, the North Gary deposit thins rapidly to a thin fringe of nodular and laminated barian feldspar (celsian) and barite less than several meters thick but at least 2 km long; the celsian may be diagenetic or reflect thermal metamorphism of barite strata.

JK stratiform barite deposit

The JK stratiform barite deposit is exposed for 2 km across a north-trending mountainous spur about 5 km west of the Jason South/Main deposit (Fig. 4), in the South Block, about 3 km south of the Hess Fault. It occurs in Dp3 carbonaceous shales near the contact with the overlying Itsi Formation. Laminated barite varies from 3 to 10 m in thickness, and minor interlaminated pyrite appears to increase to the southeast. Fetid black coarsely crystalline limestone, similar to limestone at the Pete and North Gary deposits has been noted in nearby talus. Samples from the JK deposit are finely- laminated barite with laminae definition due to variation in barite grain size (average 0.1mm) as well as variation in accessory minerals such as carbonate (1%) and pyrite (0.1%). Micro-textures suggest carbonate has replaced barite grains.

Pete stratiform barite deposit

The Pete stratiform barite deposit (63°02', 130°06'), about 15km southeast of the Jason deposit (Fig. 4), is the most southeasterly of the stratiform barite deposits of the MacMillan Fold belt. The Pete claims were staked in 1975 by Ogilvie Joint Venture; 5 holes were drilled in 1978 totalling 590 m. The Pete deposit crops out on two southwest-trending ridges and has been drilled on lower ground to the east defining a strike length of at least 3 km.

Near the Pete deposit, carbonaceous siliceous shale of Dp3 and sandstone and argillite of the Itsi Member are repeated by northwest-trending, south-dipping contractional faults.

Stratiform barite occurs in two fault-bound panels. In the lower panel, a nodular barite horizon in the west grades to the east into a laminated barite body up to 7 m thick that is both underlain and overlain by nodular barite in carbonaceous siliceous shale. The laminated barite has a strike length of at least one kilometer, contains minor disseminated sphalerite and is locally carbonate-rich. The laminated barite body overlies a dark grey limestone bed 0.5 to 1 m in thickness that locally contains nodular barite. This limestone yielded middle Frasnian conodonts similar to the limestone above the North Gary barite deposit (Dawson and Orchard, 1982).

REGIONAL FERROAN CARBONATE ALTERATION

Stratiform sulphide-barite deposits at Macmillan Pass are intimately associated with carbonatization. The proximal replacement zones of the Jason South/Main and End zones, and Tom deposits are dominated by a ferroan carbonate. Extensive ferroan carbonate alteration occurs within calcareous shales of the upper Road River Group and siltstone and conglomerates of Dp2 over a strike length of at least 5 km from the End zone area east to the South zone/Main zone along the north side of the Hess fault zone. This alteration is composed of pervasive and porphyroblastic siderite cut by siderite veins and breccias, and quartz, ankerite and pyrite veins, all associated with extensive silicification.

Ferroan carbonate alteration is also associated with mafic volcanic flows, tuffs and low-grade base metal mineralization at the Boundary Creek prospect (Turner and Rhodes, 1990), and Devonian basaltic flows/sills and volcaniclastic rocks throughout the Central Block.

The ferroan carbonate clearly represents hydrothermal alteration though the source of the carbon is ambiguous. The calculated isotopic composition of the carbon in the Devonian hydrothermal fluid based on $\delta^{13}C$ analyses of ankerites and siderites at the Jason (Turner, this volume) and Tom (Ansdell et al., 1989; Goodfellow and Rhodes, this volume) deposits is compatable with that of CO_2 degassed from the mantle or a restricted mixture of carbon from organic matter and limestone in underlying Proterozoic and Paleozoic strata.

DISCUSSION

Relationship of stratiform barite to stratiform Zn-Pb-barite deposits

Stratiform barite deposits are generally interpreted to be sedimentary in origin, related to the submarine discharge of barium-rich hydrothermal fluids (e.g. Lydon et al., 1985; Poole, 1988). Such sedimentary exhalative models include (1) barite sedimentation adjacent to a submarine exhalative vent (e.g. Turner and Goodfellow, 1990), (2) barite sedimentation distant from the exhalative vent along a redox interface between a reduced barium- rich watermass and overlying oxygenated waters creating a barite 'bathtub-ring', or (3) barite sedimentation related to overturn and oxygenation of a reduced oxygen-rich water mass (Goodfellow and Jonasson, 1986).

Stratiform barite deposits differ from the Jason South/Main and Tom stratiform Zn-Pb-barite deposits by their lack of base metal content (i.e. laminated sphalerite and galena), and the exclusive occurrence of barian rather than ferroan carbonate in the vent complexes. This absence of base metals could be due to (1) hydrothermal discharge into oxygen-rich water and dispersal of metals (Lydon et al., 1979), or (2) low temperature fluids incapable of transporting metal complexes (Lydon et al., 1985). The former hypothesis is unlikely as the carbonaceous, non-bioturbated chert and mudstone of Dp1 and Dp3 indicate barite deposits were deposited below reduced botton water conditions. However, several lines of evidence suggest formation from low temperature, metal-poor fluids: (1) the lack of ferroan carbonate and sulphides within the vent complex at the Walt; (2) the absence of pervasive silicification common in vent complexes of stratiform Zn-Pb deposits; (3) lack of association with sedimentary breccias that would reflect association with a large displacement (and therefore deeply penetrating) fault; (4) formation of the barite deposits peripheral to the base metal and volcanic deposits in the core of the geothermal system; and (5) formation of barite deposits predate and postdate the formation of stratiform sulphide deposits (the major episode of hydrothermal activity), and therefore formed during the waxing and waning stages of geothermal activity .

Relationship of base metal deposits to volcanism

Basaltic volcanism predated and continued up to the time of formation of stratiform Zn, Pb deposits and occurred intermittently throughout the western portion of the ancestral Central Block (Fig. 4). The Boundary Creek zinc deposit is associated with a volcanic center, albeit a minor one. The youngest tuffs at Boundary Creek occur at the stratigraphic level of the Jason South/Main and Tom deposits. A link is therefore apparent between the sediment-hosted stratiform deposits and volcanic processes. Injection of basaltic magmas at depth presents a mechanism for generating the hot fluids (i.e. 250°C) interpreted from fluid inclusions at the Jason and Tom deposits (Gardner and Hutcheon, 1986; Ansdell et al., 1989). Though alteration makes the protolith difficult to interpret, volcanic rocks at Boundary Creek appear to represent a submarine basaltic center dominated by pyroclastic eruptions. These volcanic rocks are probably of alkaline affinity similar to other volcanics of Paleozoic age in Selwyn Basin (e.g. Mortensen and Godwin, 1986; Turner and Abbott, 1990).

Middle and Late Devonian history of the MacMillan Fold Belt geothermal system

The complex internal stratigraphy of the Earn Group near MacMillan Pass indicates a history of Devonian tectonism and geothermal activity. Low temperature hydrothermal activity was initiated in the Middle Devonian coincident with volcanism, reached a maximum during formation of stratiform base metal deposits in early Late Devonian, and waned later in the Late Devonian.

(1) Early and Middle Devonian chert basin

Late Early to early Middle Devonian marine transgression across Selwyn Basin and the carbonate shelf to the east resulted in a starved basin environment with deposition of pelagic and hemipelagic carbonaceous shale and argillaceous chert. A stratified watermass with reduced bottom waters persisted throughout shale and chert deposition.

(2) Middle Devonian uplift, volcanism, and low temperature hydrothermal activity

Differential uplift and erosion occurred in the ancestral Central Block, with erosion of Devonian siliceous shale and chert and locally, strata as old as Ordovician. Basaltic volcanism (tuffs, breccias, flows) and associated sill emplacement occurred within the ancestral Central Block. The ancestral North and South Blocks remained relatively quiescent, but in the North Block, seafloor venting of low temperature hydrothermal fluids formed large barite-carbonate deposits (e.g. Walt, Hess).

(3) Middle to Late Devonian conglomerate influx

Erosion and volcanism in the ancestral Central Block was followed by Middle Devonian subsidence, widespread deposition of the MacMillan Pass member, and local volcanism associated with continued faulting (Boundary Creek).

Turbidites of the MacMillan Pass member, derived from an uplifted subaerial source to the west, prograded eastward within the ancestral Central Block "graben" and spilled into the margins of the ancestral North and South Blocks. Early deposition of outer fan or basin plain turbidites with local gravel-rich channel systems, was followed by very rapid progradation of a gravel blanket deposit.

(4) Late Devonian faulting and high temperature hydrothermal activity (zinc-lead deposits)

Extension on northeast-trending and possibly west northwest-trending faults created a 20 km by 7 km WNW-trending rectangular domain of extension in the Central Block. This zone of extension overlapped with the older volcanic belt. Most fault activity immediately followed the termination of conglomerate deposition.

High temperature submarine discharge, associated with the intersections of active faults within this faulted basin at a number of centers resulted in the formation of seafloor sedimentary sulphide- carbonate +/- barite deposits (i.e Jason, Tom) (Fig. 21). Similar hydrothermal fluids precipitated sulphide-carbonate in shallow sediments coincident with latest tuff eruptions at the west end of the faulted basin (i.e. Boundary Creek). Extensive silicification and ferroan carbonate metasomatism occurred along the ancestal Hess fault on the southwest margin of the faulted basin. Hydrothermal activity coincided with the end of turbidite deposition and onset of widespread siliceous pelagic and hemipelagic sedimentation.

(5) Late Devonian chert basin and low temperature hydrothermal activity (barite deposits)

Following the cessation of high temperature exhalative activity and onset of pelagic sedimentation, sedimentary barite deposits (Fig. 21) formed along small displacement faults from submarine discharge of low temperature hydrothermal fluids. Most are peripheral to the older faulted basin that had localized high temperature geothermal discharge.

(6) Late Devonian uplift(?), erosion and sandstone deposition

Local erosion of Dp2 and Dp3 predated or coincided with differential subsidence and deposition of irregular thicknesses of northerly derived sandstone, siltstone and shale of the Itsi Member in the Central and South Blocks.

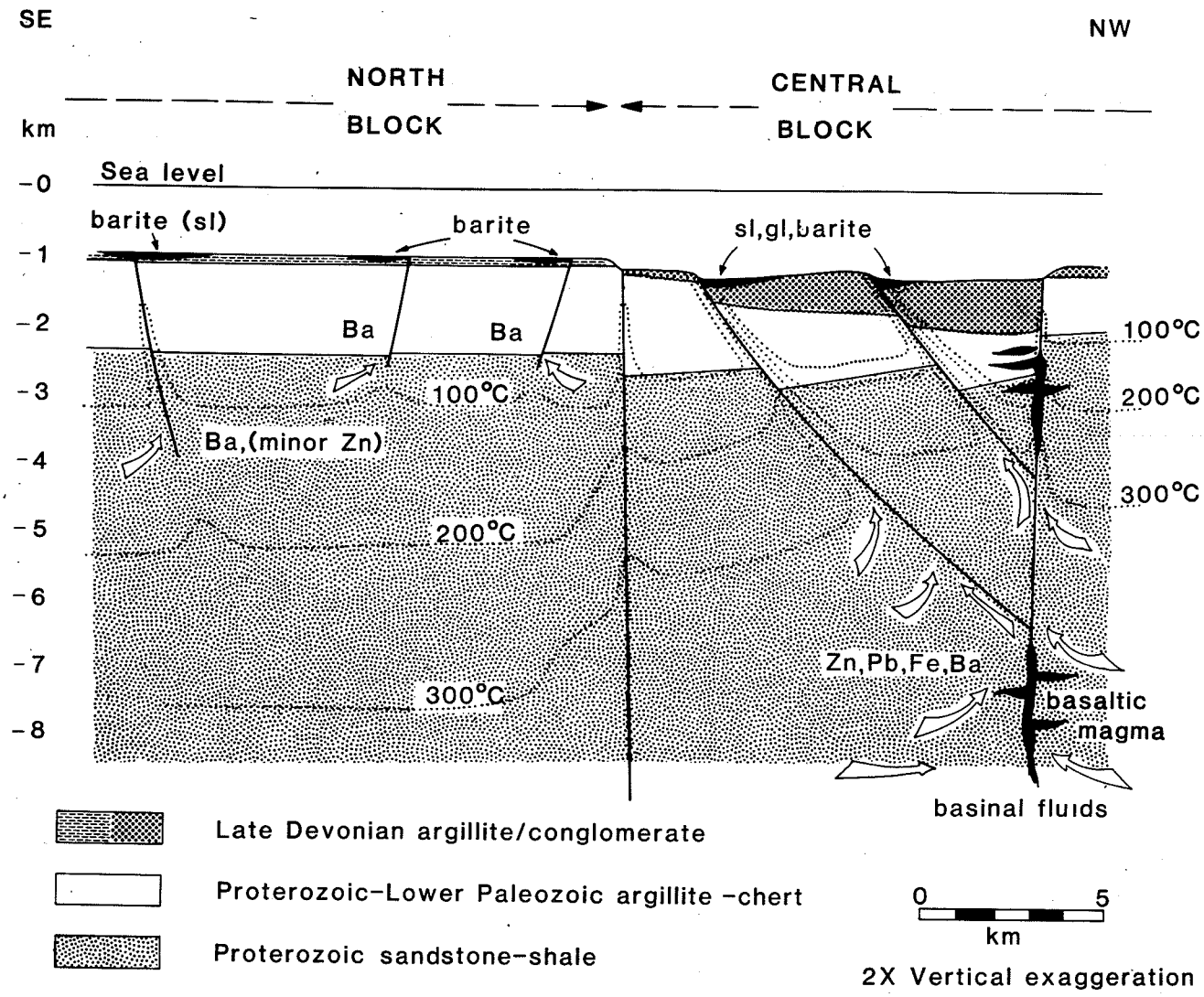

Figure 21 Schematic cross-section showing mineralizing process in the Macmillan Pass district during middle Devonian time.

REFERENCES

Abbott, J.B., 1981, Walt property description; in Yukon Geology and Exploratino 1979-80; Department of Indian Affairs and Northern Development, Canada, Whitehorse, Yukon, p. 216-217.

Abbott, J.G., 1982, Structure and stratigraphy of the MacMillan Fold Belt; evidence for Devonian faulting: in Yukon Geology and Exploration-1981; Exploration and Geological Services Division, Yukon, Indian and Northern Affairs Canada, p.22-33.

Abbott, J.G., 1983, Geology of the Macmillan Fold Belt 105O-SE and parts of 105P-SW (1:50,000): Exploration and Geological Services Division, Yukon, Indian and Northern Affairs, Canada, Open File Maps.

Abbott, J.G., in prep, Geology of the MacMillan Pass area, eastern Yukon; Exploration and Geological Services Division, Yukon, Indian and Northern Affairs, Canada pub.

Ansdell, K.M., Nesbitt, B.E., and Longstaffe, F.J., 1989, A fluid inclusion and stable isotope study of the Tom Ba-Pb-Zn deposit, Yukon Territory, Canada: Economic Geology, v.84, p.841-856.

Bailes et al., R.J.W., Smee, B.W., Blackadar, D.W., and Gardiner, H.D., 1986, Geology of the Jason lead-zinc-silver deposits, MacMillan Pass, Yukon Territory: in Morin, J.A. ed., Mineral Deposits of the Northern Canadian Cordillera, C.I.M.M., Special Volume 37.

Blusson, S.L., 1971, Sekwi Mountain map-area, Yukon Territory and District of Mackenzie; Geological Survey of Canada, Paper 71-22, 17 p.

Blusson, S.L., 1978, Regional geologic setting of lead-zinc deposits in Selwyn Basin, Yukon; in Current Research, Part A; Geological Survey of Canada, Paper 78-1A, p. 77-80.

Carne, R.C., 1979, Geological setting and stratiform mineralization Tom Claims, Yukon Territory: Exploration and Geological Services Division, Yukon, Indian and Northern Affairs Canada, Report 1979-4, 30 p.

Cecile, M.P., 1984, Geology of northeast Niddery map area; Geological Survey of Canada, open file 1006.

Cecile, M. P. and Abbott, J. G., 1989, Geology of the Niddery Lake map area (NTS 105-O) Yukon: Geological Survey of Canada Open File 2076.

Dawson, K. M. and Orchard, M. J., 1982, Regional metallogeny of the northern Cordillera: biostratigraphy, correlation and metallogenic significance of bedded barite occurrences in eastern Yukon and western District of Mackenzie: in Current Research, Part C, Geol. Surv. of Can., Paper 82-1C, p. 31-38.

Gardner, H.D. and Hutcheon, I., 1985, Geochemistry, mineralogy and geology of the Jason Pb-Zn deposits, Macmillan Pass, Yukon, Canada; Economic Geology, v. 80, p. 1257-1276.

Goodfellow, W.D., 1987, Anoxic stratified oceans as a source of sulphur: in sediment-hosted stratiform Zn-Pb deposits (Selwyn Basin), Yukon, Canada, Chemical Geology, v. 65, p. 359-382.

Goodfellow, W.D. and Rhodes, Dereck, this volume, Geological setting, geochem istry and origin of the Tom stratiform Zn-Pb-Ag-barite deposits.

Gordey, S.P., in press, Evolution of the northern Cordilleran miogeosyncline, Nahanni map area (105I), Yukon Territory and District of Mackenzie: Geological Survey of Canada, Memoir.

Gordey, S.P., J.G. Abbott and M.J. Orchard, 1982, Devono-Mississippian (Earn Group) and younger strata in east-central Yukon: Current Research, Part B, Geol. Surv. Can. Paper 82-1B, p. 93-100.

Gordey, S.P., Geldsetzer, Morrow, D.W., Bamber, E.W., Henderson, C.M., Richards, B.C., McGugan, A., Gibson, D.W., and Poulton, T.P., in press, Upper Devonian to Middle Jurassic Asemblages of Ancestral North America; in The Cordilleran Orogen; Canada, H. Gabrielse and C.J. Yorath (eds.), Geological Survey of Canada, no. 4. (also) Geological Society of America, The Geology of North America, no. G-2.

Lydon, J.W., Lancaster, R.D., and Karkkainen, P., 1979, Genetic controls of Selwyn Basin stratiform barite/sphalerite/galena deposits: an Investigation of the dominant barium mineralogy of the Tea deposit: in Current Research, Part B, Geological Survey of Canada, Paper 79-1B, p. 223-229.

Lydon, J.W., Goodfellow, W.D., and Jonasson, I.R., 1985, A general genetic model for stratiform baritic deposits of the Selwyn Basin, Yukon Territory, and District of Mackenzie: in Geol. Surv. Can., Paper 85-1A, p. 651-660.

McClay, K.R., 1983, Structure of the Tom Deposit, Yukon Territory: Geol. Assoc. of Can., Program with Abstracts v. 8. p. A45.

McClay, K.R. and Bidwell, G., 1986, Geology of the Tom Deposit, MacMillan Pass, Yukon Territory: in Morin, J.A. ed., Mineral Deposits of the Northern Canadian Cordillera, C.I.M.M., Special Volume 37, p. 100-114.

Morin, J. A., Marchand, M., and Debicki, R.L., 1980, Mineral Industry Report 1978, Yukon Territory: Exploration and Geological Services Division, Yukon, Indian and Northern Affairs Canada, 87 p.

Mortensen, J.K., and Godwin, C.I., 1982, Volcanogenic massive sulphide deposits associated with highly alkaline rift volcanic rocks in the southeastern Yukon Territory: Economic Geology, v. 77, p.1225-1230.

Poole, F. G., 1988, Stratiform barite in Paleozoic rocks of the Western United States, Proceedings of the Seventh Quadrennial IAGOD Symposium: E. Schweizerbart'sche Verlagsbuchhandlung Nagele u. Obermiller), D-7000 Stuttgart 1

Turner, R.J., 1985, Geology of the South Zone Deposits, Jason Property, MacMillan Pass Area, Yukon: in Yukon Exploration and Geology-1983, Indian and Northern Affairs Canada, p.105-114.

Turner, R.J.W., 1986, The genesis of stratiform lead-zinc deposits, Jason property, Macmillan Pass, Yukon: [unpub. Ph.D thesis], Stanford University, Stanford, 205 p.

Turner, R.J.W., this volume, Jason stratiform Zn-Pb-barite deposit, Selwyn Basin, Canada (NTS 105-0-1): Geological setting, hydrothermal facies and genesis.

Turner, R. J. W., Goodfellow, W.D., and Taylor, B.E., 1989, Isotopic geochemistry of the Jason stratiform sediment-hosted zinc-lead deposit, Macmillan pass, Yukon: in Current Research, Part E, Geological Survey of Canada, Paper 89-1E, p. 21-30.

Turner, R.J.W. and Abbott, Grant , 1990, Marg setting, structure, and zonation of the Marg volcanogenic massive sulphide deposit, Yukon: in Current Research, Part E, Geological Survey of Canada, Paper 90-1E, p. 31-41.

Turner, R.J.W. and Rhodes, Dereck, 1990, Boundary Creek zinc deposit (Nidd property), Macmillan Pass, Yukon: sub-seafloor sediment-hosted mineralization associated with volcanism along a Late Devonian syndepositional fault: in Current Research, Part E, Geological Survey of Canada, Paper 90-1E, p.321-335.

Turner, R.J.W. and Goodfellow, W.G., 1990, Barium carbonate bodies associated with the Walt (Cathy) stratiform barium deposit, Selwyn Basin, Yukon: a possible vent complex associated with a Middle Devonian sedimentary exhalative barite deposit: in Current Research, Geological Survey of Canada, Paper 90-1E, p. 309-319.

Winn, R.D., Jr. and Bailes, R.J., 1987, Stratiform lead-zinc Sulphides, mudflows, turbidites: Devonian sedimentation along a submarine fault scarp of extensional origin, Jason deposit, Yukon Territory, Canada: Geol. Soc. America Bull., v. 98, p. 528-539

Winn, R.D., Jr.,Bailes et al., R.J., and Lu, K.I., 1981. Debris Flows, turbidites, and lead-zinc sulfides along a Devonian submarine fault scarp, Jason Prospect, Yukon Territory: in Seimers, C.T., Tillman, R.W., and Williamson, C.R.; eds., Deep-water clastic sediments, a core workshop; Soc. Econ. Pal. and Min., Core Workshop No. 2, p. 396-416.

JASON STRATIFORM Zn-Pb-BARITE DEPOSIT, SELWYN BASIN, CANADA (NTS105-0-1): GEOLOGICAL SETTING, HYDROTHERMAL FACIES AND GENESIS

Robert J.W. Turner,
Geological Survey of Canada,
100 West Pender Street,
Vancouver, B.C.,
V6B 1R8

INTRODUCTION

Location

The Jason deposit is located in the Selwyn Mountains near MacMillan Pass on the border of the Yukon and Northwest Territories (63°10' N; 130°15' W; map sheet NTS 105-0-1)(Fig. 1). The Jason deposit is approximately 400 km northeast of Whitehorse, Yukon and is accessible via the North Canol Road during the summer from the town of Ross River and by air to an airstrip 6 km northeast of the Jason deposit.

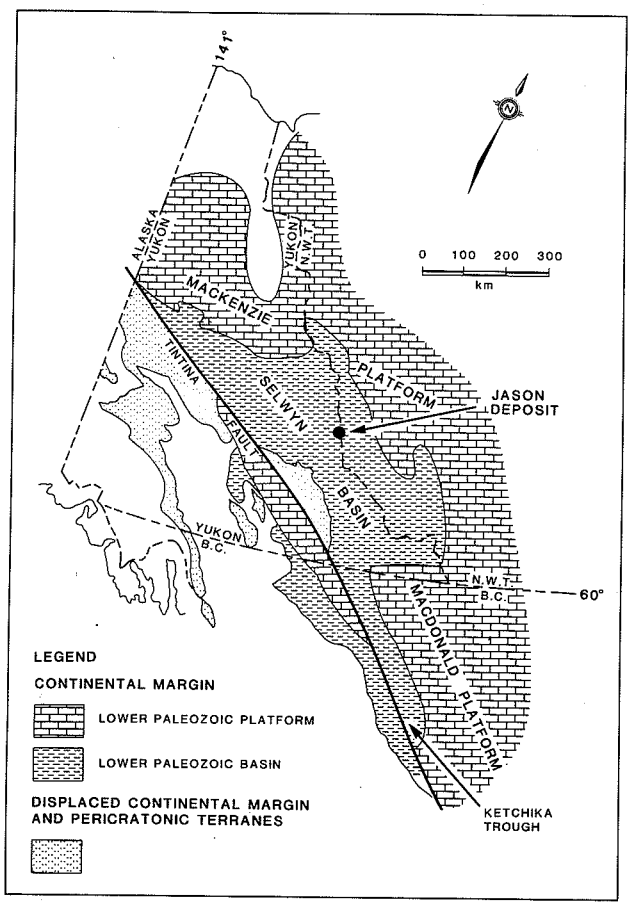

Figure 1 Map of northwestern Canada showing the location of Jason deposit within the context of Lower Paleozoic paleogeography of autochthonous North America (platform carbonate and basin shale-chert facies). Displaced terranes of North American affinity are also shown.

Exploration history

Zinc-lead mineralization was first discovered in the vicinity of MacMillan Pass at the Tom deposit in 1951. The adjacent Jason property was staked in 1975 by Clyde Smith for Ogilvie Joint Venture by following the host strata of the Tom deposit west across the South MacMillan River valley. The Jason Main zone was discovered in 1975 by drilling a geochemical anomaly on a drift covered knoll 100 m above the valley. The South zone was discovered in 1978 drill testing a geochemical anomaly 400 m to the south. The property was optioned by Abermin Corporation (then Pan Ocean Oil Ltd., and later Aberford Resources Ltd.) in 1979. The Jason End zone was discovered in 1980 4 km to the northwest below a drift covered valley slope by backhoe trenching a coincident geochemical and gravity anomaly.

Approximately 30,000 m of surface diamond drilling from 1975 to 1982 have defined total geological reserves in the South, Main and End zones of 14.1 million tonnes grading 7.09% lead, 6.57% zinc and 79.9 g/tonne silver using a cut-off grade of 8% zinc plus lead (Bailes et al., 1986).

Previous studies

The geologic setting of the Jason deposit has been discussed by Smith (1978, 1979), Teal and Teal (1978), Hubacheck (1981), Winn et al. (1981), Bailes et al., (1986), Turner (1986), Turner and Einaudi (1986) and Winn and Bailes (1987). The link betweeen syndepositional faulting and the formation of the Jason stratiform lead-zinc deposit was first pointed out by Smith (1978). The sedimentology of the sedimentary breccias was described by Winn et al. (1981); Turner (1986); and Winn and Bailes (1987). Turner (1984) recognized the Jason fault as syndepositional, and both the cause of the sedimentary breccias and the hydrothermal conduit for the Jason deposit. The mineralogy, mineral chemistry, textures and hydrothermal facies of the Jason deposit have been studied by Gardner (1983) and Turner, (1986). Other studies include isotope geochemistry (Longstaffe et al. 1982; Gardner, 1983; Gardner and Hutcheon, 1985; Turner et al., 1989) and fluid inclusion data (Gardner, 1983; Gardner and Hutcheon, 1985).

STRUCTURE

Structure of the MacMillan Fold Belt

The Jason deposit lies within the MacMillan Fold

Belt (MFB)(Abbott, 1982, 1983; Abbott and Turner, this volume), a 125 km by 30 km structural domain with an anomalous westerly trend within the northwest-trending structural grain of the Mackenzie Mountains. Outer continental margin strata of the Selwyn Basin (Fig. 1) exposed within the MFB include Upper Proterozoic and Cambrian sandstone, shale and limestone; Ordovician to Devonian shale, chert, limestone and mafic volcanic rock of the Road River Group; and Devonian carbonaceous shale, chert conglomerate and sandstone of the Portrait Lake Formation. Regional metamorphism is prehnite-pumpellyite grade except in the contact aureoles of granitic stocks of Upper Cretaceous age.

The unusual Mesozoic structural trend of the MFB reflect older Devonian faults according to Abbott (1982) who divided the MFB into three tectonostratigraphic domains (North, Central and South blocks) based on style of Mesozoic structure and Silurian-Devonian stratigraphy. The Jason and Tom stratiform Zn-Pb deposits, and the Boundary Creek zinc prospect occur within the Central Block (Fig. 2). The structure of the Central block is dominated by west-trending tight to isoclinal folds and steep contractional faults, a more complex structure than the North or South blocks. Within the Central block, Portrait Lake Formation strata overlie basaltic flows and volcaniclastic rocks as young as late Middle Devonian. Abbott recognizes three members within the Portrait Lake Formation: a lower chert member (Dp1), a middle turbidite member (MacMillan Pass Member) , and an upper siliceous shale member (Dp3) (see Abbott and Turner, this volume). A thick conglomerate unit within the MacMillan Pass member is limited largely to the Central Block reflecting deposition within a Devonian graben structure (Abbott, 1982). Also restricted to the Central Block graben are Middle to Upper Devonian volcanic rocks and syndepositional faults, and Upper Devonian base metal deposits.

Structure of the Jason syncline

The Jason stratiform Zn-Pb-Ba deposit is located near the southern margin of the Central Block near the Hess fault zone (Fig. 2). The Hess fault underlies west-trending and northwest-trending valleys covered by glacial drift. Portrait Lake strata are exposed in a series of upright tight west-trending, shallowly east-plunging folds north of the Hess fault on the Jason property (Fig. 3). Stratiform Zn-Pb-barite mineralization occurs on the north limb (Jason Main zone) and the

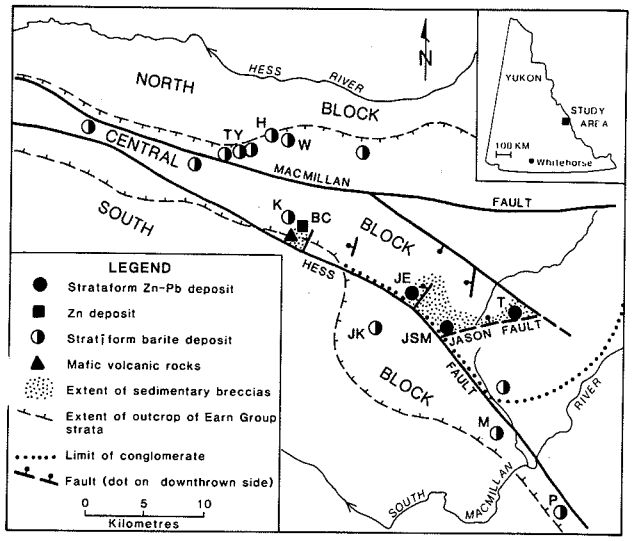

Figure 2 Distribution of Devonian age faults, sedimentary breccias, stratiform Zn-Pb-barite, stratiform barite deposits and volcanic rocks in the Macmillan Pass area. The North, Central and South blocks are separated by the Macmillan and Hess faults respectively. Zinc-lead prospects noted on the map are Jason South/Main (JSM), Jason Tyrala (TY), Hess (H), Walt (W), K (Kobuk), JK (JK), Gary (G), Moose (M), and Pete (P). Inset map shows location of Macmillan Fold Belt.

south limb (Jason South zone) of the Jason syncline, southernmost of these folds (Fig. 4, 5 and 6).

The Jason syncline subcrops below a low knoll on the northwest side of the MacMillan River valley. Strata of the Jason syncline are poorly exposed on surface; most knowledge is based on drilling and surface trenching. Strata on both the north and south limbs are steep-dipping and west-trending. Evidence for an isoclinal syncline is based on the reversal of stratigraphic tops and repetition of stratigraphy between the South zone area (south limb) and the Main zone area (north limb). A west-trending, steep-dipping penetrative cleavage is observed in surface outcrops. Westward convergence of the north and south limbs indicates the Jason syncline plunges shallowly to the east under the MacMillan River valley.

Numerous faults have been intersected during drilling (Fig. 4, 5 and 6); based on textural character, drill hole correlations, offset of surface lithologies, and air photo lineaments, these faults are divided into three

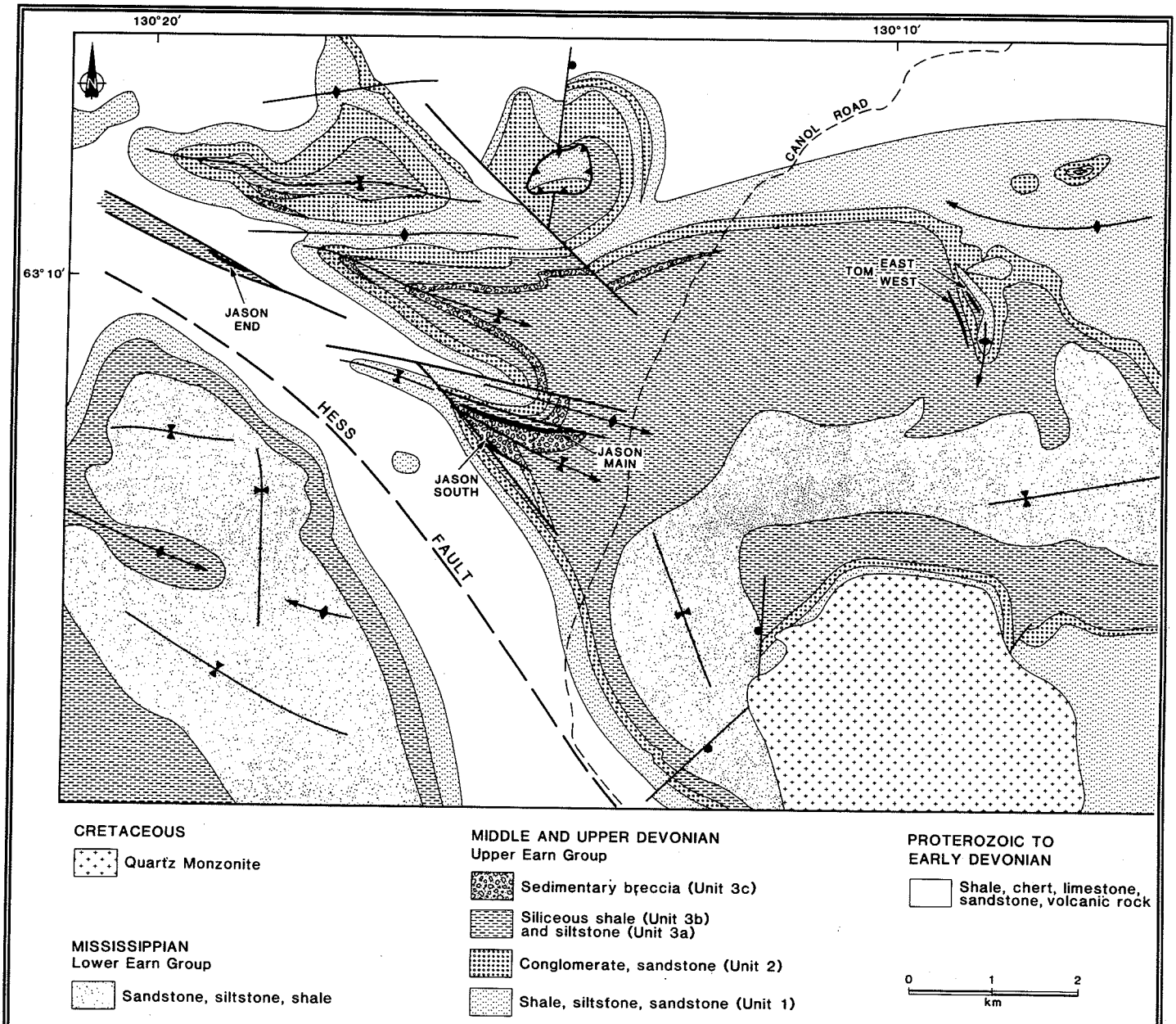

Figure 3 Bed-rock geologic map of the Jason deposit area (modified after Abbott, 1983; McClay and Bidwell, 1986). Distribution of Quaternary sedimentary cover is not shown.

sets: (1) the Jason fault, a Devonian syndepositional fault; (2) steeply-dipping, easterly-trending faults that are parallel or oblique to the axial plane of the syncline, and (3) younger steep north-trending graphitic or mud gouge faults that offset all other structures with small displacement.

Jason fault: Devonian syndepositional fault

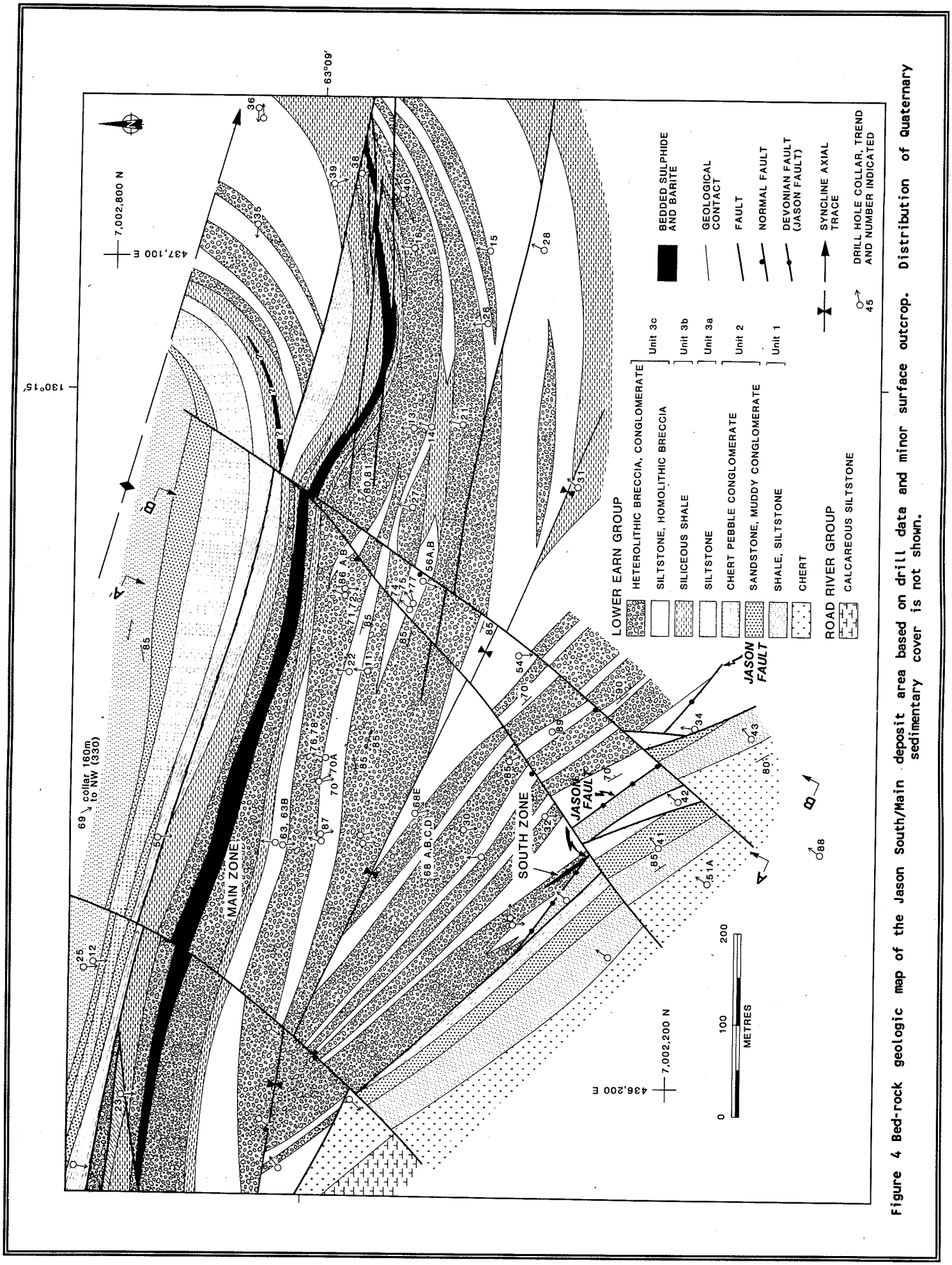

Figure 4 Bed-rock geologic map of the Jason South/Main deposit area based on drill data and minor surface outcrop. Distribution of Quaternary sedimentary cover is not shown.

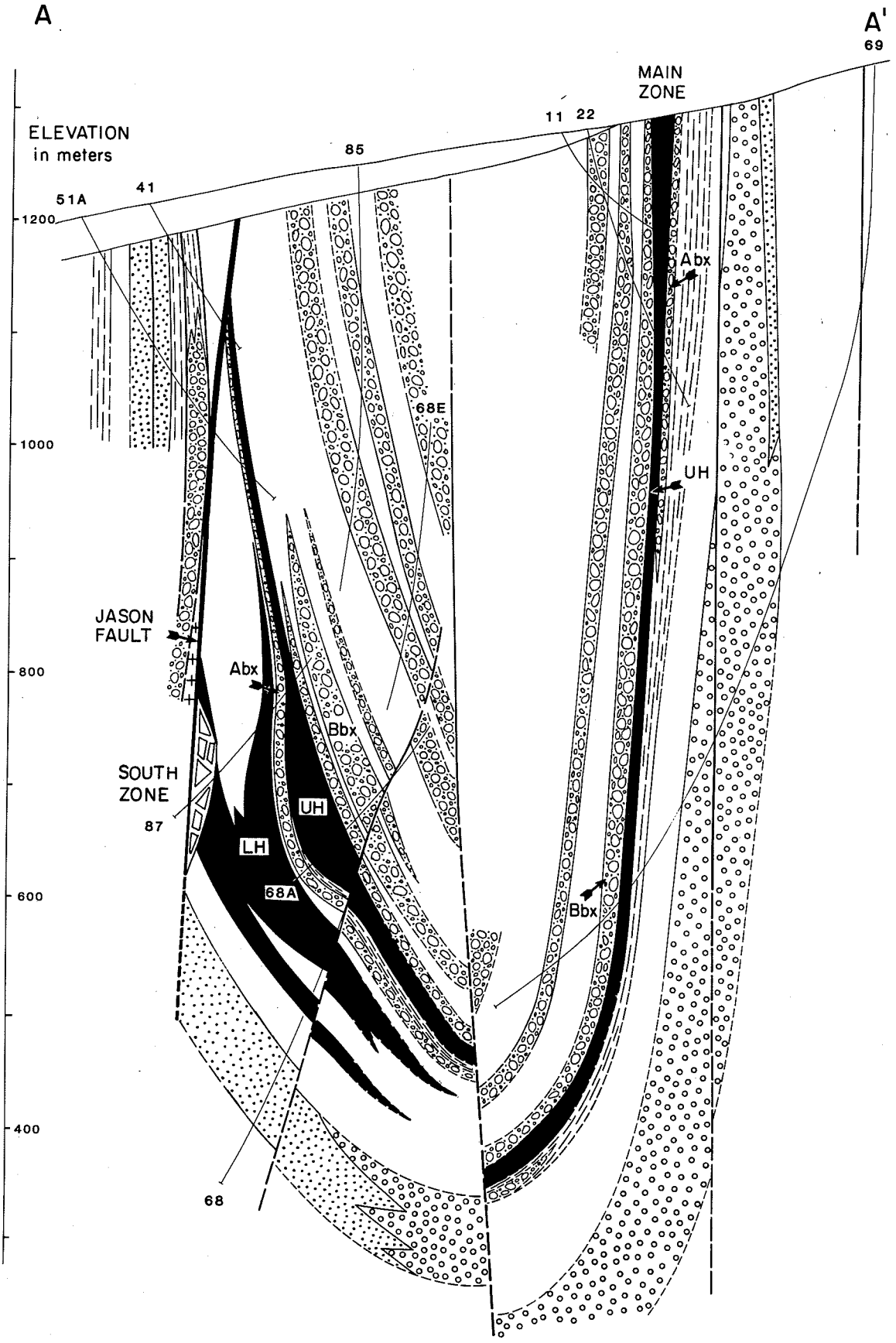

Figure 5 Geologic cross-section A-A' looking west across the South and Main zones. Several features are indicated: upper lens (UH), lower lens (LH), A diamictite unit (Abx), B diamictite unit (Bbx). Refert to Figure 4 for the location of the section and legend for lithologic symbols.

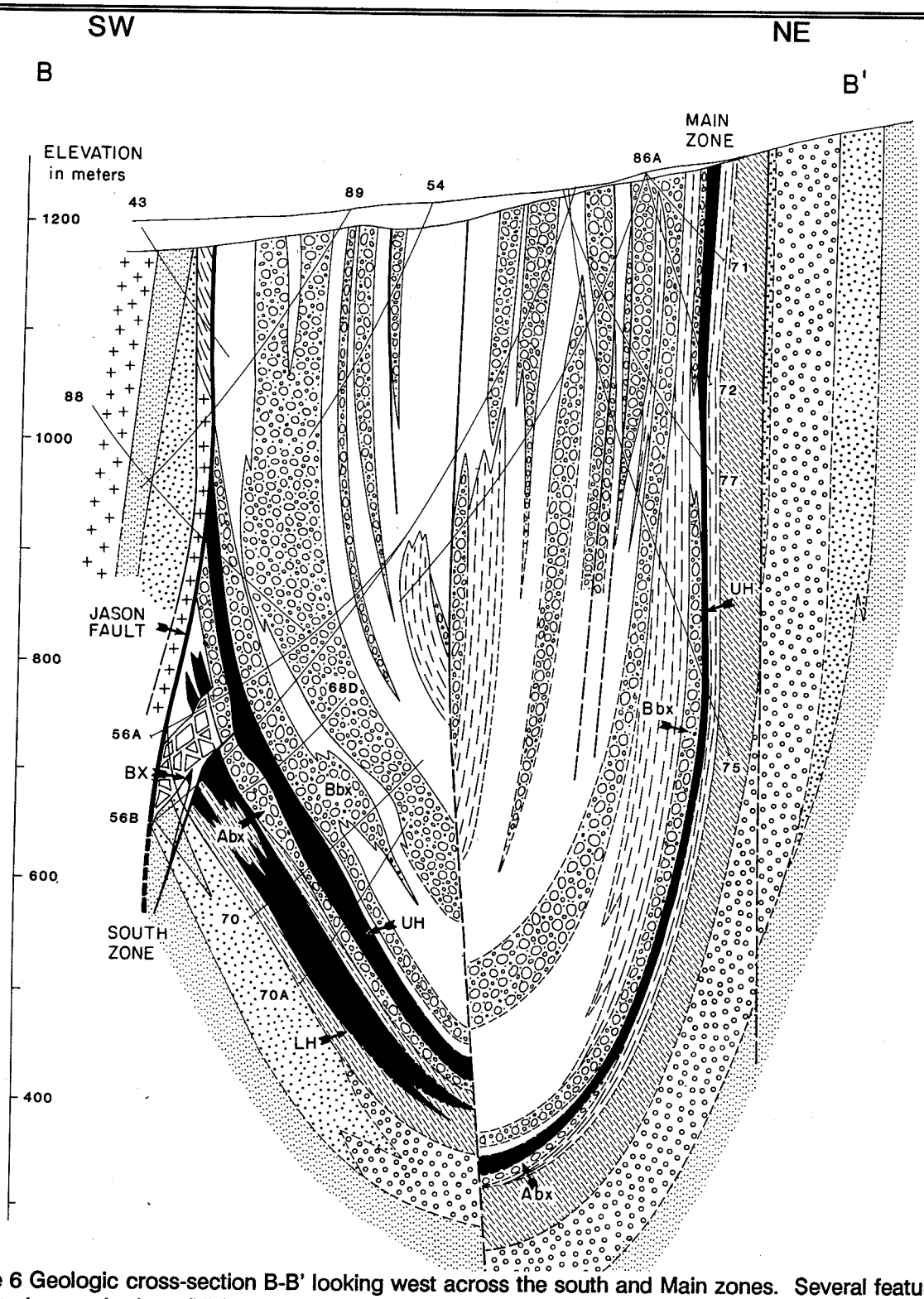

Figure 6 Geologic cross-section B-B' looking west across the south and Main zones. Several features are indicated upper horizon (UH), lower horizon (LH) and individual diamictite units (Abx, Bbx) (modified after Turner, 1986). Refer to Figure 4 for the location of the section and legend for lithologic symbols.

Geometry and offset

The Jason fault is a steep south-dipping, northwest-trending structure that offsets steep north-dipping strata on the south limb of the Jason syncline (Fig. 4, 5 and 6). The Jason fault juxtaposes older calcareous siltstone of the Road River Group, and chert of the lower member of the Portrait Lake Formation (Dp1) against younger Dp2 and Dp3 including stratiform sulphide-barite lenses and the diamictite lithofacies. South side strata occur within a thin structural sliver bound to the south by a younger subparallel fault. The stratigraphic level of the Jason deposit has not been recognized south of the Jason fault.

The Jason fault does not crop out on surface but has been intersected in 13 drill holes over a strike length of 450 m and a dip extent of 400 m (Fig. 5 and 6). Stratigraphic omission across the Jason fault indicates normal movement. Stratigraphic offset across the fault can only be indirectly calculated as no stratigraphic marker has yet been observed on both sides of the fault. Six hundred metres of displacement is estimated on the Jason fault based on apparent offset of the estimated position of the base of the MacMillan Pass Member (Fig. 6). The Jason fault is cut by younger northwest and northeast trending faults (Fig. 4).

Textural character

Younger faults in the Jason area are filled with graphitic or muddy gouge that lack significant base metal content; however the Jason fault zone is an indurated fragmental unit composed of altered mudclasts and siderite vein fragments in an altered and sulphide-bearing matrix. Clasts are rounded to subrounded coarse-grained siderite, and shale or siltstone cut by siderite veinlets or breccia. The matrix is massive fine-grained clay, quartz, muscovite and siderite with minor disseminated pyrite, sphalerite, galena, chalcopyrite and pyrrhotite.

For further discussion of the Jason fault, see "Hydrothermal facies of the Jason deposit".

STRATIGRAPHY OF THE JASON SYNCLINE

The oldest rocks exposed in the Jason syncline are fossiliferous black calcareous shales intersected on the south side of the Jason fault (DH63-587-591.6m)(Fig. 7). These strata contain Middle Devonian tentaculites and correlate with Silurian to Middle Devonian age silty limestone of the upper Road River Group (unit SIDl of Abbott, 1982).

The Portrait Lake Formation near the Jason deposit has been divided into a lower chert member (Dp1), a MacMillan Pass member of conglomerate (Dp2c,s) and siltstone (Dp2p), and an upper siliceous shale member (Dp3) (Abbott, 1982; Abbott and Turner, this volume) (Fig. 7). Dp1 has only been intersected south of the Jason fault. North of the Jason fault, the oldest strata drilled belong to the MacMillan Pass member. Upwards from its base the MacMillan Pass member is composed of a lower silty mudstone unit (Dp2p), a middle sandy conglomerate unit (Dp2c,s) and an upper siltstone unit (Dp2p). These strata are overlain by interbedded diamictite, sedimentary breccia, siltstone, siliceous shale and conglomerate that are laterally equivalent with regionally extensive siliceous shale (Dp3). Stratiform sulphide-barite-chert is interbedded with the uppermost siltstone of Dp2 and the lowermost diamictite and siliceous mudstone of Dp3.

Lower Member (Dp1)

Bedded black chert is in transitional contact with overlying silty mudstone of Dp2 south of the Jason fault (Fig. 8; DH89). Conodonts recovered from black chert of Dp1 at the Walt (Cathy) barite deposit are interpreted as early Middle to early Late Devonian age (Dawson and Orchard, 1982).

MacMillan Pass Member (Dp2)

The MacMillan Pass Member is greater than 150 m thick within the Jason syncline. North of the Jason fault, the base is not exposed. Drilling has intersected a lower silty mudstone unit, a middle conglomerate and sandstone unit, and an upper siltstone unit. The lower stratiform sulphide-barite lens of the Jason deposit is interbedded with the upper part of the upper siltstone unit. No fossils have been collected from the MacMillan Pass Member, and its age is constrained as Middle to early Late Devonian based on fossil collections from Dp1 and Dp3.

Silty mudstone unit (Dp2p)

The lower silty mudstone unit is composed of dark-grey mudstone interbedded with thin sandstone

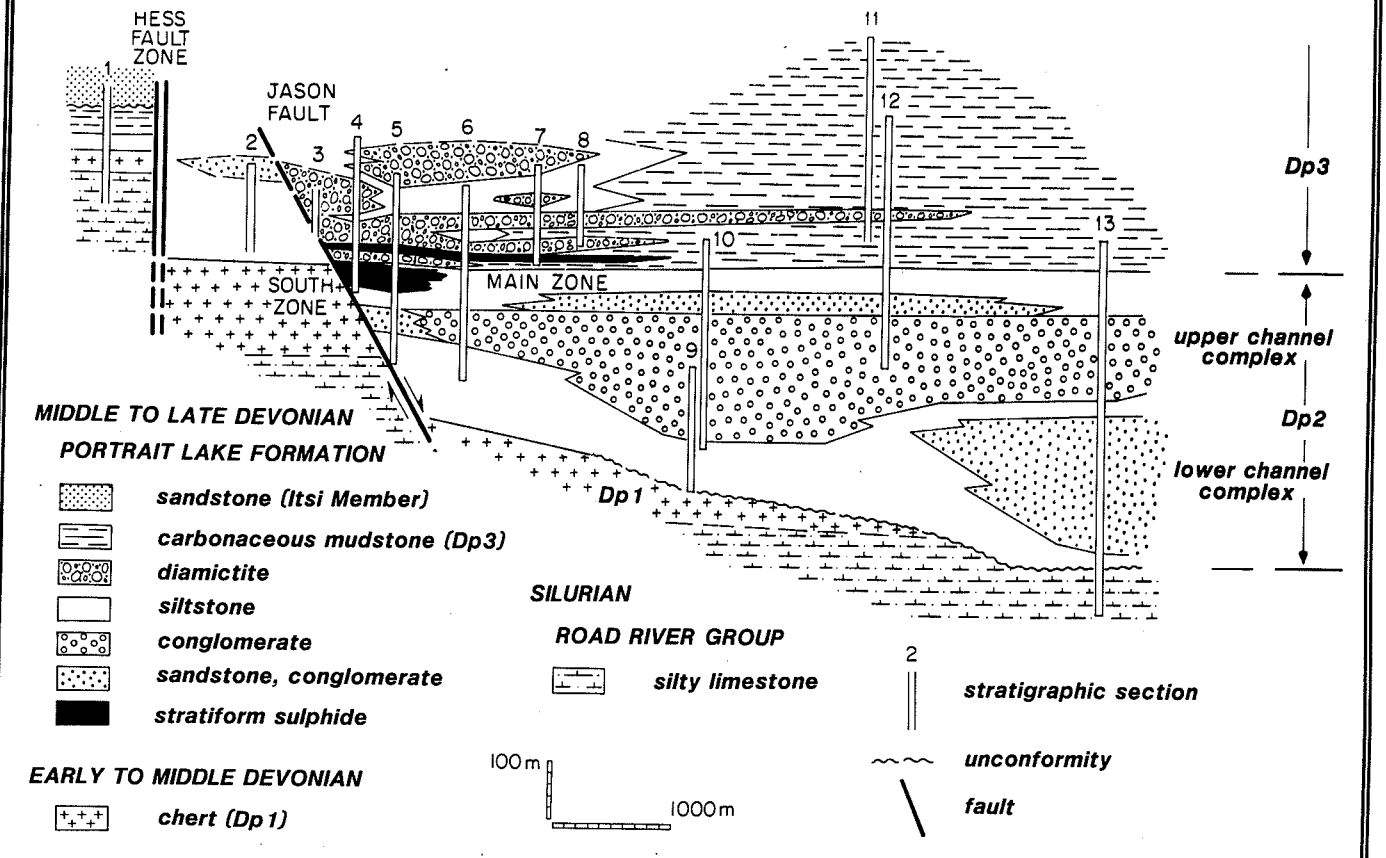

Figure 7 Stratigraphic section of the Jason deposit area with about 5X vertical exaggeration. Horizontal scale is only approximate. Stratigraphic sections are (1) Black Canyon, (2) DH-89, (3) DH-88, (4) DH-56A; (5) DH-68, (6) DH-69, (7) DH-71, (8) DH-78, (9,10) Jason knoll, (11) DH-8, (12) DH-17, and (13) Jason Mountain.

and siltstone laminae . Mudstone beds are silty, massive and typically 5 to 50 mm thick with mm-scale light-coloured less organic-rich laminae ('pinstripe' argillite of Abbott, 1982). Coarser laminations are 3 to 7 mm thick, massive or plain parallel laminated with lessor cross-lamination in preserved ripple forms ('biscuit rippled' of Teal and Teal, 1978). The lower mudstone unit represents deposition from dilute muddy turbidites.

The thickness of the lower silty mudstone unit is unclear. A gradational contact with underlying chert of Dp1 occurs in DH 89 (Fig. 6). The lower silty mudstone unit is best exposed in DH 69 below the conglomerate on the north limb of the syncline.

Conglomerate/sandstone unit (Dp2c,s)

The middle conglomerate and sandstone unit is up to 100 m thick on the north limb where it is composed of up to 30 m of medium-bedded graded sandstone turbidite overlain by 60 m of massive conglomerate (Fig. 6). Chert pebble conglomerate consists of rounded to angular, grey, black and white chert and minor quartz sandstone pebbles and cobbles in a chert and quartz sandstone matrix. The conglomerate is massive and internal stratification has not been recognized. On the south limb, the

conglomerate unit is 60 m thick and composed of a thinning and fining-upward sequence of 6-8 m thick fining-upward conglomerate-sandstone units.

Upper siltstone unit (Dp2p)

The upper siltstone unit is a sequence of thin-bedded siltstone and carbonaceous mudstone with minor sandstone. Siltstone beds are 1 to 3 cm thick, ungraded, with sharp upper and basal contacts and composed of chert and quartz silt. Siltstone beds commonly have a basal sandstone laminae with occasional grading, cross lamination, and load casts (T_{c-e} or T_{d-e} turbidite beds of Bouma,1962; or T_{0-4} beds of Stow and Shanmugam, 1980). Pinch and swell, cross-laminated sandstone (starved ripple trains) up to 5 cm thick, and graded sandstone beds up to 30 cm thick (T_{abe}, T_{ae} turbidites) are locally important. The upper siltstone unit thickens from 50 m thick on the north limb to 100 m thick on the south limb due to interbedding with sulphide-barite laminae of the lower stratiform lens of the Jason deposit.

Upper member (Dp3): Diamictite lithofacies

Throughout the MacMillan Fold Belt, the MacMillan Pass Member is overlain by black siliceous shale (uDpt of Abbott, 1983; Dp3 of Abbott and Turner, this volume). Conodonts from coarsely crystalline limestone beds within the Dp3 overlying the Tom deposit are early Late Devonian (early Frasnian) age (Abbott, 1982). However, the MacMillan Pass Member in the Jason syncline is overlain by a diamictite lithofacies of interbedded matrix-rich heterolithic diamictites, matrix-poor sedimentary breccias, and conglomerate interbedded with siltstone and siliceous shale (Fig. 4, 5, 6 and 7). Stratiform sulphide-barite of the upper lens of the Jason deposit is interbedded with diamictite beds and carbonaceous siliceous shale at the base of the diamictite lithofacies. The thickness of the diamictite lithofacies is at least 270 m thick.

Matrix-rich heterolithic diamictite

Diamictites ("heterolithic breccias" of Winn et al., 1981; Winn and Bailes, 1987) include a diverse suite of coarse-grained, poorly sorted fragmental rocks composed of angular to subrounded intraclasts of siltstone, argillite, sandstone and chert conglomerate, and rounded chert pebbles, in a poorly sorted carbonaceous mud-rich matrix. Diamictites include intraclast-rich breccias, pebbly mudstones, muddy conglomerates, and sandy mudstones. The diverse clasts of the diamictite lithofacies could have all been derived from underlying Portrait Lake strata.

Intraclasts commonly range in diameter up to 20 cm, but may exceed a meter. Some mudstone and siltstone clasts have ductile or brittle shear strain along their margins. White and grey chert pebbles to 3 cm in diameter commonly compose up to 10 percent of diamictite beds. Chert pebbles often have replacement rims or disseminations of pyrite or minor sphalerite and galena. Sulphides tend to be distinctly more abundant in chert pebbles than intraclasts or in the matrix of a diamictite bed. Given the additional fact that come chert pebble conglomerate fragments are cemented by ferroan carbonate, pyrite, sphalerite and galena, it is clear that hydrothermal fluid infiltration and mineral deposition took place within permeable gravel beds prior to resedimentation. Diamictite immediately overlying the upper stratiform sulphide lens contains intraclasts of massive sphalerite-galena-pyrite similar to massive sphalerite-galena beds within the upper stratiform lens.

Conglomerate and sandstone

Beds of chert-pebble conglomerate to 10 m thick, sandy conglomerate and pebbly sandstone to 5 m thick, and massive sandstone with weak parallel laminaetion to 3 m thick (T_{abe} of Bouma,1962) are intimately interbedded with beds of diamictite. A continuum exists between well-sorted conglomerate, muddy conglomerate/sandstone, and pebbly/sandy mudstone, as well as between conglomerate, intraclast-rich conglomerate and intraclast-rich pebbly mudstone. Conglomerate beds are often gradational upwards into diamictite.

Diamictite units: Lobes of interbedded diamictite, conglomerate and sandstone

Interbedded diamictite, conglomerate and sandstone beds that form discrete stratigraphic units are referred to as "diamictite units". Three such diamictite units can be correlated throughout the Jason syncline based on position with respect to sulphide-barite lenses and distinctive sandstone marker beds. Use of marker sandstone beds for stratigraphic correlation on the north limb was developed by K. I. Lu. The 'A' diamictite unit occurs between the lower and upper stratiform sulphide lens; the 'B' diamictite unit between the upper stratiform

lens and the 'O' sandstone marker, and the 'C' diamictite lies immediately above the 'O' marker (Fig. 5, 6). Isopachs of the A, B and C units within the Jason syncline, based on 57 drill hole intersections in an area 1200 m by 1200 m indicate that these units trend normal to that of the Jason fault (Fig. 8). Individual lobes exceed 800 m in length, vary from 200 to 600 m in width and thicken to as much as 90 m where they terminate against the Jason fault. These patterns suggest that the source of the diamictite lobes was across the Jason fault to the east. Given the textural and compositional character of the Jason fault (see discussion under "Hydrothermal facies of the Jason deposit") that suggests it was syndepositional, it is interpreted that the submarine scarp of the Jason fault was the source of the diamictite lobes.

Diamictite lobes are wedge-shaped in longitudinal profile (Fig. 9a); where they are thickest adjacent to the Jason fault they are composed of massive intraclast-rich pebbly mudstone. With increasing distance from the Jason fault, diamictite beds thin, the average clast size decreases, and the amount of interbedded siltstone and siliceous shale increases. In the distal parts of some lobes, cycles up to 4 m thick of conglomerate are overlain gradationally by intraclast-rich conglomerate or diamictite. Lateral to the axis of the lobe, diamictite beds thin and interfinger with mudstone or siltstone beds (Fig. 9b). Massive to bedded conglomerate, sandy conglomerate, intraclast-rich conglomerate and sandstone occur as lenticular, channel-like bodies that trend parallel to the axis of the breccia lobe, predominantly in the intermediate to distal parts of the breccia lobes. Conglomerate lenses pass laterally into carbonaceous mudstone in the proximal lobe but into siltstone in the distal lobe.

Interbedded siltstone/mudstone

Thin-bedded siltstone similar to the upper siltstone in the MacMillan Pass Member is the most common fine-grained lithology in the diamictite lithofacies. However, carbonaceous mudstone is dominant in the basal portion of the diamictite lithofacies associated with the upper sulphide-barite lens (Fig. 6); mudstone thickens from less than 10 m on the south limb to over 50 m on the north limb. Mudstone is also important in the axial zone of the syncline near the presumed top of the diamictite lithofacies.

Matrix-poor homolithic breccia

Sequences of siltstone interbedded with diamictite units are locally disrupted into matrix-poor siltstone clast breccia (Winn et al., 1981, Winn and Bailes, 1987). Intraclasts are angular to subangular in shape, average 0.1 to 0.3 m in diameter, and compose 50 to 95 percent of the breccia. A continuum exists between homolithic breccia, contorted and faulted strata and undisturbed siltstone strata; rapid lateral change from breccia to undisturbed siltstone is common.

Correlation between Jason syncline and regional strata

Correlation of the Jason syncline stratigraphy with regional Portrait Lake stratigraphy is critical for the understanding the stratigraphic position of the Jason deposit. The MacMillan Pass Member and upper siliceous shale member (Dp3) typical of the regional Portrait Lake Formation, are well exposed on Jason Mountain three kilometres northwest of the Jason deposit.

MacMillan Pass Member (Dp2)

On Jason Mountain , the MacMillan Pass Member is dominated by two easterly-trending lenticular bodies of conglomerate and sandstone, the upper and lower channel complexes (Fig. 7; section 13). The upper channel complex (UCC) is a widespread conglomerate unit 60 to 300 m thick (muDcg of Abbott, 1982) that can be followed in outcrop south to the conglomerate/ sandstone unit on the north limb of the Jason syncline. Paleocurrent indicators suggest west to east flow (Bailes et al., 1986). The southward thinning and fining of the UCC in the Jason syncline and absence south of the Hess fault suggests the Jason syncline lies along the margin of the channel.

The lower channel complex (LCC) is composed of two southeast trending lobes (Bailes et al., 1986). The southwestern lobe is exposed on Jason Mountain unconformably overlying Road River Group. The LCC is 300 m thick on Jason Mountain and composed of beds of sandstone, pebbly sandstone, massive conglomerate, and thin-bedded siltstone in fining- and thinning-upwards sequences 5 to 20 m thick (Fig. 7; section 13). Massive conglomerate beds up to 5 m thick are interbedded with pebbly sandstone beds to several metres thick that locally have parallel or inclined stratification. The latter suggest deposition on gravel bars within a braided complex of turbidite channels

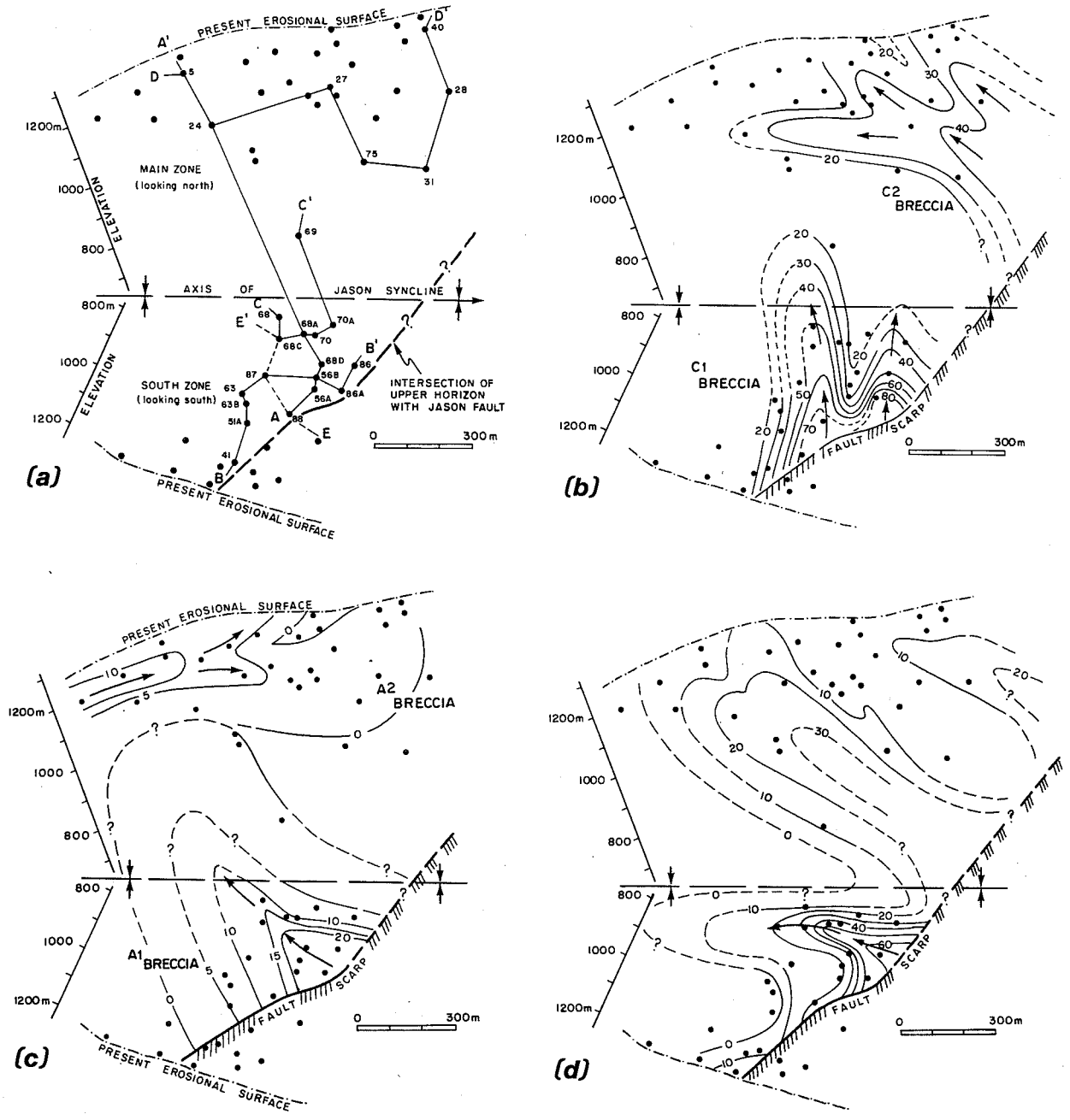

Figure 8 Isopach maps of the thickness of individual diamictite units (in metres) on a structurally restored plan view of the Jason syncline. Strata on the north (Main zone) and south (South zone) limbs of the Jason syncline have been unfolded about the estimated position of the southeast plunging syncline axis. The area east of the intersection of the Jason fault with the diamictite unit was the submarine fault scarp and diamictite source area during depostion of the diamictite. Location of the piercing points of drill holes with the diamictite are indicated. (a) Lines of stratigraphic sections A-A', B-B', C-C' and D-D' across the Jason deposit (Fig. 12), (b) Isopach of A diamictite unit; (c) Isopach of B diamictite unit; and (d) Isopach of C diamictite unit.

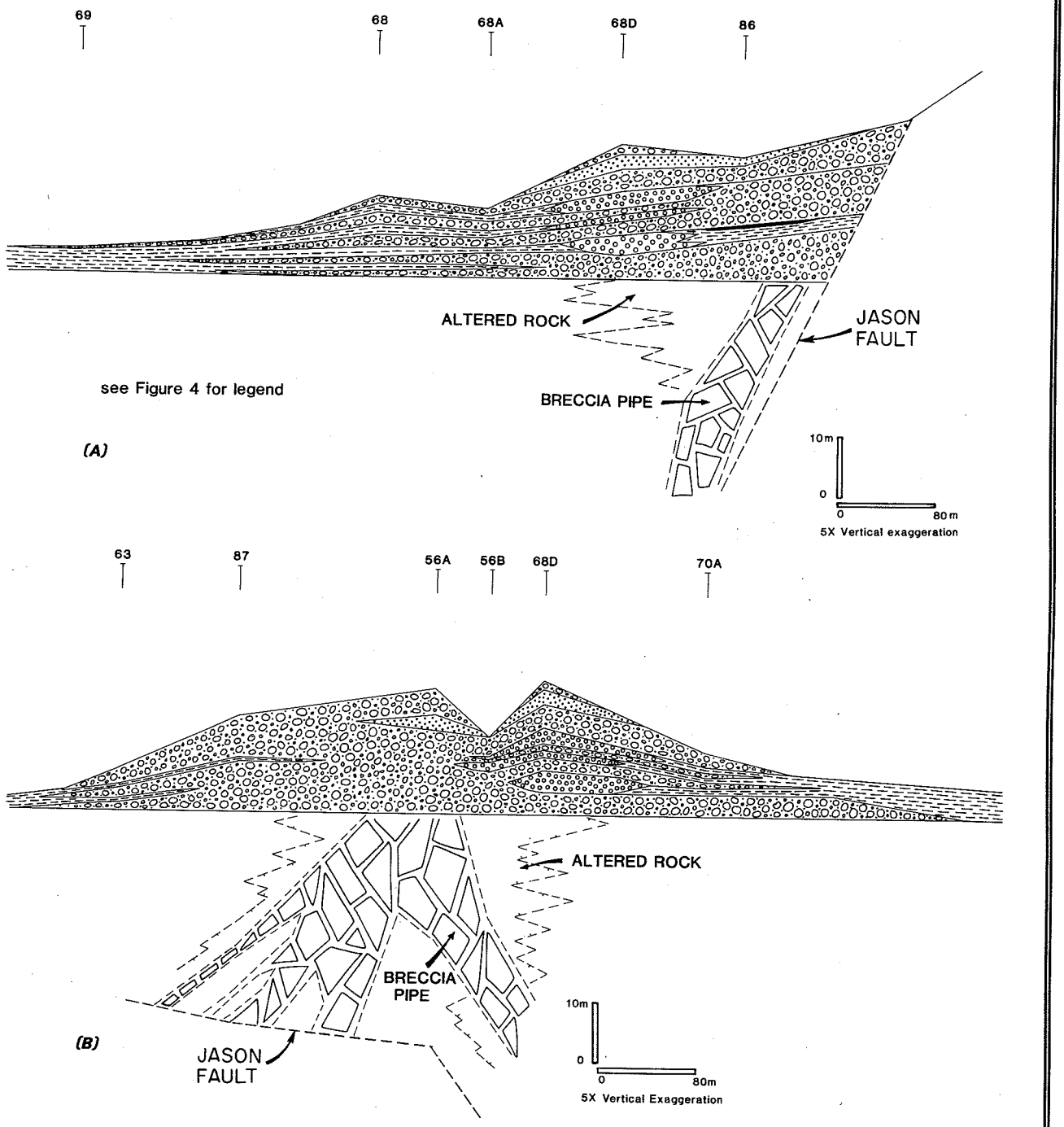

Figure 9 Restored stratigraphic cross section of the A1 diamictite unit (a) parallel to the axis of the lobe and perpendicular to the Jason fault; and (b) transverse to the axis of the breccia lobe and sub parallel to the Jason fault the location of drill hole control is shown.

(Winn et al., 1981). Sandstone beds are graded with plane and cross lamination, and sole marks ($T_{a,ab,bcd}$ beds of Bouma, 1962). These sandstone- conglomerate beds thin and pass into sand-banded argillite to the south.

The channel complexes occur within a widespread siltstone lithofacies. Siltstone lithofacies above the UCC (Unit 3A of Carne, 1979) (Fig. C1) correlates with the upper siltstone that hosts the lower sulphide-barite lens in the Jason syncline. The LCC is facies equivalent to the silty argillite underlying the conglomerate/sandstone unit in the Jason syncline; the latter is equivalent to Unit 1 of Teal and Teal (1978) and Carne, (1979), and forms much of the Dp2p unit of Abbott (1982, 1983). Sand-rich siltstones lateral to the channel complexes likely represent channel lateral or levee facies to the turbidite channel system; siltstones underlying and overlying the channel complexes are distal turbidites deposited downstream from channel gravel deposition.

Upper member and diamictite lithofacies

The diamictite lithofacies is largely limited to the Jason syncline and pinches out rapidly to the north within a thick unit of carbonaceous mudstone of the upper member (Fig. 7). Northeast of the Jason deposit below the MacMillan River valley, a thick sequence of carbonaceous mudstone overlies the MacMillan Pass member (Fig. 7; sections 11,12). A thin diamictite unit 20 m thick occurs 80 m above the top of the MacMillan Pass Member; this diamictite unit also crops out in the syncline north of the Jason syncline (Fig. 3) and appears to represent the distal edge of the diamictite lithofacies. Similar diamictite lithofacies also occur associated with other base metal deposits in Central Block (see Abbott and Turner, 1990). A sequence of diamictite up to 30 m thick occurs at the contact of the MacMillan Pass Member and overlying upper member siliceous shales a kilometre north and a kilometre east of the Jason End zone stratiform sulphide prospect (Fig. 3). Diamictite, conglomerate, and volcanic rocks are associated with the Nidd zinc prospect west of Jason (Turner and Rhodes, 1990). Diamictite and muddy conglomerate also underlie the Tom deposit (Goodfellow and Rhodes, this volume).

STRATIGRAPHY OF THE JASON DEPOSIT

Stratigraphic correlation between Main and South zones

On the north limb of the Jason syncline, a single lens of stratiform sulphide-barite-chert up to 20 m thick (Main zone) is interbedded with carbonaceous mudstone and diamictite overlying siltstone at the top of the MacMillan Pass Member (Fig. 6). On the south limb there are two stacked stratiform sulphide-barite lenses ("South zone"); the upper lens is interbedded with mudstone and diamictite at the same stratigraphic level as the Main zone immediately above the MacMillan Pass Member. The lower stratiform lens, interbedded with the uppermost siltstone unit, is separated from the upper lens by 10 m of siliceous shale and diamictite.

Stratiform sulphide-barite on the north limb and the upper lens on the south limb are part of a single stratiform body, the "upper stratiform lens". The upper lens is up to 20 m thick and extends over 1200 m from the Jason fault on the south limb to the present erosional surface on the north limb of the syncline (Fig. 10). The lower lens, a wedge-shaped body 300 m by 400 m in extent (Fig. 11) and up to 40 m thick, occurs only on the south limb. The Jason fault juxtaposes these stratiform lenses against Road River calcareous mudstone and lower member chert to the south. Prior to the recognition of the Jason fault (Turner, 1984), workers (Winn et al, 1981; Bailes et al., 1986; Gardner and Hutcheon, 1985; Winn and Bailes, 1987) interpreted the South zone and Main zone to be separate deposits at different stratigraphic levels. While the Main zone clearly sits above the conglomerate, the South zone was interpreted to be at the base of the Portrait Lake Formation because of proximity to Road River strata underlying the updip portion of the South zone and was therefore thought to be older. In this interpretation, conglomerate units within the diamictite lithofacies above the South zone were correlated with the conglomerate unit of the MacMillan Pass Member on the north limb of the Jason syncline. However, this latter interpretation does not explain the thick conglomerate unit underlying the South zone, or the similarity of diamictite units interbedded with and overlying both the South and Main zone. In addition, the systematic changes of mineralogy and metal ratios discussed below imply that the South and Main zones are parts of a single zoned stratiform body.

Stratigraphic correlation between the Jason and Tom stratiform Zn-Pb deposits

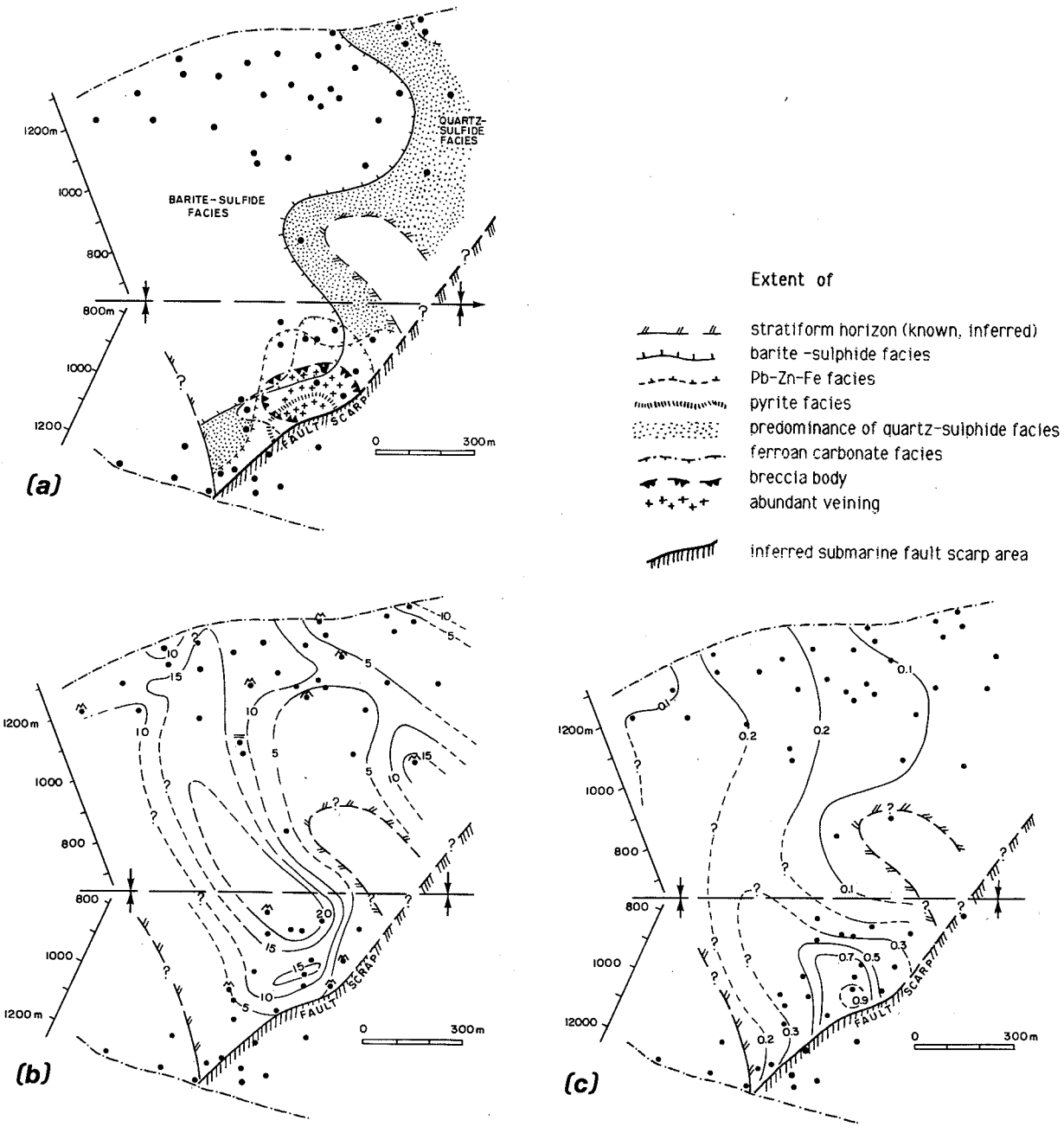

Figure 10 Structurally restored plan view of the upper stratiform lens. Piercing points of drill holes with the upper stratiform lens are shown. (a) distribution of textural facies; and (b) isopach of thickness (in metres); (c) contours of lead/(lead+zinc) based on averaged assay results for each drill intercept.

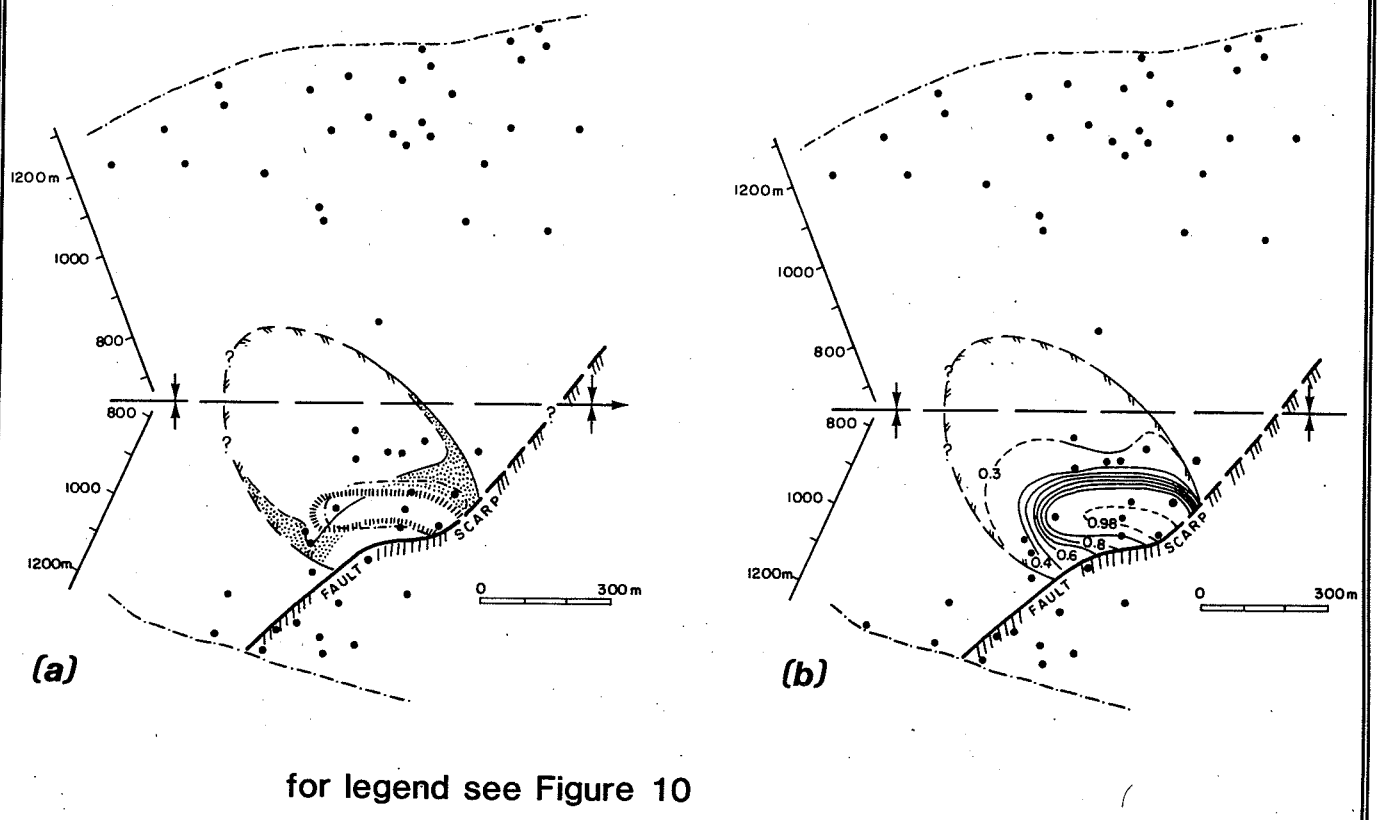

for legend see Figure 10

Figure 11 Structurally restored plan view of the lower stratiform lens. Piercing points of drill holes with the upper stratiform lens are shown. (a) distribution of textural facies; and (b) contours of lead/(lead+zinc) based on averaged assay results for individual drill intercepts of the upper lens.

The Tom stratiform Zn-Pb deposit, five kilometres north-east of the Jason deposit is interbedded with carbonaceous mudstone of the upper member just above the contact with the upper siltstone of the MacMillan Pass Member. The Jason deposit straddles this same contact and it is therefore interpreted that both deposits occur at the same stratigraphic position. Whether this contact is significantly diachronous is unclear.

HYDROTHERMAL FACIES WITHIN THE JASON DEPOSIT

The upper and lower lenses of the Jason deposit can each be divided into two major components: a blanket-like body of bedded sulphide, barite and chert, and areally restricted massive and veined ferroan carbonate and pyrite adjacent to the Jason fault (Fig. 10a). This ferroan carbonate-rich zone coincides with high lead/(lead+zinc) ratios (Fig. 10c, 11b). Away from the fault, the lead/(lead+zinc) ratio decreases systematically.

The Jason deposit can be further divided into hydrothermal facies (Fig. 11a,b,c,d). Bedded sulphide, barite and chert are subdivided into facies based on the presence and proportion of different lamina types (Fig. 12), while massive and vein mineralization is divided according to dominant mineral type.

Bedded sulphide-barite-chert ("sedimentary blanket")

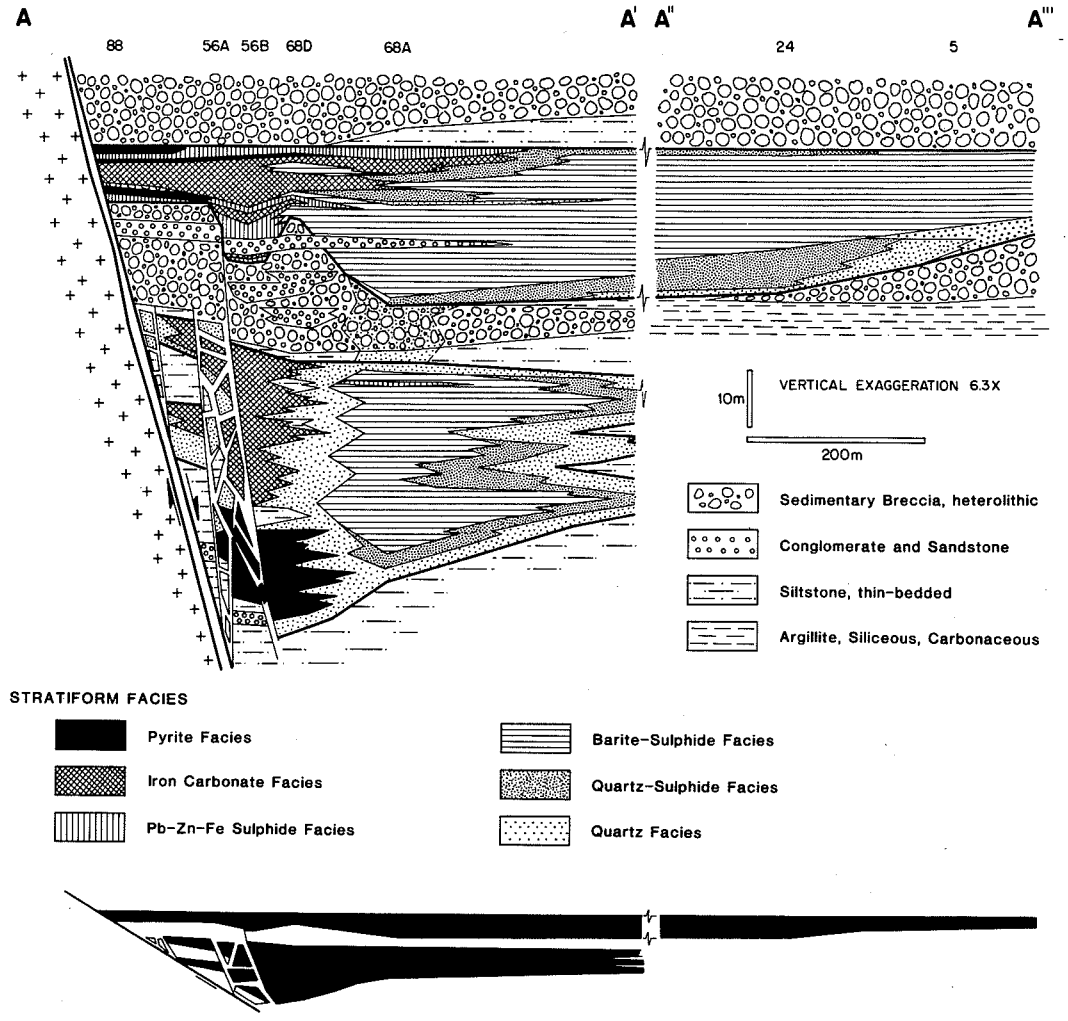

Figure 12 (a) Restored stratigraphic cross-sections illustrating distribution of internal facies within the stratiform lenses. Heavy black line encloses hydrothermal facies. Sections have 6.3X vertical exaggeration unless otherwise noted; the true scale cross-sections is shown in solid black. Location of sections shown in Fig. 8(a). (a) Section A-A' across the trend of the Jason fault. Break in section is approximately 400 m wide.

PbZnFe sulphide facies :

Thick beds of massive to banded sphalerite-galena, or massive galena-pyrite beds compose 30 to 50% of the upper lens near the Jason fault (Fig. 12a). In DH 86A, a two metre sphalerite-galena bed (667.7-669.7) is composed of four discrete depositional cycles, each with a massive galena-rich base and banded sphalerite-rich top (Fig. 12b). These textures suggest a sedimentary origin and deposition from a density flow with early rapid deposition of denser galena particulate followed by

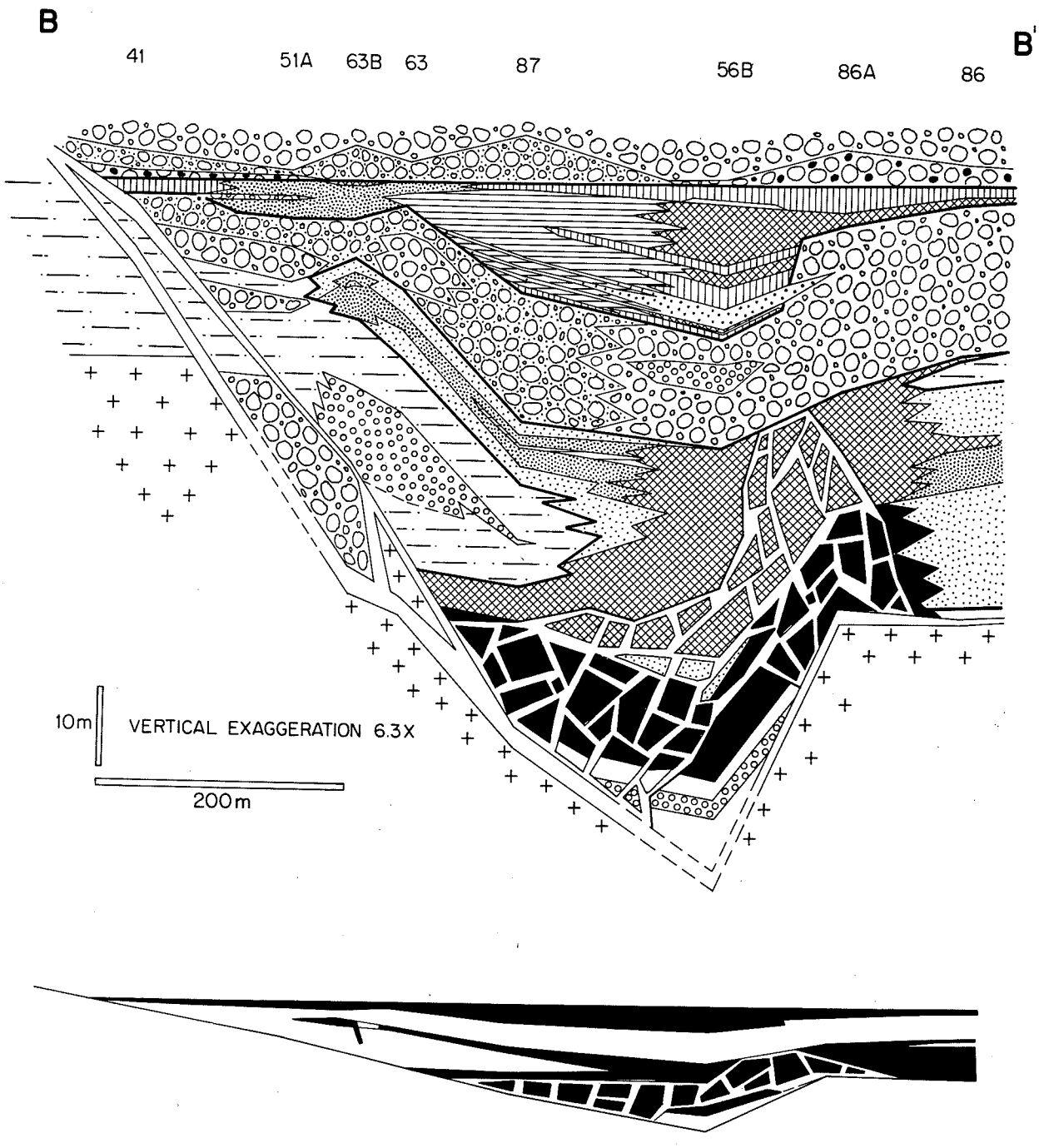

Figure 12 (b) Restored stratigraphic cross-sections illustrating distribution of internal facies within the stratiform lenses. Heavy black line encloses hydrothermal facies. Sections have 6.3X vertical exaggeration unless otherwise noted; the true scale cross-sections is shown in solid black. Location of sections shown in Fig. 8(a). Section B-B' of proximal stratiform lenses and breccia pipe along the trend of the Jason fault.

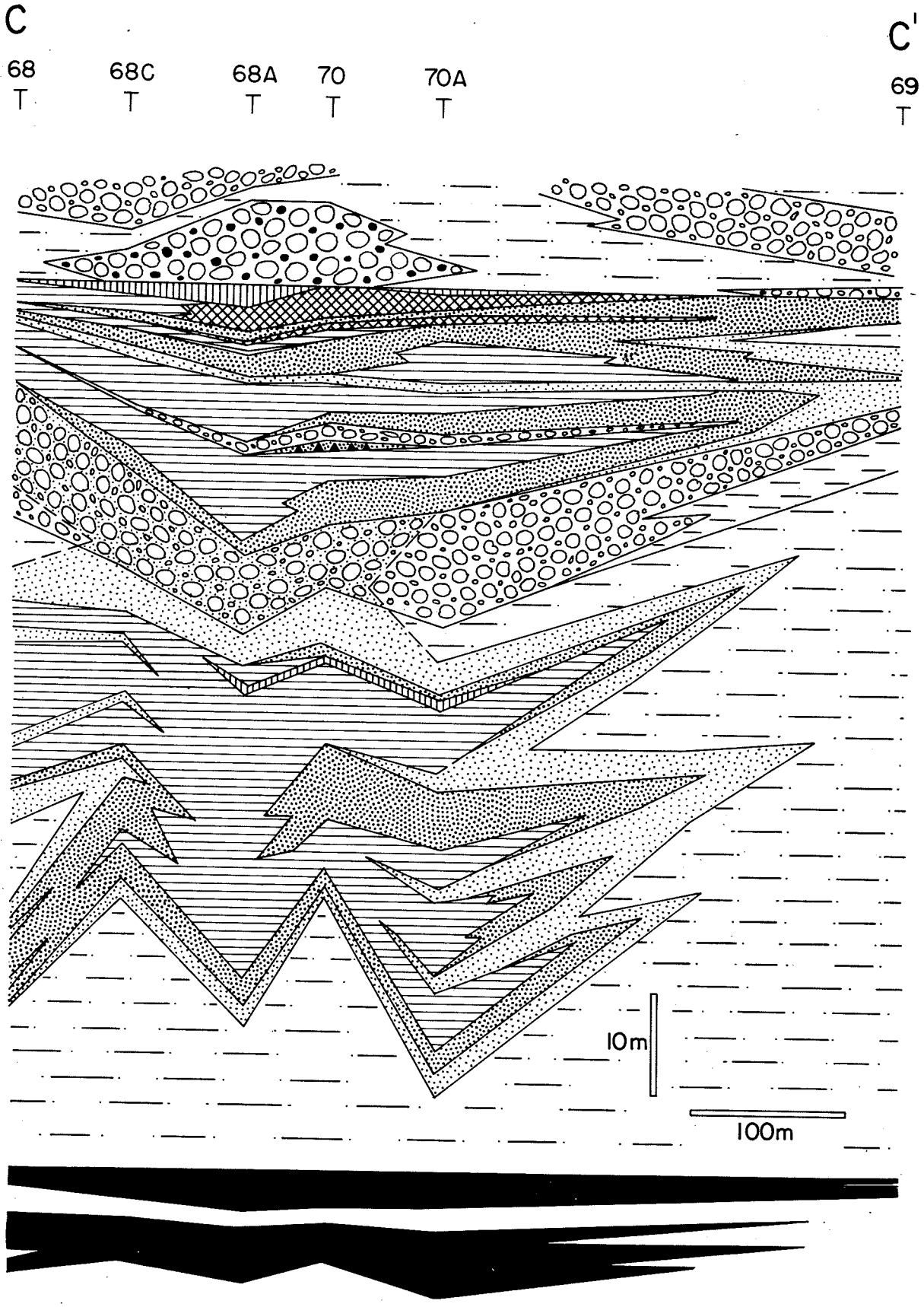

Figure 12 (c) Restored Stratigraphic cross-sections illustrating distribution of internal facies within the stratiform lenses. Heavy black line encloses hydrothermal facies. Sections have 6.3X vertical exaggeration unless otherwise noted; the true scale cross-sections is shown in solid black. Location of sections shown in Fig. 8(a). Section C-C' of proximal stratiform lenses and breccia pipe along the trend of the Jason fault.

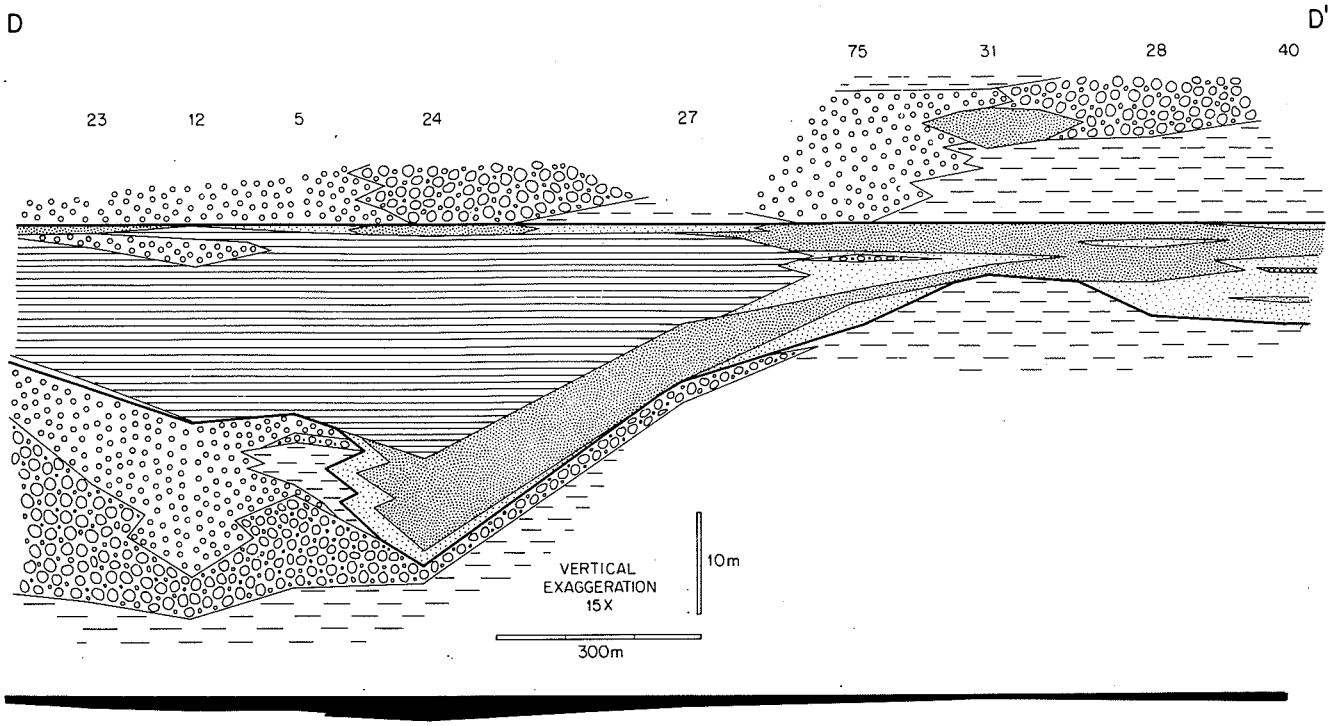

Figure 12 (d) Restored stratigraphic cross-sections illustrating distribution of internal facies within the stratiform lenses. Heavy black line encloses hydrothermal facies. Sections have 6.3X vertical exaggeration unless otherwise noted; the true scale cross-sections is shown in solid black. Location of sections shown in Fig. 8(a). Section D-D' of distal stratiform lens on north limb of syncline (Main zone). Vertical exaggeration is 15X.

slower deposition of less dense particulate. Sphalerite-galena beds at the top of the upper lens are disconformably overlain by diamictite with abundant clasts of massive sphalerite- galena that indicate seabottom erosion of the PbZnFe sulphide facies. Away from the Jason fault, some sphalerite-galena beds are barite-rich representing a transition to barite-sulphide facies (e.g. DH 68D, 680-681m). Galena-pyrite beds are more abundant in the lower part of the upper lens (e.g. DH 56A and 56B) and are composed of massive intergrown galena, pyrite and lesser ferroan carbonate and quartz. Textures suggest that galena has replaced ferroan carbonate and pyrite.

Barite-sulphide facies

The barite-sulphide facies forms the bulk of the Jason deposit and is composed of millimetre- to centimetre-scale beds of barite, chert, sphalerite, sphalerite- chert, sphalerite-galena, and barite-galena (Fig. 13). Fine (5-40μ) anhedral grains of barite, quartz, sphalerite and galena occur as a granoblastic mosaic in laminae 0.01 to 5 mm thick. No replacement textures exist among barite, quartz, sphalerite and galena. Laminae have sharply defined boundaries and mineral grains of hydrothermal origin comprise greater than 95% of individual lamina; interbeds of siltstone and mudstone typically contain less than 5% disseminated pyrite and only trace sphalerite. Disseminated anhedral grains, clots and irregular bands of barian and ferroan carbonates increase in abundance approaching the contact with ferroan carbonate facies. These carbonates occur as replacements of barite, chert and siliceous mudstone. Near the contact with the ferroan

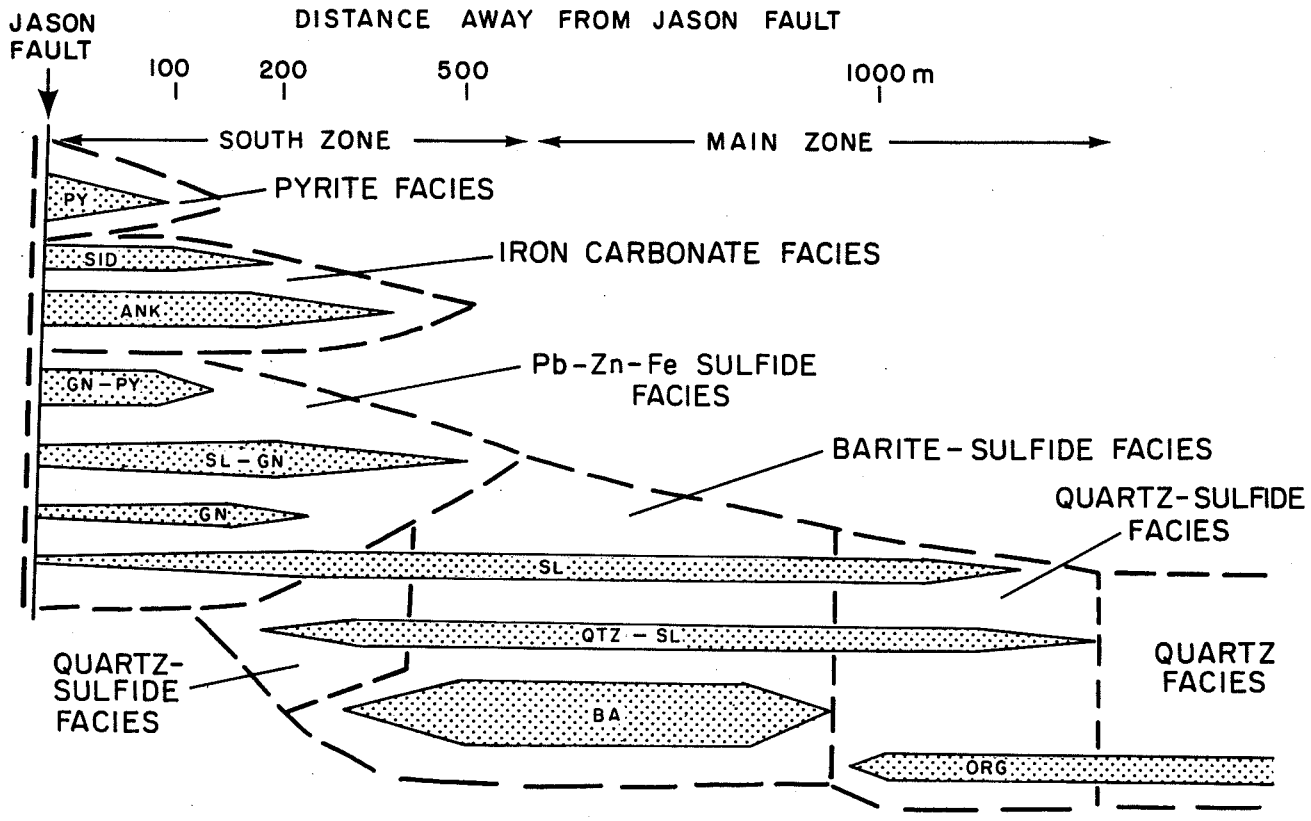

Figure 13 Distribution of lamina types within the upper stratiform lens with respect to distance from the Jason fault. Dotted lines indicate the types of laminae that compose each hydrothermal facies.

carbonate facies, banded quartz with minor sphalerite ("hazy quartz") represents silicified laminated barite-sulphide.

In the upper stratiform lens, barite-sulphide laminae are interbedded with about 10% hard, siliceous mudstone beds. These mudstone beds are distinctly harder and more siliceous than texturally similar mudstone lateral to the Jason deposit; this suggests silica addition, either during or after deposition, to the mudstone. Siliceous mudstone beds are up to 30 cm thick, and vary from pale grey colour on the south limb near the Jason fault, to black on the north limb. Relict black patches within grey siliceous mudstone beds indicate that the paler colour is due to post depositional destruction of organic matter (i.e. bleaching). Beds up to a meter thick of pale grey siliceous siltstone and mudstone clasts are interbedded with sulphide-barite strata on the south limb.

Barite-sulphide strata of the lower lens are interbedded with about 40 percent 0.5 to 3 cm thick siltstone beds. Like mudstone beds in the upper lens, siltstone turbidite beds are more siliceous within the deposit than are adjacent siltstone strata. Within the barite-sulphide facies, siltstone beds are grey and bleached of organic matter.

Pb+Zn grades diminish with increase in the proportion of barite laminae, and in the case of the lower lens, siltstone beds. The sub-economic grades of the western Main zone reflects this dilution of sulphide laminae by barite laminae; the subeconomic nature of much of the lower lense reflects dilution by both barite laminae and siltstone beds.

Quartz-sulphide facies :

Sub-millimetre laminae of pyrite, sphalerite, and quartz-sphalerite interbedded with carbonacous chert of the quartz-sulphide facies (Fig. 13) are the dominant lithologies in the eastern portion of the upper lens (Main zone) on the north limb (Fig. 12d). Disseminated framboidal, anhedral and subhedral pyrite grains tend to be concentrated within particular laminae or beds of carbonaceous mudstone. Minor fragmental beds within this facies are composed of clasts of laminated and banded chert-sphalerite within a matrix of fine-grained quartz and sphalerite that indicate resedimentation of a partially cohesive silica-sphalerite on the seafloor.

In the lower lens, the quartz-sulphide facies has a different style; discontinuous quartz-celsian bands up to 1 cm thick are flanked by disseminated pyrite and sphalerite (Fig. 14). This quartz-sulphide facies forms an envelope-like distribution around the barite-sulphide facies (Fig. 12a, c). The coarser-grained and discontinuous character of quartz-celsian bands, and the inward termination of celsian crystals from band margins suggest a diagenetic rather than sedimentary origin. Quartz-sulphide strata differ from barite-sulphide facies by the absence of barite laminae, the presence of quartz-celsian bands, presence of organic matter that darkens the rock, and the greater abundance of disseminated pyrite (Fig. 13). Disseminated grains of hyalophane, celsian and ferroan carbonate occur within interbedded siltstone (Fig. 14).

Between the ferroan carbonate facies and the barite facies in the lower lens is a "blank zone" of silicified and bleached siltstone with quartz-celsian bands and abundant leached disseminated carbonate grains (e.g. DH 87, 618-647 m). The blank zone is interpreted to represent silicification and minor carbonate alteration of barite-sulphide strata adjacent to the ferroan carbonate facies.

Quartz facies:

Surrounding and lateral to the distal lower lens, and lateral to the upper lens is siliceous pyritic mudstone or siltstone. This facies is distinguished from the quartz-sulphide facies by the absence of laminated sulphides (Fig. 13), and from regional carbonaceous shale and siltstone by a harder, siliceous nature, and elevated content of disseminated pyrite, hyalophane and ferroan carbonate. In the lower lens, there is an outward zoning from disseminated pyrite to iron carbonate (Fig. 14).

Vent complex:

The term "vent complex" is used to embrace this massive and vein mineralization as well as the associated breccia pipe and rock alteration adjacent to the Jason fault. Adjacent to the Jason fault, both stratiform lenses are composed of beds of massive ferroan carbonate and pyrite cut by irregular veinlets, pods and breccias of ferroan carbonate, galena, pyrrhotite, pyrite, quartz, muscovite, sphalerite, and chalcopyrite (Fig. 14). The abundance of replacement and vein textures, coarse grain size, and absence of bedding suggests an epigenetic rather than sedimentary origin for this part of the Jason deposit. An epigenetic origin is also supported by fluid inclusion data that gives a mean homogenization temperature of about 250° C for fluid inclusions within siderite, ankerite and quartz (Gardner and Hutcheon, 1985).

Massive pyrite facies:

Immediately adjacent to the Jason fault, the upper lens in DH 88 (Fig. 12a) is composed of pyrite beds interbedded with sphalerite-galena beds (PbZnFe facies) and chert conglomerate. Massive pyrite beds occur close to, and at the top of, the upper lens where they are in sharp contact with beds of sphalerite-galena and unaltered diamictite overlying the upper lense. This massive pyrite locally displays micro-collimorphic textures, and is cut by irregular veinlet networks of sphalerite and galena, and planar quartz-sphalerite-galena-chalcopyrite veinlets. Irregular veins contain pyrite pseudomorphic after barite laths. In the lower part of the upper lense, pyrite-rich rock is composed of a network of irregular pyrrhotite-pyrobitumen veinlets with pyrite selvages that replace conglomerate and ferroan carbonate rock (DH 88, 349-359 m).

Within the lower horizon adjacent to the Jason fault and cut by the breccia pipe are thick sequences of banded pyrite interbedded with siltstone (e.g. 86A-724-736 m). Pyrite bands are quite stratiform away from the breccia pipe; towards the breccia pipe pyrite bands become increasingly irregular and discordant with evidence of replacement of adjacent siltstone beds by pyrite. These pyrite bands may reflect:

(1) sedimentary pyrite bands remobilized by hydrothermal fluids adjacent to the breccia pipe; or

(2) a single-stage zoned epigenetic event with distal replacement by pyrite being bedding-selective, while near the breccia pipe both bed selective and discordant

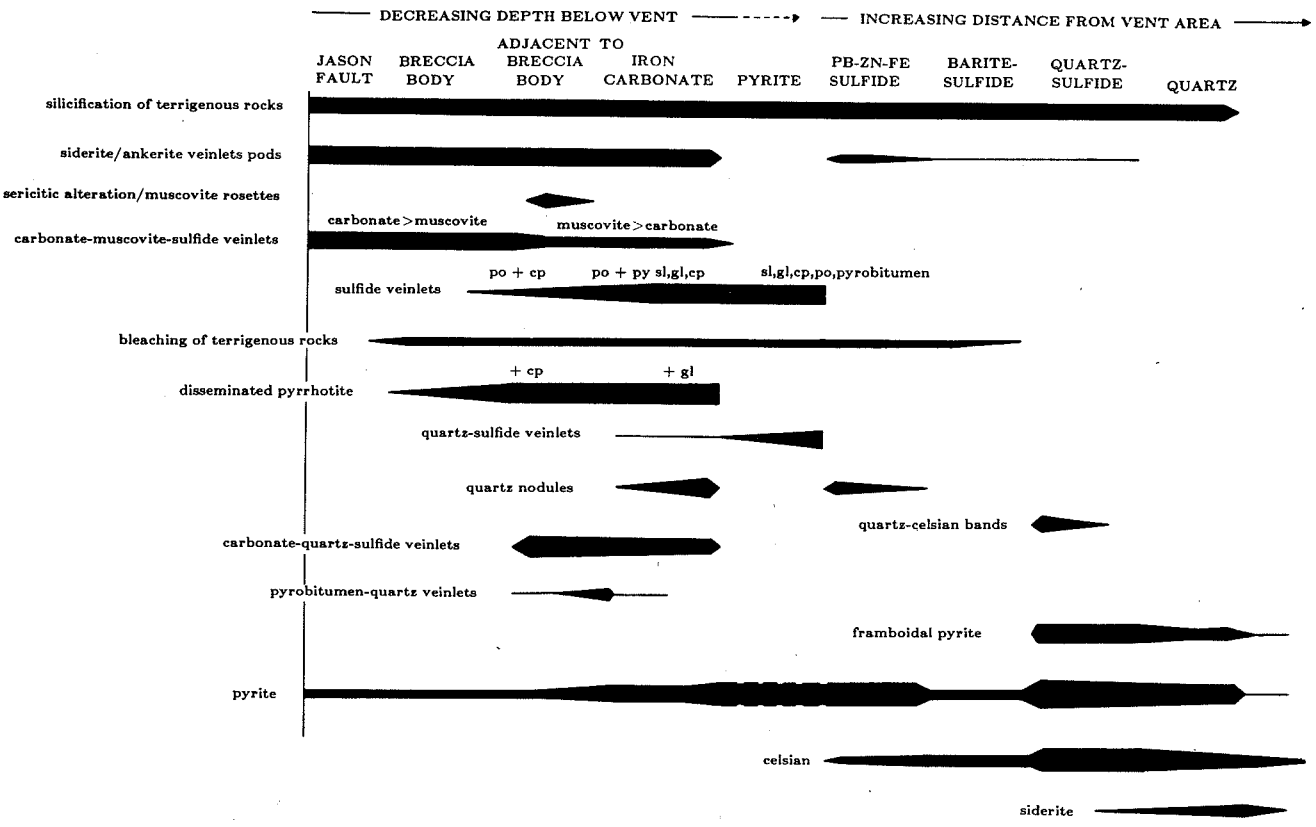

Figure 14 Distribution of discordant and non-stratiform mineral assemblages within the Jason deposit. Thickness of bar indicates variation in abundance of mineral assemblage throughout deposit. From left to right arrows indicate decreasing depth below the paleo-seabottom within the vent complex, and increasing distance along the paleo-seabottom away from the vent area.

pyrite replacement took place. Where the breccia pipe cuts the banded pyrite, the breccia matrix is composed of pyrite, siderite and pyrrhotite, with pyrite partially replaced by pyrrhotite. Abundant veins of dark sphalerite are associated with pyrite bands near the breccia body (Fig. 12b, DH 87).

Ferroan carbonate facies

Massive beds centimetres to metres in thickness of siderite and ankerite with lessor disseminations, veinlets and pods of galena, pyrrhotite, pyrite, quartz, muscovite and pyrobitumen, and minor sphalerite and chalcopyrite compose much of the upper and lower horizons near the Jason fault (Fig. 12a). In the upper horizon, this ferroan carbonate facies is composed of thick, massive medium-grained ankerite in sharp contact with overlying sphalerite-galena beds (e.g. Fig. 12b, DH 86A); contacts are more diffuse with interbedded sphalerite-galena beds. Adjacent to the Jason fault, this ankerite is largely replaced by pyrite and pyrrhotite of the massive pyrite facies (DH 88, 349-359). Disseminated and veinlet sulphides are most abundant where the ferroan carbonate facies overlies the breccia pipe, and decrease in abundance away from the Jason fault. Unlike the lower lens, siderite is not common; where siderite and ankerite are intergrown mineral textures indicate replacement of siderite by ankerite. A transgressive contact separates ferroan carbonate facies from the barite-sulphide facies in the upper part of the

upper lens (Fig. 12a,b); abundant textural evidence points to the early replacement of barite-sulphide beds by ferroan carbonates in this contact zone. Barite strata adjacent to this ferroan carbonate replacement front contain abundant disseminated barian carbonate minerals (benstonite, northesite, witherite) that replace barite.

The ferroan carbonate facies in the lower lens is spatially related to the breccia pipe (Fig. 12a,b), and differs from its counterpart in the upper horizon by its more bedded nature, abundance of clastic interbeds (siltstone), greater abundance of siderite, and lower galena content. It is overlain with sharp contact by the weakly altered 'A' diamictite unit (e.g. DH-56A), and interfingers laterally with siltstone and silicified siltstone of the Quartz facies, except at the top of the upper lens where ferroan carbonate with abundant coarse galena replaces barite-sulphide strata (e.g. DH 68A). It is interesting to note that the greatest extent of the ferroan carbonate facies occurs at the top of both the upper and lower lenses (Fig. 12a), perhaps reflecting that the maximum hydrothermal fluid flux through the hydrothermal sediments was along the base of the overlying mud-rich, and hence relatively impermeable, diamictite. Such concentration of lateral fluid flow below an aquatard has been noted in many modern geothermal systems. Such a model suggests at least some ferroan carbonate alteration following termination of hydrothermal sedimentation in the upper lens and deposition of overlying diamictite. Unlike the upper lens, a "blank zone" of silicified siltstone with diagenetic quartz-celsian bands (e.g. DH 87) or "unaltered" siltstone (e.g. DH 68D) separates most of the ferroan carbonate facies from the barite-sulphide facies. This blank zone may represent silicification of the barite-sulphide facies, perhaps as an outer silicification front related to the core of ferroan carbonate alteration.

A systematic zonation due to progressive mineral replacement characterizes much of the ferroan carbonate facies of the lower horizon adjacent to the breccia pipe. Siltstone strata show a progression of silicification, destruction of organic matter, recrystallization of clays, sequential replacement by siderite, pyrrhotite and ankerite, and veining as the breccia pipe is approached (Fig. 15).

Breccia pipe

A steeply dipping cylinder-shaped body of partially brecciated rock extends over 50 m from the Jason fault upwards to the 'A' diamictite unit, and cuts the pyrite and ferroan carbonate facies of the lower horizon (Fig. 12a,b). The breccia pipe is 300 m by 50 m in plan dimension and elongate parallel to the Jason fault. Thin zones of breccia to 1 m thick are composed of angular fragments of silicified siltstone to 10 cm in diameter that cut mineralized strata of the pyrite and overlying ferroan carbonate facies. The breccia matrix is composed of siderite, pyrrhotite, pyrite, quartz, ankerite, muscovite and galena .

The angular nature of fragments and high ratio of fragment to matrix suggests little vertical movement or milling of fragments; minor offset of strata is recognized across several narrow breccia zones suggesting normal fault movement. Siderite is commonly replaced by pyrrhotite, galena or pyrite. Where the breccia pipe cuts banded pyrite of the pyrite facies, pyrrhotite commonly has replaced pyrite. The breccia pipe is overlain by weakly-altered diamictite cut by irregular veinlets and patches of siderite, pyrrrhotite and pyrite, and massive and veined ferroan carbonate facies of the upper lens.

Altered sedimentary rock

Widespread silicification of sedimentary strata occurs adjacent to the Jason fault as well as in association with stratiform lenses. Silicified mudstone occur on the south (Devonian footwall) side of the Jason fault, within the matrix of the Jason fault at deep to intermediate levels, and in the north-side (Devonian hangingwall) strata adjacent to the breccia pipe. A silicification front discordant to bedding was noted within a large siltstone clast in diamictite overlying the Jason deposit. Across this front siltstone beds thin as they pass from silicified to non-silicified siltstone indicating silicification prior to full compaction of the sediment; the silicification also must have occured prior to resedimentation.

Whereas quartz is the cement in the conglomerate unit throughout the MacMillan Fold Belt, the conglomerate underlying the Jason deposit and thin conglomerate beds interbedded with the 'A' diamictite unit are cemented by pyrite, ankerite, quartz, galena and sphalerite (Fig. 12a,b). Clearly these permeable gravels were infiltrated by hydrothermal fluids during formation of the Jason deposit.

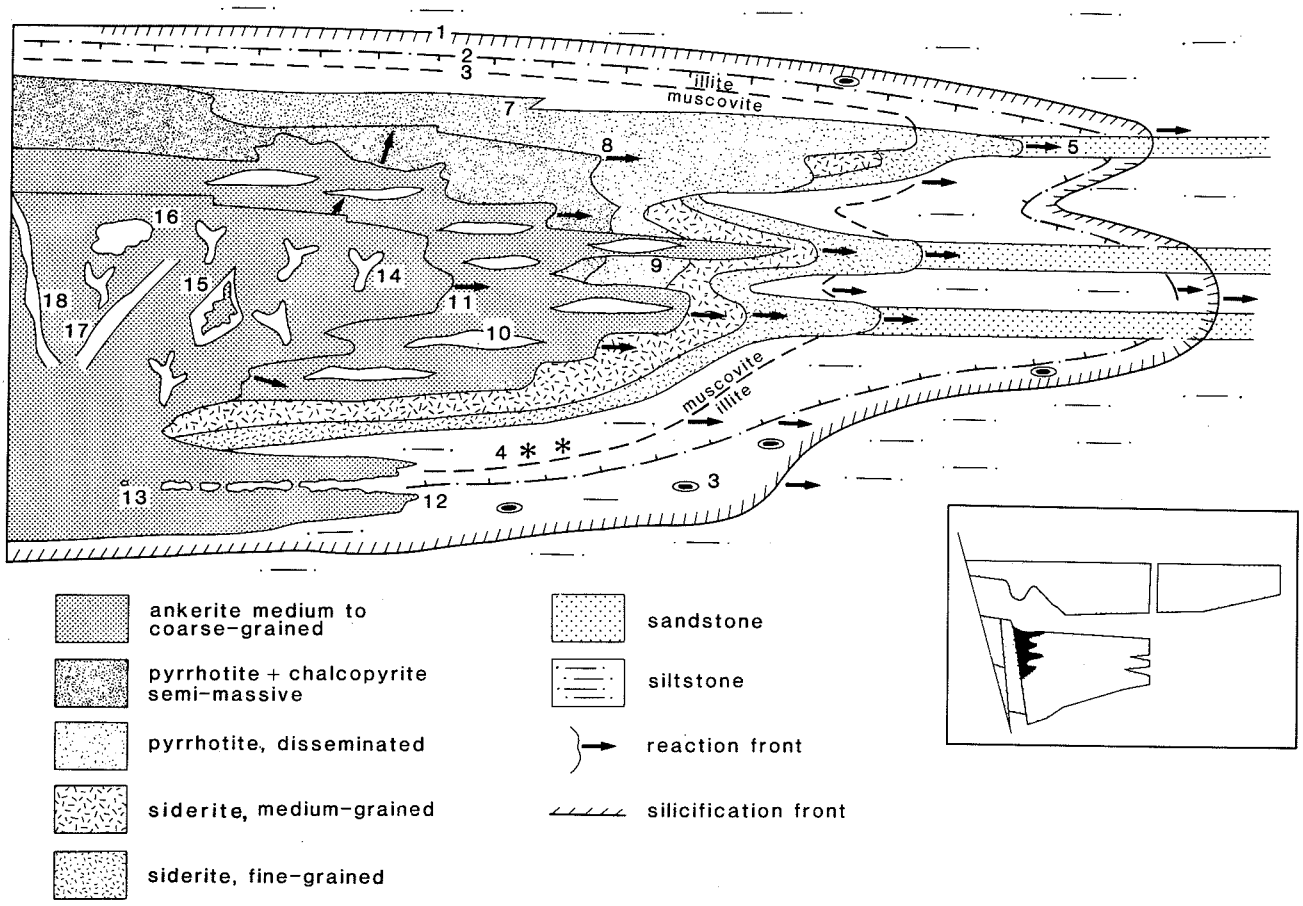

Figure 15 Schematic diagram of mineral relationships within the iron carbonate facies of the lower lens adjacent to the breccia pipe (see location on inset diagram). Numbers on the figure refer to specific relationships: (1) extent of silicification; (2) extent of destruction of organic matter; (3) extent of muscovite replacement of illite; (4) coarse-grained muscovite rosettes; (5) replacement of sandstone laminae by fine-grained siderite; (6) extent of medium-grained siderite; (7) replacement of siderite by disseminated pyrrhotite; (8) replacement of siderite by semi-massive pyrrohtite and minor chalcopyrite; (9) bedding parallel ankerite-quartz-galena veins; (10) amalgamation of parallel ankerite-quartz-galena veins; (11) extent of massive ankerite-galena; (12) replacement of siltstone by ankerite; (13) corroded fragments of siltstone in ankerite matrix; (13) galena 'lace' interstitial to ankerite; (14) irregular ankerite veins and pods; (15) ankerite-quartz-galena-pyrobitumen pod; (16) quartz nodule; (17) ankerite, galena, quartz, muscovite vein; and (18) pyrrhotite-pyrite-muscovite vein.

Jason fault: vertical zonation and Devonian orientation

Deep fault zone

The structure and composition of the Jason fault change with respect to stratigraphic level. Below the intersection of the upper lens, the fault zone is narrow, sharply defined and associated with altered and sulphide-rich wall rocks. In the deepest portion of the fault drilled (Fig. 12b, DH 87), the fault is a single 3 m thick zone of irregular to rounded fragments of

coarse-grained siderite and siderite-quartz-pyrite in a matrix of fine-grained quartz, siderite and clay with disseminated pyrite, galena, sphalerite, chalcopyrite and pyrrhotite. The north wall of the fault is brecciated and intensely silicified siltstone cut by breccias and veins of pyrrhotite, sphalerite and pyrite. The south wall of the fault is silicified Road River mudstone with abundant veinlets of ferroan carbonate. In DH 63 the Jason fault is composed of two fault strands within a broad 10 m zone of veinlets and vein-breccias of ferroan carbonate, pyrite, chalcopyrite and muscovite. The fault strands contain fragments of coarse-grained vein siderite and silicified mudstone cut by siderite veins in a fine-grained matrix of quartz, clay and ferroan carbonate. The fault in DH 41 also has two strands and includes fragments of siderite breccia, quartz-banded stratiform rock, and tube-shaped veins of siderite with selvages of ankerite-muscovite- pyrite. The tube-like shape of these veins suggest formation by fluid streaming through unconsolidated fault matrix rather than along fractures.

Shallow fault zone

Above the upper stratiform lens, the Jason fault is a broad, more diffuse zone of faults, pervasive ductile shear, spaced small-offset faults and veinlets that cut bedding at high angle. The fault zone is clay-rich and only weakly altered. Drill hole 34 , the shallowest intersection of the Jason fault zone, contains a narrow zone of pebble breccia bracketed by a broad, 10 m wide zone of small offset slip zones (with siderite vein breccias) and local penetrative shear deformation reflecting broadly distributed shear. Siderite -pyrite veins in north-side strata cut bedding at high angle, and strata are offset in a normal fault sense across some veins. Some such veins are folded suggesting veining was followed by compaction of the host sediment causing shortening and folding of the veins.

Orientation of fault prior to Mesozoic folding :

If the Jason syncline is unfolded about its gently east-plunging axis, the restored orientation of the Jason fault trends east-northeast and dips about 40 degrees northwest. This restored orientation trends toward the present location of the Tom deposit which also is situated adjacent to a west side down normal syndepositional fault (Goodfellow and Rhodes, this volume) suggesting that both the Tom and Jason deposit formed adjacent to the same ENE-trending syndepositional fault. It is likely that the original Jason fault intersected bedding more steeply than at present; the present shallower dip likely reflects flattening of the fault-bedding angle during folding (i.e. rotation of the fault towards the orientation of the axial plane of the Jason syncline).

FLUID INCLUSION STUDIES

Homogenization temperatures for 74 fluid inclusions from minerals of the vent complex of the Jason deposit indicate hydrothermal fluids were Na-Ca-Cl brines, approximately 9 weight % equivalent NaCl and 250° C (Gardner and Hutcheon, 1985). Twenty two, two-phase inclusions (vapour plus aqueous phase) were studied in siderite, ankerite and quartz within veinlets of the central ferroan carbonate facies (e.g. DH 56B); the average arithmetic mean for homogenization temperatures is 252°C and values range from 181 to 284°C. Twenty, two-phase aqueous inclusions in quartz, ankerite, barite and barytocalcite from the outer ferroan carbonate facies near the replacement front with barite-sulphide facies (DH 68A) have an average mean homogenization temperature of 219°C, while 18 three-phase CO_2-bearing (and a few CH_4-bearing) inclusions in fluorite, quartz, barytocalcite and sphalerite have a mean of 265°C. Seven, two-phase inclusions in siderite and quartz veins within the intermediate levels of the Jason fault (DH-41) have a mean homogenization temperature of 230°C. In general three-phase CO_2-bearing inclusions average 6.3 equivalent weight % NaCl, while two-phase inclusions are more saline (9.7 equiv. wt.%).

STABLE ISOTOPE GEOCHEMISTRY (Turner, Taylor and Goodfellow)

The following data are presented in preliminary form only, and draw from a current project between Robert Turner, Bruce Taylor and Wayne Goodfellow of the Geological Survey of Canada. Preliminary publication of these results includes Turner et al., (1989), and Turner et al., (1990). Isotopic analyses are reported relative to the following standards: ^{13}C, PDB; ^{34}S, CDT; ^{18}O, SMOW.

Oxygen isotope chemistry

The $\delta^{18}O$ per mil values for vein and massive minerals from the vent complex are: siderite (14.5 to 20.2; 16 samples), ankerite (10.6-20.5; 20 samples), barian carbonate (15.3 to 18.6; 2 samples), quartz (20.1 to 23.0; 19 samples) and muscovite (15.8 to 17.5; 7 samples)(Fig. 16).

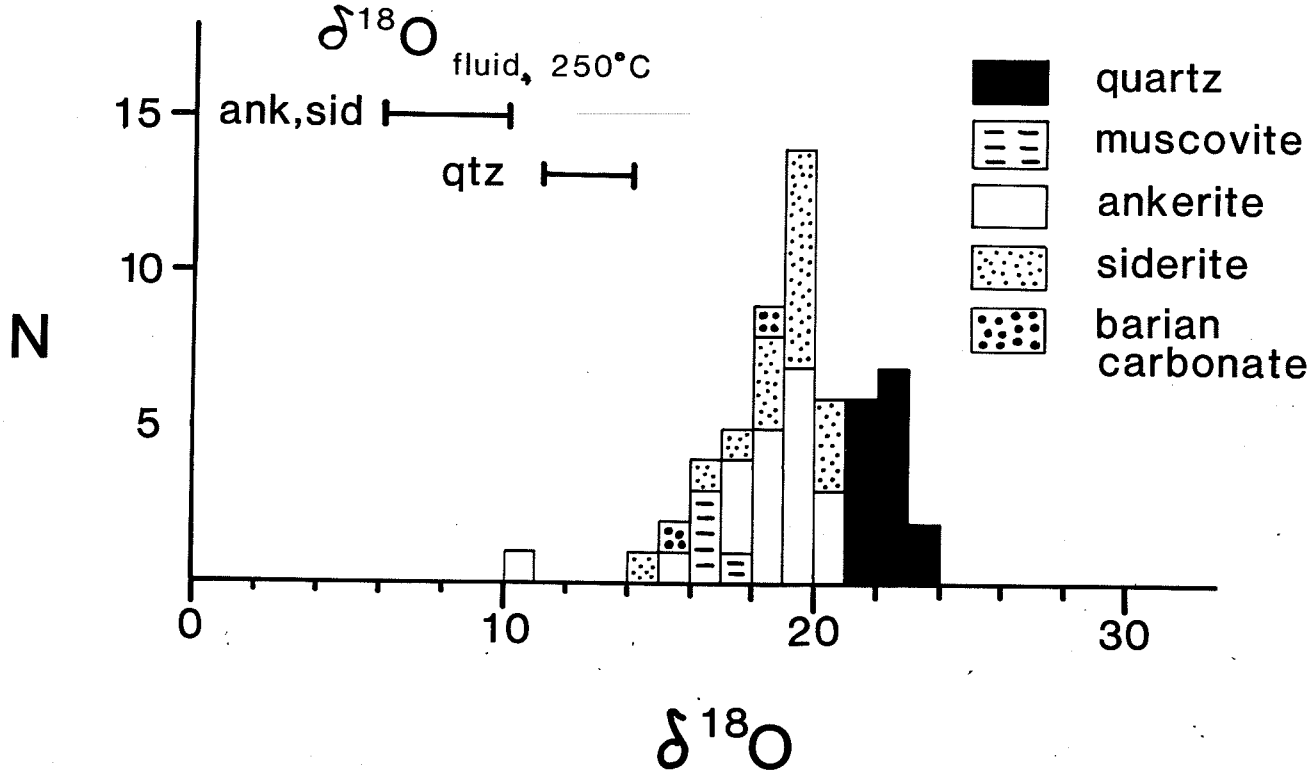

Figure 16 Histogram of $\delta^{18}O$ values for silicates and carbonates in the vent complex of the Jason deposit. The calculated range of $\delta^{18}O$ of a 250^0 C hydrothermal fluid in equilibirium with these carbonates (ank,sid) and quartz (qtz) is indicated.

The calculated oxygen isotopic composition of a 250^o C hydrothermal fluid in equilibrium with ankerite and siderite is 6.2 to 10 °/oo, and for quartz 11 to 14.1 °/oo. These high estimated $\delta^{18}O$ fluid values suggest the fluid that formed the Jason deposit was an evolved basinal fluid or metamorphic fluid (sensu lato).

Carbon isotope chemistry

The $\delta^{13}C$ values of vein and massive carbonates from the vent complex are: siderite (-7.2 to -3.2; 19 samples), ankerite (-9.1 to -1.6; 21 samples), and barian carbonate (-10.3 to -8.4; 2 samples).

The calculated isotope composition of carbon of a 250^o C fluid in equilibrium with the ankerite and siderite overlaps that of CO_2 degassed from the mantle, but could also be derived from a restricted mixture of carbon from organic matter and limestone in strata underlying the Jason deposit. The former scenario would require the mixing of mantle fluids (e.g. CO_2) with base metal-bearing fluids derived from basinal clastic rocks during formation of the stratiform Zn-Pb deposits, the latter could require just a single basinal fluid.

Sulphur isotope chemistry

Isotope chemistry of sulphides

Sulphur isotope data for the Jason deposit include 22 sulphide and 17 sulphate analyses from Gardner and Hutcheon (1985), and 53 sulphide and 9 sulphate analyses from Turner, Taylor and Goodfellow (1990) (Fig. 17). The $\delta^{34}S$ of sulphides from the Jason deposit range from 4.0 to 23.5. The $\delta^{34}S$ of replacement epigenetic sulphides in the vent complex

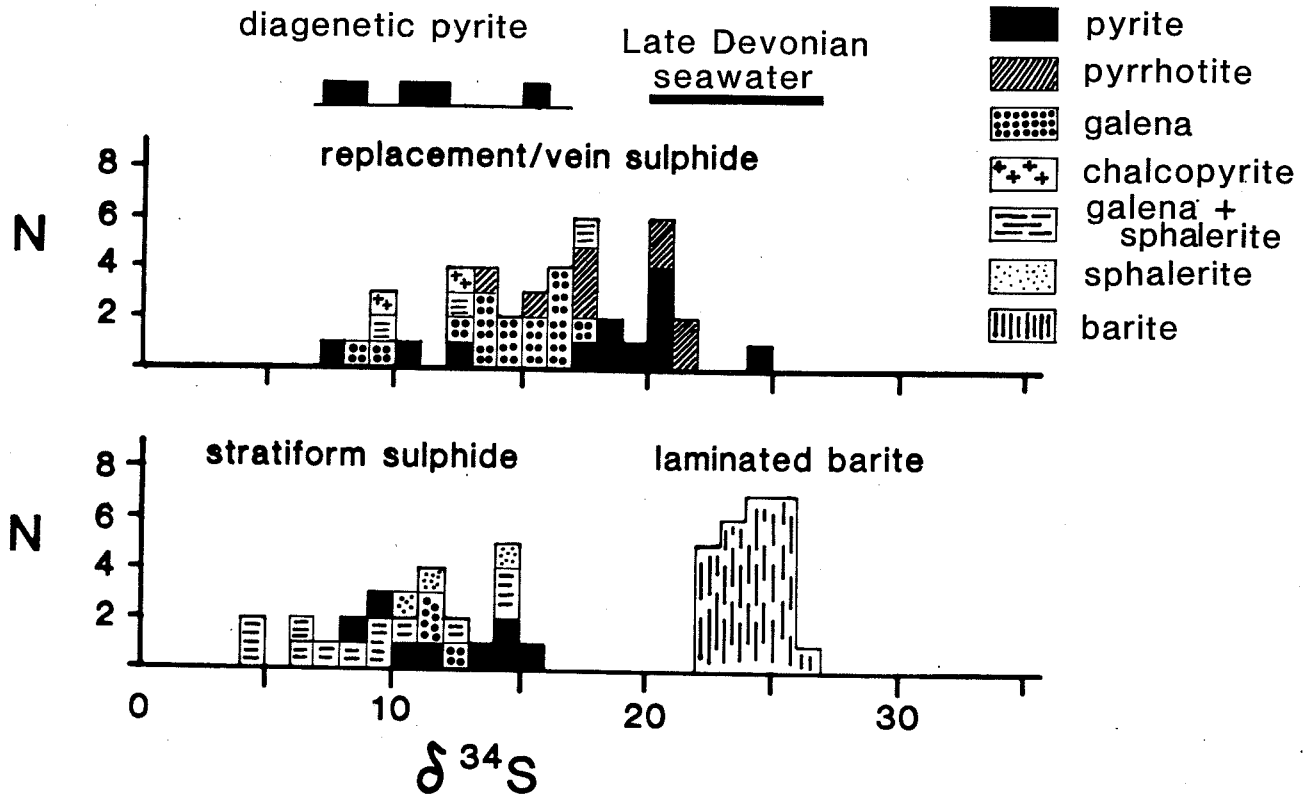

Figure 17 Histogram of $\delta^{34}S$ values for 75 sulphide and 26 barite samples from the Jason deposit. Includes data from Gardner and Hutcheon (1985). Sulphide samples have been divided into replacement and vein sulphides from the vent complex, stratiform sulphides in the bedded sedimentary lenses, and laminated pyrite in mudstone underlying and overlying the Jason deposit. Estimated $\delta^{34}S$ of Late Devonian seawater is from Claypool et al., (1980).

tend to be higher (6.7 to 23.5) than laminated sedimentary sulphides (4.0 to 15.6) (Fig. 17). Comparison of $\delta^{34}S$ values in individual minerals also show this trend; $\delta^{34}S$ for galena and pyrite samples in the vent complex are higher than laminated galena and pyrite (Fig. 17). In the drill hole 69 intersection of the Main zone, the $\delta^{34}S$ of laminated to disseminated pyrite in Dp3 carbonaceous mudstone up to 70 m above and 20 m below (4 samples) the distal part of the upper stratiform lens range from 7.2 to 15.1, compared to 8.8 to 9.2 (two samples) for laminated pyrite in the stratiform lens (quartz-sulphide facies). The similarity between the isotopic composition of these "sedimentary" pyrites in mudstone and "hydrothermal" pyrite in the stratiform lense suggests a similar sulphur source. The isotopic composition of these pyrite in mudstone is similar to that of pyrite in Dp3 above the Tom deposit ($\delta^{34}S$ = 5 to 12°/oo (Goodfellow and Rhodes, this volume).

Isotope chemistry of sulphates

Analyses of laminated barite studied by Gardner and Hutcheon (1985) yielded an average $\delta^{34}S$ of 24.4 +/-1.2; these authors noted that these values are similar to the estimated sulphur isotopic composition of Late Devonian sulphate (Claypool et al., 1980). A systematic increase in $\delta^{34}S$ occurs with increasing stratigraphic position in drill holes 81-68 (Gardner and Hutcheon,

1985) and 81-68A. The latter trend correlates with a slight but consistent shift to less radiogenic strontium isotope ratios in the same barite samples. In contrast, however, 2 sections in the Main zone appear to show a general decrease in $\delta^{34}S$ with increasing stratigraphic position (Trench 3, Gardner and Hutcheon, 1985; DH-25).

Interpretation of sulphur source

The similarity of isotopic composition of sulphur in barite to that estimated for Late Devonian seawater sulphate suggests that barite formed from the mixing of seawater sulphate and hydrothermal barium. The source of sulphide sulphur is less clear; three possible sulphur sources exist:

(1) a reduced, sulphur- and metal-bearing hydrothermal fluid (e.g. Ohmoto et al., in press),

(2) reaction between a sulphur-poor but metal-bearing fluid and H_2S-bearing anoxic bottom waters (e.g. Goodfellow and Jonasson,1984; Goodfellow, 1987), and

(3) high temperature inorganic reduction of barite sulphate by hot reduced fluid during replacement of barite in the vent complex. The organic-rich nature of, and lack of evidence of bioturbation within Portrait Lake strata suggest deposition within a reduced water column; such a water mass could have been rich in reduced sulphur (Goodfellow and Jonnason, 1984).

If the source of sulphur in laminated pyrite in mudstones above and below the deposit ($\delta^{34}S$ = 7.2 to 15.1°/oo.) was reduced seawater sulphate as is common in pyrite of slowly deposited basinal strata (see Goodfellow, 1987), then it is reasonable that the isotopically similar sulphur in the bedded sulphides of the Jason deposit ($\delta^{34}S$ = 4 to 15.6°/oo) could also have been derived from seawater sulphate. The higher $\delta^{34}S$ values of sulphides in the vent complex ($\delta^{34}S$ = 6.7 to 23.5°/oo) must represent an additional sulphur source such as (1) high temperature inorganic reduction of sulphate in laminated barite during replacement, or (2) the introduction of reduced sulphur with the hydrothermal fluids. This second reduced sulphur likely mixed with sulphur derived from remobilized sedimentary sulphides (e.g. sphalerite). It is important to note that most of the reduced sulphur in the Jason deposit occur in the volumetrically large stratiform lenses rather than in epigenetic sulphides of the much smaller vent complex. Therefore, regardless of the source of the vent complex sulphides, the great portion of the reduced sulphur in sulphides of the Jason deposit appears to reflect a seawater sulphur source.

STRONTIUM ISOTOPE GEOCHEMISTRY

The $^{87}Sr/^{86}Sr$ ratio of four siderite and five ankerite samples from the vent complex range of from 0.7137 to 0.7221 (Fig. 18). The $^{87}Sr/^{86}Sr$ ratio of siderite samples, which are largely from the Jason fault and the deeper portions of the vent complex, tend to be more radiogenic (0.7160 to 0.7221) than ankerite samples from the shallower portions of the vent complex (0.7135 to 0.7185). High Rb/(Rb+Sr) ratios (0.38 and 0.55) were measured for 2 siderites which had high $^{87}Sr/^{86}Sr$ ratios (i.e. 0.7196 and 0.7221), perhaps suggesting contamination by radiogenic strontium.

Eighteen of twenty barite samples from laminated barite over the entire stratigraphic thickness of the Jason deposit have a narrow range of strontium isotope ratios, ($^{87}Sr/^{86}Sr$ = 0.7126-0.7144); two samples fall outside this tight cluster (i.e. 0.7085, 0.7107) (Fig. 18). Detectable rubidium occurred in only one barite sample. The $^{87}Sr/^{86}Sr$ ratio in barites from two vertical sections through the bedded ores shows a general increase with increasing stratigraphic position (DH 68A, DH 23); in the case of DH 68A this upward trend coincides with a systematic increase in $\delta^{34}S$ in sulphate.

Interpretation of mixing processes :

Strontium isotopic data provide insight into mixing processes during ascent of the hydrothermal fluid through the vent complex, and at the seafloor. Siderite in the Jason fault and "deep" vent complex has higher $^{87}Sr/^{86}Sr$ ratios than ankerites in the "shallower" vent complex. Bedded sedimentary barite is the least radiogenic. The $^{87}Sr/^{86}Sr$ of Late Devonian seawater is estimated as 0.7082 (Burke et al., 1982). This general trend of decreasing $^{87}Sr/^{86}Sr$ ratio with decreasing depth below the Devonian seabottom is interpreted to reflect mineral precipitation during the progressive mixing of a radiogenic hydrothermal fluid with less radiogenic Late Devonian seawater.

The broad range of values for carbonates in the vent complex suggest that this mixing involved not only strontium in seawater but also strontium derived from barite during replacement by carbonate. It has been noted that siderite, whether banded, massive or vein is early in the paragenesis with respect to massive or vein

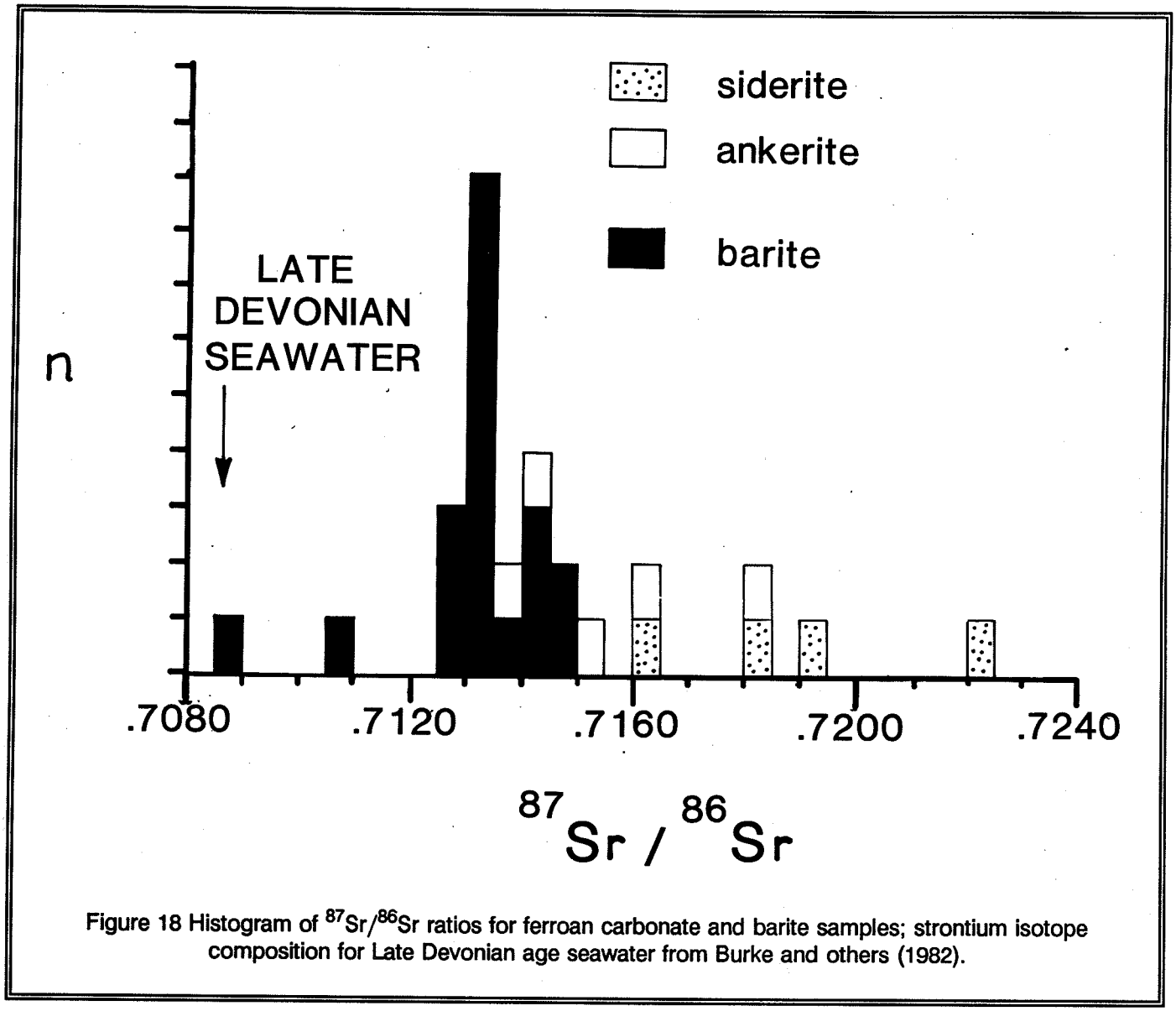

Figure 18 Histogram of $^{87}Sr/^{86}Sr$ ratios for ferroan carbonate and barite samples; strontium isotope composition for Late Devonian age seawater from Burke and others (1982).

ankerite. Siderite replacement bands in siltstone cut by later less radiogenic ankerite veins may suggest less mixing with seawater during siderite precipitation than vein ankerite, or reaction during siderite formation with a radiogenic clastic sediment.

The narrow range of $^{87}Sr/^{86}Sr$ values for barite suggests simple mixing between this modified hydrothermal fluid discharging from the vent complex, and seawater. The distinct shift of $^{87}Sr/^{86}Sr$ ratio in barite from Late Devonian seawater ($^{87}Sr/^{86}Sr$ = 0.7083; Burke and others,1982) suggests precipitation of barite during initial mixing with seawater. However, one barite sample has a $^{87}Sr/^{86}Sr$ value very close to that of seawater. A plot of $^{87}Sr/^{86}Sr$ versus 1/Sr for barite samples is a linear trend suggesting simple two component mixing of a more radiogenic, strontium-rich hydrothermal fluid with less radiogenic, strontium-poor seawater.

Interpretation of fluid source:

Siderite precipitated in the Jason fault and the deep part of the vent complex is considered to have

mixed least with seawater based on geologic setting; hence this mineral is considered the most representative of the hydrothermal fluid. The very radiogenic strontium (i.e. 0.7160 to 0.7221) reflects a radiogenic hydrothermal fluid derived from continental crustal rocks or derived sediments.

DISCUSSION ON THE CHARACTER OF THE JASON DEPOSIT :

Syndepositional nature of the Jason fault and fault scarp apron sediments

Diamictites represent debris derived from the submarine scarp of the Jason fault. The conformable nature, great lateral extent, heterolithic composition, and sharp sedimentary contacts indicate the diamictites were transported and deposited on the seafloor as sediments, rather than formation by in situ fragmentation. The source of diamictites was east of the Jason fault based on thickening and coarsening of the diamictite lobes up to the Jason fault. The compositional similarity of diamictite fragments to MacMillan Pass Member strata that are now elevated by the the Jason fault, the unique indurated and mineralized nature of the Jason fault relative to other local faults, and the change in structure, texture, alteration and mineralization of the fault with depth suggests that the Jason fault was syndepositional and the source of the diamictite lobes.

Sediments eroded from the scarp of the Jason fault were variably lithified and in some cases hydrothermally altered. Deformation of the margins of mudstone and siltstone clasts suggest that mud and silt beds were still plastic when deposited (Winn and Bailes, 1987). It is likely that gravels exposed on the fault scarp were largely uncemented because within the diamictite beds separate chert pebbles are far more abundant than clasts of chert pebble conglomerate. That pyrite and ferroan carbonate commonly cement the conglomerate clasts reflects early hydrothermal cementation of permeable gravels adjacent to the vent complex.

Homolithic breccias represent partial slumping or in situ disruption of silts and muds. Lack of clast mixing and comminution of the clasts suggests little lateral transport. Sudden change along a stratigraphic horizon from homolithic siltstone breccia to undeformed bedded siltstones indicates insitu disruption, perhaps caused by cross-stratal fluid flow due to seismic activity or elevated fluid pressures associated with the hydrothermal system.

Sedimentary origin of the bedded sulphide-barite-quartz

The Jason deposit formed from fluids that rose along an active syndepositional fault and exhaled onto the seafloor (Fig. 19). The bulk of the deposit formed as a stratiform body of hydrothermal sediments. Where this upflow zone along the Jason fault crossed earlier-formed sediments, widespread metasomatism hydrothermal has occurred (vent complex). Seawater was reduced, and likely rich in reduced sulphur.

Beds of fragmented laminated suphide-chert interbedded with laminated sulphide-barite, and clasts of massive sphalerite-galena overlying bedded sphalerite-galena indicates the resedimentation of bedded sulphide and laminated sulphide-quartz on the seafloor and hence, an origin as hydrothermal sediments. Resedimented barite-sulphide has not been recognized but a similar origin is presumed based on the interlamination of barite with sulphides and chert. Interbedded siltstone and mudstone reflect non-hydrothermal clastic deposition. Such a sedimentary origin of hydrothermal laminae explains sharp compositional changes across lamina boundaries and the absence of replacement textures. An origin by hydrothermal fluid infiltration during diagenesis has been advocated for some stratiform zinc-lead deposits; however such an hypothesis is not advocated for the Jason deposit.

Origin of zoning in hydrothermal sediments

Hydrothermal sedimentation likely occurred from a laterally migrating hydrothermal plume, possibly at the top of a ponded brine pool or at a density contrast within the seawater. It is difficult to assess these two possibilities (Fig. 19). In order of maximum relative abundance (with respect to other hydrothermal sediments), the zoning outward from the vent area is galena, barite, sphalerite, and pyrite. The PbZnFe facies reflects rapidly sedimented galena-sphalerite in the immediate vent area. The barite-sulphide facies represents a broad intermediate region of barite sedimentation away from the vent. The absence of barite in the vent area is likely the result of replacement of barite by quartz, ferroan carbonate and sulphide, rather than lack of deposition. The outer limit of barite deposition likely reflects the limit of physical transport of

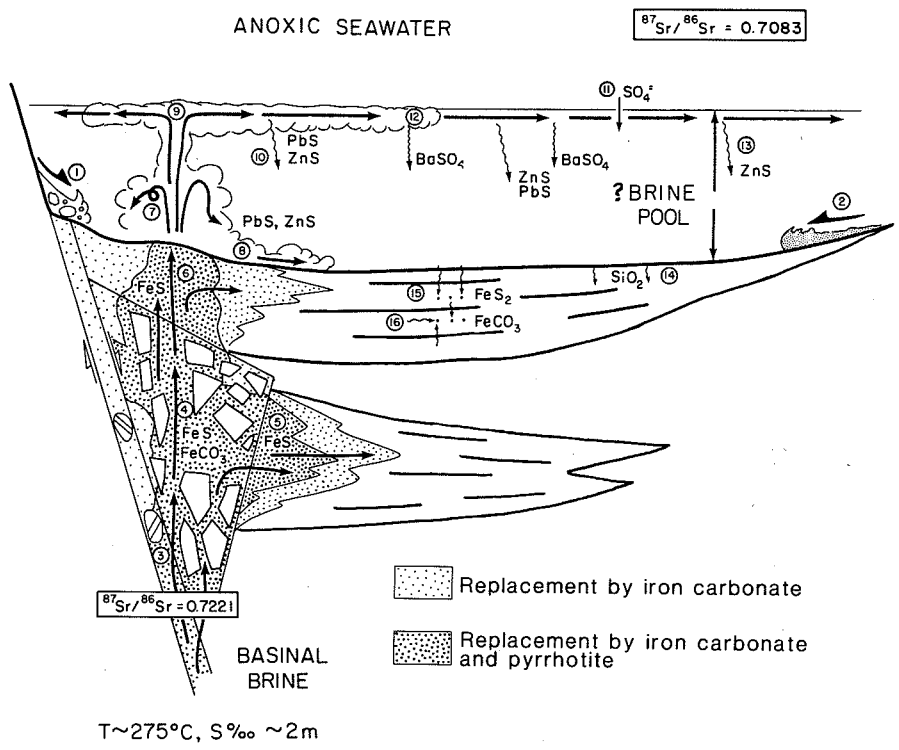

Figure 19 Interpretive cross-section illustrating processes during formation of the Jason deposit: (1) debris flow (diamictite) from active fault scarp; (2) chert-slit turbidity flow; (3) upflow of reduced metal-rich hydrothermal fluid; (4) brecciation of indurated sediments, precipitation of ferroan carbonate, pyrrhotite, quartz and muscovite; (5) lateral infiltration causing silicification, recrystallization of clays, and progressive replacement of barite-sulphide facies and siltstone by siderite and pyrrhotite; (6) replacement of laminated barite, silica and sphalerite sediments by massive and veined ferroan carbonate, pyrrhotite, galena and pyrite; (7) venting of hydrothermal fluids; quenching of fluids causing rapid sedimentation of sphalerite and galena; (8) resedimentation of sulphides from vent mound; (9) entrainment of sulphide particulate in bouyant hydrothermal plume that spreads laterally along a density interface, possibly the top of a brine pool; (10) sedimentation of entrained sulphide during lateral spread of plume; segregation of mineral particulate due to differental settling rates, (11) mixing of hydrothermal barium, zinc, lead and iron with seawater sulphate and sulphide; (12) intermediate deposition of barite; (13) continued deposition of sphalerite and pyrite in distal area, pyrite in most distal area; (14) diffusion of silica into shallow sediments and consequent precipitation; and bacterial sulphate reduction coupled with oxidation of organic matter forming pyrite (15) and carbonate precipitation.

barite particulate by the spreading plume. As at modern seafloor hydrothermal sites, quenching of the hydrothermal fluid and mineral precipitation must have taken place immediately upon mixing with seawater in the vent area. Therefore, zoning of hydrothermal minerals must represent the relative settling rate of different hydrothermal minerals. That sulphide sedimentation is more extensive than barite sedimentation likely reflects a higher settling rate of barite relative to sphalerite and pyrite, possibly due to coarser particulate size as noted in some modern seafloor vent sites. The zoning of sulphide minerals from proximal galena to sphalerite to distal pyrite is also interpreted to reflect relative settling rates; proximal

galena likely reflects the high specific gravity of galena.

Origin of quartz-rich sediments

The ubiquitous association and co-extensive distribution of siliceous and/or silicified siltstone and mudstone with hydrothermal sediments suggest that silica precipitation either occurred:

(1) above the seafloor and was deposited as a sediment;

(2) in pore fluids below the seafloor due to diffusion of silica from an overlying silica-rich watermass (e.g. brine pool); and/or

(3) in pore fluids below the seabottom due to lateral infiltration of hydrothermal fluids from the vent complex area throughout the hydrothermal sedimentary body. Sedimentary or seabottom diffusion processes are felt to be the cause of siliceous sediments throughout the bulk of the stratiform bodies distal from the vent area (e.g. Main zone), while the lateral infiltration process was likely important near the vent complex, particularly where silicification is associated with destruction of organic matter (e.g South zone). Mixing of silica-rich hydrothermal fluids with seawater does not lead to saturation with respect to amorphous silica because dilution offsets the decreasing solubility of silica (Janecky and Seyfried, 1984). However, hydrothermal fluids ponded as brine pools do precipitate amorphous silica (Shanks and Bishoff, 1977). Therefore, a fossil brine pool environment should be characterized by silica-rich hydrothermal sediments, while a fossil seawater plume environment would likely be silica deficient. This line of arguement favors the formation of the Jason deposit within a brine pool rather than an open seawater plume.

Fault movement, deposition of diamictite, and hydrothermal activity

The wedge-shaped cross-sectional profile of the Jason deposit (Fig. 12a) likely reflects hydrothermal deposition within a bathymetric low adjacent to the Jason fault scarp. The occurrence of diamictite interbedded with and overlying (but not below) the Jason deposit, indicates that hydrothermal activity coincided with early movement on the fault and formation of an unstable submarine fault scarp. Based on the thickness of diamictite stratigraphically above the Jason deposit, most fault movement followed the termination of hydrothermal sedimentation. It is possible that rapid deposition of diamictite could have physically blocked exhalative discharge, causing the end of hydrothermal sedimentation. One could speculate that hydrothermal discharge then shifted to the northeast along the Jason fault to form the Tom deposit, whose mineralogy, textures, hydrothermal facies, isotopic chemistry, fluid chemistry and temperature are strikingly similar to that of the Jason deposit (see Carne, 1979; Ansdell et al., 1989, Goodfellow and Rhodes, this volume).

Vent complex: fossil hydrothermal upflow zone

The abundance of replacement and vein textures, coarse grain size and absence of evidence of bedding indicates an epigenetic origin of the ferroan carbonate facies. This facies formed by replacement of earlier formed hydrothermal sediments based on the discordant replacement contact between the ferroan carbonate and barite-sulphide facies. The massive micro-colliform texture of pyrite at the top of the upper lens suggests formation by in situ precipitation from rising fluids immediately below the seafloor. The ferroan carbonate and pyrite facies, together with the breccia pipe, represent the paleo-upflow zone or vent complex for hydrothermal fluids that formed the Jason deposit. Thick-bedded massive sphalerite-galena beds reflect the quenching of hydrothermal fluids in seawater and rapid fallout of sulphide particulate, or the resedimentation of this sulphide sediment.

Processes within the vent complex

Fluids rising on the Jason fault were focussed by the higher permeability breccia pipe resulting in localized discharge at the seafloor. The steeper attitude of the breccia pipe (with respect to bedding) relative to the Jason fault, and evidence for normal fault displacement in breccia zones of the breccia pipe suggest that the latter developed along shallow, antithetic splay faults as commonly noted in listric growth faults. Baritic, sulphidic and siliceous hydrothermal sediments in and adjacent to the upflow zone were susceptible to replacement by ferroan carbonate, pyrrhotite and pyrite. Reduction of sulphate in barite may have provided the reduced sulphur for some vent complex sulphides. Quartzose siltstone beds were also prone to dissolution and replacement by siderite and iron sulphides. The ferroan carbonate facies has much higher lead/(lead+zinc) ratios than adjacent barite-sulphide facies suggesting preferential

remobilization of sphalerite during metasomatism and the consequent enrichment in residual galena. High lead/lead + zinc values also define the interpreted paleo-vents of other stratiform zinc-lead deposits (Carne, 1979; Taylor and Andrew, 1978). It is important to note that the vent complex is almost exclusively superimposed on earlier-formed sulphide-rich hydrothermal sediments that may have been the sulphur source for epigenetic sulphides; this is distinct from the sulphide-rich footwall breccias that comonly underlie Cu-Zn volcanogenic massive sulphide deposits. Whereas the case of such volcanic-hosted deposits suggests reduced sulphur was introduced with the hydrothermal fluid, the character of the Jason deposit does not require it.

It is anticipated that the vent complex formed under steep physical-chemical gradients (e.g., temperature, $^{f}O_2$, $^{f}S_2$, pH) in which the hydrothermal fluid evolved rapidly, and that these conditions varied markedly over the life of the hydrothermal system. Brecciation and ferroan carbonate precipitation followed earlier silicification of the sediments, perhaps reflecting rupture of a silicified cap coincident with CO_2 effervescence in the hydrothermal fluids. In the lower lens, early-formed alteration was both pervasive (e.g. silicification) and bedding controlled (e.g. siderite); superposed alteration (e.g. ankerite-galena) replaced early bedding-controlled alteration and developed along fractures during progressive induration of the sediments. This textural evolution suggest progressive induration of the sediment and a change with time from pervasive fluid infiltration of sediments to fracture-controlled permeability.

Fluid chemistry :

The Jason deposit formed from a 250°C Na-Ca chloride brine about 3 times seawater salinity (9 equiv. wt%) (Gardner and Hutcheon, 1985). The fluid was a reduced, CO_2-rich, radiogenic basinal fluid that transported significant Fe, Ba, Zn, Pb, and lessor Cu, Ag, As and Hg. The predominance of pyrrhotite and ferroan carbonates as iron-bearing phases in the vent complex suggest a low activity of sulphur, and a low activity ratio of reduced sulphur to carbon in the fluid. The dominance of CO_2 over CH_4 in three-phase fluid inclusions (Gardner and Hutcheon, 1985) indicates CO_2 as the dominant carbon species. However, the widespread distribution of pyrobitumen and pyrrhotite in the vent complex argues for a reduced fluid with an oxygen fugacity buffered by reduced carbon species (e.g. methane). Given the radiogenic nature and high calculated values of $\delta^{18}O$, the hydrothermal fluids must have been basinal or metamorphic fluids that had intimately reacted with continental crust or derivative clastic rocks, such as the thick sequence of Late Proterozoic feldspathic quartz grits that occur beneath the Selwyn Basin.

Carbonate-rich vent complexes like those of the Jason deposit are typical of other Upper Devonian and Lower Mississippian exhalative deposits within the Selwyn Basin. Other such deposits include the Marg volcanogenic massive sulphide deposit (Turner and Abbott, 1990), the Walt stratiform barite deposit (Turner and Goodfellow, 1990), the Tom stratiform Zn-Pb deposit (Ansdell et al., 1989), and the Boundary Creek zinc deposit (Turner and Rhodes, 1990). Carbon dioxide-rich hydrothermal fluids were characteristic of all exhalative deposits, regardless of whether the deposit was volcanogenic or sediment-hosted, or formed by lower temperature (e.g. barite deposits) or higher temperature fluids (e.g. base metal deposits), . It should be noted that mafic volcanic rocks of Devonian age in the MacMillan Fold Belt and elsewhere in Selwyn basin are commonly altered to ferroan carbonate. Based on the estimated $\delta^{13}C$ of the fluids at the Jason, the source of the carbon in the fluid may reflect mantle degassing of CO_2, or a mix of organic and limestone carbon from strata of Selwyn Basin.

ACKNOWLEDGEMENTS

This paper is drawn largely from my Ph.D studies at Stanford University. That work benefited greatly from the supervision of Marco T. Einaudi. This paper also incorporates results from ongoing research on the genesis of the Jason deposit; in this regard I would like to acknowledge particularily the value of my discussions with Wayne Goodfellow of the GSC. Stable isotopic data are drawn from current research with Bruce Taylor and Wayne Goodfellow of the Geological Survey of Canada. Preparation and stable isotopic analyses of selected samples were carried out in laboratories at the GSC and the Ottawa-Carleton Centre for Geoscience Studies/GSC Stable Isotope Laboratory, Ottawa University. Determination of $^{87}Sr/^{86}Sr$ of carbonates and barite was conducted by Geochron Labratories Ltd., Cambridge, Mass.; and at the Geochronology Laboratory, Lithosphere and Canadian Shield Division, GSC, Ottawa. My understanding of the

Jason deposit has also benefited greatly from discussions with Grant Abbott, Rick Bailes, Don Blackadar, Dave Gardner, Peter Hubacheck, K. I. Lu, Dereck Rhodes, Barry Smee, Clyde Smith, Bruce Taylor and Rob Zierenberg. I would like to thank Abermin Resources Ltd. for their continued support of this project. Thanks also go to Cal Shannon and others at the Jason camp who have over the years made it such an enjoyable place to work.

REFERENCES

Abbott, J. G., 1982, Structure and stratigraphy of the Macmillan Fold Belt: evidence for Devonian faulting, in Yukon Geology and Exploration 1981: Dept. of Indian Affairs and Northern Development (Canada), Northern Affairs Program, Expl. and Geol. Serv. Div., Whitehorse, Yukon, p. 22-33.

Abbott, J G., 1983, Geology of the Macmillan Fold Belt 105O-SE and parts of 105P-SW (1:50,000), Dept. of Indian Affairs and Northern Development (Canada), Northern Affairs Program, Expl. and Geol. Serv. Div., Whitehorse, Yukon, Open File Maps.

Abbott, J. G., and Turner, R. J. W., (this volume) Late Devonian tectonic setting of stratiform ZnPb deposits, MacMillan Fold Belt, Yukon, in Abbott, J. G. and Turner, R. J. W., eds., Mineral deposits across the northern Canadian Cordillera, Yukon-northeastern British Columbia, IAGOD Field Guide, Excursion 14.

Ansdell, K.M., Nesbitt, B.E. and Longstaffe, F.J., 1989, a fluid inclusion and stable isotope study of the Tom Ba-Pb-Zn deposit, Yukon Territory, Canada, Economic Geology, v. 84, p. 841-856.

Bailes, R. J., Smee, B. W., Blackadar, D. W., Gardner, H. D., 1986, Geology of the Jason lead-zinc-silver deposits, Macmillan Pass, Yukon Territory, in Morin, J. A., ed., Mineral deposits of the northern Cordillera: Canadian Institute of Mining and Metallurgy, Special Volume 37, p. 87-99.

Bouma, A. H., 1962, Sedimentology of some flysh deposits, Elsevier, Amsterdam, 168 p.

Burke, W. H., Denison, R. E., Hetherington, E. A., Koepnick, R. B., Nelson, H. F. and Otto, J. B., 1982, Variation of seawater $^{87}Sr/^{86}Sr$ throughout Phanerozoic time, Geology, p. 516-519.

Carne, R. C., 1979, Geological setting and stratiform mineralization, Tom claims, Yukon Territory: Dept. Indian Affairs Northern Devel. Open-File Rept. EGS 1979-4, 30 p.

Claypool, G. E., Holser, W. T., Kaplan, I. R., Sakai, H., and Zak, I., 1980, The age curves of sulfur and oxygen isotopes in marine sulfate and their mutual interpretation: Chem. Geology, v. 28, p. 199-260.

Dawson, K. M. and Orchard, M. J., 1982, Regional metallogeny of the northern Cordillera: biostratigraphy, correlation and metallogenic significance of bedded barite occurrences in eastern Yukon and western district of MacKenzie, in Current Research, Geological Survey Canada, Paper 82-1C, p. 31-38.

Gardner, H. D., 1983, Petrologic and geochemical constraint on genesis of the Jason Pb-Zn deposits, Yukon Territory, unpub. M. Sc. thesis, University of Calgary, 212 p.

Gardner, H. D. and Hutcheon, I., 1985, Geochemistry, mineralogy and geology of the Jason Pb-Zn deposits, Macmillan Pass, Yukon, Canada: Economic Geology, v. 80, p. 1257-1276.

Goodfellow, W. D., 1987, Anoxic stratified oceans as a source of sulphur in sediment-hosted stratiform Zn-Pb Deposits (Selwyn basin, Yukon, Canada): Chemical Geology, v. 65, p. 359-382.

Goodfellow, W. D., and Rhodes, D., (this volume), Geological setting, geochemistry and origin of the Tom Zn-Pb-Ag-barite deoposits, in Abbott, J.G. and Turner, R.J.W., eds., mineral deposits of the northern Canadian Cordillera, Yukon-northeastern British Columbia, IAGOD Field Guide, Excursion 14.

Goodfellow, W. D. and Jonasson, I. R., 1984, Ocean stagnation and ventilation defined by $\delta^{34}S$ secular trends in pyrite and barite, Selwyn Basin, Yukon: Geology, v. 12, p. 583-586.

Hubacheck, P. C., 1981, Report on stratigraphic sections, Jason property, Yukon Territory, unpublished report for Ogilvie Joint Venture, 18 p.

Janecky, D.R., and Seyfried, Jr., 1984, Formation of massive sulfide deposits on oceanic ridge crests: Incremental reaction models for mixing between hydrothermal solutions and seawater, Geochim. Cosmochim. Acta, 48, 2723-2738.

Longstaffe, F. J., Nesbitt, B. E., and Muehlenbachs, K., 1982, Oxygen isotope geochemistry of the shales hosting Pb-Zn-Ba mineralization at the Jason prospect, Selwyn basin, Yukon, in Geol. Survey Canada Paper 82-1C, p.45-49.

McClay, K.R., and Bidwell, G.E., 1986, Geology of the Tom Deposit, Macmillan Pass, Yukon, in Morin, J.A., ed., Mineral Deposits of the Northern Cordillera: Canadian Institute of Mining and Metallurgy, Special Volume 37, p. 100 - 114.

Ohmoto, H., Kaiser, C.J., and Geer, K.A., in press, Systematics of sulphur isotopes in recent marine sediments and ancient sediment-hosted basemetal deposits: Int. Conf. on Stable Isotopes and Fluid Processes in Mineralization, Geological Society of Australia, Special Publication.

Shanks, W. C., and Bishoff, J. L., 1977, Ore transport and deposition in the Red Sea geothermal system: a geochemical model, Geochim. Cosmochim. Acta, 41, 1507-1519.

Smith, C. L., 1978, Geological setting of Jason and Tom deposit, Macmillan Pass area, Eastern Yukon: summary of presentation, Whitehorse Geoscience Forum 1978, 6p.

Smith, C.L., 1979, Ogilvie Joint Venture exploration results, 1978 season and summary of results 1974 through 1977; unpublished report, 46 p.

Stow, D. A. V., and Shanmugam, G., 1980, Sequence of structures in fine-grained turbidites: comparison of Recent deep sea and ancient flysch sediments, Sedimentary Geology, 25, p. 23-42.

Taylor, S., and Andrew, C. J., 1978, Silvermines orebodies, Co. Tipperary, Ireland, Inst. Mining Metallurgy Trans., 87, Sec. B, 111-124.

Teal, P.R., and Teal, S.E., 1978, Geology and sedimentary interpretation of the MacMillan Pass area (Jason and Tom properties), Yukon Territory, unpublished report for Ogilvie Joint Venture, 60 p.

Turner, R.J.W., 1984, Geology of the South Zone Deposits, Jason Property, Macmillan Pass Area, Yukon: Yukon Exploration and Geology 1983, p.105-115.

Turner, R.J.W., 1986, The genesis of stratiform lead-zinc deposits, Jason property, Macmillan pass, Yukon: unpub. Ph.D thesis, Stanford University, Stanford, 205 p.

Turner, R.J.W., and M. T. Einaudi, 1986, The geological setting and genesis of the South Zone stratiform Pb-Zn-barite deposits, Macmillan Pass, Yukon in Turner, R.J.W. and Einaudi, M. T., eds., The Genesis of Stratiform Sediment-Hosted Lead and Zinc Deposits: Conference Proceedings, Stanford University Publications, Geological Sciences, Vol. XX. p. 5-12.

Turner, R.J.W., Goodfellow, W.D., Taylor, B.E., 1989, Isotopic geochemistry of the Jason stratiform sediment-hosted zinc-lead deposit, Macmillan Pass, Yukon; in Current Research, Geological Survey of Canada, Paper 89-1E, p. 21-30.

Turner, R.J.W. and Abbott, Grant , 1990, Setting, structure, and zonation of the Marg volcanogenic massive sulphide deposit, Yukon, in Current Research, Geological Survey of Canada, Paper 90-1E, p. 31-41.

Turner, R.J.W. and Rhodes, Dereck, 1990, Boundary Creek zinc deposit (Nidd property), Macmillan Pass, Yukon: sub-seafloor sediment-hosted mineralization associated with volcanism along a Late Devonian syndepositional fault; in Current Research, Part E, Geological Survey of Canada, Paper 90-1E, p.321-335.

Turner, R.J.W. and Goodfellow, W.G., 1990, Barium carbonate bodies associated with the Walt (Cathy) stratiform barium deposit, Selwyn Basin, Yukon: a possible vent complex associated with a Middle Devonian sedimentary exhalative barite deposit; in Current Research, Part E, p. 309-319.

Turner, R. J. W., Taylor, B. E., and Goodfellow, W. D., 1990, Jason stratiform ZnPb deposit: Exhalative and replacement processes along a syndepositional fault (Abstr.): Paper presented at Geological Survey of Canada Minerals Colloquium, Ottawa.

Winn, R.D., Jr., and R.J. Bailes, and K.I. Lu, 1981, Debris flows, turbidites and lead-zinc sulfides along a Devonian submarine fault scarp, Jason prospect, Yukon Territory, in Seimers, C.T., Tillman, R.W., and Williamson, C.R., eds., Deep-water clastic sediments, a core workshop, Society Economic Paleontologists Mineralogists, p. 396-416.

Winn, R.D., Jr., and Bailes, R.J., 1987, Stratiform lead-zinc sulphides, mudflows, turbidites: Devonian sedimentation along a submarine fault scarp of extensional origin, Jason deposit, Yukon Territory, Canada: Geol. Soc. America Bull., v. 98, p. 528-539.

GEOLOGICAL SETTING, GEOCHEMISTRY AND ORIGIN OF THE TOM STRATIFORM Zn-Pb-Ag-BARITE DEPOSITS

Wayne D. Goodfellow
Geological Survey of Canada
601 Booth Street
Ottawa, Ontario, Canada K1A 0E8

and
Dereck Rhodes
Cominco Exploration Limited
700-409 Granville Street
Vancouver, British Columbia V6C 1T2

TABLE OF CONTENTS

INTRODUCTION

The Tom stratiform Zn-Pb-Ag deposits are located at latitude $63^0$10'N, longitude $130^0$10'W approximately 9 km southwest of the Yukon-NWT border at MacMillan Pass (Fig. 1). The property is accessible by the North Canol Road, a narrow clay-gravel road maintained only during the summer months (mid-June to mid-October). The nearest town and supply center is Ross River, 226 km southeast on the Canol Road. The road distance to Whitehorse via Ross River and Carmacks is 630 km. Total distance to tidewater at Skagway, Alaska, is 810 km by road. A 550 meter long unlicensed gravel airstrip, built by Hudson Bay Mining and Smelting (HBM&S) in 1969 is located along the Canol Road about 2.7 km west of the Tom deposit.

EXPLORATION HISTORY

Three zones, Tom East, Tom West and Tom Southeast, have been delineated to date on the Tom property. HBM&S have calculated mining reserves of 9,283,700 tonnes of 69.4 g/t Ag, 7.5% Pb and 6.2% Zn using a 7% Zn+Pb cutoff, a 15% dilution factor and 90% recovery for the Tom East and West Zones (McClay and Bidwell, 1986). The galena, sphalerite and barite mineralization occur in fine grained black clastic rocks of the Middle-Upper Devonian Earn Group of the Selwyn Basin (Abbott, 1982; Gordey et al., 1982).

The Tom deposit was discovered in 1951 by prospectors working for Hudson Bay Exploration and Development. Surface exposures of the East and West zones were located and 36 drill holes totalling 5,400 m were diamond drilled in 1952-53. No exploration was carried out on the property between 1954 and 1966. In 1967-68, an additional 4,800 m of diamond drilling was carried out and underground evaluation commenced in 1969. In the period 1970-71, some 1,887 m of underground development was completed on the 1,440 m level. Both the Tom East and the Tom West Zones were further evaluated with 3,617 m of underground diamond drilling. The property then lay idle until 1976 when exploration activity renewed. Surface diamond drilling was carried out in 1978 and 1979 resulting in discovery of the thin but high grade Southeast Zone. The underground exploration commenced in 1981 with the driving of a decline to the 1,300 m level. Development ceased in March, 1982, and the underground workings below 1,440 m are now flooded.

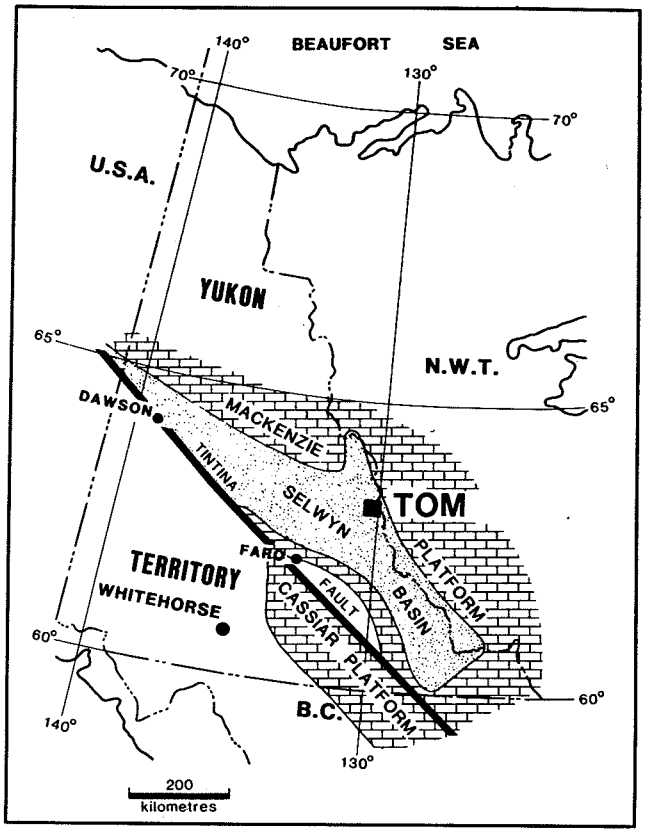

Figure 1 Map showing the location of the Tom deposit within the Selwyn Basin.

In 1988, Cominco Ltd. optioned the Tom property and began a program of surface drilling the depth extension of the West and Southeast Zones. This program drilled 2226 metres in 1988 and 2175 metres in 1989 with further drilling planned for 1990.

In terms of geological work, the Niddery Lake 1:250,000 map-sheet (105 O) was mapped at a reconnaissance scale by Blusson (1974). Geological studies by Carne (1976, 1979) established a stratigraphic framework, characterized the different stratigraphic units and described sedimentary sulphides and a feeder zone within the West Zone. During the seventies, surface maps of the Tom deposit were produced by Hudson Bay Exploration and Development at 1:5000 and 1:2500 scales. The Tom deposit was placed into its regional context with 1:50,000 scale mapping of the Macmillan Fold Belt (Abbott, 1982). More recently, McClay and

Bidwell (1986) have unravelled the structural history of the deposit and further mapping by Cominco Limited has subdivided Unit 3b of Carne (1976) into four units. Genetic aspects of the deposit were addressed by Large (1981) who placed geological and geochemical constraints on ore formation and by Ansdell et al. (1989) who used isotopic and fluid inclusion data to constrain the hydrothermal system.

This paper presents a summary of the data derived by Hudson Bay Exploration and Development, Cominco Limited and the Geological Survey of Canada.

REGIONAL GEOLOGICAL SETTING

In the Macmillan Pass area, a 30 km-wide by 60 km-long belt of Late Proterozoic to Triassic strata tends west-northwest across the more northerly regional structural grain of the Selwyn Basin (Fig. 2). This belt, referred to as the "Macmillan Fold Belt" (Abbott, 1982), has been divided into the North, Central and South blocks on the basis of outcrop pattern, north-south lithofacies variations and structural style. All of the Macmillan Pass Pb-Zn deposits fall within the Central Block. The distinctive lithofacies and structure of the Central Block is thought to represent a zone of faulting in Devonian times. While previous workers (Smith, C.L., Carne, R.C.) have talked of the Macmillan Pass "graben" it is probable that the Central Block is more complex than a single palaeo-graben as demonstrated by both structure and facies.

Abbott (1982) has recognized five main subdivisions of the sedimentary succession. These include (a) Hadrynian ("Grit" unit) clastic rocks and shaly equivalents (Cambrian-Ordovician) of the Mackenzie Platform; (b) Lower Cambrian to Middle Devonian carbonate units of the Mackenzie Platform found to the east and northeast of Macmillan Pass; (c) Ordovician-Devonian shales, cherts and minor limestones of the Road River Group; (d) Earn Group black clastic rocks (Devonian-Mississippian); and (e) Post-Earn Group sediments including Carboniferous quartz arenites, Permian cherts and shales, and Triassic sandstones and shales (Abbott, 1982; Gordey et al., 1982).

All of the Zn-Pb deposits at Macmillan Pass are hosted within Devonian lower Earn Group rocks. These rocks and particularly their equivalents within the Nahanni map sheet (N.T.S. 105 I) have recently been given formational status as the Portrait Lake Formation (Gordey, in prep.). The Portrait Lake Formation has been subdivided by Abbott and Turner (this volume) into the Macmillan Pass Member, a thick sequence of coarse grained black clastic rocks at the base of the Formation, and the Itsi Member, a package of brown and rusty weathering siltstones, sandstones and mudstone at the top of the Formation (Table 1). Sandwiched between the Macmillan Pass Member and Itsi Member is an unnamed succession of carbonaceous cherty mudstone and chert referred to here as the Tom Sequence. The Tom Zn-Pb-barite deposit occurs within the Tom Sequence.

The Macmillan Pass Member consists of a thick sequence of westerly-derived Late Devonian clastics deposited on the Canadian Cordilleran miogeosyncline. The clastics consist of silt and sand laminated mudstone, chert conglomerates, chert-quartz sandstones and siltstone which formed local massive deposits up to 800 m thick on submarine fans and in narrow grabens formed during rifting of the Cordilleran passive margin (Gordey et al. 1987). Horst-graben structures formed during rifting have produced large thickness variations, local unconformities and diachronous stratigraphic relationships. Stratigraphic correlations on a regional scale are hampered further by few stratigraphic marker units and a paucity of diagnostic fossils. As a result, the time span represented by particular clastic units is not known in most areas. This is particularly true of the Tom property (Fig. 3) where the only fossils precisely dated thus far come from a limestone bed within the Tom sequence (Table 1).

All known mineralization at Macmillan Pass occurs in areas of major facies and thickness changes, demonstrating a relationship of mineralization to areas of maximum syndepositional tectonism. Often in these areas multiple chert pebble conglomerate horizons occur along with locally derived diamictites composed of grit to boulder size clasts floating in a mudstone matrix. Alkalic basaltic flows and pyroclastics overlap in time the Tom, Jason and Boundary Creek deposits, and are spatially associated with the Jason and Boundary Creek deposits.

At the Tom property all the mineralization occurs at or near the contact of the coarse clastics of the Macmillan Pass Member with the overlying blue grey weathering carbonaceous mudstone and chert of the Tom Sequence. On the adjacent

Jason property mineralization seems to occur at or close to the same stratigraphic horizon however this

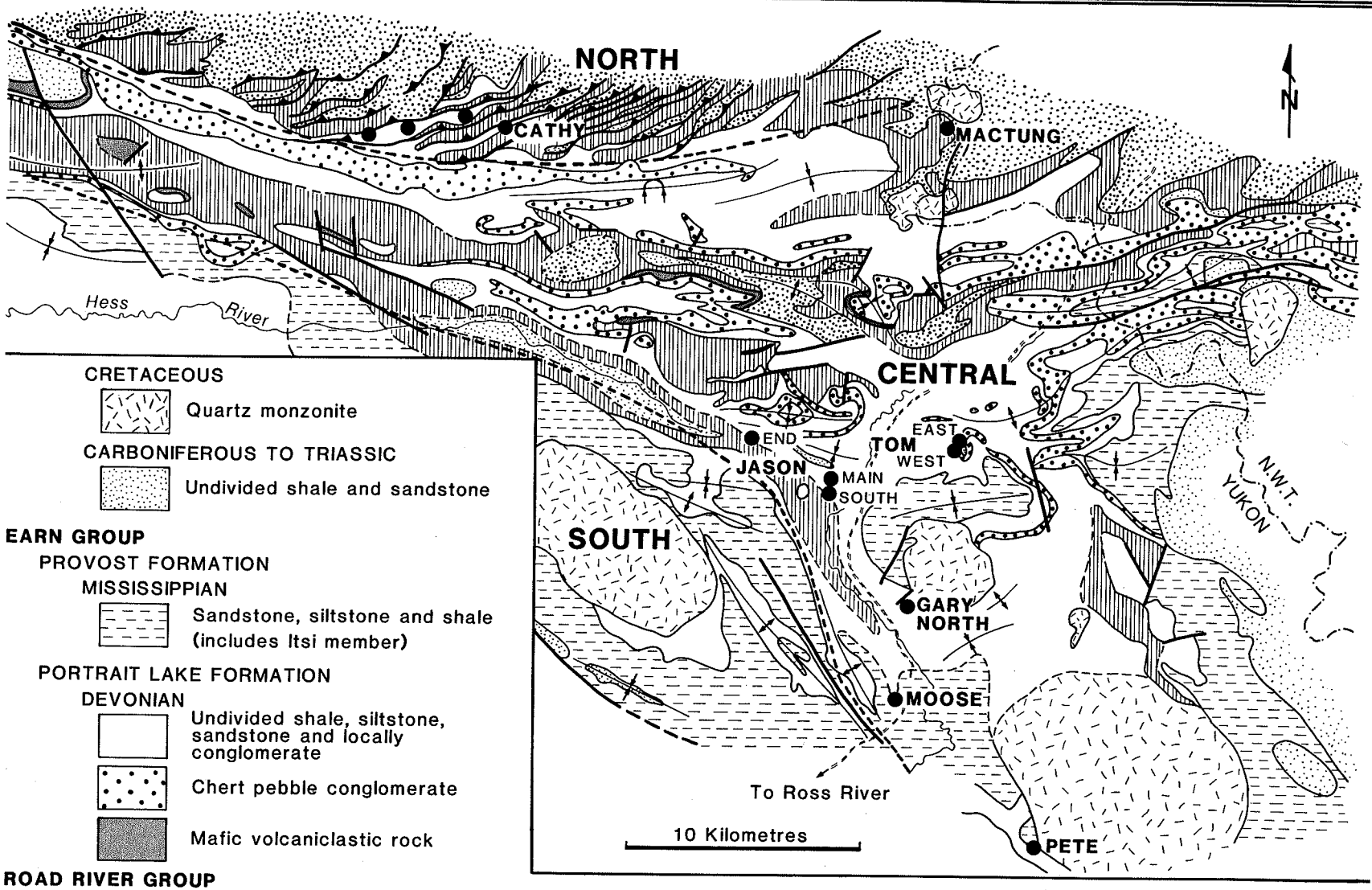

Figure 2 Macmillan Fold Belt and the location of sedimentary Zn-Pb-Ag-barite and barite deposits (from Abbott, 1982).

Table 1 Table of formations, members, units, lithologies, conodont ages (cross referenced to the terminology of earlier studies).

GP	FM	PERIOD/ STAGE			ABBOTT (1990)	CARNE (1979)	MAJOR UNITS	CORE UNITS	CORE DESCRIPTIONS	SURFACE MAP UNITS	SURFACE MAPPING DESCRIPTIONS
EARN GROUP		ITSI MEMBER	MISSISSIPPIAN		Dp4	4	THIS REPORT		Brown, dark brown and rusty brown weathering siltstones, sandstone and mudstone		
	PORTRAIT LAKE FORMATION	TOM SEQUENCE	DEVONIAN	Middle Frasnian →	Dp3	3b	TE	NO CORE	Interbedded siliceous mudstone rich in pyrite/ barite nodules and wavy laminated pyritic siliceous mudstone.	TE2	Dark grey to rusty weathering siliceous, pyritic black siltite with abundant white barite nodules
										TU	Light bluish grey weathering black cherty mudstone with thin interbeds of chert
								TE		TE1	Same as TE2 except stratigraphically below unit Tu
							TH	THpl	Threefold subdivisions evident in mapping not recognized in core. Siliceous, carbonaceous mudstone commonly with stylolite enhanced laminae. Over the west ore zone, the following units have been recognized: THpl -10 to 30 cm intervals of finely laminated pyrite; THa - calcareous siltstone above a 0.5 to 1.0 m thick limestone bed(THm); THnbp -wispy nodular barite/pyrite.	TH3	Light bluish grey weathering radiolarian chert with thin carbonaceous mudstone interbeds
								THa		TH2	Light bluish grey weathering medium bedded blocky black chert with thin interbeds of carbonaceous mudstone
								THm		TH1	Similar to TH3 except thicker chert beds
								THnbp			
							TG	TG	Radiolarian, commonly pyritic, carbonaceous thinly laminated mudstone.	TG	Silvery grey weathering, recessive, thinly bedded siliceous, pyritic mudstone with scattered radiolaria
							TC	TCnbp	Black carbonaceous mudstone with thin intervals of fine wispy barite nodules, absent above S.E. Zone		
								TCc/ TCd	Clastic striped black carbonaceous mudstone and diamictite		
								TCh	Black carbonaceous siliceous mudstone and chert with variable amounts of sulphide and barite laminae		
								TB	SEDIMENTARY FACIES: Interbedded barite, chert, sphalerite, galena and pyrite	TB	SEDIMENTARY FACIES
								TS	VENT FACIES: Veins, breccias and replacements of sulphides, ferroan carbonate and quartz	TS	VENT FACIES
								TCh	Black carbonaceous siliceous mudstone and chert with variable amounts of pyrite and barite laminae	TG	Described above
		MACMILLAN PASS MEMBER			Dp2p	3a	MMa	MMa	Black carbonaceous mudstone with light grey sand and silt interbeds	MMa	Brown to rusty brown weathering silt and sand striped carbonaceous mudstone
					Dp2s/ Dp2c	2	MD	MD	Diamictite consisting of chert pebble conglomerate, sandstriped mudstone and mudstone clasts in a mudstone matrix	MCg/ MG	Grey weathering chert pebble conglomerate(MCg) and chert clast grits(MG)
							MCg/ MG	MCg/ MG	Chert pebble conglomerate(MCg) and chert clast grits(MG)		
				Middle Emsian →	Dp2p	1	MMa	MMa	Black carbonaceous mudstone with light grey sand and silt interbeds	MMa	Brown to rusty weathering silt and sand striped carbonaceous mudstone

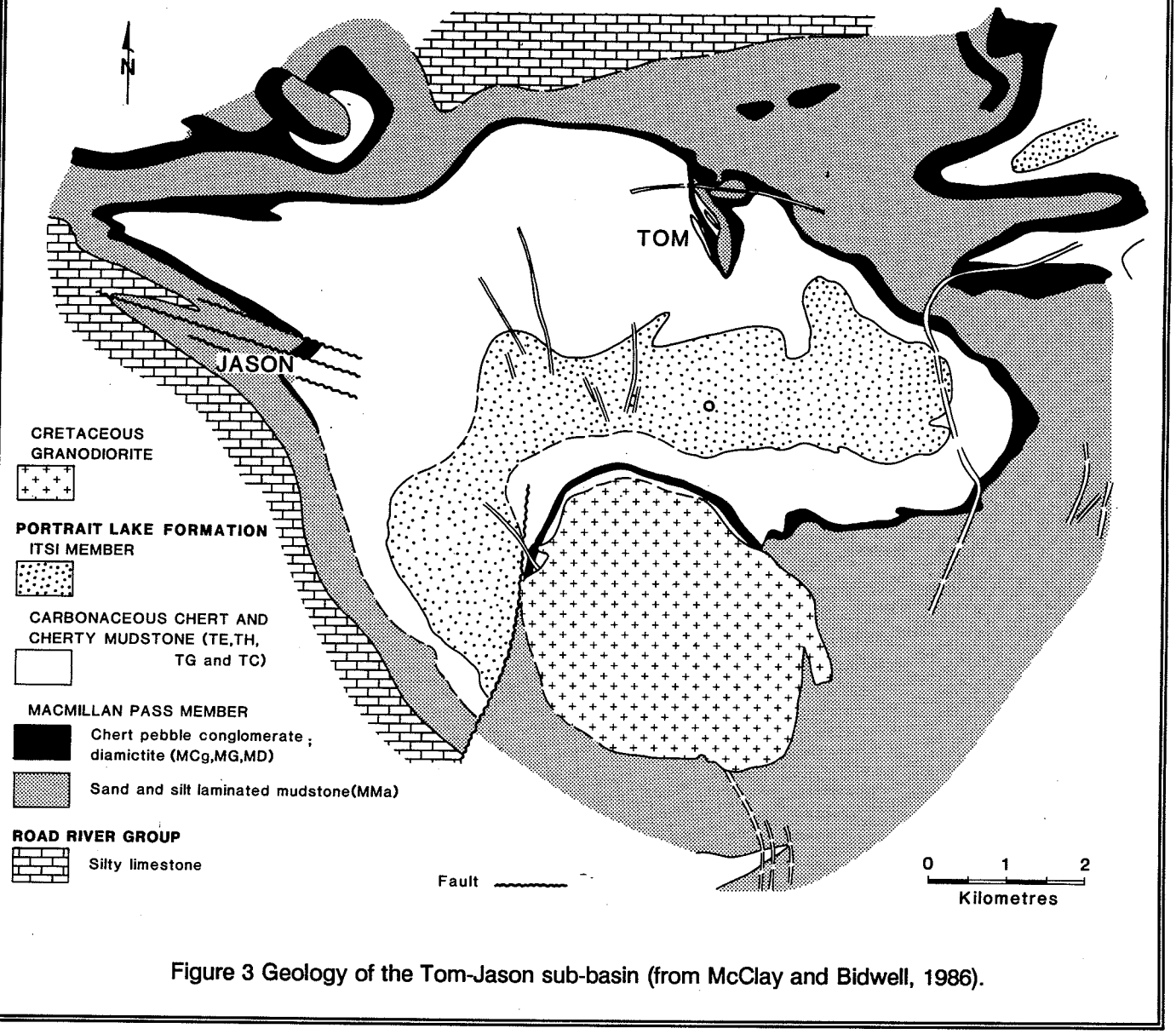

Figure 3 Geology of the Tom-Jason sub-basin (from McClay and Bidwell, 1986).

interpretation is complicated by multiple chert pebble conglomerates and diamictites in the section above the ore (Turner, 1986). Mineralization has been traced in a "feeder zone" at the Jason deposit down to the upper contact of Road River Group (Turner, 1986).

At Boundary Creek no bedded mineralization has been encountered. Clastic rocks of the Macmillan Pass Member, however, have been hydrothermally altered, and extensively replaced and veined by sulphides, ferroan carbonate and quartz. The hydrothermal alteration extends down to the upper portions of the Road River Group (Turner and Rhodes, 1989).

In general terms there appears to be a spatial zonation from Boundary Creek to Tom deposit in deposit characteristics. They are:

(1) diminishing syndepositional tectonism from major

disturbances at the Boundary Creek deposit with associated volcanism, less intense tectonism with nearby volcanic rocks at Jason, and moderate tectonic activity with no associated volcanic rocks at the Tom deposit;

2) progressively younger (higher stratigraphic levels) mineralization from the Boundary Creek to Tom deposit;

(3) progressively less replacement and/or poorly bedded mineralization from the Boundary Creek to Tom deposit.

The implications of the above are that the Tom depositional environment is probably more quiescent permitting greater development of extensive "sheets" of bedded barite and sulphides. The converse of this is that there is probably less replacement and early epigenetic mineralization.

PROPERTY GEOLOGY

Introduction

The Tom deposit occurs on the northern margin of a small sub-basin within Earn Group rocks (Fig. 3). This sub-basin is delineated by the outcrop pattern of chert-pebble conglomerates (MCg) of the Macmillan Pass Member and an increase in the thickness of mudstone and chert (Tom Sequence) which overlie conglomerate units and mineralized zones. The dominant structure is a north-northwest-trending broad syncline with north-south re-entrants caused by faulting and fold interference patterns (Fig. 3). The basin margins are characterized by tight folding and thrust faulting.

Stratigraphy

The rocks exposed on the Tom property consist entirely of Middle Devonian to Mississippian sedimentary rocks of the Portrait Lake Formation (Table 1). The Portrait Lake Formation has been divided into a lower clastic package referred to as the Macmillan Pass Member, an overlying unnamed carbonaceous mudstone and chert sequence (referred to as the Tom Sequence), and the Mississippian Itsi Member. Drilling and mapping by Cominco Limited has provided a detailed stratigraphic break down of these rocks. Table 1 presents the stratigraphic column (with relevant field descriptions) as it is now recognized at the Tom property. The terminology used in this report is cross-referenced with the earlier terminology of Carne (1979) and the regional nomenclature of Abbott et al. (this guidebook).

In general, sedimentary and diagenetic textures, structures and minerals are better preserved in core than in surface exposures. This is particularly true for fine grained and delicately textured mudstones of the Tom Sequence. Consequently whereas the units of the Macmillan Pass Member logged in core and mapped at the surface are the same, detailed textures and finer subdivisions have been recognized in core than in surface exposures of the Tom Sequence. A comparison of the stratigraphy observed in surface exposures and fresh drill core of the Tom property is given in Table 1.

PORTRAIT LAKE FORMATION

The local stratigraphy of the Tom deposit presented in this paper is taken largely from Carne (1979) with modification from recent surface mapping and logging of diamond drill core by the Cominco Limited geologists and the authors. Carne's (1979) terminology, however, has been replaced because of the recognition of new units and the subdivision of others. The major change in stratigraphy is the recognition of diamictitic units stratigraphically below and above the deposit, and the subdivision of Carne's (1979) Unit 3b, the Tom Sequence, into four units. In earlier studies, footwall diamictites have been included with the more regional chert pebble conglomerate (Unit 2 of Carne, 1979, and muDcg of Abbott, 1982) although the high mud content, syn-emplacement deformation of mudstone clasts and its restriction to the Tom deposit area supports a local derivation.

Macmillan Pass Member

Regionally, the Macmillan Pass Member consists dominantly of sand and silt laminated mudstones and fine siltstone (MMa) of turbidite origin. The rocks are recessive brown weathering and dark grey on fresh surfaces. The silt and sand laminae range in thickness from 2 mm to 10 cm and are separated by 1 to 10 cm of mudstone. Where delicate laminae of silt or fine sand alternate rhythmically and are evenly spaced, the rock has been referred to as a "pin-striped" argillite (Abbott, 1982). Inter-bedded chert sandstone, chert grit and chert pebble conglomerate occur locally (McClay and

Plate 1. Photographs of clastic sedimentary rocks from the Macmillan Pass Member and Tom Sequence. (a) Sand-laminated dark grey mudstone from unit MMa showing cross-laminations. (b) Chert- and mud-clast breccias with a mudstone matrix. Mudclasts are flattened parallel to bedding planes and the matrix is infilled with pyrite (white specks) and ferroan carbonate. Sample PH1-05 (44.4 m). (c) Diamictite (DM) consisting of flattened mud-clasts suspended in a mudstone matrix. Sample TS70-12. (d) Diamictite from the Tom Sequence consisting of flattened mudstone and chert clasts suspended in a black mudstone matrix. Sample T88-1-47.

Bidwell, 1986).

Chert Pebble Conglomerate (Mcg), Chert Grit (MG) and Silt and Sand Laminated Mudstone (MMa)

Chert pebble conglomerate (MCg) and chert grits (MG) typically form units of variable thickness within the silt and sand striped mudstone (MMa), enabling subdivision of unit MMa into a lower (MMa1) and upper (MMa2) unit. Although the chert pebble conglomerate is fairly continuous in the Macmillan Pass area, there are local areas where it does not occur. In these areas, it is impossible to subdivide unit MMa. Because the lithologies are essentially identical, there are problems defining pre- and post-conglomerate silt and sand laminated mudstones, particularly instructurally complex areas.

Unit MMa consists of 50 to 300 m of recessive brown-weathering dark grey, sand and silt laminated mudstone and siltstone (McClay and Bidwell, 1986). Sand laminae range up to a few cm in thickness and are separated by 1 to 10 cm of mudstone. Local beds of chert grit, chert sandstone and chert pebble conglomerate occur within this unit (McClay and Bidwell,1986). Based on limited fossil collections, this unit has been shown to range in age from late Middle Devonian to early Upper Devonian (Abbott 1982; Gordey et al., 1982).

The chert pebble conglomerate (MCg) and chert grit (MG) units consist of 0.3 to 10 m beds with total thicknesses ranging up to 200 m. The MCg units consists commonly of coarse and fine grained conglomerates interbedded with lesser contents of chert grit and chert sandstone, and sporadic sand laminated mudstone. The chert pebble conglomerate is composed predominantly of pale to dark grey, well rounded to sub-rounded chert clasts which are typically well sorted. Throughout most of the unit, it is clast supported except near the base and top where mud-stone clasts become more abundant and chertclasts are commonly supported by a mudstone matrix. Flattened and contorted mudstone clasts indicate that the mudstone clasts consisted of soft mud when deposited.

The silt and sand laminated mudstones (MMa) above and below the chert pebble conglomerate vary greatly in thickness as does the conglomerate sequence (MCg). Below the conglomerates, unit MMa1 ranges in thickness between 50 and 300 m. Above the conglomerate, the silt and sand laminated mudstones (MMa2) range up to 200 m in thickness. Locally, the silt and sand laminated mudstones host primitive plant fossils that are late Middle Devonian to Early Devonian in age (Abbott, 1982; Gordey et al., 1982).

Diamictite (MD)

Unit MD consists of 0.3 to 10 m diamictite beds which form lenses several 100 m long and up to 140 m thick. Diamictites occur interbedded with minor pebbly mudstone, chert pebble conglomerate and sand laminated mudstone. The breccia clasts are typically mud-supported, poorlysorted, angular to subrounded and compositionally variable (Plate 1b, 1c and 1d). Dominant clast lithologies include mudstone, chert, conglomerate and sandstone. Mudstone clasts also display soft sediment compactional textures (Plate 1d). Interbedded sand laminated mudstones are disrupted due to slumping. Although thicknesses are not well constrained, they generally increase away from the synsedimentary fault in the Tom sub-basin.

Several lines of evidence indicate that this unit was derived locally. These are:

1) the local distribution of diamictites, typically in areas of synsedimentary faulting;

2) the predominance of angular, commonly very coarse and poorly sorted mud clasts;

3) the high mud content of the matrix.

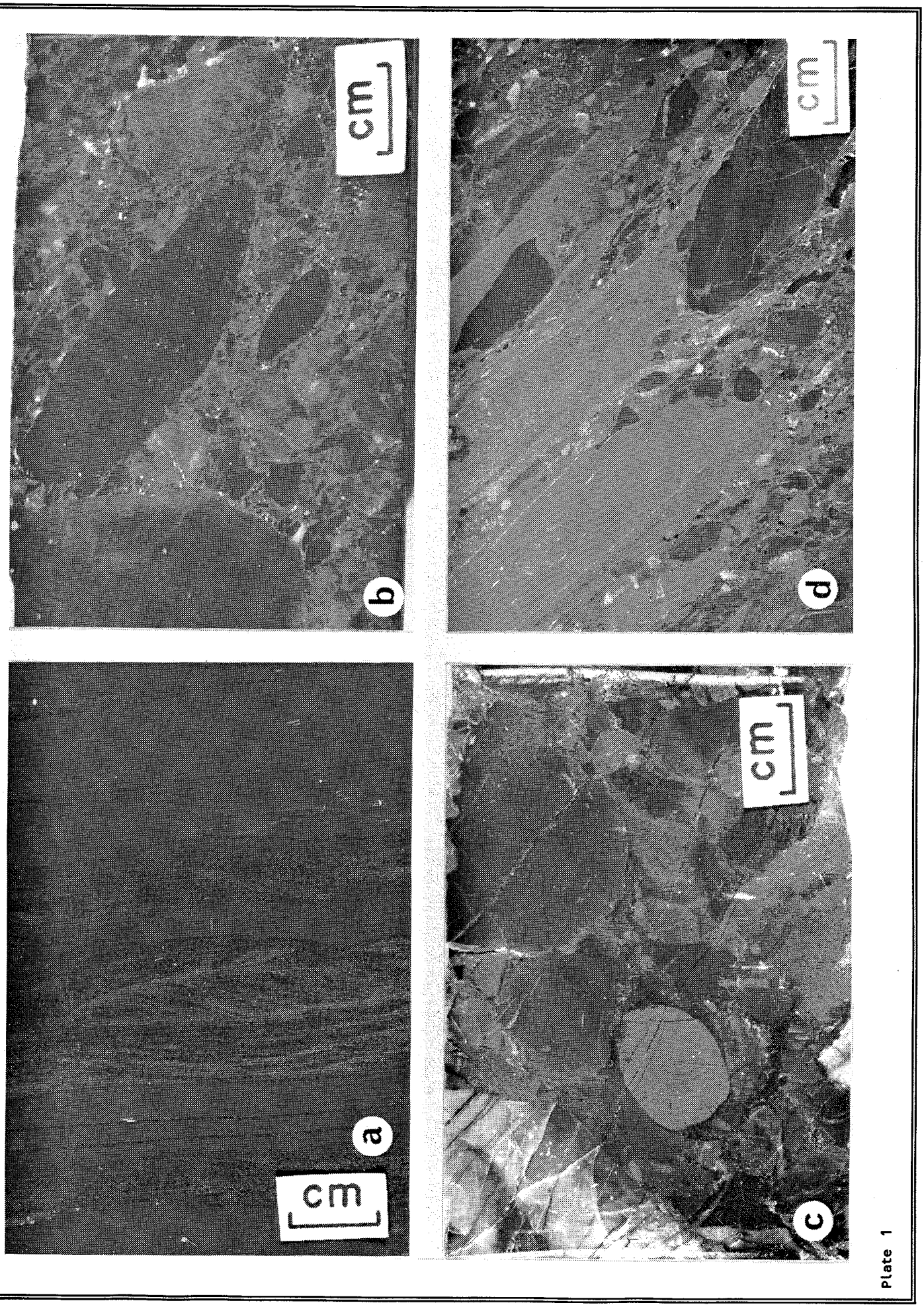

Plate 1

4) the presence of diamictites flanking either side of the Tom conglomerate high and its interpreted growth fault margins.

A decrease in thickness towards the Tom synsedimentary fault, the slumping of interbedded mudstone and the absence of this unit in the interpreted upthrown block support a fault-scarp breccia origin for this unit. Furthermore, the presence of chert pebble conglomerate clasts demonstrates that this unit consists in part of resedimented conglomerate and post-dates chert pebble conglomerates of the Macmillan Pass Member.

Tom Sequence (Carbonaceous Chert Mudstone and Radiolarian Chert)

Throughout the Macmillan Fold Belt, a succession of blue grey and platy weathering, thinly laminated black carbonaceous and very siliceous mudstones occur stratigraphically between rocks of the Macmillan Pass Member and Itsi Member. This succession ranges in thickness from 200 m to 1500 m over a relatively short lateral distance of 1 to 2 km. Recent mapping and drilling of these rocks by Cominco Limited has defined a more detailed stratigraphy in the area of the Tom deposit (Fig. 4 and 5).

For this report, these rocks are informally referred to as the Tom Sequence. Within the area of the Tom deposit, the Tom Sequence shows very abrupt facies and thickness changes about a paleobathymetric high (i.e., conglomerate high) which occurs at the nose of the Tom anticline. This high is flanked by two separate sub-basins or troughs corresponding to the West Zone and Southeast Zone. Although broadly defined stratigraphic units can be traced throughout the area and within each sub-basin, there are substantial differences within each unit between the West Zone and Southeast Zone (Fig. 5). For example, a number of lithologies are found in the West Zone "sub-basin" but are absent in the Southeast Zone "sub-basin".

Four major stratigraphic units are described in the following section with separate descriptions for lithologies that are part of each unit but are not continuous between the West Zone and Southeast Zone. These descriptions are based on core from seven holes drilled about the Tom anticline and collared high in the Tom Sequence (Fig. 4). The stratigraphic relationships are shown in figure 5.

Unit TC

This unit includes the host rocks for the Tom deposit. In general,these rocks are very black, highly carbonaceous, relatively massive and competent. They lack the thinner more fissile bedding textures of overlying units and are not speckled with silt size radiolaria which are common in higher units. The rock is typically enriched in fine grained pyrite (3-8 %) which occurs evenly disseminated imparting a distinctive sparkle and less commonly as pyrite laminae and concretions.

The lower part of this unit has been subdivided into a more siliceous or cherty subunit (TCh). The more siliceous character of this subunit imparts a smooth glossy appearance to the core when wet. It is this basal part of TC that is the immediate host for the Tom deposit.

Except for subunit TCh, several subunits that are not continuous between the West Zone (DDH's T88-1, T88-4 and T88-7) and the Southeast Zone (DDH's T89-5, T88-3 and T88-6) (refer to Fig. 5 for DDH locations) have been described. Except for subunit TCh, there is virtually no similarity between West Zone and Southeast Zone rocks despite the fact they are approximately temporally equivalent and are separated by a strike length of only 500 m. The various laterally discontinuous lithofacies are described below.

TChbp1: Symmetrically distributed above and below stratiform sulphide/barite mineralization of the West Zone are black carbonaceous cherty mudstones and chert that are delicately laminated with fine grained pyrite (Plate 2b, 2c) and white barite (Plate 2a). In the immediate vicinity of the high barite ore facies, these rocks are strongly laminated with white barite and fine grained pyrite and sphalerite, and are transitional into the Black and Grey Facies described below under mineralization.

The contact between the ore zones and this unit is gradational and characterized by an upward increase in clay minerals at the expense of quartz and a decrease in the density of sphalerite, pyrite and barite laminae. It is noteworthy that this mudstone (TChbp1) contains 2 to 5 % barite, even in samples that are not obviously laminated with barite (Fig. 10).

Pyrite in TChpb1 rocks underlying the West

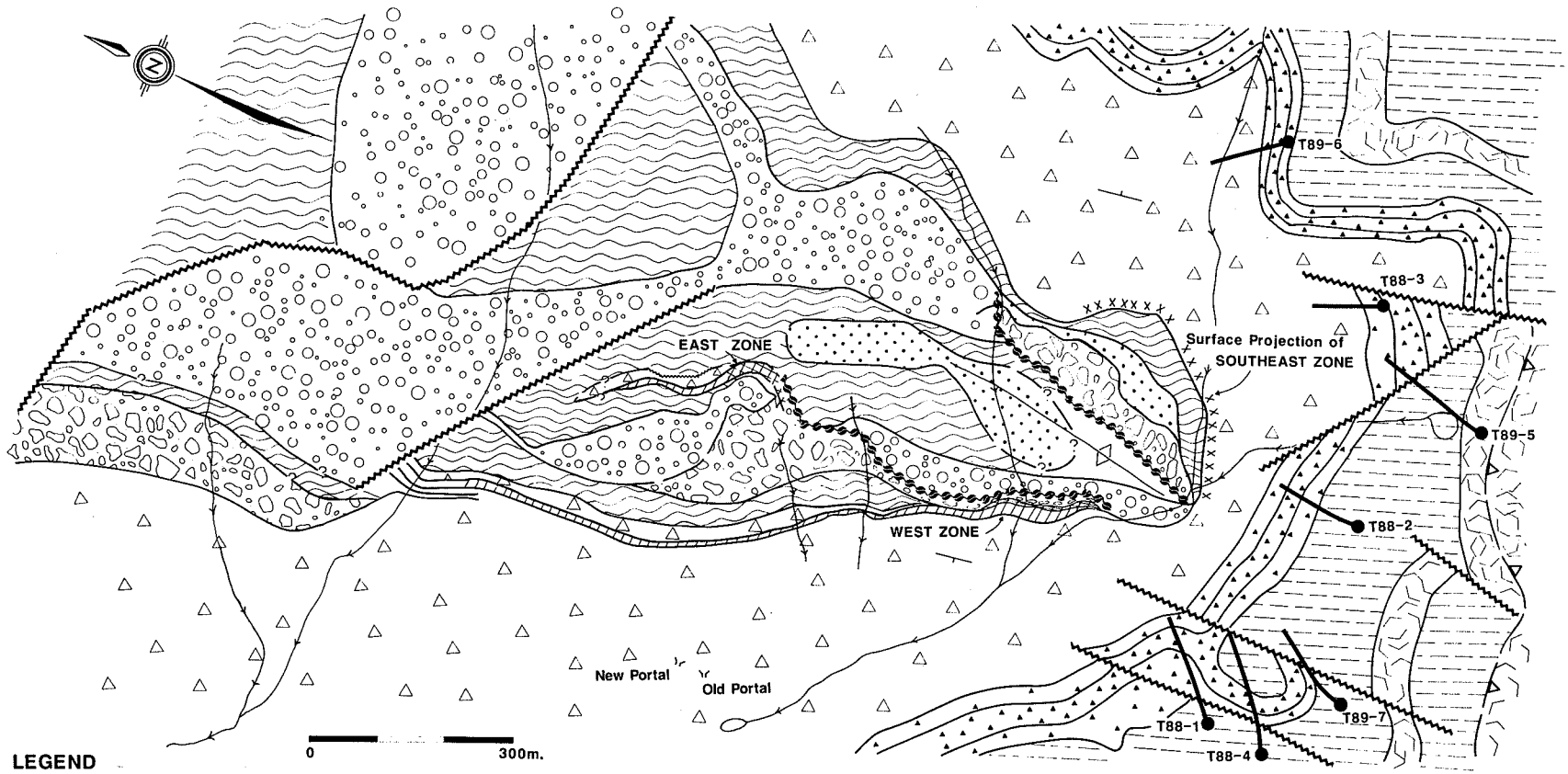

LEGEND

Portrait Lake Fm. P

Tom Sequence (T) Black carbonaceous package

- TU Unit – Upper Cherts
- TE Unit Laminated Cherty Mudstone with Barite Nodules
  - 2 Upper (above Tu)
  - 1 Lower
- TH Unit – Carbonaceous Radiolarian Cherts
  - 3 Upper Cherty Black Mudstone
  - 2 Central Blocky Black Chert
  - 1 Lower Cherty Black Mudstone
- TG/C Units – TG Radiolarian Speckled Cherty Mudstone
  - TC Very Carbonaceous Cherty Mudstone
- TB Laminated Barite / Sulphide rock
- TS Vent Facies – Sulphide / Siderite rock & Sulphide / Siderite stockwork

Macmillan Pass Member (M) Coarse clastic package

- MD Diamictite
- MCg Chert Pebble Conglomerate
- MMa 1,2 Mudstone, arenaceous, striped with silt to thin sand laminae
- MMa 3,4,5, Mudstone, arenaceous, striped with medium to coarse sand bands and grit beds

- geological contact
- growth fault
- fault
- anticline
- bedding
- drill hole location
- creek
- portal

Figure 4 Geology of the Tom anticline and immediate area about the ore zones.

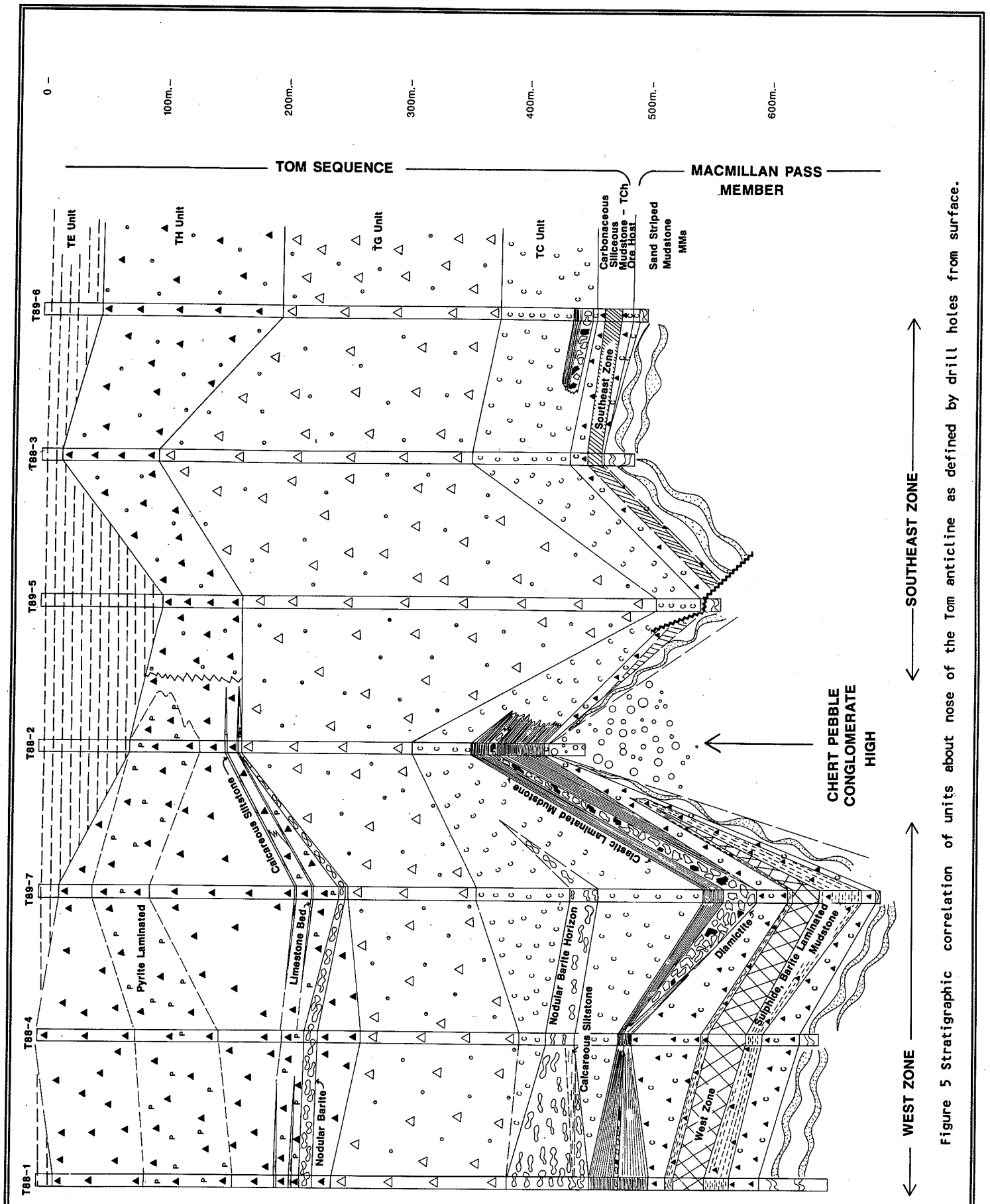

Figure 5 Stratigraphic correlation of units about nose of the Tom anticline as defined by drill holes from surface.

Zone forms coarser grained bands and blebs. The coarser grained pyrite commonly displays diffuse contacts with the enclosing rocks and in some areas it appears to cross-cut the mudstone. This pyrite is therefore of secondary diagenetic or hydrothermal origin. The fine pyrite laminae, however, is probably of sedimentary origin and formed by the influx of hydrothermal iron during the early stages of hydrothermal activity.

The mineralized interval and enclosing TChbp1 rocks have a true maximum thickness of about 100 m which decreases southward reaching zero on the northern flank of the conglomerate high. Isopachs of the cherty carbonaceous mudstone (TCh) and mineralized interval (Fig. 6 and 8, respectively) suggest a bathymetric low (i.e., a basin or trough) flanking the conglomerate high.

TChp: A much thinner (1-5 m) unit of pyrite laminated cherty mudstone (TChp1) sandwiches and/or overlies the Southeast Zone. These rocks are characterized by a relatively marked increase in the density of delicate pyrite laminae immediately adjacent to the Southeast Zone. Unlike mudstones flanking the West Zone, the Ba content is generally low, ranging from (<0.5 %) adjacent to the conglomerate high to 2-3 % in the more distal parts of Southeast Zone.

TCc/TCd: The sand and silt striped mudstone (TCc) and diamictite (TCd) occur in the hanging wall of the West Zone and to a lesser extent the Southeast Zone; the latter is remarkably similar to diamictitic units (MD) of the Macmillan Pass Member. These units are typically less than a meter in thickness, and span a stratigraphic interval of 5 to 30 m. The diamictite consists of angular to subrounded chert and deformed mudstone clasts supported by a mudstone matrix. The presence of post-ore sedimentary breccias indicates movement on the growth faults and the shedding of clastics from the conglomerate high well after the major episode of hydrothermal activity.

TCnbp: This lithology consists of mudstones with variably sized barite nodules aligned along bedding planes. It occurs as distinctive and correlatable intervals which form part of the hanging wall stratigraphy of the Tom West Zone and are absent above the Southeast Zone.

The nodules (Plate 2d) are composed of white barite which is variably replaced by Ba-feldspars, principally celsian and hyalophane. Interbedded with the barite is delicately laminated microframboidal pyrite. The alignment of barite along bedding planes suggests that the nodules represent boudins formed by soft sediment deformation of hydrothermal barite beds.

The replacement of barite by Ba-feldspars has been observed for barite hosted in carbonaceous sediments. During diagenesis, bacterial sulphate reduction decreases the sulphate activity below the solubility of barite, barite dissolves and barium released to pore waters precipitates as a feldspar under what were probably elevated geothermal gradients. The amount of barite dissolved is limited by the content of organic matter which serves as an essential nutrient source for sulphate-reducing bacteria.

Unit TG

Unit TG consists of silvery grey weathering, pale to dark grey, moderately siliceous and carbonaceous mudstone and radiolarian chert with variable amounts of pyrite laminae. Pyrite also occurs disseminated throughout and forms concretions. This unit is generally finely bedded (0.5 to 4 cm) and breaks down into thin fissile felsenmeer. The most distinctive feature of this lithology is the speckling of the rock with 5 to 20% white silt size radiolaria. These radiolaria tend to pluck out of the core and weather out of surface exposures, resulting in a pinpoint porosity and gritty texture.

Bedding plane parallel styolites containing black organic residues left behind by pressure dissolution of silica give the rock a banded appearance in places. Styolites are variably spaced from 0.5 cm to 10 cm. Commonly, a distinctive 1-5 mm grey striping is evident in this rock due to the alternation of radiolarian-rich and radiolarian-poor mudstones. This unit does not change appreciably between the West Zone and Southeast Zone. Subtle variations in texture and composition occur but are not sufficiently distinctive to allow subdivision of this relatively homogeneous unit.

Unit TH

This unit is distinguished by its particularly high silica content. At the surface, this unit has been subdivided into two subunits of light blue grey weathering radiolarian chert (TH3 and TH1) which are separated by black cherty mudstone (TH2). This three-fold division, however, has not been recognized in core.

Plate 2. Photographs of pyritic and baritic black cherty mudstone from the Tom Sequence. (a) Black Facies: interlaminated and thinnly beds of white barite, sphalerite, galena and black chert. Top of the West Zone, transitional into the overlying balck cherts of Unit TC. Represents the wanning stages of the Tom hydrothermal system. Sample T88-1-69. (b) Black carbonaceous cherty mudstone delicately laminated and thinnly bedded with framboidal pyrite. The pyrite in the thicker beds is coarser grained due to recystallization. Sample T88-1-45. (c) Black carbonaceous chert delicately laminated with microframboidal pyrite. The high pyrite content and sedimentary textures indicate formation in the water column during the wanning stages of the hydrothermal system. Sample T88-1-07. (d) White streaks of barite and Ba-feldspar containing pyrite oriented parallel to bedding planes. Sample T88-1-38.

In the core, unit TH consists of carbonaceous, cherty mudstone commonly with delicate styolite enhanced laminae. The styolites are marked by residues of black amorphous carbon. Over the West Zone, this unit thickens and several lithofacies are defined. These include the following: THnbp - one or more intervals of wispy nodular barite and laminated pyrite; THm - 0.5 to 1.0 m thick, fetid limestone beds variably silicified. Conodonts extracted from one limestone bed has been dated as Middle Frasnian, Late Devonian (M.Orchard, per. comm.); THa - Laminated calcareous siltstone overlying the limestone at the base of unit TH; and THp1 which consists of 10 to 30 cm thick intervals of delicately laminated carbonaceous mudstone above the West Zone. Over the Southeast Zone, this unit is thinner, slightly less siliceous but more speckled with radiolarian.

Unit TE

In core, this unit is very distinctive and consists of alternating intervals of siliceous carbonaceous mudstone with nodular barite and pyrite, and wavy laminated pyritic siliceous mudstone. It is the upper-most stratigraphy drilled thus far in the Tom area and only the lower-most intervals of this unit have been cored. From surface mapping, this unit has been subdivided into two subunits (TE1 and TE2) of dark grey to rusty weathering, thin bedded, brittle, black, pyritic siltite with abundant barite nodules separated by subunit (TU) of light bluish grey weathering, black cherty mudstone with thin interbeds of chert and fine laminae of siltstone and sandstone.

Itsi Member

The Itsi Member is an informal name applied by Abbott (1983) to a sequence of clastic rocks which overlies siliceous mudstone and siltite (Unit TE).

The basal part of the Itsi Member consists of approximately 40 m of rusty weathering dark grey sand-laminated micaceous siltstone which unconformably overlies the Tom Sequence (McClay and Bidwell, 1986).

This basal unit is overlain by thick bedded buff grey weathering plane-laminated, cross-laminated and ripple drift-laminated sandstone. The thickness of the sandstone sequence is at least 150 m thick (Abbott 1982).

This Member is distinguished from other rocks of the Portrait Lake Formation by its distinctive rusty grey weathering, the absence of chert and the high mica content of the basal unit.

Palaeobathymetry and Facies Variations

All of the known mineralized zones occur about the nose of a tightly folded south plunging anticline (the Tom anticline). Figure 4 is a surface map of this whereas figure 5 presents the stratigraphic associations and correlations observed in Cominco Ltd. holes drilled about the flanks of the Tom anticline. Both the mapping and drilling demonstrate rapid lateral and vertical facies changes in the Macmillan Pass Member and Tom Sequence.

Three discrete areas of chert pebble conglomerate distributed about the nose of the Tom anticline were defined during mapping (Fig. 4). A central area of chert pebble conglomerate extends for about 500 meters from the nose of the anticline along the southern limb of the anticline. This conglomerate is separated on both the north and south limbs from the other masses of chert pebble conglomerate by two discrete prism-like accumulations of sedimentary rocks. These prisms consist at their base of massive beds of

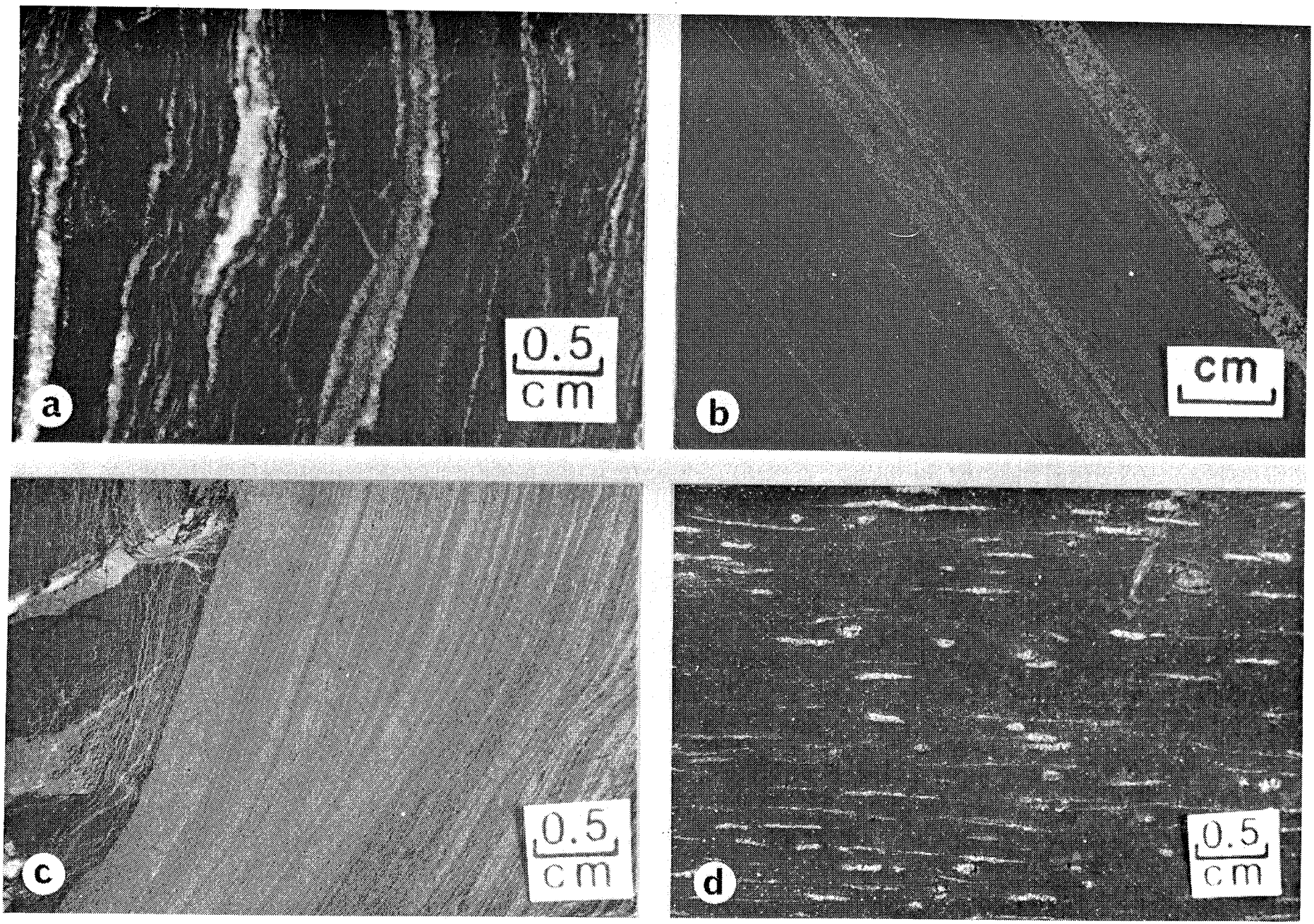

Plate 2

diamictite giving way upward to interbedded diamictites, carbonaceous grits and sand-striped mudstones, and to progressively finer grained sand- and silt-striped mudstones. The prisms of sediments on the east limb of the fold consist of coarser grained diamictites, grits and sandstones and thicker beds than similar clastic rocks on the west limb. The two sedimentary prisms, which underlie the Southeast Zone and West Zone, indicate trough-like areas or basins of subsidence on either side of a paleobathymetric high of chert pebble conglomerate.

Figure 5 shows the stratigraphic variations about the fold nose as indicated by drilling. This figure reveals a stratigraphic column associated with the West Zone on the west limb of the anticline that is significantly different from the stratigraphic column associated with the Southeast Zone on the east limb. Abrupt thinning and pinching out of the footwall strata of the West zone and of the ore itself against a chert pebble conglomerate "high" are evident. A similar pinch out of footwall strata is evident in the Southeast Zone. Isopach maps of the ore (TB and TS, Fig. 6), the footwall sand-striped mudstone unit (MMa, Fig. 7), and the footwall siliceous carbonaceous mudstones (TCh, Fig. 8) projected onto a longitudinal section constructed about the fold nose show a clear pinching out of these strata against a chert pebble conglomerate high. They also show a corresponding thickening into what appear to be sub-basins peripheral to the high. These basins coincide with the thick prisms of diamictite, sand-striped mudstones and cherty mudstones mapped on surface. Drill hole intercepts of the mineralized zones with identification numbers projected onto a longitudinal section about the nose of the Tom anitcline are shown in figure 9.

Figure 5 also demonstrates that the Tom paleo-high exerted an important control on sedimentation for several hundred metres above the mineralized zones. The stratigraphic column is appreciably thinned over the conglomerate high. Above the West Zone the strata exhibit considerably more stratigraphic diversity than the more homogeneous mudstones that comprise the hanging wall rocks of the Southeast Zone basin. These facies variations are remarkable considering that the rocks show these changes over a strike length of less than 500 metres.

From the marked sedimentary facies and thickness changes, it is clear that a major syndepositional structure is exposed at the nose of the Tom anticline. The structure appears to be a narrow horst-like feature cored by chert pebble conglomerate and flanked on either side by two lenticular sub-basins. This structure controls the marked facies variations seen over 600 metres of true stratigraphic thickness along the two kilometres of strike length of strata distributed about the nose of the Tom anticline. It has also controlled the venting of metalliferous fluids at the Tom deposit.

Geochemical profiles of Ba, Zn and SiO_2 (Figs. 10, 11 and 12) plotted onto a longitudinal section of the West and Southeast zones show a marked Ba decrease in rock of the Tom Sequence in the Southeast Zone compared to correlative rocks from the West Zone. This indicates that Ba was partly restricted to the West Zone sub-basin, perhaps by a paleobathymetric barrier such as the conglomerate high. Furthermore, intervals of elevated Ba and Zn contents (compared to background shale and chert) throughout the Tom Sequence overlying the mineralized zones indicates that the hydrothermal system continued to vent fluids well after the formation of the Tom deposits. The distribution of SiO_2 (Fig. 12), however, varies stratigraphically, increasing in the radiolarian cherts, but does not display any obvious lateral variations between the Southeast and West Zones. The lack of significant lateral variability of silica may be controlled by sluggish kinetics and high residence times of silica in the water column than by the lack of major hydrothermal silica input. High residence times would allow silica to be dispersed more widely in the basin.

Figure 13 is a schematic diagram portraying stages of development of the conglomerate high and flanking basins at the Tom deposits. The evolutionary stages are:

1) uplift of the chert pebble conglomerate in a horst structure during block faulting;

2) the formation of depositional basins flanking the horst structure;

3) the shedding of unconsolidated chert pebble conglomerate, sand striped mudstone and carbonaceous mudstone off the fault scarps;

4) the formation of clastic prisms of diamictite which terminate against the conglomerate high; and

5) the venting of hydrothermal fluids along bounding faults and/or through highly permeable conglomerates uplifted during block faulting. Indicated on figure 4 are

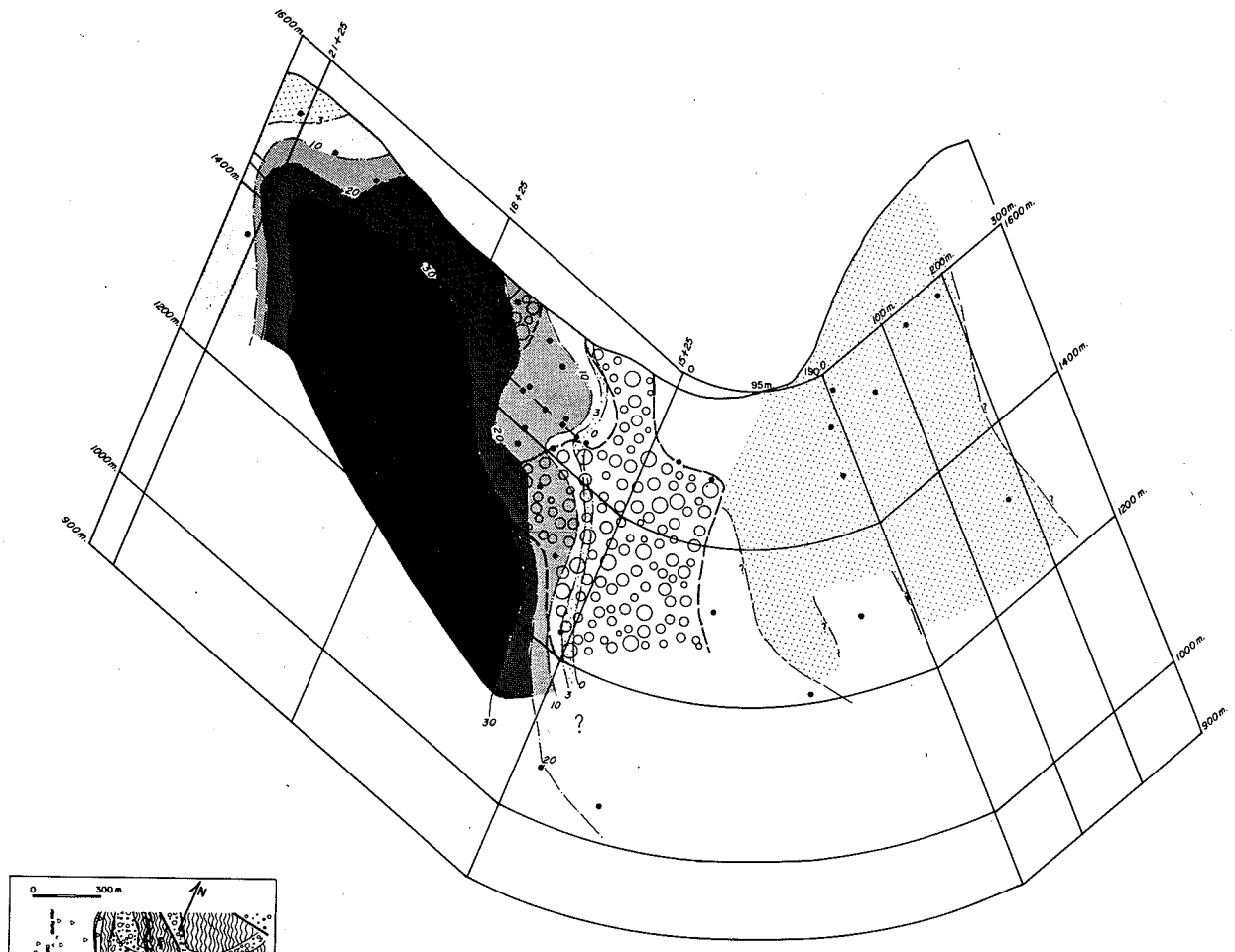

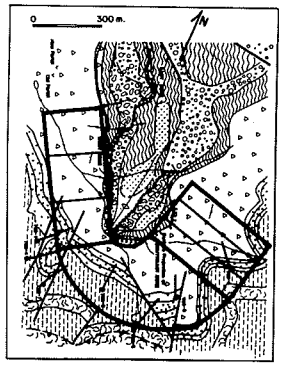

Inset showing location of panels of West Zone – Southeast Zone Horizon projected onto longitudinal section.

LEGEND

- Drill hole intercept of mineralized horizon
- Isopachs of mineralized intersection thickness
- Underground workings
- Chert Pebble Conglomerate high as defined by pinch out of sand striped mudstones (MMa)

- 0–3m.
- 3–10m.
- 10–20m.
- 20–30m.
- >30m.

Figure 6 Isopach of the Tom West and Southeast Zones projected onto a longitudinal section about the nose of the Tom anticline.

the interpreted growth faults that offset the chert pebble conglomerate and truncate the margins the sub-basins.

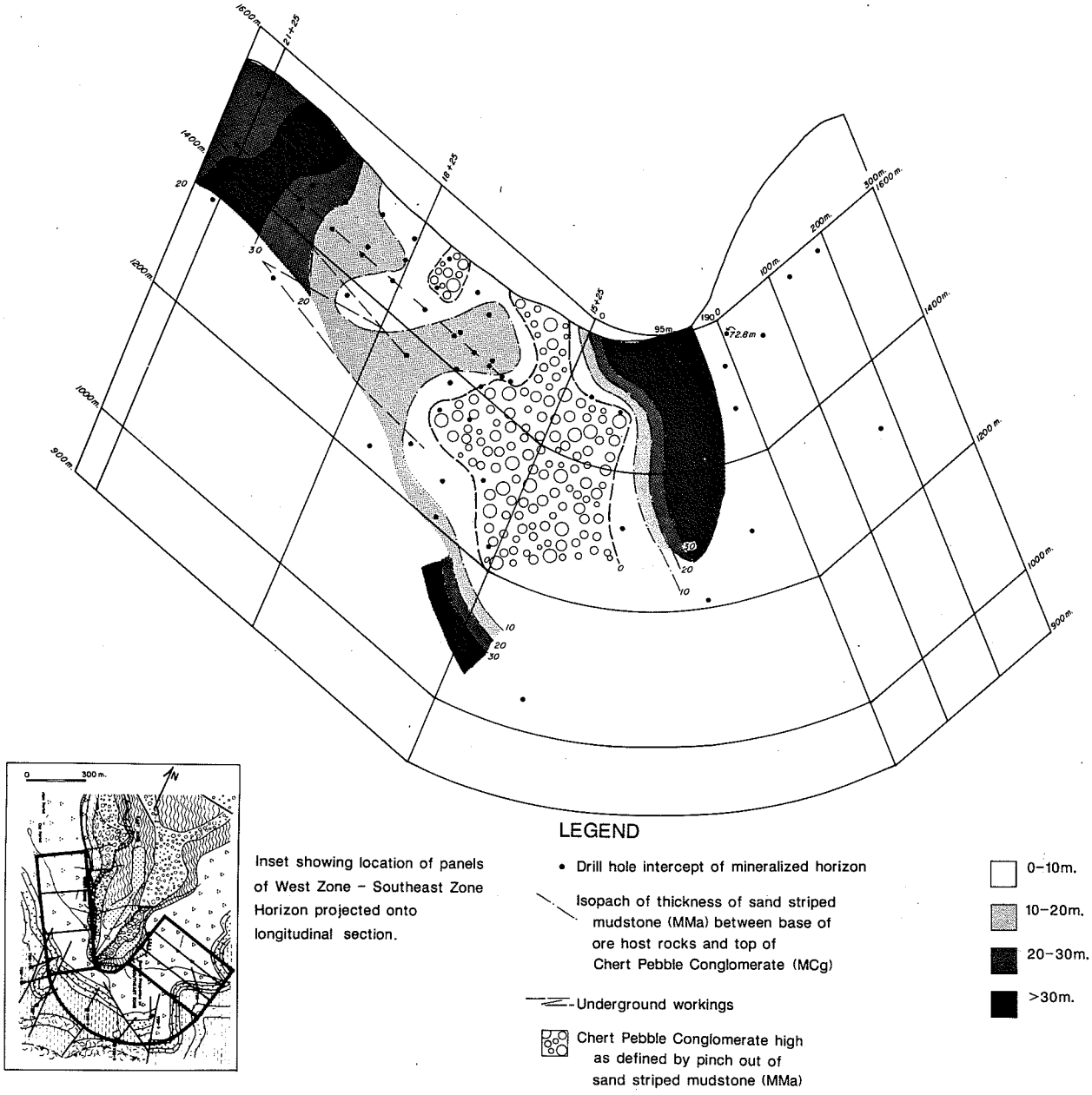

Figure 7 Isopach of the upper sand-striped mudstones (MMa) projected onto a longitudinal section about the nose of the Tom anticline.

Structure

The structure of the Tom area is complex. Detailed mapping and structural analysis (McClay, 1983; unpublished data) has revealed three phases of folding and faulting.

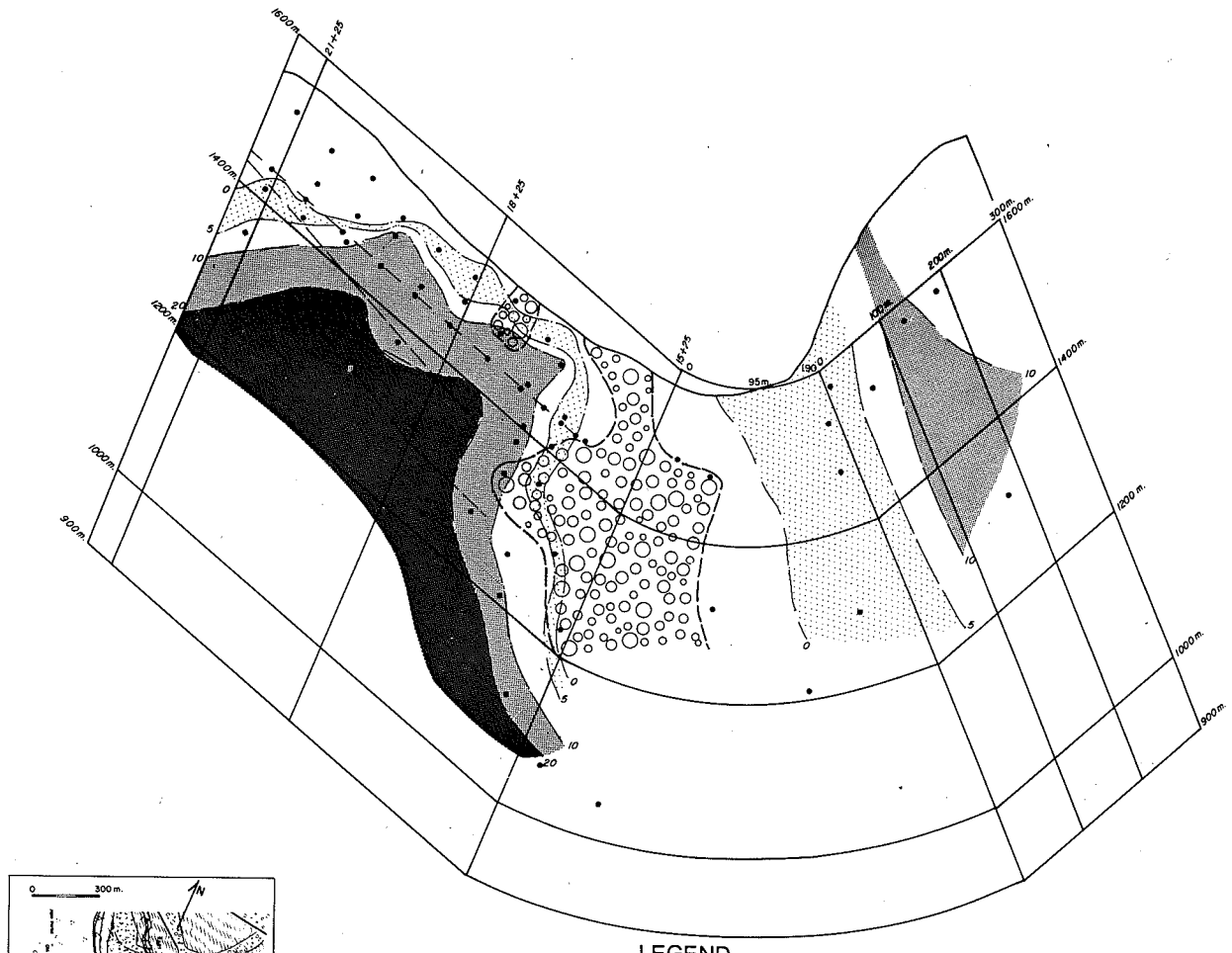

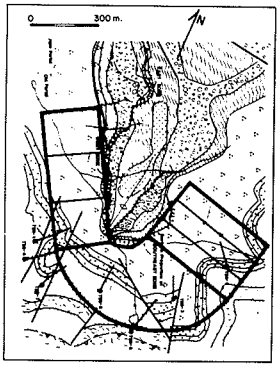

Inset showing location of panels of West Zone – Southeast Zone Horizon projected onto longitudinal section.

LEGEND

- Drill hole intercept of mineralized horizon
- Isopachs of footwall Cherty Carbonaceous Mudstone (TCh) between base of mineralized horizon and top of sand striped mudstone (MMa) or Chert Pebble Conglomerate (MCg)
- Underground workings
- Chert Pebble Conglomerate high as defined by pinch out of sand striped mudstone (MMa)

0 – 5 m.
5 – 10 m.
10 – 20 m.
> 20 m.

Figure 8 Isopach of the footwall siliceous carbonaceous mudstone TCh projected onto longitudinal section about the nose of the Tom anticline.

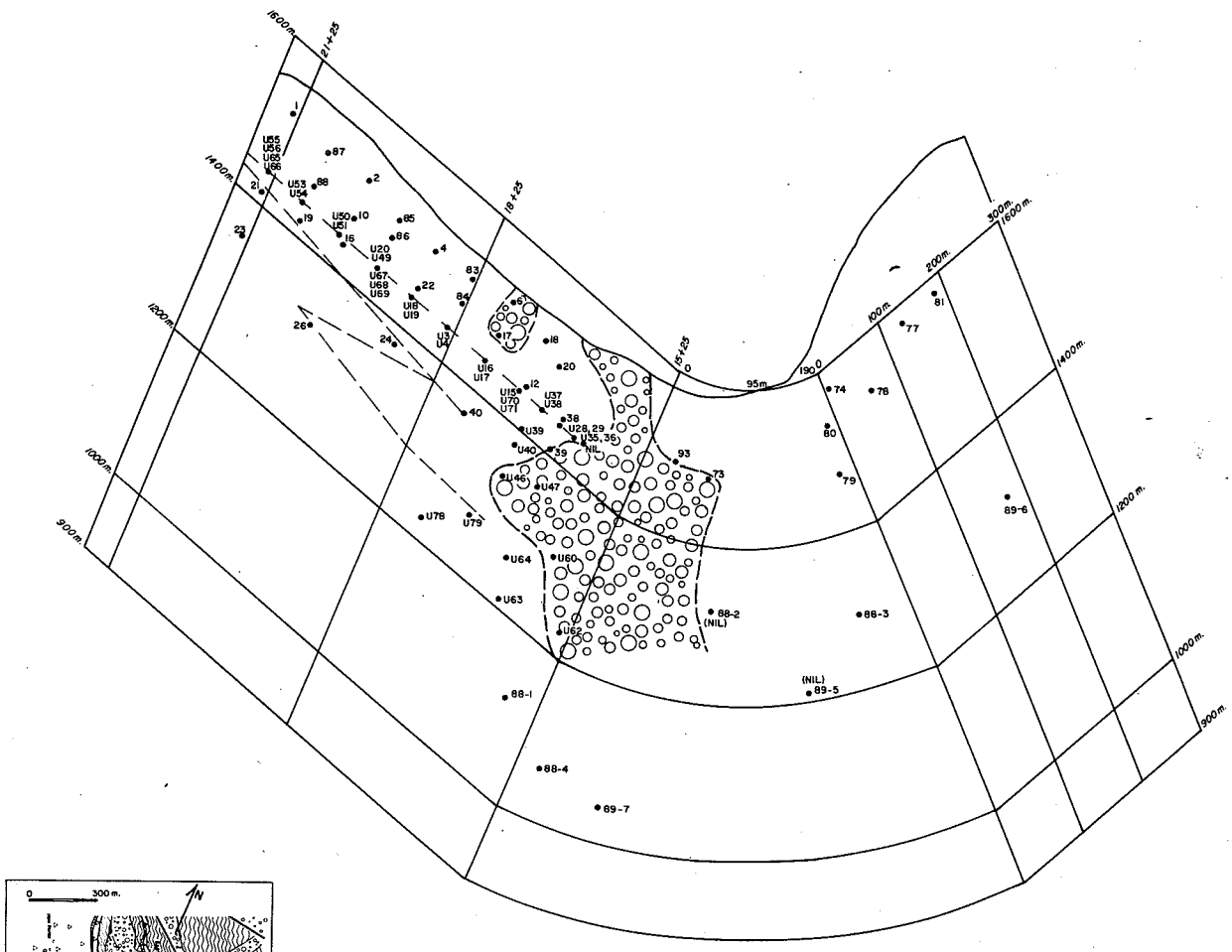

Inset showing location of panels of West Zone – Southeast Zone Horizon projected onto longitudinal section.

LEGEND

- Drill hole intercept of mineralized horizon with identification number
- Underground workings
- Chert Pebble Conglomerate high as defined by pinch out of sand striped mudstone (MMa)

Figure 9 Drill hole intercepts of mineralized horizon with identification number projected onto a longitudinal section about the nose of the Tom anticline.

Phase 1 structures are localized, tight to near isoclinal north-south plunging folds with associated bedding plane thrust faults of which the Tom anticline and associated faults are the most important. The major

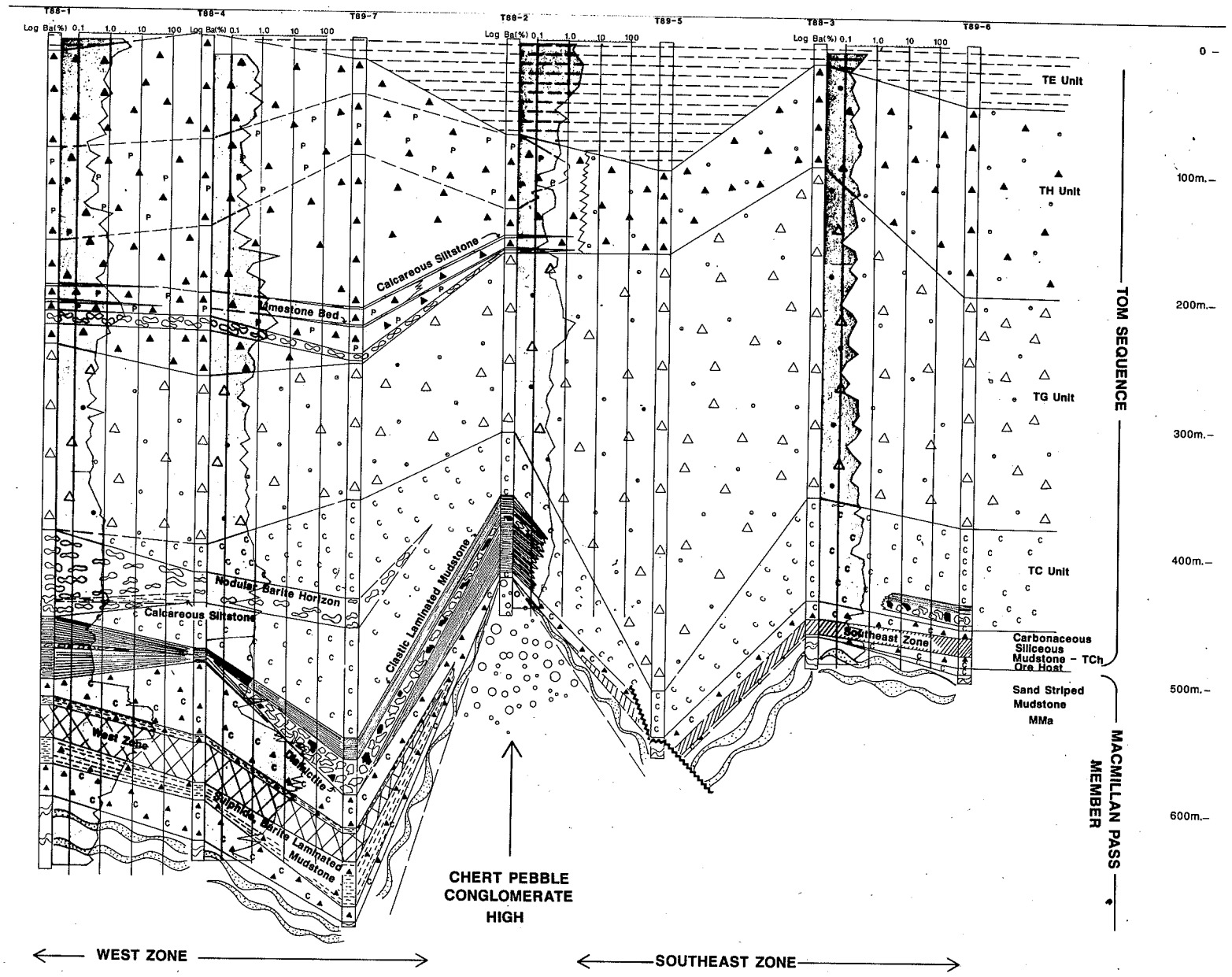

Figure 10 Barium content of drill holes spanning the Tom Sequence plotted on a longitudinal section of the West and Southeast Zones (based on analyses of samples taken every 3 or 4.5 m).

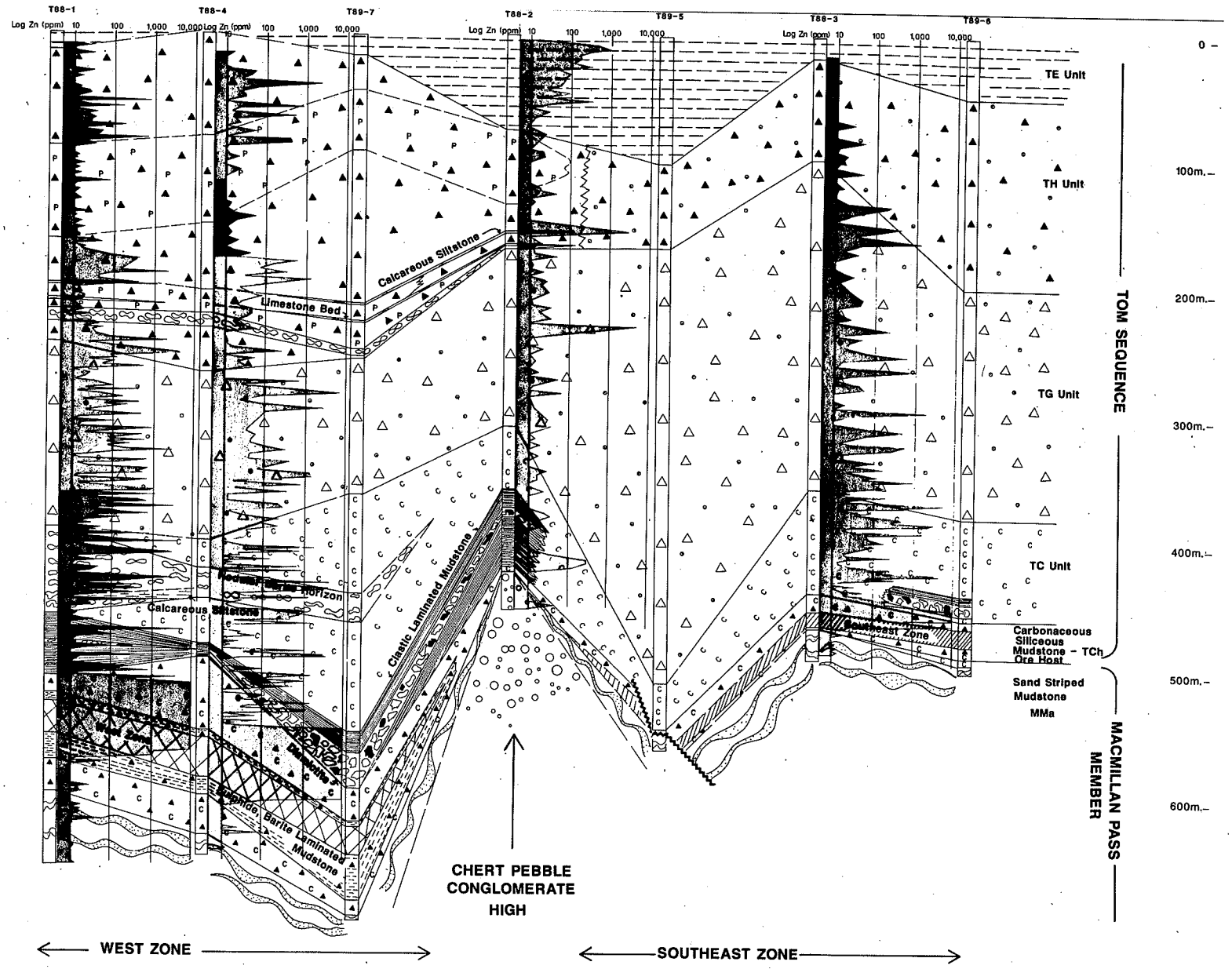

Figure 11 Zinc content of drill holes spanning the Tom Sequence plotted on a longitudinal section of the West and Southeast Zones (based on analyses of samples taken every 3 or 4.5 m).

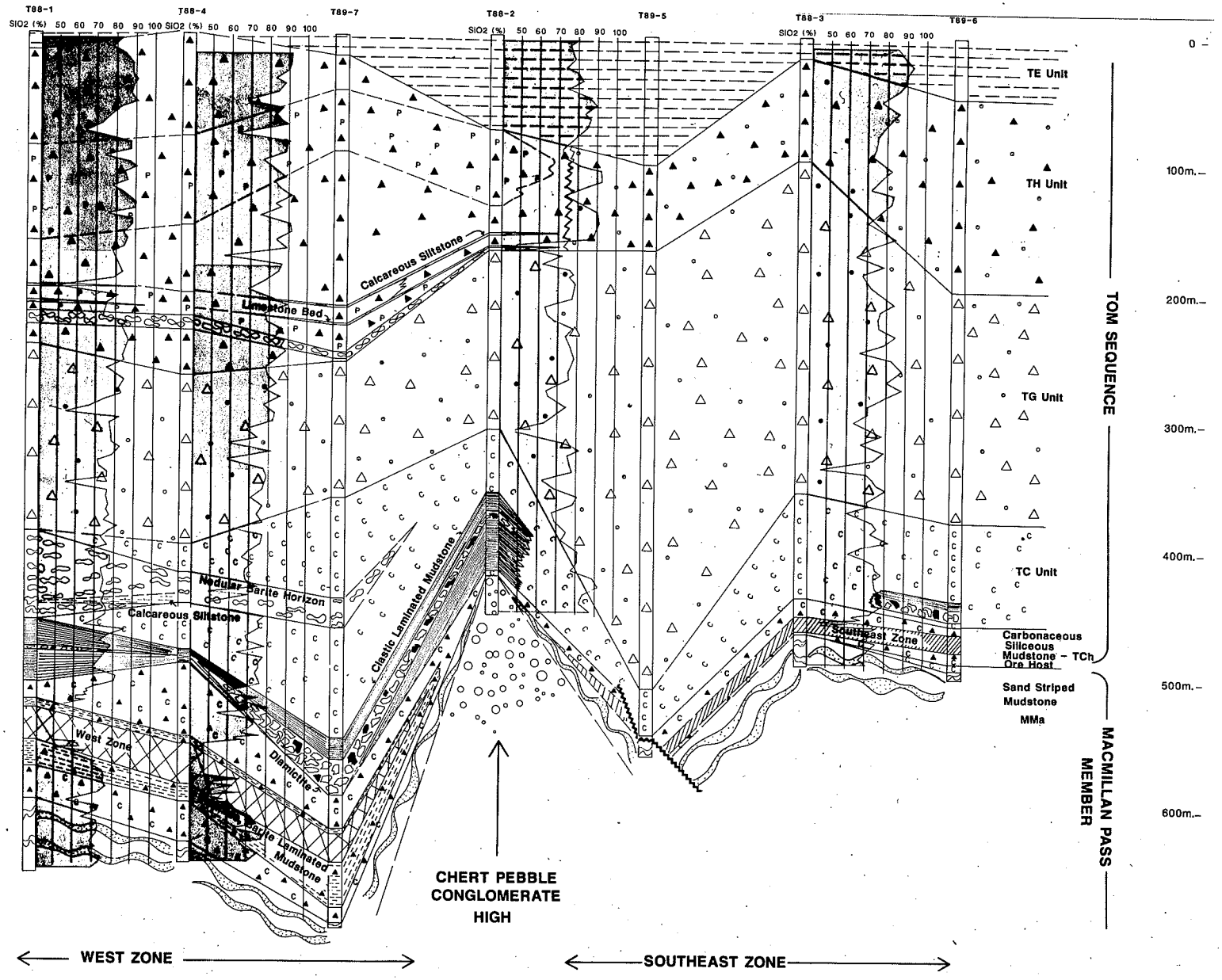

Figure 12 Silica (SiO_2) contents of drill holes spanning the Tom Sequence plotted on a longitudinal section of the West and Southeast Zones (based on samples taken every 3 or 4.5 m).

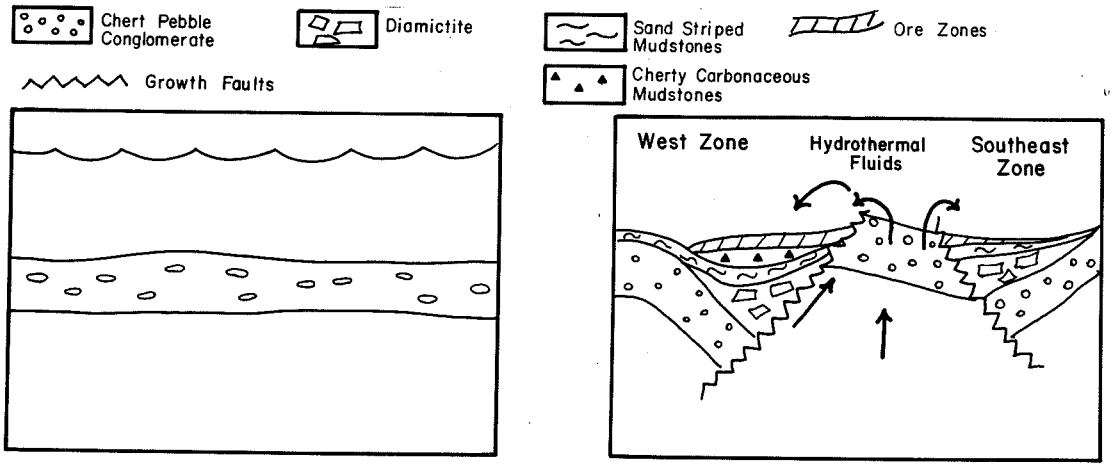

1 Sectional View - Chert Pebble Conglomerate laid down as horizon.

4 Greater subsidence on West Zone side with cherty carbonaceous mudstone. Hydrothermal venting along growth faults and/or through chert pebble conglomerate aquifer deposits West Zone, Southeast Zone.

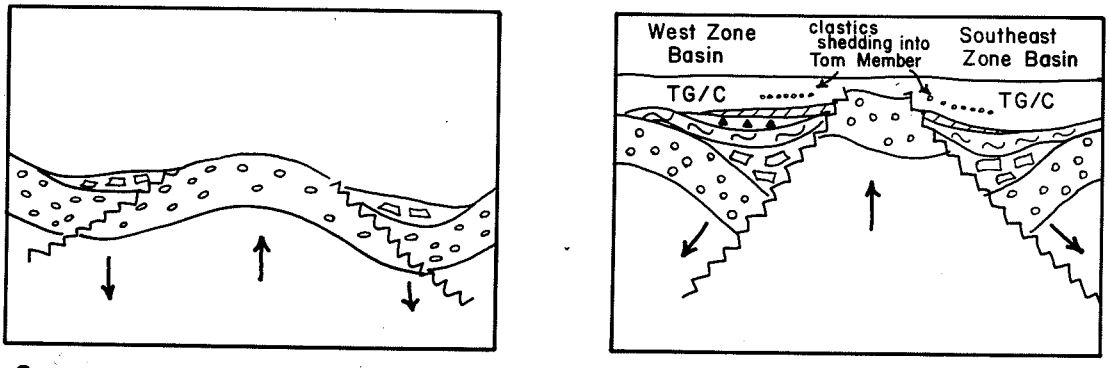

2 Ridge/Dome develops due to underlying stresses (Magma chamber?). Low angle growth faults develop on flanks of dome. Differential subsidence on flanks - infill with coarse diamictites.

5 Conglomerate high still exerts influence during lower Tom Member sedimentation. Differences in sediments laid down between West Zone and Southeast Zone. Clastic unit developed in Carbonaceous Submember.

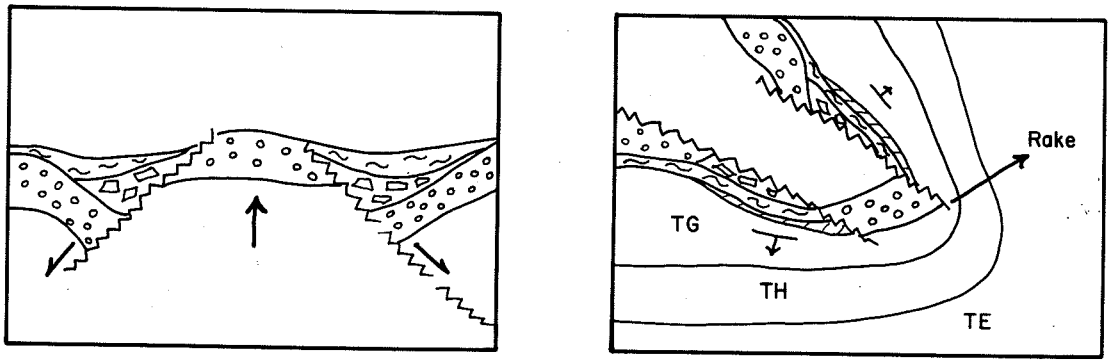

3 Ongoing subsidence and uplift. Thickened sand striped mudstone deposited above conglomerate.

6 Plan View - System in 5 is tilted on end and folded to give present configuration. Seems likely that folding was controlled by syndepositional high and basins that would impart strong structural anisotropy.

Figure 13 Schematic diagram of the Tom area showing the stages of development of the chert pebble conglomerate high and flanking sub-basins.

F1 fold (Tom anticline) and associated parasitic folds plunge gently northward in the northern part of the map area and steeply southward in the south. Phase 1 structures involve the Macmillan Pass Member and overlying Tom Sequence but are not found in the Itsi Formation.

Phase 2 structures have an east-west to northwest-southeast orientation and consist of open upright folds with associated low-angle thrust faults. These are the dominant structures in the area; they refold F1 folds and they have a well developed, east-west cleavage. Phase 2 thrust faults are found around the margins of the sub-basin. In the vicinity of the Tom deposit, F2 folds are small (1-20 m), open, steeply west plunging and superimposed on the F1 north-south anticline. The F2 folds affect all stratigraphic units.

Phase 3 structures are generally open, north-south-oriented buckle folds which fold the second phase slaty cleavage (S2). Small Phase 3 folds are found in Tom Sequence and both small and large (up to 0.5 km wave length) F3 folds are found in Itsi Member.

Locally complex outcrop patterns result from interference of F1 and F2 folds.

MINERALIZATION

Introduction

The Tom deposit consists of three mineralized zones - the West Zone, East Zone and Southeast Zone (Fig. 4). Sedimentary sphalerite-galena-barite mineralization in each of the ore zones occupies a stratigraphic position near the contact between a succession of argillaceous-arenaceous turbidites, chert pebble conglomerate and sedimentary breccias, and an overlying sequence of pyritic and carbonaceous siliceous shales and chert (Table 1). Stratigraphic correlations and structural analysis indicate that the West Zone and East Zone were initially part of the same ore lens before being folded into a south-plunging anticlinal structure and partly eroded. Although the East Zone has been more intensely deformed, the stratigraphic relationships are similar and it contains mineralized facies which are identical to mineralized facies documented for the less deformed West Zone. Similar to the West Zone, the East Zone was deposited in a sub-basin which was formed by down-faulting along the Tom extensional fault. Both zones are truncated, therefore, to the south by a horst structure formed during block faulting.

The Southeast Zone, by contrast, appears to have formed during the same hydrothermal episode which generated the West Zone and East Zone but in a sub-basin formed on the southeast margin of the horst structure. Except for bedding plane-parallel faulting which locally removes part of the sulphide zone, this Zone has a tabular shape, is laterally continuous and does not appear to have been intensely deformed.

The Tom East and West Zones outcrop at surface (Fig. 4). The Southeast Zone has no surface expression and may not subcrop. It was discovered in 1979 by shallow surface drilling of the east limb of the Tom anticline. The Tom West and Southeast Zones lie at or about the same stratigraphic horizon on either flank of the Tom anticline. They form sheet-like bodies that are relatively undeformed and present a cohesive picture relative to the structure, stratigraphy and paleobathymetry. The East Zone lies in the core of the anticline in strongly faulted and folded ground and is less readily understood. In the following sections, the West and Southeast Zones are described in some detail from ongoing study by the authors. The East Zone is described largely from the work of McClay and Bidwell (1986).

Tom West Zone

The Tom West Zone is a slightly folded, tabular body dipping 70^0 to the west. It is up to 41 m thick, 1,000 metres long and is continuous from the surface for 360 metres down dip. Near the southern limit of West Zone, a brecciated vent complex is associated with scarp talus breccias (i.e., diamictite, unit MD) suggesting that both the hydrothermal vents and abrupt southerly termination of stratiform mineralization are controlled by synsedimentary faulting. Distinct mineral zonation occurs in the deposit which is described more fully below. This zonation results in only the more southern 300 metre-long portion of the West Zone having grades in excess of 10% Pb+Zn, which can be regarded as the economic cutoff for ore at Macmillan Pass. The high grade portion of the West Zone lies at the southern end of the Tom anticline on the western limb of the fold within the carbonaceous cherty

mudstones (TCh) of the Tom Sequence.

ORE FACIES

The West Ore Zone consists of four distinct ore facies which are zoned with respect to the hydrothermal vent complex (Fig. 14 and 15). These facies, from south to north away from the hydrothermal vent, are: 1) Vent Facies; 2) Pink Facies; 3) Grey Facies; and 4) Black Facies. The different ore facies are distinguished from each other by the relative proportions of hydrothermal and epiclastic minerals, sulphide textures, the degree of replacement of earlier formed hydrothermal sediments above and adjacent to the vent, and the bulk mineral and isotopic chemistry.

Vent Facies

This Facies consists of a vein network of pyrite, pyrrhotite, galena, sphalerite, ankerite, siderite and quartz with variable but generally minor chalcopyrite, arsenopyrite and tetrahedrite. In some parts of the vent complex, sedimentary barite, sphalerite and galena have been extensively replaced by mostly pyrrhotite, pyrite and ferroan carbonates. In other areas, sulphides have been brecciated possibly by the rapid discharge of hydrothermal fluids or by a sudden volume expansion accompanying the release of CO_2 from the fluid. The low ratio of epiclastic to hydrothermal components and the complex mineral paragenesis indicates multiple episodes of hydrothermal discharge from the same vent complex and rapid fluid evolution within the vent complex.

The Vent Facies is best developed where hydrothermal sedimentary rocks overlie the hydrothermal fluid discharge conduit. In hole U63W, high grade ore of the Pink Facies is veined and partly replaced by ferroan carbonate. The upper portion of the Vent Facies is commonly higher grade with grades of 15-30% Pb+Zn and 150-200 g/T Ag that are common. The lower portions of the Vent Facies are often high in iron sulphides and siderite with sub-ore grades of lead and zinc (2-5% combined).

Below the contact of the West Zone with the underlying sedimentary sequence, the density and thickness of sulphide veins decrease markedly and the vent complex is represented by an anastomosing network of ferroan carbonate-quartz veins containing minor pyrite, chalcopyrite and sphalerite. The Vent Facies formed therefore where vent fluids invaded, brecciated and reacted with hydrothermal sediments deposited earlier in the history of hydrothermal activity.

The Vent Facies has been divided into several types of mineralization on the basis of vein mineralogy and textures. The different types are zoned from the core to the margins of the vent complex.

Type 1, at the core of the complex, is a stockwork and massive replacement zone consisting of massive pyrrhotite and pyrite with blebs of chalcopyrite, sphalerite and galena (Plate 3a). Patches of quartz probably represent remnants of the original sediment. This rock is commonly extremely high grade (30-50% Pb+Zn) with very high silver contents.

Type 2 is characterized by veins and replacement zones of medium grained masssive crystalline pyrite with a ferroan carbonate matrix and blebs and veinlets of sphalerite and galena (Plate 3c). Most of the galena is coarse grained. The pyrite is characterized by a mosaic of coalescing pyrite cubes.

Type 3 consists of massive crystalline ferroan carbonate and coarse grained galena cut by coarse grained galena and brown sphalerite veins. Minor pyrrhotite occurs in places (Plates 3b, 3d).

Type 4 is composed of brecciated chert and silicified mudstone that is cemented and veined by pyrite, brown sphalerite, coarse grained galena and ferroan carbonate (Plate 4a). Chert clasts have been rounded, presumably by silica dissolution during hydrothermal fluid discharge.

The most distal type (Type 5) is characterized by veinlets of pyrite, sphalerite and galena cutting the footwall chert and silicified mudstone.

The Vent Facies is underlain by an anastomosing network of coarse grained cream ankerite and quartz veins (Plates 4b, 4c) which are best developed in the chert- and mudstone-clast breccia and the chert pebble conglomerate. The veins range up to several cm in thickness, are oriented sub-vertical to the paleo-seafloor, and contain sericite, euhedral pyrite, minor chalcopyrite and brown sphalerite. In the area of ankerite-quartz veining, highly permeable coarse grained clastic rocks have been invaded by hydrothermal fluids which deposited ankerite, quartz, sericite, pyrite, chalcopyrite and sphalerite in open space between clasts and replaced the matrix and some clasts with

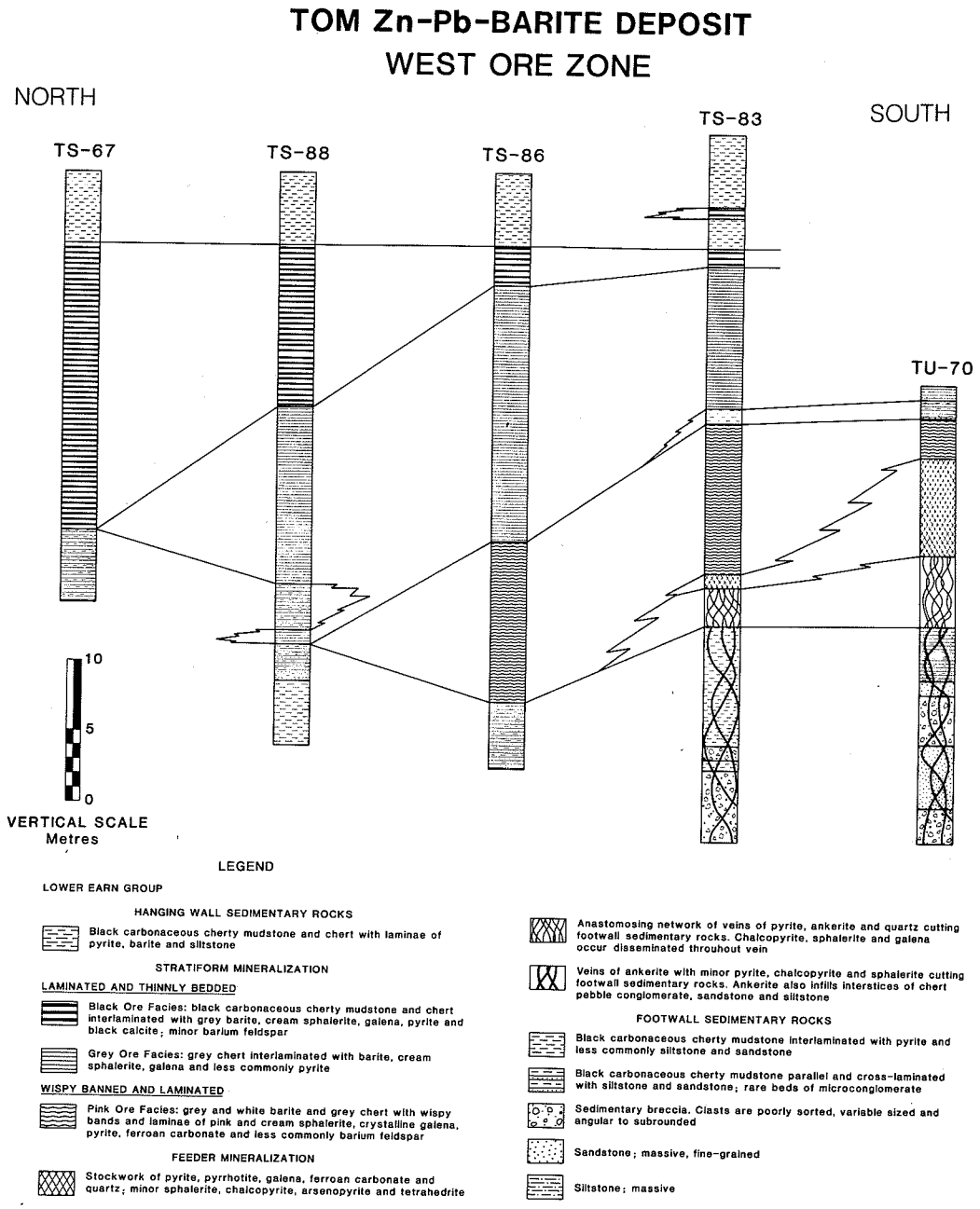

Figure 14 Geological cross-section of the Tom West Zone showing the distribution of the Vent, Pink, Grey and Black facies about the vent complex.

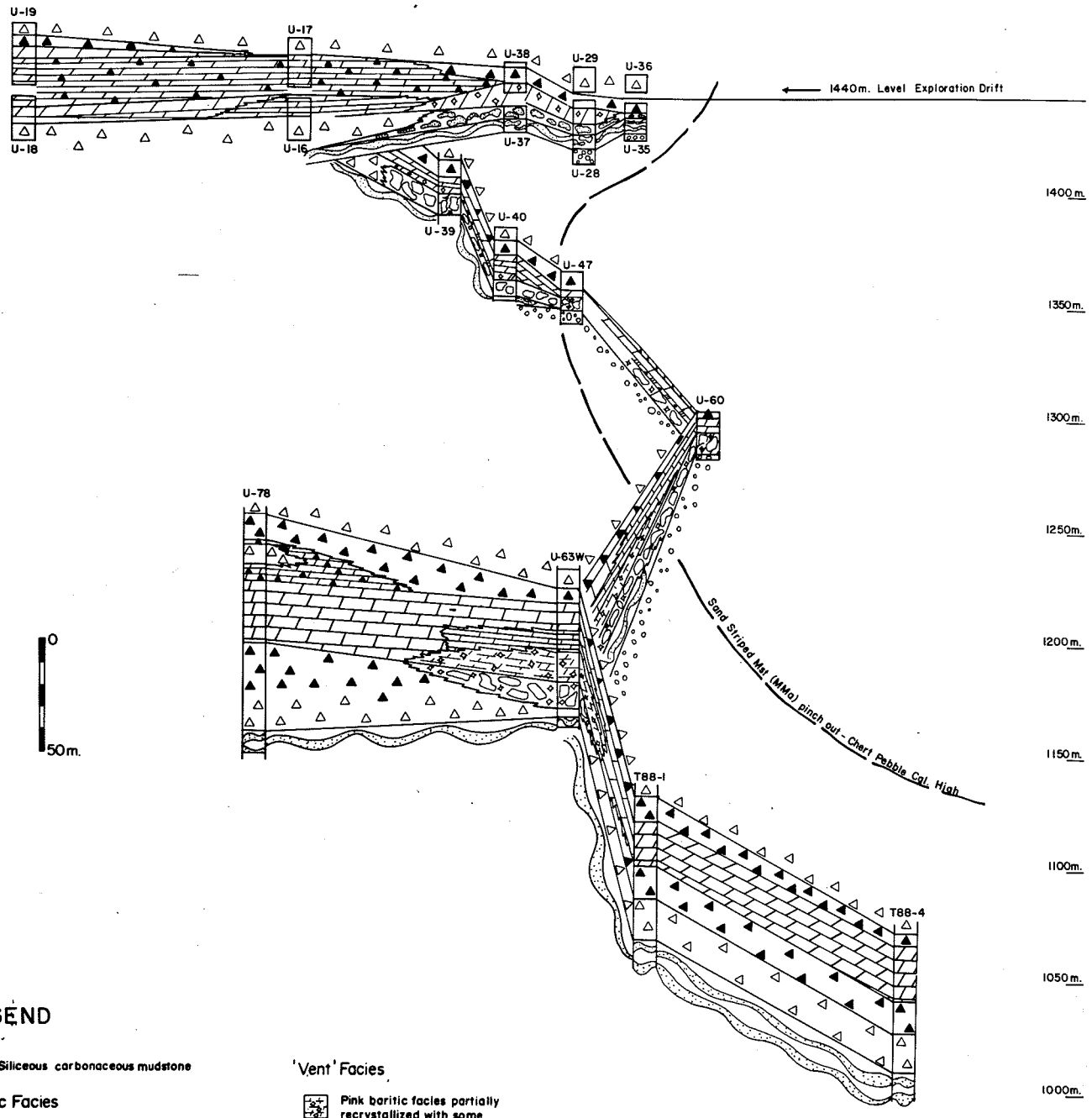

LEGEND

Siliceous carbonaceous mudstone

Baritic Facies

Siliceous carbonaceous mudstone striped with 10-20% barite/ witherite laminae and bands, and laminae of very fine grained sulphides. "BLACK ORE"

Finely interlaminated siliceous mudstone with barite/ witherite laminae and bands in about 50:50 ratio. "GREY ORE"

Pink and blue-grey barite witherite laminae and bands, lesser light grey chert interbeds hosting fine disseminated lead and zinc sulphides. Low grade "PINK ORE"

As above, but with intense pink-orange colours due to abundant sphalerite. Wisps, bands and irregular swirls, patches of galena common. High grade "PINK ORE"

'Vent' Facies

Pink baritic facies partially recrystallized with some replacement and veining by iron carbonate.

Sulphide/siderite rock. Mix of siderite, galena, sphalerite, lesser pyrite, generally in swirled mix of constituents with no well defined texture.

Stockwork/breccia mineralization. Fragments and blocks of siliceous mudstone commonly bleached and partially replaced by siderite in siderite and sulphide matrix, variable proportions of iron sulphides: pyrite (minor pyrrhotite), sphalerite, galena, siderite generally lower grade.

Sulphide Facies

Laminae and bands of abundant sphalerite and galena in siliceous mudstone host.

Macmillan Pass Member

Diamictite. Blocks and fragments of sand bands in mudstone matrix appears slumped and disrupted nearly insitu since train of fragments is often evident.

Sand striped mudstone - Typical, only moderately siliceous mudstone with 1 to 50mm. thick laminae and bands of fine to medium grained sandstone. Sandstones are commonly impregnated with siderite.

Chert pebble conglomerates and grits. Rock composed of subrounded to rounded silica 'chert' clasts varying from 1mm. to 50mm. in silica matrix. Individual beds usually show good sorting with clasts of similar size. Siderite is common as veins and interstitial impregnations.

Figure 15 Fence diagram showing the distribution of ore facies at the south (vent proximal) end of the Tom west Zone.

Plate 3 Photographs of rock slabs from the West Zone. (a) Vent Complex: massive pyrite (light grey) and pyrrhotite (medium to dark grey) with remanent black chert (black specks). Patch in the center consists of chalcopyrite, pyrite and ferroan carbonate, and probably represents a clast of mineralized feeder pipe rebrecciated and partly replaced during hydrothermal discharge. Chalcopyrite also occurs disseminated throughout. Sample TOM87-04. (b) Vent Complex: massive crystalline galena (medium grey) with bands of pyrite (light grey) and ferroan carbonate. White veins and patches consist of ferroan carbonate. Sample TOM87-03D. (c) Vent Complex: Massive crystalline pyrite (pale grey) intermixed with galena and sphalerite (medium grey). White patches consist of ferroan carbonate. Sample TOM 87-02D. (d) Vent Complex: swirls and bands of crystalline galena (medium grey), ferroan carbonate and pyrite (light to medium grey) and white quartz. Sample TOM87-12.

Plate 4 Photographs of the veined, brecciated and replacedsedimentary rocks underlying the massive replacement vent complex. (a) Brecciated black chert clasts that are variably replaced by pyrite, pyrrhotite, galena, arsenopyrite and ferroan carbonate, and cut by galena-sphalerite followed by white ferroan carbonate veins. Sample TOM 105O-01. (b) Sedimentary breccia consisting of variably sized, poorly sorted, angular to subrounded chert and mudstone clasts cemented, veined and partly replaced by ankerite (white). Breccia probably represents resedimented chert pebble conglomerate and mudstone. Sample TS83-36. (c) Sedimentary breccia cut by veins of ankerite and infilled and partly replaced by ankerite. The ankerite typically contains euhedral pyrite and minor chalcopyrite. Sample TU69-17. (d) Chert pebble conglomerate infilled and partly replaced by ankerite (white). Pyrite occurs disseminated throughout the matrix and most clasts. Most clasts have ragged margins due to the replacement by ferroan carbonate. Sample PH1-02.

Plate 5 Photographs of polished slabs of the sedimentary-hydrothermal facies, West Zone. (a) Pink Facies: interbanded white barite, pink, pale green and black sphalerite, and grey chert. Diffuse contacts between bands, recrystallized sphalerite and high contents of vent-proximal elements indicate that the sedimentary textures have been partly overprinted by hydrothermal replacement textures in areas flanking the Vent Complex. (b) Grey Facies: Interbedded white barite, cream sphalerite (medium grey) and mudstone (dark grey). Galena occurs finely disseminated in sphalerite-rich laminae. Beds are intensely folded and offset along small faults. Sample TOM 87-05. (c) Grey Facies: Interbedded grey chert (medium grey), white barite, and cream and pink sphalerite (pale to medium grey). Chert beds display tension gashes filled with carbonate minerals. Dark grey tabular structures consist in part of Ba-feldspar. Cream sphalerite laminae and beds have generally diffuse contacts compared to chert bed contacts which are sharp. Sample T88-1-62. (d) Black Facies: Black carbonaceous chert finely laminated with white chert and sphalerite. Minor microframboids of pyrite aligned along bedding planes. Sample TOM 87-03.

ankerite (Plate 4d). Away from the vent zone, quartz, sericite, chalcopyrite and sphalerite decrease until the hydrothermal minerals are represented by what is probably a lower temperature ankerite-pyrite assemblage.

Sand laminated mudstone (MMa) has also been flooded by hydrothermal fluids which appear to have migrated laterally along more permeable sandstone and siltstone laminae. Within these laminae, quartz grains are cemented and partly replaced by cream ankerite containing pyrite euhedra (Plate 1a). Ankeritic sandstone and siltstone weather a distinctive rusty brown. Interbedded mudstone, presumably due to its low relative permeability, has not been significantly affected by hydrothermal processes except near the center of fluid discharge where it is silicified and cut by ankerite-quartz-sulphide veins.

The stratabound ankerite-pyrite which cements quartz grains in coarser grained clastic units is restricted to the footwall sequence and extends laterally beyond the known limits of the sulphide zones. The restriction of ankerite and pyrite to pre-ore, permeable units, an increase in the content of these minerals with proximity to the feeder zone and the mineralogical similarity to veins forming part of the vent complex all indicate that ankerite and pyrite were precipitated from ore-forming

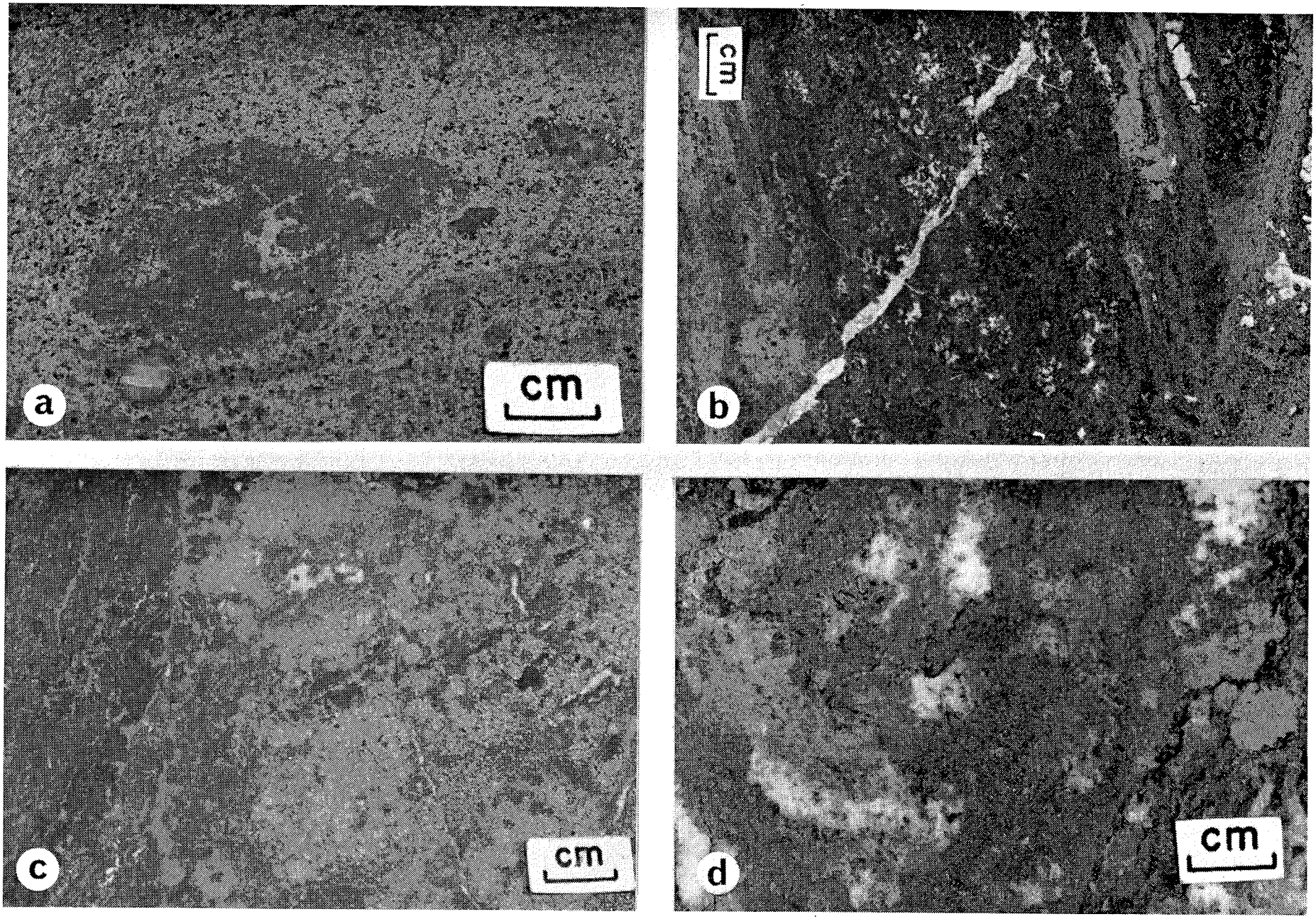

Plate 3

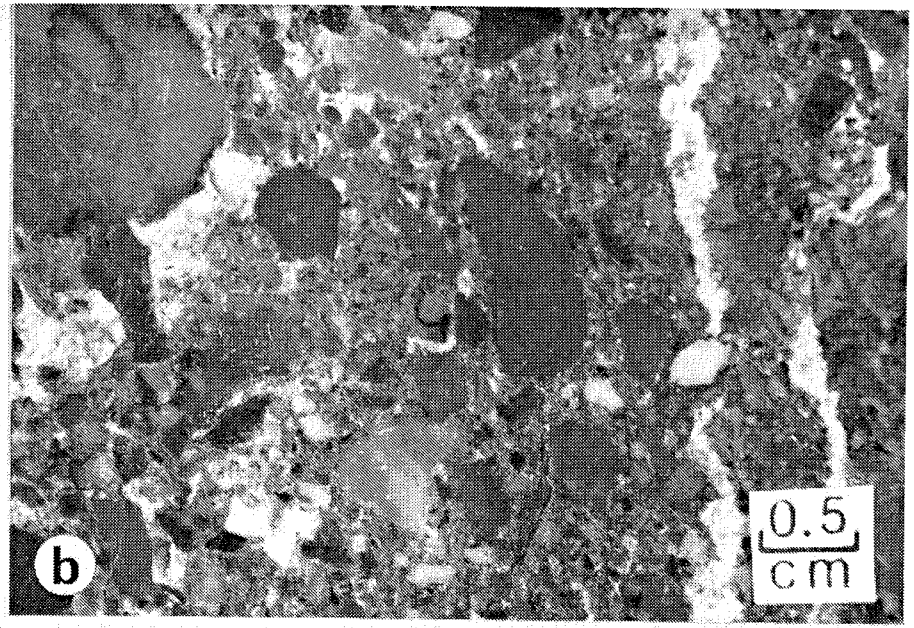

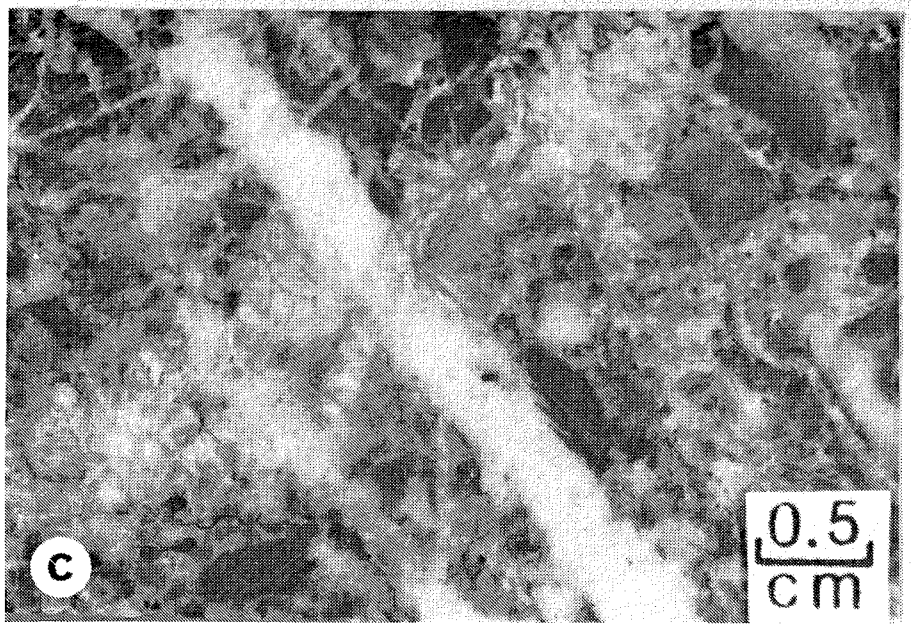

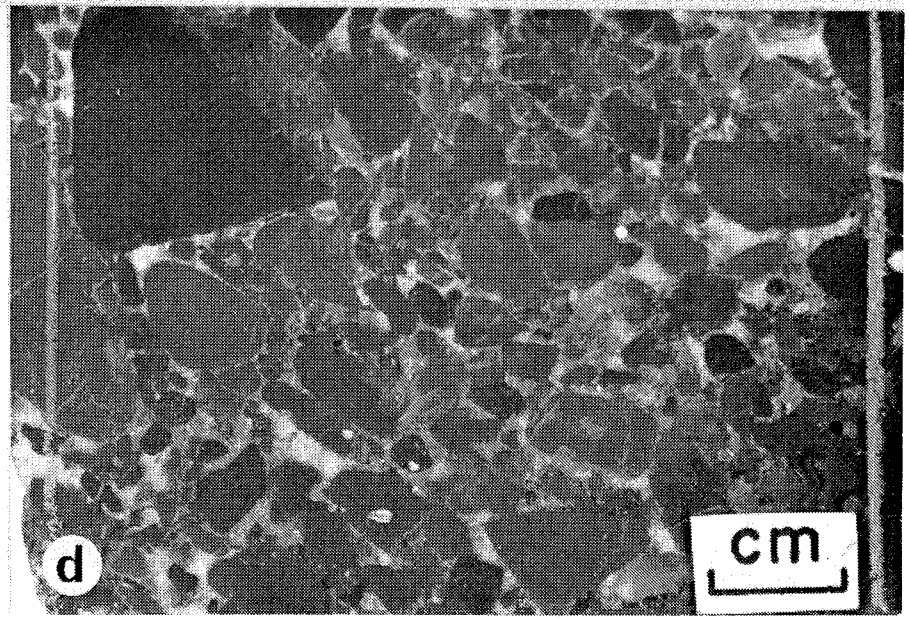

Plate 4

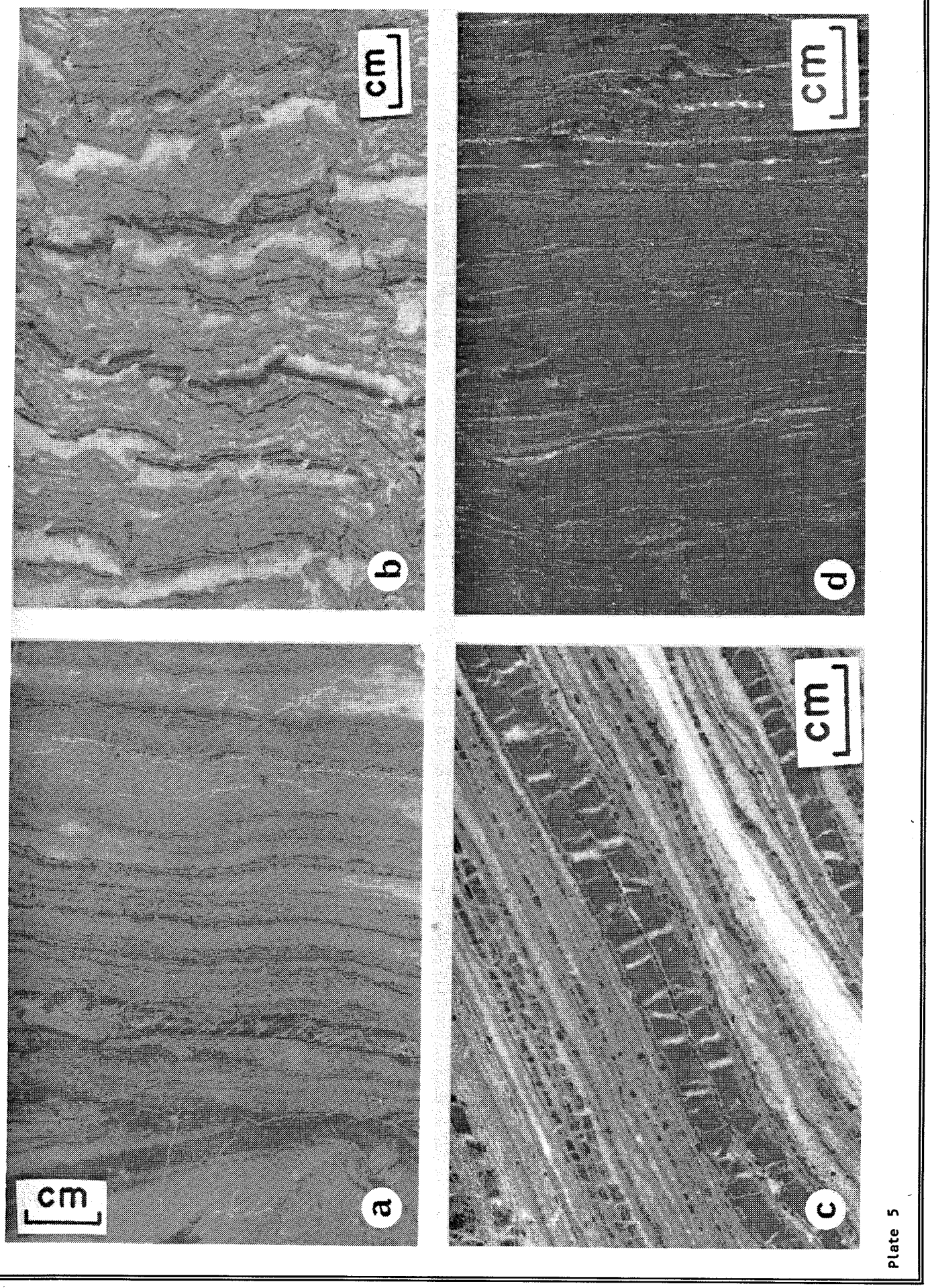

Plate 5

Plate 6 Photographs of polished ore slabs from the West Zone. (a) Grey Facies: Intensely folded interbedded chert (medium grey), barite (white), cream and pale pink sphalerite and galena. Tension gashes in chert beds filled with carbonate minerals. Sample T88-1-62. (b) Grey facies: Interbedded chert (medium grey), barite (white), cream and pale pink sphalerite (pale to medium grey and finely laminated) and galena. Sample T88-1-62. (c) Weak Pink Facies: Interbedded chert (pale grey), pink and cream sphalerite (pale to medium grey), white barite and galena. Chert various in thickness from several centimetres to millimetres. Sample T88-1-57. (d) Chert beds (medium grey) with black spherical patches (not identified but may be radiolaria) and wavy laminae of cream sphalerite (pale to medium grey) and barite (white). Dark grey tabular areas aligned along bedding planes consist partly of Ba-feldspar. Sample TOM 87-05D

hydrothermal fluids which had evolved during migration from the vent complex.

Pink Facies

Because this ore facies is situated adjacent to the Vent Facies, it has been partly replaced by hydrothermal fluids and is therefore transitional between the Vent Facies and hydrothermal sedimentary facies. The sedimentary components of this facies consist mostly of interbedded grey to white barite, pale grey chert, cream sphalerite, fined grained pyrite, and black Ba-carbonate (Plate 5a). These beds retain sedimentary textures such as sharp bedding contacts. Overprinting hydrothermal sediments by wispy bands of silicified pink and yellow sphalerite, and coarser grained brown sphalerite, crystalline galena, and ferroan carbonate, has increased the grain size, metal grades, and Pb/Pb+Zn ratios. Bedding textures have been obliterated by a combination of replacement processes and disruption of sediments by rapid hydrothermal discharge near the vent. It seems likely that a significant part of the 10-30% Pb, Zn grades that are common to this Facies come from late introduction of sulphides into a low grade parent rock.

Replacement minerals are localized along original bedding planes due to a high stratal permeability. The ferroan carbonate partly replaces barite, and the black Ba-carbonate beds commonly form boudins which are variably replaced by Ba-feldspar. The organic matter in chert beds has been destroyed, presumably by thermal degradation by hydrothermal fluids.

Low grade Pink Ore refers to the more banded barite/witherite rock that is composed predominantly of yellow, orange and pink sphalerite laminae and bands alternating with sphalerite-poor blue grey to white laminae and bands. The bands range in thickness from less than 1 mm to 50 mm and are composed of barite/witherite with finely disseminated sphalerite/galena. The witherite content varies but seems to be higher in the blue grey bands and more common distal to the vent area. Light grey chert beds and black mudstone laminae are more common in areas transitional to the grey ore. The low grade Pink Ore is commonly sub-ore with grades of 1-2% Pb, 2-6% Zn and low silver abundances.

Grey Facies

This Facies along with the Black Facies constitutes the bulk of Tom deposit although the Zn and Pb content is generally lower due to 1) the dilution effect of high barite and 2) the low level of replacement by sphalerite and galena. Typically this mineralization is sub-ore grade with 0-2% Pb, 4-5% Zn and negligible silver. This barite type occurs distal to the Vent Facies on the 1440 m level and forms the low grade non-ore portion of the Tom West Zone separating HBM&S Hanging Wall and Footwall Ore Zones (see U18, U19 and U17, U16). Higher grade Grey Ores can occur in the immediate hanging wall as variants of the Black Ore described below.

The Grey Facies consists predominantly of interbedded cream to pale pink sphalerite, fine grained galena, fine grained pyrite, white to pale grey barite, pale grey chert and blue grey to white Ba-carbonate and Ba-feldspar (Plate 5b, 5c, 6a, 6b, 6c, 6d). The Ba-carbonate is partly replaced by Ba-feldspar and form boudins distributed discontinuously along bedding planes (Plate 5c). Chert beds have also been pulled apart and infilled with quartz (Plate 5c). Other than replacement by Ba-feldspar, the only other alteration this Facies appears to have undergone is the destruction of ambient marine organic matter which rained from the overlying water column and accumulated during an hiatus of the hydrothermal system. As a result, pale grey chert occurs instead of what would have been a typical black chert (Plate 6c).

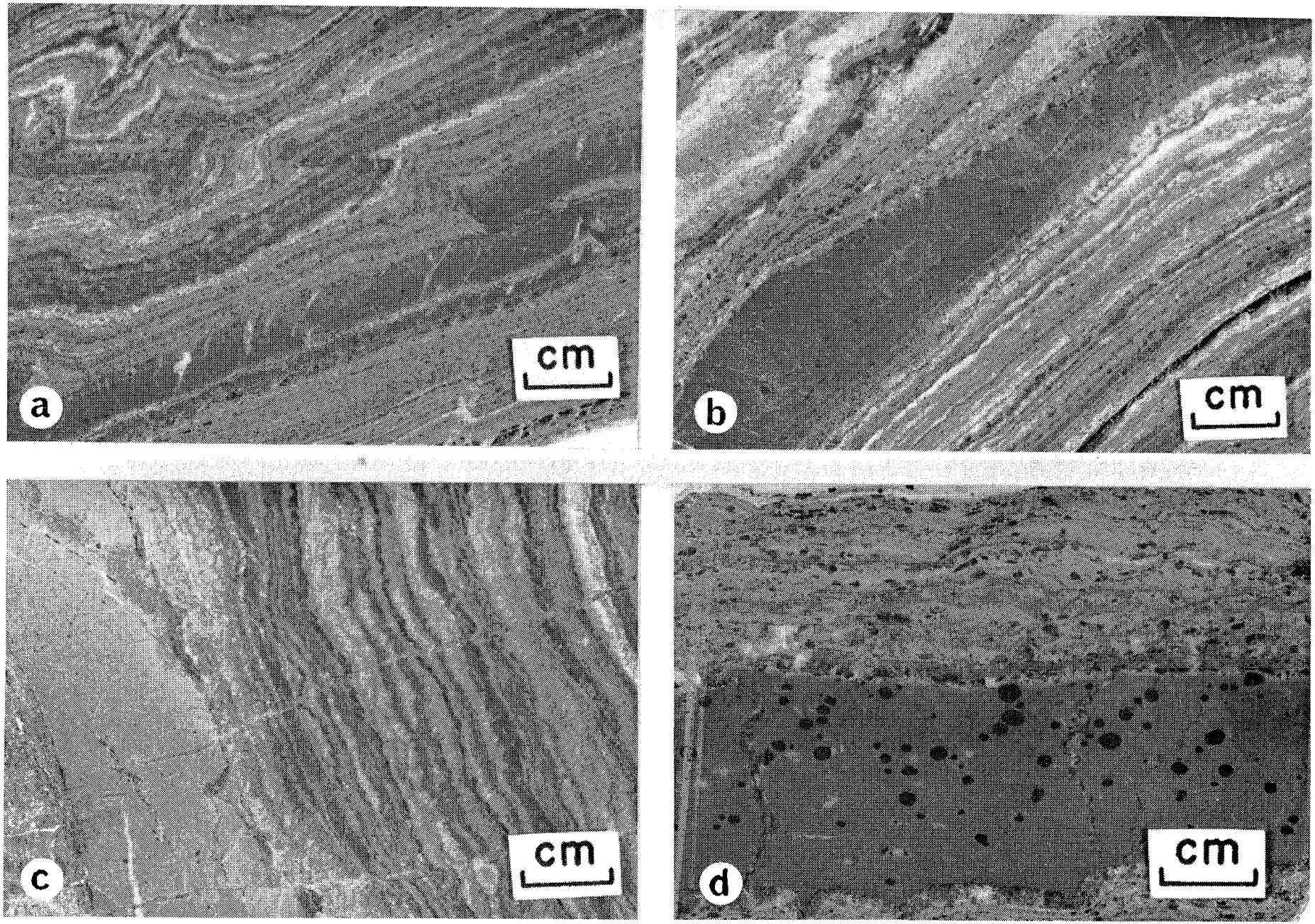

Plate 6

Black Facies

Black ore refers to black cherty mudstone and chert that are delicately striped with white barite/witherite laminae and fine grained sphalerite, galena and pyrite laminae (Plate 5d). The sphalerite is typically cream colour. These laminae range in thickness from <0.1 mm to more prominent 1-5 mm and commonly comprise 10-20% of the rock. This "ore" type particularly in the hanging wall zone can be of much higher grade than the more massive barite types. While very low in silver and hosting only 1-2% Pb, the Black Facies commonly contains 7-12% Zn in the few metres immediately above the more massive barite facies. For the most part this grade is not immediately obvious due to the very fine grain size and light colour of the sphalerite. It is this high grade Black Facies which constitutes the Hanging Wall Zone included by HBM&S in ore reserves. Away from the Hanging Wall Zone this Facies is generally of sub-ore grade (i.e. 4-10% Pb+Zn).

This Facies occurs in the uppermost part and distal margin of the deposit where the barite content relative to sphalerite, the duration of hydrothermal discharge within a pulse and the frequency of hydrothermal pulses all decrease. The transition from the Black Facies into the overlying sediments is gradational and characterized by a rapid decrease in the thickness and frequency of barite and sphalerite laminae; pyrite laminae with minor sphalerite and barite however persist 100's of m into the overlying chert and mudstone. A decrease in the barite content relative to sphalerite has resulted in an increase in Zn grades; Pb/Pb+Zn ratios are however very low and characteristic of distal mineralization. Although the Tom deposit has been tectonically deformed, bedding textures are well preserved and consist of distinct bedding contacts.

On a microscopic scale, the barite appears recrystallized and consists of a mosaic of subhedral barite grains aligned along bedding planes. In detail, the sphalerite also appears fine grained and displays diffuse contacts with the enclosing rocks. Pyrite laminae are composed of pyrite framboids which are commonly overgrown by euhedral pyrite.

Sulphide Facies

Laminated sulphides or sulphide laminated mudstone is not common in the West Zone but is occasionally evident as in the bottom of drill hole TU18. Where present it often resembles Southeast Zone sulphides described below.

Metal Contents

Each of the Tom West Zone ore types shows varying metal contents. The higher grade "vent" facies are not only richer in Pb, Zn and Ag but also contain significantly higher Cu and such deleterious metals as Hg, As and Sb.

Tom Southeast Zone

The Tom Southeast Zone is a relatively undeformed tabular body dipping 60-70^0 to the east. It ranges from 0.5 to 6 m thick, 400 m long and extends from 50 m below surface down dip for at least 350 m. No surface expression of the zone has been encountered and it may be that it does not breach the subcrop surface. Alternatively being a very thin Zone, it may be completely masked by felsenmeer and talus cover. The Zone lies on the southern end of the Tom anticline but on the eastern limb of the anticline opposite to that of the Tom West zone. The Southeast Zone forms an integral part of another sub-basin flanking the chert pebble conglomerate high but on the side opposite the Tom West and East Zones.

ORE FACIES

The Southeast Zone is characterized by finely interlaminated sphalerite, galena, pyrite and black cherty mudstone. Close to the nose of the Tom anticline the sulphides are contorted, swirled and incorporate boudins that suggest structural disturbance.

There is a major change in ore facies about the conglomerate high, particularly as it relates to the amount of barite present. Barium contents, which range from 0.6% in the southernmost, vent proximal area to 3.0% in the more northern vent distal part of the Southeast Zone, are markedly lower than in the West and East Zone. For the most part, the Southeast Zone consists of delicately laminated sulphides without evidence of the type of hydrothermal replacement that characterizes the West Zone. In the basal sections of the mineralized zone in DDH T88-3, however, there is evidence for minor hydrothermal replacement. This evidence includes rare swirled tectures, high Pb contents, traces of chalcopyrite associated with pyrrhotite and siderite rhombs in mudstone. The drilling control of this zone is too limited to permit any

significant appraisal of the mineral zonation in relation to hydrothermal vent processes.

METAL CONTENT

The ore isopach, Pb contour and Pb/Pb+Zn ratio longitudinal sections (Fig. 6, 16 and 17, respectively) show the Southeast Zone to be thinner but of generally higher grade than most of the West Zone. Based on limited drilling, Pb grades (8-13%) and Pb/Pb+Zn ratios (0.4-0.5) increase towards the chert pebble conglomerate high.

Silver contents and Ag/Pb ratios are highest near the chert pebble conglomerate high (8.1 oz/T) but again the data is scanty. Overall Zn grades, by contrast, do not change appreciably (8-12% average) and the change in Ag/Pb ratios is due to the varying proportions of argentiferous galena present in the ore.

Isopachs of the footwall carbonaceous cherty mudstones (Fig. 8) and mineralized zones (Fig. 6) show that the rate of both epiclastic and hydrothermal sedimentation was less southeast of the conglomerate high. This suggests that there was probably less subsidence and a diminished sediment supply in this area. As a result, the Southeast Zone is thinner but of higher grade due in part perhaps to less dilution by normal marine sediments. An increase of Pb and Ag contents towards the conglomerate high suggests that hydrothermal venting was focussed along the faulted margins of the horst structure.

The Southeast Zone is markedly depleted in Ba compared to the West Zone (Fig. 10). This has the effect of increasing the metal contents of the Southeast Zone since barite is the major dilutant in the West and East Zones, particularly in barite-rich facies. Although the low Ba content of the Southeast Zone is not well understood, it is unlikely to reflect a different fluid chemistry but instead relate to the paleobathymetry of the basin and the vertical distribution of quenched minerals in the hydrothermal plume. Because barite has a high specific gravity and forms large crystals when quenched, it is unlikely to be carried as high in the hydrothermal plume as finer grained sulphide particulates. As a result, the lateral distribution of barite may be restricted by the conglomerate high whereas finer grained sulphides carried higher in the hydrothermal plume would probably be dispersed more widely.

Tom East Zone

The East Zone has not been appreciably studied by the authors nor explored to date by Cominco Limited. The following descriptions by McClay and Bidwell (1986) remain valid.

The East Zone is a series of intensely contorted, fault bounded pods of high-grade (22% Zn-Pb, 165 g/t Ag) laminated and thinly bedded barite, chert, sphalerite and galena. The mineralization is overlain in part by black carbonaceous chert. Detailed mapping and structural analysis (McClay, unpublished data) has shown that the East Zone occurs near the hinge of the Tom anticline which, in this part of the structure, plunges gently northward. Stratigraphically, the East Zone lies above the sand-banded mudstone (MMa) and occurs at the same stratigraphic level as the West Zone.

The East Zone is texturally and mineralogically similar to ore facies described for the Tom West Zone. This similarity indicates that the East Zone and West Zone formed part of the same mineralized zone before being folded about the Tom anticline and eroded.

GEOCHEMISTRY

Element Zonation

To establish element abundances in the different mineralized facies, and document element zonation about the vent complex, major, minor and trace elements were determined in bulk samples collected at approximately one meter contiguous intervals from drill hole core of the West Ore Zone. Since most of the chemical changes are gradational due to temporal evolution of the hydrothermal fluids and variable degrees of hydrothermal replacement within the vent complex, geochemical results for samples from drill holes used to construct a longitudinal cross-section of the West Zone (Fig.13) were contoured.

Base Metals

The stratigraphic and lateral zonation of Zn, Pb, Cu and Ag is illustrated by contour maps of these elements plotted on a longitudinal section of the West Zone (Fig. 18, 19, 20 and 21, respectively). Zinc (Fig. 18) is enriched in two zones: Zone I coincides with the Pink Facies (Fig. 14) and Zn contents reach maximum values near the transition between this Facies and the

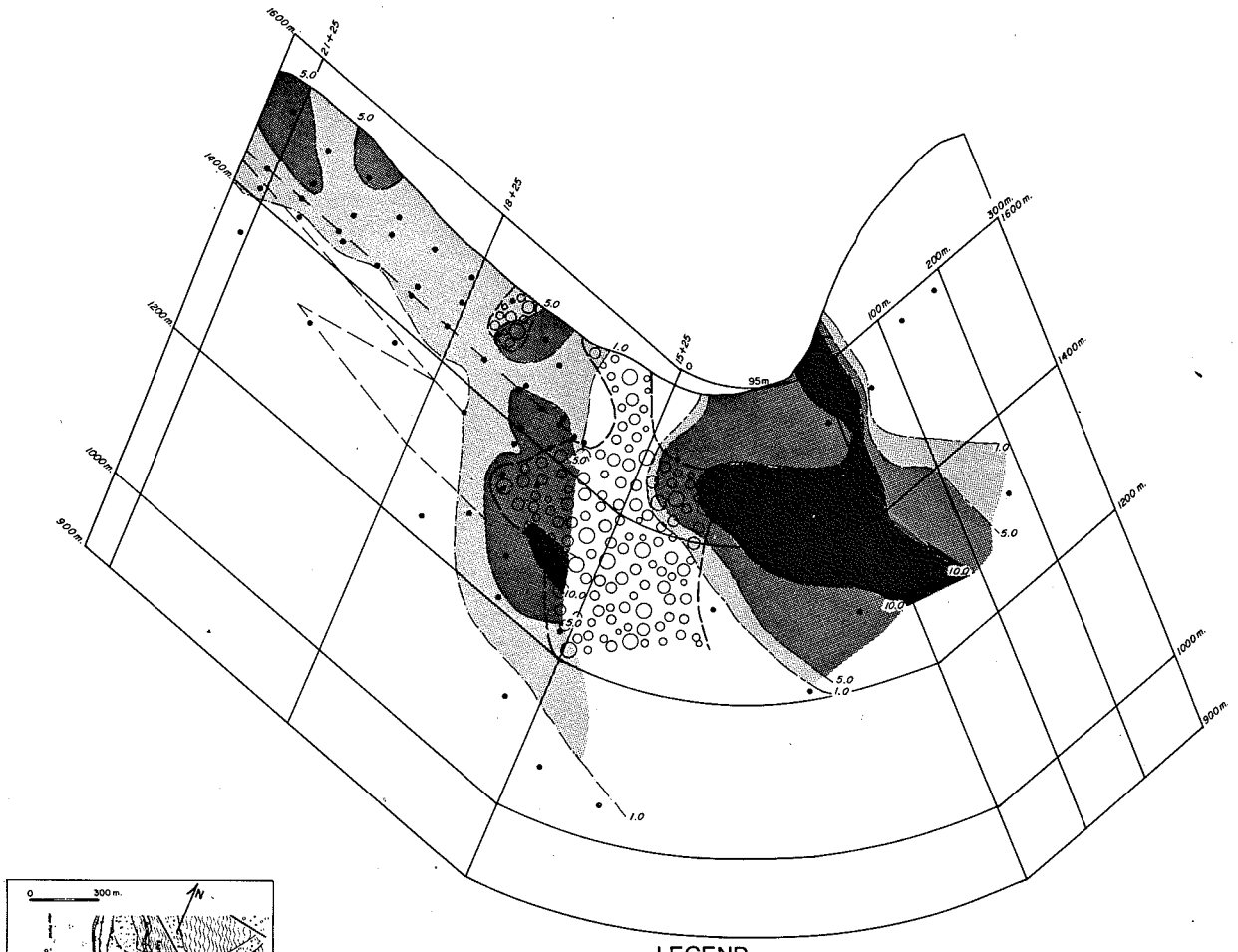

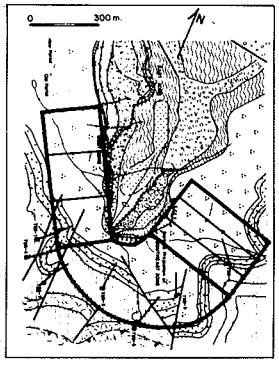

Inset showing location of panels of West Zone - Southeast Zone Horizon projected onto longitudinal section.

LEGEND

- Drill hole intercept of mineralized horizon
- Pb countours, values in %, averaged over interval included in mineralized intercept.
- Underground workings
- Chert Pebble Conglomerate high as defined by pinch out of sand striped mudstone (MMa)

- 1.0–5.0%
- 5.0–10.0%
- >10%

Figure 16 Lead assay contours of the West and Southeast Zones projected onto a longitudinal section about the nose of the Tom anticline.

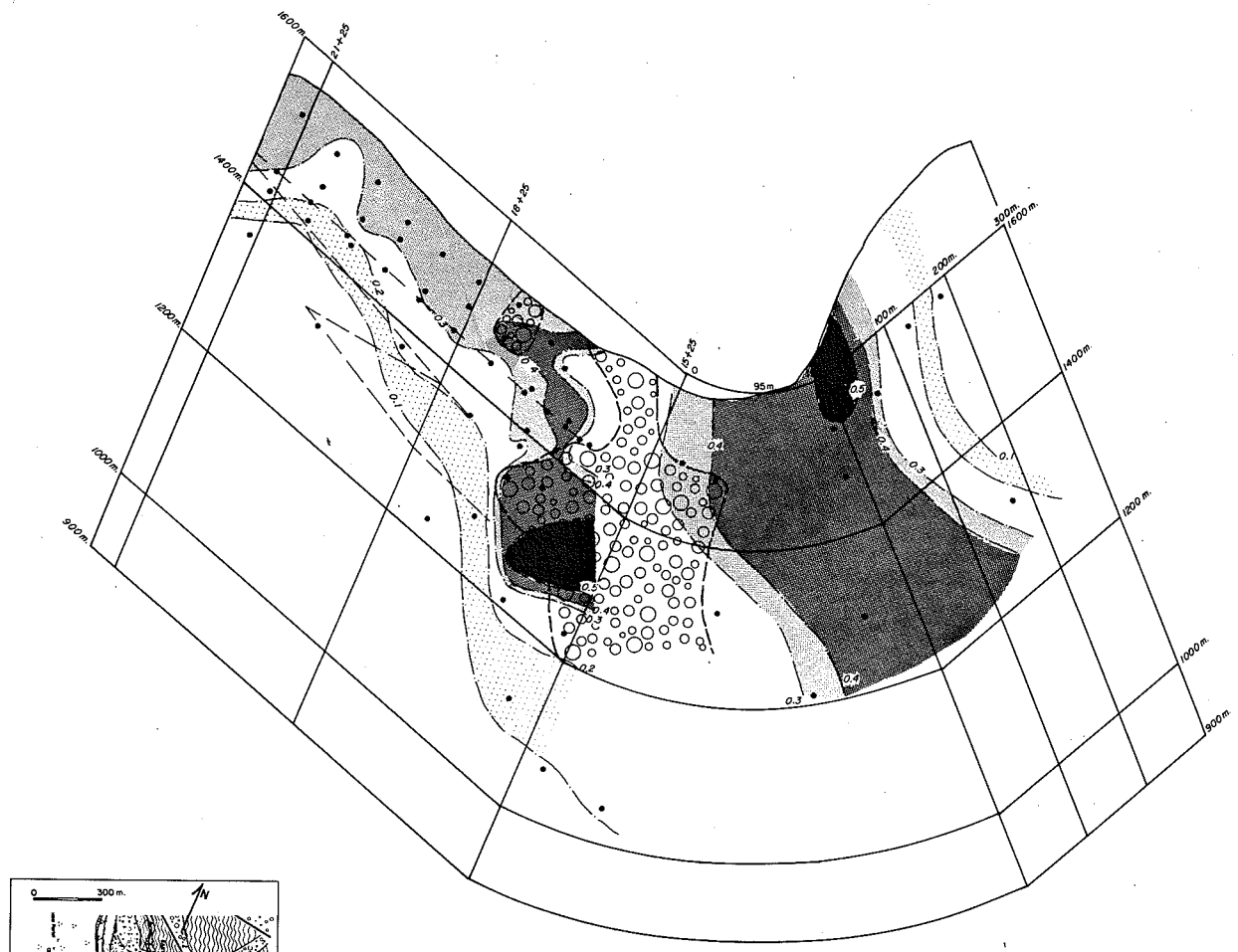

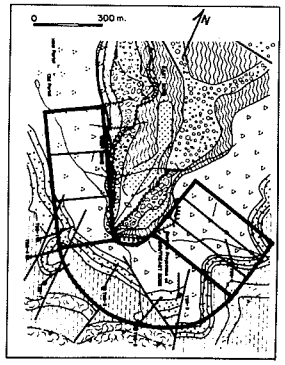

Inset showing location of panels of West Zone – Southeast Zone Horizon projected onto longitudinal section.

LEGEND

- Drill hole intercept of mineralized horizon
- Contours of Pb to Pb+Zn ratios in mineralized intersections
- Underground workings
- Chert Pebble Conglomerate high as defined by pinch out of sand striped mudstone (MMa)

- 0.1–0.2
- 0.2–0.3
- 0.3–0.4
- 0.4–0.5
- >0.5

Figure 17 Contours of Pb/(Pb/+Zn) ratios of the West and Southeast Zones projected onto a longitudinal section about the nose of the Tom anticline.

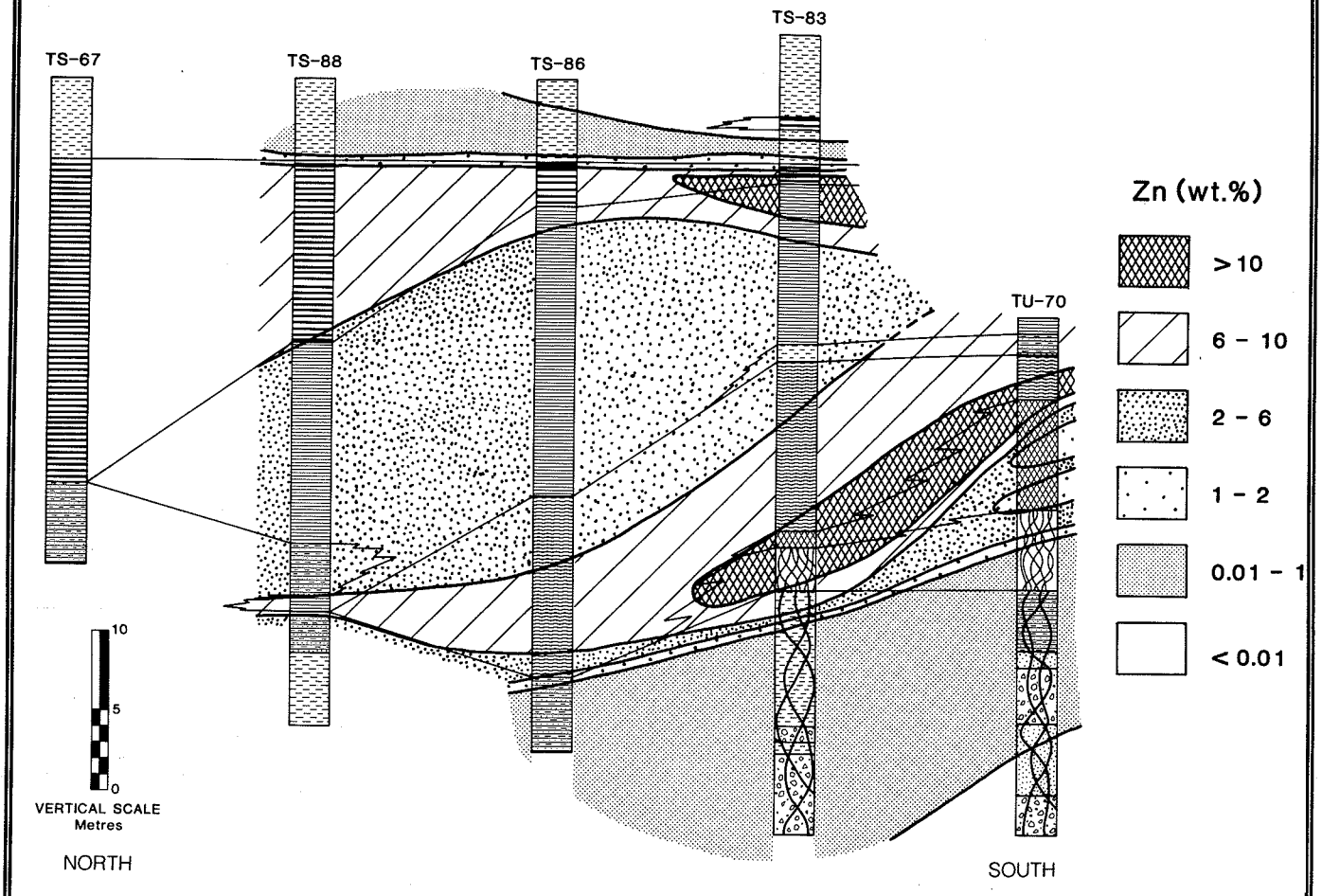

Figure 18 Contours of Zn contents plotted on a cross-section of the Tom West Zone.

Vent Facies. Zinc abundances within the Vent Facies are generally low, between 1 and 6 weight %, and were probably depleted during the replacement of hydrothermal sediments in the vent complex. This is supported by textures showing galena replacing sphalerite within the Vent Facies. Zinc dissolved from the core of the vent complex moved outward and precipitated in the transition zone between the Vent Facies and sedimentary-hydrothermal facies. Evidence for a non-sedimentary origin for some of the sphalerite in this zone of high Zn includes 1) a coarser grain size, 2) wispy laminae with diffuse contacts, 3) an unusual colouration not typical of sedimentary sphalerite from the deposit, and 4) highly silicified sphalerite bands indicating the introduction of hydrothermal silica. Furthermore, this zone of Zn enrichment corresponds to some of the highest Hg contents and Hg/Zn atomic ratios > 60 (Fig. 22). The close correlation of high Hg/Zn ratios with the Pink Facies suggests that Hg substitutes for Zn in the sphalerite lattice. Because of its high volatility, Hg was probably driven out of the high-temperature vent complex and concentrated in adjacent hydrothermal sediments.

Zone II coincides with the Black Facies near the top and distal margins of the West Zone. It is distinguished from Zone I by generally low Pb and Hg contents. As discussed earlier, most of the sphalerite is a cream colour and of sedimentary origin. The high Zn in this Zone II is controlled more by a decrease in barite,

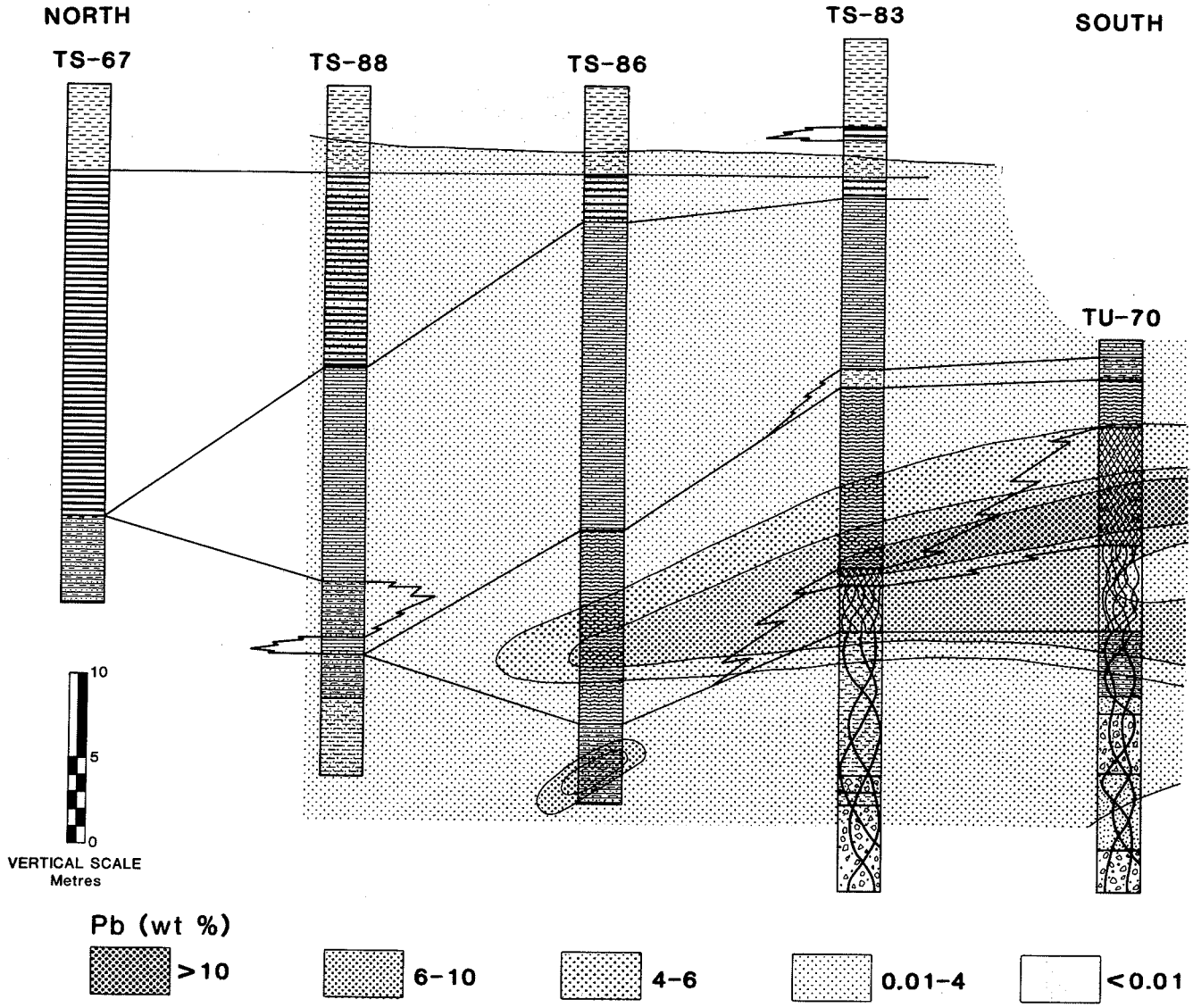

Figure 19 Contour of Pb contents plotted on a cross-section of the Tom West Zone.

the dominant gangue mineral, during the waning stages of the hydrothermal system than by an increase in Zn. This is illustrated by a contour plot of the Ba/(Ba+Al) ratio (Fig. 23) which shows hydrothermal Ba relative to Al in epiclastic clays reaching maximum values in the Pink and Grey Facies and decreasing in the Black Facies. In fact, a decrease in the thickness and frequency of sphalerite laminae relative to epiclastic sediments demonstrates that sphalerite and barite depositional rates both decrease in the Black Facies except barite drops off faster than sphalerite.

Lead (Fig. 19) displays a zonal pattern similar to Zn except that maximum values coincide with the Vent Facies instead of the Pink Ore Facies. This pattern is consistent with the post-sedimentary deposition of

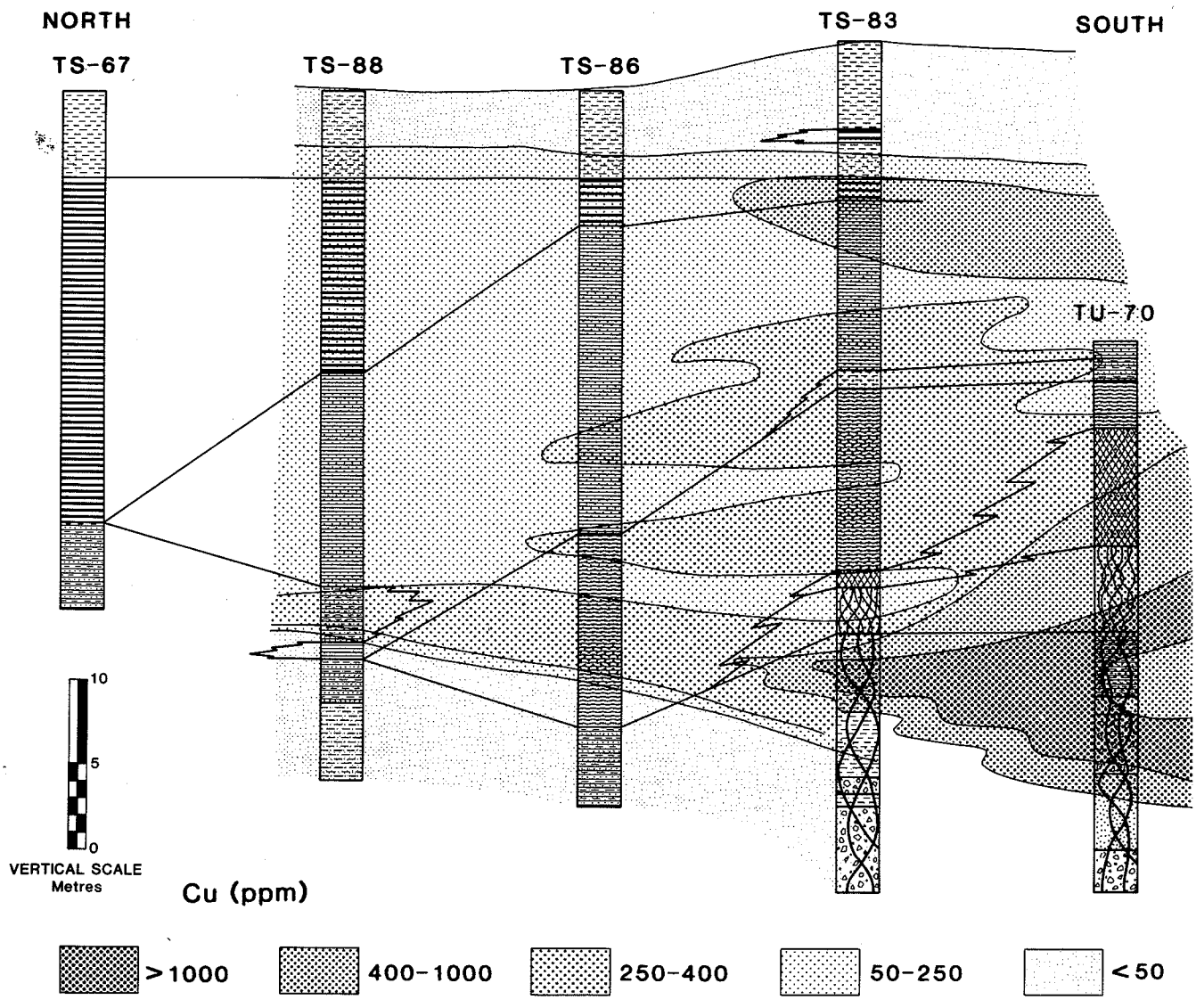

Figure 20 Contours of Cu contents plotted on a cross-section of the Tom West Zone.

coarse grained galena in veins and replacement zones during the reaction of hydrothermal sediments with metalliferous fluids in the areas of active venting. This is shown by contours of Pb/(Pb+Zn) ratios (Fig. 24) which display maximum values in the Vent Facies and decrease gradually in the Pink and Grey Facies reaching minimum ratios in the most distal Black Facies. The relationship of metal ratios to the different ore facies and the degree of carbonate replacement is illustrated with Pb/(Pb+Zn) versus CO_2 plot in figure 25.

Similar to Pb, Ag (Fig. 21) is concentrated in the Vent Facies although the contour pattern is slightly different. Furthermore, the high correlation of Ag with Sb (Fig. 26) indicates that a major portion of the Ag resides in tetrahedrite which is known to occur in the Vent

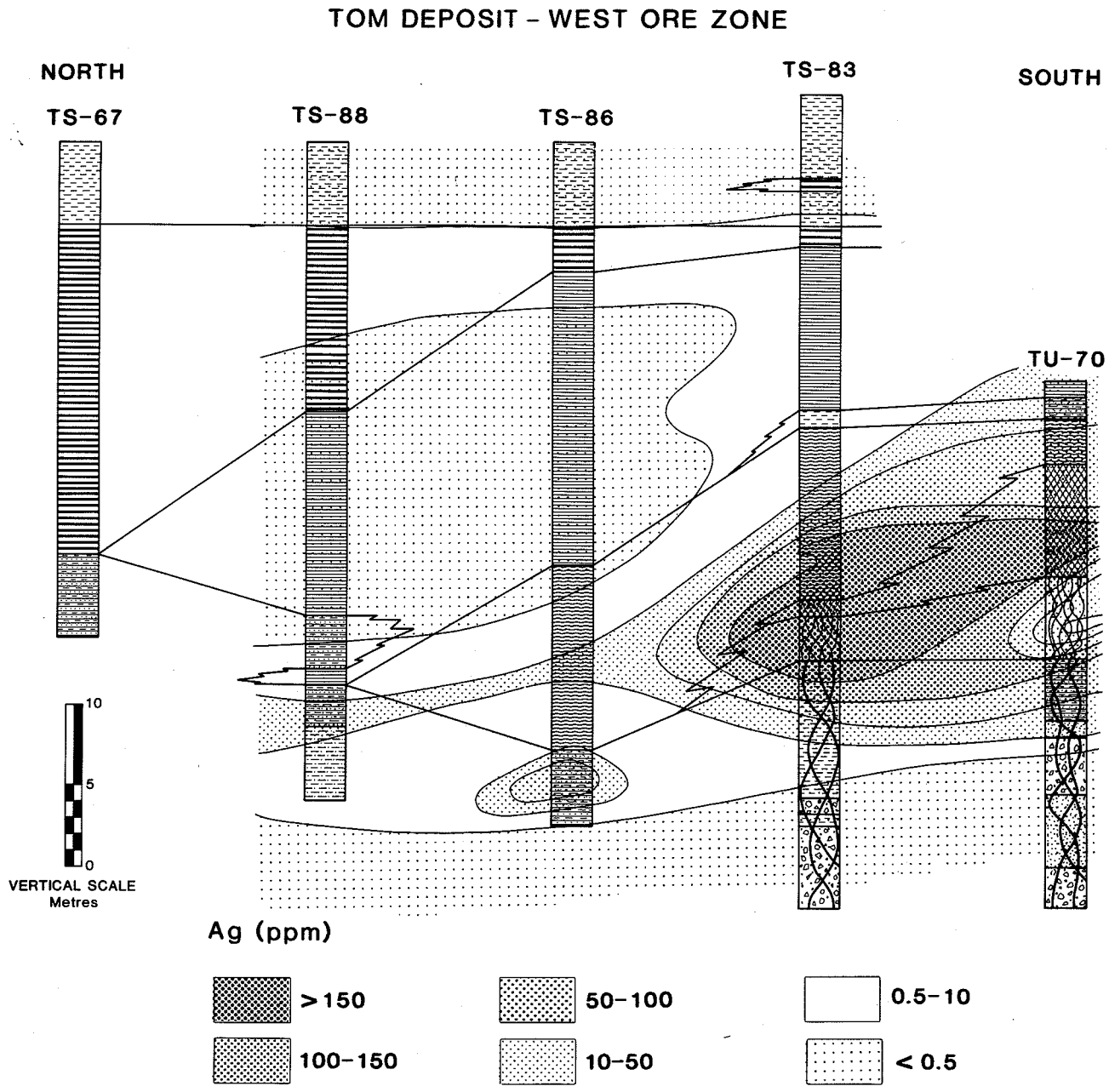

Figure 21 Contours of Ag contents plotted on a cross-section of Tom West Zone.

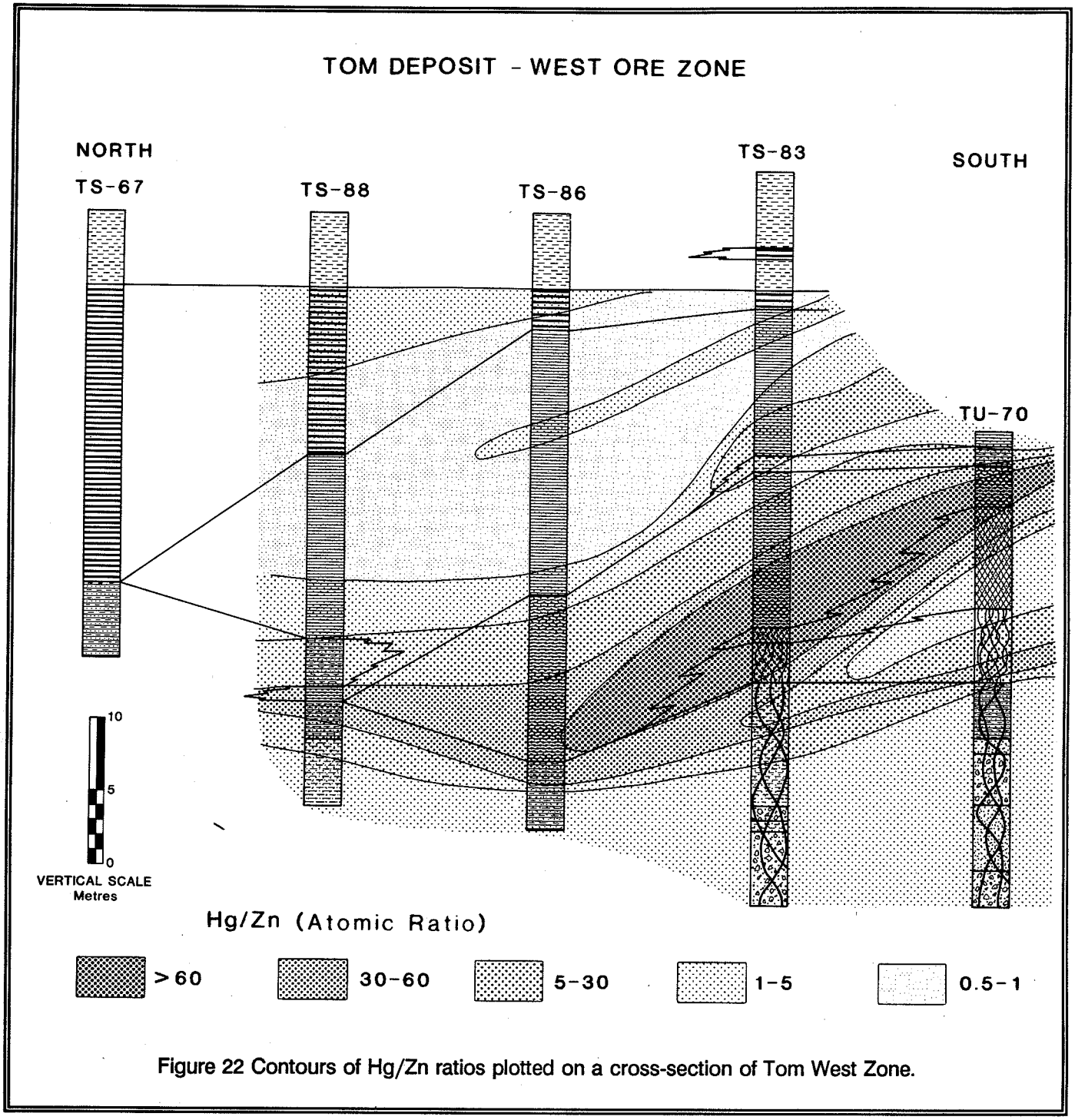

Figure 22 Contours of Hg/Zn ratios plotted on a cross-section of Tom West Zone.

Facies. The correlation of Ag with Pb is only moderate indicating that galena is not an important host for Ag in the West Zone.

Copper contents (Fig. 19) exceed 0.1 wt. % in the Vent Facies and the underlying feeder zone. Cu values in the sedimentary-hydrothermal facies are

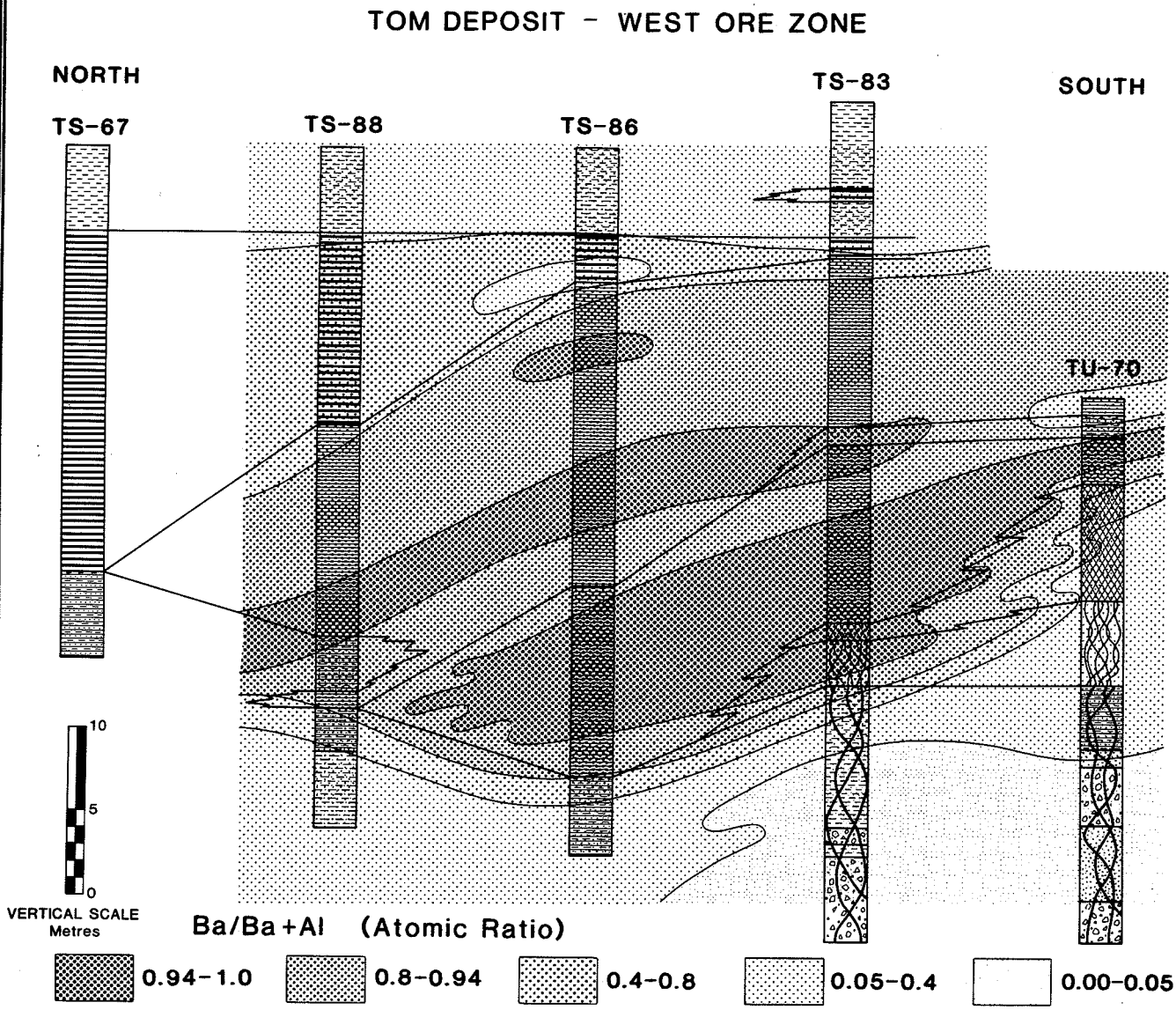

Figure 23 Contours of Ba/(Ba+Al) ratios plotted on a cross-section of the Tom West Zone.

typically less than 400 ppm. The Cu in the Vent Facies is partitioned between tetrahedrite and chalcopyrite. The chalcopyrite is commonly associated with pyrrhotite within the massive sulphide replacement zone and with ankerite-quartz veins cutting the underlying sedimentary rocks. Tetrahedrite is concentrated in the massive sulphide replacement zone.

Volatile Elements

The zonal distributions of Hg, As, Sb, Se and Cd about the vent complex are illustrated with contours plotted on a longitudinal sectional of the West Ore Zone. Mercury (Fig. 27), similar to Hg/Zn ratios, is spatially zoned about the vent complex and reaches contents

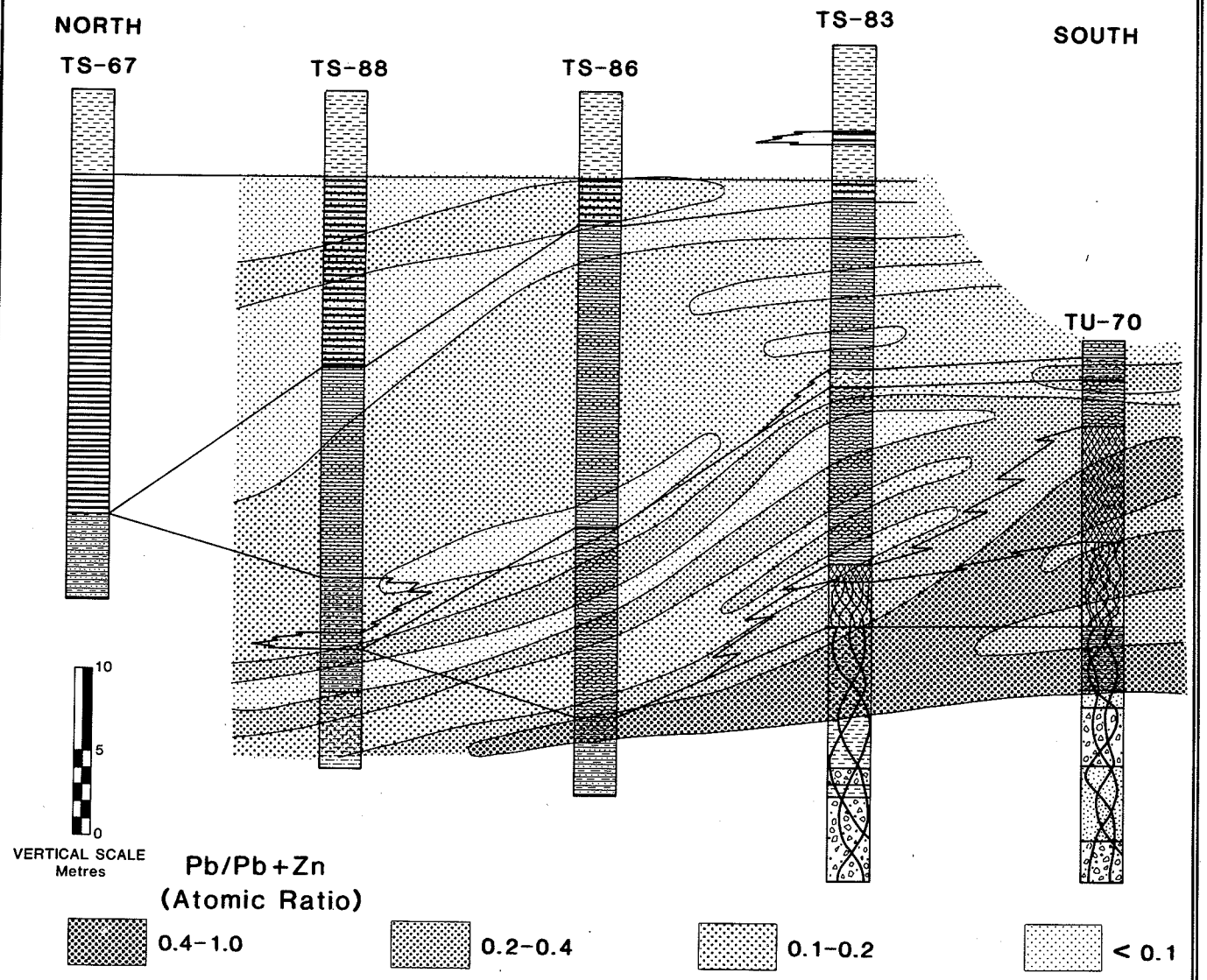

Figure 24 Contours of Pb/Pb+Zn ratios plotted on a cross-section of the Tom West Zone.

greater than 200 ppm in the Pink Facies. As stated earlier, most of the Hg resides in sphalerite formed during the partial replacement of hydrothermal sediments near the vent complex.

Antimony (Fig. 28) and As (Fig. 29) are concentrated within the Vent Facies where their abundances exceed 500 and 2500 ppm, respectively. Most of the Sb resides in tetrahedrite whereas As is bound by arsenopyrite.

Selenium shows a weak enrichment in the Pink Facies where Se contents can exceed 10 ppm. The form in which Se occurs is unknown. In other mineralized facies, the Se content is generally less than a local background value of 5 ppm for the enclosing sedimentary rocks.

Carbonate-associated Elements

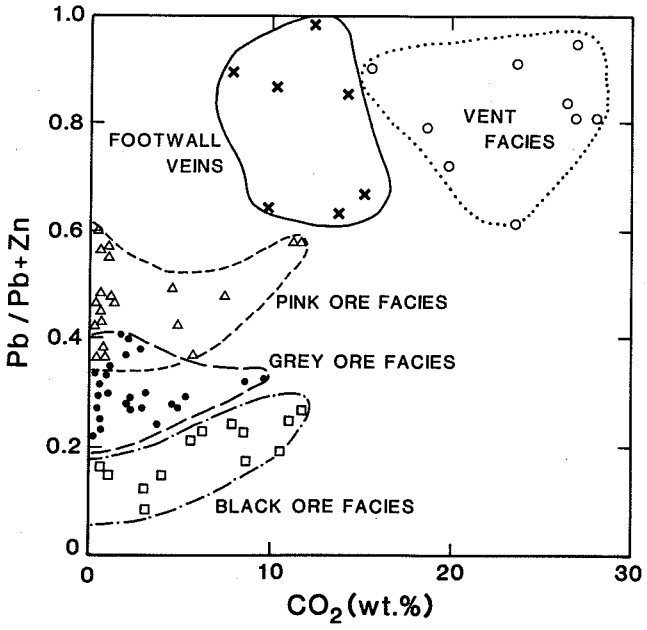

Figure 25 Binary plot of Pb/Pb+Zn versus CO_2 showing the chemical differences between the different ore facies and footwall feeder zones.

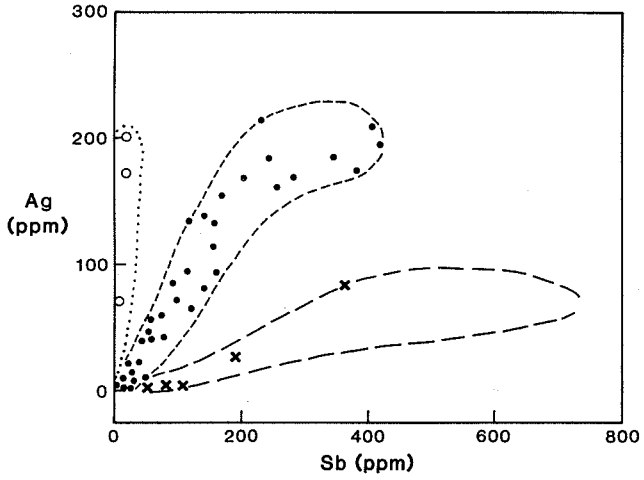

Figure 26 Binary plot of Ag versus Sb for all ore facies, Tom West Zone.

Elements forming or bound in carbonates include Fe^{2+}, Ba, Ca, Mg, Mn and Sr. This is an important suite of elements because of extensive carbonate replacement and veining in the vent complex. Siderite and ankerite are the dominant carbonates, particularly in the Vent Facies where barite is replaced by ferroan carbonates.

Contour plots of CO_2 on the West Zone longitudinal section (Fig. 30) reveal two areas of high carbonate content. The first area coincides with ferroan carbonate replacement within the vent complex and ankeritic sandstone beds in the footwall sand banded mudstone. The extent of carbonate replacement is shown by CO_2 values which exceed 20 wt. % in the Vent Facies (Fig. 30). The close spatial association of Mg, Ca and Mn (Fig. 31, 32, 33) with high CO_2 abundances reflects the occurrence of these elements in ferroan carbonates. The second area, located near the top of the West Zone, coincides with elevated Ca contents (Fig. 32) due to dominance of calcite over other carbonate minerals.

Strontium displays zonal patterns which are unique when compared to other carbonate-bound elements. Some of the highest Sr contents (up to 4900 ppm in DDH TS-86) coincides with calcium carbonate enrichment in a zone straddling the contact between the West Zone and the overlying carbonaceous mudstone. A second area of Sr enrichment corresponds to the Pink Facies near the margins of the vent complex where CO_2 gradients are large. The mineral hosting Sr in this area is unknown although barium carbonates have been documented in the Pink Facies. Bulk chemical distributions for Ba are difficult to interpret in terms of the controlling mineralogy because of the partitioning of Ba into barite, carbonates and feldspars.

Lithophile Elements

The major lithophile elements are bound for the most part in ambient marine sediments which occur interbedded with hydrothermal sediments within the mineralized zones. These sediments are composed of biogenic and inorganic silica precipitates and detrital minerals, the most important of which are clays. The contribution of hydrothermal silica is difficult to determine although the prograde solubility of quartz under hydrothermal conditions indicates a significant flux of hydrothermal silica into the water column from the Tom vents. The sluggish kinetics of silica precipitation coupled with the probable undersaturated nature of the water column with respect to dissolved silica would have delayed silica precipitation and

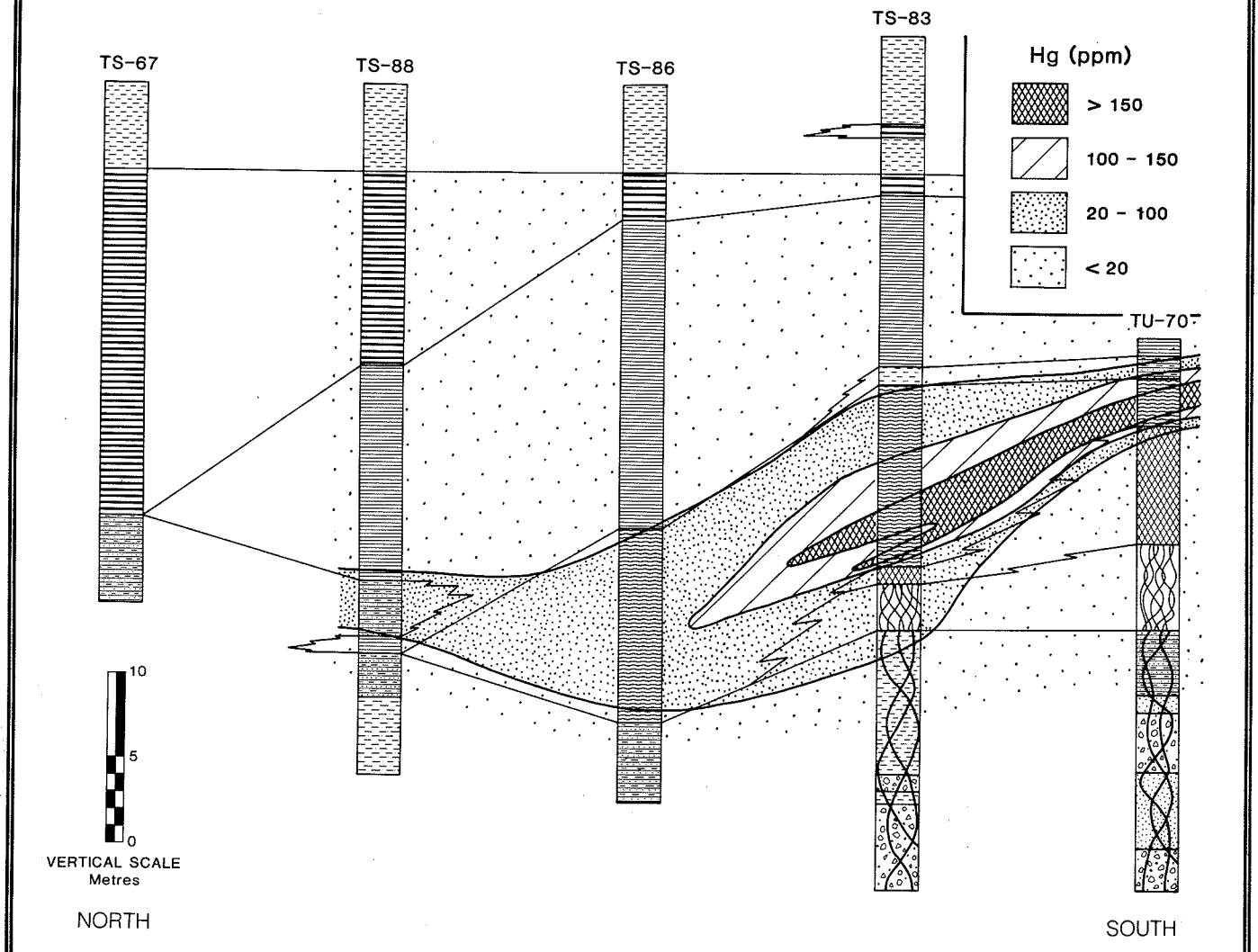

Figure 27 Contours of Hg contents plotted on a cross-section of the Tom West Zone.

therefore dispersed silica over a large area. As a result, the spatial relationship of hydrothermal-sedimentary silica to seafloor vents may be extremely subtle.

Within the vent complex, however, quartz in chert beds interbedded with hydrothermal sediments and in the underlying sedimentary rocks has clearly been dissolved by hydrothermal fluids. This is shown in a plot of $SiO_2/(SiO_2+Al_2O_3)$ ratios for a longitudinal section of the Tom West Zone (Fig. 34). SiO_2 was normalized to Al_2O_3 to remove the dilution effects of carbonate-sulphide flooding in the feeder zone. Al_2O_3 was selected as a normalizing major oxide because it is not easily mobilized under hydrothermal alteration. Uniform Al_2O_3 (Fig. 35), TiO_2 and K_2O contents across the vent complex support this interpretation. Furthermore, Ti/Al ratios in the mineralized facies (Fig. 36) which are the same as those in the enclosing sediments is further evidence that Al was not significantly redistributed during hydrothermal alteration.

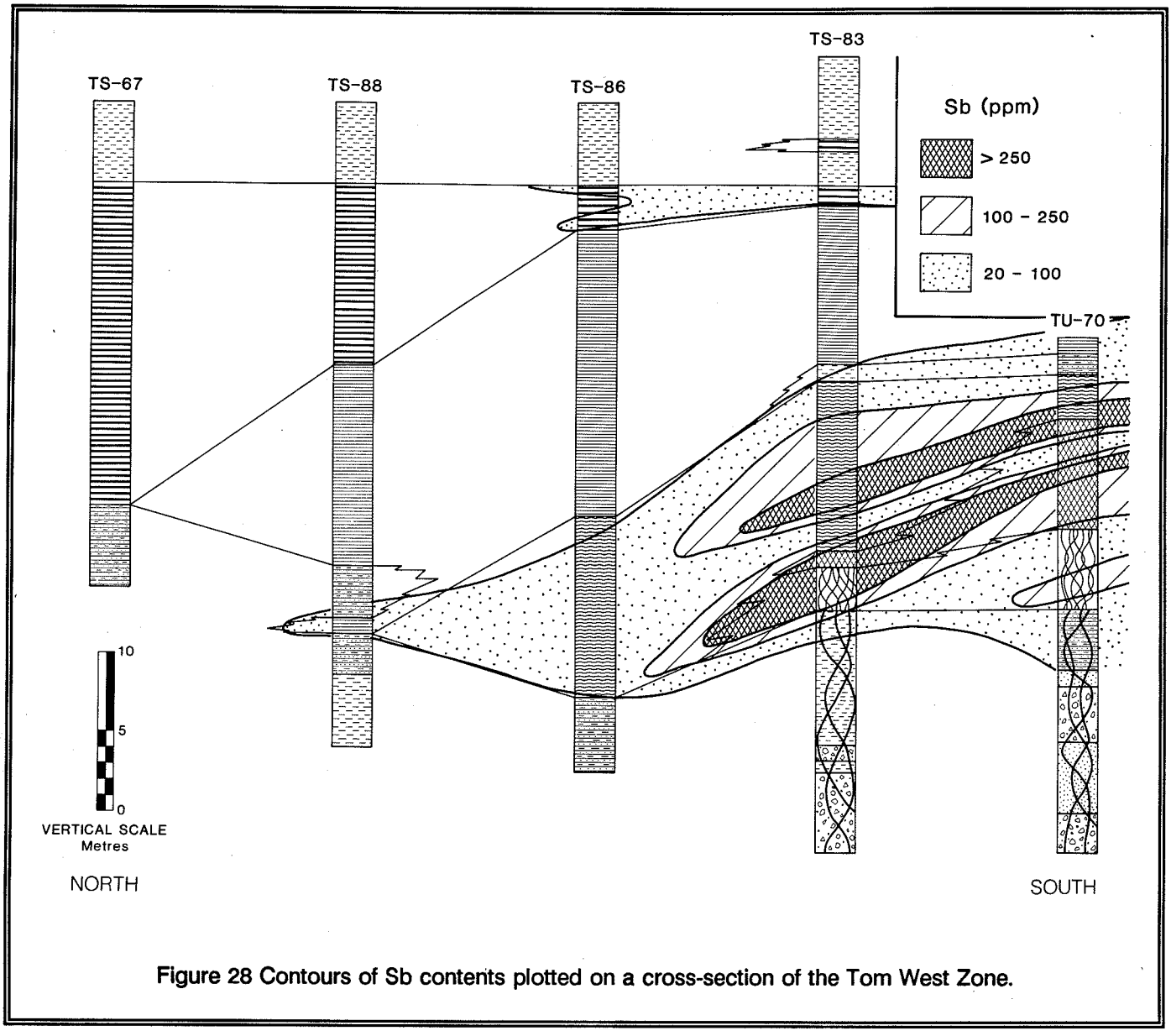

Figure 28 Contours of Sb contents plotted on a cross-section of the Tom West Zone.

Barium is enriched in the Pink and Grey Facies and depleted in the Black Facies and Vent Facies. The decrease in the Black Facies is controlled by a decrease in hydrothermal flux in the waning stages of the hydrothermal system. As a result, the proportion of this Facies represented by epiclastic sediment increases stratigraphically upwards and away from the vents. This is illustrated by contours of Ba/Ba+Al ratios plotted on a longitudinal section of the West Zone (Fig. 23). Within the Vent Facies, however, a decrease of barium is due to the replacement of barite by ferroan carbonates and sulphides as described earlier.

Isotopes

Sulphur Isotopes

$\delta^{34}S$ values were determined in galena, pyrite, pyrrhotite and barite from the West Zone and enclosing sedimentary rocks. Within the bedded barite-sulphide

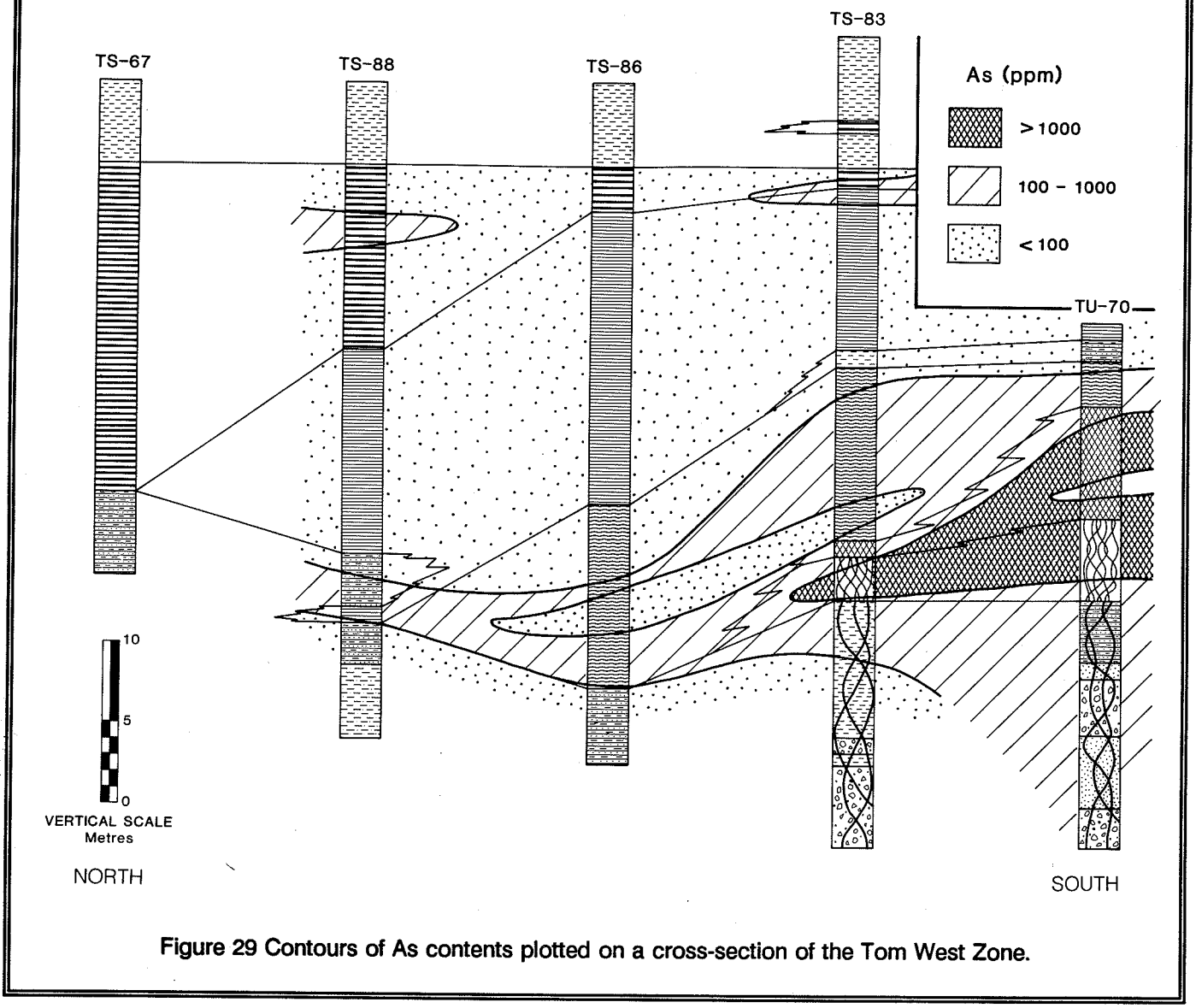

Figure 29 Contours of As contents plotted on a cross-section of the Tom West Zone.

facies, $\delta^{34}S$ values range between 17.7 and 25.7 per mil and fall within the range of Middle to Late Devonian seawater (Claypool et al. 1980; Goodfellow, 1987). Contours of sulphur isotope values for barite define two broad zones within the West Zone (Fig. 37), one with values greater than 22 per mil and a second with values greater than 20 per mil, separated by barite with values less than 20 per mil.

Within the Vent Facies, one sample from the outer margin has a value of 12.6 per mil which is considerably less positive than for barite from sedimentary-hydrothermal facies. The similarity of this value to $\delta^{34}S$ values for hydrothermal sulphides from the vent complex indicate that the sulphur in this barite sample probably formed by the oxidation of hydrothermal sulphides.

Values of $\delta^{34}S$ in galena, contoured on the West Zone longitudinal section, show a consistent trend from values less than 6 per mil in the Grey Facies to values greater than 12 per mil in the Vent Facies (Fig.

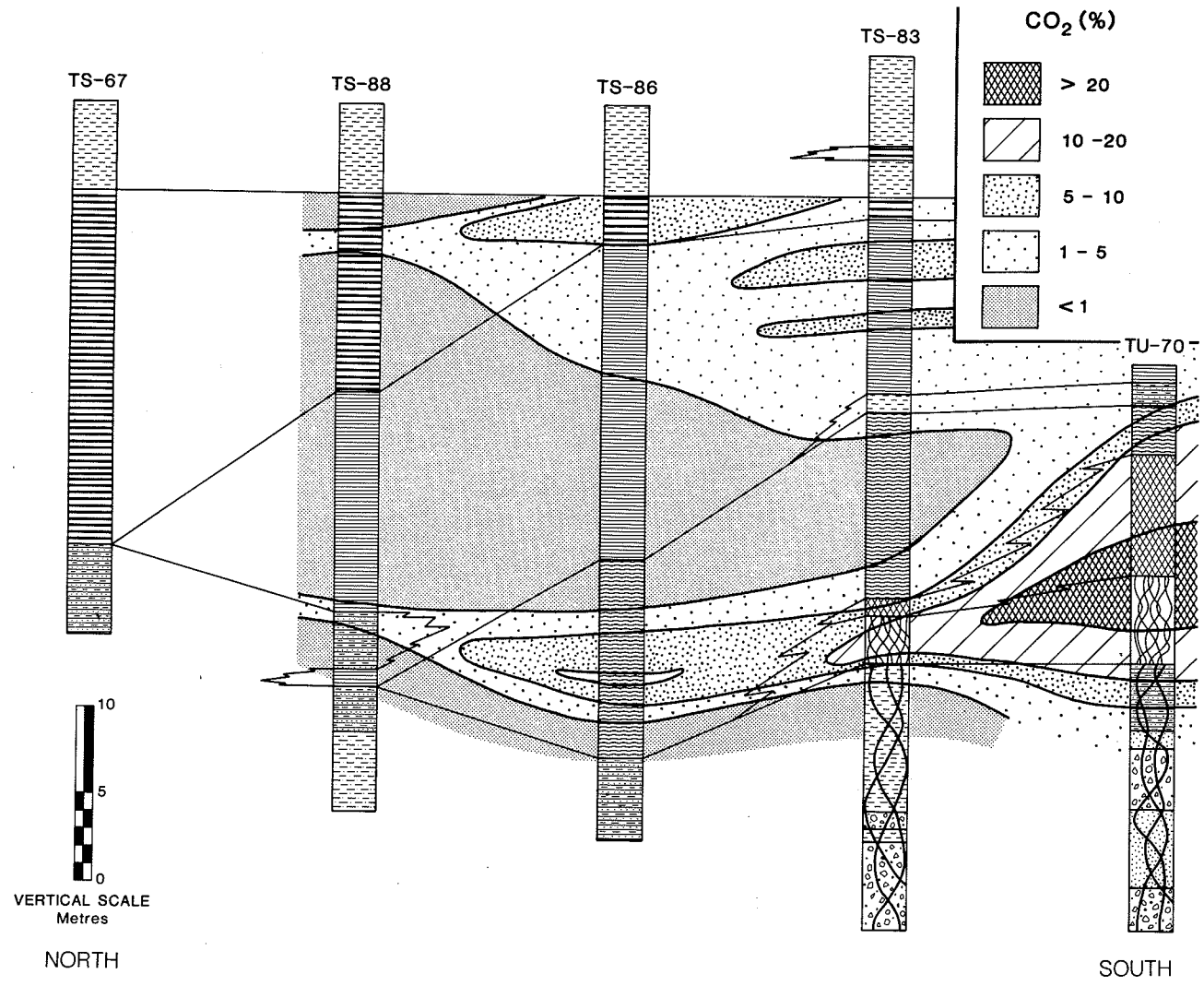

Figure 30 Contours of CO_2 contents plotted on a cross-section of the Tom West Zone.

38). This pattern of increasing values towards the vent complex is similar to the pattern for Pb/Pb+Zn ratios and corresponds to increased replacement of barite by galena. Values for pyrrhotite and pyrite within the Vent Facies are also isotopically heavy, ranging between 13.8 and 16.7 per mil, and 12.5 and 15.9, respectively.

Values of $\delta^{34}S$ in sedimentary pyrite range between 8 and 12 per mil in the underlying carbonaceous mudstone, the Grey and Black Facies, and the overlying cherty mudstone (TCh). The similarity of $\delta^{34}S$ values in pre-ore, post-ore and syn-ore sedimentary pyrite indicates that most of the sulphur was derived from the ambient water column. The fact that sulphur isotope values for galena and sedimentary pyrite are similar argues further for an ambient water column for sulphur bound in galena.

Within the Tom Sequence, $\delta^{34}S$ values in sedimentary pyrite increase systematically upwards, reaching maximum values of +28 per mil in the siliceous and carbonaceous mudstone unit (Unit TH). This trend

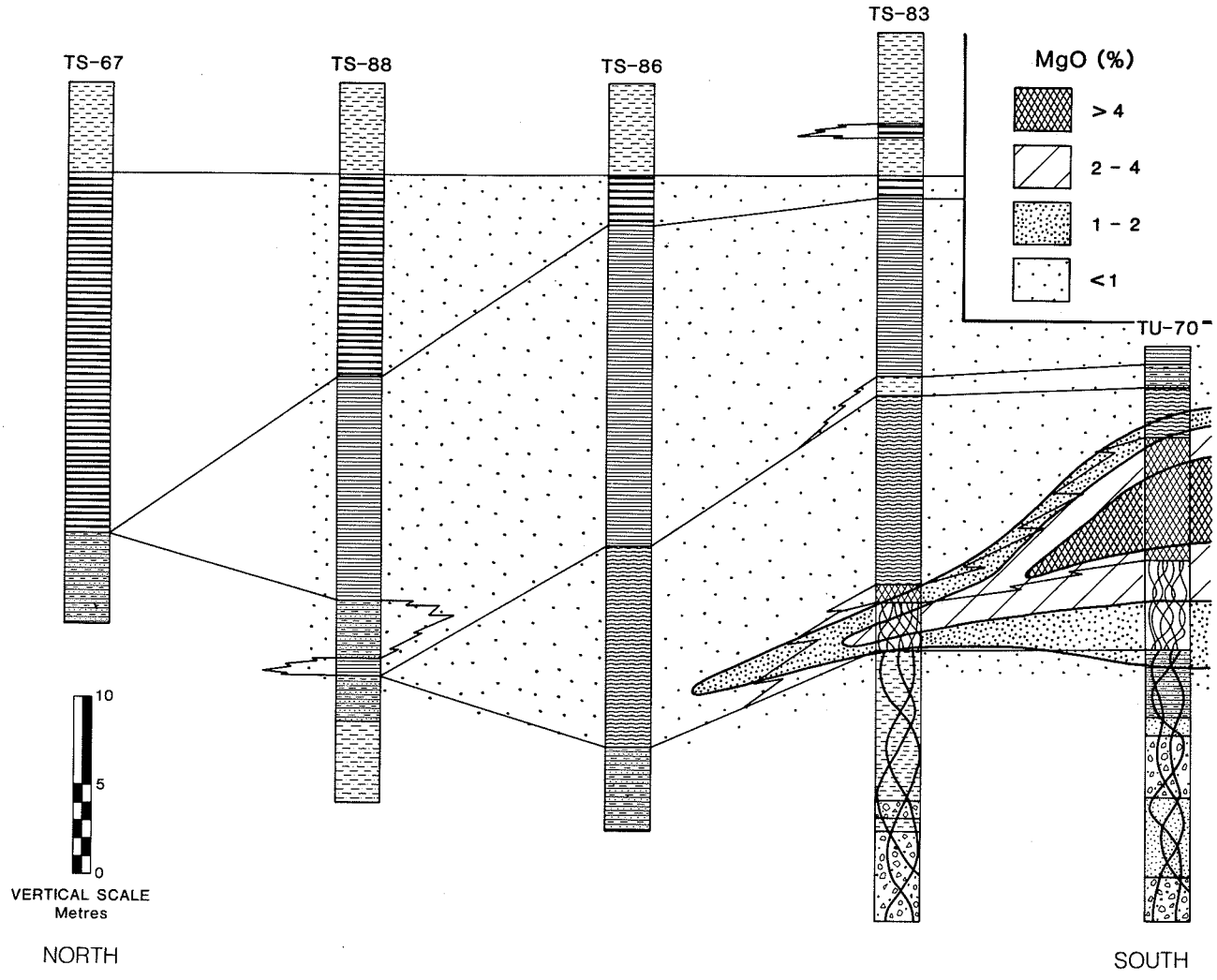

Figure 31 Contours of MgO contents plotted on a cross-section of the Tom West Zone.

of upward increasing $\delta^{34}S$ values in Middle-Late Devonian pyrite has been documented previously (Goodfellow and Jonasson, 1984) and interpreted to result from closed system bacterial sulphate reduction within the anoxic portions of a stratified and reduced water column.

The most likely source of heavy sulphur in sulphides from the Vent Facies is barite sulphate which was reduced to sulphide by reaction with a low fO_2, organic-buffered ore-forming fluid. This would account for the close correspondence of positive $\delta^{34}S$ values with low barite contents and replacement sulphides in the Vent Facies, and the marked increase of values towards the vent complex. Organic compounds were the most likely reductants because of the availability organic matter in the thick sequences of syn- and post-rift sedimentary rocks underlying the Selwyn Basin and the common association of high dissolved organic carbon contents with basinal sedimentary metalliferous fluids formed in cratonic settings. Negative $\delta^{13}C$ values in ferroan carbonates from the vent complex are direct

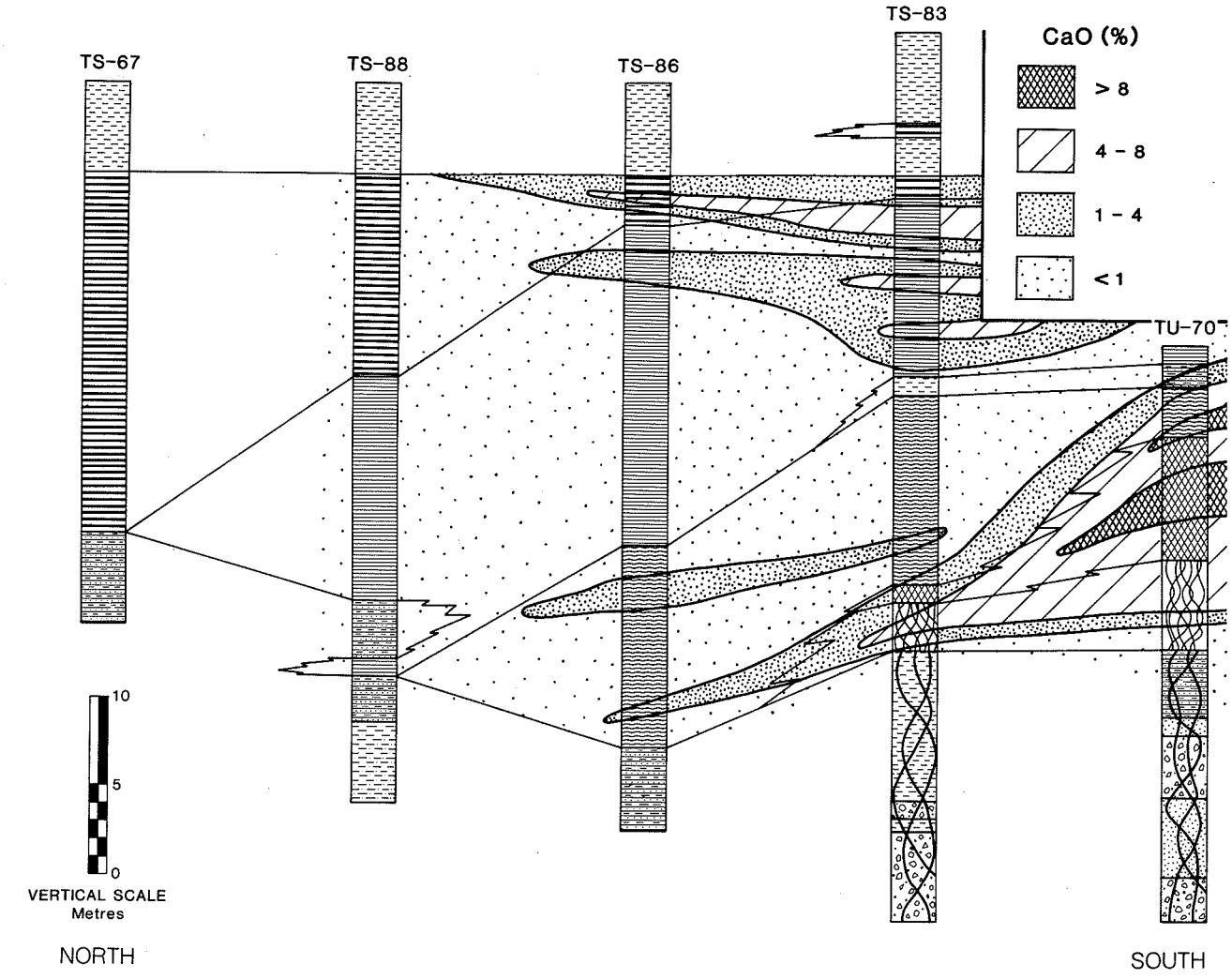

Figure 32 Contours of CaO contents plotted on a cross-section of the Tom West Zone.

evidence for organic carbon oxidation which probably accompanied the reduction of sulphate to sulphide.

The only other possible interpretation is that isotopically heavy sulphur was introduced with the hydrothermal fluids although there are several arguments against a hydrothermal source. First, if $\delta^{34}S$ values in dissolved sulphide were highly positive, than this isotopic signature should also be reflected in sedimentary sulphides. Instead, values in sedimentary sulphides are considerably less. Second, if the hydrothermal fluid was carrying reduced sulphur, then more sulphides would have been deposited in the feeder zone when the fluid chemistry changed rapidly due presumably to mixing with entrained seawater in the upflow zone. Third, the occurrence of pyrrhotite veins and the replacement of pyrite by pyrrhotite in the feeder zone indicates a low sulphur activity in the mineralizing fluids. And, fourth, the content of reduced sulphur that can be transported at moderate temperatures in the presence of base metals and at neutral pH is very limited (Goodfellow, 1987). It is unlikely therefore that

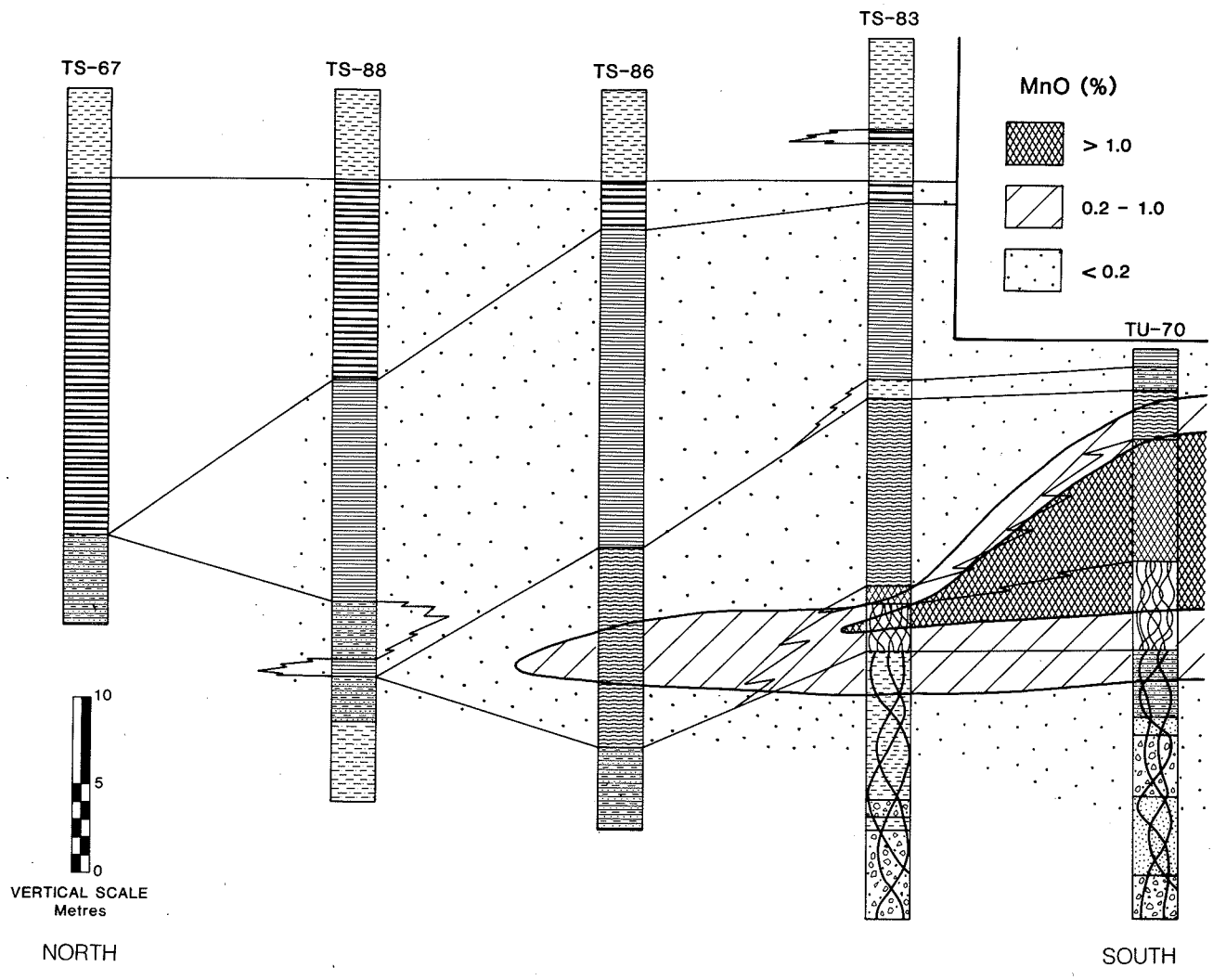

Figure 33 Contours of MnO contents plotted on a cross-section of the Tom West Zone.

reduced sulphur in the Vent Facies is of hydrothermal origin.

Carbon Isotopes

Values of $\delta^{13}C$ in ankerite range between -5.4 and -6.1 per mil. These values are considerably more negative than for Devonian seawater. Because of the preferential uptake of ^{12}C by organisms during CO_2 metabolism, Paleozoic organic matter typically displays δ^{13} C values that range between -22 and -32 per mil PDB (Schidlowski, 1982). Devonian organic carbon from the Selwyn Basin has values which range between -27.1 and -30.2 (Goodfellow and Jonasson, 1986). Carbonate minerals precipitated from dissolved carbonates produced by oxidation of organic matter will, therefore, have negative $\delta^{13}C$ values.

It is likely therefore that negative $\delta^{13}C$ values in ankerite from the Vent Facies reflect the oxidation of organic matter. Whether or not this reduction took place within the vent complex during bacterial sulphate

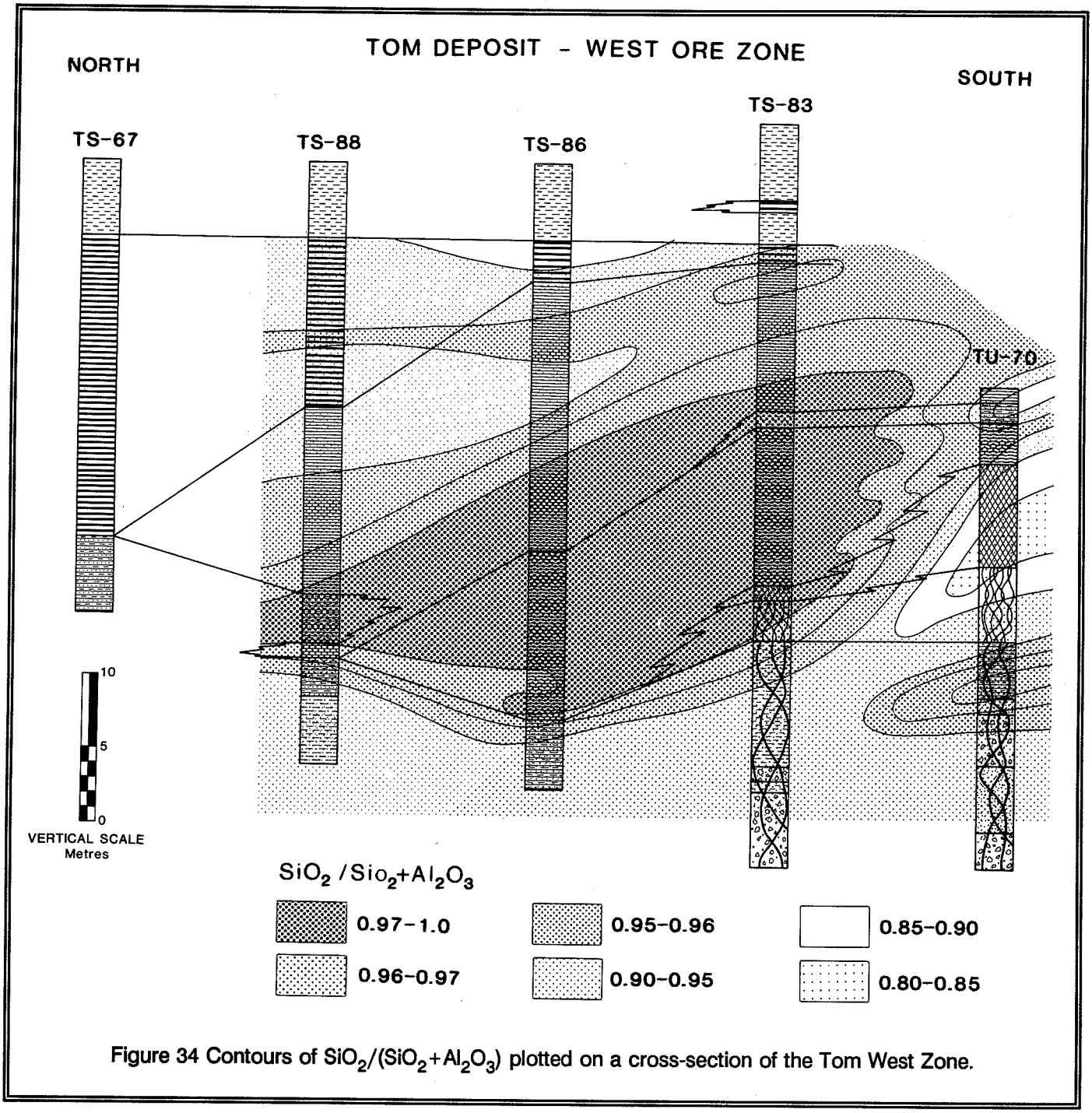

Figure 34 Contours of $SiO_2/(SiO_2+Al_2O_3)$ plotted on a cross-section of the Tom West Zone.

reduction, or in the hydrothermal fluid reaction zone is difficult to determine. The association of isotopically light ferroan carbonate with heavy sulphides and barite replacement supports the former.

Strontium Isotopes

Strontium isotope values in sedimentary barite from the West Zone range between 0.71298 and

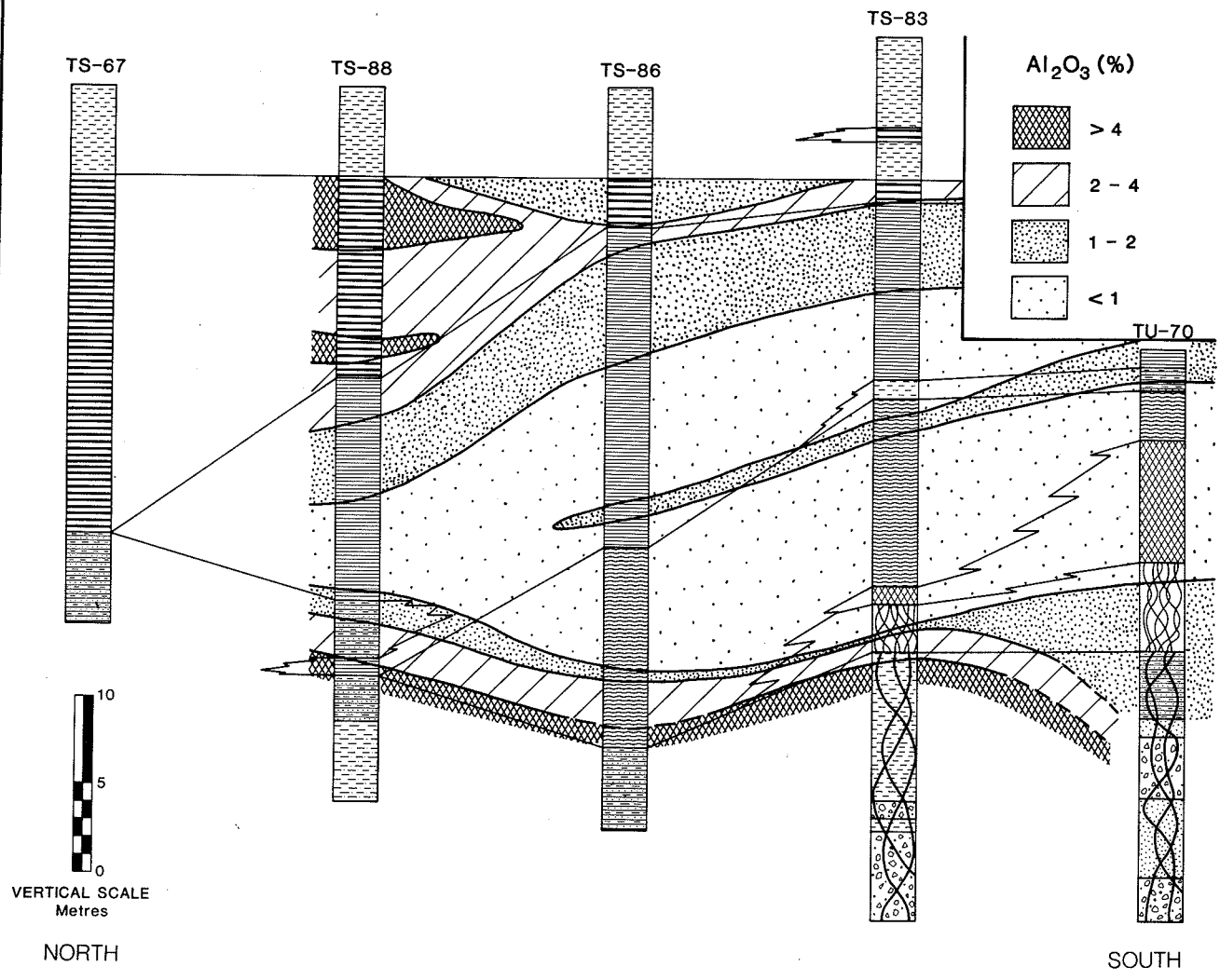

Figure 35 Contours of Al_2O_3 plotted on a cross-section of the Tom West Zone.

0.71511. These $^{87}Sr/^{86}Sr$ values, which can be regarded as an initial value because of the low Rb/Sr ratio of hydrothermal barite, are significantly more radiogenic than contemporaneous seawater and are similar to values for continental crust-derived Paleozoic shales in the Selwyn Basin. The highly radiogenic character of the Sr is further evidence for hydrothermal fluid generation in continental crust or, what is more likely, sediments derived from continental crust.

Within the West Zone, $^{87}Sr/^{86}Sr$ values display a gradual and systematic decrease from the base to the top of the mineralized zone, and from the vent complex to the distal margins. The zonation of $^{87}Sr/^{86}Sr$ ratios in the West Zone is controlled by the mixing of radiogenic Sr of hydrothermal origin with Sr in the ambient water column. An increase in the Sr(seawater)/Sr (hydrothermal fluid) mixing ratio away from the vent explains the decrease in isotopic ratios from proximal to

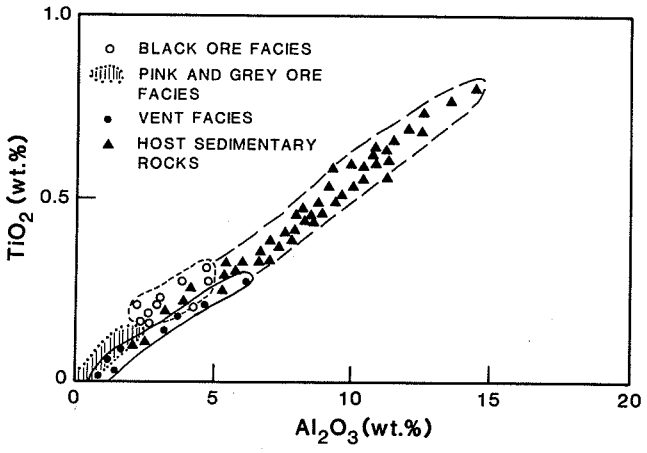

Figure 36 Binary plot of TiO_2 versus Al_2O_3 for mineralized and host rocks from the Tom West Zone.

distal barite facies.

The systematic upward decrease in $^{87}Sr/^{86}Sr$ ratios is, however, more difficult to explain. If the hydrothermal fluid behaved as a buoyant plume as indicated by the fluid inclusion measurements (Ansdell et al., 1989), then the systematic upward decrease could be controlled by a temporal decrease in Sr activity in the hydrothermal fluid which may reflect a gradual decrease in the temperature of the hydrothermal system. A decrease in the Sr activity of the hydrothermal fluid would increase the a(seawater Sr)/a(hydrothermal fluid) ratio at the time of barite precipitation and generate barite with less radiogenic initial strontium ratios. A decrease in the temperature of the hydrothermal system with time is supported by upward decreasing Pb/Pb+Zn and Ba/Zn+Pb ratios.

Lead Isotopes

Large (1981) reported $^{206}Pb/^{204}Pb$ ratios of 18.7-18.83, $^{207}Pb/^{204}Pb$ ratios of 15.7-15.81 and $^{208}Pb/^{204}Pb$ ratios of 38.67-38.92 for galena from the Tom deposit. These radiogenic ratios are consistent with the derivation of Pb from a radiogenic source. Although Large (1980) suggested that shales of the Selwyn Basin were the source of Pb, older continental sediments such as the Grit Unit cannot be ruled out on the basis of these data.

Fluid Inclusions

Ansdell et al. (1989) described two distinctive types of fluid inclusions in quartz and ankerite veins from the Vent Facies, Tom deposit. Type I consists of aqueous, two-phase inclusions which are dominant in ankerite, and Type II are CO_2-bearing, aqueous inclusions which are dominant in quartz; both types display highly variable degrees of filling.

Homogenization temperatures (T_h) in ankerite and quartz range from 194^0C to 272^0C (average = 258^0C +/-$33C^0$) and 157^0C to 335^0C (average = +/-$31C^0$), respectively. These results have been interpreted by Ansdell et al. (1989) in two ways. First, the T_h values give a measure of the temperature of the mineralizing fluids; and, second, the large range of T_h values may reflect variable leakage from the inclusions during deformation. The second interpretation appears to be preferred by the authors although the evidence supporting this choice is not given. If there has been significant leakage during subsequent tectonism, then the temperatures of the mineralizing fluids were probably considerably lower than measured T_h.

Aqueous inclusions in ankerite range in salinity between 5.0 and 18.3 equivalent wt. % NaCl with an average of 9.1 +/- equivalent wt. % NaCl. These salinities are similar to salinities of 4.1 to 14.1 equivalent NaCl (average = 9.4 +/- 1.7 equiv. NaCl) determined by Gardner and Hutcheon (1985) for the nearby, temporally equivalent Jason SEDEX deposit. The presence of other salts (e.g. $MgCl_2$, $CaCl_2$, $FeCl_2$) in both the Tom and Jason deposits is indicated by the lowering of the first melting temperature of ice.

GENESIS OF TOM DEPOSITS

The Tom Zn-Pb-Ag-barite sedimentary-hydrothermal deposits formed during a period of extensional tectonism in the Selwyn Basin. Regionally within the Selwyn Basin, tectonic instability is marked by abrupt thickness and facies changes, major gaps in the stratigraphic record and associated unconformities, diachronous stratigraphic relationships, the influx of coarse clastics derived from lower Paleozoic cherts uplifted elsewhere in the Basin, and the extrusion of mafic alkalic rocks during Middle and Late Devonian.

During the Middle to Late Devonian, the Selwyn Basin was bounded by the Mackenzie Carbonate

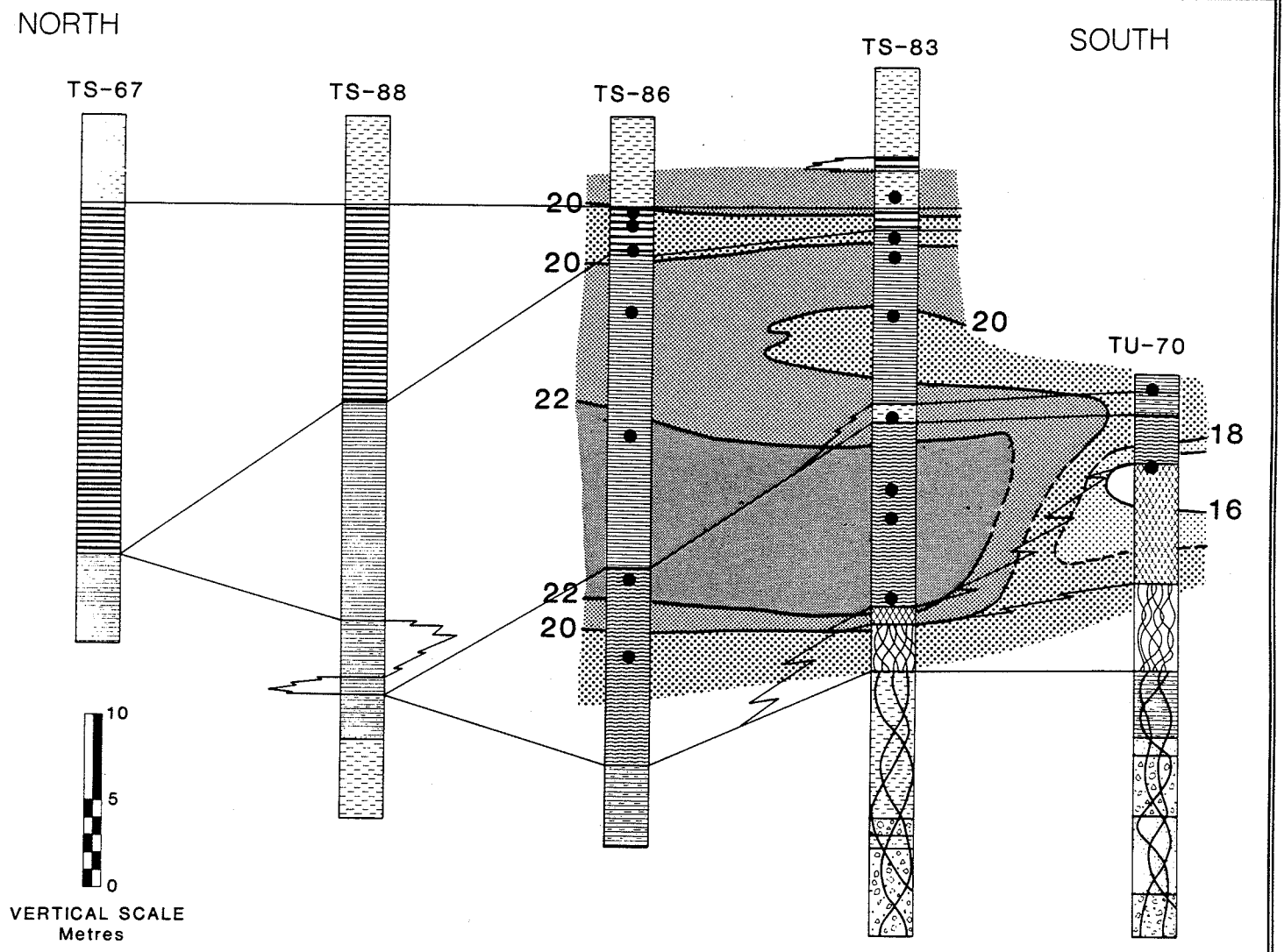

Figure 37 Contours of $\delta^{34}S$ values in barite plotted on a cross-section of the Tom West Zone.

Platform on the east and north, and by the Cassiar Platform to the west. The facies boundaries between shallow water carbonates and deeper water basinal sediments probably reflected a basin and arch geometry formed during the rifting of the craton in the Late Proterozoic and Early Cambrian. The sedimentary environment during the Middle and Late Devonian was characterized by starved sedimentation (except during episodes of turbidite influx) and anoxic (and H_2S-rich) bottom water conditions. Evidence for stagnant conditions during this time interval includes the absence of bioturbation, high organic carbon contents and S/C ratios, the paucity of bottom dwelling organisms and positive, upward increasing $\delta^{34}S$ values in pyrite (Goodfellow, 1987).

Locally within the Tom area, tectonic instability is marked by abrupt thickness and facies changes about a paleobathymetric high cored by chert pebble conglomerate. The juxtaposition of chert pebble conglomerate against younger sediments indicates major uplift in this area. This high, which probably

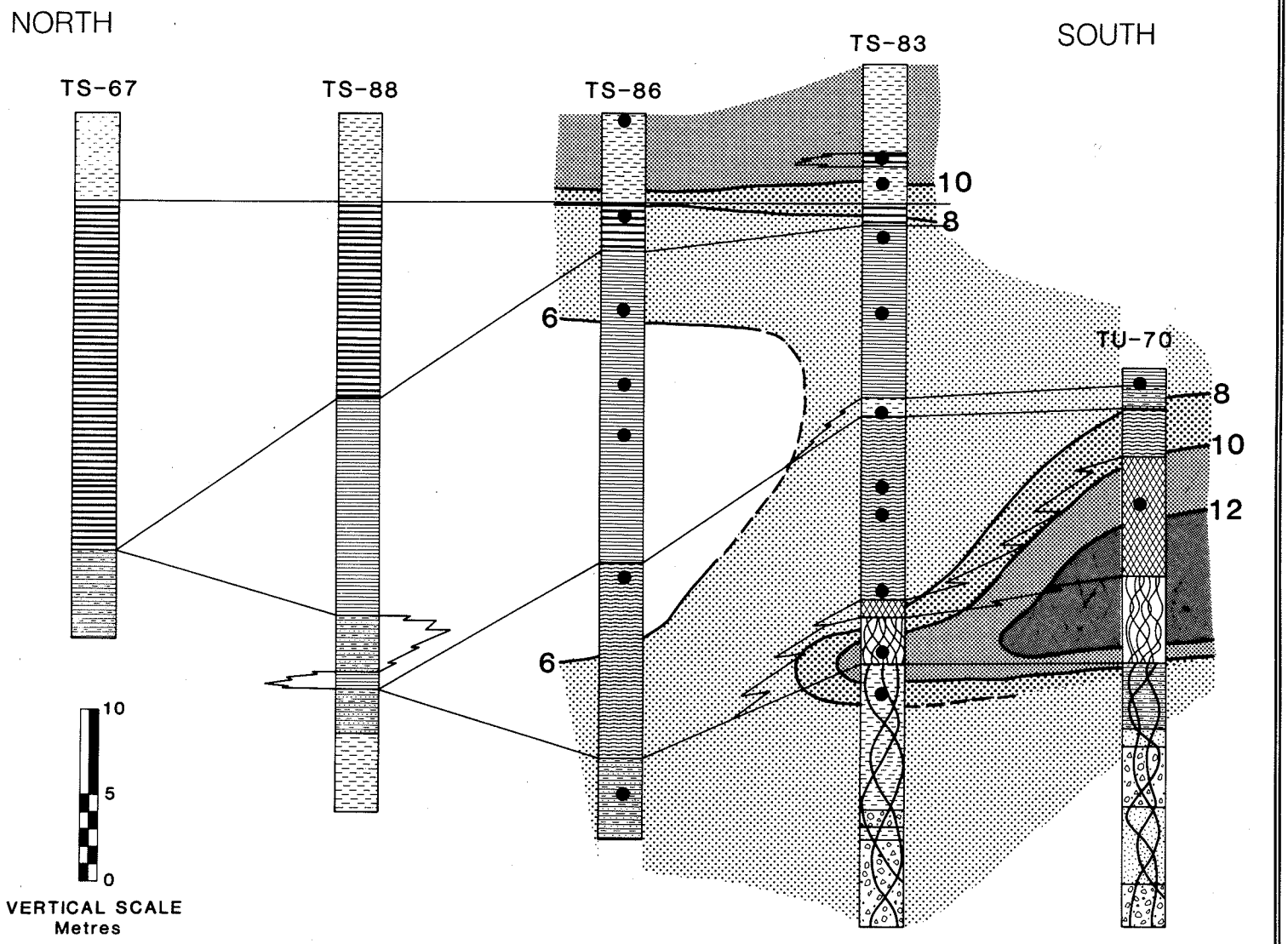

Figure 38 Contours of $\delta^{34}S$ values in galena plotted on a cross-sectoin of the Tom West Zone.

represents a horst structure formed during a period of widespread block faulting in the Selwyn Basin, exerted an important control on the sedimentation and the sites of venting and associated sulphide formation. This horst structure, which became a positive feature during sedimentation of the sand-banded mudstone overlying the chert pebble conglomerate, is reflected by wedges of locally derived debris flows which pinch out against this high and major slumping in the underlying sand-banded mudstone.

Stratiform sulphides formed in bathymetric lows on either side of the conglomerate high. Isopachs of sand-banded mudstone between the sulphide zones and underlying diamictite indicate a thickening of this lithology adjacent to the conglomerate high. Isopachs of the footwall cherty mudstone (Fig. 8) and the West Zone both show a maximum thickness flanking the conglomerate high. In the case of the cherty mudstone, this indicates a basinal control on the thickness of hemipelagic sediments.

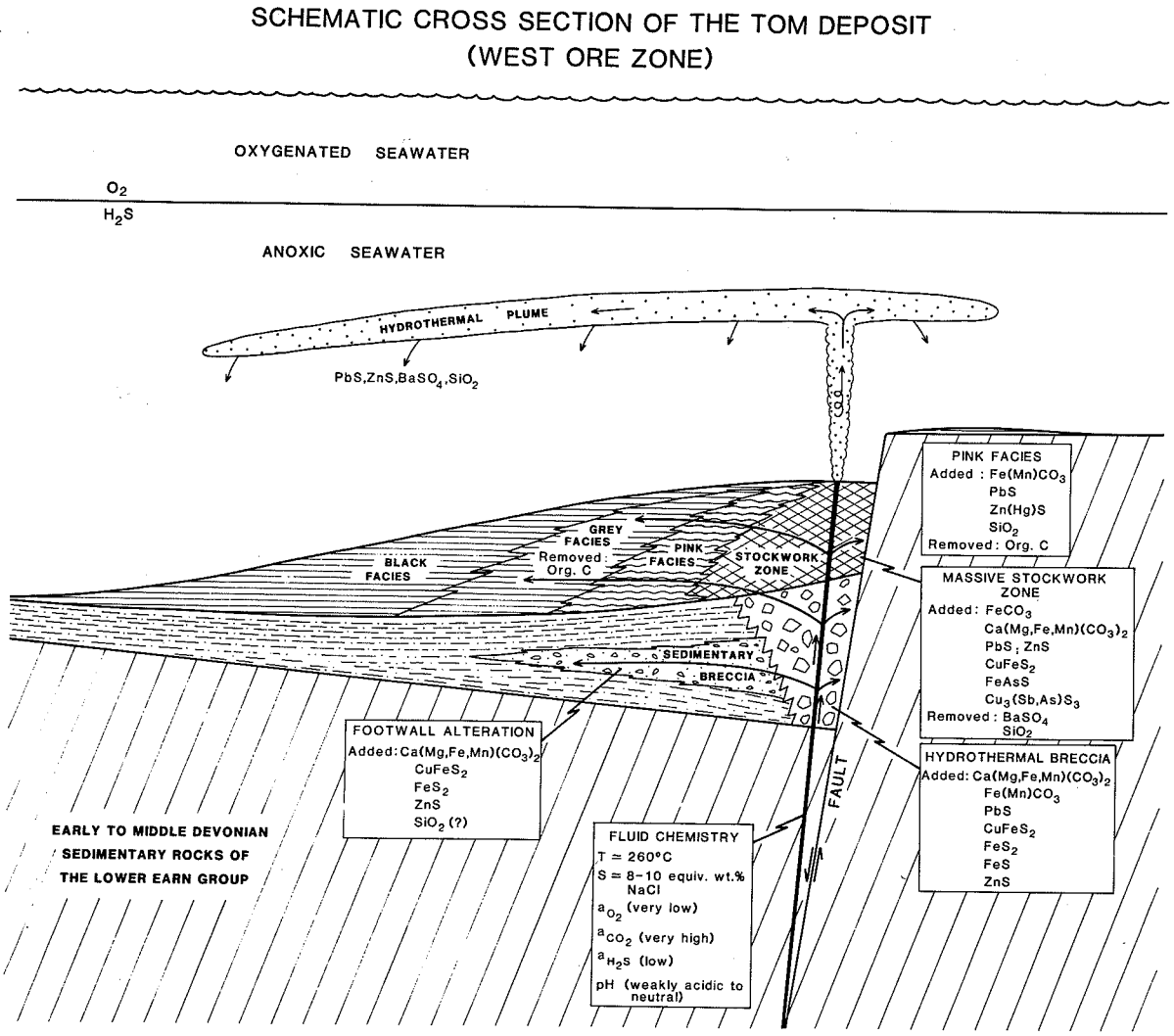

Figure 39 Schematic model of the Tom deposit highlighting the important processes including: a) block faulting, subsidence, fault scarp breccias, and basins formation; b) hydrothermal fluid venting along synsedimentary faults; c) hydrothermal alteration of the underlying sequence; d) replacement of sedimentary hydrothermal products overlying the vent and the formation of a replacement vent complex; e) fluid behavior upon discharge at seafloor, as constrained by fluid inclusion salinity/temperature data; f) hydrothermal depositional processes at the seafloor; and g) sources of metal, S, C, Sr and Ba (Goodfellow).

Although the West Zone thickens away from the paleo-high, reaches maximum thicknesses before thinning to the north, this does not necessarily indicate a basinal control. The fact that the geometry of the West Zone does not conform to the paleobathymetry during deposition of the sand-banded mudstone suggests that the deposits may represent mounds as opposed to sulphides filling depressions on the seafloor. This interpretation is supported by hydrothermal fluid densities measured from fluid inclusions which indicate that these fluids would behave as buoyant plumes and not bottom hugging brines. If the fluids were buoyant,

the major control on sulphide morphology is the position of the vent and not the seafloor bathymetry.

From the distribution of Vent Facies, venting was localized along a lenticular structure which extended for 100's of meters and defined the northern margin of the paleo-high. Although it is unlikely that the entire strike length of this structure was hydrothermally active at the same time, it is likely that hydrothermal fluids were discharged over a large strike length from vents that migrated or were active at different times. Sealing and capping the hydrothermal vent complexes would cause the sites of venting to migrate along the structure to vent sites less restricted.

The discharge of hydrothermal fluids into the Macmillan Pass graben has resulted in the formation of blanket deposits of sedimentary-hydrothermal sulphides and barite above and lateral to hydrothermal vents (Fig. 39). Based on densities measured in fluid inclusions, the vent fluids most likely behaved as buoyant plumes from which sulphides and barite precipitated during catastrophic mixing with ambient seawater. This is consistent with the sulphur isotope results which indicates an ambient seawater origin for sulphur bound in sedimentary barite and sulphides. As a result, it is possible that the Tom deposits formed mound-like bodies localized at and about vents. The lateral dimensions of the sulphide zones would then be controlled by the shape of the plume which in turn relates to density contrast, basinal currents and physical barriers such as the conglomerate high.

Sedimentary barite and sulphides deposited above active vents have been veined, brecciated and replaced by ferroan carbonate, pyrrhotite, galena, chalcopyrite, tetrahedrite and arsenopyrite during protracted flow-through of hydrothermal fluids. This has resulted in marked increases in ore grades and Pb/Pb+Zn ratios, and the contents of carbonate components (i.e., Ca, Mg, Sr, Mn, and CO_2) and volatile elements (i.e., As and Sb), and Pb/Pb+Zn ratios, and the removal of barite and silica. Highly positive $\delta^{34}S$ values in galena from the replacement zone (compared to sedimentary-hydrothermal galena distal to the vent) indicates that a significant component of this sulphur originated from the inorganic reduction of sedimentary barite sulphate during reaction with low-f_{O2} hydrothermal fluids. Further evidence for low contents of reduced sulphur include:

1) the predominance of ferroan carbonate over Fe sulphides in the vent complex,

2) the replacement of pyrite by pyrrhotite in the vent complex,

3) the low contents of hydrothermal sulphides in the underlying feeder zone despite evidence for rapid fluid evolution during fluid discharge, and

4) the limitation of transporting reduced sulphur and base metals together in moderate temperature basinal metalliferous fluids buffered at a high pH by sediments eroded from a sialic craton.

The lateral migration of hydrothermal fluids from the vent zone has resulted in the partial replacement of hydrothermal sediments by coarse grained Hg-rich sphalerite, crystalline galena and ferroan carbonate (Pink Facies) and the destruction of organic matter (Pink and Grey Facies). Below the massive replacement zone, the footwall sequence has been locally brecciated and silicified, and cut by veins of ferroan carbonate and minor sulphides. Furthermore, permeable chert pebble conglomerate and sand-banded mudstone have been invaded by hydrothermal fluids and cemented and partly replaced by ankerite and euhedral pyrite. Because the area of ankerite/pyrite alteration below the deposits is large, extending beyond the lateral limits of the deposit, it provides a large exploration target. Furthermore, an increase in the content of ankerite and pyrite towards the vent suggests that it may be used to pinpoint vent sites.

The hydrothermal system at Tom deposits was extremely long-lived, reaching a maximum during the formation of the bedded sulphide-barite ores and decaying gradually over the millions of years represented by the overlying cherty mudstones and cherts. As a result, the hanging wall sequence is characterized by intervals of delicately interlaminated pyrite and barite with sphalerite. Zinc contents, which range up to thousands of ppm, are considerably elevated compared to background shales from the Selwyn Basin (Goodfellow et al., 1983), and probably formed by the discharge of low-temperature hydrothermal fluids into the basin. The non-uniform distribution of sulphide/ barite laminae indicates that the hydrothermal system behaved episodically throughout most of the Frasnian. From an exploration viewpoint,

the mineralogically and geochemically anomalous sedimentary rocks overlying the Tom deposit constitute a large exploration target. Furthermore, anomalous post-ore sediments are products of a prolonged hydrothermal system which characterizes many SEDEX deposits, including the Howards Pass (Goodfellow and Jonasson, 1986) and Sullivan (Hamilton et al., 1983) Zn-Pb deposits.

ACKNOWLEDGEMENTS

The work of many geologists with H.B.M. and S. Ltd., Cominco Ltd. and the Geological Survey of Canada has contributed to the data presented here. Our thanks are given to Hudson's Bay Mining and Smelting Ltd. and Cominco Ltd. for permission to publish this paper. We especially want to thank Bob Turner and John Lydon for stimulating discussions on the Tom deposit in particular and SEDEX deposits in general.

We are also grateful to Jennifer Shaw, Andy Douma and the cartography group at the Geological Survey of Canda for diagram preparation, to Conrad Gregoire and Gwendy Hail for supervising chemical analyses, and to Kate Grapes and Dan Richardson for providing able field assistance.

REFERENCES

Abbott, J.G., 1982, Structure and stratigraphy of the Macmillan fold belt: evidence for Devonian faulting. Open File Report, Exploration and Geological Services Division, Department of Indian and Northern Affairs, Whitehorse, Yukon, 16p.

Abbott, J.G., 1983. Geology of the Macmillan fold belt. Open File Report, Exploration and Geological Services Division, Department of Indian Affairs and Northern Development, Whitehorse, Yukon, 3 maps and legend, scale 1:50,000.

Abbott, J.G., Gordey, S.P., and Tempelman-Kluit, D.J. 1986: Setting of stratiform sediment-hosted lead-zinc deposits in Yukon and northeastern British Columbia; in Mineral Deposits of Northern Cordillera, J.A. Morin (ed.), Canadian Institute of Mining and Metallurgy, Special Volume 37, p. 1-18. (this volume): Setting of stratiform, sediment-hosted lead-zinc deposits in Yukon and northeastern British Columbia.

Ansdell, K.M., Nesbitt, B.E. and Longstaffe, F.J., 1989. A fluid inclusion and stable isotope study of the Tom Ba-Pb-Zn Deposit, Yukon Territory, Canada. Economic Geology, v. 84, p. 841-856.

Blusson, S.L., 1974. Operation Stewart (northern Selwyn Basin): Mount Edni (106A), Bonnet Plume Lake (106B), Nadaleen River (106C), Lansing (105 N) and Niddery Lake (105O). Geological Survey of Canada, Open File 205.

Carne, R.C., 1976, Stratabound barite and lead-zinc-barite deposits in eastern Selwyn Basin, Yukon Territory. Open File Repor EGS 1976-16, Dept. of Indian and Northern Affairs, 41 pp.

Carne, R.C., 1979. Geological setting and stratiform mineralization, Tom claims, Yukon Territory. Department of Indian and Northern Affairs, Report 1979-4, 30p.

Claypool, G.E., Holser, W.T., Kaplan, I.R., Sakai, H. and Zak, I., 1980, The age curves of sulfur and oxygen isotopes in marine sulfate and their mutual interpretation: Chem. Geology, v. 28, p. 199-260.

Gardner, H.D., and Hutcheon, I., 1985, Geochemistry, minerology and geology of the Jason Pb-Zn deposits, Macmillan Pass, Yukon, Canada: Econ. Geol., v. 80, p. 1257-1276.

Goodfellow, W.D., Jonasson, I.R. and Morganti, J.M., 1983. Zonation of chalcophile elements about the Howards Pass (XY) Zn-Pb deposit, Selwyn Basin. Journal of Geochemical Exploration, v. 19, p.503-542.

Goodfellow, W.D. and Jonasson, I.R., 1984. Ocean stagnation and ventilation defined by $\delta^{34}S$ values in pyrite and barite, Selwyn Basin, Yukon. Geology, v. 12, p. 583-586.

Goodfellow, W.D. and Jonasson, I.R., 1986. Environment of formation of the Howards Pass (XY) Zn-Pb deposit, Selwyn Basin, Yukon. In J.A. Morin (Ed.), Minerla Deposits of the Northern Cordillera, Canadian Institute of Mining and Metallurgy, Special Volume 37, p. 19-50.

Goodfellow, W.D., 1987. Anoxic stratified oceans as a source of sulphur in sediment-hosted stratiform Zn0Pb Deposits (Selwyn Basin, Yukon, Canada), Chemical Geology, v. 65, p.359-382.

Gordey, S.P., 1981. Geology of the Nahanni map area, Yukon Territory and District of Mackenzie. Geological Survey of Canada, Open File 780.

Gordey, S.P., Abbott, J.G. and Orchard, M.J., 1982. Devono-Mississippian (Earn Group) and younger strata in east-central Yukon. In Current Research, Part B, Geological Survey of Canada, paper 82-1B, p. 93-100.

Gordey, S.P., Abbott, J.D., Tempelman-Kluit, D.J. and Gabrielse, H., 1987. "Antler" clastics in the Canadian Cordillera. Geology, V. 15, p. 103-107.

Hamilton, J.M., Bishop, D.T., Morris, H.C., and Owens, O.E., 1982, Geology of the Sullivan orebody, Canda, in Precambrian sulphide deposits (H.S. Robinson Memorial Volume): Hutchinson, R.W., Spence, C.D., and Franklin, J.M., eds., Geological Association of Canada, Special Paper 25, p. 597-665.

Large, D., 1981, On the geology, geochemistry and genesis of the Tom Pb-Zn-Barite deposit Yukon Territory, Canada, unpublished Ph.D thesis, Technischen Universität Carolo-Wilhelmina Zu Braunschweig, 153 p.

McClay, K.R. and Bidwell, G.E., 1986. Geology of the Tom deposit, Macmillan Pass, Yukon. In J.A. Morin (Ed.), Mineral Deposits of the Northern Cordillera, The Canadian Institute of Mining and Metallurgy, Special Volume 37, p. 100-115.

Schidlowski, M., 1982. Content and isotopic composition of reduced carbon in sediments. IN: Mineral Deposits and the Evolution of the Biosphere, H.D. Holland and M. Schidlowski (Editors), Spinger Verlag:New York, p. 103-122.

Turner, R.J.W., 1986. Genesis of stratiform lead-zinc deposits, Jason property, Macmillan Pass, Yukon. Ph.D. thesis, Stanford University, Stanford, 205 p.

Turner, R.J.W. , Goodfellow, W.D. and Taylor, B.E., 1989. Isotopic geochemistry of the Jason stratiform sediment-hosted zinc-lead deposit, Macmillan Pass, Yukon. In: Current Research, Part E, Geological Survey of Canada, Paper 89-1E, p. 21-30.

Turner, R.J.W. and Rhodes, D., 1990. Geology of the the Boundary Creek deposit. In: Current Research, Part E, Geological Survey of Canada, Paper 90-1E, p.

RECENT DEVELOPMENTS IN THE GEOLOGIC UNDERSTANDING OF THE MACTUNG TUNGSTEN SKARN DEPOSIT[1]

DOROTHY ATKINSON
Department of Indian Affairs and Northern Development
Exploration and Geology
Box 150, Yellowknife
Northwest Territories
X1A 2R3

DONALD J. BAKER
Hornestake Mining Company
1726 Cole Boulevard
Golden, Colorado 80401

ABSTRACT

Tungsten-bearing skarn at MacTung, located on the Yukon-Northwest Territories border at latitude 63° 17', is hosted by Cambrian and Lower Ordovician limestones. The Lower ore zone occurs within a limestone slump breccia which directly overlies early Cambrian clastic rocks. The Upper ore zone, located approximately 100 m above the Lower ore zone, is composed of three skarn lenses developed within limestone beds interbedded with unmineralized pelite.

Low-grade regional metamorphism and deformation prior to skarn formation produced weak recrystallization and development of a locally pronounced slaty cleavage and a large overturned asymmetric fold. Hydrothermal activity is evidenced at the weakest stage by bleaching of otherwise black marbles and metaclastic rocks. Approaching the ore zones, hydrothermal alteration of marbles produced three distinct, concentric skarn zones: a peripheral zone of garnet and garnet-pyroxene skarn with abundant remnant bleached marble; an intermediate zone of pyroxene skarn, with negligible remnant marble; a central zone of pyrrhotite-pyroxene skarn. Scheelite and chalcopyrite abundance increases progressively toward the central pyrrhotite-pyroxene skarn zone.

The Cirque Lake stock, a composite biotite quartz monzonite intrusion exposed north and up-dip of the deposit, has previously been considered the source of hydrothermal fluids. Recent data suggest that the MacTung deposit is only coincidentally located near the margin of this stock. Quartz vein densities and orientations, location of pegmatites and aplites, patterns of skarn zoning, alteration and bleaching of metaclastic rocks and the systematic up-dip, up-section stacking of mineralization in each limestone-rich unit all indicate hydrothermal fluids were derived from a source at depth, south of the deposit.

Introduction

MacTung is the largest tungsten deposit in the free world. Located 255 km northeast of Ross River, 11 km off the North Canol road, it crops out on Mt. Allen in the Selwyn Mountains on the Yukon-Northwest Territories border at latitude 63° 17'. The deposit was discovered in 1962 during a regional exploration program by Southwest Potash Corporation, a subsidiary of American Metals Climax, now AMAX Inc. Subsequent surface and underground geologic work on the property has identified Lower and Upper ore zones in which scheelite occurs within skarned limestone within a Lower Paleozoic pelitic-limestone sequence.

The sequence is intruded by a composite biotite quartz monzonite stock of Cretaceous age, the MacTung pluton of Anderson (1982, 1983) or the Cirque Lake stock of Harris (1977).

---

[1] (Reprinted from Atkinson and Baker, 1986)

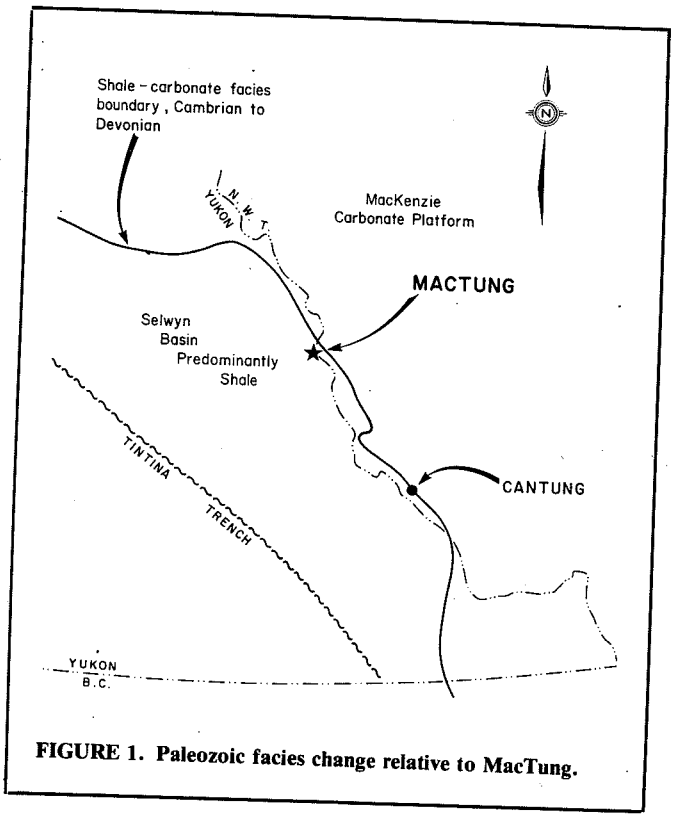

FIGURE 1. Paleozoic facies change relative to MacTung.

The close spatial association with the tungsten deposit, the presence of abundant accessory garnet and quartz-tourmaline veins within the Cirque Lake stock led previous workers to suggest that hydrothermal fluids originated from this stock. During 1982 and 1983, the authors conducted a detailed study of the deposit and concluded that this simple interpretation is inconsistent with four critical geological observations:

1. No ore is developed in contact with the stock.

2. Hydrothermal alteration is relatively weak adjacent to the stock, and alteration zones are discordant to the stock.

3. Veining and alteration of the stock margin itself is rare close to the ore zones.

4. The stock has steeply dipping contacts, with the apex of the stock, where hydrothermal fluids would be expected to have accumulated, located hundreds of metres up-section and up-dip of ore.

Regional Geology

MacTung is located within a facies change that defines the Paleozoic continental margin. To the northeast are Lower Cambrian - Middle Devonian shelf carbonates of MacKenzie Platform and to the southwest are Early Ordovician - Devonian fine-grained pelites of Selwyn Basin (Abbott, 1982) (Fig. 1). At MacTung, the zone of transition is marked by alternating beds of pelite, limestone and limestone slump breccia which make up a highly condensed Cambro-Ordovician succession.

Orogeny during the Jura - Cretaceous included regional folding, metamorphism and development of slaty cleavage throughout Selwyn Mountains. MacTung is located in a mildly folded area between an imbricately thrusted zone to the west and a strongly folded zone to the south (Fig. 2). Numerous late-to-post-tectonic granitic plutons intrude this orogenic belt. A number of skarn tungsten deposits are associated with these Cretaceous plutons and collectively define the Selwyn Tungsten Belt (Cathro, 1969; Dick and Hodgson, 1982.

Stratigraphy

The sedimentary sequence at MacTung consists of nine mappable units designated alpha-numerically 1, 2B, 3C, 3D, 3E, 3F, 3G, 3H and 4 (Fig. 3).

Unit 1, the lowermost unit exposed on the property, is a heterogeneous brown to grey, thinly to moderately bedded clastic unit composed of interbedded mudstone, shale, siltstone and greywacke. The unit is considered to be of lowermost Cambrian age (Abbott, 1983, pers. comm.). However, confirmation of this age must await more definite work on the Hadrynian - Cambrian contact.

Unit 2B, host to the Lower ore zone, is highly variable in thickness and composition. The unit is characterized by the presence of limestone slump breccias which appear to have formed as a series of coalescing debris fans at this stratigraphic level. It is correlated with the Lower Cambrian Sekwi Formation. In outcrops on the North Face of Mt. Allen, 20 m of dominantly well-bedded, fine-grained limestones and clastics with interbedded slump breccias are interpreted to represent the upslope extension of 35 m of chaotic, medium to light grey limestone slump breccia exposed in underground workings. Down dip, these slump breccias abruptly thin and fragment size decreases as

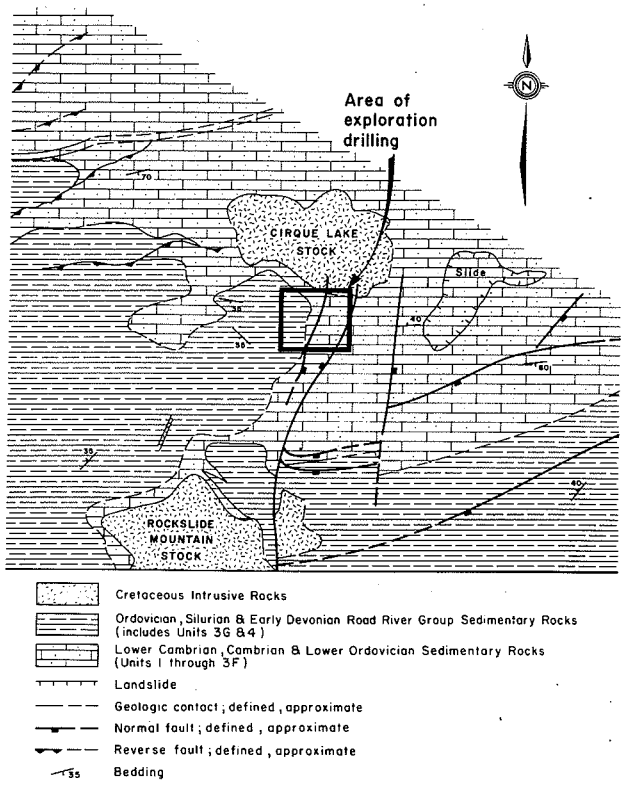

FIGURE 2. Generalized geologic map.

the slumps grade into a few centimetres of calcareous pelite as seen in southern drill holes. South of these drill intersections, additional slump breccias also outcrop. Slumps are chiefly lime or locally mud hosted. Fragments include: limestone clasts which may be fossiliferous containing Archaeocyathids, well-bedded or breccias; calcareous pisolites and ooids; phosphatic nodules; and various siliciclastic rocks including fragments of Unit 1. Clasts are generally elongate and range from a few millimetres up to 10 m in diameter. Slumps rest locally with erosional unconformity on Unit 1, although, in southern drill intersections, the calcareous pelites of Unit 2B appear to conformably overlie shales of Unit 1.

Unit 3C is in gradational contact with Unit 2B. It consists of 100 m of black, pyritic, carbonaceous, fine-grained clastic rocks and rare thin limestone beds. Numerous elongate clasts of mudstone, shale, siltstone and collophane occur as separate distinct clasts, as intraformational conglomerates and as boudinaged beds presumably disrupted by soft sediment deformation. This unit separates the Lower and Upper ore zones.

Siliceous sponge spicules found in Unit 3C have been identified as Protospongia of broad Early to Middle Cambrian age (Abbott, pers. comm., 1983).

Unit 3D consists of 20 m of repetitively intercalated 2 cm to 1 m thick beds of calcic and phosphatic limestone slump breccias, mudstone, shale and siltstone that conformably overlie Unit 3C. Slump breccias contrast with Unit 2B in that the breccia beds are characteristically thin and contain smaller, compositionally less variable, well sorted and bedded fragments.

Fragments include limestone clasts, black phosphatic nodules and siliciclastic rocks. Metasomatized calcic limestones within Unit 3D form the basal unit of the Upper ore zone.

Unit 3E is in gradational contact with Unit 3D, as slump breccias die out and the sequence becomes dominantly pelitic. The unit consists of 60 m of finely interbanded black to brown mudstones, shales and siltstones with limestone beds scattered throughout. The central portion of Unit 3E, with up to 20% limestone beds, hosts the middle part of the Upper ore zone.

Unit 3F is similar to Unit 3E, consisting of 30 m of intercalated compositionally distinct layers commonly less than 10 cm in thickness. The central part of Unit 3F contains up to 35% limestone beds which are host to the upper part of the Upper orebody.

Unit 3G, a 20 m thick, cliff forming unit of light coloured talc-tremolite dolomite with thin shale interbeds conformably caps the Upper ore zone.

Unite 3H consists of 90 m of black, carbonaceous, pyritic, fissile shale which is characterized by strong limonite staining on surface exposures.

Unit 4 consists of at least 50 m of black, carbonaceous, fossiliferous flagstones and shale. Abundant graptolite fossils include late Ordovician

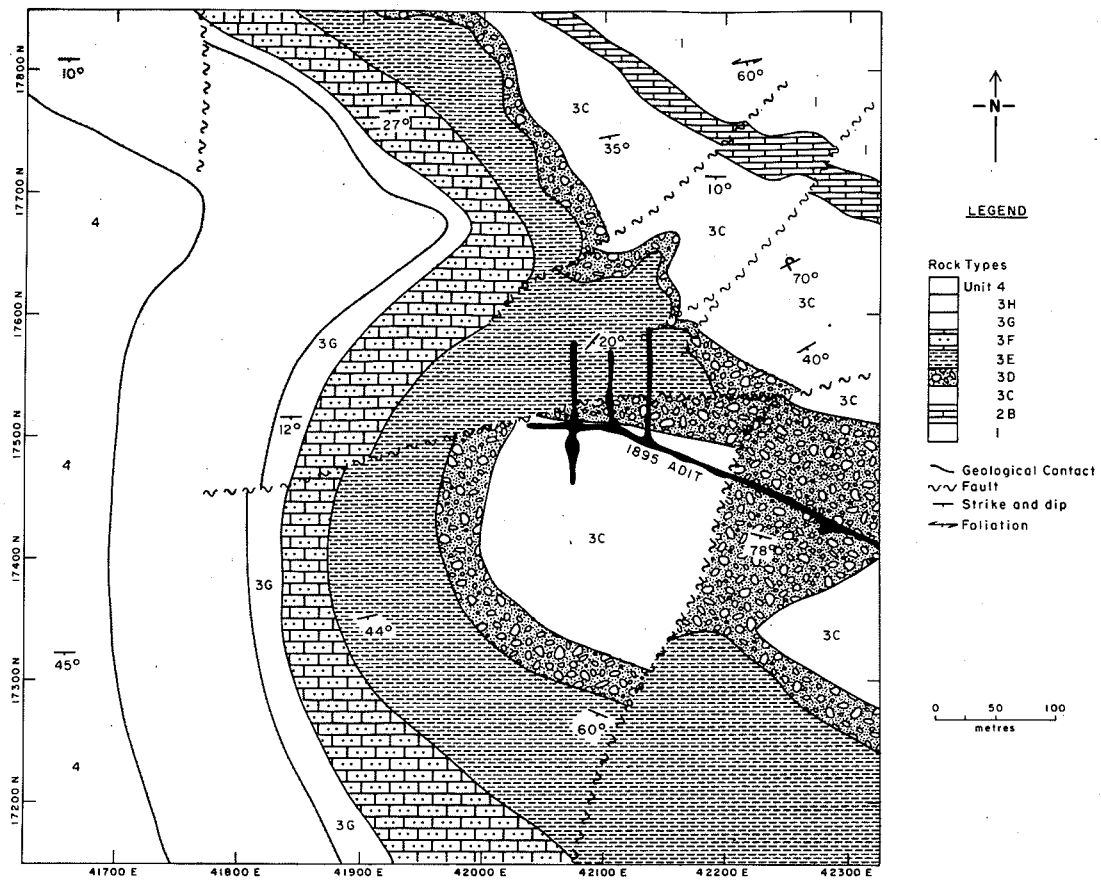

FIGURE 3. Geologic map and detailed cross section locations.

species (Abbott, 1983, pers. comm.).

Igneous Rocks

Two Cretaceous biotite quartz monzonite stocks and associated, locally abundant, dykes occur in the MacTung area: the Cirque Lake stock east of the deposit, the Rockslide Mountain stock to the south and a prominent east-trending biotite quartz monzonite and quartz latite porphyry dyke northwest of the deposit (Fig. 2). The stocks are composite, as evidenced by numerous igneous textural varieties for which crosscutting relationships can be documented. Textural varieties include medium- to coarse-grained, equigranular biotite quartz monzonite, quartz monzonite porphyries and rare quartz latite porphyry. Within the Cirque Lake stock, garnet is a local, conspicuous accessory and tourmaline forms impressive coatings on fracture surfaces. Tourmalinized halos envelope dykes and quartz veins that extend out into country rock.

Porphyry dykes occur south of the ore zones and in core from southern drill holes. They are characterized by phenocrysts of euhedral, white feldspar to 5 mm, quartz and brown biotite. Groundmass is aphanitic to fine-grained and is commonly extensively sericitized. Aplitic and pegmatitic textural varieties are

also recognized and are associated with quartz veins.

Structural Geology

At MacTung, a strong slaty to fracture cleavage trends east to northeast and may dip to the north or south. Within the ore zones and hornfels zones, this cleavage is rarely documented and may have been obliterated by post-tectonic thermal metamorphism associated with Cretaceous igneous activity.

Bedding generally dips gently to moderately south (Fig. 3). A megascopic isoclinal fold is documented in the lowermost units including Unit 2B, by drilling, mapping of underground workings and surface mapping of the north face of Mt. Allen. The axial surface of this structure is inclined gently to moderately south and is at a low angle to bedding. The hinge plunges gently to the west on the west end of the explored area and gently to the east on the east end. Thickening of Unit 2B in hinge zones and abrupt attenuation in the intermediate asymmetric limb are indicative of plastic deformation. In cross section, the fold is S-shaped (Fig. 4). Although this structure is considered a systematic part of a regional strain pattern, it may have resulted, at least in part, from soft sediment stresses. Synsedimentary deformation of pelites and limestones is well demonstrated within the sequence exposed at MacTung by erratic fold symmetry, internal folding of layers, boudinaged slabs of relatively competent beds outlining folds or occurring as breccia fragments in flow matrix.

Two prominent high-angle normal fault trends are mapped at MacTung (Fig. 3), a relatively older, east-trending, north side-down set and a relatively younger, northeast to east-northeast-trending, west side-down set. These faults offset both intrusive contacts and skarn.

Regional and Contact Metamorphism

Jura-Cretaceous deformation and associated metamorphism resulted in weak recrystallization to produce micaceous pelites and marbles with pervasive cleavage. Subsequent intrusion of Late Cretaceous plutons produced narrow overprinting contact aureoles of biotite ± andalusite ± cordierite ± feldspar ± quartz hornfelsed pelitic rocks (Anderson, 1982), calc-silicate minerals in hornfelsed limy pelitic rocks and recrystallization of marbles to form coarser-grained, locally garnetiferous marbles.

Prograde Hydrothermal Alteration

The style, degree and nature of alteration by hydrothermal fluids at MacTung reflects the primary composition, competency, structure and porosity of the metasomatized rock. Thus, non-reactive and non-porous pelitic rocks which fractured in a brittle manner are crosscut by quartz veins with accessory scheelite and are enveloped by relatively narrow alteration halos, whereas highly reactive and permeable calcic limestones are pervasively skarned and contain economic concentrations of scheelite.

During the 1982 and 1983 field programs, the property was mapped at a scale of 1:1000 and core from drill holes on representative cross sections was logged (Fig. 3). Each 5 m (25 ft) core interval was described and physically measured for limestone-pelite ratio, percentage of limestone that is remnant, phosphatic or skarned and the percentage of core that is quartz vein or dyke material. A visual estimate was also made of the garnet, pyrrhotite and biotite content within skarn.

Alteration in Pelitic Rocks

Prograde hydrothermal alteration in pelitic rocks consists largely of bleaching to browning and cream hornfels or to green aphanitic calc-silicate rocks which generally contain no disseminated scheelite. This is especially apparent in narrow pelitic beds or fragments within predominantly limestone (e.g. Unit 2B) or within narrow pelitic beds rhythmically intercalated with limestone (e.g. Units 3D, 3E or 3F). Within thick pelitic sequences, bleaching occurs largely as halos enveloping quartz veins. Bleached halos up to one metre wide crosscut bedding and cleavage. Where quartz veins are abundant, overlapping bleached halos form a pervasive alteration, however, where quartz veins are sparse, remnant black pelitic rocks or brown and purple hornfels are preserved.

Quartz veins are generally oriented parallel to bedding or cleavage in pelitic rocks. Crosscutting quartz veins terminate against skarn beds or change vein mineralogy abruptly at limestone contacts to a pyroxene-garnet assemblage, presumably as a result of reaction with limestone wall rocks. Thus, quartz veins with bleached halos in pelitic rocks are considered hydrothermally analogous to skarn in limestone, the difference reflecting host rock composition rather than process.

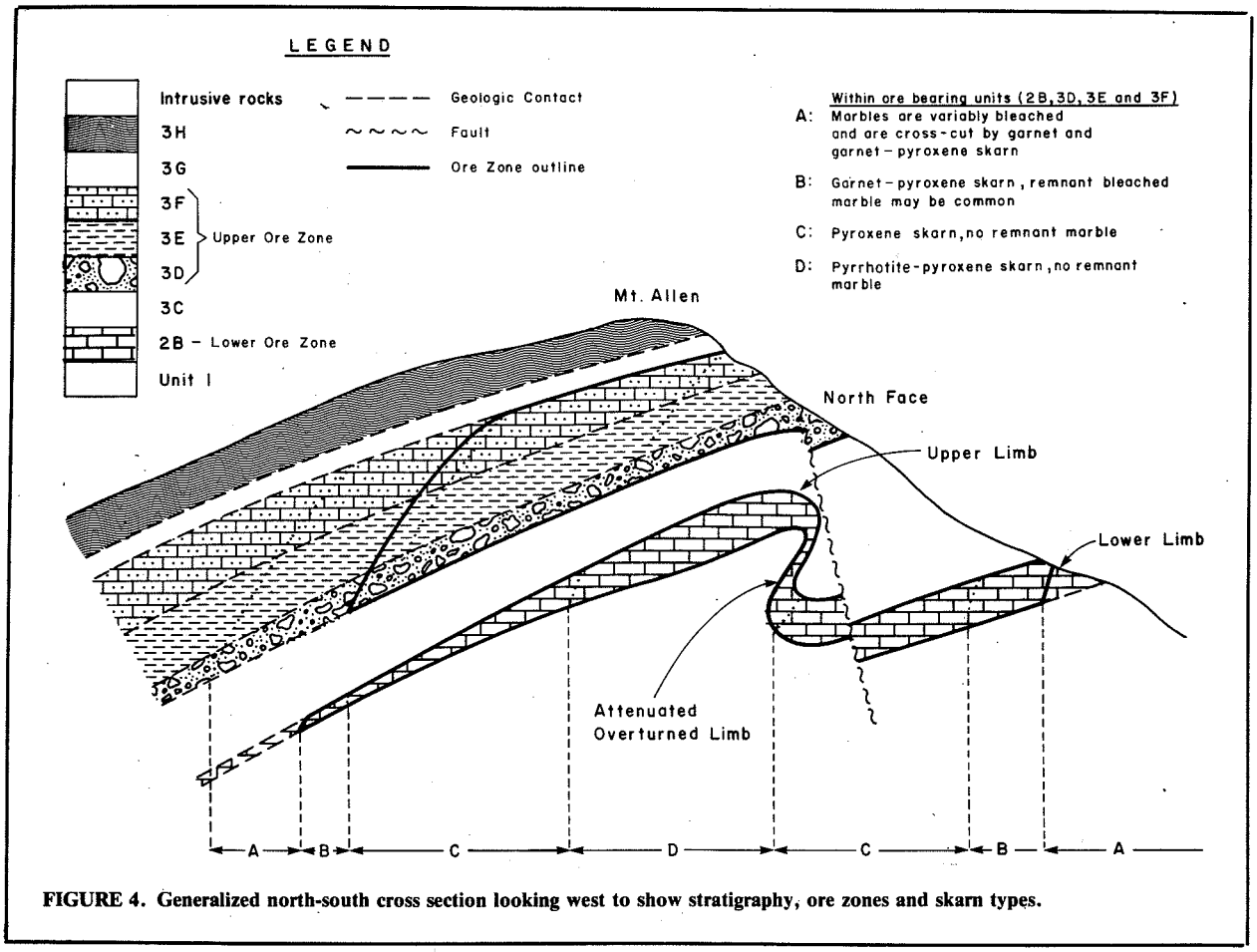

FIGURE 4. Generalized north-south cross section looking west to show stratigraphy, ore zones and skarn types.

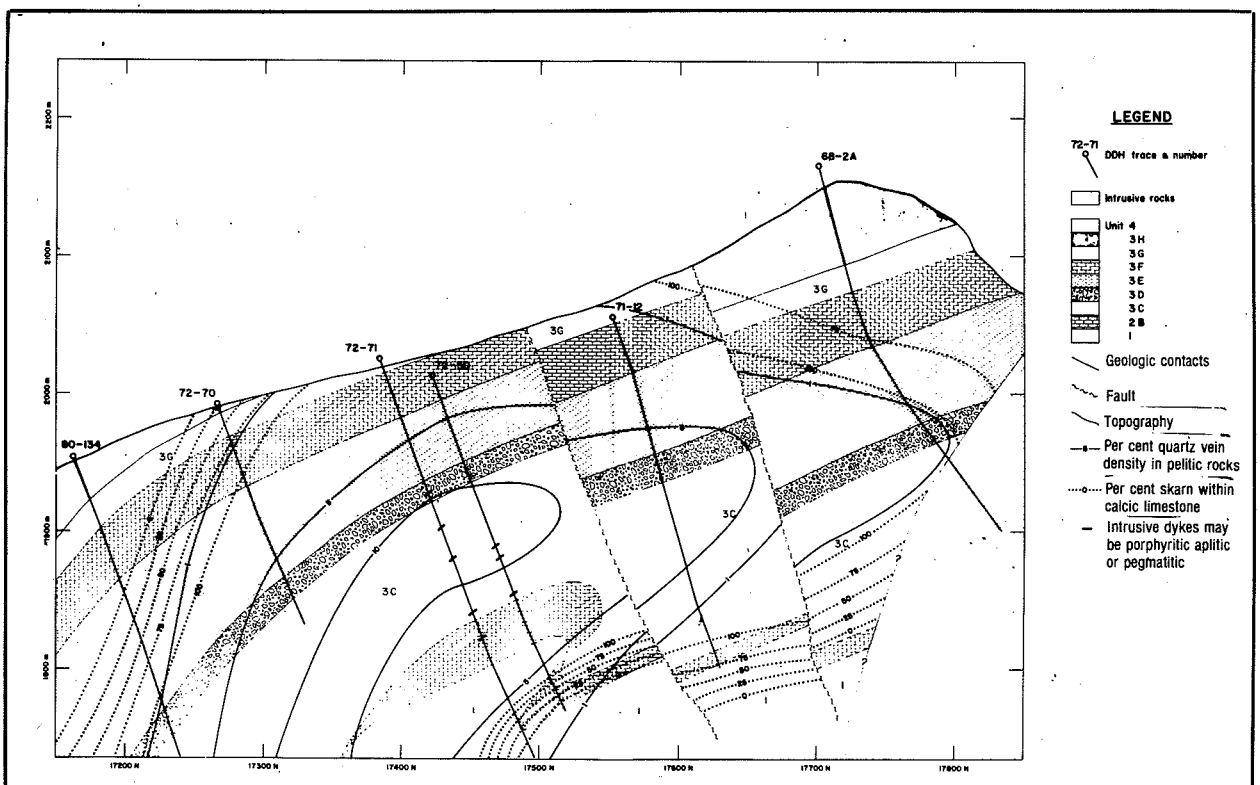

FIGURE 5. N-Section 41850E looking west. Distribution of quartz vein densities, skarned calcic limestone and intrusive dykes.

Another product of hydrothermal alteration of pelitic rocks is brown hydrothermal biotite, occurring as elongated aggregates on bedding and foliation planes, particularly in Unit 1 where they form a distinct zone up to 50 m below the Lower ore zone.

Alteration in Limestone

Prograde hydrothermal alteration of limestone includes bleaching, observed up to 400 m laterally from ore, and pervasive skarn development within calcic limestones. As economic concentrations of scheelite occur only in skarn, the percentage of skarn that has replaced calcic limestone delimits the ore zones (Fig. 5, 7, 9, 11 and 13). On the periphery of the deposit, bleached limestone is crosscut by garnet and garnet-pyroxene skarn veins. Skarn containing greater than 5% garnet is indicative of the outer limit of mineralization (Fig. 6, 8, 10, 12 and 14). Progressing into the deposit, remnant limestone becomes increasingly rare, garnet-pyroxene skarn grades into pyroxene skarn and, toward the core of the deposit, pyrrhotite-pyroxene skarn (Fig. 4). A similar zoning pattern occurs within limestone crosscut by veins.

Garnet-skarn is minor in amount, occurring in pods and veins within limestone. Pods are often drusy with red, enhedral garnet crystals up to 3 mm in size intergrown with glassy or white quartz and trace amounts of scheelite.

Garnet-pyroxene skarn is characterized by fine-grained, green pyroxene with red to reddish brown garnet, abundant remnant calcite, scheelite and traces of pyrrhotite. The average WO_3 grade is less than one per cent.

Pyroxene skarn is the most common skarn type in both the Lower and Upper ore zones. It is fine- to rarely coarse-grained. Dark green pyroxene is the most abundant mineral, remnant calcite is minor, pyrrhotite content varies from a trace to several per cent and scheelite is abundant. WO_3 grades are better than one per cent.

Pyrrhotite-pyroxene skarn is gradational with pyroxene skarn and is distinguished visually by pyrrhotite content exceeding 15%. This is the most altered skarn, contains the least calcite and is characterized by WO_3 and Cu grades of better than 1.5% and 0.2% respectively. Grain size including that of scheelite is generally coarser than other skarn types. Five per cent and 20% pyrrhotite content contours are shown in figures 6, 8, 10, 12 and 14. Primary sedimentary structures are commonly preserved even in pyrrhotite skarn. Under ultraviolet light, scheelite can be seen preferentially concentrated on such primary sedimentary features as clast rims and bedding planes.

Other skarn types include biotite skarn and quartz skarn. Biotite skarn consists of massive aggregates of fine- to coarse-grained, dark brown biotite present within argillaceous limestone beds of both the Lower and Upper ore zones, especially at the base of the slump breccia within Unit 2B and extending out into basinal equivalents (Fig. 6, 8, 10, 12 and 14). Where biotite is associated with quartz and/or pyrrhotite, coarse-grained scheelite is commonly present. Infrequent quartz flooding of skarn forms erratic pods, rootless veins or zones of quartz skarn. Quartz is milky and contains abundant, euhedral, large scheelite crystals. Grades of WO_3 may exceed 5% in this rare skarn type.

Ore Zones

Geologic work on the property includes mapping, 14 000 m of diamond drilling in 90 holes from surface, 2300 m of diamond drilling in 51 holes from underground and 800 m of underground development. This has defined geologic reserves of 32 million tonnes grading 0.92% WO_3. The Lower ore zone, localized within isoclinally folded limestone slump breccia of Unit 2B, contains one-third of defined geologic ore reserves and will be mined by underground methods. The remainder of the ore is contained within the Upper ore zone which consists of three separate stratiform zones within Units 3D, 3E and 3F, the majority of which will be mined by open-pit methods. The relative abundance of barren interbedded pelites within the Upper ore zone accounts for grade differences between the Upper and Lower ore zones and between 3D, 3E and 3F. It is anticipated that detailed mapping and logging of barren pelitic interbeds or fragments in slump breccias will be required for grade control during mining of MacTung.

Post-mineral and Retrograde Alteration

Late quartz veins crosscut skarn, with the characteristic development of coarse-grained scheelite in skarn adjacent to these veins. Crosscutting, late-stage, calcite-filled faults and fractures are enveloped by clay alteration zones, producing locally incompetent rocks. Manganese oxides released during clay

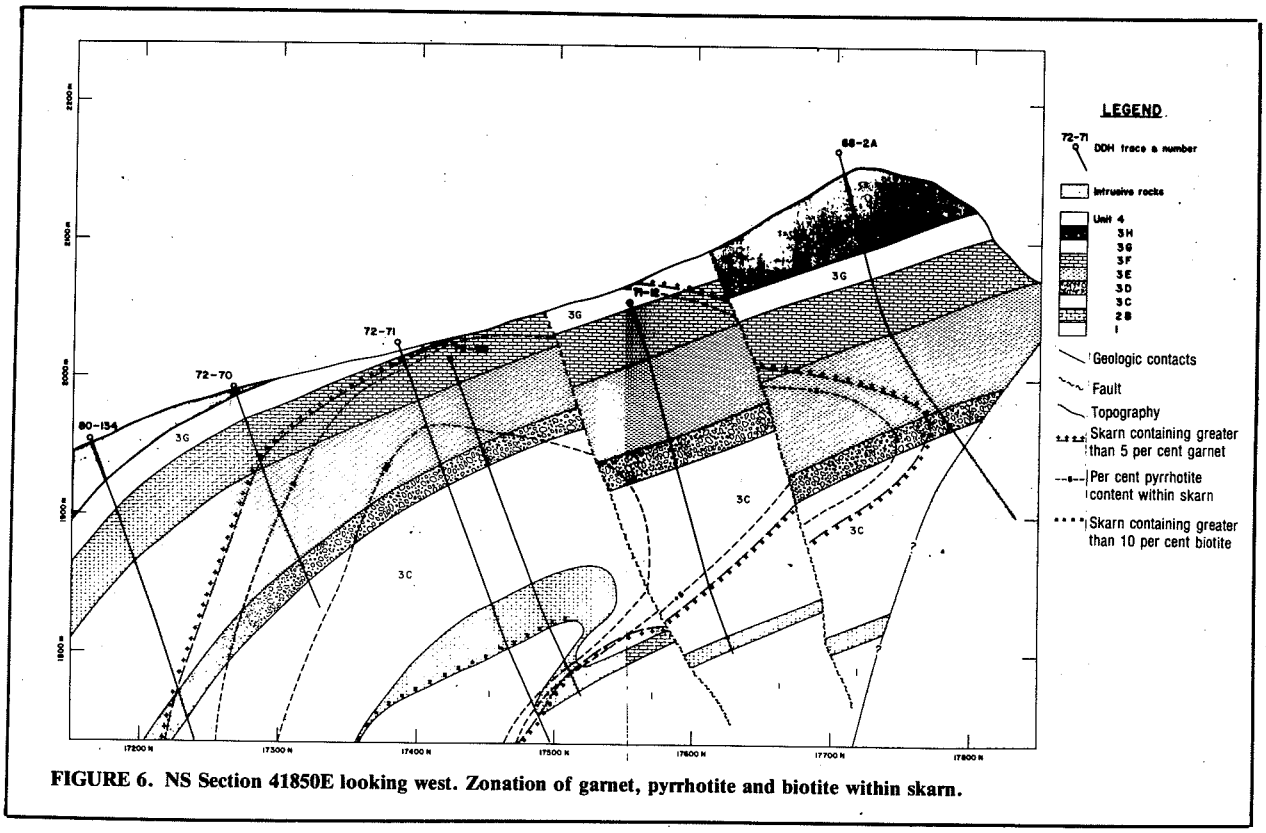

FIGURE 6. NS Section 41850E looking west. Zonation of garnet, pyrrhotite and biotite within skarn.

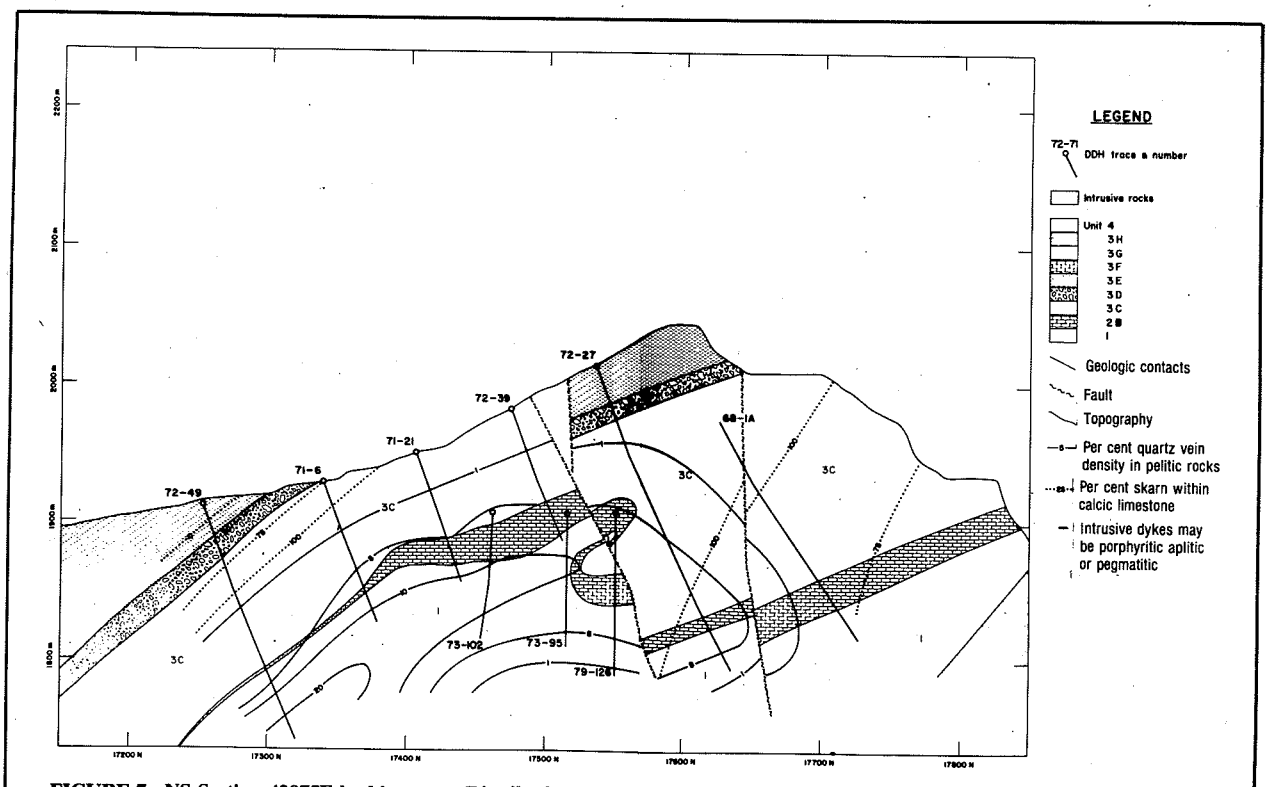

FIGURE 7. NS Section 42075E looking west. Distribution of quartz vein densities, skarned calcic limestone and intrusive dykes.

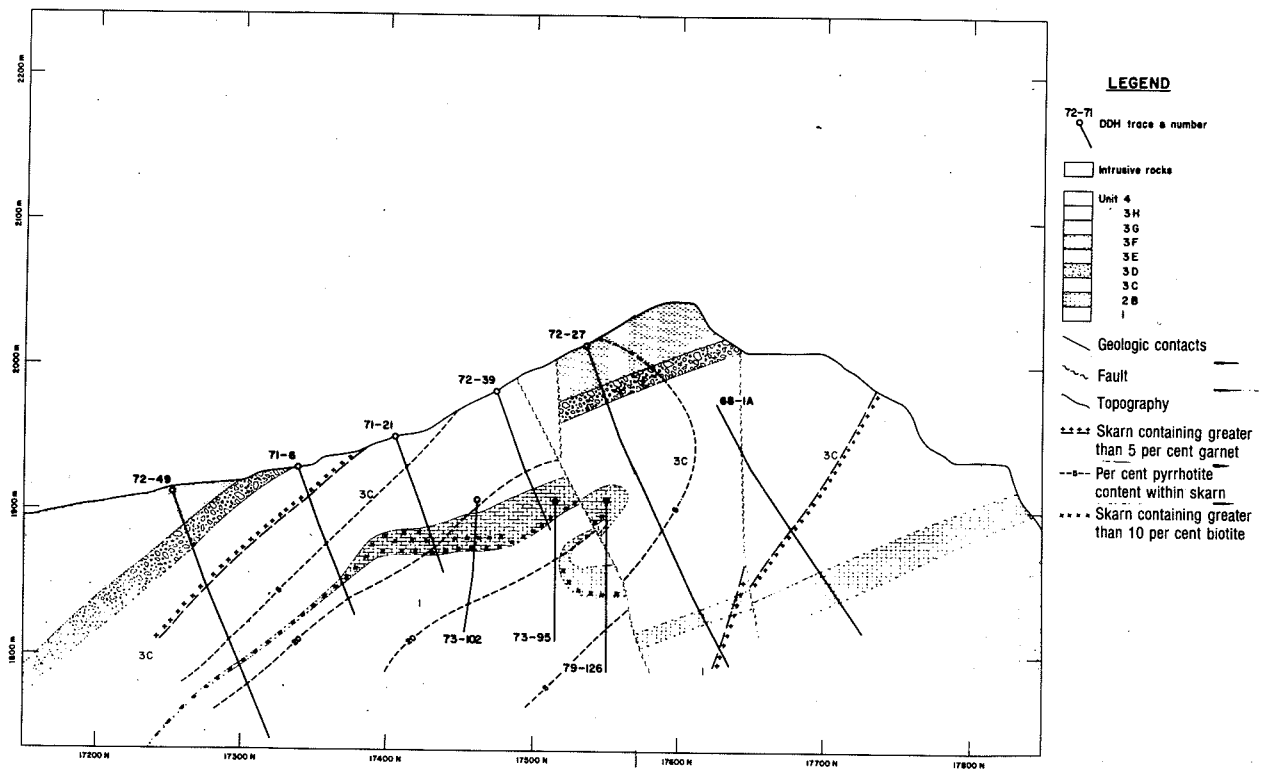

FIGURE 8. NS Section 42075E looking west. Zonation of garnet, pyrrhotite and biotite within skarn.

alteration form abundant massive fracture coatings. Hydrous skarn, characterized by isolated coarse-grained masses of amphibole and rarely observed within pyroxene skarn, is assumed to represent local retrograde alteration.

Source of the Hydrothermal Fluids

The following observations indicate that magmatic hydrothermal fluids originated from a stock at depth south of the deposit rather than from the Cirque Lake stock and that mineralizing fluids migrated up-dip and up-section to react with marbles and form ore-bearing skarns. The hypothesized source stock and fluid migration route are shown schematically in Figure 15.

1. The Lower ore zone and the three individual horizons comprising the Upper ore zone are stacked up-dip and up-section (Fig. 4). Thus, the Lower ore zone is furthest south and the uppermost ore horizon (within Unit 3F) of the Upper ore zone is furthest north.

2. Hydrothermal alteration of pelitic rocks and marbles including the distribution of garnet and pyrrhotite is zoned up-dip and up-section parallel with the stacking of the ore zones (Fig. 5 through 14). Hydrothermal alteration zones as shown are obviously discordant to the contact of the Cirque Lake stock.

3. Quartz veins within pelitic rocks, described previously, are interpreted to represent fossilized hydrothermal fluid channel-ways. The veins are orientated parallel to bedding or cleavage, rarely forming stockworks. They range in widths of up to one metre, averaging 2 cm to 5 cm. Accessory minerals indicate

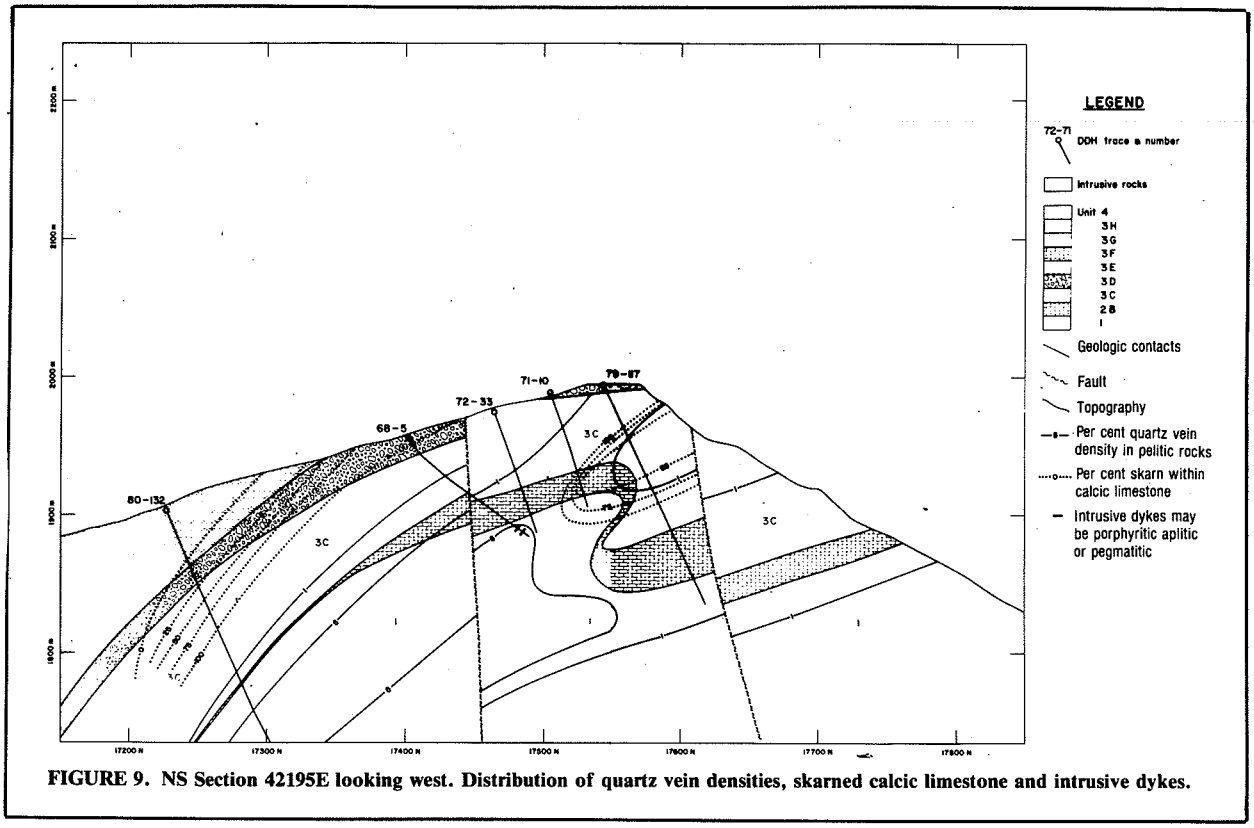

FIGURE 9. NS Section 42195E looking west. Distribution of quartz vein densities, skarned calcic limestone and intrusive dykes.

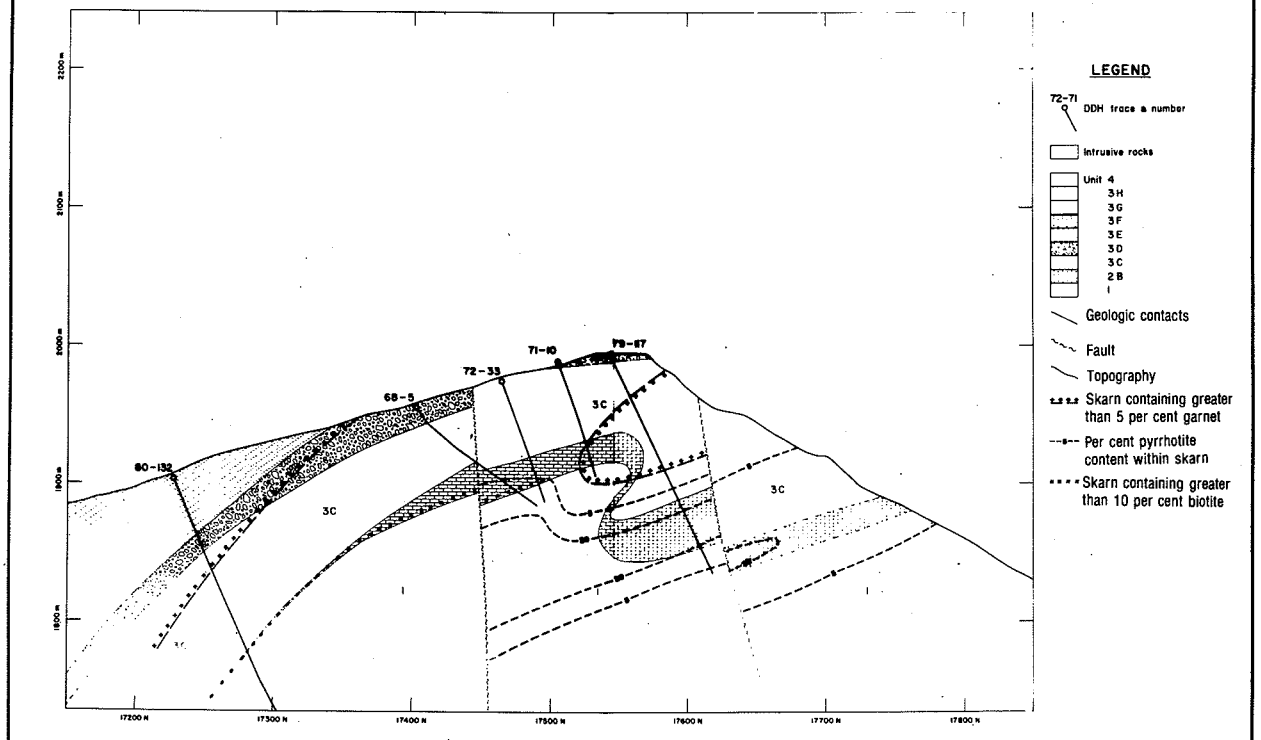

FIGURE 10. NS Section 42195E looking west. Zonation of garnet, pyrrhotite and biotite within skarn.

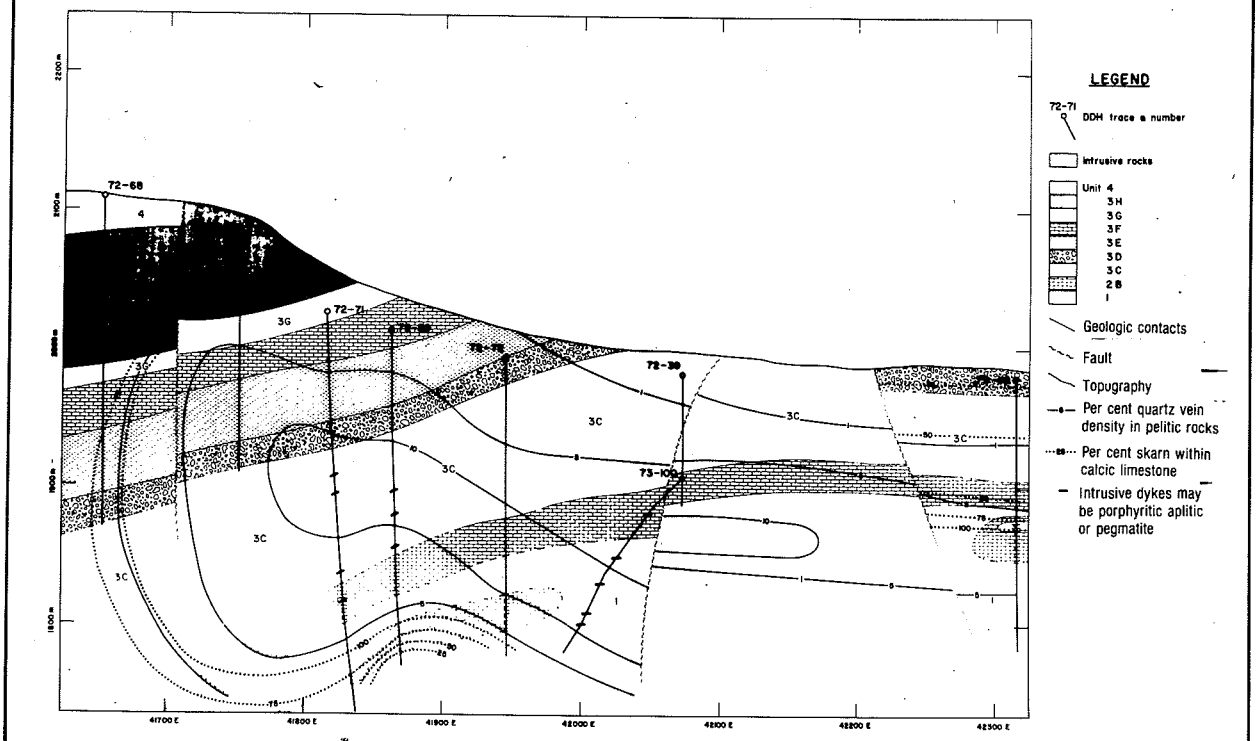

FIGURE 11. NS Section 17500N looking west. Distribution of quartz vein densities, skarned calcic limestone and intrusive dykes.

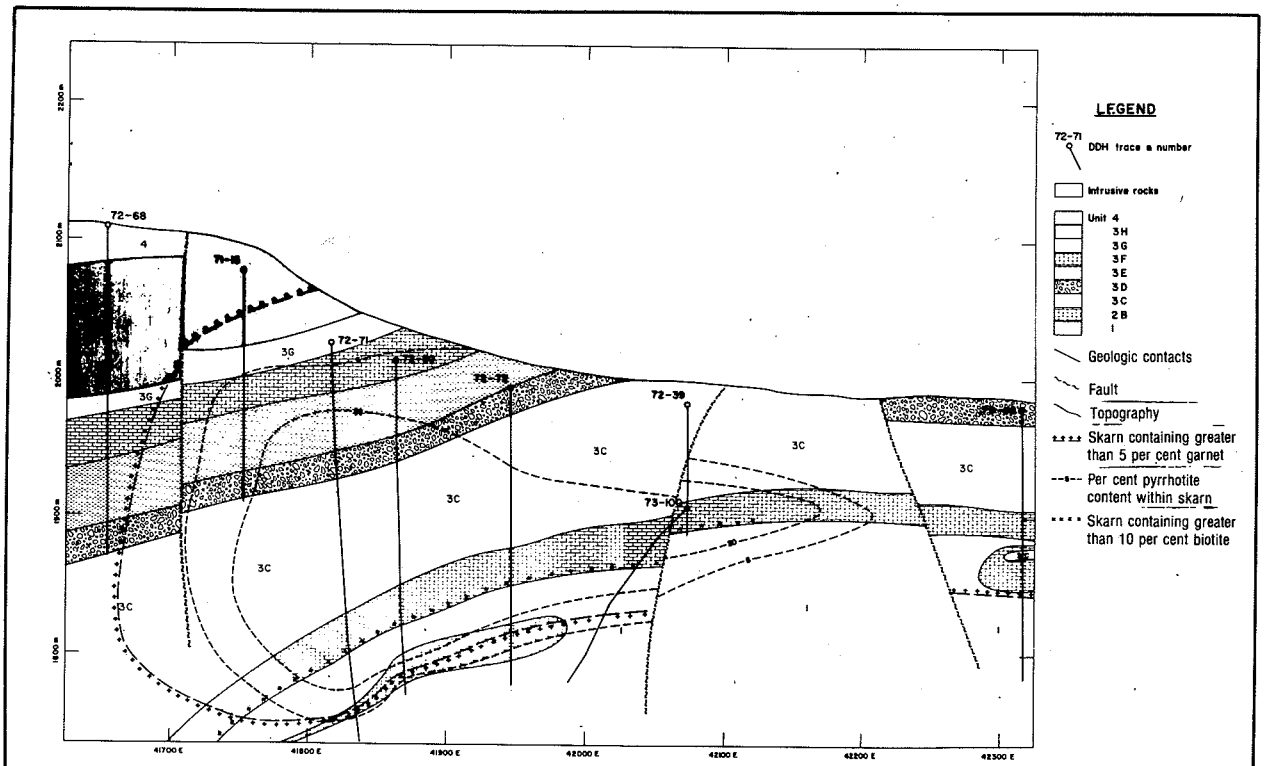

FIGURE 12. NS Section 17500N looking west. Zonation of garnet, pyrrhotite and biotite within skarn.

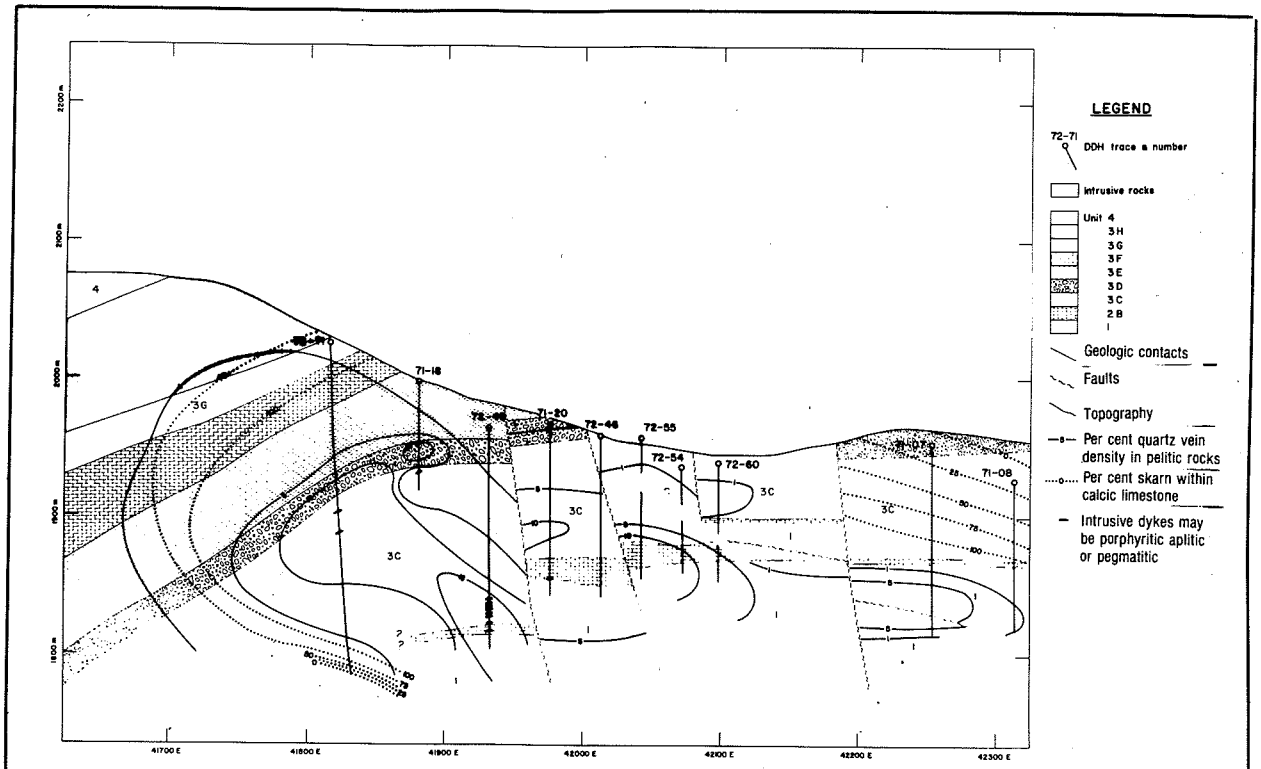

FIGURE 13. EW Section 17400N looking north. Distribution of quartz vein densities, skarned calcic limestone and intrusive dykes.

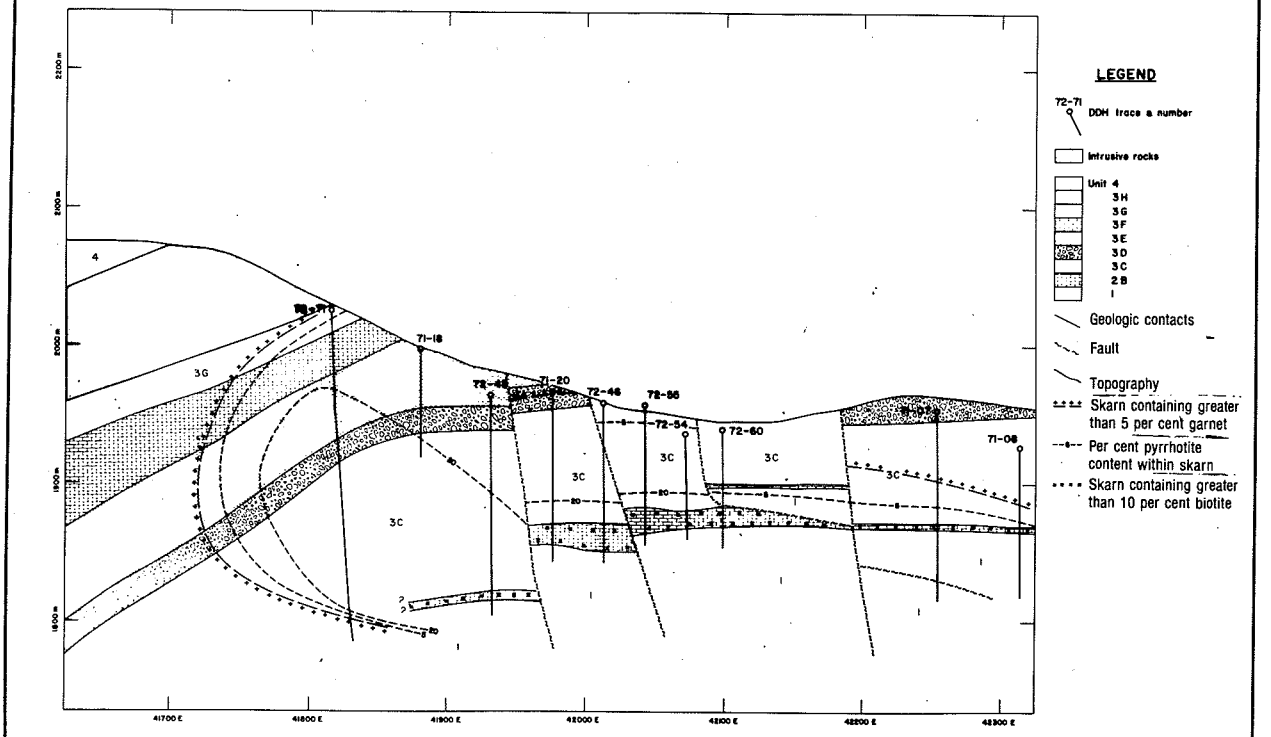

FIGURE 14. EW Section 17400N looking north. Zonation of garnet, pyrrhotite and biotite within skarn.

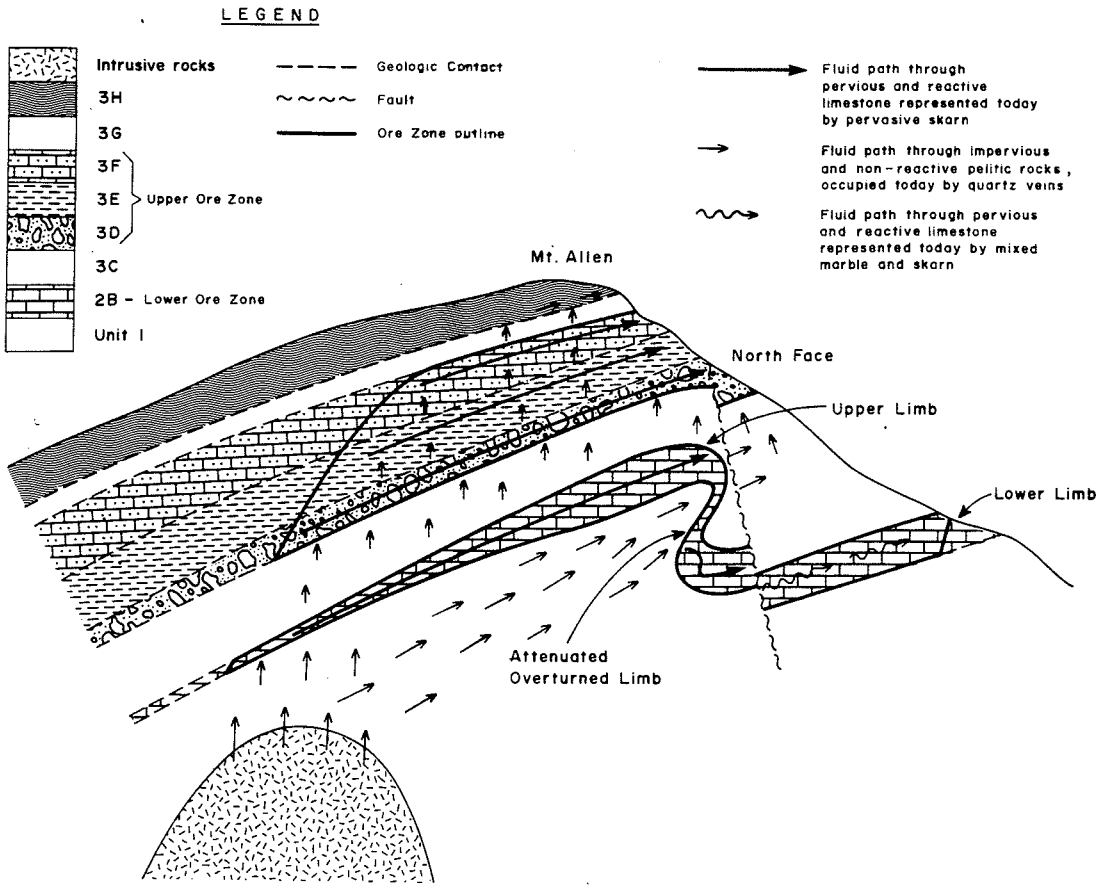

FIGURE 15. Proposed hydrothermal fluid migration pattern.

scheelite, feldspar, biotite, molybdenite, tourmaline, pyrrhotite, chalcopyrite, sphalerite and pyroxene. It became evident during mapping and logging that quartz veins vary systematically in abundance such as to allow contouring of vein densities within thick pelitic sequences such as Units 1 or 3C. The resultant density contours are approximately parallel to bedding, are most abundant beneath the Lower and Upper ore zones and decrease up-section and up-dip in tandem with the distribution of garnet and pyrrhotite (Fig. 5, 7, 9, 11 and 13).

4. Pegmatite, aplite and porphyry dykes are common in deep drill holes south of the ore zones, indicating the presence of an intrusion at depth (Fig. 5, 9, 11 and 13). As observed in core, many of the quartz veins are texturally gradational with these intrusive dykes with increase in feldspar and biotite content. Such veins are often zoned with feldspar edges and quartz centres. Quartz veins also occur with euhedral quartz edges and aplite centres, indicating that hydrothermal and magmatic fluids utilized common channelways. Generally quartz veins crosscut dykes, although some

dykes brecciate quartz veins and have complex age relationships. Thus, a close relationship is established between igneous activity, quartz veining and mineralization in deep drill holes south of the ore zones.

5. The distribution of accessory molybdenite and sphalerite is consistent with a source stock south of the ore zones. Molybdenite is abundant within quartz veins beneath ore, particularly beneath the Lower orebody. Sphalerite occurs in quartz veins peripheral to ore, in base metal skarns immediately south of the deposit within a lateral equivalent of the Lower ore zone and as microscopic disseminations within pelitic rocks overlying ore.

Conclusions

Detailed work during 1982 and 1983 has led the authors to a new interpretation of the origin of the mineralizing solutions of MacTung.

It is believed that the MacTung deposit is only coincidentally located near the contact with the Cirque Lake stock and that the source of mineralizing fluids is a blind stock immediately south of MacTung. Magmatic-hydrothermal fluids gathered at the apex of this unexposed stock during crystallization of the magma and the fluids gathered at the apexof this unexposed stock during crystallization of the magma and the fluids then migrated out of the stock and moved up-dip and up-section, utilizing weaknesses along bedding or foliation planes within pelitic rocks, and infiltrated permeable limestones. Reactions between hydrothermal fluids and limestone produced prograde skarn minerals, garnet, pyroxene and pyrrhotite and deposited scheelite and chalcopyrite. Reactions between hydrothermal fluids and pelitic rocks produced bleached halos and calc-silicate rocks.

Abundant quartz veins in pelitic rocks at MacTung represent a fossil plumbing system for the hydrothermal fluids and although they are roughly parallel and concordant with bedding, they are the equivalent of stockwork within porphyry Mo-W systems.

The hydrothermal system was probably short-lived; retrograde alteration is minimal, being confined largely to late faults and fractures. The Cirque Lake stock, although probably of the same general age as the hypothesized stock south of MacTung deposit, may post- or pre-date skarn formation and tungsten mineralization.

From an exploration point of view, although outcropping biotite quartz monzonite stocks and dykes provide exploration targets for contact skarn deposits, more importantly, they may provide evidence for more widespread unexposed igneous activity which could have given rise to magmatic-hydrothermal fluids.

Acknowledgements

We gratefully acknowledge the many geologists who have provided us with stimulating discussions, both on site and in the office.

Thanks are extended to C.J. Hodgson of Queen's University for editorial comments and J. Adams of AMAX of Canada for typing the manuscript.

BIBLIOGRAPHY

Abbott, J.G., 1982, Structure and stratigraphy of the MacMillan Fold Belt: evidence for Devonian faulting in Yukon Exploration and Geology 1981, Department of Indian Affairs and Northern Development, Northern Affairs Program - Yukon, Exploration and Geological Services Division, Whitehorse.

Anderson, R.G., 1982, Geology of the MacTung pluton in Niddery Lake map area and some of the plutons in Nahanni map area, Yukon Territory and District of MacKenzie; in Current Research, Part A, Geological Survey of Canada, Paper 82-1A, p. 229-304.

Anderson, R.G., 1983, Selwyn plutonic suite and its relationship to tungsten skarn mineralization, southeastern Yukon and District of MacKenzie; in Current Research, Part B, Geological Survey of Canada, Paper 83-1B, p. 151-163.

Atkinson, D. and Baker, D.J., 1986, Recent developments in the geologic understanding of MacTung, in Morin, J. (ed.), Mineral Deposits of the Northern Canadian Cordillera; Canadian Institute of Mining and Metallurgy, Special Volume 37, p. 234-244.

Cathro, R.J., 1969, Rungsten in Yukon, Western Miner, April 1969, p. 23-40.

Dick, L.A., and Hodgson, C.J., 1982, The MacTung W-Cu (Zn) contact metasomatic and related deposits of the northeastern Canadian Cordillera, Economic Geology, Vol. 7, p. 845-867.

Harris, F.R., 1977, Geology of the MacMillan tungsten deposit, Mineral Industry Report, 1976; Department of Indian Affairs and Northern Development, EGS 1977-1, p. 20-32.

GEOLOGY OF THE KETZA RIVER GOLD MINE

Shirley M. Abercrombie
Chief Geologist
Ketza River Mine

INTRODUCTION

Exploration activity began in the Ketza River district in 1947 with the discovery of silver-lead veins on the nearby Iona property by Hudson Bay Mining and Smelting Company Limited. On the Ketza property to the west, gold was discovered in 1954 and 1955 by prospectors working for Conwest Exploration Company Limited. Conwest explored the Ketza River sulphide gold deposit with trenching and 59 drill holes from 1955 until 1960 and outlined 75,000 tonnes grading 12 g/t Au. Work completed by Conwest was conducted under frequently harsh conditions, often involving a two-day sled dog or packhorse trip to and from the site for supplies. Packhorses were also used for drill moves. Given a $35 gold price and difficulties in working in this remote location, the project was mothballed.

The Ketza River Property was optioned by Pacific Trans-Ocean Resources in late 1983. Pacific Trans-Ocean and Canamax entered a joint venture agreement to explore and develop the property in early 1984, with Canamax the operating partner. After three years of aggressive exploration, including 12,669 metres of diamond drilling and 1.6 km of underground development, an oxide reserve totalling 495,800 tonnes at 18.0 grams gold per tonne was established. A sulphide reserve of equal size but lower grade was delineated. A production decision based solely on the oxide reserve, was approved early in 1987. Facilities for a 320 tonne-per-day mining and milling operation were constructed in 1987. The first gold bar was poured on April 28, 1988 and the mine was officially opened on July 21, 1988. In April 1989 Canamax Resources Inc. purchased Pacific Trans-Ocean's share of the property and is now 100% owner of the Ketza River Mine.

A work force of 110 is employed at Ketza, working a series of rotating shifts. Crews are transported between Ross River and Whitehorse by aircraft.

Mining is being carried out on three underground levels (1430m, 1510m, 1550m) using modified cut and fill and square set mining methods. Several small open pits are also being mined. The mill is currently operating at 400 tonnes per day with a budgeted grade of 11.3 g/t. Reserves include 105,000 tonnes of mineable oxide at 12.8 g/t and significant drill indicated sulphide reserves. Approximately 36,000 tonnes of the oxide reserve will be mined by open pit during the summer of 1990. Assuming diamond drilling results are favourable, sulphide mining will commence in late 1990 around the time the underground oxide reserves are exhausted. To date 56,500 ounces of gold have been produced.

PROPERTY GEOLOGY

Only Cambrian strata are preserved in five main units on the Ketza River property (Fig. 1). A westward-plunging anticline, with its axis in the Peel Creek Valley (see Cathro, this volume; 1986), exposes a thick sequence of argillites, phyllite and quartzites that is overlain by Lower Cambrian limestone and pelitic mudstone. upper Cambrian black shales unconformably overlie the lower Cambrian rocks.

Unit 1a, (> 300 m thick) the oldest, comprises interbedded brown to rusty weathering argillite and fine grained thin to thick bedded impure quartzite. Much of this unit has been altered to a rusty weathering purple-brown hornfels which typically breaks in 2-10 cm blocks.

Unit 1b is a thin interval (25 to 60 m thick) of resistant dark grey to black, well laminated, silty limestone, containing archeocyathids and local irregular bands of oncoids or ooids.

Unit 1c, (75-105 metres thick) is composed of greyish green to brown, recessive weathering, calcareous phyllitic mudstone with minor argillaceous limestone. Large pyrite cubes are common. The upper

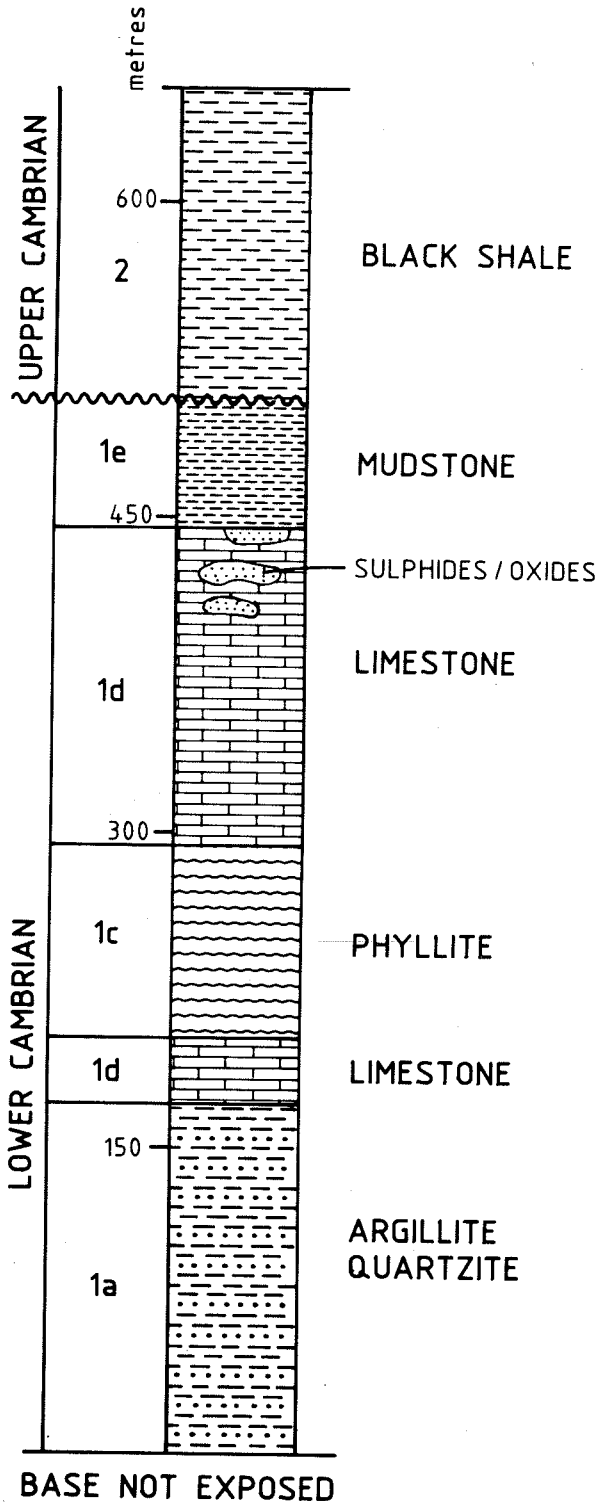

Figure 1. Generalized stratigraphic section for the Ketza River Mine, Yukon. Sulphide and oxide manto deposits occur at the upper contact of the unit 1d limestone.

contact with Unit 1d is gradational and is defined as the point where carbonate is greater than half of the rock.

Unit 1d, (120 to 180 m thick) the main host for gold mineralization, is distinctive grey-blue, thickly bedded to massive archeocyathid-bearing, cliff-forming carbonate. Limestone dominates, but 10-15% of the unit is orange-brown weathering ferroan dolomite. Large archeocyathid buildups and irregular bands of oncoids are locally present at the top of this unit. Calcite-quartz veins and dry fractures are abundant.

Unit 1e (0 to 50 m thick) is light green weakly to non-calcareous phyllitic green mudstone. Where unaltered, it is well laminated to massive with numerous hairline cracks and blocky fractures. Lenses and beds 2 cm to 3 m thick of unit 1d carbonate occur sporadically in the basal part of the mudstone. This unit locally forms the hangingwall in the Peel Zone. Near mineralization, the mudstone is altered to light green clay or talc that vary from thin coatings on fractures to pervasive alteration.

Unit 2 is black, locally carbonaceous shale of upper Cambrian age. The top of the unit is not exposed on the property and thickness is unknown. Minor fine grained pyrite is the only significant alteration. Slatey cleavage is well developed and the shale in drill core tends to break into thin "poker chip" sized plates. Small structural blocks of shale occur in the footwall of the Ridge Zone. Relief on the erosional surface separating unit 2 from the lower Cambrian units 1d and 1e is up to 40 metres and the unconformity surface transgresses the 1d/1e contact.

STRUCTURE

Faults are the dominant structures on the property. North-eastward-directed thrusts with stratigraphic throws of up to 450 metres are the oldest faults. Numerous high angle reverse, normal and strike-slip faults disrupt the thrusts and related folds. High angle block faults related to local doming and uplift are the most prominent. These faults are usually of limited strike length and frequently show movement of a pivotal nature, with variable displacement and a changing sense of movement along strike.

Faults are documented on a more detailed scale in the Peel and Ridge zones (Fig. 2) where surface and underground mapping has revealed a number of faults which post-date thrusting and folding and pre-date high-angle block faulting. These faults are of varied attitudes and unlike the generally planar high angle block faults, have changing dips and curvilinear traces.

The Peel oxide deposit and the Ridge Zone lie within a panel of intense structural preparation bounded by two NW-striking block faults. The Peel Fault pre-dates these block faults, strikes ENE and juxtaposes unit 1d to the south and unit 1a to the north. This fault represents the northern limit of limestone replacement mineralization and localizes the Ridge Zone. The north trending Boundary Fault dips steeply east and forms the western limit of the Peel Zone. All of the faults within the structural panel pre-date mineralizing events and served as conduits for the ore forming fluids. The NW trending structures pre-date or are coeval with mineralizing events.

A local apophysis of a mid-Cretaceous stock is postulated to lie beneath the core of the anticline in the Peel Creek Valley (see Cathro, this volume; 1988). Supporting evidence includes a halo of intense hornfels in the argillites, a broad aeromagnetic feature centered about the fold axis, and a concentration of gold mineralization along the flanks of the structure. A strong fissure pattern related to the anticline is believed to have been responsible for the primary localization of the gold deposit.

MINERALIZATION

On the Ketza River property, gold deposits are of two general types: limestone replacement sulphide/oxide deposits, referred to as mantos and chimneys; and, quartz-sulphide fissure vein and stockwork systems. The mantos and chimneys are hosted by unit 1d limestone on the southern flank of the westerly plunging Peel Creek Anticline. The vein and stockwork deposits occur in unit 1a argillite and phyllite on its northern limb.

The most important deposits on the property are sulphide/oxide mantos and chimneys. The mantos are generally stratabound and concordant, but in detail, show extreme variability in thickness with sharp discordance to bedding.

The Peel and Ridge Zones form a contiguous manto and chimney body. Figure 3 is a perspective drawing illustrating the 3-dimensional geometrical relationship between the Peel and Ridge oxide zones. The Peel Oxide Zone, a gently dipping lens or tube like body, is adjacent to a larger sulphide manto located to the west. At its northern end, the Peel Oxide Zone joins

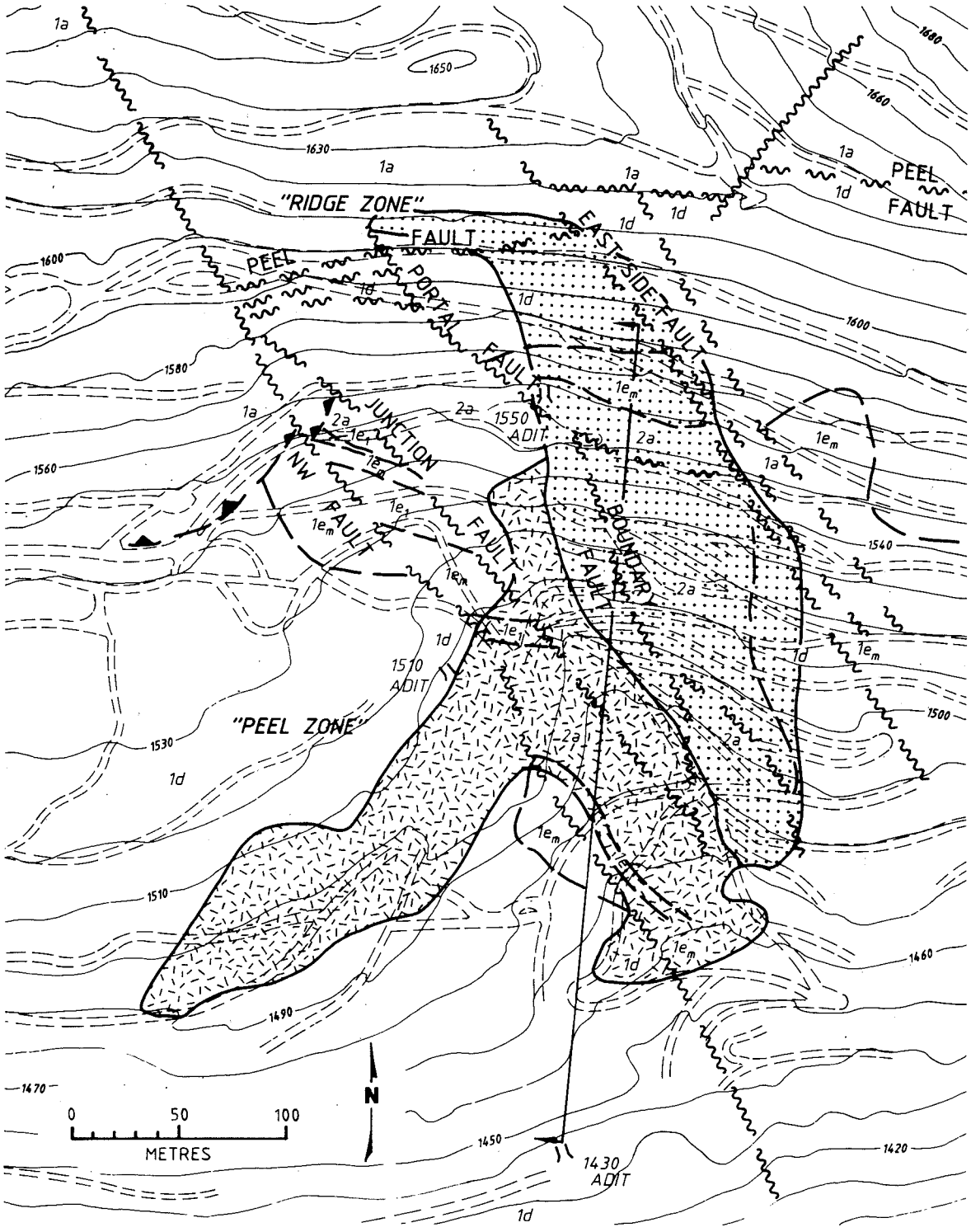

Figure 2. Geological map of the Peel and Ridge Zones.

LEGEND
(to accompany Figure 2)

UPPER CAMBRIAN

2a Black carbonaceous shale

Unconformity

LOWER CAMBRIAN

1e$_1$ Upper grey limestone member

1e$_m$ Laminated greenish-grey mudstone

1d Thin bedded to massive grey limestone

1c Thin bedded brown to greenish-grey calcareous argillite and agrillaceous limestone

1b Laminated dark grey to black carbonaceous limestone

1a Thin bedded grey argillite and phyllite

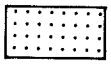
Sulphide body

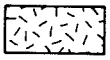
Oxide body

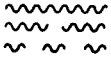
Fault (defined, approximate, assumed)


Thrust Fault

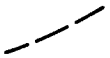
Geological Contact


Adit

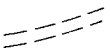
Road

Figure 2 Legend

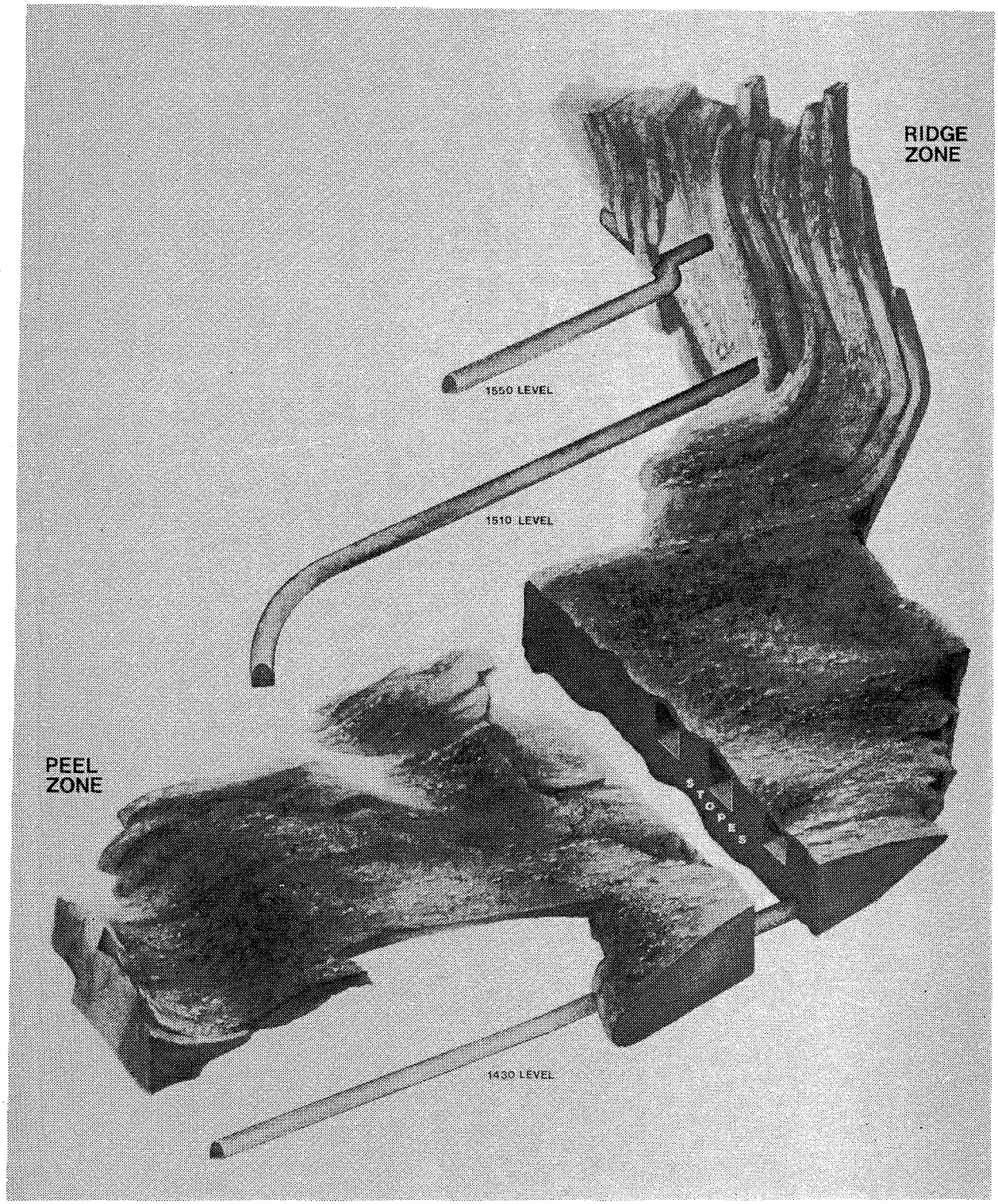

Figure 3. A perspective drawing illustration the 3-dimensional geometrical relationship between the Peel and Ridge oxide zones. The Peel sulphides lie west (left) of the Peel oxides.

a steeply plunging oxide chimney referred to as the Ridge Zone.

The Peel Zone is unique in that its western half issulphide and its eastern half has been deeply and thoroughly oxidized. Oxidation is, in places, deep and depth of oxidation is unrelated to existing topography. The major oxide deposits actually occur below or are encompassed by sulphides.

The Peel Sulphide Zone consists of irregular, interconnected veins and pods of auriferous pyrrhotite-pyrite-arsenopyrite in a body 600 metres long by 100 metres wide. Thickness varies from one to twenty-five metres and is stratabound, near the upper contact of the unit 1d limestone. Alteration of the limestone adjacent to the deposit is almost non-existent. Sulphide-limestone contacts are sharp with only the slightest sign of bleaching.

The sulphide ore is primarily pyrrhotite with an average of about 10% arsenopyrite, 5% pyrite and 2% chalcopyrite. Galena and sphalerite are rare. The sulphides are zoned from an arsenopyrite rich core grading out to pyrrhotite dominated fringes. A thin zone of galena and sphalerite locally rims the gold bearing section and calcite forms the margin of the deposits. Non-sulphide gangue minerals include quartz, calcite and sericite.

Native gold or, less commonly, electrum forms finely disseminated grains up to 25 microns in size. The gold is commonly associated with chalcopyrite and native bismuth and occurs mainly in fractures in arsenopyrite and pyrite or along sulphide grain boundaries. Less commonly, it is in pyrrhotite. Gold is erratically distributed, showing no preference for the hangingwall or footwall of the sulphide deposit.

The sulphide manto changes abruptly to oxide across a steeply dipping, northwest-trending fault called the Junction Fault (Fig. 2). Where seen in the underground workings, the contact between oxide and sulphide is sharp and distinct.

The Peel Oxide Zone is an elongated, sheet-like body approximately 60 metres wide by 280 metres long and about 5 metres thick on average. It dips from 10 to 30 degrees to the east, perpendicular to the long axis of the deposit. Virtually no sulphides remain in the oxidized portion of the deposit. The oxides generally show sharp contacts with the host limestone, with only a weak limonitic alteration of the limestone. The hangingwall is rubbly limestone with blocks of limestone up to 1 metre in diameter suspended in either oxide or distinct, light gray, strongly laminated clay.

Goethite and hisingerite (a rare form of hydrous iron silicate) are the main minerals within the oxide. Trace amounts of clay, quartz crystals and a small percentage of pyrite are also present. Most of the oxide minerals appear to be intimately mixed or amorphous. Goethite, hematite and scorodite have been identified by x-ray powder diffraction. The term limonite is used to describe the oxide material in general.

Gold occurs as free grains up to 25 microns in diameter within the oxide minerals. Metallurgical results suggest submicroscopic gold is present. The oxide includes two distinct textures and colours. Massive to boxwork textured brown oxide is located primarily in the footwall of the Peel Zone and is, generally barren of gold. Fine grained, locally colloform bright red-orange oxide occurs near the hangingwall and contains hisingerite. Gold is usually associated with the bright coloured, colloform banded texture, hisingerite, fine grained oxide and 'veins' of quartz sulphide sand.

The Peel Zone hangingwall is a lithologic contact whereas the footwall is an assay grade cutoff. The best grade assays occur at the hangingwall contact, with the gold grade decreasing downward. Gold distribution is markedly different in relation to the sulphide protore where gold is erratically distributed throughout the deposit.

The Ridge Oxide Zone, is roughly oval in cross-section, approximately 90 metres long down dip and 20 metres by 50 metres in horizontal section. The Ridge Oxide Zone has the same mineralogy as the Peel Oxide Zone. There is no unoxidized sulphide mineralization in this deposit. Both the hangingwall and the footwall of the Ridge are assay grade cut-offs. Ore grade material tends to occur as colourful, locally banded oxides near the center of the oxide deposit, surrounded by boxwork textured oxides.

The Ridge Zone is surrounded by irregular fault slices of limestone, mudstone and black shale. The Junction and Peel Faults (Fig. 2) are the key structures which disrupt the stratigraphy in this area and their intersection likely provided a major control on the position of the Ridge Zone.

The other sulphide/oxide mantos and chimneys in the Cache Creek Valley are smaller than the Peel and

Ridge Zones but have similar characteristics.

In addition to the manto-chimney deposits, several large but as yet sub-economic fissure veins occur on the property (see Cathro, this volume; 1988). All are hosted by hornfelsed argillite-quartzite (Unit 1a). The fissure vein deposits are composed of gold bearing quartz-arsenopyrite-pyrite. Quartz is generally the major constituent and arsenopyrite the most abundant sulphide.

The veins contain two types of oxide mineralization. One type resembles the manto and chimney oxides and has essentially the same constituents. More common are greenish oxides of arsenic-rich sulphides, scorodite, mixed with abundant clay. When the two oxide types occur in the same vein, a broad, banded texture often results. Gold does not appear to prefer one type of oxide over the other. The gold occurs as free milling grains.

In contrast to the weak hydrothermal alteration of limestone near mantos, argillite is intensely clay altered or pervasively silicified within several meters of veins.

GENESIS OF THE DEPOSIT

The gold deposits at Ketza are thought to be genetically related to a blind mid-Cretaceous stock centered beneath the core of the district. Steeply dipping faults coeval with uplift and doming during intrusion of this stock are believed to have been the principal ore localizing features.

The style of sulphide emplacement was controlled by the local structural intensity and by the competency and chemical reactivity of the host rocks. The brittle hornfelsed argillite allowed the formation of large and complex vein systems with numerous stringer off-shoots and stockworks along their margins.

In chemically reactive limestone, mantos and chimneys developed hydrothermal boring or corrosion by ore-forming fluids. Upon gaining access to the limestone along major fissure conduits, these fluids were guided by a myriad of smaller scale structural openings including secondary faults, minor thrusts, fractures, joints and bedding surfaces. The Peel and Ridge Zone oxides lie within an intensely faulted and fractured panel. As the rate of replacement depended to a large degree on the surface area available for reaction, the thickest and most extensive mineralization was emplaced in areas with the highest density of structural discontinuities. Some of these structural openings may have been enlarged by groundwater dissolution prior to the introduction of hydrothermal fluids.

In order for deep supergene oxidation to occur, as it did in the Peel and Ridge Zones, the primary sulphide deposits must have been accessible to subterranean watercourses carrying a strong flow of oxygenated water. Oxides underlie sulphides suggesting oxygenated groundwater must have utilized the hydrothermally created channels to oxidize the sulphides. Gold had reconcentrated near the hangingwall of the mantos implying that significant remobilization of gold occurred with oxidation. The average grade of the Peel Zone Oxide is approximately double that of the sulphide protore. Heat or a chemical gradient was required to achieve this upward remobilization. Perhaps oxidation and sulphide formation were closely overlapping, continuous events and that the heat of the hydrothermal process resulted in remobilization, or perhaps heat was released through oxidation of pyrrhotite.

The strongly laminated clays along the oxide hangingwall and the limestone rubble along the contact are evidence of groundwater deposition and of open space in waning stages of the oxidation process.

REFERENCES

Cathro, M.S., 1988, Gold and silver lead deposits of the Ketza River District, Yukon: Preliminary results of field work. in Yukon Geology, Vol. 2, Exploration and Geological Services Division, Yukon, Indian and Northern Affairs Canada, p. 8-25.

GOLD AND SILVER, LEAD DEPOSITS OF THE KETZA RIVER DISTRICT, YUKON: PRELIMINARY RESULTS OF FIELD WORK (modified from Cathro, 1988)

Michael S. Cathro
Department of Geology and
Geological Engineering
Colorado School of Mines
Golden, Colorado 80401

ABSTRACT

The Ketza River gold deposits, in central Yukon, are gold-bearing, massive sulphide mantos and chimneys in Lower Cambrian limestone. Mining is presently confined to oxidized portions of the deposits. The deposits are bounded on three sides by silver-rich veins. Metal zoning corresponds to a pronounced domal uplift that is thought to be related to a buried Cretaceous intrusion. The zoning may partly reflect stratigraphic control, but distance from the buried intrusion is considered the prime control.

INTRODUCTION

The Ketza River gold deposit, jointly owned by Canamax Resources Inc. and Pacific Trans-Ocean Resources Ltd. is the largest lode gold deposit discovered in Yukon to date, and is the Yukon's next gold mine. The Ketza River deposit is bounded on three sides by numerous silver-lead veins informally known as the "Iona Silver Property". Together, these deposits comprise the Ketza River District.

Two aspects of the geology are of particular interest. Firstly, the style of gold mineralization is new to Yukon. Auriferous epigenetic massive iron, arsenic and copper sulphides or supergene, iron oxides occur mainly as stratabound "mantos" (or blankets) in thickly bedded Lower Cambrian limestone. Lead and zinc minerals are rare and silver values low. The mantos comprise a previously unrecognized type of gold deposit in the northern Cordillera, and perhaps present a gold-rich analogue of the silver-rich replacement deposits at Midway, British Columbia; Leadville, Colorado; Bingham and Tintic, Utah; and Santa Eulalia, Mexico.

Secondly, the district exhibits an obvious concentric zoning pattern of metals and style of mineralization, with gold occurring near the centre of a conspicuous, domal uplift, and silver-lead mineralization occurring more distally. The zoning may be partly the result of stratigraphic control of mineralization. The uplift is probably underlain by a Middle Cretaceous stock although no intrusive rocks have been located. Mineralization in the Ketza River District is thought to be genetically related to this stock.

This report is modified slightly from Cathro, 1988, and presents the preliminary results of field work which will form the basis of a Master of Science thesis at the Colorado School of Mines. It is based on outcrop, drill-core and underground examinations of the Ketza River gold deposits during the 1984 and 1986 field seasons. Study of the surrounding silver-lead occurrences during 1986 was confined to examination of surface exposure and dump material because most of the workings are inaccessible and drill-core is not available.

LOCATION AND HISTORY

The Ketza River District (Fig. 1) covers an area roughly 10 km by 10 km. It is centered 50 km south of the town of Ross River in the rugged St. Cyr Range of the Pelly Mountains (N.T.S. 105 F 09, 61°32'N, 132°15'W). A 45 km gravel road connects the Canamax camp with the Robert Campbell Highway at a point 23 km southeast of

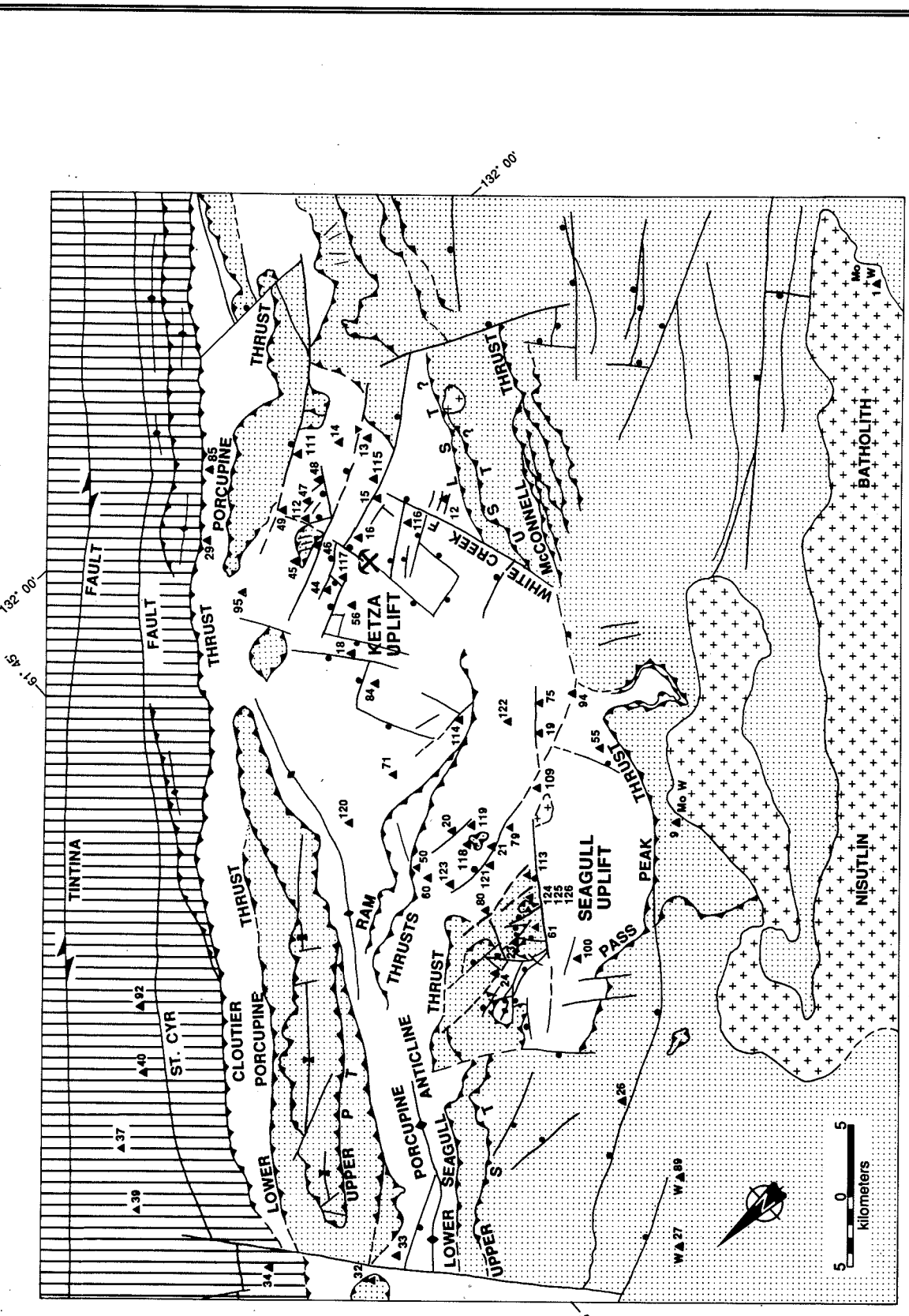

Figure 1. Structural setting of epigenetic mineral occurrences in the central Pelly Mountains (modified from Abbott, 1986). Most occurrences are associated with two domal structures, the Ketza and Seagull Uplifts, which together form Ketza-Seagull Arch. Ketza-Seagull Arch is a window through the Seagull-Porcupine-Pass Peak Thrust, and includes the unpatterned area southwest of the Porcupine Thrust, and southeast of the Porcupine Anticline. The Arch and Uplifts are defined by the window, by the pattern of normal faults in it, and by the distribution of map units, which are not shown here (see Tempelman-Kluit, 1977). Abbreviations include Lower Seagull Thrust (LST), (Upper Seagull Thrust (UST), Porcupine Thrust (PT). Numbers refer to mineral occurences. The crossed hammers show the location of the Ketza Mine.

Ross River.

The first discovery in the district was a silver-lead vein found in 1947 by HudsonBay Mining and Smelting Co. Ltd. The Ketza River gold deposit (formerly known as the BOOM or WOODCOCK showing) and many of the larger silver-lead occurrences, were discovered by Conwest Exploration Co. Ltd. and others in 1954 and 1955. The silver-lead veins have been intermittently explored with trenching, drilling, and underground work (12 short adits) by various interests until the present with only limited success. Only very minor production of hand cobbed ore has taken place. The STUMP (or 1) vein, discovered in 1966, is the best explored and by far the largest of the veins with probable reserves of 49 800 tonnes grading 20.0% Pb and 719.9g/t Ag (Orssich et al., 1985).

Conwest explored the Ketza River gold deposit with trenching and 59 drill holes from 1955 until 1960, and outlined sulphide reserves of 68 000 tonnes grading 12 g/t Au (Rotherham, 1958). The property then lay dormant until 1984 when Pacific Trans-Ocean Resources Ltd optioned the property from Conwest and entered into a joint venture agreement with Canamax Resources Ltd. Aggressive drilling and underground development to the end of 1986 had delineated reserves of 1.0 million tonnes averaging 13.7 g/t Au (Northern Miner, February 9, 1987).

Two factors have been primarily responsible for the greatly increased tonnage and economic viability of the Ketza River gold deposit: 1) appreciation by Canamax geologists of the geometry and ore controls of similar deposits in the U.S. and 2) recognition of the potential for large tonnages of metallurgically superior oxide mineralization in structurally prepared zones.

REGIONAL GEOLOGY

This summary of the regional geology is based on published descriptions of the geology of the Pelly Mountains and Ketza River District, including Wheeler et al. (1960), Tempelman-Kluit (1977a, 1977b, 1979, in prep.), Tempelman-Kluit et al. (1975, 1976), Read (1980), and Abbott (1986). The Ketza River district is underlain by moderately folded and faulted Paleozoic miogeoclinal strata of the Pelly-Cassiar Platform which are interpreted as autochthonous and parautochthonous to the North American craton by Tempelman-Kluit (1977a).

Four significant thrust faults, the McConnell, Porcupine-Seagull, Cloutier, and St. Cyr Thrusts, run parallel to the Tintina Fault and dip generally southwest (Fig. 1). Most rocks in the Ketza River District are part of the Cloutier Thrust Sheet although two small klippen belong to the overlying Porcupine-Seagull Thrust Sheet. Thrusting probably occured during the Late Jurassic and Early Cretaceous (Tempelman-Kluit, 1979). The northwest-trending Tintina Fault located 15 km northeast of the District, has experienced at least 450 km of dextral, transcurrent offset since the middle Cretaceous (Gabrielse, 1985).

The most prominant structural feature in the Pelly Mountains is the Ketza-Seagull Arch (Abbott, 1986), an elongate, northwest-trending window through the Porcupine-Seagull Thrust that is probably underlain by, and related to buried Cretaceous intrusions. Abbott considered the Arch to be made up of two smaller domal structures, the Seagull Uplift and Ketza Uplift (Fig. 1). Structure in the window is characterized by steeply dipping normal faults.

The Ketza Uplift, situated in the centre of the Ketza River District (Fig. 3, was first postulated to be underlain by an intrusion by Parry et al. (1984). This theory is supported by the presence of a magnetic anomaly, hornfelsing, and hydrothermal alteration immediately north of the Ketza River gold deposit. The hornfels has been dated by whole-rock K-Ar as Middle Cretaceous (101 +4 Ma; K.M. Dawson, G.S.C., 1986, pers. comm. to S.E. Parry).

LOCAL GEOLOGY

The Ketza River District is underlain by five main units that range in age from Lower Cambrian to Mississippian. These are shown in Figures 2 (generalized stratigraphic column) and 3 (simplified geology map). Cambrian through Mississippian strata of units 1 to 4 belong to the Cloutier Thrust Sheet and strata of unit 5 belong to the structurally overlying Porcupine-Seagull Thrust Sheet.

An excellent description of the Lower Cambrian sedimentary rocks (Unit 1) near the Ketza River gold deposit has been presented by Read (1980). His terminology of subunits within Unit 1 is adopted here with minor modifications. The other units are mainly modified after Tempelman-Kluit (1977a) and unpublished company maps.

Unit 1: Lower Cambrian

The Lower Cambrian succession has been split into five lithostratigraphic subunits (1a through 1e) with

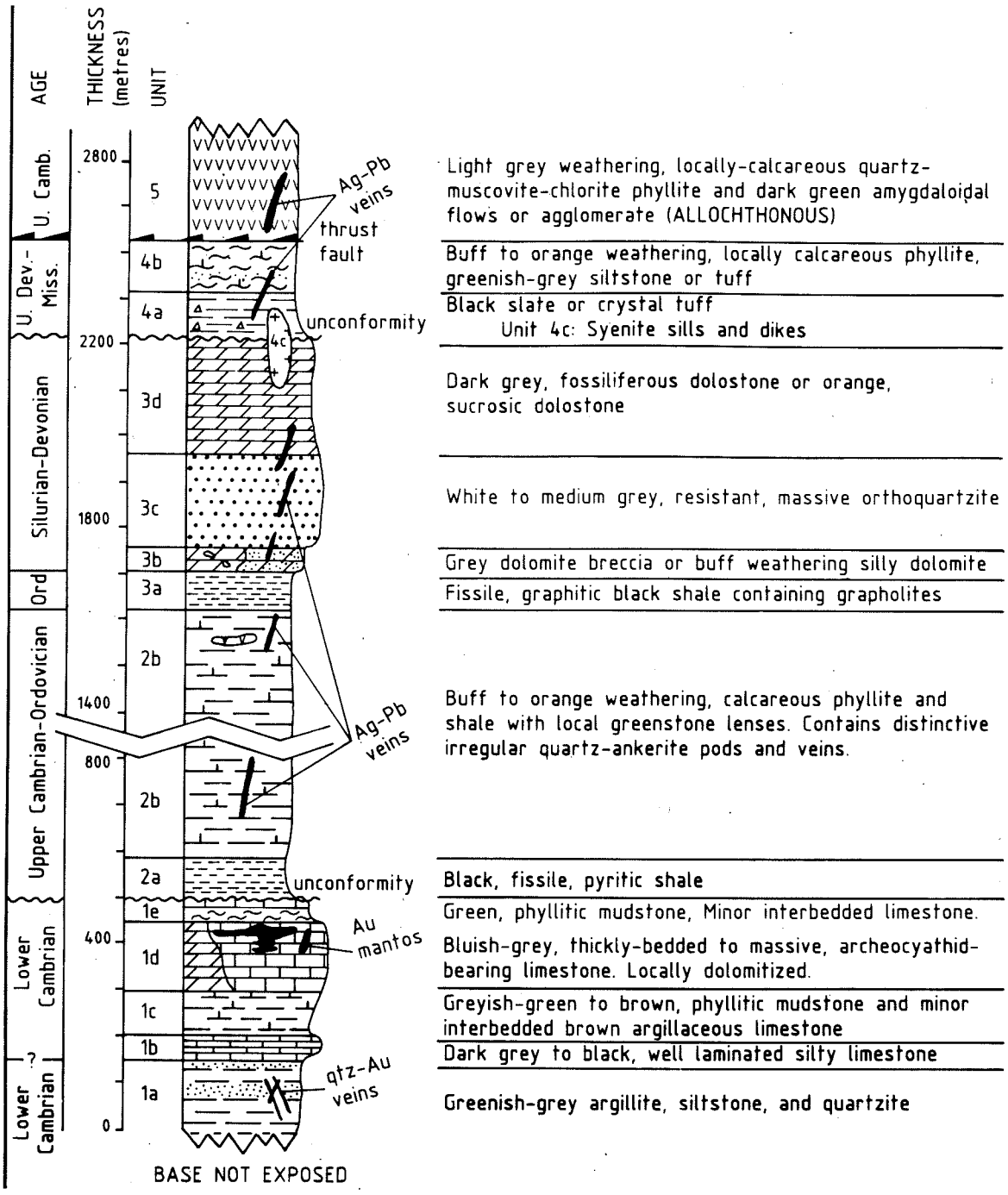

Figure 2. Generalized stratigraphic column for the Ketza River District including the relative positions of important mineral deposit types (modified after Tempelman-Kluit, 1977a; Read, 1980; and unpublished Canamax Resources reports).

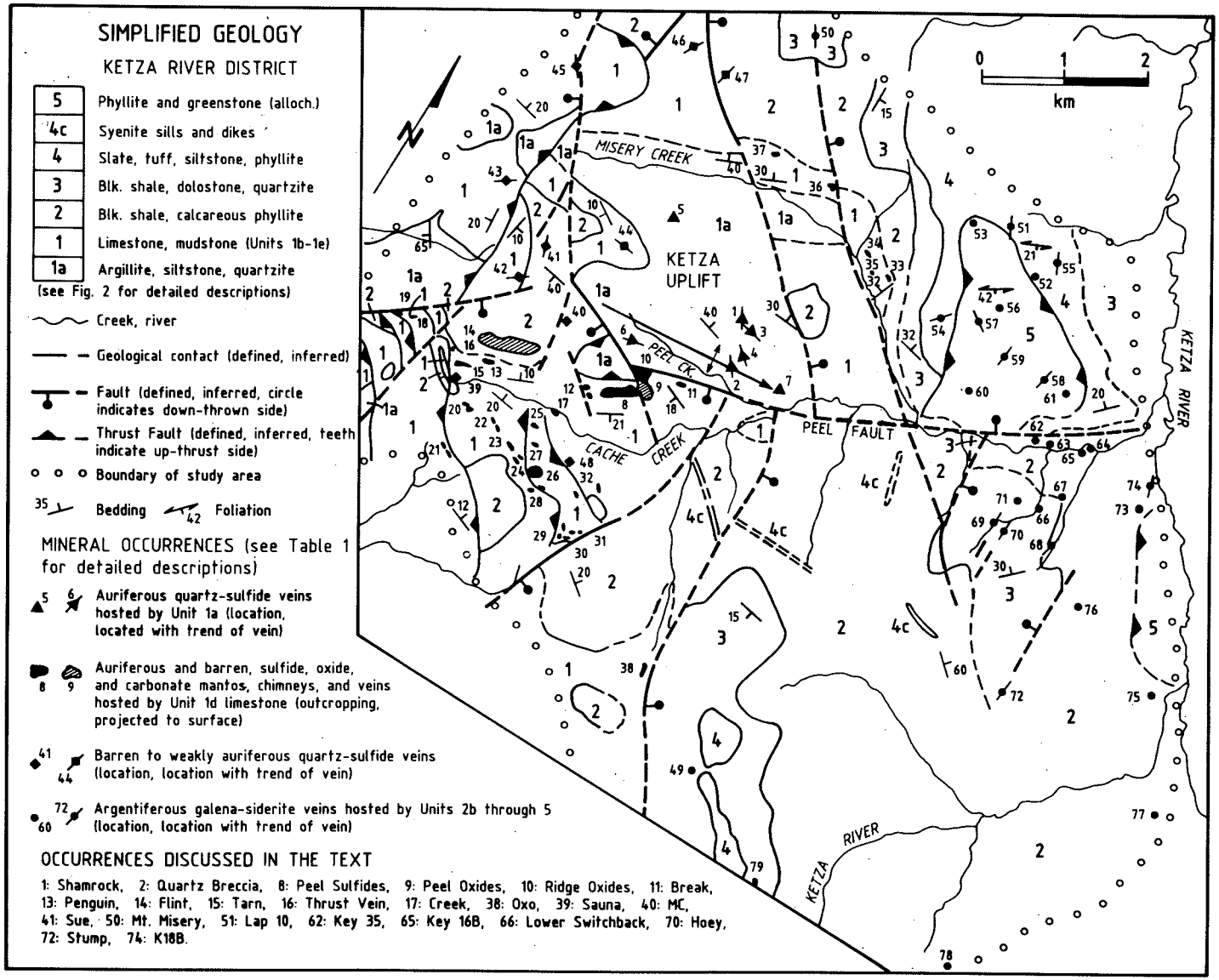

Figure 3. Simplified geology map of the Ketza River District including the locations of mineral occurrences discussed in this paper. Summary descriptions of all occurrences are given in Table 1. (Geology modified after Tempelman-Kluit, 1977a; 1980; and unpublished Canamax Resources maps).

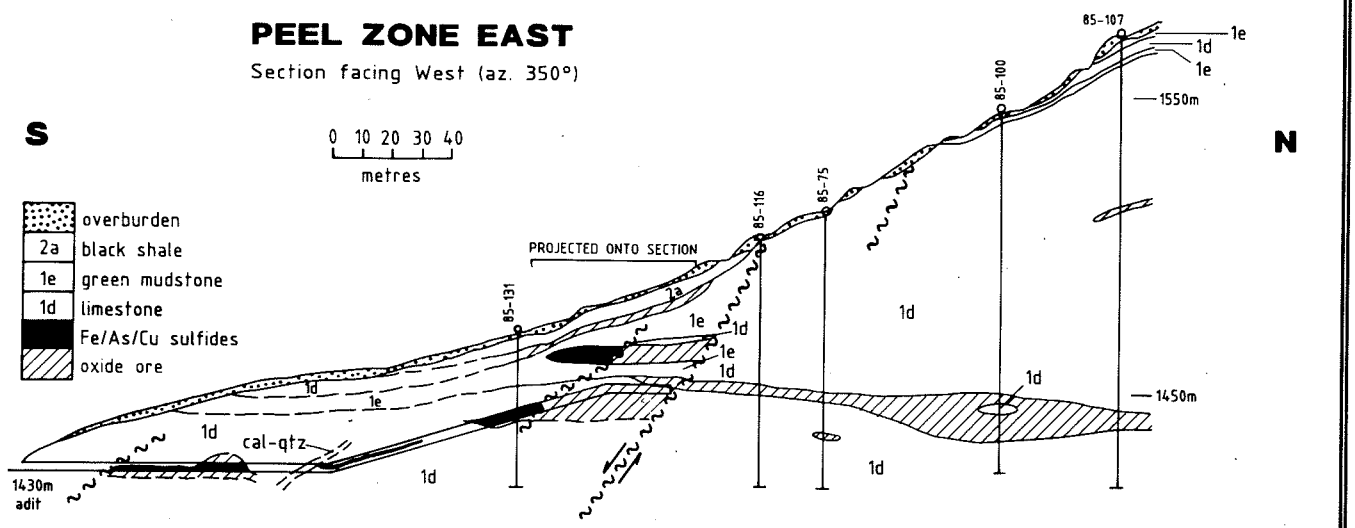

Figure 4. Cross section facing west through the Peel gold zone. See Fig. 2 in Abercrombie (This volume), for location.

an aggregate thickness greater than 500 m. The lower contact is not exposed and the upper contact is an unconformity of probable Upper Cambrian age.

Unit 1a contains the oldest rock exposed and comprises green argillite, siltstone, and quartzite. The unit contains a strong hornfels on the north side of the ridge that hosts the Ketza River gold deposits.

Unit 1b, a narrow bed (25 to 60 m thick) of resistant, dark grey to black, well laminated, silty limestone conformably overlies Unit 1a. Contacts are sharp and the unit is an excellent marker.

Unit 1c contains Early Cambrian fossils and is composed of greyish green to brown, recessive-weathering, calcareous, phyllitic mudstone with minor interbedded argillaceous limestone. Large pyrite cubes may be present. This unit may be as much as 100 m thick. The upper contact with Unit 1d is gradational and arbitrary since it is defined as the point where carbonate makes up more than half of the rock (Read, 1980).

Unit 1d, the main host for gold mineralization, is distinctive grey-blue, thickly bedded to massive, archeocyathid-bearing, cliff-forming limestone (Fig. 4). The unit is 120 to 180 m thick and made up predominantly lime mudstones with argillaceous interbeds near its base. Large archeocyathid buildups (archeocyathid bindstone and skeletal sand) are reported near the bottom of Unit 1d along the southern edge of the district (Read, 1980). Bedding attitudes are generally difficult to determine because the rocks are strongly bioturbated. To the west and north of the main Ketza River gold deposit, the limestones are strongly dolomitized and are blocky and orange weathering.

Unit 1e, a narrow (0 to 50 m thick) marker bed of non-calcareous, phyllitic green mudstone is interbedded with limestone within 10 m of the top of Unit 1d . In places, the upper limestone and green mudstone are completely missing, suggesting that the upper contact is an unconformity.

Unit 2: Upper Cambrian-Ordovician

Cambro-Ordovician rocks in the Ketza River District comprise a lower unit of black shale (Unit 2a) and a thick, upper unit of buff weathering, calcareous phyllite or shale (Unit 2b). Both weather recessively, making thicknesses and contact relations difficult to determine.

Drilling has shown Unit 2a to be at least 30 to 100 m thick. Unit 2b is at least 1000 m thick. A major unconformity probably exists beneath the black shale (Unit 2a). This unit was not described by Tempelman-Kluit (1977a), or Read (1980). This age,

though uncertain, is probably Upper Cambrian. In this study, it is grouped with Unit 2b. Unit 2b is strongly deformed and contains small, distinctive, irregular quartz-ankerite veins. Near large quartz veins, the calcareous phyllite is altered to blocky weathering, sucrosic dolomite. Large galena-siderite veins are hosted by Unit 2b.

Unit 3: Ordovician-Silurian-Devonian

Unit 3 includes four distinctive subunits that range in age from Ordovician to Devonian. Most host galena-siderite veins.

Unit 3a, the lowermost member, is recessive, fissile, graphitic, black graptolitic shale with minor interbedded calcareous, silty, and muddy beds. It is 50 to 100 m thick and Ordovician to Silurian in age.

Unit 3b, overlying the black shale, is a thin discontinuous interval of buff weathering, grey, silty dolomite and well indurated dolomite breccia with a dark grey dolomite matrix. Large coral fragments have been found at one location. This unit hosts weakly disseminated and vein-type Ag-Pb mineralization at the LOWER SWITCHBACK showing.

Unit 3c is distinctive white to medium grey, massive, resistant orthoquartzite. In many places it lies directly on Unit 3a black shale. It is at least 150 m thick and is Silurian. It hosts galena-siderite and quartz-pyrite-gold mineralization at the MT MISERY and HOEY showings.

Unit 3d is predominantly well-bedded, dark grey fossiliferous dolostone of Devonian age. On Mt. Misery, fine to medium-grained sucrosic, orange weathering dolomite overlying the quartzite (Unit 3c) is probably equivalent to Unit 3d.

Unit 4: Devonian-Mississippian

These rocks are equivalent to the Earn Group of Gordey et al. (1987) and consist of a lower member (Unit 4a) of black slate and dark grey to black, cherty siltstone or crystal tuff with minor interbedded chert, sandstone, chert pebble conglomerate and green tuff. The lower contact with carbonate is usually unconformable (Gordey et al., 1987).

Unit 4b overlies the black slate and includes buff-orange weathering, locally calcareous phyllite, and greenish-grey siltstone or tuff of unknown thickness.

Mississippian intrusive rocks (Unit 4c), consist of rare syenitic sills and dykes. A small diorite plug near the KEY 3 showing is surrounded by a pyrite aureole and alteration in overlying Mississippian volcanic rocks.

Unit 5: Upper Cambrian and Ordovician

Two klippen of volcanic rocks belonging to the Porcupine-Seagull Thrust Sheet occur near the junction of Cache Creek and the Ketza River. They are predominantly recessive, light grey weathering, locally calcareous, quartz- muscovite-chlorite phyllite, and green, moderately foliated, amygdaloidal volcanic flows and agglomerate. Minor chert and dark green diorite has also been reported (Orssich et al., 1985). The larger of the two klippen occurs north of Cache Creek, dips gently to the south, and is in contact with all rocks types from the Upper Cambrian phyllite to Mississippian volcanic rocks. The unit exceeds 200 m in thickness.

STRUCTURE

As stated above, the Ketza Uplift dominates the Ketza River District. The most obvious structures are southwest-dipping thrust faults with relatively small displacements, and steeply dipping, east, north and northwest trending normal faults. Most strata are gently folded and moderately dipping except near thrusts, where drag folding has occurred.

Northeast-directed thrusts other than the Porcupine-Seagull Thrust are only documented in the well studied Lower Cambrian rocks. The highly contorted nature of the Cambro-Ordovician calcareous phyllite (Unit 2b) suggests that this unit may also have been imbricated by thrusting. Thrust-related folds have gently dipping axial planes and upright to overturned forelimbs.

At least three sets of steeply dipping faults cut the thrust faults. These faults form the eastern, western and southern margins of the Ketza Uplift and are thought to reflect intrusion-related doming.

The Peel Fault is an east-trending, steeply north-dipping reverse fault located immediately north of the Ketza River gold deposit. The fault extends down Cache Creek and is responsible for the 200 to 300 m of offset of strata on either side of the Cache Creek valley.

Northwest-trending faults are nearly vertical. The fault east of the SHAMROCK zone with at least 400 m offset is one of the largest and may be the offset extension of the fault east of the OXO showing. Most of the silver-lead occurrences occur near vertical

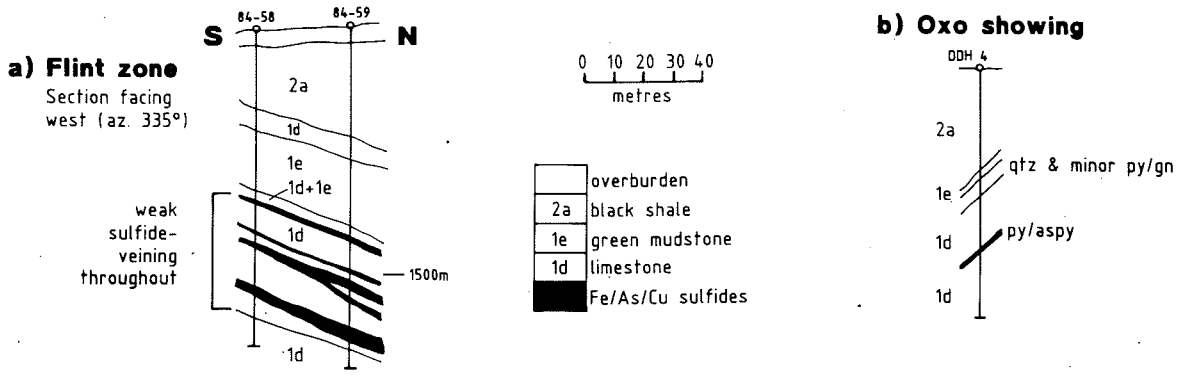

Figure 5. a) Cross section facing west through the Flint zone.
b) DDH #4, OXO showing.

north-trending faults of relatively small displacement (Fig. 5).

Faults near the Ketza River gold deposit are complex and are an important control on mineralization. The strong northwest-trending fault set crosscuts the east-trending Peel Fault and thrust faults.

MINERALIZATION

Over a hundred mineral showings occur in the Ketza River District. These can be broadly classified into four main types as follows:

1. auriferous quartz-arsenopyrite + pyrite veins cutting Lower Cambrian argillite/quartzite (Unit 1a),

2. auriferous and barren sulphide, carbonate and oxide mantos, chimneys and veins hosted in Lower Cambrian limestone (Unit 1d),

3. barren to weakly auriferous quartz + arsenopyrite veins and stockworks cutting Lower Cambrian limestone (Unit 1d) and Cambrian-Ordovician calcareous phyllite (Unit 2b),

4. argentiferous galena-siderite veins cutting Upper Cambrian through Mississippian strata (Unit 2b to Unit 5).

These deposit types are zoned and coincide with the distribution of rock types about the Ketza Uplift. Type 1 gold-rich quartz veins are surrounded by Type 2 gold-rich mantos which are in turn surrounded by Type 4 silver-lead veins. Type 3 veins show an erratic distribution. For simplicity, the types are described in this order.

Locations of the showings are shown on Figure 3 and some of the important features (mineralogy, attitude, host rock, etc.) are given in Table 1.

(1) Gold in Proterozoic argillite

Important gold-bearing quartz-arsenopyrite veins at the SHAMROCK and QUARTZ BRECCIA zones (Fig. 3) occur in argillically-altered argillite and quartzite of Unit 1a near the approximate centre of the Ketza Uplift. The QUARTZ BRECCIA zone is a vein zone 200 m long by 24 m wide that strikes 300° and dips moderately east just north of Peel Creek. At surface, veins are composed of coarse, granular quartz, scorodite, and minor arsenopyrite. In the SHAMROCK zone 700 m farther north, similar veins also trend northwesterly. Surface samples containing mostly scorodite have

returned assays up to 1000 g/t au (Northern Miner Magazine, March, 1987, p. 35).

FRED'S VEIN occurs approximately 500 m north of the Ketza River gold deposit in hornfelsed argillite of Unit 1a. It trends east-northeast, dips steeply and has a higher sulphide content than the Shamrock-type veins. Locally, this vein contains massive pyrrhotite-arsenopyrite not unlike the sulphide mantos and veins in Lower Cambrian limestone.

(2) Gold in lower Cambrian limestone

Lower Cambrian limestones of Unit 1d host the Ketza River gold deposit and similar but smaller, lower grade occurrences over an area of 6 km by 4 km (Fig. 3). The deposits consist of massive sulphide, carbonate, or oxide mantos, chimneys, and veins. The largest deposits (the TARN, PENGUIN, FLINT, BREAK and PEEL zones (occurrences 8 to 15) fall along a 2 km lineament trending 080° (Fig. 3) suggesting structural control. All deposits occur in the upper 100 m of the Lower Cambrian limestone, indicating that stratigraphy is also an important ore control.

The deposits are either sulphide-rich or oxide-rich. The latter appear to be in situ supergene replacements of the sulphides. Their superior metallurgical properties and grade (average 18 g/t versus 9 g/t for sulphides), make the oxides the most economically important. The sulphides, are more common and better exposed.

Sulphide mineralogy

The mineralogy of the sulphide bodies is simple, consisting mainly of semi-massive to massive pyrrhotite, with variable quantities of arsenopyrite, pyrite and minor chalcopyrite. Some deposits south of Cache Creek contain significant siderite.

Arsenopyrite averages 5 to 10% by volume and forms large (2 to 5 mm) euhedral grains disseminated throughout the pyrrhotite. Arsenopyrite also locally forms narrow (5 mm) bands around remnant limestone clasts enclosed in pyrrhotite. In some places massive pyrrhotite contains small (3 m by 20 m) discrete lenses of massive (90%) arsenopyrite.

Pyrite is common as large (to 5 cm) subhedral masses but rarely makes up more than 50% of the total sulphides. Chalcopyrite is common as a fine network between other sulphide grains and makes up 0.5 to 1% of the sulphides by volume.

Gold is irregularly distributed but correlates best with arsenopyrite and total sulphide content. Only in the PEEL zone are sulphides consistently auriferous. Only erratic high values have been encountered in showings distal from the PEEL zone. Toohey (1986) determined that gold generally occurs as 0.5 to 25 micron grains associated with native bismuth and chalcopyrite which fill fractures in other sulphides. Spheroidal gold inclusions in pyrrhotite and pyrite were also noted.

Galena and sphalerite are extremely rare in most sulphide deposits, with small amounts noted in the PEEL zone and the CREEK showing and significant quantities in the OXO showing (Fig. 5).

Oxide mineralogy

Gold-bearing oxide material is composed of limonite, hematite, other unidentified hydrous iron oxide minerals and quartz. Gold grades are often highest where an unusual yellow, orange, red or brownish black, conchoidally-fracturing amorphous mineral is present (Fig. 7). Conwest geologists referred to this as "hisingerite" which is actually a mineraloid. This material resembles yukonite in appearance.

Shape and size of ore bodies

The auriferous bodies vary in shape and size. All crosscut the enclosing limestone and are clearly epigenetic. The largest and most continuous of the sulphide bodies are conformable, nearly flat-lying blankets or "mantos". The deposits occur near the top of the massive Lower Cambrian limestone (Fig. 8), from 0 to 100 m beneath the green mudstone (Unit 1e). The thickness of the mantos varies greatly, from less than 10 cm to greater than 30 m. Vertical stacking of parallel lenses (Fig. 4) is common. The maximum drilled dimensions of the PEEL zone (sulphides plus oxides) are approximately 500 m by 300 m. The FLINT zone may be larger, with a drilled thickness of over 30 m (Fig. 5) and a possible strike length of over 1500 m based on geophysical data.

Mantos are extremely irregular in detail despite their strong overall stratigraphic control. Massive sulphides pinch and swell and inter- finger with barren limestone or weakly sulphide-veined limestone. Locally, mantos become calcite and quartz-rich at their margins.

Sulphides consistently crosscut earlier-formed irregular calcite veins (5 - 20% of host limestone) proving that the deposits are epigenetic.

Contacts between sulphides and limestone are invariably sharp; only faint bleaching of limestone is occasionally visible. In some places, irregular sulphide veins form a strong crackle breccia. As sulphide content approaches 30 to 40%, incipient brecciation is evident, with no appreciable rotation of limestone clasts. The clasts have irregular, rounded outlines. These textures suggest gradual replacement of limestone by sulphides.

Crosscutting chimneys and irregular sulphide veins are common and have a variety of orientations. The THRUST vein and a number of unnamed crosscutting bodies south of Cache Creek are the best exposed. The BLUFF zone may be a vein occurrence.

The THRUST VEIN is a 2 m wide vein of pyrrhotite-pyrite-quartz- calcite striking northwest and dipping moderately south. It is in a thrust fault which juxtaposes Unit 1d (limestone) against Unit 2a (black shale) and has a strike length of over 100 m. At its west end, the THRUST VEIN changes to quartz and calcite with no sulphides. Similar veins occupy thrust faults in the cliffs south of Cache Creek, roughly 1 km south of the PEEL zone.

Auriferous iron oxide deposits (RIDGE, BREAK and PEEL OXIDE zones) can have the same general shape as sulphide bodies although they show a greater affinity for structurally disrupted sites.

The PEEL OXIDE zone is a flat-lying manto contiguous with the PEEL SULPHIDE zone but generally lies east of the major NW Fault. In some places, unoxidized sulphides are above the oxides suggesting that groundwater flow patterns the position of oxide mineralization.

The RIDGE zone (Fig. 3) is an irregular, northwest-plunging, pipe-shaped oxide body up to 30 m by 100 m across and at least 100 m below surface. It appears to occupy the junction between the PEEL Fault and the NW Fault. The RIDGE zone is mainly in limestone (Unit 1d) and merges with the PEEL OXIDES.

The BREAK zone, discovered in 1986, is 500 m east of the RIDGE zone in a similar structure and appears to be oriented in an easterly direction. The mineralogy and grade are similar to the RIDGE zone.In summary, pyrrhotite, arsenopyrite, siderite and iron oxide mantos, veins and chimneys are in Lower Cambrian limestone (Unit 1d) beneath a layer of green mudstone (Unit 1e). The deposits are gold-rich only near the junction between the PEEL fault and the NW fault. Oxide deposits are developed in zones of structural complexity which apparantly controlled groundwater flow and in situ oxidation sulphides. The sulphide deposits, although stratabound, are clearly epigenetic.

(3) Quartz-sulphide veins

Barren to weakly auriferous quartz-sulfide veins and stockworks are common. They are economically unimportant, and have not received much attention but may indicate a large intrusion-centreed hydrothermal system. The SAUNA, MC and SUE showings are the best example. Similar but unnamed showings occur south and west of the MT MISERY showing and north and west of the OXO showing (Fig. 3).

The veins are randomly oriented and are predominantly quartz with subordinate (less than 2%), chalcopyrite or arsenopyrite, accessory pyrrhotite, pyrite, galena or tetrahedrite. Strong dolomitization of host carbonate rocks is ubiquitous near the veins. At the MC zone where a stockwork of small quartz veins is developed in Lower Cambrian limestone, chalcopyrite is the predominant sulphide. The SUE showing is a large (up to 3 m wide) quartz vein, with very minor disseminated chalcopyrite, in Upper Cambrian calcareous phyllite.

The relationship of the veins to pyrrhotite-arsenopyrite mantos and the auriferous quartz sulphide veins is not well understood. They may simply represent quartz-rich examples of the former, or gold-poor examples of the latter.

(4) Silver-lead veins in Upper Cambrian and younger rocks

At least thirty silver-lead-bearing veins have been discovered in the Ketza River District. Most are shown on Figure 3. All occur in Upper Cambrian to Mississippian strata. Fissure vein fillngs predominate although wall rock adjacent to the veins contains weak disseminations and stringers. The gangue is mainly siderite (some may be ankerite) with lesser, but locally abundant quartz, calcite and fragments of wallrock.

Coarsely disseminated galena and pyrite form shoots in the siderite veins or massive veins up to 50 cm wide. Chalcopyrite, tetrahedrite, arsenopyrite, sphalerite and pyrrhotite are accessory. Silver grades up to 17 000 g/t have been reported from tetrahedrite-rich material (Woodcock, 1955) but hand-picked, massive galena typically assays between 1000 to 4000 g/t Ag. When sampled over the entire width, siderite-galena veins generally grade 10 to 25% Pb, 300 to 800 g/t Ag, and trace to 2 g/t Au (Green, 1966; Findlay, 1967, 1968, 1969; Orssich et al., 1985).

Several veins contain significant gold. The HOEY showing (Fig. 18) consists of galena and siderite on surface but drilling and underground development have intersected a gold-bearing quartz-pyrite vein (21.6 g/t Au over 0.70 m for a length of 9.15 m) (Findlay, 1969; Orssich et al., 1985). Silurian quartzite encloses the vein at depth. Moderate gold values in a lens of pyrite and arsenopyrite have also been reported from the K16B zone (Orssich et al., 1985).Vein-faults generally strike within 20° of north and dip steeply, either east or west. The orientations of most veins are given in Table 1. A few veins have slightly different attitudes. At the KEY 3 showing, a siderite- quartz-galena-tetrahedrite vein has an attitude of 010/30W, the LAP 10 vein is oriented between 030/15W and 010/45W, and a pyritic fault zone at the KEY 35 showing is oriented at 057/68N (Orssich et al., 1985). Dolomite breccia (Unit 3a) nearby contains narrow galena veins trending 350°.

The amount and direction of movement on the vein-faults is difficult to estimate but most displacement is probably vertical. The fault at the MT MISERY vein moved east side down by as much as 100 m. The HOEY vein is in a steep, east-dipping, reverse fault with an offset of at least 20 m. Offset on many of the other vein-faults is probably minimal. Some veins show good continuity. The STUMP vein can be traced on surface for 250 m while the HOEY and LAP 10 veins have been traced for 275 m and 140 m respectively. The MT. MISERY vein can be traced for 60 m and is covered by scree at both ends.

The veins vary in width from a few cm to more than 5 m but average 2 m, of which 15 to 60 cm may be galena. The galena tends to split into parallel bands, 10 to 20 cm wide. The only veins with defined tonnages are the STUMP vein (49 800 tonnes grading 20% Pb and 719 g/t Ag) and the KIBB vein (8065 tonnes grading 14.4% Pb and 873 g/t) (Orssich et al., 1985).

Galena-siderite veins cut nearly all rock types from Unit 2b (Upper Cambrian-Ordovician) to Unit 4 (Mississippian) as well as Unit 5 Upper Cambrian. Clearly the veins were emplaced after thrusting (Mesozoic) since they show no change in orientation or mineralogy across the thrust fault. Mineralization must also postdate formation of the north-trending fault set. It is not known whether these north-trending faults are related to the formation of the Ketza Uplift.

DISCUSSION AND CONCLUSIONS

Ore controls and mode of formation

Stratigraphy, thrust faults and steep faults control the pyrrhotite- arsenopyrite $\pm$ siderite manto and vein showings. Gold-rich deposits of this class are confined to the area adjacent to the PEEL fault, particularly where this structure intersects northwest-trending cross-faults. Detailed mapping has shown that the sulphide deposits are clearly discordant and therefore epigenetic. Sulphide textures include vein stockworks, incipient breccia, and massive sulphide lenses suggesting variable replacement of limestone along bedding and fractures. Open-space textures, such as colloform banding are poorly developed and rubble breccias and laminated silt are absent. For these reasons, karst solution channels are not thought to have played an important role in controlling ore deposition. The author believes that pyrrhotite- arsenopyrite + siderite were deposited from hydrothermal solutions that gained access to the Lower Cambrian limestone along steep faults (i.e. the PEEL fault and cross-faults). These structures are thought to have formed in response to Middle Cretaceous intrusion and doming which has resulted in the Ketza Uplift. The hydrothermal solutions were confined beneath a thick sequence of impermeable shales (Units 1e, 2a, 2b) and therefore travelled laterally away from the faults. The gold-poor and siderite-rich mantos located far from the PEEL Fault may reflect the expected drop in temperature and pressure of fluids moving away from the intrusion.

The important gold-rich, iron oxide deposits of the RIDGE, BREAK, and PEEL OXIDE zones occur in strong fault zones. These deposits are believed to have formed by the in situ, supergene oxidation of primary sulphide mantos and veins in zones of high groundwater flow.

Silver-bearing galena-siderite veins follow north-trending, steeply dipping faults in Upper Cambrian (Unit 2b) and younger rocks. The faults may also be

middle Cretaceous in age. No regional zoning of galena-siderite vein mineralogy has been recognized.

Quartz-sulfide mineralization occurs in Proterozoic to Upper Cambrian strata but is only gold-rich in the Proterozoic rocks. These auriferous veins generally strike northwest and dip moderately east. Barren and weakly auriferous quartz-sulfide veins and stockworks in Cambrian limestone and calcareous phyllite (Units 1d and 2b) are randomly oriented.

Metal zoning and relative timing

Metals and occurrence types are zoned about the center of the Ketza Uplift from: quartz-arsenopyrite-gold veins; to auriferous pyrrhotite-arsenopyrite mantos and veins; to barren pyrrhotite-siderite mantos and veins; and finally, to galena-siderite veins on the perimeter. The zonation can be partly explained by strong stratigraphic control. This control can be summarized as follows:

1. quartz-arsenopyrite gold veins, mainly in Proterozoic argillite- quartzite (Unit 1a)

2. golg-ridrpyrrhotite-arsenopyrite mantos and veins (or their oxidized equivalents), mainly in Lower Cambrian limestone (Unit 1d)

3. barren pyrrhotite-pyrite-siderite mantos and veins in Lower Cambrian limestone (Unit 1d)

4. silver-rich galena-siderite veins, mainly in Upper Cambrian and younger strata (Unit 2b through Unit 5).

An alternate exploration for the observed concentric zonation proposes that the different types of mineralization may all be part of a large, district-scale hydrothermal system. The change from gold and arsenic-rich, to silver and lead-rich deposits may be a direct result of a decrease in fluid temperature and pressure of the hydrothermal fluids as they migrated away from the heat source. In this case the heat source is a Middle Cretaceous stock, postulated to underlie the Ketza Uplift. The relative ages of the deposit types are unclear because they occur in different rock units and no cross- cutting relationships are seen. Isotopic studies and geothermomentry may help sort out these problems.

Implications for exploration

The suggestion that the various deposit types in the Ketza River District are related to a common source has important implications for exploration in the district and elsewhere. If silver-lead veins can be proven to be distal to a large intrusion-centred hydrothermal system with gold mineralization near the centre, then silver veins are a useful exploration guide for quartz-sulfide vein or sulphide manto deposits. Other silver camps in the Cordillera such as Keno Hill, Plata, Tintina, Quartz Lake and Midway should be re-evaluated with the Ketza zoning model in mind, especially if carbonate rocks are present.

ACKNOWLEDGEMENTS

Financial support for this study has been provided by the Exploration and Geological Services Division of Indian and Northern Affairs Canada. I am grateful to Grant Abbott and Jim Morin of INAC for advice and encouragement. Thanks are also extended to the management of Canamax Resources Inc. for accommodation in field, access to drill core, underground workings, and confidential exploration data, and for permission to publish. Special thanks must go to Canamax geologists Steve Parry, Jeff Toohey, Fred Harris, and Cyrril Orssich for inspiring and critical discussion. Kate Rodd and Karen Smith helped with proof-reading, typing and drafting and their assistance is greatly appreciated.

REFERENCES

Abbott, J.G., 1986, Epigenetic mineral deposits of the Ketza-Seagull district, Yukon; in Yukon Geology, Vol. 1, Exploration and Geological Services Division, Yukon, Indian and Northern Affairs Canada, p. 56-66.

Cathro, M.S., 1988, Gold and silver, lead deposits of the Ketza River District, Yukon: Preliminary results of field work; in Yukon Geology, Vol. 2; Exploration and Geological Services Division, Yukon, Indian and Northern Affairs Canada, p. 8-25.

Findlay, D.C., 1967, The mineral industry of Yukon Territory and southwestern District of Mackenzie, 1966; Geological Survey of Canada, Paper 67-40, p. 56-58.

Findlay, D.C., 1968, The mineral industry of Yukon Territory and southwestern District of Mackenzie, 1967; Geological Survey of Canada, Paper 68-68, p. 75-77.

Findlay, D.C., 1969, The mineral industry of Yukon Territory and southwestern District of Mackenzie, 1968; Geological Survey of Canada, Paper 69-55, p. 44-46.

Gabrielse, H., 1985, Major dextral transcurrent displacements along the Northern Rocky Mountain Trench and related lineaments in north-central British Columbia; Geological Society of America Bulletin, Vol. 96, p. 1-14.

Gordey, S.P., Abbott, J.G., Tempelman-Kluit, D.J. and Gabrielse, H., 1987, "Antler" clastics in the Canadian Cordillera in Geology, Vol. 15, p. 103-107.

Green, L.H., 1966, The mineral industry of Yukon Territory and southwestern District of Mackenzie, 1965; Geological Survey of Canada, Paper 66-31, p. 64-68.

Orssich, C.N., Harris, F.R. and Watts, A.C., 1985, Iona Silver Property: 1985 property report; Unpublished company report, Canamax Resources Inc., 59 p.

Parry, S.E., Harris, F.R. Cathro, M.S. and Wytrwal, Z.J., 1984, Ketza River Property: 1984 summary report; Unpublished company report, Canamax Resources Inc., 41 p.

Read, B.C., 1980, Lower Cambrian archeocyathid buildups, Pelly Mountains, Yukon; Geological Survey of Canada, Paper 78-18, 54 p.

Rotherham, D.C., 1959, Report on the Ketza River Property; Unpublished company report, Conwest Exploration Co. Ltd.

Tempelman-Kluit, D.J., 1977a, Geology of Quiet Lake and Finlayson Lake map areas, Yukon Territory (105 F and G); Geological Survey of Canada, Open File 486.

Tempelman-Kluit, D.J., 1977b, Stratigraphic and structural relations between the Selwyn Basin, Pelly-Cassiar Platform and Yukon crystalline terrane in the Pelly Mountains, Yukon; in Report of activities, Part A: Geological Survey of Canada, Paper 77-1A, p. 223-227.

Tempelman-Kluit, D.J., 1979, Transported cataclasite, and granodiorite in Yukon: Evidence of arc-continent collision; Geological Survey of Canada, Paper 79-14, 27 p.

Tempelman-Kluit, D.J., Abbott, G., Gordey, S. and Read, B.C., 1975, Stratigraphic and structural studies in the Pelly Mountains, Yukon Territory; in Report of activities, Part A: Geological Survey of Canada, Paper 75-1A, p. 45-48.

Tempelman-Kluit, D.J., Gordey, S.P. and Read, B.C., 1976, Stratigraphic and structural studies in the Pelly Mountains, Yukon Territory; in Report of activities, Part A: Geological Survey of Canada, Paper 76-1A, p. 97-106.

Toohey, J., 1986, Geology and ore controls of the Ketza River gold deposits, Yukon; Unpublished term project report, Queen's University, Kingston, Ontario, 111 p.

Wheeler, J.O., Green, L.H. and Roddick, J.A., 1960, Quiet Lake, Yukon Territory; Geological Survey of Canada, Map 8-1960.

Woodcock, J.R., 1955, Ketza River Area, Yukon Territory: 1955 Field Season; Unpublished company report, Conwest Exploration Co. Ltd., 60 p.

FIELD GUIDE ANVIL PB-ZN-AG DISTRICT YUKON TERRITORY, CANADA

Lee C. Pigage
CURRAGH RESOURCES INC.
117 Industrial Road
Whitehorse, Yukon Territory
Canada Y1A 2T8

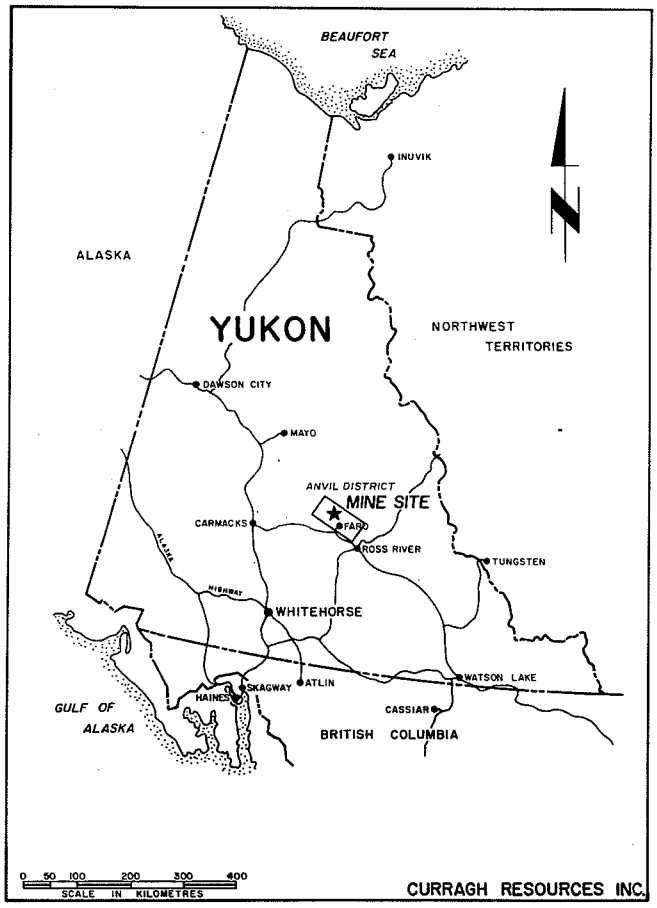

Figure 1 Location map of Anvil District in Yukon Territory, Canada. Concentrates are trucked to tidewater at Skagway, Alaska through Carmacks and Whitehorse.

INTRODUCTION

The Anvil Pb-Zn-Ag District is located near the town of Faro in central Yukon Territory 200 kilometers northeast of Whitehorse (Figure 1). Five deposits of the stratiform, massive pyritic sulphide type (Gustafson and Williams, 1981) have defined reserves within the district (Table 1). The mineral deposits define a curvilinear trend in plan (Figure 3) and occur within a 150 meter thick upper Proterozoic to Cambrian stratigraphic interval (Jennings and Jilson, 1986). The total geological reserves for the district is similar to that for other major stratiform Pb-Zn deposits (Figure 4). If all sulphide lithologies are considered, irrespective of grade, the district contains an estimated total of 225 million tonnes of sulphide-bearing rock (Jennings and Jilson, 1986).

Intensive exploration within the district began after Al Kulan discovered the Vangorda deposit in 1953 using conventional prospecting. Exploration methods are discussed by Aho (1966, 1969), Brock (1973), Chisholm (1957), and 1 Morton (1973). Anvil Mining Corporation began open-pit mining of the Faro deposit at rates of up to 10,000 tonnes per day in late 1969. The mine is currently owned and operated by Curragh Resources Inc. Open pit mining of the Faro deposit is continuing on a year-round basis with the concentrator processing 13,500 tonnes of ore per day. Concentrates from the mine are trucked to Skagway, Alaska (Figure 1) and then shipped to markets around the world.

Curragh Resources Inc. is also working on developing several additional mines in the district. Underground exploration has begun on a high grade portion of the Faro deposit. Pre-development and environmental studies are being undertaken for the Vangorda and Grum deposits. These latter two deposits will be open pit mines with the ores being processed at the Faro mine concentrator. The remaining deposits have not yet been developed, although a pilot drill hole is being planned for the Dy deposit.

This paper will discuss the general nature of the deposits including ore types, zoning patterns, alteration patterns, and subsequent metamorphism and deformation. The field trip will look first at the ore types and metamorphism-deformation in the Faro underground mine. Additional stops at the Grum and

Table 1 Summary of tonnage and grade figures for Anvil district ore deposits as of June 1983*

	Tonnage X 10^6 tonnes	Pb (%)	Zn (%)	Ag (g/mt)	Cutoff (%Pb+ Zn)
Faro (1)**					
Geological reserves before mining	57.6	3.4	4.7	--	5.0
Remaining geological reserves (1983)	33.0	3.0	4.6	36	4.0
Remaining open pit reserves (1983)	25.2	2.9	4.3	36	4.0
Grum (2)					
Geological reserves	30.8	3.1	4.9	49	4.0
Open pit reserves	16.9	3.0	4.9	47	4.0
Vangorda (3)					
Geological reserves	7.1	3.4	4.3	48	4.0
Open pit reserves	5.2	3.4	4.2	47	4.0
Dy (4)					
Geological reserves	20.3	5.7	7.0	82	9.0
Swim (5)					
Geological reserves	4.3	3.8	4.7	42	6.0
Total					
Geologcial reserves before mining	120.1	3.7	5.6	--	N/A
Remaining geological reserves (1983)	95.5	3.7	5.2	51	N/A
Remaining open pit reserves (1983)	47.3	3.0	4.5	41	4.0

* Compiled from various "in house" reports of Cyprus Anvil Mining Corp. and Kerr Addison Mines.
** Refers to the number on Figure 3

Vangorda deposits are planned depending on time constraints and development progress for these deposits.

REGIONAL GEOLOGY

Roddick and Green (1961) first systematicaly mapped the Anvil District. After discovery of the Vangorda, Swim, and Faro deposits, Tempelman-Kluit (1972) undertook a more detailed geological study. More recently Gordey (1983) and Gordey and Irwin (1987) correlated rock units in the district with previously mapped areas to the east and southeast.

The Anvil District is part of Selwyn Basin (Figure 2), a large area of central Yukon where deep water clastics, chert, and minor carbonate accumulated along the ancient North American continental margin during late Proterozoic and Paleozoic (Gabrielse, 1967). Sediments in the basin contain several large-scale compositional sequences which reflect its evolutionary development. An excellent summary of these stages is presented in Abbott et al. (1986).

The late Proterozoic to early Cambrian "Grit Unit" (Gabrielse et al., 1973) is the oldest unit exposed in the basin. It consists of a thick sequence of

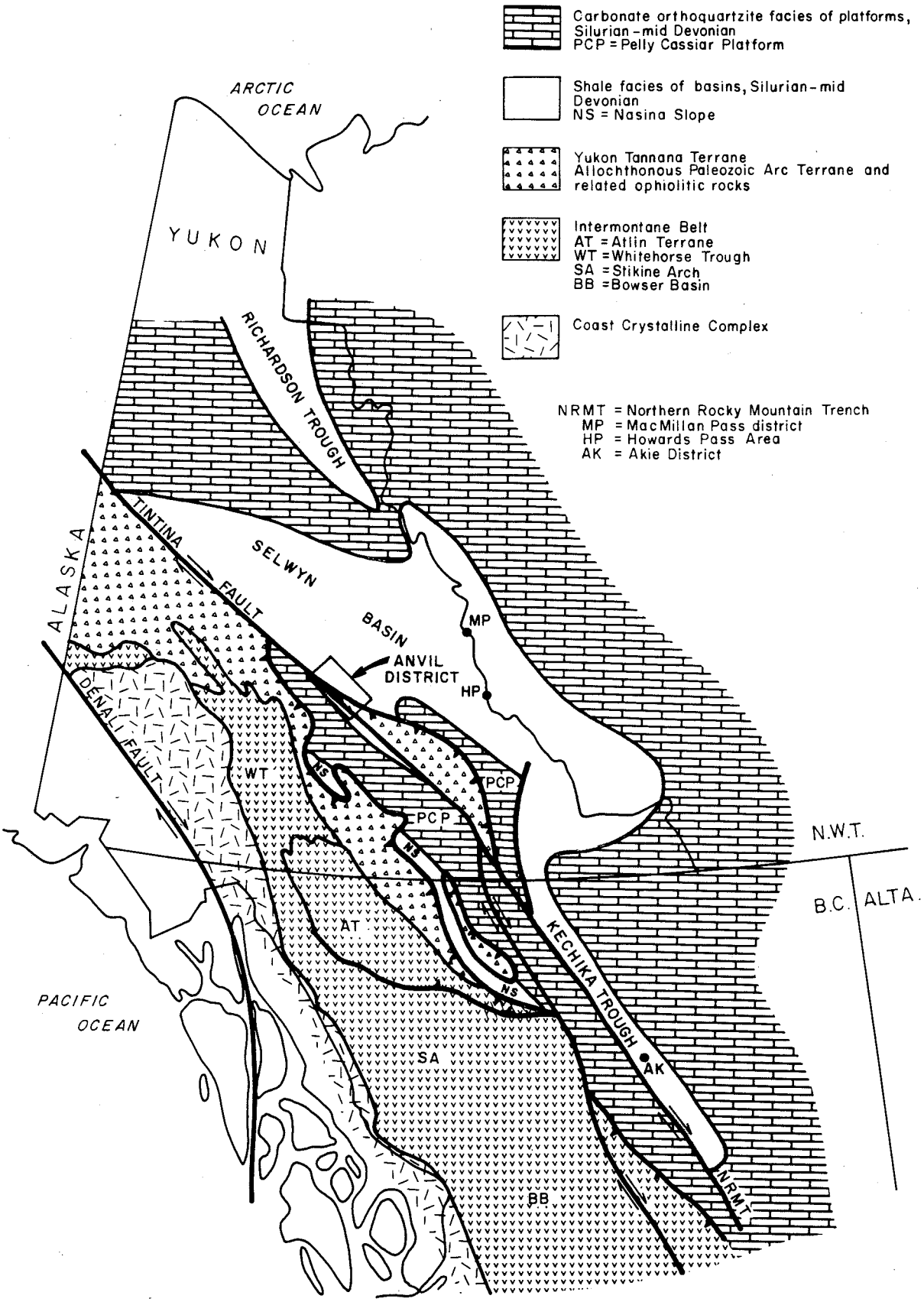

Figure 2 Location map of Anvil District. The major sulphide deposits are indicated in tectonic features of northwestern Canada.

quartzofeldspathic turbidites and shales. The lowermost portion of the sequence reflects initial rifting forming the ancient continental margin (Eisbacher, 1981).

During the interval early Cambrian to middle Devonian the basin is characterized by passive continental margin sedimentation of dominantly carbonaceous fine clastics and chert with a shallow carbonate platform to the northeast (Mackenzie Arch) (Abbott et al., 1986). Scattered occurrences of Ordovician basaltic flows, volcaniclastic breccias, and tuffs indicate intermittent extension within the basin.

A transgressive shale and chert sequence replaced carbonate platform sedimentation in the Mackenzie Arch during middle Devonian to Mississippian time. Intrabasinal or westerly derived chert and quartz-rich coarse clastics interbedded with carbonaceous shales and cherts in Selwyn Basin indicate a tectonic event during this interval which resulted in local extension (Abbott et al.,1986). Extension is also indicated by the local occurrence of felsic volcanics and plutonics during this interval (Mortensen, 1982).

Locally preserved Mississippian to Triassic fine grained shallow water clastics and cherts delineate a return to an oxygenated, stable, marine continental margin depositional pattern.

Selwyn Basin is immediately northeast of the Yukon-Tanana suspect terrane (Coney et al., 1980), a mid-Paleozoic volcanic-plutonic assemblage built on continental crust (Mortensen and Jilson, 1985). At least part of the Yukon-Tanana terrane was emplaced as an allochthon overlying North American rocks along the outboard edge of Selwyn Basin. This structure is thought to be part of a transpressive suture developed during oblique collision of the suspect terrane with North America in Jurassic through Cretaceous (Mortensen and Jilson, 1985). This collision initiated metamorphism and deformation of the basin with development of northeast directed thrusting and folding. Collisional deformation culminated with the intrusion of mid-Cretaceous granites.

Right lateral, transcurrent movement along the Tintina Fault in latest Cretaceous or early Tertiary time completed the deformation history of Selwyn basin. Estimates of offset along the Tintina Fault range from 450 kilometers (Tempelman-Kluit, 1970a) to 750 kilometers (Gabrielse, 1985).

The clastics of Selwyn Basin host most of Canada's large stratiform lead-zinc deposits, making it a metallogenic province of world-wide significance (Carne and Cathro, 1982). Mineral deposits within the basin range from Cambrian through Devonian in age. The Anvil District differs from the remainder of the Selwyn Basin because the rocks and ore deposits are metamorphosed and significantly recrystallized. This has resulted in coarser grain size with improved metallurgical performance. This geologic factor and the size and location of the Faro deposit have combined to determine that Faro is as yet the only producer of Selwyn Basin.

DISTRICT STRATIGRAPHY

The stratigraphic sequence of Anvil District ranges in age from latest Precambrian to Permian (Figure 3). The lower part of the sequence is divisible into three major mappable units. From the base these are noncalcareous metapelite of the Mount Mye formation, calcareous pelite of the Vangorda formation, and basalt of the Menzie Creek formation (Figures 4, 5; Jennings and Jilson, 1986). All formational names in this interval are informal. The aggregate thickness for this pre-Silurian sequence is approximately 5 kilometers.

The overlying sequence is characterized by shale, chert, basalt, minor limestone, and coarse clastics rich in chert fragments. Strata of the Earn Group (Gordey et al., 1982) and Anvil Range Group (Tempelman-Kluit, 1972) are present. This sequence ranges in age from Devonian to Permian. All or part of this upper sequence may be allochthonous with respect to the underlying units. The Earn Group locally contains stratiform barite deposits.

The Devonian and younger rocks are not related to the ore deposits in the district and consequently are not discussed further. The three older units either host the ore deposits or bear a possible relationship to the ore and are considered in more detail below.

Mount Mye formation

The Mount Mye formation (Figure 5) consists dominantly of noncalcareous, biotite-muscovite-andalusite-staurolite +/- garnet schist in areas of amphibolite facies metamorphism and noncalcareous, weakly carbonaceous, light to medium

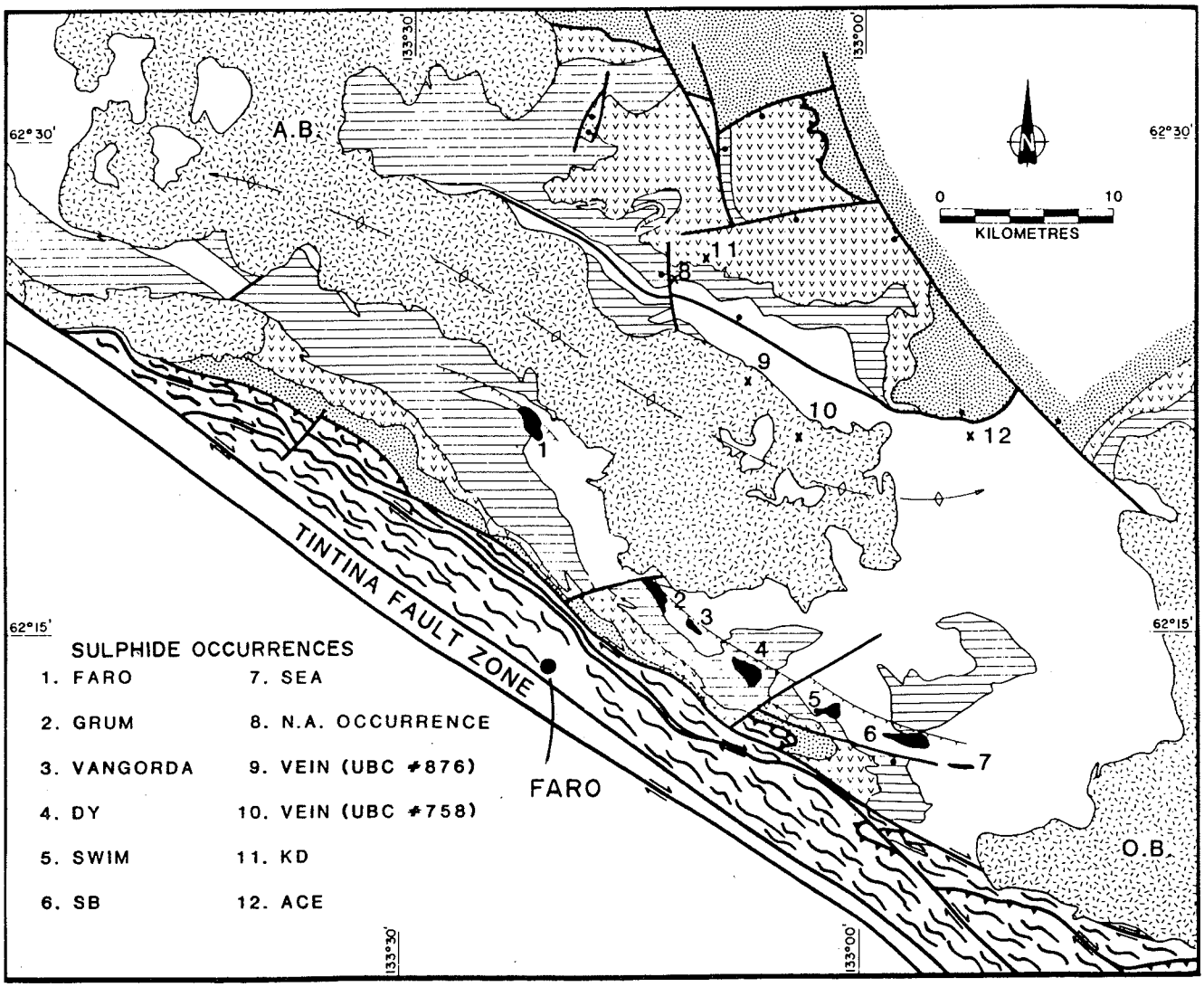

contact

strike slip fault

normal fault

thrust fault

axis of Anvil Arch

northeast edge of subbasin

granodiorite and quartz monzonite AB = Anvil Batholith OB = Orchay Batholith

EARN GROUP black shale, chert, chert pebble conglomerate, limestone, quartzite (includes undifferentiated Askin Group, Silurian and Devonian dolomite and quartzite locally)

MENZIE CREEK FORMATION metabasalt flows breccias and tuffs, graphitic phyllite (includes undifferentiated Road River Group black shales locally)

VANGORDA FORMATION calcareous phyllite and equivalent calcsilicates, metabasite

MOUNT MYE FORMATION non calcareous phyllite and schist

undifferentiated rocks southwest of Finlayson Lake fault zone includes rocks of Yukon Cataclastic complex, Triassic sedimentary rocks, ultramafic and mafic plutonic rocks and basalt and varicolored chert of Permian or Pennsylvanian Anvil Range Group.

Figure 3 Geology map of Anvil District. The major sulphide deposits are indicated in black.

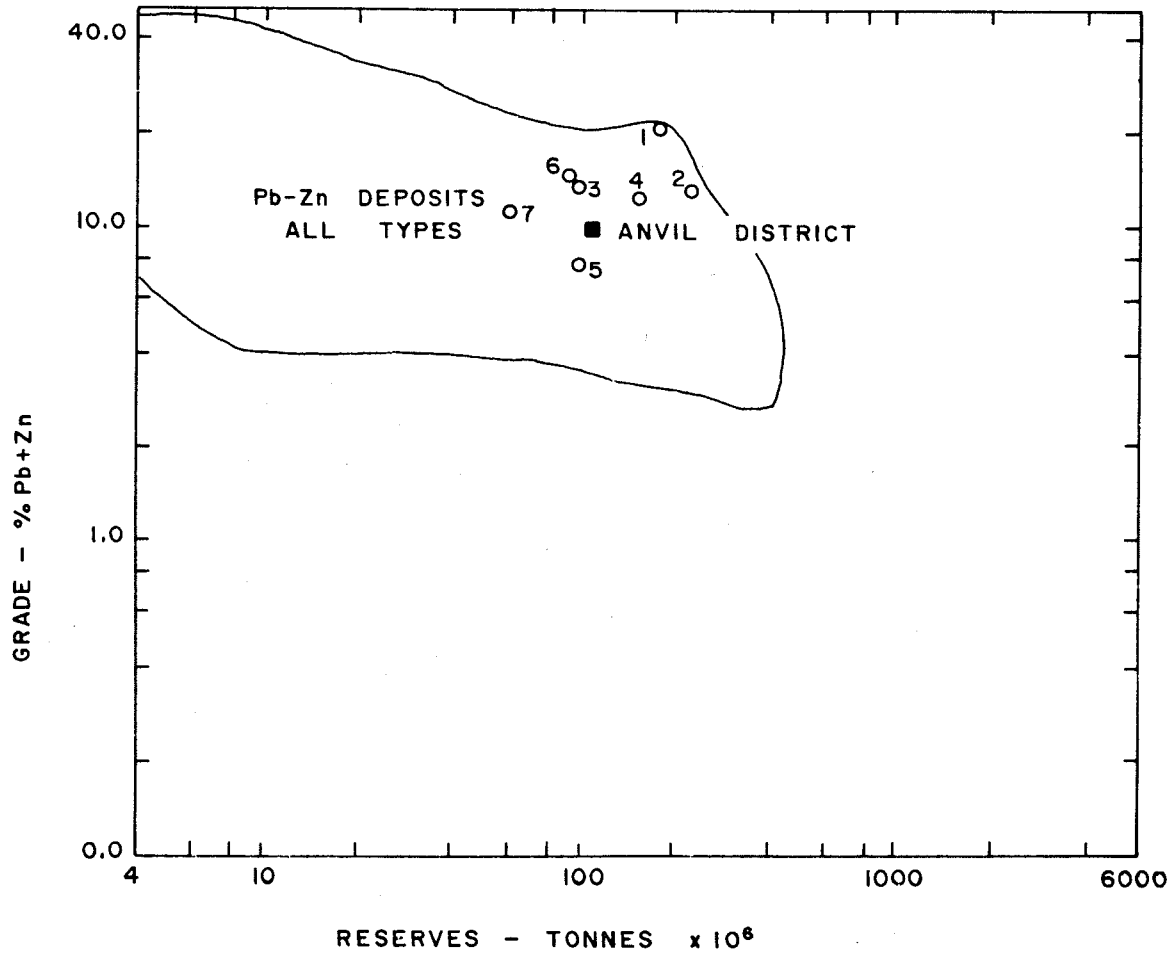

1 BROKEN HILL, AUSTRALIA
2 McARTHUR RIVER, AUSTRALIA
3 MT. ISA, AUSTRALIA
4 SULLIVAN, CANADA
5 HOWARDS PASS, CANADA
6 RED DOG, ALASKA
7 MEGGEN, WEST GERMANY

Figure 4 Comparison of size-grade characteristics of some major lead-zinc deposits. Modified from Gustafson and Williams (1981).

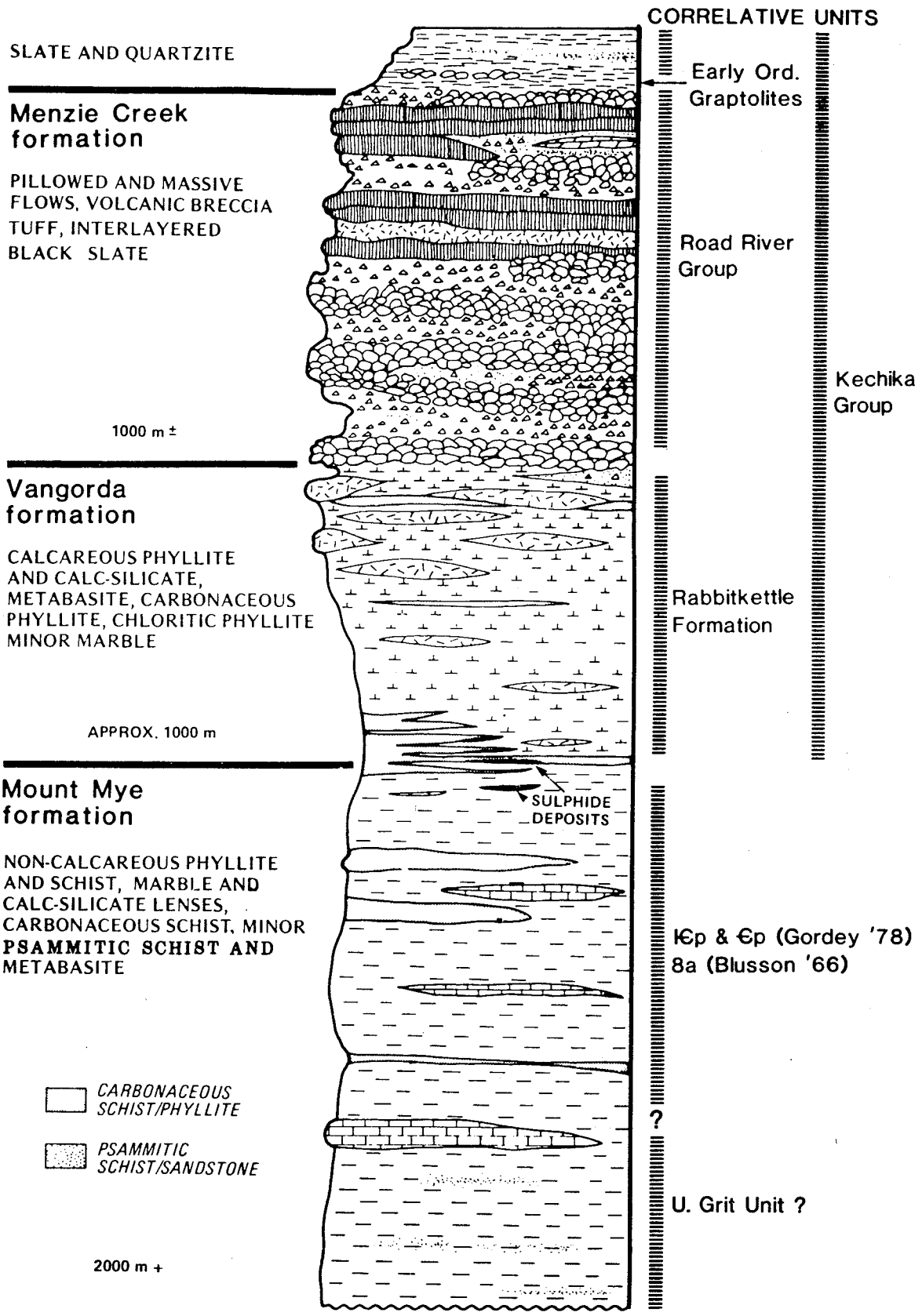

Figure 5 Stratigraphic column of the older portion of the rock units in the Anvil District.

gray muscovite-chlorite phyllite in areas of greenschist facies metamorphism. It contains lesser, interlayed, black carbonaceous phyllite or schist, calcitic marble, calc-silicate phyllite or schist, metabasite, and psammitic schist. The unit has a structural thickness of at least 2 kilometers with the base not being exposed. The reddish brown weathering color of the unit is characteristic and helps distinguish it from noncalcareous portions of the overlying Vangorda formation.

Dark grey to black carbonaceous phyllite or schist members comprise about 10 per cent of the formation. They are more abundant in the upper 200 meters of the unit.

Calcitic marble and calc-silicate schist or phyllite also constitute about 10 per cent of the Mount Mye formation. The marble is light grey, medium crystalline calcite with boudins of pelite, amphibolite, and calc-silicate. Marble bodies may be up to 75 meters thick but are generally only a few tens of meters thick; they can be traced laterally for several kilometers. The calc-silicate lithology is a thinly interbanded sequence of purplish brown biotite pelite and pale green actinolite-epidote calc-silicates. Typically the calc-silicates are spatially associated with the marbles. A persistent marble and calc-silicate horizon occurs about 200 to 400 meters below the top of the Mount Mye formation.

Metabasite bodies are generally only a few meters thick and have small to moderate lateral dimensions. Volumetrically they constitute less than 1 per cent of the Mount Mye formation. They are generally strongly foliated, dark green amphibolites lacking relict igneous texture. Compositions are similar to basalts of the Menzie Creek formation (Jennings and Jilson, 1986). They are interpreted as subvolcanic feeder dykes and sills of the Menzie Creek basalts.

The upper portion of the Mount Mye formation is very similar to the buff weathering mudstone and blue-gray mudstone units described by Gordey (1978) to the east near Howards Pass and to unit 8A of Blusson (1966). Correlation with these units would imply the top of the formation is lower Cambrian or possibly middle Cambrian. Jennings and Jilson (1986) suggested that the persistent marble and calc-silicate package may correlate with the widespread early Cambrian limestone conglomerate of Selwyn Basin. Parts of the Mount Mye formation also resemble rocks underlying those presumed correlative units, implying that the Mount Mye probably includes rocks as old as Hadrynian.

Vangorda formation

The Vangorda formation is characterized by light to medium-gray, calcareous, phyllitic rocks made up of very thin (0.1-2 cm) interlayers of medium grey, non-calcareous, weakly carbonaceous, muscovite-chlorite pelite and light grey, generally calcareous quartz-calcite +/- dolomite siltstone. At the higher metamorphic grade of amphibolite facies, the Vangorda phyllites are transformed to a thinly banded, pervasively foliated, green, cream, and purplish brown, calc-silicate. Major interbanded units include metabasite, carbonaceous pelite, and phyllitic limestone. The Vangorda formation varies between 0.5 and 2 kilometers in apparent thickness. The formation becomes more calcareous up section. The light grey to tan colored drusy weathering of the formation is characteristic both within the district and elsewhere.

The metabasite bodies range from 1 to 100 meters in thickness and are up to several kilometers in length. They comprise approximately 15 per cent of the Vangorda formation and are more prevalent near the top of the formation. Whole rock analyses show that the metabasites are compositionally similar to the overlying Menzie Creek basalts (Jennings and Jilson , 1986). Locally the metabasites contain coarsely crystalline serpentinized pyroxenite subunits. Most metabasite bodies have medium-grained, equigranular centres with strongly foliated margins. Although marginal contacts of the bodies are superficially conformable, detailed inspection indicates the units are locally slightly crosscutting. The metabasites are thus interpreted as subvolcanic dyke and sill feeders to the Menzie Creek formation.

Typically the Vangorda formation adjacent to the metabasites is a thinly banded, hard, pale green, calcareous, chloritic phyllite. Originally this lithology was interpreted as a marginal tuff adjacent to basaltic flows. More extensive drill intersections and additional outcrop exposures indicate that instead it represents a slight contact metamorphic aureole caused by intrusion of the metabasite bodies.

Black, slightly calcareous to dolomitic, carbonaceous pelite members occur throughout the

Vangorda formation. Dimensions and lateral continuity of these members are poorly known. The thickest and most extensive of these occurs at the base of the formation; it ranges from only a few tens of meters to 100 meters in thickness. This basal member becomes thicker in the immediate vicinity of the ore deposits and appears to be laterally equivalent to black, sulphide-bearing, ribbon-banded, carbonaceous, quartzite ores within the mineral deposits.

The Vangorda formation is lithologically similar to, though more argillaceous than the Rabbitkettle Formation seen to the east (Gordey, 1978; Gabrielse et al., 1973). Based on this correlation the Vangorda formation may range in age from middle or late Cambrian through early Ordovician.

Menzie Creek formation

The Menzie Creek formation is a unit of basaltic metavolcanic rocks consisting of pillowed and massive flows with comparable amounts of massive, coarse, monolithic breccias and lesser, thin-bedded, tuff and/or volcanic sandstone and siltstone. The formation reaches a maximum structural thickness of 1.5 kilometers in the district. Whole rock major element and trace element data (Jennings and Jilson, 1986) imply that the flows of the Menzie Creek volcanic unit are dominantly alkali basalt erupted in a within-plate setting. Similar major and minor element compositions for the metabasites in the Mount Mye and Vangorda formations suggest the metabasites are subvolcanic feeders for the Menzie Creek formation.

Carbonaceous phyllite and brown siltstone immediately overlying the Menzie Creek formation northeast of the Anvil Batholith contain graptolites of middle Ordovician or early Silurian age (Tempelman-Kluit, 1972; Gordey, 1983) suggesting correlation of the Menzie Creek volcanics with the widespread Road River Formation black shale and chert to the northeast. The Menzie Creek formation has been traced for 100 kilometers along strike and 30 kilometers across strike, showing that it is one of the largest of several basaltic units of its age in Yukon.

Relation of Stratigraphy to Ore Deposits

The ore deposits of Anvil District are stratiform and confined to an approximately 150 meter thick interval straddling the contact of the Mount Mye and Vangorda formations (Figure 5). This stratigraphic position indicates the mineralization is Cambrian in age. The deposits consist of one to five sheets of sulphide mineralization with interbanded metasedimentary rocks. For those deposits with more than one sulphide horizon, the mineralized horizons are generally stacked one above the other. At least three of these mineralized horizons appear to be laterally equivalent to part of the basal carbonaceous pelite member of the Vangorda formation. Unlike other sedimentary exhalative deposits of Selwyn Basin, the Anvil deposits are not characterized by a host stratigraphic section dominated by black carbonaceous rocks. Instead the carbonaceous rocks in the district are thin and subordinate or locally not even present.

DEFORMATION, METAMORPHISM and PLUTONISM

The structural and metamorphic history of the Anvil District is complex and of considerable significance to the present form and nature of the ore deposits. Five deformation phases have been recognized within the metasedimentary and metavolcanic rocks of the district. The first two are periods of intense mid-Mesozoic fold deformation and concurrent metamorphism which determined the gross structure of the mineral deposits (see Figure 6). The remaining deformations are only locally developed and do not generally form large or significant structures.

The first deformation (D1) produced a regional metamorphic foliation (S1) axial planar to tight to isoclinal mesoscopic folds (F1) in bedding (S0). Mesoscopic D1 early folds are rarely preserved in the district; they are ubiquitously north-easterly inclined to upright, northeasterly verging structures with shallow northwesterly or southeasterly plunging axes (Figure 6).

During the second deformation event (D2), S1 was strongly crenulated and ubiquitous close to tight mesoscopic folds (F2) in S1 were produced. S0 primary bedding was transposed into near parallelism with the S1 foliation. Parallel to the axial planes of the D2 folds is a crenulation cleavage (S2) which imparts a well developed lithon structure to most rocks of the district, especially the strongly banded phyllites of the Vangorda formation. F2 axial planes and S2 axial plane foliations dip shallowly to the southwest or northeast, with fold axes subparallel to F1 fold axes. Southwest of the Anvil batholith (see Figure 3) the S2 surfaces dip dominantly southwest, and F2 minor folds have southwest

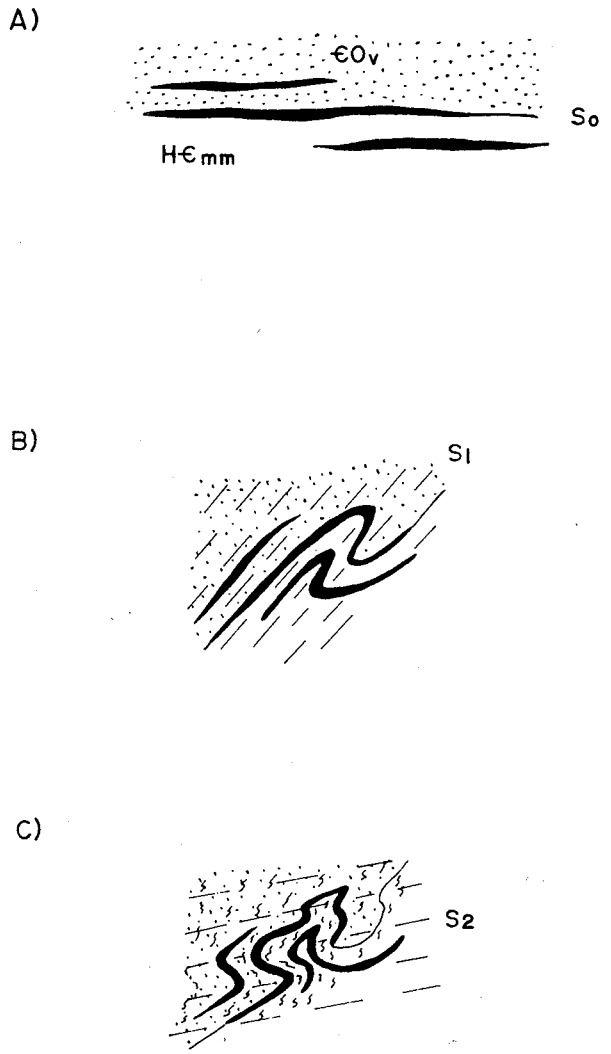

Figure 6 Schematic cross-section through the Grum deposit. Section oriented SW-NE and looking northwest. Stacked en echelon ore horizons are shown in black. This section shows the sequential development of the type 3 interference pattern between D_1 and D_2 folding deformations.

A) Deposition of sulphide ore horizons parallel to S_0.

B) Formation of northeast-verging, steeply dipping, D_1 minor folds.

C) Formation of type 3 interference pattern with development of southwest-verging, shallowly dipping, D_2 minor folds.

vergence. Northeast of the batholith S2 surfaces dip dominantly northeast, and F2 minor folds have northest vergence.

The largest megascopic folds known to have been formed during D2 are those at the Grum Deposit (Figures 10, 11) and comparable folds in the Swim Deposit. Three later, less intense periods of folding and associated faulting followed. The later events (D3 through D5) generally produced open folds and weak crenulations in S2 related to broad, regional structures. An important exception to this general rule is found in the vicinity of the Faro deposit where the fourth event (D4) is intense with tight mesoscopic folds developed in nearly pervasive S2. D4 minor folds have appreciable mica growth along S4 axial plane crenulation cleavages (see Figures 8 and 9 for examples of fourth phase folds affecting the outline of the Faro deposit).

During the later stages of this deformation history a large granitic body (Anvil batholith) was intruded into the metamorphic sequence. Anvil batholith ranges in composition from a biotite-muscovite peraluminous granite to a metaluminous to peraluminous hornblende-biotite granodiorite (Pigage and Anderson, 1985). Textures include equigranular massive, megacrystic massive, and various strongly to weakly foliated variants. Foliation within the intrusive rocks is concordant with S2 surfaces in the surrounding metasediments. Several K-Ar ages on the granitic rocks yielded ages of 85-100 Ma (Templeman-Kluit, 1972). Rb-Sr isochron ages of 99-100 Ma (Pigage, and Anderson, 1985) are concordant with the K-Ar ages and indicate rapid cooling after high-level emplacement.

Intrusion of the Anvil batholith further deformed the metamorphic sequence so that the overall structure of the district is an elongate dome cored by the batholith (Figure 3). In the later stages of emplacement large extensional fault displacement occurred along the margins of the batholith (Pigage and Jilson, 1985). S-C mylonitic banding within these fault zones is consistent with development of the faults during late D2 deformation. These faults determine the present day limits of several of the deposits.

Anvil batholith and surrounding metasedimentary rocks are crosscut by two general types of post-tectonic dykes. The majority of the dykes are northeast-trending, medium to dark green, porphyritic, unfoliated, hornblende-biotite quartz diorite. These quartz diorite

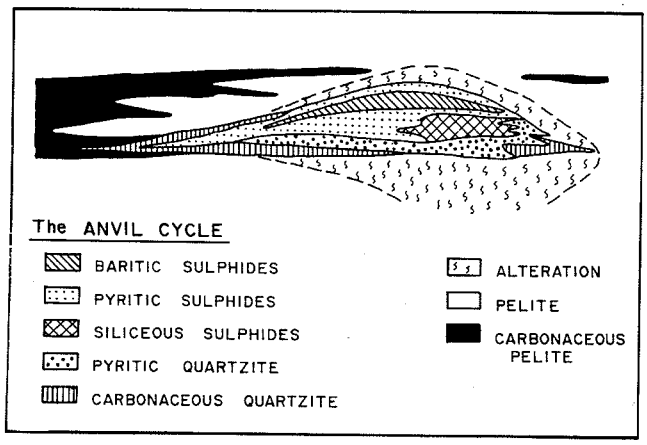

Figure 7 Idealized Anvil cycle of ore type facies variatinos based largely on the Faro and Vangorda deposits. The section is greatly vertically exaggerated.

dykes appear to be associated with late extensional faults. Unfoliated, pale tan, smoky quartz-feldspar porphyry also occurs as late crosscutting dykes. These dyke suites have not been isotopically dated; their absolute ages are uncertain.

Metamorphism was concurrent with deformation and was most intense during the major D1 and D2 folding deformations. D1 metamorphism has been largely overprinted by the later D2 metamorphism. Metamorphic grades during these two events appear to be comparable since mica mineral assemblages between microlithons (i.e. S1 foliations) are similar to those defining the S2 foliation surfaces. The rest of the discusion will focus on the D2 metamorphism.

Metamorphic grade ranges from upper amphibolite facies (sillimanite-muscovite zone) to lower greenschist facies (muscovite-chlorite zone) in a low pressure Buchan type facies series. In pelites adjacent to the intrusions the typical assemblage is andalusite-staurolite-garnet-biotite-muscovite-quartz-plagioclase with laocal fibrolite and cordierite. Lower greenschist facies pelites contain the assemblage muscovite-chlorite-quartz-plagioclase.

Metamorphic isograds are roughly concentric about the Anvil batholith. Locally isograds are truncated and juxtaposed by the late D2 extensional faults. The Faro deposit (closer to the batholith) is metamorphosed to amphibolite facies. All other deposits are only weakly metamorphosed to lower greenschist facies. This difference in metamorphism is reflected in decreased grain size and increased degree of mineral intergrowth in the less metamorphosed deposits (Tempelman-Kluit, 1970b). This has a significant impact on metallurgical response of Anvil district ores.

ORE DEPOSITS

General Description

The lead, zinc, silver deposits of Anvil District are of the sediment hosted, stratiform, massive pyritic sulphide type (Gustafson and Williams, 1981; Large, 1980) or sedimentary exhalative (sedex) type (Carne and Cathro, 1982). They occur either as a thick sulphide lens with little or no interbanded metasedimentary rocks (e.g. Faro) or as several thinner lenses stacked approximately one above the other with substantial metasedimentary interlayers (e.g. Grum and Dy).

There are presently five known lead-zinc bearing mineral deposits along a curvilinear trend on the south flank of the Anvil batholith (Figure 3). From northwest to southeast they are Faro, Grum, Vangorda, Dy, and Swim. Additionally two base metal deficient sulphide occurrences, the SB and Sea, are also known.

The Anvil deposits are distributed through a 150 meter thick stratigraphic interval straddling the boundary of the Mount Mye and Vangorda formations. They are associated with the regionally developed, but laterally discontinuous carbonaceous pelite unit forming the base of the Vangorda formation. Some sulphide lenses are, or appear to be, the lateral facies equivalent of this carbonaceous pelite. Some lenses (such as the upper horizons of Grum) are at the base of fingers of the carbonaceous pelite unit on a local scale as well as being its lateral equivalent on a more regional scale. In other cases, the ore lenses occur at lower or higher stratigraphic intervals than the carbonaceous pelite.

Detailed mapping and drilling suggest the linearly distributed deposits lie close to a northeasterly "pinch out" or "zero edge" of the associated carbonaceous pelite (the basal member of Vangorda formation). To date, no sulphide deposit lithofacies have been encountered in a moderate number of drill holes through the ore-bearing horizon southwest or northeast of the deposit line. Taken together, these observations suggest some relationship between sulphide deposits

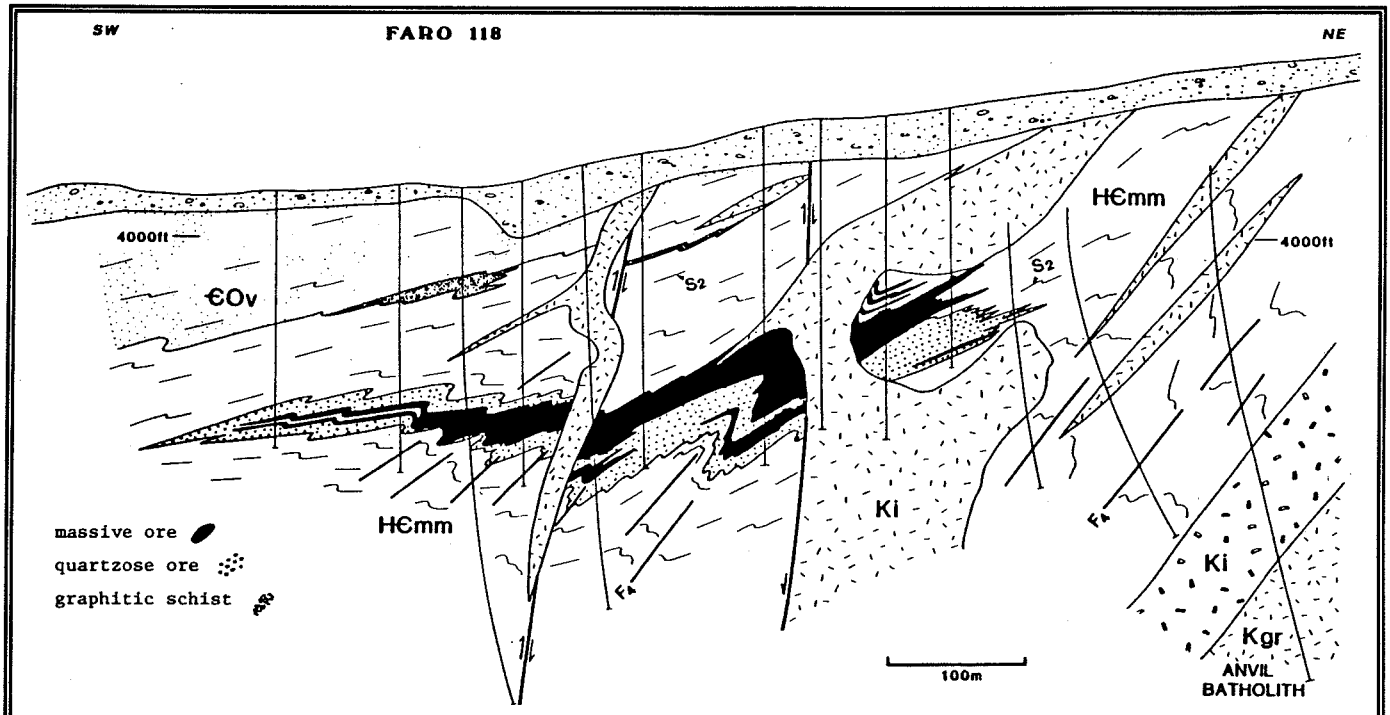

Figure 8 Vertical cross section 118+000 through Faro deposit. Section is oriented SW-NE looking northwest. Northeast-verging D_4 folds strongly affect the shape of the ore body. Deposit is generally concordant with S2 foliation. Ki are massive hornblende-biotite and smokey quartz feldspar porphyry dykes which postdate the Anvil batholith.

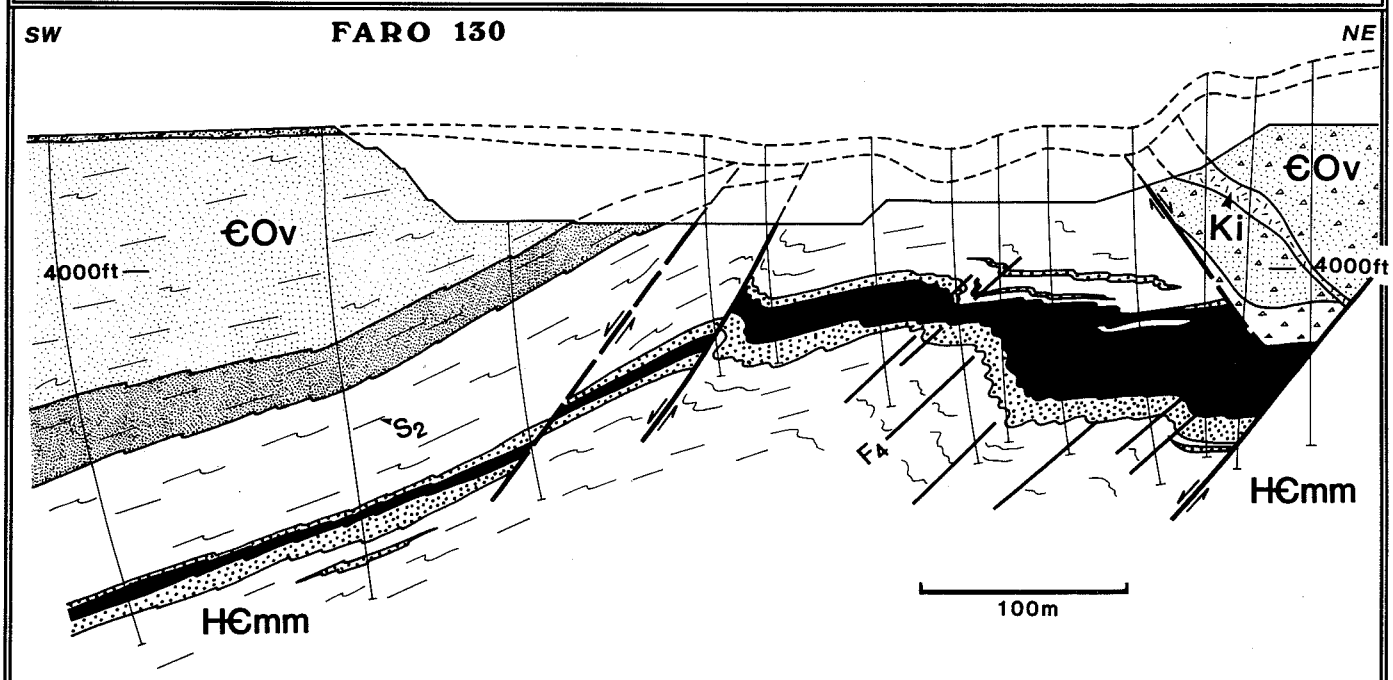

Figure 9 Vertical cross section 130+000 through Faro deposit. Section is oriented SW-NE looking northwest. Rock unit patterns are the same as in Figure 8. Triangles in far right unit indicate the breccia cap (see text).

and facies changes at a reduced basin margin.

All deposits are composed of a small number of different ore types. The ore types are broadly divisable into massive sulphides and quartzose disseminated sulphides. There are pyritic, baritic, pyrrhotitic and carbonate bearing variants of the massive sulphide ore types and carbonaceous and non-carbonaceous variants of the quartzose ore types.

Lead-zinc grade and metallurgical performance varies by ore type. The baritic massive sulphides are high grade, easily grindable and yield good grade concentrates with good recoveries. On the other hand carbonaceous quartzites are typically low grade, hard, and produce lower grade concentrates with low recoveries. Other ore types exhibit intermediate grade and recovery characteristics and performance.

These sulphide sheets or horizons are deformed into complex fold structures. The deposits are elongate parallel to the D2 fold axes and associated lineations in the host metasediments. The Faro deposit, which superficially does not appear to be complexly folded, actually shows great internal complexity in the geometry of high grade and waste layers.

Present deposit lengths are generally two to three times widths; unfolded, the deposits have an ameboid shape with diameters up to 4000 meters. Individual sulphide horizons commonly are 10 to 40 meters in thickness. The upper and lower contacts of sulphide horizons are invariably sharp while lateral extensions grade into the enclosing host rocks.

All deposits show a variably developed, white mica-dominant, alteration overprint in the wallrocks. At lower metamorphic grade this alteration is footwall biased. For the Faro deposit, this alteration encloses the entire mineralized sulphide lens.

Description of Sulphide Lithofacies

All ore types in the Anvil District are completely recrystallized metamorphic tectonites containing well developed S1 and/or S2 foliations. In the following sections the general characteristics of the massive and quartzose ores are described.

Massive Sulphide Ores

Massive Pyritic Sulphides

The massive pyritic sulphides consist of banded to homogenous, usually weakly foliated and/or lineated, massive pyrite with lesser sphalerite and galena. Total sulphide content is at least 60%, generally greater than 80% and commonly nearly 100%. Gangue consists of quartz and/or barite and/or carbonates (calcite, dolomite, ankerite). Accessory minerals include pyrrhotite, chalcopyrite, magnetite, arsenopyrite and marcasite. At amphibolite facies metamorphic grade, variants of this rock type with high lead-zinc grades commonly develop a porphyroblastic buckshot texture of pyrite in a matrix of dark reddish brown to black base metal sulphides.

Baritic, Massive Pyritic Sulphides

This ore type is a strongly and thinly banded massive sulphide/sulphate rock consisting of pyrite, galena, sphalerite and commonly magnetite in a gangue of off-white barite and lesser carbonates (calcite, dolomite, ankerite, and probably barytocalcite). Barite content ranges up to 50%; non-sulphide bearing, massive barite does not occur in the Anvil deposits. There is a complete gradation between this ore type and the massive pyritic sulphide ore type. Lead-zinc grade is typically high (10-15% combined Pb+Zn). Sphalerite is characteristically honey coloured to reddish brown. Pyrrhotite is not commonly seen in the baritic facies except in the Faro deposit where pyrrhotite is more abundant overall.

Carbonate-bearing, Massive Pyritic Sulphides

This ore type is similar to the massive pyritic sulphides but contains 10% carbonate (calcite, dolomite, ankerite) either as interstitial gangue or as coarse patches and irregular blebs. It is a minor facies and is not known with certainty to always be an original composition variant. The most common occurrence of coarse pinkish beige to tan, ankerite patches may represent recrystallized original carbonate or re-worked pre/syn-metamorphic veins.

Pyrrhotitic Massive Sulphides

This ore type consists of massive, finely crystalline, usually well foliated pyrrhotite with less than 50% pyrite porphyroblasts and highly variable amounts of sphalerite and galena. Minor chalcopyrite is characterisistic of this relatively copper-rich facies. Rounded to angular, rotated, foliated quartzite or quartz-vein clasts 2 cm or less in diameter are typical. This is a minor facies and

is not known with certainty to be primary as some pyrite in the massive sulphide ore types may invert to pyrrhotite during regional metamorphism. The pyrrhotitic facies is volumetrically more important in Faro than other deposits. At Faro pyrrhotite-rich ores are generally much finer grained than non pyrrhotitic ores.

General Comments on Massive Sulphides

Breccia textures are more common in the massive pyritic and pyrrhotitic facies than in the barite or carbonate bearing facies. Pyritic breccias generally involve fragments of more quartzose or less base metal rich pyritic facies in a massive pyrite plus base metal sulphide matrix. Fragments are be angular to subrounded, poorly sorted, and either clast or matrix supported. In some cases, margins of fragments can be fit back together. In all cases, the breccias are post-metamorphic since they involve variably oriented, foliated clasts. The origin of the breccias appears to be related to ductility contrasts between the affected lithologies during sulphide flow induced by deformation ad metamorphism. These are clearly not primary breccias related to feeder zones or paleoslumps prior to sulphide lithification.

Friable and porous massive sulphides are relatively common and when strongly developed often degenerate to pyrite sand. The porous massive sulphides are commonly carbonate or barite bearing and originate by post-metamorphic groundwater leaching and oxidation, especially near faults.

Quartzose Disseminated Sulphide Ores

Post-metamorphic breccias are also common in the quartzose disseminated sulphide ore types. Pyritic quartzite breccias are often spectacularly developed in the sphalerite-rich high grade facies where ductility contrasts between the sulphides and quartzite bands dictate ductile flow in the sulphides and brittle failure, rotation and brecciation in the quartzites. Where less intensively developed, the breccias grade into examples of sulphide mobilization into D2 or later cleavages.

Ribbon banded, "Graphitic", Pyritic Quartzite

This ore type is a dark grey to black, well banded, sulphide-bearing quartzite (metamorphic usage). Bands are:

(a) dark grey, very fine grained, carbonaceous, phyllitic quartzite to siliceous phyllite (presumed metachert),

(b) light grey, more coarsely crystalline, quartz-sulphide (pyrite-sphalerite-galena) interbands.

Banding is on a scale of 0.2-2.0 centimeters. Total sulphide content usually is between 10% to 30% although the entire range encompasses 2% to 60%. Pyrite is usually the dominant sulphide species but higher grade examples have sub-equal pyrite and lead-zinc sulphides ranging to lead-zinc dominant variants with little pyrite. Strong sulphide species differentiation between bands, such that barren pyrite bands are adjacent to or near sphalerite or galena rich bands, occurs but is uncommon.

S_0 bedding is typically transposed into the S1 cleavage. Microlithon textures with S2 forming a spaced carbonaceous parting with intervening folded S0-1 surfaces are typically well developed. Possibly the prominent ribbon-banding is a transposed primary stockwork veining (?).

Pyritic Quartzite

This ore type consists of a light grey, generally poorly banded, moderately to weakly foliated, micaceous quartzite with highly variable base metal and pyrite contents. Pyrite contents are generally 10% to 40% ranging between 2 and 60%. Although there is a complete gradation from massive sulphide ores to quartzose ores, there is usually little problem in separating this facies from the massive pyritic sulphides as the vast majority of the quartzite examples have less than 40% total sulphides. A minor variant of this facies contains low pyrite (5%) content with base metal sulphides predominant. Barite in major amounts is uncommon in this facies; carbonate species are not typical but are locally abundant. Chalcopyrite, pyrrhotite and magnetite-bearing varieties are common. Sphalerite in the high grade examples is characteristically a vibrant reddish brown.

In the Grum and Vangorda deposits, detailed drill hole intersections have shown that adjacent to metabasites the carbonaceous ribbon-banded pyritic quartzites show a gradual alteration to pyritic quartzites. This decarbonization represents a contact metamorphic

effect adjacent to the metabasite sills and dykes cutting through the ore deposit.

At Faro the northeast edge of the deposit contains a thick interval of extremely pyritic quartzite. This quartzite is spectacularly barren of lead and zinc but contains elevated copper contents and is rich in magnetite. A similar facies is developed at Vangorda where it is quite gold rich (1 gram/tonne) and more clearly occurs in the deposit footwall.

Idealized Anvil Deposit (Anvil Cycle)

All deposits have a distinct arrangement of sulphide ore types. This arrangement in a vertical and lateral sense is so commonly seen within and between deposits, it has been termed the Anvil Cycle (Jennings and Jilson, 1986). Figure 7 is a generalized, pre-deformation, vertically exaggerated cross-section of an ideal Anvil District deposit. It is based largely on the Faro and Vangorda deposits.

The base of the cycle is marked by ribbon-banded, carbonaceous, pyritic quartzites. The carbonaceous quaratzites are succeeded upward by pyritic quartzites, siliceous pyritic sulphides, massive pyritic sulphides and baritic massive pyritic sulphides. This array is also seen laterally with ribbon-banded, carbonaceous, pyritic quartzites forming the marginal or distal facies of a deposit progressing inward to the baritic massive pyritic sulphide facies.

It is important to note that Anvil cycles are developed on a wide variety of scales and to varying degrees of completeness. The most common scale is that of a cross-section through an entire deposit making recognition in individual boreholes or exposures often difficult. A series of complete and partial cycles may cumulatively form a mega-cycle on the scale of a complete horizon (e.g. Faro) or on the scale of a single sulphide horizon within a multilayered deposit (e.g. Grum or Dy). Complete cycles are also seen over a one meter or less stratigraphic interval, emphasizing the wide range of scales at which facies ordering can occur.

Facies zoning can be used in a tenuous way as top indicators in poly-deformed ore horizons to decipher fold patterns. This facings indicator is used with a greater degree of confidence if the complete Anvil cycle is present. It is stressed that stratigraphic tops directions defined by the unambiguous distribution of Mount Mye and Vangorda formation lithologies always take precedence over those interpreted from sulphide facies ordering.

Metal zoning crudely complements this facies distribution pattern. The quartzose disseminated sulphide facies at the base of an ideal cycle tend to be zinc enriched. The upper, massive sulphide facies are slightly lead-silver enriched, with the uppermost baritic facies containing the highest lead and silver grades. On the basis of scanty and preliminary data, copper and to a lesser extent gold are preferentially distributed in the siliceous facies of the footwall-biased alteration overprint and in the pyritic quartzite and siliceous pyritic sulphides facies of the stratiform ore types.

Individual horizons, however,do not commonly show any evidence of zonation in the assays. Studies of metal zoning are greatly hampered by the structural complexity of the Anvil deposits.

Alteration

Both wallrocks and certain ore facies of the Anvil deposits are overprinted by a prominent, easily recognized, light beige, white mica dominant, alteration assemblage. This overprint facies is not a depositional unit and may have formed as a reaction product between wallrocks and deposit forming hydrothermal fluids, as a metamorphic reaction envelope between sulphides and silicates (unrelated to ore forming fluids), or as a combination of these processes.

Many mineralogical variants of the alteration facies are recognized including siliceous, carbonate-bearing, talcose, chloritic, pyritic, pyrrhotitic, chalcopyrite-bearing, magnetite-bearing and lead-zinc bearing species. Careful attention has been paid to the distribution of these facies in an attempt to define feeder zones for each deposit. To date, no unequivocal feeder zones have been recognized. Recognition of a feeder zone is considerably hampered in this terrane by the polydeformational overprint. Several instances of suspected pre-D2 quartz-chlorite- pyrrhotite-chalcopyrite veinlets or stringers have been observed in the altered stratigraphic footwalls of several horizons (Swim deposit in particular) but not in sufficient abundance to define a stringer or feeder zone comparable to volcanogenic deposits.

In the multi-layered deposits at greenschist facies metamorphic grade, all mineralogical variants of the alteration facies are commonly recognized, often with

the best degree of development in the footwall of a mineralized horizon. This alteration overprint commonly appears discontinuous.

The only amphibolite grade example, the Faro deposit, shows a much less varied alteration assemblage (muscovite- quartz-pyrite + marcasite) with development of a substantial hanging wall as well as footwall alteration envelope. This simplified phase assemblage may be due to re-equilibration of the greenschist facies alteration assemblage to higher grades of metamorphism. The prominant hanging-wall alteration may be related to continued post-deposition hydothermal activity or to sulphurization or other metasomatic reactions in the wallrocks during metamorphism. These metamorphic reactions may be coupled with the occurrence of mobile sulphur caused by the inversion of pyrite to pyrrhotite within the deposit. It is interesting to note that the Faro deposit shows the greatest development of the massive pyrrhotitic ore facies and also the most well defined, broadest, and most symmetrical alteration envelope.

Genetic Model

The Anvil deposits are examples of synsedimentary, stratiform, massive sulphide deposits considered to be syngenetic/diagenetic and dominantly submarine exhalative in origin. Evidence for their essentially synsedimentary origin includes:

1. The prevalent and well developed compositional layering or banding in many or most sulphide facies, commonly with large variation in proportions of sulphide species between bands.

2. Thin interlayering of sulphides with totally unmineralized metasedimentary rocks, commonly on a scale of centimeters.

3. The occurrence of all deposits within a relatively restricted vertical stratigraphic interval.

4. The curvilinear depositional trend crudely associated with a carbonaceous pelite facies change.

5. The metamorphic and deformational overprints which clearly show the ores are pre-metamorphic.

No unequivocal evidence supporting the notion of an exhalative origin is preserved in the district. Alternative interpretations of some of the ore facies in the deposits are possible. For example, all or part of the footwall siliceous ore and alteration facies could be silicified and sulphidized host sediments rather than exhalative cherty sediments.

Reconnaissance studies by Kuo (1976) demonstrated the presence of chloride-rich fluid inclusions in barite, quartz, and sphalerite of several of the Anvil deposits, implying that metalliferous brines played a role in deposit formation. The ubiquitous development of generally footwall biased alteration envelopes further suggests that these brines were relatively hot. The curvilinear distribution of the deposits suggests a synsedimentary fault which could have provided the conduit for exhalative ore fluids reaching the sea floor.

In summary, the ore deposits are thought to have formed from hot metalliferous brines discharged from submarine fumaroles localized along a synsedimentary fault or hinge line which developed in response to lower Cambrian extensional tectonism. This tectonism influenced basinal geometry resulting in reduced second order basins truncating against the hinge line. Hydrothermal fluids moved up this fault zone and exhaled into a relatively deep water reduced marine basin which was otherwise receiving distal turbidite sediments. Sulphides may have been deposited from plumes along the hinge line or from relatively dense exhaled brines ponded in local topographic depressions near the hinge line.

This model accounts for the crude associations of known deposits with apparent depositional limits of reduced, carbonaceous sediments. The hinge line or related fault sets could have provided the channelways for the first pulse of basaltic volcanism associated spatially with the deposits. A regular and repetitive change in the environment of deposition or of the ore fluid composition is required to explain the origin of the Anvil cycle.

DESCRIPTIONS OF DEPOSITS TO BE VISITED

Faro

History

The Faro deposit was discovered in 1964 by the drill testing of airborne electromagnetic anomalies

supported by other indications. Mining at Faro began in late 1969 and continued until 1982 when high costs and falling prices forced temporary closure of the mine.

In November 1985, Curragh Resources Inc. bought the Faro mine and other deposits in the Anvil District from Cyprus Anvil Mining Corporation. Waste removal from the Faro Pit resumed in early 1986. The Faro concentrator resumed production in June 1986.

General Geology

The Faro deposit occurs in the Mount Mye formation approximately 100 meters structurally beneath the Vangorda formation. Strati- graphically this may equate to the position of the lowest horizons in the Grum, Vangorda, and Dy deposits.

The orebody is hosted by biotite-muscovite-andalusite schist. With increasing metamorphic grade this schist changes into a coarse, gneissic biotite-muscovite schist. The Vangorda formation at Faro is represented by hard, dense, banded calc-silicates.

Post-metamorphic igneous intrusive rocks are more widely developed at Faro than any of the other deposits. There are two clans of dykes:

a) equigranular to subporphyritic hornblende-biotite quartz diorite,

b) smoky quartz-feldspar porphyry.

The hornblende-biotite quartz diorite forms large dykes at the northwest and northeast margins of the deposit. These dykes appear to be associated with extensional faults. The smoky quartz-feldspar porphyry is associated with an extensional fault bounding the deposit on the southeast side.

A large mass of heavily silicified post-metamorphic breccia occurs at the northeast edge of the central part of the deposit. This "breccia cap" is associated with irregular dykes belonging to both of the above clans and with the intersection of two extensional faults. The hornblende-biotite quartz diorite also occurs as clasts within the breccia. The deposit has been disrupted by the breccia and ore clasts occur within it. This breccia presumably resulted during intrusion of the dykes as the vapour pressure of the intrusive melts exceeded the confining pressure of the overlying metasedimentary sequence.

Before mining, the Faro deposit was 2000 meters along strike, 800 meters across strike and about 70 meters thick. The deposit is a flat-lying, elongate, asymmetric lens with a thick northeast side and a thin tapering southwest side (Figures 8, 9). The deposit is cut by several extensional faults which form a graben structure with the central portion of the deposit being downthrown. This central portion contained the majority of the remaining reserves when Curragh Resources Inc. acquired the deposit.

The Faro deposit exemplifies the classic Anvil cycle. It contains a massive sulphide variably baritic upper portion and a quartzose variably carbonaceous lower and peripheral part (Figure 8). In addition there is a prominent very low grade semi-massive siliceous pyritic sulphides zone along the northeast edge of of the deposit. Unusually abundant (compared to other Anvil district deposits), but erratically distributed, pyrrhotitic mineralization occurs in the southwest part of the deposit, especially where the deposit thins dramatically.

Grade zoning follows ore type zoning so that the base and northeast edge of the deposit contains the lower grade mineralization and the upper and southwest portion of the deposit contains the higher grade mineralization. In plan the deposit was also zoned with the northwest part of the deposit consisting largely of baritic massive sulphides with high lead-zinc grades, and the southeast part consisting dominantly of carbonaceous quartzose ores with low lead-zinc grades.

Gold grades in the Faro deposit are significantly lower than other deposits in the Anvil District. Gold distribution is erratic with a few high values associated with fractures. This erratic distribution and lower grade is related to the amphibolite facies metamorphic grade for the deposit.

The southwest thinning and southwest dip of the deposit combine to make the southwest edge of the orebody uneconomic for mining by open pit methods. A small southwest extension of the deposit immediately southwest of the ultimate pit walls is being mined by room and pillar underground methods from a ramp developed into the pit wall.

Field Trip Stops

An overview of the Faro deposit will be presented from the lookout point on the southwest edge of the present open pit. This overview will discuss metamorphic grade, ore type distibution, metal zoning patterns, fault and fold patterns, and mining history.

A more detailed look at ore types and deformation patterns is planned by viewing exposures in the underground mine developed in the southwest tail of the deposit.

Grum

History

The Grum deposit was discovered in 1973 by AEX Minerals in joint venture with Kerr Addison Mines. Discovery was through drill testing a gravity anomaly in an area structurally down fold plunge from the Vangorda deposit.

Surface drilling in 1973 and 1974 indicated significant mineralization; in 1975 and 1976 an underground sampling and drilling program was carried out to further define the deposit. Kerr Addison sold the deposit, along with the Vangorda and Swim deposits, to Cyprus Anvil Mining Corporation in 1979. From 1980 to 1982 Cyprus Anvil drilled additional holes in and around the deposit and relogged all existing holes. All available sulphide intersections were re-sampled and re-assayed at that time. In 1985 Curragh Resources Inc. purchased the deposit from Cyprus Anvil. Limited surface drilling programs in 1987-89 further refined the locations of mineralized horizons in near surface areas.

Curragh Resources Inc. is currently preparing plans for the development and operation of the Grum deposit. Development of the Grum and Vangorda deposits will supplement and eventually replace production from the nearly exhausted Faro pit. A haul road has been constructed between the Grum deposit and the Faro concentrator. Curragh Resources Inc.has also constructed a mine dry and water treatment plant for the Grum and Vangorda deposits. An Initial Environmental Evaluation has been prepared to identify environmental problems and directly related socio-economic impacts of the development.

General Geology

The Grum deposit subcrops beneath morainal tills and glaciofluvial silts, sands, and gravels. Overburden is thin to absent in the northwest end of the deposit and thickens to 100 meters towards the southeast.

It consists of three to five layers of massive and disseminated sulphide mineralization with interbanded pelitic phyllites. The most important mineralized horizon occurs just beneath the basal carbonaceous pelite member of the Vangorda formation. There are thin low grade horizons within the Vangorda formation and more important horizons in the upper part of the Mount Mye formation.

At Grum, the Vangorda formation consists of soft, highly fissile, calcareous, muscovite-chlorite phyllites. Metabasites are minor and tend to be highly foliated chlorite phyllite rather than the blocky, massive greenstones that typify the Vangorda metabasites elsewhere. The basal carbonaceous pelite member of the Vangorda formation thickens across the deposit from about 10 meters in the northeast to as much as 80 or 100 meters southwest of the deposit. The sulphide horizons appear to be associated with the northeast pinchout of this unit. Immediately above the main ore horizon the carbonaceous rocks are soft and highly sheared and gouged. Elsewhere they are moderately hard, highly fractured, black, siliceous phyllites.

The Mount Mye formation consists of soft muscovite-chlorite phyllites. They are distinguished from the Vangorda formation phyllites by being noncalcareous. The ore layers at Grum are define a complex, shallowly northwest plunging, polyphase fold structure (Figure 10, 11, 12). The prominant S-shaped folds (in cross section looking northwest, see Figure 10) are second phase structures. They are superimposed on a larger Z-shaped first phase fold (Figure 10). The dominant plane of fissility (S2) in the phyllites at Grum is axial planar to the second phase folds and dips shallowly (10o-30o), generally to the southwest. This fissility is a major factor in assessing slope stability for a Grum pit. The overall deposit elongation parallels the axial direction of the second phase folds. The first and second phase folds plunge towards the northwest with a dip of approximately 12o (Figure 12).

There are several important extensional faults at Grum. The largest displacements occur on moderately (35o-45o) dipping structures that truncate the deposit at

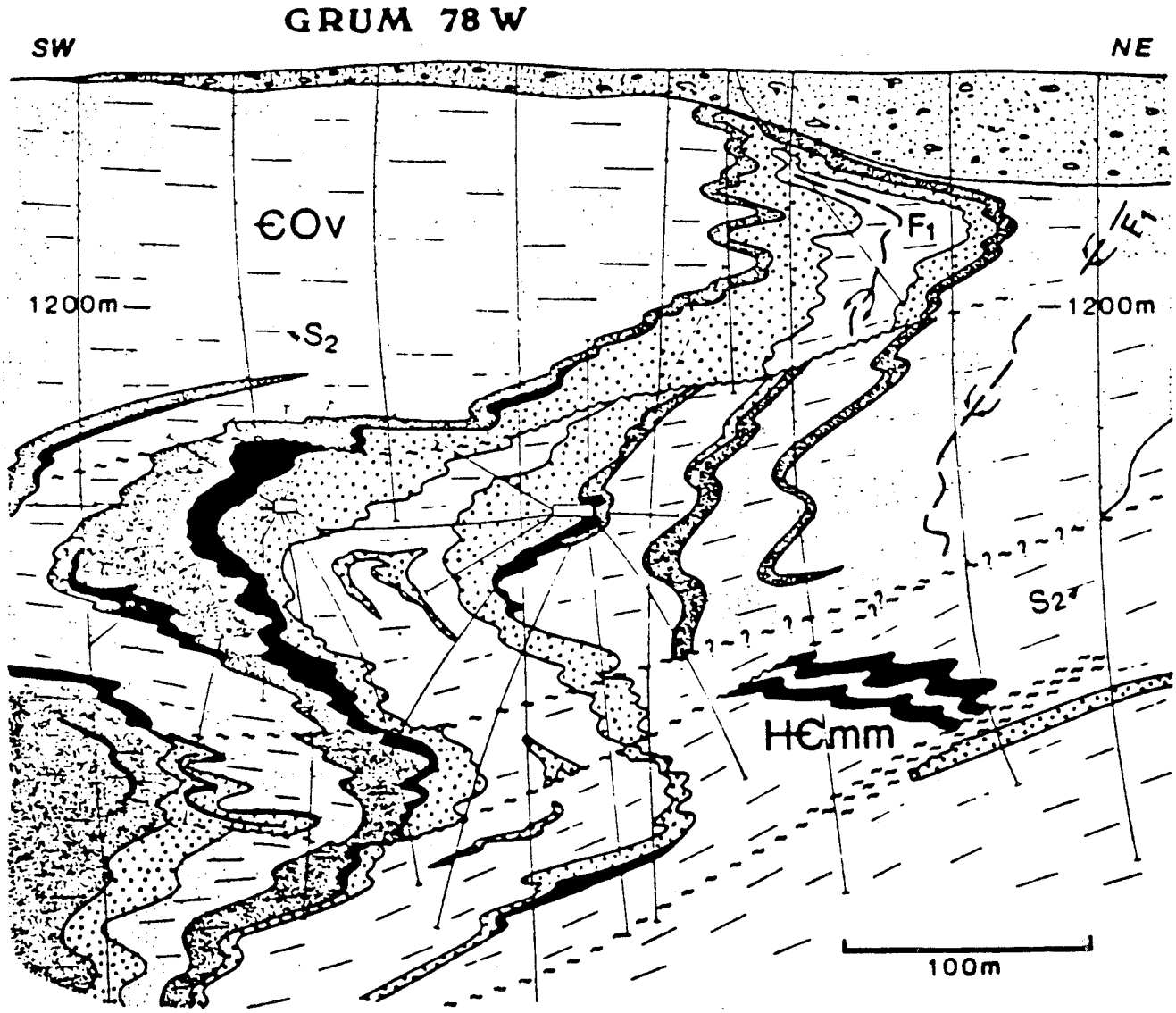

Figure 10 Vertical cross section 78+00W through Grum deposit. Section is oriented SW-NE looking northwest. Rock unit patterns are the same as in Figure 8. Section shows type 3 interference pattern between D^1 and D^2 fold structures. Anvil cycle is also evident with massive sulphides overlying quartzose sulphides.

both its northwest and southeast ends (Figure 12). The extensional fault on the northwest end has a minimum displacement of one kilometer. Fabrics in these fault zones indicate they formed late during the D2 deformation with emplacement and uplift of the Anvil batholith. Neither of these major structures would crop out in an open pit.

Several smaller subparallel faults will be found in the proposed Grum pit. A myriad of smaller faults were

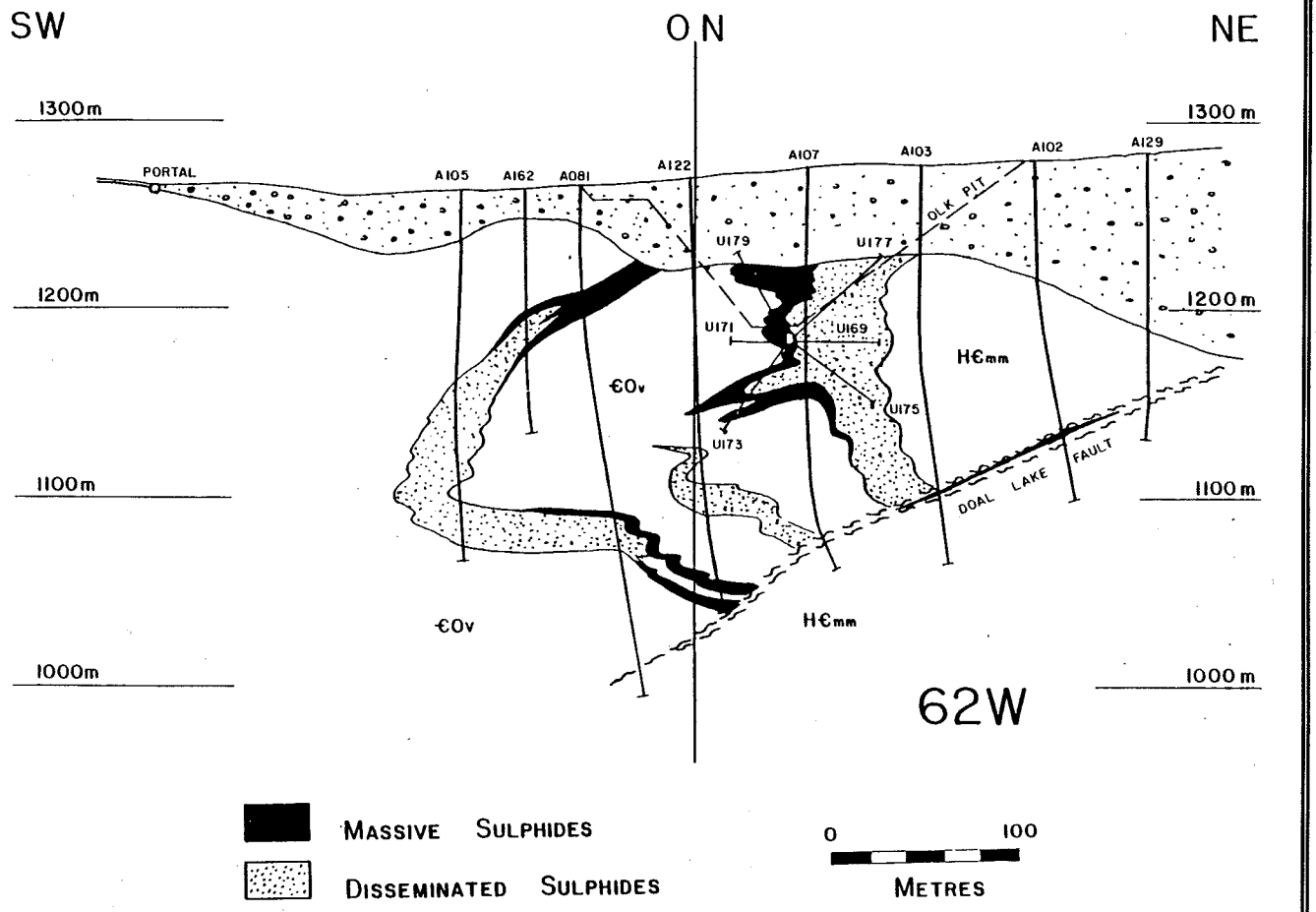

Figure 11 Vertical cross section 62+00W through Grum deposit. Section is oriented SW-NE looking northwest. Type 3 interference pattern is less obvious because D^1 fold closure has been eroded. Doal Lake Fault is a large extensional fault which forms the southeast boundary of the Grum deposit.

mapped underground by Kerr Addison trending on the average 080° and dipping steeply. One of these faults has an interpreted normal displacement of 60 meters. Points mapped underground and on surface tend to strike 060° and dip subvertically.

As with other deposits in the Anvil Range a given ore horizon at Grum has a massive sulphide upper portion and a quartzose, disseminated sulphide lower portion. The horizons can be up to 30 meters thick but are mostly 15 meters or less in thickness. The sulphide horizons are separated by significant thicknesses of barren phyllite. Interfaces between ore and waste tend to be sharp at the stratigraphic hanging wall and gradational both at the footwall and laterally. Quartzose ore types at Grum constitute about 50% of the deposit; this proportion is significantly higher than the other deposits.

As with all Anvil District deposits, overall grade is strongly partitioned into massive, particularly baritic, sulphides. Therefore the stratigraphic tops of horizons tend to have high Pb+Zn grade and stratigraphic bottoms low Pb+Zn grade. The average gold content of Grum is several times higher than Faro. The sphalerite at Grum is richer in zinc. Both of these

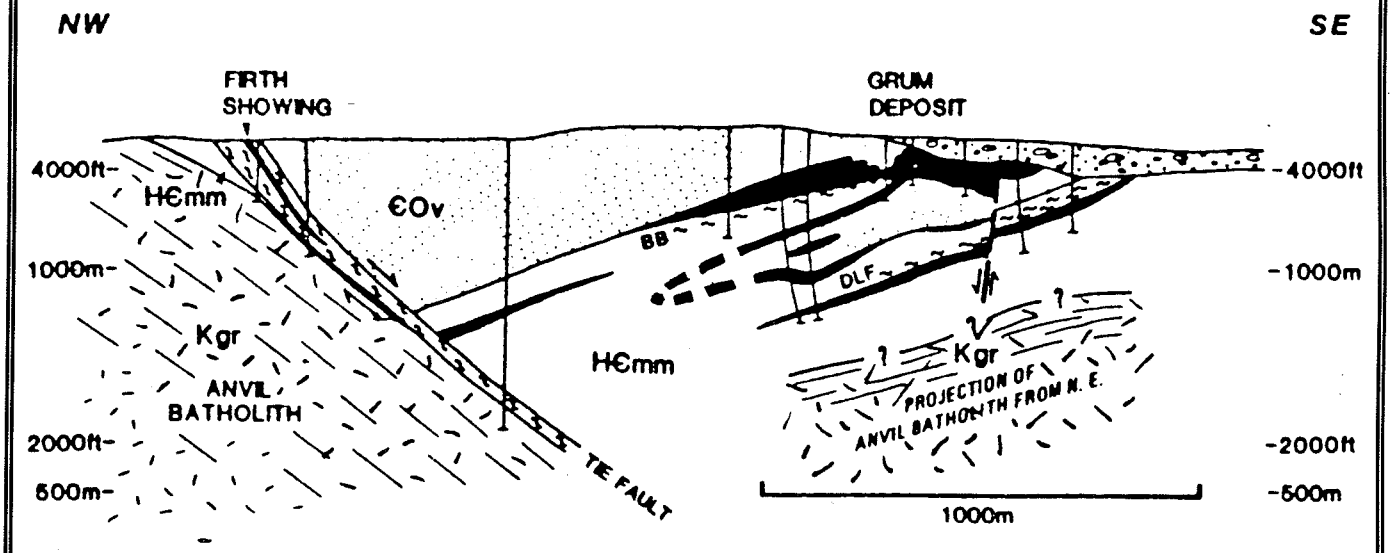

Figure 12 Vertical long section through Grum deposit. Section is oriented NW-SE looking northeast. Section shows the northwest plunge of the Grum fold structure. Firth showing represents slivers of Grum mineralization in the Tie Fault, a large extensional fault zone that juxtaposes footwall amphibolite facies rocks against hanging wall greenschist facies rocks.

variations are due to the lower metamorphic grade at Grum.

Grum ores also have a finer grain size and more complex mineral intergrowth than the Faro deposit. This necessitates finer grinding than Faro ores. Cyprus Anvil Mining Corporation had already made modifications to its mill to accommodate this fine grind prior to shutdown in 1982.

Locally drill holes within the deposit contain substantial metabasite intersections. The metabasites are typically substantially altered to a pale beige or grey muscovite-carbonate (calcite, dolomite, ankerite)-quartz assemblage. Typcially the carbonated metabasites units are highly foliated. Extremely altered metabasites also contain scattered occurrences of a bright green mica. XRD and SEM work indicated that this micaceous mineral is a chromium-rich kaolinite or serpentine (Modene, 1982).

Field Trip Stops

The Grum deposit will not be exposed at the time of the field trip. A brief stop will be made to look at the typical mesoscopic type 3 interference pattern for the D_1 and D_2 minor folds and axial plane surfaces. The fold patterns will be exposed in the calcareous phyllites of the Vangorda formation.

If time permits, core intersections of some of the typical rock types in the Anvil District will be viewed.

Vangorda

History

Vangorda was the initial discovery in the Anvil Range. Attention was drawn to the area by a small stream exposure of highly oxidized sulphides with a prominent red iron oxide stain in Vangorda Creek. The deposit was drill tested from 1953 to 1955 by Prospector Airways, a predecessor to Kerr Addison Mines. This drilling outlined a significant deposit, but a production decision was not warranted at that time. The deposit remained idle for the following decade. Minor additional drilling was done by Kerr Addison largely for metallurgical sampling. In 1979 Kerr Addison sold the

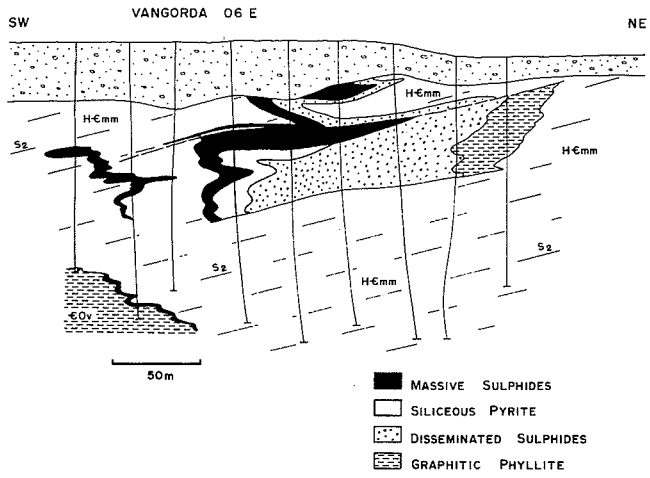

Figure 13 Vertical cross section 06+00E through Vangorda deposit Section is oriented SW-NE looking northwest. Upper part of deposit is overturned with quartzose ores structurally overlying massive sulphides. Major portion of deposit is upright. Quartzose ores and siliceous pyrite underlying massive sulphides show gradational transition to underlying altered Mount Mye phyllites.

deposit to Cyprus Anvil Mining Corporation.

Cyprus Anvil geologists examined the available drill core and concluded that it would be necessary to redrill the deposit to provide adequate material for re-evaluating it. In 1979 the northwest portion of the deposit was re-drilled with NQ core holes. Scattered core holes were put down in the southeast part of the deposit. Because of anticipated poor recoveries in this area it was judged advisable to drill this part of the deposit with rotary methods. This fill in drilling was done in 1981.

Curragh Resources Inc. acquired the Vangorda deposit in 1985. In 1987 selected fill-in diamond drill holes were completed. Test holes were also completed in the southeast portion of the deposit at this time. Because the test holes showed good recovery, the remainder of the deposit was redrilled in 1988 using NQ core holes.

General Geology

The Vangorda deposit is quite shallow, in most places subcropping beneath glacial till. It has been traced over a 1300 meter by 200 meter area. The till blanket is up to about 30 meters thick in the northwest part of the deposit and thins to less than 5 meters in the southeast. Northwest of Vangorda Creek the till cover is also quite thin. Locally the basal overburden and uppermost broken bedrock are cemented by iron oxides into a tough "ferricrete" breccia.

The deposit consists of one major sulphide horizon structurally located about 50 to 120 meters beneath the basal carbonaceous pelite member of the Vangorda formation. Several thin horizons occur above the main horizon. One of these occurs at the base of the Vangorda formation basal carbonaceous pelite member. This ore horizon may equate to the main horizon at Grum. In general these upper horizons are too thin or low grade to be mineable.

The host rocks for the deposit are dominantly noncalcareous phyllites, presumably part of the Mount Mye formation. Formational assignments near this deposit, however, are ambiguous due to the strong wall rock alteration. Most phyllites in the deposit footwall are bleached, locally silicified and/or chlorite and sulphide bearing.

The Vangorda deposit occurs in the hinge of a large second phase fold. Overall the deposit has the shape of a reclining "M" or a "three" in cross section (Figure 13). The major part of the deposit is structurally and stratigraphically upright. There is considerable uncertainty, however, in the details of fold morphology. The deposit is elongate in the northwest-southeast direction parallel to F_2 fold axes. The northwest half of the deposit plunges about 10o towards the northwest, and the southeast half is subhorizontal. The S_2 foliation generally dips shallowly southwest; its orientation is locally quite variable.

The deposit is truncated by a steep normal fault at its northwest end. Displacement along this fault is uncertain; it has been correlated with similar normal faults in the district (such as the faults truncating the Grum deposit). Many other gouge zones were observed in drill core but the orientation of the structures responsible for them is not known.

A number of faults parallel to S_2 are predicted. These are "required" to make the structure and stratigraphy fit (see Figure 13). These low angle structures are best thought of as sheared out fold limbs. They are not generally gouge zones and will probably

pose no more serious a problem for slope stability than the S_2 foliation and the myriad of small gouge zones that parallel it. Several analogous structures are thought to be present at Grum.

The deposit consists of the same sulphide rock types as the other deposits. Two ore types are particularly prominant. The massive sulphides forming the stratigraphically highest portion of the deposit are commonly baritic and rich in lead and zinc. This unit is actually a mixture of about 50% pyritic massive sulphide and 50% baritic massive sulphide ore types. Within a given drill hole the two ore types are interbanded on a scale of 0.5-5 meters. Immediately underlying themassive sulphides is a very pyrite-rich quartzite. This quartzite grades downwards sequentially into pyritic quartzite, siliceous phyllite, and ultimately altered phyllite of the Mount Mye formation. Concordant with this downward decrease in silica is a similar downward decrease in the abundance of sulphides from quartz rich semi-massive pyrite at the top to slightly pyritic altered phyllite at the base. Although pyrite is the dominant sulphide in the quartzite, pyrrhotite is generally present and locally abundant or dominant. Magnetite is also unusually well developed in the pyritic portion of the quartzite. The quartzite contains only minor lead and zinc but is relatively rich in copper and unusually high in gold. This pyritic quartzite to siliceous pyrite is similar to the semi-massive zone along the northeast edge of the Faro deposit.

Of the other ore rock types only the carbonaceous ribbon-banded pyritic quartzite occurs to any greatextent. This carbonaceous quartzite tends to have low Pb+Zn grades and is peripheral to the deposit.

The gradational and conformable change from the extremely pyritic quartzite immediately beneath the massive sulphides to slightly altered Mount Mye footwall phyllites has important implications concerning ore genesis. This pattern strongly suggests that the quartzose ores in the Vangorda deposit are not exhalative in origin. Rather they represent a strongly silicified and sulphidized footwall to the massive sulphides. In this scenario the only exhalative mineralization in the Anvil cycle would be the massive sulphides. Feeder zones for the exhalative mineralization would ideally be demarcated by the quartzose ores.

Field Trip Stops

There is a strong possibility that the southeast portion of the Vangorda deposit will be partially exposed at the time of the field trip. If this is the case then it will be possible to view a complete Anvil cycle from the massive sulphides through the quartzose ores into the altered footwall phyllites. It will present an excellent opportunity to discuss zoning patterns, deformation textures, and genetic models.

SELECTED REFERENCES

Abbott, J.G., Gordey, S.P., and Tempelman-Kluit, D.J., 1986, Setting of stratiform, sediment-hosted lead-zinc deposits in Yukon and northeastern British Columbia. IN J.A. Morin (ed.) Mineral Deposits of Northern Cordillera. Canadian Institute Mining Metallurgy, Special Paper 37, 1-18.

Aho, A.E., 1966, Exploration methods in Yukon with special reference to Anvil District. Western Miner, 39, 127-148.

Aho, A.E., 1969, Base metal province of Yukon. Canadian Institute Mining Metallurgy Bulletin, vol. 62, no. 684, 397-409.

Brock, J.S., 1973, Geophysical exploration leading to the discovery of the Faro Deposit. Canadian Institute Mining Metallurgy Bulletin, vol. 66, no., 97-116.

Blusson, S.L., 1966, Frances Lake, Yukon Territory and District of Mackenzie. Geological Survey Canada, Map 8-1967.

Carne, R.C. and Cathro, R.J., 1982, Sedimentary exhalative (sedex) zinc-lead-silver deposits, northern Canadian Cordillera. Canadian Institute Mining Metallurgy Bulletin, Vol. 75, no. 840, 66-78.

Chisholm, E.O., 1957, Geophysical exploration of a lead-zinc deposit in Yukon Territory. In Methods and case histories in mining geophysics, Sixth Commonwealth Mining and Metallurgy Congress, 269-277.

Coney, P.J., Jones, D.L., and Monger, J.W.H., 1980, Cordilleran suspect terranes. Nature, 288, 329-333.

Eisbacher, 1981, Sedimentary tectonics and glacial record in the Windermere Supergroup, Mackenzie Mountains, northwestern Canada. Geological Survey Canada, Paper 80-27.

Gabrielse, H., 1967, Tectonic evolution of the northern Canadian Cordillera. Canadian Journal Earth Sciences, 4, 271-298.

Gabrielse, H., 1985, Major dextral transcurrent displacements along the northern Rocky Mountain trench and related lineaments in north-central British Columbia. Geological Society America Bulletin, 96, 1-24.

Gabrielse, H., Blusson, S.L., and Roddick, J.A., 1973, Geology of Flat River, Glacier Lake and Wrigley Lake map areas; Geological Survey Canada, Memoir 366, 153 p.

Gordey, S.P., 1978, Stratigraphy and structure of the Summit Lake area, Yukon and Northwest Territories. In Current Research, Part A, Geological Survey Canada, Paper 78-1A, 3-48.

Gordey, S.P., 1983, Thrust faults in the Anvil Range and a new look at the Anvil Range Group, south Central Yukon Territory. In Current Research, Part A, Geological Survey Canada, Paper 83-1A, 225-227.

Gordey, S.P., Abbott, J.G., and Orchard, M.J., 1982, Devono- Mississippian (Earn Group) and younger strata in east central Yukon. In Current Research, Part B, Geological Survey Canada, Paper 82-1B, 93-100.

Gordey, S.P. and Irwin, S.E.B., 1987, Geology, Sheldon Lake and Tay River map areas, Yukon Territory. Geological Survey Canada, Map 19-1987 (3 sheets), scale 1:250 000.

Gustafson, L.B., and Williams, N., 1981, Sediment-hosted stratiform deposits of copper, lead, and zinc. Economic Geology, 75th Anniversary Volume, 139-178.

Jennings, D.S. and Jilson, G.A., 1986, Geology and sulphide deposits of Anvil Range, Yukon. In J.A. Morin (ed.), Mineral Deposits of Northern Cordillera. Canadian Institute Mining Metallurgy, Special Paper 37, 319-361.

Kuo, S.L., 1976, Geology and geochemistry of stratabound ore deposits in south central Yukon Territory and southwestern District of Mackenzie, Northwest Territories. Unpublished Ph.D dissertation, University of Alberta, Edmonton, 597 p.

Large, D., 1980, Geological parameters associated with sediment-hosted submarine exhalative Pb-Zn deposits. Geologisch, J., Reike, D. Heft 40, 49-129.

Modene, J.S., 1982, Origin and sulfur isotope geochemistry of the Grum deposit, Yukon Territory, Canada. Unpublished M.Sc dissertation, University of Wisconsin, 158 p.

Mortensen, J.K., 1982, Geological setting and tectonic significance of Mississippian felsic metavolcanic rocks in the Pelly Mountains, southeastern Yukon Territory. Canadian Journal Earth Sciences, 19, 8-22.

Mortensen, J.K. and Jilson, G.A., 1985, Evolution of the Yukon-Tanana terrane: evidence from southeastern Yukon Territory. Geology, 13, 806-810.

Morton, P., 1973, Geochemistry of bedrock and soils in the vicinity of the Anvil mine, Yukon Territory. Unpublished M.Sc dissertation, University of British Columbia, 207 p.

Pigage, L.C. and Anderson, R.G., 1985, The Anvil plutonic suite, Faro, Yukon Territory. Canadian Journal Earth Sciences, 22, 1204-1216.

Pigage, L.C. and Jilson, G.A., 1985. Major extensional faults, Anvil Pb-Zn district, Yukon. Geological Society America, Abstracts with Programs-Cordilleran Section, 17, 400.

Roddick, J.A., and Green, L.H., 1961, Tay River, Yukon Territory. Geological Survey Canada, Map 13-1961.

Sato, T., 1972, Behaviors of ore forming solutions in seawater. Mining Geology, 22, 31-42.

Tempelman-Kluit, D.J., 1970a. Stratigraphy and structure of the "Keno Hill Quartzite" in Tombstone River - Upper Klondike River map areas. Yukon Territory. Geological Survey Canada, Bulletin 180, 102 p.

Tempelman-Kluit, D.J., 1970b, The relationship between sulphide grain size and metamorphic grade of host rocks in some stratabound pyritic ores. Canadian Journal Earth Sciences, 7, 1339-1345.

Tempelman-Kluit, D.J., 1972, Geology and origin of the Faro, Vangorda and Swim concordant zinc-lead deposits, central Yukon Territory. Geological Survey Canada, Bulletin 208, 73 p.

ADDITIONAL REFERENCES ON ANVIL DISTRICT GEOLOGY

Campbell, F.A., and Ethier, V.G., 1974, Sulfur isotopes, iron content of sphalerites, and ore textures in the Anvil Ore Body, Canada. Economic Geology, 69, 482-493.

Campbell, R.B., 1967, Geology of Glenlyon map-area. Geological Survey Canada, Memoir 352, 92 p.

Godwin, C.I., and Sinclair, A.J., 1982, Average lead isotope growth curves for shale-hosted zinc-lead deposits, Canadian Cordillera. Economic Geology, 77, 675-690.

Gondie, J., 1972, Geology of the Anvil Mine. In D.J. Glass (ed.) Major lead-zinc deposits of Western Canada. International Geological Congress, 14th Session, Guidebook.

Johnston, J.R., 1936, A reconnaissance of Pelly River between Macmillan River and Hoole Canyon, Yukon. Geological Survey Canada, Memoir 200, 19 p.

Kuo, S.L. and Folinsbee, R.E., 1974, Lead isotope geology of mineral deposits spatially related to the Tintina Trench, Yukon Territory. Economic Geology, 69, 806-813.

Lecouter, P., 1973, A lead isotope study of ore deposits from the East Kootenay District, B.C. and the Anvil District, Yukon Territory. Unpublished PhD dissertation, University of British Columbia.

Roddick, J.A., 1967, Tintina Trench. Journal Geology, 75, 23-33.

Shanks, W.C. III, Woodruff, L.G., Jilson, G.A., Jennings, D.S., Modene, J.S., and Ryan, B.D., 1987, Sulfur and lead isotope studies of stratiform Zn-Pb-Ag deposits, Anvil Range, Yukon: basinal brine exhalation and anoxic bottom-water mixing. Economic Geology, 82, 600-634.

Tempelman-Kluit, D.J., 1968, Geological setting of the Faro, Vangorda and Swim base metal deposits, Yukon Territory. Geological Survey Canada, Paper 68-1 Part A, 43-52.

Tempelman-Kluit, D.J., 1970, An occurrence of eclogite near Trench, Yukon. Geological Survey Canada, Paper 70-1B, 19-22.

THE GREW CREEK GOLD-SILVER DEPOSIT IN SOUTH-CENTRAL YUKON TERRITORY

Jesse L. Duke
Noranda Exploration Company Ltd.
Whitehorse, Yukon

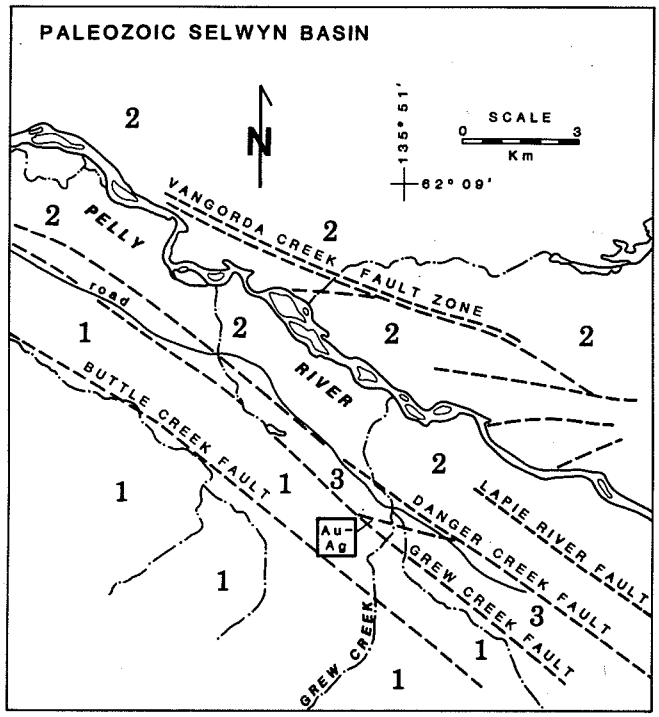

Figure 1 Grew Creek regional geological setting. 1 - unit 1, early Paleozoic Pelly-Cassiar Platform phyllite and chert. 2 - unit 2, Anvil Allochthon metabasalt and marble. 3 - unit 3, Eocene volcanic, volcaniclastic, and fluvial clastics. Grew Creek is marked as Au-Ag occurrence.

INTRODUCTION

The Grew Creek property lies between Ross River and Faro in central Yukon Territory. The block of 332 claims that cover the zone of mineralization lie on the western flank of the broad valley which marks the Tintina Trench. This valley was scoured by Pleistocene glacial ice and is extensively covered by till, drumlins and small lakes. The epithermal style gold and silver mineralization is hosted in Eocene felsic crystal lithic lapilli tuff. The Grew Creek discovery is important as the first reported Tertiary volcanic-hosted epithermal gold occurence in the Tintina Trench.

Between June 1987 and September 1988 19,173 metres of diamond drilling and 1,651 metres of reverse circulation drilling were completed on the property as part of a joint venture agreement between Goldnev Resources Inc. and Noranda Exploration Company Ltd. Goldnev is continuing exploration on the property.

REGIONAL SETTING

The Grew Creek deposit is in an Eocene volcanic assemblage that is preserved in a graben in the Tintina Trench. The Trench reflects the Tintina Fault, a major northwest trending structure with at least 450 km of Late Cretaceous and early Tertiary right-lateral displacement (Gabrielse, 1985). In the Grew Creek area, a complex array of faults that comprise the Tintina Fault system (Fig. 1), juxtopose autochthonous Pelly-Cassiar Platform on the south side against the Anvil Allochthon on the north side. Late Miocene or Pliocene block faulting preserved part of the Eocene volcaniclastic and sedimentary package between these major tectonic elements.

LOCAL GEOLOGY

The Grew Creek deposit is in a steep north dipping sequence of rhyolitic crystal-lithic lapilli tuff which has been intruded by quartz-feldspar porphyry dykes of the same composition, and minor andesite (Fig. 2). These rocks form a fault bounded wedge with Paleozoic metasediments to the south and interbedded Eocene fluvial sediments and volcanics to the north. Felsic quartz-porphyry intrusions in the sediments appear to be limited to the area immediately north of the

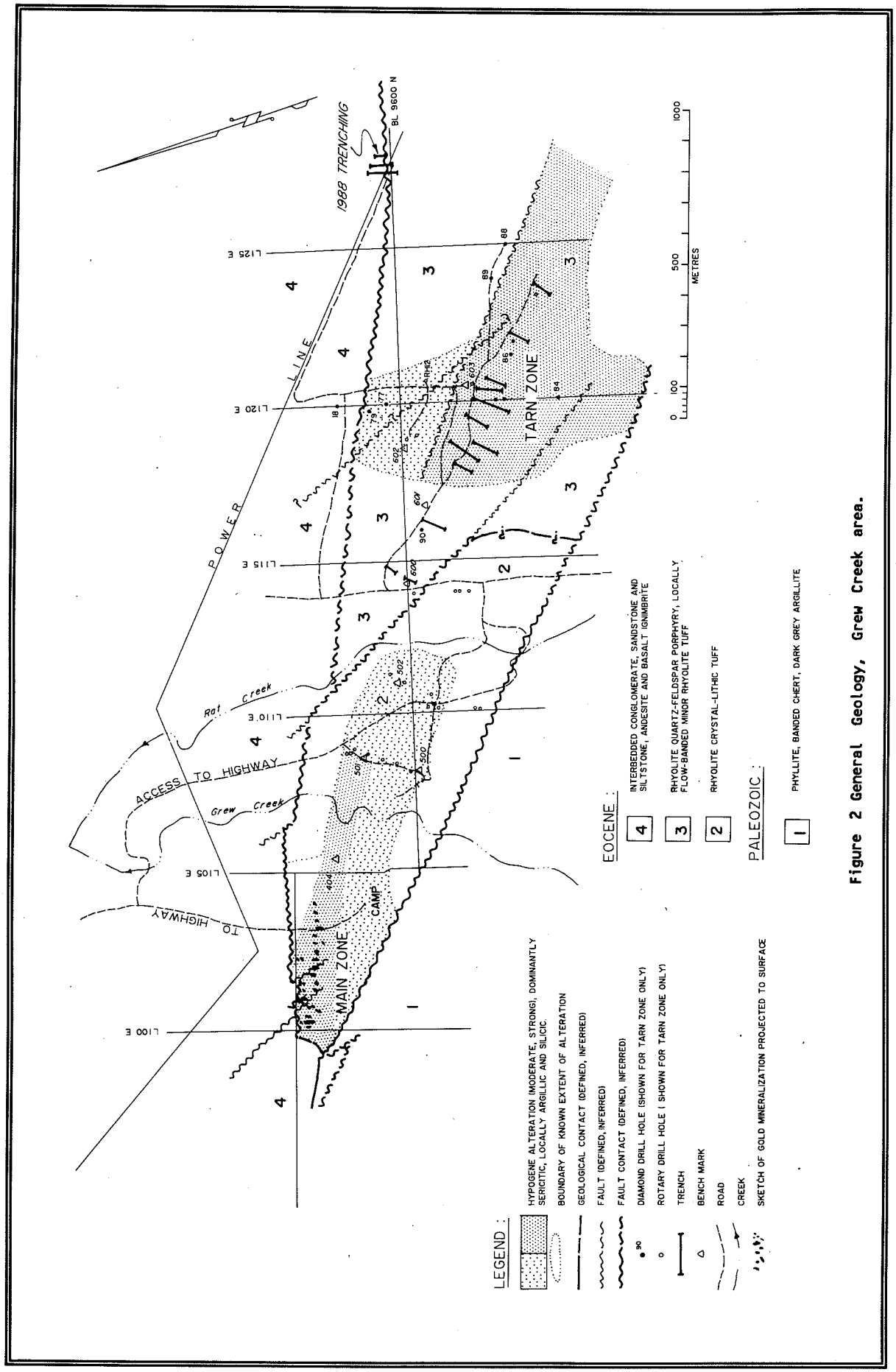

Figure 2 General Geology, Grew Creek area.

Main Zone mineralization.

STRUCTURE

The Main Zone is interpreted to lie at the intersection of the northwest-southeast trending compressional Grew Creek Fault and a north-south trending extensional structure. The Grew Creek Fault is a zone of gouge and rock fragments over 10 metres wide. The north-south trending structure is defined by a physiographic linear visible on airphotos. This structure has the same orientation as several prominent faults within the Main Zone that control the distribution of mineralization. One of these faults forms the western boundary of the Main Zone.

Some of the north-south trending faults appear to offset mineralization whereas gold and silver is localized along others. This suggests the timing of mineral deposition and normal extensional faulting was close.

High-grade mineralization does not appear to extend to the bedrock surface. A leached cap may be present. The bedrock is covered by up to 59 metres of glacial till.

MINERALIZATION

The Main Zone comprises a stockwork of chalcedonic and fine to medium grained veins of quartz +/- clay +/- calcium carbonate +/- adularia that dips vertically or steeply to the northeast. Vuggy, crustiform and banded textures in open space fillings are characteristic and suggest repeated cycles of mineral deposition. Gold and silver are irregularly distributed through the stockwork. Gold occurs as very fine grained electrum in quartz. Gold to silver ratios very greatly. Silver also occurs in acanthite, amalgam and with selenides. Pyrite and trace amounts of arsenopyrite and chalcopyrite are also found in the deposit.

The stockwork zones that contain the ore body are closely-spaced and funnel-shaped with the wide end pointed upward. They dip about 75 degrees north and have a strike length of 400 metres with a vertical extent of about 150 metres and a maximum width of about 110 m. Values up to 2.86 oz/ton gold and 21.6 oz/ton Ag occur within the deposit. Geological reserves estimated in 1988 prior to 1989 core zone drilling are 852,100 tons grading 0.26 oz/ton Au and 0.98 oz/ton Ag.

Oxygen isotope studies show some enrichment with values ranging between 2.1 and 7.7 $\delta^{18}O$ values for quartz and 5.6 to 11 for carbonate (Duke and Godwin, 1986). This suggests a deep, hot, magmatic source for the mineralized fluid.

K-Ar age dating of the volcanic host rock and sericite from altered samples of the deposit; and palynological dating of pollen spores within the volcanic package have established the timing of volcanism and mineralization as mid Eocene (Duke and Godwin, 1986).

ALTERATION

Intense argillic alteration of the wall rock along mineralized veins is typical and strong sericitic and argillic alteration is widespread throughout the felsic volcanics. In the Main Zone both the footwall and hanging wall exhibit the strong sericitic and argillic alteration with no clear sense of zoning. Silicification of tuff near mineralization is common. A 10 to 80 metre wide zone with 3-5% pyrite occurs as a hangingwall to the stockwork mineralization. The gold/silver mineralization is at the western end of a hypogene sericite and clay alteration zone which ranges up to 500 metres wide and has been traced for 3 kilometres toward the east. The Tarn Zone (Fig. 3) is the eastern portion of the alteration zone.

FIELD TRIP VISIT
DISCOVERY OUTCROP

A short walk over the Main Zone will take you to the Discovery Outcrop. Note the mineralized banded veining and carbonized plant fragments exposed. The bulk of the deposit lies under the swampy ground immediately to the south east of the outcrop.

This small silicified and mineralized knoll survived the extensive glacial scouring in this area. Originally it formed a small patch of indurated volcaniclastic rock exhibiting distinctive yellow and orange alteration colors. Its occurrence here has been interpreted as part of a silicified cap that may have formed as the result of the boiling at depth of hydrothermal waters. Note the extreme clay alteration in rhyolite in the trench immediately west of the outcrop. This could be the result of acid sulphate leaching

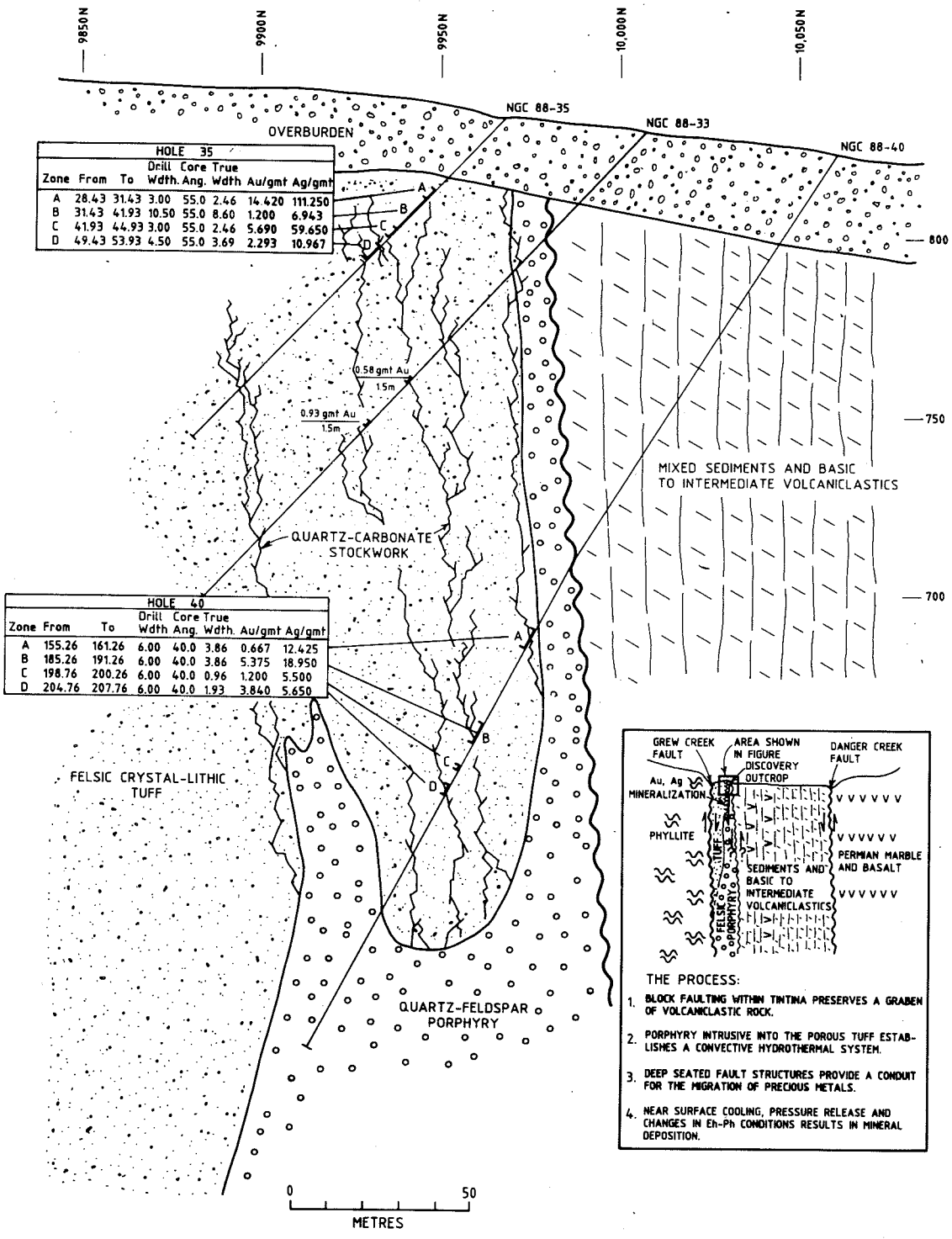

Figure 3 Cross-section (10125 East on Fig. 2) through the Grew Creek deposit.

associated with the boiling of rising sulphur-bearing hydrothermal waters.

DRILL CORE

A good example of the mineralization can be viewed in Hole 29 between 69.5 metres and 101.0 metres. This 31.5 metre interval contained 0.34 oz/ton Au and 4.41 oz/ton Ag.

GEOLOGY OF THE ROSS RIVER COAL DEPOSITS[1]

D.G.F. LONG, D. HUGHES AND J.G. ABBOTT

INTRODUCTION

In the Ross River area coal-bearing rocks are exposed along Lapie River and near Ross River townsite (Kindle, 1946; Milner and Craig, et al. 1973; Wheeler et al., 1960; Hughes and Long, 1980). They occur within two fault-bounded blocks referred to as the Lapie River and Ross River blocks. The inferred distribution of these rocks and structural relations within the area are shown in Figure 1. The geometry of these fault blocks is uncertain, owing to extensive surficial cover, hence other areas underlain by early Tertiary strata may be present in this vicinity.

The field trip will visit a small open pit in the Ross River block where between 1986 and 1989, 87,000 tonnes of coal were mined from two seams. The coal is fuel for the concentrate dryer at the Faro zinc, lead mine.

LAPIE RIVER BLOCK

Early Tertiary strata along Lapie River abut older metamorphic and igneous rocks to the northeast and southwest along two major northwest-trending faults (Fig. 1). Vertical separation on these faults is in the order of several hundred metres. Strike-slip cannot be demonstrated as the fault zones are poorly exposed; horizontal slickensides on small parallel fractures near the southwest fault, however, suggest strike-slip could have been a significant or even dominant component of movement. The position of these faults away from Lapie River as shown on figure 1 is conjectural owing to extensive surficial cover.

Over 400 m of well-indurated conglomerate, sandstone, siltstone and shale along with minor coal are partially exposed along Lapie River between the faults. The strata generally dip southwest at from 25 to 35^0, but are gently folded midway between the bounding faults and dip steeply near the fault zones. The lowermost 120 m of section is dominated by laminated claystone and siltstone and contains two thin lenticular coal seams with maximum thicknesses of 30 cm. Minor sandstone and conglomerate beds are present in the middle part of this unit within both coarsening and fining upwards sequences. Conglomerates associated with the latter are distinctly lenticular, and occur within channels up to 12 m wide characterized by rapid lateral facies changes. Above this is a 35 m thick unit of massive to weakly stratified, medium to small pebble conglomerates with minor flat bedded and planar cross-stratified sandstones; a poorly exposed 175 m thick unit of sandstone, siltstone and claystone with minor conglomerate beds near the base and top and a thin (0.1 m) coal seam in the upper part; and an upper unit, at least 100 m thick, in which massive to stratified medium to small pebble conglomerates are exposed between extensive covered intervals.

Conglomerates within the Lapie River section occur in bed sets up to 15 m thick which commonly have well-defined lower contacts. Clasts are subangular to rounded with maximum size between 1 and 7 cm. They consist mainly of resistant lithologies, including tectonized chert and cherty siltstone, grey and white quartzites, vein quartz and lesser amounts of other metamorphic rock fragments, set in a matrix of medium to coarse-grained sandstone. Plane bedded and cross-stratified, medium to very coarse sandstone occurs, in association with small pebble and granule conglomerate, in filling small channels within the finer grained parts of the section, and as more laterally extensive beds in association with the coarser conglomerates. Sandstones within coarsening upwards sequences in the lowermost unit are flat laminated and in part ripple cross-laminated. The horizontally laminated claystones and siltstones are commonly micaceous and fissile and in places contain well preserved plant remains. Mudrocks in close association with sandstone and conglomerate units appear more massive and contain plant remains, rooted zones and

[1] Modified from Hughes and Long, 1980

BIBLIOGRAPHY

Duke, J.L., and Godwin, C.I., 1986, Geology and alteration of the Grew Creek epithermal gold-silver prospect, south-central Yukon; in Yukon Geology, Vol. 1; Exploration and Geological Services Division, Yukon, Indian and Northern Affairs Canada, p. 72-82.

Gabrielse, H., 1985, Major transcurrent displacements along the northern Rocky Mountain trench and related lineaments in north-central British Columbia; Geol. Soc. of Am. Bull., Vol. 96, p. 1-14.

Gordey, S.P., and Irwin, S.E.B., 1987, Geology, Sheldon Lake and Tay River map areas, Yukon Territory; Geological Survey of Canada, Map 19-1987 (3 sheets), scale 1:250,000.

Jackson, L.E., Gordey, S.P., Armstrong, R.L. and Harakal, J.E., 1986, Bimodal Paleogene volcanics near Tintina Fault, east-central Yukon, and their possible relationship to placer gold; in Yukon Geology, Vol. 1; Exploration and Geological Services Division, Yukon, Indian and Northern Affairs Canada, p. 139-147.

Pride, M.J., 1988, Bimodal volcanism along the Tintina Trench near Faro and Ross River; in Yukon Geology, Vol. 2; Exploration and Geological Services Division, Yukon, Indian and Northern Affairs Canada, p. 69-80.

Tempelman-Kluit, D.J., 1972, Geology and origin of the Faro, Vangorda, and Swim concordant zinc-lead deposits, central Yukon Territory; Geological Survey of Canada, Bulletin 208, 73 p.

Tempelman-Kluit, D.J., 1979, Transported ophiolite, cataclastic, and granodiorite in Yukon: evidence of arc-continent collision; Geol. Surv. Can., Paper 79-14, 27 p.

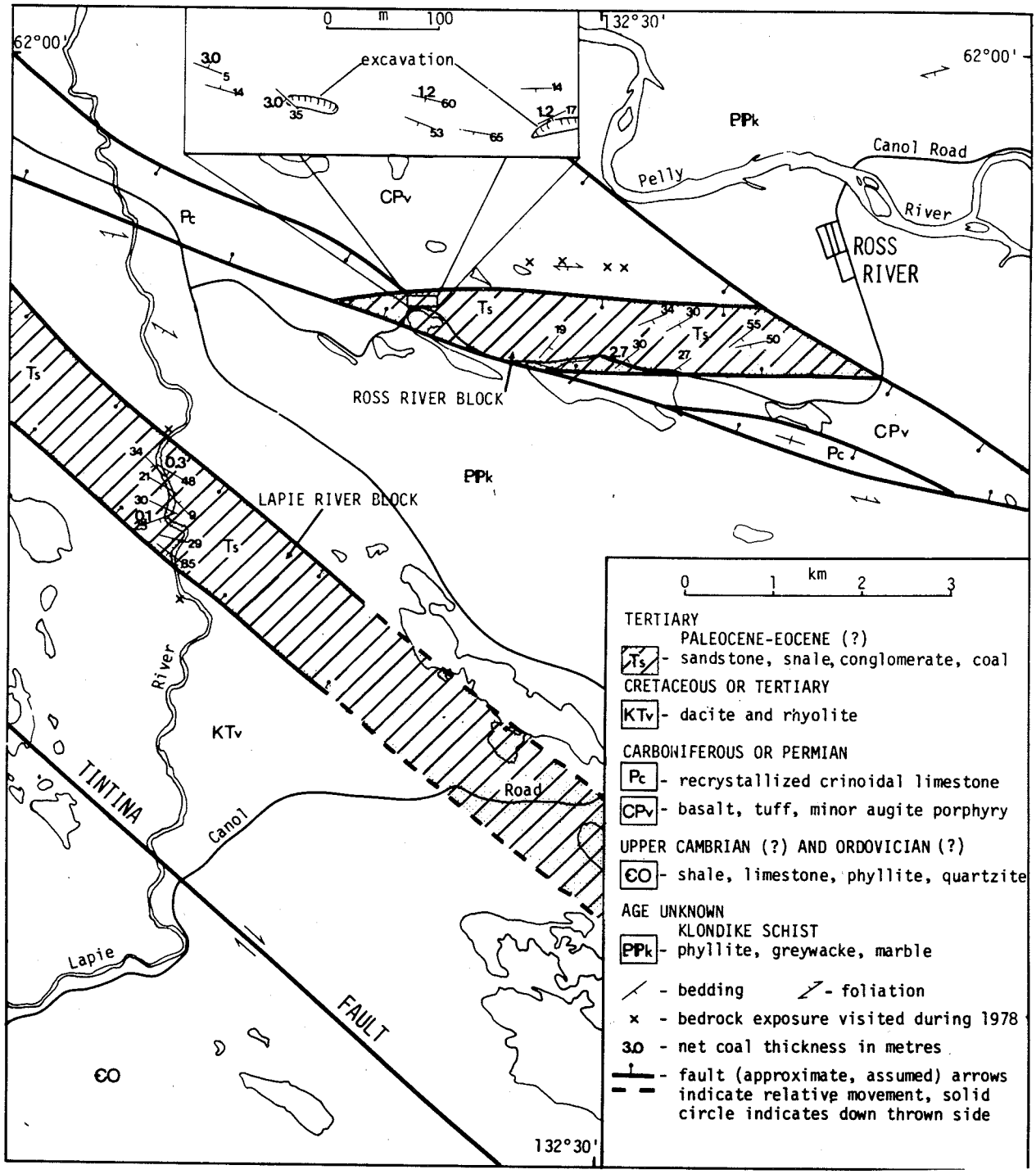

Figure 1 Generalized geology of Ross River area showing net coal thickness (modified from Tempelman-Kluit, 1977, pers. com., 1979 by Hughes and Long 1980).

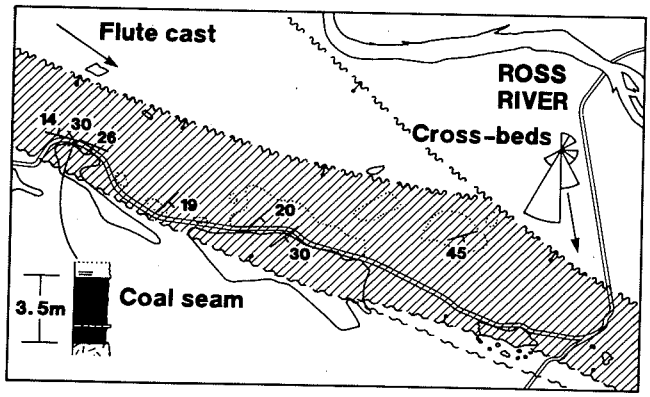

Figure 2 Geology of the Ross River Block, based on Hughes and Long (1980). Insert shows the stratigraphy of a thick coal seam at the western end of the block. The seam is underlain by mudrocks of floodplain origin and overlain by laminated mudrocks of pond or lake origin. Paleocurrent rose at right in from the upper part of the measured section shown in Figure 3.

minor carbonaceous partings.

ROSS RIVER BLOCK

The Ross River block is bounded by faults with large vertical separations which may have strike-slip displacements. The position of faults shown on Figure 5 east of Ross River townsite and south of the Canol Road is conjectural, owing to extensive surficial cover.

Early Tertiary strata in the Ross River block are exposed within a small area near its western extremity, and along and north of the Canol Road, 1.5 km further east (Fig. 1). Unlike the Lapie River block, which is covered by thick deposits of glacial and lacustrine material in areas away from the river, resistant strata in the central part of this block have only a thin veneer of surficial material.

At the western locality, scattered exposures of siltstone, sandstone, claystone and coal occur within an area 300 m by 100 m (Fig. 1, 2). They are strongly folded and probably lie close to one of the bounding faults. Two coal seams, 3 m and 1.2 m thick, are exposed in an open cuts near the Canol Road. These coal seams were estimated to contain an "inferred" (Energy, Mines and Resources, 1977) resource of 370 kilotons at depths of less than 50 m (Hughes and Long, 1980). Other seams of low to medium volatile bituminous coal higher in this sequence (Fig. 3) were considered too thin to meet current resources criteria. Two other seams of similar thickness are exposed in nearby trenches and, although lack of exposure prevents definite correlation, their proximity to the excavated seams suggests they may be lateral equivalents.

Further east a homoclinal succession, at least 400 m thick, is partially exposed along the north side of the Canol Road (Fig. 3). This sequence is largely undeformed, and dips southwest at 10 to 30°. The section, from its base, comprises a recessive, poorly exposed 200 m thick unit of massive to laminated claystone, siltstone, and minor sandstone; a more resistant 110 m thick unit of sandstone, siltstone, claystone, coal (five seams) and, in the lower part, massive to stratified units of conglomerate and sandstone up to 12 m thick; and a resistant unit, at least 100 m thick , of massive to crudely stratified and in part cross-stratified conglomerate and minor sandstone. Parts of this upper conglomeratic unit and some of the more resistant beds in the underlying unit are exposed between the road section and the bounding faults to the north.

The conglomerates are similar in character to the thicker units in Lapie river section; they range from granule to large pebble grade, with maximum clast size up to 9 cm. Individual beds may be up to 4.5 m thick, although composite bed sets may be thicker. Lenticular sandstones intercalated with conglomerats are of medium to very coarse sand grade and exhibit plane bedding and trough and planar cross-stratification. Finer grained sandstones in the more shaly parts of the section are ripple cross-laminated. In the lower parts of the section the mudrocks are commonly laminated with few plant remains, whereas in the central part of the section they tend to be massive to laminated with more abundant plant remains, rooted zones and thin carbonaceous partings.

Coal seams 0.3, 0.4, 0.65, 0.9 and 2.65 m thick were recorded at 231, 235, 241, 264 and 286 m respectively from the base of section. Covered intervals within the central and lower units may conceal additional seams.

AGE AND CORRELATION

The ages of the coal-bearing strata in this area have been determined approximately from examination

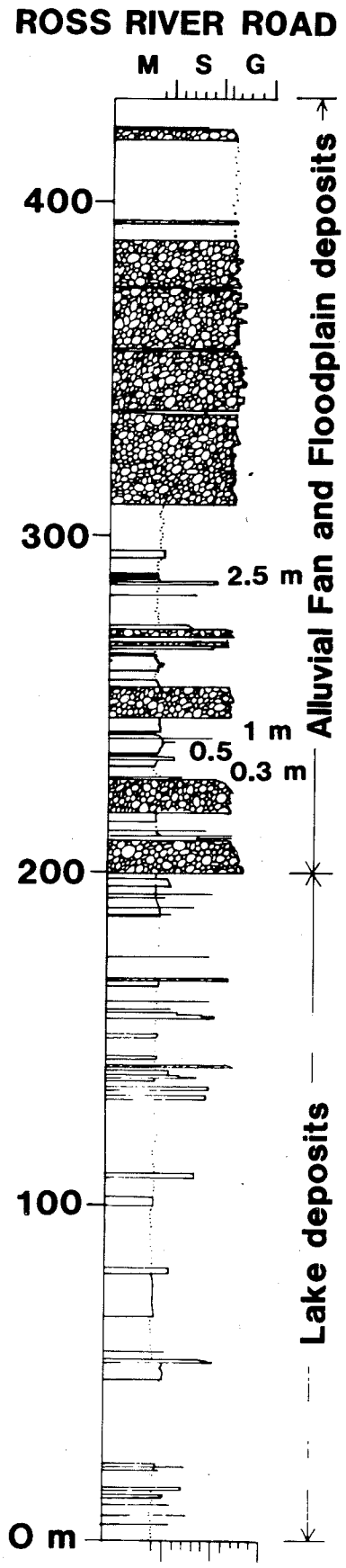

Figure 3 Stratigraphic section exposed along Canol Road, from 61°58'10"E, 132°32'56"W to 61°58'08"W. M=mudstone, S=sandstone, C=conglomerate. Thickness of coal seams in metres.

of macro- and microflora. Kindle (1946) reported a Paleocene age for a collection of plant remains from the Lapie River section. Microflora examined by Hopkins (1979) in the study by Hughes and Long (1980) are poorly preserved, but suggest an Early or possibly Middle Eocene age for a sample collected from the basal part of the Lapie River section, and an age no younger than Eocene and probably Early Eocene or Lower Middle Eocene for two samples from the Canol Road section.

Both the Lapie River and Canol Road sections show gross coarsening upwards trends, from shale at the base to conglomerate at the top, and are of comparable thickness. Absence of marker horizons precludes direct correlation of these two sections. Correlation between the sections based on palynomorph assemblages is not possible other than to suggest a broad age equivalence, due to the small number of palynomorphs present and their poor state of preservation. Coal rank, as determined from vitrinite reflectance (measured by A.R. Cameron of the Geological Survey of Canada), is markedly higher in the Ross River area than within equivalent sediments elsewhere in the Trench. Coals from the Lapie River section are of high volatile bituminous A rank (1.0 - 1.25% R) and coals from the road section and western part of the Ross River block are respectively of low volatile bituminous (1.6 - 1.7%) R) and semi-anthracite (1.9% R) rank. This elevation in rank suggests an abnormally high geothermal gradient during much of the burial period of these coals, probably a result of local heating related to intrusions emplaced at relatively shallow depth subsequent to their deposition. These rank variations can be used to suggest a correlation if strike-slip movement between the two blocks was relatively minor. If the two blocks were close during coalification and experienced similar thermal histories, and if most of the coalification preceded deformation, a relatively constant increase in rank with depth would be expected. This would suggest that the Lapie River sediments are younger than those in the Ross River block, and that the western coals of the Ross River block underlie or correlate with the lower part of the Canol Road section. If linear rank gradients of 0.1 to 0.2% R /100 m are assumed (a range which includes the highest gradients yet noted in western Canadian coals), and if the above assumptions are valid, correlations between the two sections ranging from 200 m of missing strata (if the low gradient is selected) to a slight overlap (if the high gradient is selected) are indicated. These correlations imply a minimum

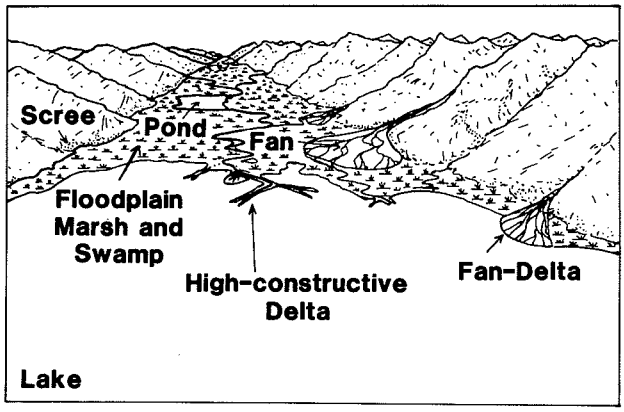

Figure 4 Depositional model of the Ross River Basin in Eocene times. The thickest coal seams would have developed in areas of high subsidence, and low fluviatile input.

thickness of between 800 and 1100 m of early Tertiary strata may be present in this area.

DEPOSITIONAL ENVIRONMENT

The Tertiary coal deposits at Ross River appear to have accumulated in a linear fault controlled basin which developed in response to trans-tensional stresses caused by strike-slip movement along the Tintina Fault system in Early to lower Middle Eocene times (Long, 1980, 1981a, 1981b, 1986; Hughes and Long, 1980).

High rates of subsidence led to deposition of thick sequence of laminated mudrocks along the basin axis, while thick sequences of massive and planar cross stratified granule to large pebble conglomerates were deposited by alluvial fans along the margins of the basin (Fig. 4). Progradation of fluvial facies from the valley walls led at first to development of fan-deltas where alluvial fans entered the lakes. This is best seen in the section along Lapie River (Long, 1981b), but is indicated in the lower half of the road section in the Ross River Block (Fig. 2, 3) by grainflow deposits of medium pebble grade. Further infilling of the trench led to development of extensive wetlands along the trench axis, with deposition of floodplain soils in drier sections, and marsh, pond and swamp deposits where high water tables were maintained. Trunk rivers were confined by extensive vegetation, leading to low rates of lateral migration (c.f. Long, 1984). Where these low gradient, high-construction rivers debouched into lakes, elongate deltas were developed.

While coal seams may have developed in several settings in the Ross River basin, thicker seams appear to be associated with areas of high subsidence n the floodplain, away from major riverine influence. Selective preservation of thinner coal seams (up to 2.5 m) in association with alluvial fan deposits in the upper part of the sequence in the Ross River Block (Fig. 2, 3), may reflect deposition on abandoned sections of fans, or on distal parts of the fans, where subsidence of older gravels into the underlying muddy sequence allowed selective preservation of thick peats.

REFERENCES

Energy, Mines and Resources, 1977, 1976 assessment of Canada's coal resources and reserves; Department of Energy Mines and Resources, Report EP77-5, 20 p.

Hopkins, W.S., Jr., 1979, Geological Survey of Canada, Internal Report No. T-03-WSH-1979.

Hughes, J.D. and Long, D.G.F. 1980, Geology and coal resources potential of early Tertiary strata along Tintina Trench, Yukon Territory Geological Survey of Canada Paper 79-32, 21 pp.

Kindle, E.D., 1946, Geological reconnaissance along the Canol Road, from Teslin River to MacMillan Pass, Yukon; Geological Survey of Canada, Paper 45-21.

Long, D.G.F., 1980, Sedimentary and tectonic framework of fresh-water intermontain coal basin of the Canadian Cordillera; Resumes Abstracts, 26th Congress Geologique International 3:1058.

Long, D.G.F., 1981a, The relation of clastic basins to major structures in the Canadian Cordillera; in The last 100 million years (Mid Cretaceous to Holocene) of Geology and mineral deposits in the Canadian Cordillera; Program with Abstracts, Cordilleran Section, Geological Association of Canada (February 13-14) Vancouver, B.C.

Long, D.G.F., 1981b, Dextral strike slip faults in the Canadian Cordillera and depositional environments of related fresh-water intermontain coal basins; in A.D. Miall (editor), Sedimentation and Tectonics in alluvial basins; Geological Association of Canada, Special Paper 23:153-186.

Long, D.G.F., 1984, Rock River basin (NTS 95D, 11 and 14); Department of Indian and Northern Affairs, Canada, Yukon Exploration and Geology 1983, p. 60-68.

Long, D.G.F., 1986, Coal in the Yukon; in J.D. Morin (editor) Mineral Deposits of the Northern Cordillera. Canadian Institute of Mining and Metallurgy, Special Paper 37 p. 311-318.

Milner, M. and Craig, D.B., 1973, Coal in the Yukon; Department of Indian and Northern Affairs, unpublished manuscript, 27 p.

Tempelman-Kluit, D.J., 1977, Quiet Lake (105 F) and Finlayson Lake (105 G) map-areas, Yukon; Geological Survey of Canada, Open File 486.

Wheeler, J.O., Green, L.H. and Roddick, J.A., 1960, Quiet Lake map- area, Y.T.; Geological Survey of Canada, Map 7-1980.